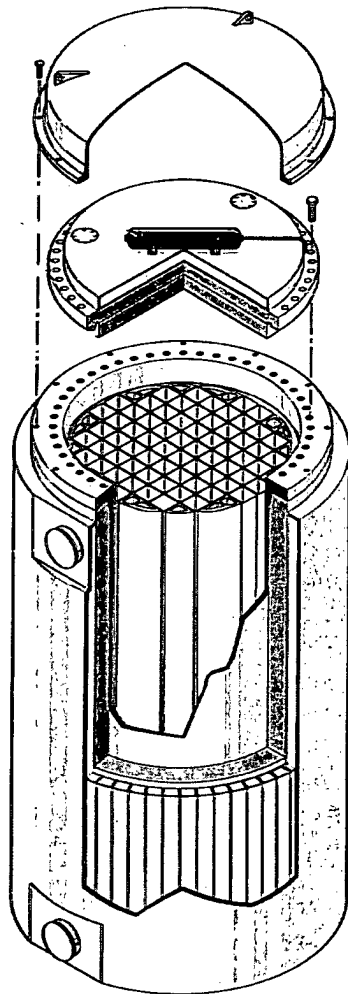


Enclosure 3 to TN E-26455

Full version of TN-68 UFSAR Revision 4 (Public Version)

A
TRANSNUCLEAR



Non-Proprietary

**TN-68 DRY STORAGE
CASK**

UPDATED FINAL SAFETY ANALYSIS REPORT

Rev. 4 5/08



NON-PROPRIETARY

**TN-68 DRY STORAGE CASK
UPDATED FINAL SAFETY ANALYSIS
REPORT**

Transnuclear, Inc.
7135 Minstrel Way, Suite 300
Columbia, Maryland 21045

Rev. 4 5/08

TN-68 SAFETY ANALYSIS REPORT MASTER TABLE OF CONTENTS

1 GENERAL DESCRIPTION

1.1	Introduction.....	1.1-1
1.2	General Description of the TN-68	1.2-1
1.2.1	Cask Characteristics.....	1.2-1
1.2.2	Operational Features.....	1.2-3
1.2.2.1	General Features.....	1.2-3
1.2.2.2	Sequence of Operations.....	1.2-3
1.2.2.3	Identification of Subjects for Safety and Reliability Analysis	1.2-4
1.2.3	Cask Contents	1.2-5
1.3	Identification of Agents and Contractors	1.3-1
1.4	Generic Cask Arrays	1.4-1
1.5	Supplemental Data	1.5-1
1.6	References.....	1.6-1

2 PRINCIPAL DESIGN CRITERIA

2.1	Spent Fuel To Be Stored	2.1-1
2.2	Design Criteria for Environmental Conditions and Natural Phenomena.....	2.2-1
2.2.1	Tornado Wind and Tornado Missiles	2.2-1
2.2.1.1	Applicable Design Parameters	2.2-1
2.2.1.2	Determination of Forces on Structures.....	2.2-1
2.2.1.3	Tornado Missiles	2.2-9
2.2.2	Water Level (Flood) Design	2.2-13
2.2.2.1	Flood Elevations.....	2.2-13
2.2.2.2	Phenomena Considered in Design Load Calculations.....	2.2-14
2.2.2.3	Flood Force Application.....	2.2-14
2.2.2.4	Flood Protection	2.2-14
2.2.3	Seismic Design	2.2-14
2.2.3.1	Input Criteria	2.2-15
2.2.3.2	Seismic-System Analysis	2.2-15
2.2.4	Snow and Ice Loading	2.2-17
2.2.5	Combined Load Criteria	2.2-17
2.2.5.1	Introduction	2.2-17
2.2.5.2	TN-68 Cask Loading.....	2.2-18
2.2.5.3	Bounding Loads for Design and Service Conditions	2.2-21
2.2.5.4	Design Loads.....	2.2-22
2.3	Safety Protection Systems.....	2.3-1
2.3.1	General.....	2.3-1
2.3.2	Protection By Multiple Confinement Barriers and Systems.....	2.3-2
2.3.2.1	Confinement Barriers and Systems	2.3-2
2.3.2.2	Cask Cooling.....	2.3-4
2.3.3	Protection by Equipment and Instrument Selection.....	2.3-5
2.3.3.1	Equipment	2.3-5
2.3.3.2	Instrumentation.....	2.3-5
2.3.4	Nuclear Criticality Safety	2.3-5
2.3.4.1	Control Methods for Prevention of Criticality	2.3-5

**TN-68 SAFETY ANALYSIS REPORT
MASTER TABLE OF CONTENTS**

2.3.4.2	Error Contingency Criteria	2.3-6
2.3.4.3	Verification Analysis-Benchmarking	2.3-6
2.3.5	Radiological Protection	2.3-6
2.3.5.1	Access Control	2.3-6
2.3.5.2	Shielding.....	2.3-7
2.3.5.3	Radiological Alarm System.....	2.3-7
2.3.6	Fire and Explosion Protection.....	2.3-7
2.4	Decommissioning Considerations.....	2.4-1
2.5	Summary of Cask Design Criteria	2.5-1
2.6	References.....	2.6-1

3 STRUCTURAL EVALUATION

3.1	Structural Design	3.1-1
3.1.1	Discussion.....	3.1-1
3.1.2	Design Criteria.....	3.1-2
3.1.2.1	Confinement Boundary	3.1-3
3.1.2.2	Non-Confinement Structure	3.1-3
3.1.2.3	Basket	3.1-4
3.1.2.4	Trunnions.....	3.1-5
3.2	Weights and Centers of Gravity.....	3.2-1
3.3	Mechanical Properties of Materials	3.3-1
3.3.1	Cask Material Properties.....	3.3-1
3.3.2	Basket Material Properties.....	3.3-1
3.3.3	Material Properties Summary	3.3-1
3.3.4	Material Durability	3.3-1
3.4	General Standards for Casks.....	3.4-1
3.4.1	Chemical and Galvanic Reactions	3.4-1
3.4.1.1	Cask Interior	3.4-1
3.4.1.2	Cask Exterior.....	3.4-5
3.4.1.3	Lubricants and Cleaning Agents	3.4-6
3.4.1.4	Hydrogen Generation	3.4-6
3.4.1.5	Effect of Galvanic Reactions on the Performance of the Cask	3.4-7
3.4.2	Positive Closure	3.4-8
3.4.3	Lifting Devices	3.4-8
3.4.3.1	Trunnion Analysis	3.4-8
3.4.3.2	Local Stresses in Cask Body at Upper Trunnion Locations	3.4-9
3.4.3.3	Trunnion Bolt Stresses	3.4-10
3.4.4	Heat.....	3.4-11
3.4.4.1	Summary of Pressures and Temperatures	3.4-11
3.4.4.2	Differential Thermal Expansion	3.4-11
3.4.4.3	Stress Calculations.....	3.4-12
3.4.4.4	Comparison with Allowable Stresses.....	3.4-13
3.4.5	Cold	3.4-13
3.4.6	Fire Accident	3.4-14
3.5	Fuel Rods	3.5-1
3.5.1	Fuel Rod Temperature Limits.....	3.5-1
3.5.2	Thermal Stress of Fuel Cladding due to Unloading Operations.....	3.5-1

**TN-68 SAFETY ANALYSIS REPORT
MASTER TABLE OF CONTENTS**

3.6	Supplemental Information.....	3.6-1
3.6.1	Supplemental Information from Reference 12	3.6-1
3.6.2	Supplemental Information from Reference 18	3.6-13
3.6.3	Supplemental Information from Reference 19	3.6-17
3.7	References.....	3.7-1

3A STRUCTURAL ANALYSIS OF THE TN-68 STORAGE CASK BODY

3A.1	Introduction.....	3A.1-1
3A.2	Cask Body Structural Analysis	3A.2-1
3A.2.1	Description.....	3A.2-1
3A.2.2	ANSYS Cask Model.....	3A.2-1
3A.2.3	Individual Load Cases	3A.2-2
3A.2.3.1	Normal Conditions	3A.2-2
3A.2.3.2	Accident Conditions	3A.2-5
3A.2.3.3	Summary of Individual Load Cases	3A.2-6
3A.2.3.4	Fire Accident	3A.2-7
3A.2.4	Additional Cask Body Analyses	3A.2-8
3A.2.4.1	Trunnion Local Stresses	3A.2-8
3A.2.4.2	Tornado Missile Impact.....	3A.2-8
3A.2.4.3	Impact on a Trunnion	3A.2-9
3A.2.5	Evaluation (Load Combinations Vs. Allowables)	3A.2-11
3A.3	Lid Bolt Analyses	3A.3-1
3A.3.1	Introduction.....	3A.3-1
3A.3.2	Bolt Load Calculations	3A.3-2
3A.3.3	Load Combinations.....	3A.3-6
3A.3.4	Bolt Stress Calculations.....	3A.3-7
3A.3.5	Results	3A.3-9
3A.3.6	Minimum Engagement Length, L_e For Bolt and Flange.....	3A.3-9
3A.3.7	Conclusions.....	3A.3-10
3A.4	Outer Shell	3A.4-1
3A.4.1	Description.....	3A.4-1
3A.4.2	Materials Input Data	3A.4-1
3A.4.3	Applied Loads.....	3A.4-1
3A.4.4	Method of Analysis.....	3A.4-2
3A.4.5	Results	3A.4-3
3A.5	References.....	3A.5-1

3B STRUCTURAL ANALYSIS OF THE TN-68 BASKET

3B.1	Introduction.....	3B.1-1
3B.1.1	Geometry	3B.1-1
3B.1.2	Weight	3B.1-2
3B.1.3	Temperature.....	3B.1-2
3B.2	Basket Finite Element Model Development (For Side Impact Analysis).....	3B.2-1
3B.3	Basket Under Normal Condition Loads.....	3B.3-1
3B.3.1	Description.....	3B.3-1
3B.3.2	Basket Analysis Under 1G Side Load	3B.3-1

**TN-68 SAFETY ANALYSIS REPORT
MASTER TABLE OF CONTENTS**

3B.3.3	Basket Analysis Under Vertical Load	3B.3-2
3B.3.4	Basket Thermal Expansion Analysis	3B.3-3
3B.3.5	Design Criteria.....	3B.3-6
3B.3.6	Evaluation.....	3B.3-7
3B.4	Basket Under Accident Condition Loads - Stress Analysis.....	3B.4-1
3B.4.1	Basket Analysis Under 60 g Bottom End Drop.....	3B.4-1
3B.4.2	Basket Analysis Under Tipover Side Impact.....	3B.4-2
3B.4.3	Design Criteria For Impact Accident.....	3B.4-2
3B.4.4	Evaluation.....	3B.4-3
3B.5	Basket Under Accident Condition Loads-Buckling Analysis.....	3B.5-1
3B.5.1	Analysis of Basket To Determine the Buckling Loads.....	3B.5-1
3B.5.2	Analysis Results.....	3B.5-3
3B.5.3	Evaluation.....	3B.5-5
3B.5.4	Analysis of the Aluminum Rails to Determine the Buckling Loads.....	3B.5-5
3B.5.5	Evaluation.....	3B.5-8
3B.6	Summary of Basket Structural Analysis	3B.6-1
3B.6.1	Stresses Due To Normal Condition Service	3B.6-1
3B.6.2	Stresses Due To Accident Condition.....	3B.6-2
3B.7	References.....	3B.7-1

3C MODAL ANALYSIS OF THE TN-68 BASKET

3C.1	Introduction.....	3C.1-1
3C.1.1	Modal Analysis.....	3C.1-1
3C.1.2	Results	3C.1-2
3C.1.3	Conclusion.....	3C.1-4
3C.2	References.....	3C.2-1

3D TIPOVER AND END DROP ANALYSES OF TN-68 STORAGE CASK

3D.1	Tipover Analysis of TN-68 Storage Cask.....	3D.1-1
3D.2	Finite Element Model For Analysis.....	3D.2-1
3D.2.1	TN-32 Model	3D.2-1
3D.2.2	TN-68 Model	3D.2-1
3D.2.3	BNFL Model.....	3D.2-2
3D.3	Description of Tipover Analysis.....	3D.3-1
3D.3.1	Analysis Program.....	3D.3-1
3D.3.2	Material Properties.....	3D.3-1
3D.3.3	Loading and Boundary Conditions	3D.3-4
3D.4	Tipover Analysis Verification.....	3D.4-1
3D.4.1	Analysis Assumptions	3D.4-1
3D.4.2	Experimental Validation.....	3D.4-1
3D.4.3	TN-32 Tipover Analysis Validation	3D.4-2
3D.4.4	DaDisp Program Validation.....	3D.4-4
3D.5	TN-68 Tipover Analysis Results.....	3D.5-1
3D.5.1	Results of TN-68 Tipover Analysis	3D.5-1
3D.5.2	Dynamic Amplification Calculation.....	3D.5-1

**TN-68 SAFETY ANALYSIS REPORT
MASTER TABLE OF CONTENTS**

3D.6	Summary of G Loads For Cask and Basket Side Impact Analyses	3D.6-1
3D.6.1	Equivalent Side Drop G Load For The Cask to Envelop The Tipover Accident	3D.6-1
3D.6.2	Equivalent Side Drop G Load For The Basket to Envelop The Tipover Accident.....	3D.6-1
3D.7	End Drop Analysis of TN-68 Storage Cask	3D.7-1
3D.7.1	General Approach.....	3D.7-1
3D.7.2	Cask and Concrete Pad/Soil Description	3D.7-2
3D.7.3	End Impact Analysis.....	3D.7-2
3D.8	References.....	3D.8-1
3E	FRACTURE TOUGHNESS EVALUATION OF TN-68 CASK	
3E.1	Introduction.....	3E-1
3E.1.1	Fracture Toughness Evaluation of Confinement Boundary.....	3E-1
3E.1.2	Fracture Toughness Evaluation of Gamma Shield	3E-2
3E.1.3	References.....	3E-13
4	THERMAL EVALUATION	
4.1	Discussion	4.1-1
4.2	Summary of Thermal Properties of Materials.....	4.2-1
4.3	Thermal Evaluation for Normal and Off-Normal Conditions.....	4.3-1
4.3.1	Thermal Model for Normal and Off-Normal Storage Conditions	4.3-1
4.3.2	Maximum Temperatures for Normal Storage Conditions	4.3-4
4.3.3	Minimum Temperatures for Normal Storage Conditions	4.3-4
4.3.4	Maximum Internal Pressures for Normal Storage Conditions.....	4.3-5
4.3.5	Thermal Stresses for Normal Storage Conditions	4.3-5
4.3.6	Evaluation of Thermal Performance for Normal Storage Conditions	4.3-7
4.4	Thermal Evaluation for Accident Conditions	4.4-1
4.4.1	Thermal Models for Accident Conditions	4.4-1
4.4.2	Maximum Temperatures for Accident Conditions	4.4-3
4.4.3	Maximum Internal Pressures for Accident Conditions.....	4.4-4
4.4.4	Thermal Stresses for Accident Conditions	4.4-4
4.4.5	Evaluation of Thermal Performance for Accident Conditions	4.4-4
4.5	Thermal Evaluation for Loading and Unloading Conditions.....	4.5-1
4.5.1	Vacuum Drying	4.5-1
4.5.2	Reflooding	4.5-5
4.6	Thermal Evaluation of TN-68 Cask Containing Damaged Fuel.....	4.6-1
4.6.1	Normal Storage Conditions	4.6-1
4.6.2	Accident Conditions	4.6-1
4.6.3	Evaluation of the Thermal Performance with Damaged Fuel.....	4.6-2
4.7	Maximum Internal Pressure	4.7-1
4.7.1	Average Gas Temperature	4.7-1
4.7.2	Amount of Initial Helium Backfill.....	4.7-2
4.7.3	Free Gas within Fuel Assemblies	4.7-2
4.7.4	Total Amount of Gases within Cask Cavity	4.7-3
4.7.5	Maximum Cask Internal Pressure.....	4.7-3
4.8	Effective Fuel Properties.....	4.8-1

**TN-68 SAFETY ANALYSIS REPORT
MASTER TABLE OF CONTENTS**

4.8.1	Discussion.....	4.8-1
4.8.2	Summary of Material Properties.....	4.8-1
4.8.3	Effective Fuel Conductivity.....	4.8-2
4.8.4	Effective Fuel Density and Specific Heat.....	4.8-4
4.8.5	Conclusion.....	4.8-4
4.9	Axial Decay Heat Profile.....	4.9-1
4.10	Heat Transfer Coefficients.....	4.10-1
4.10.1	Total heat Transfer Coefficient to Ambient (Free Convection).....	4.10-1
4.10.2	Total heat Transfer Coefficient to Ambient for Fire.....	4.10-5
4.10.3	Free Convection Coefficients.....	4.10-6
4.11	Radial Hot Gap between the Basket Rails and the Cask Inner Shell.....	4.11-1
4.12	Supplemental Data.....	4.12-1
4.12.1	ANSYS Macros.....	4.12-1
4.13	References.....	4.13-1
4A	HEAT GENERATION RATE AS A FUNCTION OF SPENT FUEL PARAMETERS	
4A.1	Introduction.....	4A-1
4A.2	Calculational Methodology and Input Models.....	4A-1
4A.3	Mathematical Function to Determine Heat Generation.....	4A-1
4A.4	Sample Fuel Qualification Table for the Assembly Heat Load of 441 Watts.....	4A-2
4A.5	References.....	4A-3
5	SHIELDING EVALUATION	
5.1	Discussion and Results.....	5.1-1
5.2	Source Specification.....	5.2-1
5.2.1	Axial Source Distribution.....	5.2-3
5.2.2	Gamma Source.....	5.2-4
5.2.3	Neutron Source.....	5.2-4
5.2.4	Fission Gas Release and Airborne Radioactive Material Sources.....	5.2-4
5.2.5	Fuel Qualification for 7x7 Fuel.....	5.2-5
5.2.6	Fuel Qualification for 8x8, 9x9 and 10x10 Fuel.....	5.2-6
5.3	Model Specification.....	5.3-1
5.3.1	Description of the Radial and Axial Shielding Configurations.....	5.3-1
5.3.2	Shield Regional Densities.....	5.3-3
5.4	Shielding Evaluation.....	5.4-1
5.4.1	Computer Programs.....	5.4-1
5.4.2	Spatial Source Distribution.....	5.4-1
5.4.3	Cross-Section Data.....	5.4-1
5.4.4	Flux-to-Dose-Rate Conversion.....	5.4-2
5.4.5	Model Geometry.....	5.4-2
5.4.6	Methodology.....	5.4-2
5.4.7	Assumptions.....	5.4-2
5.4.8	Near Field Dose Rate Calculations.....	5.4-4

**TN-68 SAFETY ANALYSIS REPORT
MASTER TABLE OF CONTENTS**

5.4.9	Far Field Dose Rate Calculations	5.4-4
5.5	Supplemental Data	5.5-1
5.5.1	Sample Input Files	5.5-1
5.6	References.....	5.6-1
6	CRITICALITY EVALUATION	
6.1	Discussion and Results.....	6.1-1
6.2	Spent Fuel Loading	6.2-1
6.3	Model Specification	6.3-1
6.3.1	Description of Calculational Model.....	6.3-1
6.3.2	Cask Regional Densities	6.3-2
6.4	Criticality Calculation	6.4-1
6.4.1	Calculational or Experimental Method.....	6.4-1
6.4.2	Fuel Loading or Other Contents Loading Optimization	6.4-4
6.4.3	Criticality Results	6.4-12
6.5	Critical Benchmark Experiments	6.5-1
6.5.1	Benchmark Experiments and Applicability	6.5-1
6.5.2	Results of the Benchmark Calculations	6.5-2
6.5.3	Modeling Bias.....	6.5-2
6.6	Supplemental Data	6.6-1
6.6.1	Sample Input File, Most Reactive Lattice Evaluation	6.6-1
6.6.2	Variable Enrichment Patterns, Uniform Enrichment Validation	6.6-3
6.6.3	Sample Input Files, Uniform Enrichment Model Validation.....	6.6-9
6.6.4	Sample Input Files, Most Reactive Intact Assembly Configuration, Scoping Model	6.6-13
6.6.5	Sample Input Files, TN-68 Final Criticality Evaluation.....	6.6-18
6.7	References.....	6.7-1
6A	EVALUATION OF UNDAMAGED FUEL UNDER ACCIDENT ACCELERATIONS	
6A.1	Side Drop Analysis	6A.1-1
6A.2	Bottom End Drop Analysis	6A.2-1
6A.3	Material Properties of High Burnup Fuel.....	6A.3-1
6A.4	Determination of Side Drop g-Loading with Dynamic Load Factor	6A.4-1
6A.5	References.....	6A.5-1
6B	DAMAGED FUEL CLADDING STRUCTURAL EVALUATION	
6B.1	Introduction.....	6B.1-1
6B.2	Design Input / Data	6B.2-1
6B.3	Loads.....	6B.3-1
6B.4	Evaluation Criteria	6B.4-1
6B.5	One Foot End Drop Damaged Fuel Evaluation	6B.5-1

**TN-68 SAFETY ANALYSIS REPORT
MASTER TABLE OF CONTENTS**

6B.6	One Foot Side Drop Damaged Fuel Evaluation.....	6B.6-1
6B.7	Evaluation of Zircaloy Fuel Cladding Material Fracture Toughness.....	6B.7-1
6B.8	Fracture Mechanics Evaluation.....	6B.8-1
6B.9	Conclusions.....	6B.9-1
6B.10	References.....	6B.10-1
7	CONFINEMENT	
7.1	Confinement Boundary	7.1-1
7.1.1	Confinement Vessel.....	7.1-1
7.1.2	Confinement Penetrations.....	7.1-2
7.1.3	Seals and Welds.....	7.1-2
7.1.4	Closure.....	7.1-4
7.1.5	Monitoring of System Confinement	7.1-4
7.2	Requirements for Normal Conditions of Storage.....	7.2-1
7.2.1	Release of Radioactive Material	7.2-1
7.2.2	Pressurization of Confinement Vessel.....	7.2-1
7.3	Confinement Requirements for Hypothetical Accident Conditions	7.3-1
7.3.1	Source Terms for Confinement Calculations.....	7.3-1
7.3.2	Release of Contents	7.3-3
7.3.3	Latent Seal Failure.....	7.3-7
7.4	References.....	7.4-1
8	OPERATING PROCEDURES	
8.1	Loading the Cask	8.1-1
8.1.1	General Description	8.1-1
8.1.2	Flow Sheets.....	8.1-2
8.1.3	Vacuum Drying System.....	8.1-2
8.1.4	Leak Detection.....	8.1-3
8.1.5	Major Tools and Equipment	8.1-3
8.2	Unloading the Cask.....	8.2-1
8.3	Surveillance and Maintenance	8.3-1
8.4	Contingency Actions.....	8.4-1
8.5	Preparation of the Cask.....	8.5-1
8.6	References.....	8.6-1
9	ACCEPTANCE CRITERIA AND MAINTENANCE PROGRAM	
9.1	Acceptance Criteria.....	9.1-1
9.1.1	Visual Inspection	9.1-1
9.1.2	Structural.....	9.1-1
9.1.3	Leak Tests.....	9.1-2
9.1.4	Components.....	9.1-2
9.1.4.1	Valves.....	9.1-2

**TN-68 SAFETY ANALYSIS REPORT
MASTER TABLE OF CONTENTS**

9.1.4.2	Gaskets	9.1-2
9.1.5	Shielding Integrity	9.1-3
9.1.6	Thermal Acceptance	9.1-4
9.1.7	Neutron Absorber Tests	9.1-4
9.1.7.1	Boron Aluminum Alloy (Borated Aluminum)	9.1-4
9.1.7.2	Boron Carbide/Aluminum Metal Matrix Composites (MMC).....	9.1-5
9.1.7.3	Boral®	9.1-6
9.2	Maintenance Program	9.2-1
9.3	Marking.....	9.3-1
9.4	Specification for Neutron Absorbers	9.4-1
9.4.1	Specification for Thermal Conductivity Testing of Neutron Absorbers.....	9.4-1
9.4.2	Specification for Acceptance Testing of Neutron Absorbers by Neutron Transmission...	9.4-1
9.4.3	Specification for Qualification Testing of Metal Matrix Composites	9.4-3
9.4.3.1	Applicability and Scope	9.4-3
9.4.3.2	Design Requirements.....	9.4-3
9.4.3.3	Durability.....	9.4-4
9.4.3.4	Required Qualification Tests and Examinations to Demonstrate Mechanical Integrity.	9.4-4
9.4.3.5	Required Tests and Examinations to Demonstrate B10 Uniformity	9.4-5
9.4.3.6	Testing for Other Design Properties.....	9.4-5
9.4.3.7	Approval of Procedures.....	9.4-5
9.4.4	Specification for Process Controls for Metal Matrix Composites.....	9.4-5
9.4.4.1	Applicability and Scope	9.4-5
9.4.4.2	Definition of Key Process Changes.....	9.4-6
9.4.4.3	Identification and Control of Key Process Changes.....	9.4-6
9.5	Alternate Acceptance Testing for Neutron Absorbers for TN-68-01 through -44.....	9.5-1
9.5.1	Test Coupons	9.5-1
9.5.2	Acceptance Testing.....	9.5-1
9.6	References.....	9.6-1

9A TRANSNUCLEAR TN-68 RADIAL NEUTRON SHIELD MATERIAL

Thermal Stability	9A-1
Radiation Stability	9A-1
References.....	9A-3

10 RADIATION PROTECTION

10.1	Ensuring that Occupational Radiation Exposures are As Low As Is Reasonably Achievable (ALARA).....	10.1-1
10.1.1	Policy Considerations	10.1-1
10.1.2	Design Considerations	10.1-1
10.1.3	Operational Considerations.....	10.1-2
10.2	Radiation Protection Design Features.....	10.2-1
10.2.1	Cask Design Features	10.2-1
10.2.2	Radiation Dose Rates.....	10.2-1
10.3	Estimated Onsite Collective Dose Assessment.....	10.3-1

**TN-68 SAFETY ANALYSIS REPORT
MASTER TABLE OF CONTENTS**

10.4 References..... 10.4-1

11 ACCIDENT ANALYSES

11.1 Off-Normal Operations..... 11.1-1

11.1.1 Loss of Electric Power..... 11.1-1

11.1.1.1 Postulated Cause of the Event..... 11.1-1

11.1.1.2 Detection of Event..... 11.1-1

11.1.1.3 Analysis of Effects and Consequences..... 11.1-2

11.1.1.4 Corrective Actions..... 11.1-2

11.1.1.5 Radiological Impact from Off-Normal Operations..... 11.1-2

11.1.2 Cask Seal Leakage..... 11.1-2

11.1.2.1 Postulated Cause of the Event..... 11.1-2

11.1.2.2 Detection of Event..... 11.1-2

11.1.2.3 Analysis of Effects and Consequences..... 11.1-3

11.1.2.4 Corrective Actions..... 11.1-4

11.1.2.5 Radiological Impact..... 11.1-4

11.1.3 Overpressure Tank Needs Refilling..... 11.1-5

11.1.3.1 Postulated Cause of the Event..... 11.1-5

11.1.3.2 Detection of Event..... 11.1-5

11.1.3.3 Analysis of Effects and Consequences..... 11.1-5

11.1.3.4 Corrective Actions..... 11.1-5

11.1.3.5 Radiological Impact..... 11.1-5

11.2 Accidents..... 11.2-1

11.2.1 Earthquake..... 11.2-1

11.2.1.1 Cause of Accident..... 11.2-1

11.2.1.2 Accident Analysis..... 11.2-1

11.2.1.3 Accident Dose Calculations..... 11.2-1

11.2.1.4 Corrective Actions..... 11.2-1

11.2.2 Extreme Wind and Tornado Missiles..... 11.2-1

11.2.2.1 Cause of Accident..... 11.2-1

11.2.2.2 Accident Analysis..... 11.2-2

11.2.2.3 Accident Dose Calculations..... 11.2-2

11.2.2.4 Corrective Actions..... 11.2-2

11.2.3 Flood..... 11.2-2

11.2.3.1 Cause of Accident..... 11.2-2

11.2.3.2 Accident Analysis..... 11.2-3

11.2.3.3 Accident Dose Calculations..... 11.2-3

11.2.3.4 Corrective Actions..... 11.2-3

11.2.4 Explosion..... 11.2-3

11.2.4.1 Cause of Accident..... 11.2-3

11.2.4.2 Accident Analysis..... 11.2-3

11.2.4.3 Accident Dose Calculations..... 11.2-4

11.2.4.4 Corrective Actions..... 11.2-4

11.2.5 Fire..... 11.2-4

11.2.5.1 Cause of Accident..... 11.2-4

11.2.5.2 Accident Analysis..... 11.2-4

11.2.5.3 Accident Dose Calculations..... 11.2-5

11.2.5.4 Corrective Actions..... 11.2-5

11.2.6 Inadvertent Loading of a Newly Discharged Fuel Assembly..... 11.2-6

**TN-68 SAFETY ANALYSIS REPORT
MASTER TABLE OF CONTENTS**

11.2.6.1	Cause of Accident.....	11.2-6
11.2.6.2	Accident Analysis.....	11.2-6
11.2.6.3	Accident Dose Calculations	11.2-6
11.2.6.4	Corrective Actions.....	11.2-6
11.2.7	Inadvertent Loading of a Fuel Assembly with a higher initial Enrichment than the Design Basis Fuel.....	11.2-7
11.2.7.1	Cause of Accident.....	11.2-7
11.2.7.2	Accident Analysis.....	11.2-7
11.2.7.3	Accident Dose Calculations	11.2-7
11.2.7.4	Corrective Actions.....	11.2-7
11.2.8	Hypothetical Cask Drop and Tipping Accidents	11.2-8
11.2.8.1	Cause of Accident.....	11.2-8
11.2.8.2	Accident Analysis.....	11.2-8
11.2.8.3	Accident Dose Calculations	11.2-9
11.2.8.4	Corrective Actions.....	11.2-9
11.2.9	Loss of Confinement Barrier	11.2-9
11.2.9.1	Cause of Accident.....	11.2-9
11.2.9.2	Accident Analysis.....	11.2-10
11.2.9.3	Accident Dose Calculations	11.2-10
11.2.9.4	Corrective Actions.....	11.2-10
11.2.10	Buried Cask	11.2-10
11.2.10.1	Cause of Accident.....	11.2-10
11.2.10.2	Accident Analysis.....	11.2-10
11.2.10.3	Accident Dose Calculations	11.2-11
11.2.10.4	Corrective Actions.....	11.2-11
11.3	References.....	11.3-1
12	OPERATING CONTROLS AND LIMITS	
B 2.0	FUNCTIONAL AND OPERATIONAL LIMITS	B 2.0-1
B 3.0	LIMITING CONDITION FOR OPERATION (LCO) APPLICABILITY.....	B 3.0-1
B 3.0	SURVEILLANCE REQUIREMENT (SR) APPLICABILITY.....	B 3.0-5
B 3.1	CASK INTEGRITY.....	B 3.1.1-1
B 3.1.1	Cask Cavity Vacuum Drying	B 3.1.1-1
B 3.1.2	Cask Helium Backfill Pressure.....	B 3.1.2-1
B 3.1.3	Cask Helium Leak Rate	B 3.1.3-1
B 3.1.4	Combined Helium Leak Rate	B 3.1.4-1
B 3.1.5	Cask Interseal Pressure	B 3.1.5-1
B 3.1.6	Cask Minimum Lifting Temperature.....	B 3.1.6-1
B 3.2	CASK RADIATION PROTECTION	B 3.2.1-1
B 3.2.1	Cask Surface Contamination	B 3.2.1-1
13	QUALITY ASSURANCE	
14	DECOMMISSIONING	
14.1	Decommissioning Considerations.....	14.1-1
14.2	Supplemental Information.....	14.2-1

**TN-68 SAFETY ANALYSIS REPORT
MASTER TABLE OF CONTENTS**

14.2.1 SASI Input File..... 14.2-1
14.3 References..... 14.3-1

TN-68 SAFETY ANALYSIS REPORT

MASTER TABLE OF CONTENTS

List of Tables

1.2-1	Nominal Dimensions and Weight of the TN-68 Cask
2.1-1	Fuel Assembly Types
2.1-2	Design Basis Fuel Assembly Parameters
2.1-3	Thermal, Gamma and Neutron Sources for the Design Basis 8x8 General Electric Fuel Assembly
2.1-4	Cooling Time as a Function of Maximum Burnup and Minimum Initial Enrichment 7x7 Fuel
2.2-1	Summary of Internal and External Pressures Acting on TN-68 Cask
2.2-2	Summary of Lifting Loads Used in Upper Trunnion ANSI N14.6 Analysis
2.2-3	Summary of Loads Acting on TN-68 Cask Due to Environmental and Natural Phenomena
2.2-4	TN-68 Cask Loading Conditions
2.2-5	TN-68 Cask Design Loads (Normal Conditions)
2.2-6	Level A Service Loads (Normal Conditions)
2.2-7	Level D Service Loads (Accident Conditions)
2.2-8	Normal Condition Load Combinations
2.2-9	Accident Condition Load Combinations
2.3-1	Classification of Components
2.5-1	Design Criteria for TN-68 Casks
3.1-1	Individual Load Cases Analyzed
3.1-2	Confinement Vessel Stress Limits
3.1-3	Confinement Bolt Stress Limits
3.1-4	Non Confinement Structure Stress Limits
3.1-5	Basket Stress Limits
3.2-1	Cask Weight and Center of Gravity
3.3-1	Mechanical Properties of Body Materials
3.3-2	Temperature Dependent Body Material Properties
3.3-3	Reference Temperatures for Stress Analysis Acceptance Criteria
3.3-4	Mechanical Properties of Basket Materials
3.3-5	Temperature Dependent Basket Material Properties
3.3-6	TN-68 Cask Components and Materials
3.4-1	Upper Trunnion Section Properties and Loads
3.4-2	Upper Trunnion Stresses When Loaded by 6 and 10 Times Cask Weight
3.4-3	Upper Trunnion Loadings on TN-68 for Use in Cask Body Evaluation
3.4-4	Bijlaard Computation Sheet
3.4-5	Comparison of Actual with Allowable Stress Intensity - Confinement Vessel
3.4-6	Comparison of Actual with Allowable Stress Intensity - Gamma Shielding
3.4-7	Summary of Maximum Stress Intensity and Allowable Stress Limits for Lid Bolts
3.4-8	Comparison of Actual with Allowable Stress Intensity in Basket (Normal Conditions)
3.4-9	Comparison of Actual with Allowable Stress Intensity in Basket (Accident Conditions)
3.4-10	Comparison of Maximum Stress Intensity with Allowables in Outer Shell
3A.2.3-1	Bolt Preload (Shell Elements)
3A.2.3-2	Bolt Preload (Solid Elements)
3A.2.3-3	One (1) G Down (Shell Elements)
3A.2.3-4	One (1) G Down (Solid Elements)
3A.2.3-5	Internal Pressure - 100 PSI (Shell Elements)
3A.2.3-6	Internal Pressure - 100 PSI (Solid Elements)
3A.2.3-7	External Pressure - 25 PSI (Shell Elements)
3A.2.3-8	External Pressure - 25 PSI (Solid Elements)

**TN-68 SAFETY ANALYSIS REPORT
MASTER TABLE OF CONTENTS**

List of Tables

3A.2.3-9	Thermal Stress (Shell Elements)
3A.2.3-10	Thermal Stress (Solid Elements)
3A.2.3-11	Six (6) G on Trunnion (Shell Elements)
3A.2.3-12	Six (6) G on Trunnion (Solid Elements)
3A.2.3-13	One (1) G Side Drop - Contact Side (Shell Elements)
3A.2.3-14	One (1) G Side Drop - Contact Side (Solid Elements)
3A.2.3-15	One (1) G Side Drop - Side Opposite Contact (Shell Elements)
3A.2.3-16	One (1) G Side Drop - Side Opposite Contact (Solid Elements)
3A.2.3-17	Seismic Load - 2G Down + 1G Lateral (Shell Elements)
3A.2.3-18	Seismic Load - 2G Down + 1G Lateral (Solid Elements)
3A.2.5-1	Normal Condition Load Combinations
3A.2.5-2	Bolt Preload + 100 PSI Internal Pressure + 1G Down (Shell Elements)
3A.2.5-3	Bolt Preload + 100 PSI Internal Pressure + 1G Down (Solid Elements)
3A.2.5-4	Bolt Preload + 100 PSI Internal Pressure + 1G Down + Thermal (Shell Elements)
3A.2.5-5	Bolt Preload + 100 PSI Internal Pressure + 1G Down + Thermal (Solid Elements)
3A.2.5-6	Bolt Preload + 100 PSI Internal Pressure + Thermal + 6G Up + Trunnion Local Stress (Shell Elements)
3A.2.5-7	Bolt Preload + 100 PSI Internal Pressure + Thermal + 6G Up + Trunnion Local Stress (Solid Elements)
3A.2.5-8	Bolt Preload + 1G Down + 25 PSI External Pressure (Shell Elements)
3A.2.5-9	Bolt Preload + 1G Down + 25 PSI External Pressure (Solid Elements)
3A.2.5-10	Bolt Preload + 1G Down + 25 PSI External Pressure + Thermal (Shell Elements)
3A.2.5-11	Bolt Preload + 1G Down + 25 PSI External Pressure + Thermal (Solid Elements)
3A.2.5-12	Bolt Preload + 25 PSI External Pressure + Thermal + 6G Up + Trunnion Local Stress (Shell Elements)
3A.2.5-13	Bolt Preload + 25 PSI External Pressure + Thermal +6G Up + Trunnion Local Stress (Solid Elements)
3A.2.5-14	Accident Condition Load Combinations
3A.2.5-15	Bolt Preload + 60G Down End Drop + 100 PSI Internal Pressure (Shell Elements)
3A.2.5-16	Bolt Preload + 60G Down End Drop + 100 PSI Internal Pressure (Solid Elements)
3A.2.5-17	Bolt Preload + 60G Down End Drop + 25 PSI External Pressure (Shell Elements)
3A.2.5-18	Bolt Preload + 60G Down End Drop + 25 PSI External Pressure (Solid Elements)
3A.2.5-19	Bolt Preload + Tipover(65G) + 100 PSI Internal Pressure - Opposite Contact Side (Shell Elements)
3A.2.5-20	Bolt Preload + Tipover(65G) + 100 PSI Internal Pressure - Opposite Contact Side(Solid Elements)
3A.2.5-21	Bolt Preload + Tipover(65G) + 100 PSI Internal Pressure - Contact Side(Shell Elements)
3A.2.5-22	Bolt Preload + Tipover(65G) + 100 PSI Internal Pressure - Contact Side(Solid Elements)
3A.2.5-23	Bolt Preload + Tipover(65G) + 25 PSI External Pressure - Opposite Contact Side (Shell Elements)
3A.2.5-24	Bolt Preload + Tipover(65G) + 25 PSI External Pressure - Opposite Contact Side (Solid Elements)
3A.2.5-25	Bolt Preload + Tipover(65G) + 25 PSI External Pressure - Contact Side (Shell Elements)
3A.2.5-26	Bolt Preload + Tipover(65G) + 25 PSI External Pressure - Contact Side (Solid Elements)
3A.2.5-27	Bolt Preload + 100 PSI Internal Pressure + Seismic(Tornado, Flood) (Shell Elements)
3A.2.5-28	Bolt Preload + 100 PSI Internal Pressure + Seismic(Tornado, Flood) (Solid Elements)
3A.2.5-29	Bolt Preload + 25 PSI External Pressure+ Seismic(Tornado, Flood) (Shell Elements)
3A.2.5-30	Bolt Preload + 25 PSI External Pressure+ Seismic(Tornado, Flood) (Solid Elements)
3A.3-1	Design Parameters for Lid Bolt Analysis
3A.3-2	Bolt Data (Ref. 10, Table 5.1)

TN-68 SAFETY ANALYSIS REPORT

MASTER TABLE OF CONTENTS

List of Tables

3A.3-3	Allowable Stresses in Closure Bolts for Normal Conditions
3A.3-4	Allowable Stresses in Closure Bolts for Accident Conditions
3A.4-1	Stress In Outer Shell and Closure Plates
3B.3-1	Summary of Basket Stress Analysis - Normal Condition (1G Side Load)
3B.3-2	Linearized Stress Intensities of Aluminum Rail - Normal Condition (0° Side Load)
3B.3-3	Linearized Stress Intensities of Aluminum Rail - Normal Condition (30° Side Load)
3B.3-4	Linearized Stress Intensities of Aluminum Rail - Normal Condition (45° Side Load)
3B.4-1	Summary of Basket Stress Analysis - Accident Condition (Side Drop)
3B.4-2	Linearized Stress Intensities of Aluminum Rail - Accident Condition (0° Side Drop)
3B.4-3	Linearized Stress Intensities of Aluminum Rail - Accident Condition (30° Side Drop)
3B.4-4	Linearized Stress Intensities of Aluminum Rail - Accident Condition (45° Side Drop)
4.3-1	Maximum Temperatures for Normal Storage Conditions, 100°F Ambient
4.3-2	Maximum Temperatures for Normal Storage Conditions, -20°F Ambient
4.4-1	Maximum Temperatures for Hypothetical Fire Accident
4.4-2	Maximum Temperatures for Postulated Buried Cask Accident
4.5-1	Average Heat up Rates
4.5-2	Temperatures for the Vacuum Drying Process Without Helium Backfill
4.5-3	Temperatures for Vacuum Drying with Helium Backfill at 30 Hours
4.6-1	Minimum Height of Fuel Rubble
4.6-2	Maximum Temperature for the Cask with 8 Damaged Fuel Assemblies, Normal Storage Conditions
4.6-3	Maximum Temperature for the Cask with 8 Damaged Fuel Assemblies, Accident Conditions
4.8-1	Effective Properties for Intact Fuel Assembly
4.8-2	Effective Conductivity for Damaged Fuel Assembly
4.9-1	Average Peaking Factors
4.9-2	Peaking Factors Applied in Finite Element Model
4.10-1	Total Heat Transfer Coefficient during Fire
4.10-2	Calculated View Factors
4.10-3	Maximum Component Temperatures for Sensitivity Analysis
4.11-1	Hot Gap between the Basket and the Cask Inner Shell
4A.3-1	Results of the Decay Heat Calculation
4A.4-1	Sample Fuel Qualification Table For Tn-68 Cask (441 Watts Per Fuel Assembly)
5.1-1	TN-68 Cask Shield Materials
5.1-2	Summary of Average Dose Rates
5.1-3	Direct Dose Rates at Postulated Site Boundary from One Cask
5.2-1	BWR Fuel Assembly Design Characteristics
5.2-2	BWR Fuel Assembly Hardware Characteristics ^a
5.2-3	Material Compositions for Fuel Assembly Hardware Materials
5.2-4	BWR Fuel Assembly Source (with Channels)
5.2-5	Peaking Factor and Water Density Input for Determination of Axial Source Distribution
5.2-6	Gamma and Neutron Axial Distributions
5.2-7	Gamma Source Terms for 8x8 Design Basis Fuel
5.2-8	Source Term for Design Basis Fuel Assembly
5.2-9	Neutron Source Terms for the 8x8 Design Basis Fuel

TN-68 SAFETY ANALYSIS REPORT

MASTER TABLE OF CONTENTS

List of Tables

5.2-10	Radioactive Inventory for Verification of Bounding Irradiation History
5.2-11	Fission Gas Inventory for 8x8 Design Basis Fuel
5.2-12	Fuel Qualification for Uniform Heat Load (441 Watts per Assembly)
5.2-13	Verification of Fuel Qualification Surface Dose Rate Comparison
5.2-14	Verification of Fuel Qualification 2 M Dose Rate Comparison
5.2-15	Fuel Qualification for TN-68 Cask (Modified to Take Shielding Qualification into Account)
5.3-1	ANSI Standard-6.1.1-1977 Flux-to-Dose Factors
5.3-2	Material Compositions for the BWR Fuel Assembly
5.3-2a	Hardware Elemental Distribution for the BWR Fuel Assembly
5.3-3	Atomic Fractions for the Homogenized Design Basis 8x8 Fuel Without Channel
5.3-4	Atomic Fractions for the Homogenized Design Basis 8x8 Fuel with a 0.065-Inch Channel
5.3-5	Material Properties for the TN-68 Cask MCNP Models
5.4-1	TN-68 Near Field Dose Rates – Normal and Off-Normal Conditions (Without the Auxiliary Shield Ring)
5.4-2	TN-68 Near Field Dose Rates – Normal and Off-Normal Conditions (With 1" Auxiliary Shield Ring)
5.4-3	TN-68 Near Field Dose Rates – Normal Conditions (Dose Rates Above and Below the Neutron Shield)
5.4-4	TN-68 Near Field Dose Rates – Accident Conditions
5.4-5	TN-68 - Single Cask Farfield Dose Rates
6.1-1	Maximum Initial Enrichment for both Intact and Damaged Fuel Assemblies
6.1-2	Summary of Limiting Criticality Evaluations for the TN-68 Cask
6.2-1	Fuel Characteristics for Criticality
6.3-2	TN-68 Fixed Poison Loading Requirements
6.3-3	Description of the KENO Model Units
6.3-4	Comparison of KENO Models
6.3-5	Material Property Data
6.4-1	Results, Most Reactive Lattice Evaluation
6.4-2	Results, Uniform Enrichment Model Validation
6.4-3	TN-68 Most Reactive Intact Configuration – Scoping Results
6.4-4	TN-68 Intact Assembly Criticality Analysis - Final Results
6.4-5	Results of the Single Ended Rod Shear Scoping Studies
6.4-6	Results of the Double Ended Rod Shear Scoping Studies
6.4-7	TN-68 Damaged Assembly Criticality Analysis - Final Results
6.5-1	Benchmark Results
6.5-2	USL-1 Results
6.5-3	USL Determination for Criticality Analysis
6A-1	Maximum Overhang Length of Fuel Assembly
6A-2	Fuel Assembly Data for Side Drop
6A-3	Finite Element Model Data for Side Drop
6A-4	Summary of Stress Results for 75g Side Drop
6A-5	Modulus of Elasticity and Yield Stress (0.5 s^{-1} Strain Rate)
6A-6	Finite Element Model Data for End Drop
6B-1	Maximum Computed Fuel Rod Stresses and their Ratio to Yield Strength
6B-2	Zircaloy-2 Fracture Toughness Data for Axial Crack from Coleman [15]
6B-3	Zircaloy-2 Fracture Toughness Data for Circumferential Crack from Coleman [15]
6B-4	Fracture Toughness of Irradiated Zircaloy-2 Pressure Tubes, Huang [16]

TN-68 SAFETY ANALYSIS REPORT

MASTER TABLE OF CONTENTS

List of Tables

6B-5	Fracture Toughness of Irradiated Zircaloy-2 Pressure Tubes, Huang [16]
6B-6	Fracture Toughness (ksi- $\sqrt{\text{in}}$) Estimate Comparison of Zircaloy-2 Correlation Models
6B-7	Material Fracture Toughness (ksi- $\sqrt{\text{in}}$) vs Temperature and Fluence (Zr-2)
6B-8	Cladding Failure Modes on Selected Experiments [25]
6B-9	Summary of Fracture Test Results for Zircaloy-4 Spent Fuel Cladding [26]
6B-10	Summary of Zircaloy Tube Fracture
6B-11	Stress Intensity Factor for a Through-wall Axial Crack in Cylinder
6B-12	Allowable Through-wall Circumferential Half Crack Length for Zr-2
7.3-1	TN-68 Releasable Source Term for Off-Normal Conditions – Design Basis 8x8 Fuel (DBF-68)
7.3-2	TN-68 Releasable Source Term for Accident Conditions - Design Basis 8x8 Fuel (DBF-68)
7.3-3	Off-Site Airborne Doses From Off-Normal Conditions at 100 M From the TN-68 Cask
7.3-4	Off-Site Airborne Doses From Accident Conditions at 100 M From the TN-68 Cask
8.1-1	Sequence of Operations - Loading
8.2-1	Sequence of Operations - Unloading
9.1-1	Boron Content of Neutron Absorbers
9.4-1	Thermal Conductivity as a Function of Temperature for Sample Absorbers
9.4-2	Sample Determination of Thermal Conductivity Acceptance Criterion
9A-1	Quantitative Analysis of Gases Released from Neutron Shield Test Resin
10.2-1	Total and Direct Dose Rates as a Function of Distance for a Single TN-68 Cask
10.2-2	Skyshine Dose Rates as a Function of Distance for a Single TN-68 Cask
10.2-3	Mathematical Functions for Dose Rates as a Function of Distance for a Single TN-68 Cask
10.2-4	Blocking Factors for use in the Side (Shorter and Longer) Dose Rate Calculations
10.2-5	Blocking Factors for use in the Corner Dose Rate Calculations
10.2-6	Dose Rate as a Function of Distance for the ISFSI (Blocking Factor Method)
10.2-7	Dose Rate as a Function of Distance for the ISFSI (MCNP Array Method)
10.2-8	ISFSI Annual Doses as a Function of Distance for 20 TN-68 Casks
10.3-1	Design Basis Occupational Exposures for Cask Loading, Transport, and Emplacement (One Time Exposure, 30 kW Contents)
10.3-2	Design Basis ISFSI Maintenance Operations Annual Exposures for 30 kW Contents
10.3-3	Measured Operational Doses from TN-68 Cask Loading
13-1	Quality Assurance Criteria Matrix
14.1-1	Data for TN68 Activation Analysis
14.1-2	Results of ORIGEN2 Activation Analysis
14.1-3	Comparison of TN-68 Activity with Class A Waste Limits

TN-68 SAFETY ANALYSIS REPORT

MASTER TABLE OF CONTENTS

List of Figures

1.2-1	TN-68 Confinement Boundary Components
1.4-1	Typical ISFSI Vertical Storage
2.1-1	Decay Heat 7x7 GE Fuel Assembly 3.3 wt% U-235 Maximum Initial Bundle Average Enrichment, 40,000 MWD/MTU, 10 Year Cooled
2.1-2	Gamma Source 7x7 BWR Fuel Assembly 3.3 wt% U-235 Maximum Initial Bundle Average Enrichment, 40,000 MWD/MTU, 10 Year Cooled
2.1-3	Neutron Source 7x7 BWR Fuel Assembly 3.3 wt% U-235 Maximum Initial Bundle Average Enrichment, 40,000 MWD/MTU, 10 Year Cooled
2.1-4	Fuel Qualification Flowchart for 8x8, 9x9, and 10x10 Fuel
2.2-1	Earthquake and Wind Loads
2.2-2	Tornado Missile Impact Loads
2.2-3	Lifting Loads
2.3-1	TN-68 Cask Seal Pressure Monitoring System
2.3-2	Long Term Leak Test Results on Metallic Seals
2.3-3	Long Term Leak Test Results on Metallic Seals
2.3-4	Long Term Leak Test Results on Metallic Seals
3.4-1	Trunnion Geometry
3.4-2	Cask Body Key Dimensions
3.4-3	Standard Reporting Locations for Cask Body
3.4-4	Weld Stress Locations
3.4-5	Potential Versus pH Diagram for Aluminum-Water System
3.4-6	Effect of pH on Corrosion of Iron in Aerated Soft Water, Room Temperature
3.5-1	Finite Element Model
3.5-2	Nodal Temperature Used for Thermal Analysis
3.5-3	Temperature Distribution Resulting from Thermal Analysis
3.5-4	Nodal Stress Intensity
3A.1-1	Cask Body Key Dimensions
3A.2-1	Cask Body - Finite Element Model
3A.2-2	Cask Body - Bottom Corner
3A.2-3	Cask Body - Top Corner
3A.2-4	Cask Lid to Shield Plate Connection
3A.2-5	Fourier Coefficients for 1 g Lateral
3A.2-6	Bolt Preload and Seal Reaction
3A.2-7	Design Internal Pressure (100 PSIG)
3A.2-8	External Pressure Loading (25 PSIG)
3A.2-9	1g Down Loading
3A.2-10	Lifting: 6g Vertical Up
3A.2-11	1g Lateral
3A.2-12	Standard Reporting Locations for Cask Body
3A.2-13	Weld Stress Locations
3A.2-14	Fourier Series Approximation of the Footprint Pressure for the Side Drop
3A.2-15	Trunnion Geometry
3A.3-1	TN-68 Cask Lid Closure Arrangement
3A.3-2	TN-68 Cask Lid Bolt
3A.4-1	Cask Outer Shell and Connection with Cask Body
3A.4-2	Finite Element Model Outer Shell
3A.4-3	Finite Element Model Bottom Corner

TN-68 SAFETY ANALYSIS REPORT

MASTER TABLE OF CONTENTS

List of Figures

3A.4-4	Finite Element Model Top Corner
3A.4-5	Internal Pressure (25 psi)
3A.4-6	3G Down
3B.1-1	Representative Basket Wall Panel
3B.2-1	Axial View of Basket
3B.2-2	Geometry for ANSYS Model
3B.2-3	Finite Element Model and Element Types
3B.2-4	Basket Finite Element Model - Stainless Steel Boxes
3B.2-5	Basket Finite Element Model - Stainless Steel Plates
3B.2-6	Basket Finite Element Model - Aluminum Rails
3B.3-1	Loading and Boundary Conditions - 0° Drop
3B.3-2	Loading and Boundary Conditions - 30° Drop
3B.3-3	Loading and Boundary Conditions - 45° Drop
3B.3-4	Membrane Stress Intensity (SS Plate) - 0 Degree Drop
3B.3-5	Membrane + Bending Stress Intensity (SS Plate) - 0 Degree Drop
3B.3-6	Membrane Stress Intensity (SS Box) - 0 Degree Drop
3B.3-7	Membrane + Bending Stress Intensity (SS Box) - 0 Degree Drop
3B.3-8	Membrane Stress Intensity (SS Plate)-30 Degree Drop
3B.3-9	Membrane + Bending Stress Intensity (SS Plate) - 30 Degree Drop
3B.3-10	Membrane Stress Intensity (SS Box) - 30 Degree Drop
3B.3-11	Membrane + Bending Stress Intensity (SS Box) - 30 Degree Drop
3B.3-12	Membrane Stress Intensity (SS Plate)- 45 Degree Drop
3B.3-13	Membrane + Bending Stress Intensity (SS Plate) - 45 Degree Drop
3B.3-14	Membrane Stress Intensity (SS Box) - 45 Degree Drop
3B.3-15	Nodal Stress Intensity (SS Plate) - 45 Degree Drop
3B.3-16	Nodal Stress Intensity (Aluminum Rails) - 0 Degree Drop
3B.3-17	Nodal Stress Intensity (Aluminum Rails) - 30 Degree Drop
3B.3-18	Membrane + Bending Stress Intensity (Aluminum Rails) - 45 Degree Drop
3B.3-19	Basket Stress Due to 3G Vertical Load
3B.3-20	Stress Report Location (Big Rail)
3B.3-21	Stress Report Location (Small Rail)
3B.3-22	Extraction of Partial Basket Model (Fusion Welds)
3B.3-23	Basket Partial Model (Fusion Welds)
3B.3-24	Basket Full Model (Fusion Welds)
3B.3-25	Locations of Basket Support Plates
3B.5-1	Drop Orientation
3B.5-2	Finite Element Model Simulation
3B.5-3	Finite Element Model Geometry
3B.5-4	Finite Element Model Plot
3B.5-5	Loading Conditions
3B.5-6	Boundary Conditions
3B.5-7	0° Drop Buckling Analysis - ANSYS Computer Plot
3B.5-8	10° Drop Buckling Analysis - ANSYS Computer Plot
3B.5-9	20° Drop Buckling Analysis - ANSYS Computer Plot
3B.5-10	30° Drop Buckling Analysis - ANSYS Computer Plot
3B.5-11	45° Drop Buckling Analysis - ANSYS Computer Plot
3C.1-1	Basket Finite Element Model for Modal Analysis

TN-68 SAFETY ANALYSIS REPORT

MASTER TABLE OF CONTENTS

List of Figures

3C.1-2	Boundary Condition - 0° Modal Analysis
3C.1-3	0° Modal Analysis - First Mode (204 Hz)
3C.1-4	0° Modal Analysis - Second Mode (225 Hz)
3C.1-5	0° Modal Analysis - Third Mode (237 Hz)
3C.1-6	0° Modal Analysis - Fourth Mode (242 Hz)
3C.1-7	30° Modal Analysis - First Mode (195 Hz)
3C.1-8	30° Modal Analysis - Second Mode (253 Hz)
3C.1-9	30° Modal Analysis - Third Mode (258 Hz)
3C.1-10	30° Modal Analysis - Fourth Mode (264 Hz)
3C.1-11	45° Modal Analysis - First Mode (181 Hz)
3C.1-12	45° Modal Analysis - Second Mode (232 Hz)
3C.1-13	45° Modal Analysis - Third Mode (272 Hz)
3C.1-14	45° Modal Analysis - Fourth Mode (281 Hz)
3C.1-15	Maximum Dynamic Amplification Factor for a Triangular Load
3D.2-1	Weight and Dimensions of TN-32 Cask
3D.2-2	TN-32 Cask - Finite Element Model (1)
3D.2-3	TN-32 Cask - Finite Element Model (2)
3D.2-4	TN-32 Cask - Finite Element Model (3)
3D.2-5	TN-68 Cask Finite Element Model (1)
3D.2-6	TN-68 Cask Finite Element Model (2)
3D.2-7	TN-68 Cask Finite Element Model (3)
3D.2-8	Weight and Dimensions of TN-68 Cask
3D.2-9	Finite Element Grid for Cask Drop on Concrete Slab
3D.2-10	Finite Element Model of BNFL Full Scale Drop Test #4
3D.3-1	TN-32 Cask - Symmetry Boundary Conditions
3D.3-2	TN-32 Cask - Modal Analysis
3D.3-3	TN-32 Cask - Modal Analysis of the Approximate Basket Model
3D.3-4	TN-68 Cask Modal Analysis
3D.3-5	TN-68 Cask - Modal Analysis of the Approximate Basket Model
3D.3-6	BNFL Full Scale Drop Test #4 - Cask Modal Analysis
3D.3-7	Damping Ratio Data Reproduced from References 13 and 14
3D.3-8	Tipover Analysis Damping Coefficients
3D.4-1	BNFL Cask End Drop - Stress Plot
3D.4-2	BNFL Cask End Drop - Displacement Plot
3D.4-3	BNFL Cask End Drop - Displacement Time History
3D.4-4	BNFL Cask End Drop - Acceleration Time History (TN Analysis)
3D.4-5	BNFL Full Scale Drop Test #4 - Acceleration Time History (Test Data)
3D.4-6	TN-32 Cask Tipover Analysis - Acceleration Time History
3D.4-7	Verification of DADisp Program - Sine Wave Pulse
3D.4-8	18" Billet Side Drop Test Data From Channel A3 - Unfiltered and Filtered at 450 Hz (Performed by TN)
3D.4-9	18" Billet Side Drop Test Data From Channel A3 - Unfiltered and Filtered at 450 Hz (Performed by LLNL)
3D.5-1	TN-68 Cask Tipover Analysis - Displacement Time History Along the Length of the Cask
3D.5-2	TN-68 Cask Tipover Analysis - Displacement Plot (E=28.3E6 psi)
3D.5-3	TN-68 Cask Tipover Analysis - Von Mises Stress Plot (E=28.3E6 psi)
3D.5-4	TN-68 Cask Tipover Analysis - Acceleration Time History (E=28.3E6 psi)
3D.5-5	TN-68 Cask Tipover Analysis - Acceleration Time History (E=30E6 psi)

TN-68 SAFETY ANALYSIS REPORT

MASTER TABLE OF CONTENTS

List of Figures

3D.5-6	Single Degree of Freedom Model
3D.5-7	Dynamic Amplification Factor ($E = 28.3E6$)
3D.5-8	Ratio of Max. Cask/Basket Displacement vs. Time ($E=28.3E6$ psi)
3E-1	Locations of Fracture Toughness Evaluations (TN-68 Gamma Shield)
3E-2	Charpy V-Notch Test Results for SA-266 Gr. 2
4.3-1	Finite Element Model of TN-68 Cask
4.3-2	Details of the FEM, TN-68 Cask – Design Basis Basket
4.3-3	Details of the FEM, TN-68 Cask – Alternate Basket Details
4.3-4	Typical Boundary Conditions
4.3-5	Temperature Distribution in TN68 Cask – Design Basis Model
4.3-6	Temperature Distribution in TN68 Cask – Alternates
4.4-1	Cross-Section and Lid-Seal Models
4.4-2	Location of Heat Fluxes on Lid-Seal Model
4.4-3	Time-Temperature Histories for Hypothetical Fire Accident
4.4-4	Temperature Distributions for Hypothetical Fire Accident
4.5-1	Time-Temperature History for the Vacuum Drying with 30 kW Decay Heat Load
4.6-1	Location of the Damaged Fuel Assemblies
4.8-1	Comparison of the Transverse Effective Fuel Conductivities
4.9-1	Comparison of the Measured and Applied Axial Heat Profiles
4.10-1	Storage Configuration for TN-68 Cask
4.10-2	Finite Element Model for Radiosity Methodology
4.10-3	Temperature Distribution of Radial Neutron Shield Resin for Case # 4
4.11-1	Considered Basket Locations for Calculation of Hot Gap Size
5.1-1	Cask Shielding Configuration
5.1-2	TN-68 Normal Conditions Dose Point Locations
5.2-1	Axial Burnup Profile for Design Basis Fuel
5.2-2	Axial Neutron and Gamma Profiles
5.3-1	TN-68 MCNP Gamma Model
5.3-2	TN-68 Discrete Basket MCNP Model – XY Plot at $Z=0$ cm
5.3-3	TN-68 MCNP Quarter Model – XY Plot At $Z=0$ cm
5.3-4	TN-68 Discrete Basket MCNP Model – XY Plot At $Z=220$ cm
5.3-5	TN-68 MCNP Quarter Model – XY Plot At $Z=220$ cm
5.4-1	TN-68 Cask Side Surface Dose Rates Normal and Off-Normal Conditions (Without Auxiliary Shield)
5.4-2	TN-68 Cask Dose Rates 1 M from Side Surface Normal and Off-Normal Conditions (Without Auxiliary Shield Ring)
5.4-3	TN-68 Cask Dose Rates 2 M from Side Surface Normal and Off-Normal Conditions (Without Auxiliary Shield Ring)
5.4-4	TN-68 Cask Top Surface Dose Rates Normal and Off-Normal Conditions
5.4-5	TN-68 Cask Bottom Surface Dose Rates Normal and Off-Normal Conditions
5.4-6	TN-68 Cask Side Surface Dose Rates Normal and Off-Normal Conditions (With 1" Auxiliary Shield Ring)
5.4-7	TN-68 Cask Side Surface Dose Rates – Accident Conditions
5.4-8	TN-68 Cask Dose Rates 1 M from Side Surface – Accident Conditions
5.4-9	TN-68 Cask Dose Rates 2 M from Side Surface – Accident Conditions
5.4-10	TN-68 Cask Top Surface Dose Rates – Accident Conditions
5.4-11	TN-68 Cask – Dose Rate as a Function Of Distance

TN-68 SAFETY ANALYSIS REPORT
MASTER TABLE OF CONTENTS
List of Figures

6.3-1	Basket Views & Dimensions
6.3-2	Basket Model Compartment Wall (View G)
6.3-3	Basket Model Compartment Wall (View F)
6.3-4	Basket Model Compartment with Fuel Assembly (View G)
6.3-5	Basket Model Compartment with Fuel Assembly (View F)
6.3-6	KENO Plot of the Center of the TN-68 Basket with Fuel Assemblies
6.3-7	Radial Cross Section of the TN-68 Basket with Fuel Position Numbers
6.3-8	North East Quadrant of the TN68 Basket with Fuel Assemblies
6.3-9	Radial Cross Section of the TN-68 Basket with Fuel Assemblies
6.4-1	TN-68 Model Cross-Section, Most Reactive Lattice Evaluation
6.4-2	TN-68 Model Cross-Section, Uniform Enrichment Validation, Case 3var
6.4-3	Vanished Lattice Model
6.4-4	KENO Plot of Units 247 and 248 With Channel - Single Shear Rows
6.4-5	KENO Plot of Units 257 and 258 Without Channel - Single Shear Rows
6.4-6	KENO Plot of the Single Sheared Rods with 12.18" Axial Shift
6.4-7	KENO Plot of Units 247 and 248 With Channel - Double Shear Columns
6.4-8	KENO Plot of Units 257 and 258 Without Channel - Double Shear Rows
6.4-9	KENO Plot of the Double Sheared Rods with 12.18" Axial Shift
6.4-10	KENO Plot of the Design Basis Double Shear Damaged Assembly Model
6.5-1	Benchmarks – Trend Evaluation for Separation Distance
6A-1	Location of Fuel Assemblies vs. Basket during 75g Side Drop
6A-2	Finite Element Model Setup
6A-3	GE BWR 10x10 (GE12) Fuel Assembly - Boundary Conditions and Temperature Contour
6A-4	GE BWR 10x10 (GE12) Fuel Assembly - Deformation at 75g
6A-5	GE BWR 10x10 (GE12) Fuel Assembly - Bending Stress at 75g
6A-6	DLF Calculation Relationship
6A-7	End Drop Finite Element Model Setup
6A-8	GE BWR 9x9 (GE11) - 0.015 inch Bowing - Boundary Conditions
6A-9	GE BWR 9x9 (GE11) Fuel Assembly - Node Numbers for Bottom Three Spans
6A-10	GE BWR 9x9 (GE11) - 0.015 inch Bowing- Lateral Displacements at Midspans of Bottom Three Spans
6A-11	GE BWR 9x9 (GE11) - 0.015 inch Bowing - Axial Stress at 0° (Span 1)
6A-12	GE BWR 9x9 (GE11) - 0.015 inch Bowing - Axial Stress at 180° (Span 1)
6A-13	GE BWR 9x9 (GE11) - 0.015 inch Bowing - Axial Stress at 0° (Span 2)
6A-14	GE BWR 9x9 (GE11) - 0.015 inch Bowing - Axial Stress at 180° (Span 2)
6A-15	GE BWR 9x9 (GE11) - 0.039 inch Bowing - Boundary Conditions
6A-16	GE BWR 9x9 (GE11) - 0.039 inch Bowing - Lateral Displacements at the Midspans of Bottom Three Spans
6A-17	GE BWR 9x9 (GE11) - 0.039 inch Bowing - Axial Stress at 0° (Span 1)
6A-18	GE BWR 9x9 (GE11) - 0.039 inch Bowing - Axial Stress at 180° (Span 1)
6A-19	GE BWR 9x9 (GE11) - 0.039 inch Bowing - Axial Plastic Strain at 0° (Span 1)
6A-20	GE BWR 9x9 (GE11) - 0.039 inch Bowing - Axial Plastic Strain at 180° (Span 1)
6A-21	Variation of Modulus of Elasticity with Temperature
6A-22	Variation of Yield Stress with Temperature
6A-23	TN-68 Cask Tipover Analysis - Acceleration Time History (Full Scale)
6A-24	TN-68 Cask 1/3 Scale Impact Limiter Testing - Acceleration Time History

TN-68 SAFETY ANALYSIS REPORT

MASTER TABLE OF CONTENTS

List of Figures

- 6B-1 Kuroda's Statistical Correlation using Huang's Data
- 6B-2 Correlation for Zircaloy-2 Fracture Toughness Test Data
- 6B-3 Post Test Appearance of the Test Fuel Rods in Tests HBO-1, JM-4 and JM-14 [25]
- 6B-4 Morphologies of Cracks at 325°C
- 6B-5 Schematic Illustration of Microstructure, Sequence of Failure and Key Material Parameters Modeled for HBO-1 [27]
- 6B-6 SEM Micrograph of a Crack Tip in the C6 Rod [28]
- 6B-7 Overlapping Cracks in A2 Rod [28]
- 6B-8 Burst Opening Region of Specimen from Rod KJE051 [29]
- 6B-9 Fracture Behavior of Claddings by the High Pressurization-Rate Burst Test [31]
- 6B-10 Finite Element Model for Through-wall Axial Crack in Cylinder under Bending or Axial Load
- 6B-11 Through-wall Circumferential Crack under Bending or Axial Load
- 6B-12 Bending Stress in Tube with Through-wall Axial Crack
- 6B-13 Applied K for Through-wall circumferential Crack, Zr-2 Cladding Tube
- 6B-14 Allowable Through-wall Circumferential Flaw Size for Zr-2 Cladding Tube

- 7.1-1 Overpressure Monitoring System Pressure Drop With Time (Assuming Acceptance Test Leak Rate of 1×10^{-5} ref cm³ /s)
- 7.1-2 Overpressure Monitoring System Pressure Drop With Time (Assuming a Latent Seal Leak Rate of 5×10^{-4} ref cm³ /s)
- 7.1-3 Lid, Vent Port and Drain Port Metal Seals

- 8.2-1 Typical Setup for Filling Cask with Water

- 9A-1 Weight Loss Due to Thermal Aging of Neutron Shield Test Resin

- 10.2-1 ISFSI Layout with a 2x10 Array of TN-68 Casks
- 10.2-2 Total Dose Rate as a Function of Distance for a Single TN-68 Cask
- 10.2-3 Direct Dose Rate as a Function of Distance for a Single TN-68 Cask
- 10.2-4 Skyshine Dose Rate as a Function of Distance for a Single TN-68 Cask
- 10.2-5 Blocking Factor Calculation Illustration with QADS
- 10.2-6 ISFSI Side Annual Doses as a Function of Distance – 20 TN-68 Casks
- 10.2-7 ISFSI Corner Annual Doses as a Function of Distance – 20 TN-68 Casks
- 10.3-1 Dose Rates and Locations for TN-68 Occupational Exposure Assessments

**TN-68 SAFETY ANALYSIS REPORT
TABLE OF CONTENTS**

SECTION	PAGE
1	GENERAL DESCRIPTION
1.1	Introduction..... 1.1-1
1.2	General Description of the TN-68 1.2-1
1.2.1	Cask Characteristics 1.2-1
1.2.2	Operational Features 1.2-3
1.2.2.1	General Features 1.2-3
1.2.2.2	Sequence of Operations 1.2-3
1.2.2.3	Identification of Subjects for Safety and Reliability Analysis..... 1.2-4
1.2.2.3.1	Criticality Prevention 1.2-4
1.2.2.3.2	Chemical Safety 1.2-4
1.2.2.3.3	Operation Shutdown Modes 1.2-4
1.2.2.3.4	Instrumentation 1.2-5
1.2.2.3.5	Maintenance Techniques 1.2-5
1.2.3	Cask Contents 1.2-5
1.3	Identification of Agents and Contractors..... 1.3-1
1.4	Generic Cask Arrays 1.4-1
1.5	Supplemental Data 1.5-1
1.6	References..... 1.6-1

List of Tables

1.2-1 Nominal Dimensions and Weight of the TN-68 Cask

List of Figures

1.2-1 TN-68 Confinement Boundary Components
1.4-1 Typical ISFSI Vertical Storage

CHAPTER 1

GENERAL DESCRIPTION

This Updated Final Safety Analysis Report (UFSAR) (the terms UFSAR, Final Safety Analysis Report (FSAR), and Safety Analysis Report (SAR) are used interchangeably in this document) addresses the safety related aspects of storing spent fuel in TN-68 dry transport/storage casks. The format follows the guidance provided in NRC Regulatory Guide 3.61⁽¹⁾. The report is intended for review by the NRC under 10CFR72⁽²⁾. A second SAR will be submitted to address the safety related aspects of transporting spent fuel in TN-68 casks in accordance with 10CFR71⁽³⁾.

The TN-68 dry transport/storage cask provides confinement, shielding, criticality control and passive heat removal independent of any other facility structures or components. The cask also maintains structural integrity of the fuel during storage.

It is intended that a Certificate of Compliance under the requirements of 10CFR72 Subpart L be issued such that the casks can be used for the storage of spent fuel in an independent spent fuel storage installation (ISFSI) at power reactor sites under the conditions of a general license in accordance with 10CFR72 Subpart K.

1.1 Introduction

The TN-68 cask accommodates 68 BWR fuel assemblies with or without channels. It consists of the following components in its storage configuration:

- A basket assembly which locates and supports the fuel assemblies, transfers heat to the cask body wall, and provides neutron absorption to satisfy nuclear criticality requirements.
- A confinement vessel including a closure lid and seals which provides radioactive material confinement and a cavity with an inert gas atmosphere.
- Gamma shielding surrounding the confinement vessel.
- Radial neutron shielding surrounding the gamma shield which provides additional radiation shielding. This neutron shielding is enclosed in an outer steel shell.
- A top neutron shield which rests on the cask lid and provides additional neutron shielding.
- An overpressure system which monitors the pressure between the cask closure seals and provides a positive pressure differential between the seals.
- A protective cover which provides weather protection for the closure lid, top neutron shield and overpressure system.

- Sets of upper and lower trunnions which provide support, lifting and rotation capability for the cask.

The type of fuel to be stored in the TN-68 cask is light water reactor (LWR) fuel of the Boiling Water Reactor (BWR) type. The maximum allowable initial lattice-average enrichment varies from 3.7 to 4.7 wt% U235 depending on the B10 areal density in the basket neutron absorber plates. The maximum bundle average burnup, maximum decay heat, and minimum cooling time are 40 GWd/MTU, 0.312 kW/assembly, and 10 years for 7x7 fuel, 60 GWd/MTU, 0.441 kW/assembly, and 7 years for all other fuel. The cask is designed for a maximum heat load of 30 kW. Damaged fuel that can be handled by normal means may be stored in eight peripheral compartments fitted with damaged fuel end caps designed to retain gross fragments of fuel within the compartment.

The fuel which maybe stored within the TN-68 cask is determined from Table 2.1-4 and Figure 2.1-4.

The casks are intended for storage on a reinforced concrete pad at a nuclear power plant.

1.2 General Description of the TN-68

1.2.1 Cask Characteristics

Each storage cask consists of a fuel basket, a cask body (shell, bottom and lid), a protective cover, an overpressure system, four trunnions, penetrations with bolted and sealed covers for leak detection and venting, closure bolts and locating pins.

A set of reference drawings is presented in Section 1.5. The casks are self-supporting cylindrical vessels. Dimensions and the estimated weight of the cask are shown in Table 1.2-1. The materials used to fabricate the cask are shown in the Parts List on Drawing 972-70-2. Where more than one material has been specified for a component, the most limiting properties are used in the analyses in the subsequent chapters of this SAR.

The confinement boundary components are shown in Figure 1.2-1. The confinement vessel for the TN-68 cask consists of: an inner shell (1) which is a welded, low alloy steel cylinder with an integrally-welded, low alloy steel bottom closure; a welded flange forging (3); a flanged and bolted low alloy steel lid with bolts and metallic seals (2); and vent and drain covers with bolts and metallic seals (4 and 5). The overall confinement vessel length is 184 in. with a wall thickness of 1.5 in. The cylindrical cask cavity has a diameter of 69.5 in. and a length of 178 in.

There are two penetrations through the confinement vessel, both in the lid: one is for draining and the other is for venting. A double-seal mechanical closure is provided for each penetration. The confinement lid is 5 in. thick and is fastened to the body by 48 bolts. Double metallic o-ring seals with interspace leakage monitoring are provided for the lid closure. To preclude air in-leakage, the cask cavity is pressurized above atmospheric pressure with helium.

The interspace between the metallic seals is connected to an overpressure tank and a pressure monitoring system. The overpressure tank and the interspace between the metallic seals are pressurized with helium to a higher level than the cavity so that any seal leakage would be into rather than out of the cavity. A decrease in the pressure of the monitoring system would be signaled by a pressure transducer/switch wired to a monitoring/alarm panel.

For weather protection, a torispherical weather cover with an elastomeric seal is provided above the lid.

A gamma shield is provided around the walls and bottom of the confinement vessel by an independent shell and bottom plate of carbon steel which is welded to the closure flange. The gamma shield completely surrounds the confinement vessel inner shell and bottom closure. Gamma shielding is also welded to the inside of the confinement lid.

Neutron shielding is provided by a borated polyester resin compound surrounding the body. The resin compound is cast into long, slender aluminum containers. The array of resin-filled containers is enclosed within a smooth outer steel shell constructed of two half cylinders. In addition to serving as resin containers, the aluminum provides a conduction path for heat transfer from the cask body to the outer shell. A pressure relief valve is mounted on the top of

the resin enclosure for venting pressure due to heating of the resin and entrapped air after fuel loading.

A 4.0 inch disc of polypropylene is attached to the cask lid to provide neutron shielding during storage.

A shear key is welded to the inner wall of the confinement vessel to prevent the basket from rotating during normal operations. Similarly, a hold down fixture is installed above the basket after fuel loading is complete to prevent the basket from moving axially during normal handling.

The basket structure consists of an assembly of stainless steel cells joined by a proprietary fusion welding process to 1.75 in. wide stainless steel plates. Above and below the plates are slotted borated aluminum or boron carbide/aluminum metal matrix composite plates (neutron poison plates) which form an egg-crate structure. The poison plates provide the necessary criticality control and provide the heat conduction paths from the fuel assemblies to the cask cavity wall. This method of construction forms a very strong honeycomb-like structure of cell liners which provide compartments for 68 fuel assemblies. The minimum open dimension of each cell is 6.0 in. x 6.0 in. which provides clearance around the fuel assemblies. The overall basket length (164 in.) is less than the cask cavity length to allow for thermal expansion and fuel assembly handling.

Eight peripheral compartments in the basket may be outfitted to accept damaged fuel. The outfitting consists of an extension welded to the top of the fuel compartment, and end caps that slide into these compartments above and below the fuel.

The cask cavity surfaces are uncoated, but the short term exposure to water during loading and unloading is not sufficient to cause significant corrosion. The surfaces are protected by the inert gas environment inside the cask during long term storage. The external surfaces of the cask are painted for ease of decontamination and corrosion protection.

A stainless steel overlay is applied to the o-ring seating surfaces on the body and lid for corrosion protection.

Four trunnions are attached to the cask body for lifting and rotation of the cask. Two of the trunnions are located near the top of the body and two near the bottom. The upper trunnions are bolted to the gamma shielding and sized for single failure proof lifting. It is not intended to remove the upper trunnions during storage. The lower trunnions are welded to the gamma shielding and may be used for rotating the cask between vertical and horizontal positions.

Threaded holes are provided in the lid and top neutron shield for attachment of component lifting devices. These are used for attachment points for sling systems or other lifting tools.

Impact limiters are not used during storage.

During dry storage of the spent fuel, no active systems are required for the removal and dissipation of the decay heat from the fuel. The TN-68 cask is designed to transfer the decay

heat from the fuel to the basket, from the basket to the cask body and ultimately to the surrounding air by radiation and natural convection. The cask is capable of removing 30 kW of decay heat without external fins, thus providing a smooth outer surface for ease of decontamination.

Each cask is identified and marked with the empty weight in accordance with Section 9.3.

1.2.2 Operational Features

1.2.2.1 General Features

The TN-68 cask is designed to safely store 68 BWR fuel assemblies with or without channels. The TN-68 cask is designed to maintain the fuel cladding temperature below 400°C during storage and short-term fuel loading operations. It is also designed to maintain the fuel cladding temperature below 570 °C during short-term accident and off-normal conditions.

The shielding features of the TN-68 cask are designed to maintain the maximum combined gamma and neutron dose rate at accessible surfaces to less than 650 mrem/hr under normal operating conditions.

The criticality control features of the TN-68 cask are designed to maintain the neutron multiplication factor k -effective less than the upper subcritical limit equal to 0.95 minus benchmarking bias and modeling bias under all conditions.

In order to prevent potential human error, prior to loading the first cask at a utility, a dry run will be performed. This dry run will be used to demonstrate that the loading and unloading processes are sound and the operations personnel are adequately trained. The loading and unloading operations which have an impact on safety will be verified and recorded. These operations include loading and identifying each fuel assembly, ensuring that the fuel assembly meets the fuel acceptance criteria, torquing of the lid and cover bolts, drying, leak testing, backfilling and pressurizing the cask and pressure monitoring system, gas sampling and flooding the cask.

1.2.2.2 Sequence of Operations

The sequence of operations to be performed in loading fuel into the TN-68 storage cask is presented in Chapter 8. These operations are summarized below.

The cask is designed to be loaded in the spent fuel pool or cask pit. Upon arrival, the empty cask is inspected, and the protective cover, overpressure tank, top neutron shield and lid are removed. The cask is then lowered into the cask pit/spent fuel pool. Fuel assemblies may be installed in each of the 68 basket compartments. If the basket is outfitted for damaged fuel, bottom end caps are installed in the compartments that will be loaded with damaged fuel, then top end caps are installed after the fuel is inserted.

The lid is installed and the cavity is vented and drained. While checking for appropriate surface radiation levels, the cask is lifted above the water and some of the lid bolts are installed hand

tight. Venting/draining may occur while lifting the cask out of the pool. The cask is moved from the cask pit/spent fuel pool to the decontamination area. The remaining lid bolts are installed. The cask cavity is then evacuated and dried by means of a vacuum system and then back-filled with helium. The lid seals and penetration cover seals are leak tested. The top neutron shield is installed on the lid. The external surface radiation levels are checked to assure that they are within acceptable limits.

The overpressure system is installed and the overpressure system and seal interspace is pressurized with helium. The protective cover may be installed either in the decontamination area or at the ISFSI.

The cask is transferred to the ISFSI by a transport vehicle. The cask is set in its storage position, and connected to the site storage cask monitoring system. A channel operational test to verify proper functioning of the pressure switch/transducer is performed.

To unload the cask, these steps are performed in reverse. The cask is brought back to the reactor building. The protective cover, pressure monitoring system, overpressure tank and top neutron shield are removed. Prior to opening the cask, the cavity gas is sampled through the vent or drain port. The cavity is depressurized and the cask is lowered into the spent fuel pool. The cask is slowly filled with pool water or demineralized water through the vent or drain port. The cask is vented during this process. The water/steam mixture from the vent line may contain some radioactive gas. If the gas is radioactive, protective measures shall be imposed in accordance with ALARA such as routing the gas through the plant gaseous radwaste system. Pressure and temperature should be monitored during this operation. When the cask is full of water, the lid is removed and the fuel is accessible for unloading.

1.2.2.3 Identification of Subjects for Safety and Reliability Analysis

1.2.2.3.1 Criticality Prevention

Criticality is controlled by utilizing neutron absorption materials in the fuel basket. These features are only necessary during the loading and unloading operations that occur in the cask loading pool (underwater). During storage, with the cavity dry and sealed from the environment, criticality control measures within the installation are not necessary because of the low reactivity of the fuel in the dry cask and the assurance that no water can enter the cask during storage.

1.2.2.3.2 Chemical Safety

There are no chemical safety hazards associated with operations of the TN-68 dry storage cask.

1.2.2.3.3 Operation Shutdown Modes

The TN-68 dry storage cask is a totally passive system so that consideration of operation shutdown modes is unnecessary.

1.2.2.3.4 Instrumentation

The only instrumentation pertinent to storage is the pressure transducers/switches which monitor the cask seals for leakage. The transducers/switches monitor the pressure in an interspace between the inner and outer seals to provide an indication of seal failure before any release is possible.

An initial functional check of the transducers/switches is performed at the manufacturer's plant and a channel operational test is performed at the commencement of storage. Two identical transducers/switches are provided to assure a functional system through redundancy.

1.2.2.3.5 Maintenance Techniques

Because of their passive nature, the storage casks will require little, if any, maintenance over their lifetime. Typical maintenance would be limited to external paint touch-up and repressurizing the overpressure system. No special maintenance techniques are necessary.

1.2.3 Cask Contents

The TN-68 cask is designed to store up to 68 Boiling Water Reactor (BWR) fuel assemblies with or without fuel channels. The maximum allowable initial lattice-average enrichment varies from 3.7 to 4.7 wt% U235 depending on the B10 areal density in the basket neutron absorber plates. The maximum bundle average burnup, maximum decay heat, and minimum cooling time are 40 GWd/MTU, 0.312 kW/assembly, and 10 years for 7x7 fuel, 60 GWd/MTU, 0.441 kW/assembly, and 7 years for all other fuel. Damaged fuel assemblies are limited to bundle average 45 GWd/MTU burnup. The cask is designed for a maximum heat load of 30 kW.

In addition to satisfying these limits, the fuel to be stored must also meet the fuel qualification requirements developed in Chapter 5. This assures that the radioactive source for shielding and confinement is bounded by the design basis fuel assembly, which is an 8x8 lattice with 63 fuel rods and with burnup, bundle average enrichment, and cooling time of 48 GWd/MTU, 2.6 wt% U235, and 7 years, respectively.

Damaged fuel that can be handled by normal means may be stored in eight peripheral compartments fitted with damaged fuel end caps designed to retain gross fragments of fuel within the compartment. A description of the fuel assemblies is provided in Section 2.1.

The quantity and type of radionuclides in the spent fuel assemblies are described and tabulated in Chapter 5. Chapter 6 covers the criticality safety of the TN-68 cask and its contents, listing material densities, moderator ratios, and geometric configurations.

1.3 Identification of Agents and Contractors

Transnuclear, Inc., (TN), provides the design, analysis, licensing support and quality assurance for the TN-68 cask. Fabrication of the cask is done by one or more qualified fabricators under TN's quality assurance program. Personnel are trained and qualified in accordance with industry standards such as SNT-TC-1A for non-destructive testing and the ASME code, Section IX for welding. TN's quality assurance program is described in Chapter 13. This program is written to satisfy the requirements of 10 CFR 72, Subpart G and covers control of design, procurement, fabrication, inspection, testing, operations and corrective action. Experienced TN operations personnel provide training to utility personnel prior to first use of the cask and prepare generic operating procedures.

The construction of the ISFSI (other than the casks) is performed by others under the direction of the utility. Cask operations and maintenance is performed by utility personnel. Decommissioning activities will be performed by utility personnel in accordance with site procedures.

Managerial and administrative controls which are used to ensure safe operation of the casks are provided by the host utility.

Modifications to the TN-68 cask design, when required, may not be performed without the concurrence of Transnuclear. The host utility may make changes to the cask as specified in 10CRF72.48, as described in the Safety Analysis Report or changes in the procedures described in the Safety Analysis Report or conduct tests or experiments not described in the Safety Analysis Report, unless the proposed change, test or experiment involves a change in the license conditions incorporated in the license, an unreviewed safety question, a significant increase in occupational exposure or a significant unreviewed environmental impact.

Transnuclear, Inc. provides specialized services for the nuclear fuel cycle that support transportation, storage and handling of spent nuclear fuel, radioactive waste and other radioactive materials. Transnuclear was incorporated in the state of New York in 1965.

Transnuclear, Inc. has been involved in the design, analysis, fabrication, testing, certification and operation of packagings for spent fuel, radioactive waste, and other radioactive materials for over three decades. Transnuclear, Inc. was granted a Certificate of Compliance under 10 CFR 72 Subpart L for the TN-24 storage cask. Transnuclear, Inc. also developed the TN-40 dry storage cask for use at Northern States Power Prairie Island Nuclear Plant and the TN-32 dry storage cask for use at Virginia Power's Surry Power Station and North Anna Power Station.

Transnuclear, Inc also maintains an NRC Quality Assurance Program Approval for Radioactive Material Transportation Packages.

1.4 Generic Cask Arrays

The installation for storing spent fuel may be designed to include one or more TN-68 casks. The casks will be stored on a concrete slab in a free standing, vertical orientation. Typically, one, two or three concrete pads are utilized at an ISFSI with each pad containing a 2 by xx array of casks. One possible configuration for a dry storage installation is shown in Figure 1.4-1. Fourteen foot spacing is assumed between casks for the thermal analysis.

1.5 Supplemental Data

The following Transnuclear Drawings are enclosed:

1. TN-68 Dry Storage Cask, General Arrangement, Drawing No. 972-70-1.
2. TN-68 Dry Storage Cask, General Arrangement Cross Section & Details, Drawing No. 972-70-2.
3. TN-68 Dry Storage Cask, Lid Assembly & Details, Drawing No. 972-70-3.
4. TN-68 Dry Storage Cask, Basket, General Arrangement, Drawing No. 972-70-4. |
5. TN-68 Dry Storage Cask, Basket, Typical Cross Section, Drawing No. 972-70-5. |
6. TN-68 Dry Storage Cask, Pressure Monitoring System, Drawing No. 972-70-6.
7. TN-68 Dry Storage Cask, Damaged Fuel Assembly, Drawing No. 972-70-7. |
8. TN-68 Dry Storage Cask, Damaged Fuel Top & Bottom Caps, Drawing No. 972-70-8. |

1.6 References

1. US Nuclear Regulatory Commission, Regulatory Guide 3.61, Standard Format and Content for a Topical Safety Analysis Report for a Spent Fuel Dry Storage Cask, February, 1989.
2. 10CFR72, Rules and Regulations, Title 10, Chapter 1, Code of Federal Regulations - Energy, U.S. Nuclear Regulatory Commission, Washington, D.C., "Licensing Requirements for the Independent Storage of Spent Nuclear Fuel and High-Level Radioactive Waste."
3. 10CFR71, Rules and Regulations, Title 10, Chapter 1, Code of Federal Regulations - Energy, U.S. Nuclear Regulatory Commission, Washington, D.C., "Packaging and Transportation of Radioactive Material."

TABLE 1.2-1

NOMINAL DIMENSIONS AND WEIGHT OF THE TN-68 CASK

Overall length (with protective cover, in)	215
Outside diameter (in)	98
Cavity diameter (in)	69.5
Cavity length (in)	178
Confinement shell thickness (in)	1.5
Confinement vessel length (in)	189
Body wall thickness (in)	7.5
Confinement Lid thickness (in)	5
Overall Lid thickness (in)	9.5
Bottom thickness (in)	9.75
Resin and aluminum box thickness (in)	6
Outer shell thickness (in)	0.75
Overall basket length (in)	164
Top neutron shield thickness (in)	4
Protective cover thickness (in)	.25
Nominal Cask weight:	
Loaded on storage pad (tons)	114.5

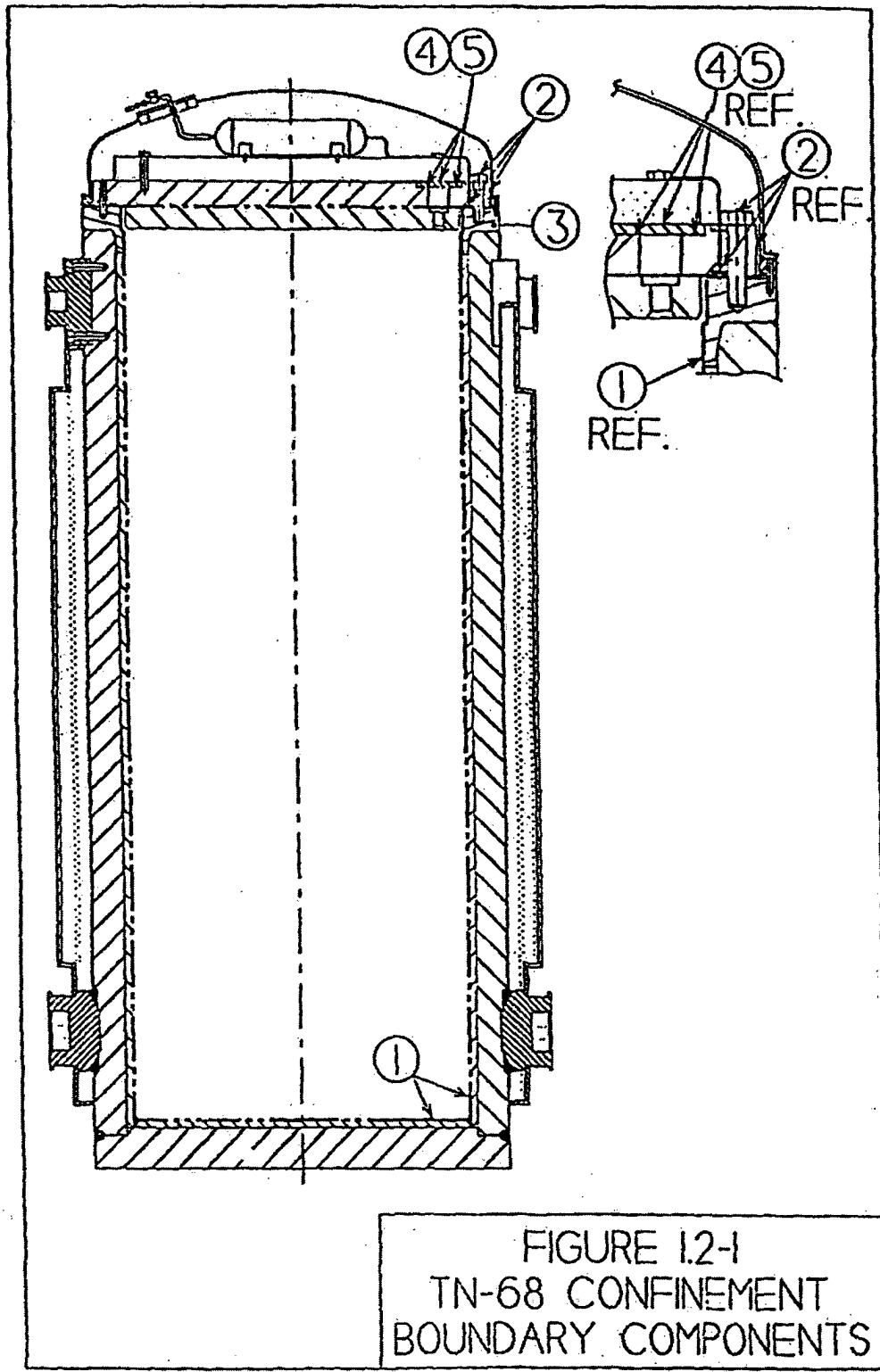


FIGURE I.2-1
 TN-68 CONFINEMENT
 BOUNDARY COMPONENTS

FIGURE 1.2-1 (Continued)

1. Figure not to scale. Features exaggerated for clarity.
2. Phantom line (--- - --- -) indicates confinement boundary.
3. Confinement boundary components are listed below:
 1. Cask body inner shell
 2. Lid assembly outer plate, closure bolts and inner o-ring
 3. Bolting flange
 4. Vent port cover plate, bolts and seals
 5. Drain port cover plate, bolts and seals

Figure 1.4-1
Typical ISFSI Vertical Storage



**TN-68 SAFETY ANALYSIS REPORT
TABLE OF CONTENTS**

SECTION		PAGE
2	PRINCIPAL DESIGN CRITERIA	
2.1	Spent Fuel To Be Stored	2.1-1
2.2	Design Criteria for Environmental Conditions and Natural Phenomena.....	2.2-1
2.2.1	Tornado Wind and Tornado Missiles	2.2-1
2.2.1.1	Applicable Design Parameters	2.2-1
2.2.1.2	Determination of Forces on Structures	2.2-1
2.2.1.2.1	Stability of the Cask in the Vertical Position Under Wind Loading	2.2-3
2.2.1.2.2	Stability of the Cask in the Vertical Position Under Missile Impact.....	2.2-4
2.2.1.2.3	Forces Applied to the Cask Due to Missile Impact	2.2-7
2.2.1.3	Tornado Missiles.....	2.2-9
2.2.1.3.1	Missile A	2.2-9
2.2.1.3.2	Missile B	2.2-10
2.2.1.3.3	Missile C	2.2-12
2.2.1.3.4	Missile D.....	2.2-13
2.2.1.3.5	Ability of Structures to Perform Despite Failure of Structures Not Designed for Tornado Loads.....	2.2-13
2.2.2	Water Level (Flood) Design	2.2-13
2.2.2.1	Flood Elevations	2.2-13
2.2.2.2	Phenomena Considered in Design Load Calculations	2.2-14
2.2.2.3	Flood Force Application	2.2-14
2.2.2.4	Flood Protection.....	2.2-14
2.2.3	Seismic Design.....	2.2-14
2.2.3.1	Input Criteria.....	2.2-15
2.2.3.2	Seismic-System Analysis.....	2.2-15
2.2.4	Snow and Ice Loading	2.2-17
2.2.5	Combined Load Criteria	2.2-17
2.2.5.1	Introduction	2.2-17
2.2.5.2	TN-68 Cask Loading.....	2.2-18
2.2.5.2.1	Normal Operation	2.2-18
2.2.5.2.2	Loading Due to Severe Natural Phenomena and Accidents	2.2-19
2.2.5.2.3	Thermal Conditions	2.2-19
2.2.5.2.4	Fuel Loading	2.2-19
2.2.5.2.5	Decay Heat/Insolation.....	2.2-19
2.2.5.2.6	Beginning of Life Unloading.....	2.2-20
2.2.5.2.7	Ambient Temperature Variations	2.2-20
2.2.5.2.8	Lightning.....	2.2-20
2.2.5.2.9	Fire	2.2-20
2.2.5.2.10	Buried Cask.....	2.2-21

**TN-68 SAFETY ANALYSIS REPORT
TABLE OF CONTENTS**

SECTION	PAGE
2.2.5.3 Bounding Loads for Design and Service Conditions.....	2.2-21
2.2.5.3.1 Dead (Weight) Loads	2.2-21
2.2.5.3.2 Lifting Loads.....	2.2-21
2.2.5.3.3 Internal Pressure.....	2.2-21
2.2.5.3.4 External Pressure	2.2-22
2.2.5.3.5 Cask Body Loads	2.2-22
2.2.5.4 Design Loads	2.2-22
2.2.5.4.1 Cask Body.....	2.2-23
2.2.5.4.2 Basket.....	2.2-24
2.2.5.4.3 Upper Trunnions	2.2-24
2.2.5.4.4 Outer Shell	2.2-25
2.3 Safety Protection Systems.....	2.3-1
2.3.1 General.....	2.3-1
2.3.2 Protection By Multiple Confinement Barriers and Systems.....	2.3-2
2.3.2.1 Confinement Barriers and Systems.....	2.3-2
2.3.2.2 Cask Cooling.....	2.3-4
2.3.3 Protection by Equipment and Instrument Selection.....	2.3-5
2.3.3.1 Equipment.....	2.3-5
2.3.3.2 Instrumentation	2.3-5
2.3.4 Nuclear Criticality Safety	2.3-5
2.3.4.1 Control Methods for Prevention of Criticality.....	2.3-5
2.3.4.2 Error Contingency Criteria	2.3-6
2.3.4.3 Verification Analysis-Benchmarking	2.3-6
2.3.5 Radiological Protection.....	2.3-6
2.3.5.1 Access Control.....	2.3-6
2.3.5.2 Shielding	2.3-7
2.3.5.3 Radiological Alarm System	2.3-7
2.3.6 Fire and Explosion Protection.....	2.3-7
2.4 Decommissioning Considerations	2.4-1
2.5 Summary of Cask Design Criteria	2.5-1
2.6 References.....	2.6-1

**TN-68 SAFETY ANALYSIS REPORT
TABLE OF CONTENTS**

List of Tables

2.1-1	Fuel Assembly Types
2.1-2	Design Basis Fuel Assembly Parameters
2.1-3	Thermal, Gamma and Neutron Sources for the Design Basis 8x8 General Electric Fuel Assembly
2.1-4	Cooling Time as a Function of Maximum Burnup and Minimum Initial Enrichment 7x7 Fuel
2.2-1	Summary of Internal and External Pressures Acting on TN-68 Cask
2.2-2	Summary of Lifting Loads Used in Upper Trunnion ANSI N14.6 Analysis
2.2-3	Summary of Loads Acting on TN-68 Cask Due to Environmental and Natural Phenomena
2.2-4	TN-68 Cask Loading Conditions
2.2-5	TN-68 Cask Design Loads (Normal Conditions)
2.2-6	Level A Service Loads (Normal Conditions)
2.2-7	Level D Service Loads (Accident Conditions)
2.2-8	Normal Condition Load Combinations
2.2-9	Accident Condition Load Combinations
2.3-1	Classification of Components
2.5-1	Design Criteria for TN-68 Casks

List of Figures

2.1-1	Decay Heat 7x7 GE Fuel Assembly 3.3 wt% U-235 Maximum Initial Bundle Average Enrichment, 40,000 MWD/MTU, 10 Year Cooled
2.1-2	Gamma Source 7x7 BWR Fuel Assembly 3.3 wt% U-235 Maximum Initial Bundle Average Enrichment, 40,000 MWD/MTU, 10 Year Cooled
2.1-3	Neutron Source 7x7 BWR Fuel Assembly 3.3 wt% U-235 Maximum Initial Bundle Average Enrichment, 40,000 MWD/MTU, 10 Year Cooled
2.1-4	Fuel Qualification Flowchart for 8x8, 9x9, and 10x10 Fuel
2.2-1	Earthquake and Wind Loads
2.2-2	Tornado Missile Impact Loads
2.2-3	Lifting Loads
2.3-1	TN-68 Cask Seal Pressure Monitoring System
2.3-2	Long Term Leak Test Results on Metallic Seals
2.3-3	Long Term Leak Test Results on Metallic Seals
2.3-4	Long Term Leak Test Results on Metallic Seals

CHAPTER 2

PRINCIPAL DESIGN CRITERIA

This chapter provides the principal design criteria for the TN-68 casks. Section 2.1 presents a general description of the spent fuel to be stored. Section 2.2 provides the design criteria for environmental conditions and natural phenomena. This section presents the analysis which shows that the casks will not tip over or move significant distances under the design basis seismic, tornado, wind and missile loadings, design basis earthquake or extreme floods. This section also contains an assessment of the local damage due to the design basis environmental conditions and natural phenomena and the general loadings and design parameters used for analysis in subsequent chapters. Section 2.3 provides a description of the systems which have been designated as important to safety. Section 2.4 provides a general discussion regarding decommissioning considerations. This is further elaborated on in Chapter 14. Section 2.5 summarizes the cask design criteria.

2.1 Spent Fuel To Be Stored

The TN-68 cask is designed to store 68 General Electric (GE) Boiling Water Reactor (BWR) spent fuel assemblies with or without fuel channels. The maximum allowable lattice-average initial enrichment varies from 3.7 to 4.7 wt% U235 depending on the B10 areal density in the basket neutron absorber plates. The maximum bundle average burnup, maximum decay heat, and minimum cooling time are 40 GWd/MTU, 0.312 kW/assembly, and 10 years for 7x7 fuel, 60 GWd/MTU, 0.441 kW/assembly, and 7 years for all other fuel. The damaged fuel assembly is limited to bundle average burnup ≤ 45 GWd/MTU. The cask is designed for a maximum heat load of 30 kW. The fuel shall have no damage to fuel grid spacers that would render the fuel outside its licensing basis for use in the reactor. Damaged fuel that can be handled by normal means may be stored in eight peripheral compartments fitted with damaged fuel end caps designed to retain gross fragments of fuel within the compartment.

Damaged fuel is defined as fuel with known or suspected cladding defects greater than pinholes or hairline cracks. Damaged fuel to be stored in the TN-68 must be capable of being handled by normal means. There must be no missing fuel pins or fuel pin segments. Fuel with missing pins that have been replaced with dummy rods that displace a volume equal to or greater than that of the original rods is not regarded as damaged. This definition is based on analysis in Appendix 6B which shows that damaged fuel so limited would be retrievable under normal and off-normal conditions. Thermal and criticality analyses assume that such fuel undergoes further damage under accident conditions.

Scoping calculations were performed to determine the fuel assembly type which was most limiting for each of the analyses including shielding, criticality, heat load and confinement. The fuel assemblies considered are listed in Table 2.1-1. The design basis fuel for decay heat, shielding and confinement is an 8x8 lattice with 63 fuel rods and with burnup, bundle average enrichment, and cooling time of 48 GWd/MTU, 2.6 wt% U235, and 7 years, respectively. The fuel qualification screening which is developed based on this fuel is conservative when applied to other fuel types with lower mass of uranium. Of the acceptable contents, only 7x7 fuel has a

greater mass of uranium, but it is not bounding because it is restricted to lower burnup, longer cooling time, and lower decay heat. It has a separate fuel qualification table. For the criticality analysis, all fuel assembly types are analyzed with 3.7% lattice average enrichment. The 10x10 assembly is most reactive and is evaluated for configurations which bound all normal, off-normal and accident conditions at various enrichments with the corresponding B10 areal density in the basket neutron absorber. The thermal and radiological characteristics for the BWR spent fuel were generated using the SAS2H/ORIGEN S modules of SCALE⁽¹⁶⁾. These characteristics for the design basis 8x8 fuel assembly are shown in Table 2.1-2. The thermal analysis uses the 10x10 fuel assembly model with the 8x8 design basis decay heat. Justification for the selection of the most limiting fuel assembly is presented in Chapters 4, 5, 6 and 7 for the thermal, shielding, criticality and confinement analyses, respectively.

Fuel with various combinations of burnup, specific power, enrichment and cooling time can be stored in the TN-68 cask as long as the combination results in decay heat, surface dose rates, and radioactive sources for confinement that are bounded by the design basis fuel. For reference, Figure 2.1-1 shows the relationship between cooling time and decay heat for a typical BWR fuel assembly. As discussed in Chapter 5, an evaluation was performed to determine various combinations of burnup, enrichment and cool time that would be acceptable for the TN-68. Table 2.1-4 provides the minimum cooling time required for various combinations of minimum initial enrichment and maximum burnup for 7x7 fuel. Figure 2.1-4 presents a fuel screening flow chart and a decay heat formula for all other fuel. The 8x8 design basis fuel is evaluated in Chapter 7 to ensure that the off-site airborne dose limits of 10 CFR 72.104 and 72.106 are met. Figures 2.1-2 and 2.1-3 show the relationship between the gamma and neutron source terms and decay time for 7x7 fuel.

Specific gamma and neutron source spectra for the design basis 8x8 fuel are given in Table 5.2-7 and 5.2-9, respectively, and the fission product gas inventory is given in Table 5.2-11.

2.2 Design Criteria for Environmental Conditions and Natural Phenomena

The storage cask design ensures that fuel criticality is prevented, cask integrity is maintained, and fuel is not damaged so as to preclude its ultimate removal from the cask. The conditions under which these objectives are met are described below.

The casks are self-contained, independent, passive systems, which do not rely on any other systems or components for their operation. The criteria used in the design of the casks ensure that their exposure to credible site hazards do not impair their safety functions.

The design criteria satisfy the requirements of 10 CFR Part 72⁽³⁾. They include the effects of normal operation, natural phenomena and postulated man-made accidents. The criteria are defined in terms of loading conditions imposed on the storage cask. The loading conditions are evaluated to determine the type and magnitude of loads induced on the storage cask. The combinations of these loads are then established based on the number of conditions that can be superimposed. The load combinations are then classified as Service Conditions consistent with Section III of the ASME Boiler and Pressure Vessel Code⁽⁴⁾. The stresses resulting from the application of these loads are then evaluated based on the rules of the ASME Code as defined herein.

2.2.1 Tornado Wind and Tornado Missiles

The TN-68 storage cask is designed to resist tornado loadings resulting from those in the most tornado prone regions of the United States as defined in NRC Regulatory Guide 1.76⁽⁵⁾. An analysis of impact on the cask by tornado missiles in accordance with NUREG-0800⁽⁶⁾ Section 3.5.1.4, is presented in this Safety Analysis Report. Non-tornado wind loading is not significant in comparison to that due to tornadoes; therefore, the wind loading is conservatively taken to be the same as the tornado loading.

2.2.1.1 Applicable Design Parameters

The design basis tornado wind velocity and external pressure drop based on NRC Regulatory Guide 1.76 are 360 mph and 3 psi respectively. The external pressure drop of 3 psi associated with passing of the tornado is small and, when combined with the other internal pressure loads is far exceeded by the design internal pressure (100 psig) for the cask.

2.2.1.2 Determination of Forces on Structures

The 360 mph tornado wind loading is converted to a dynamic pressure (psf) acting on the cask by multiplying the square of the wind velocity (in mph) by a coefficient (0.002558 at ambient sea level condition) dependent on the air density, based on data presented in a paper by T.W. Singell⁽⁷⁾. The result is a pressure of 332 psf (Figure 2.2-1a). The net force acting on the cask is obtained by multiplying this pressure by the product of the area of the cask projected onto a plane normal to the direction of wind times a drag coefficient. A drag coefficient of 1 is used based on the geometric proportions of the cask (i.e. length to diameter ratio of approximately 2) and the conservative assumption that the cask surface is rough.

An additional type of load on the structure is that created by the impact of tornado missiles on the cask. These impacts are analyzed for 4 types of missiles:

- Missile A: high energy deformable type missile (4000 lb. automobile) impacting the cask
 - a) horizontally at normal incidence at 35% of the design basis tornado horizontal wind speed.
 - b) vertically at normal incidence at 70% of the horizontal component (24.5% of the design basis tornado horizontal wind speed).
- Missile B: rigid missile (276 lb., 8 inch diameter armor piercing artillery shell) impacting the cask:
 - a) horizontally at normal incidence at 35% of the design basis tornado horizontal wind speed.
 - b) vertically at normal incidence at 70% of the horizontal component (24.5% of the design basis tornado horizontal wind speed).
- Missile C: small rigid steel sphere 1 inch in diameter impinging upon the barrier openings in the most damaging direction at 35% of the design basis tornado horizontal wind speed.
- Missile D: a 4 inch thick by 12 inch wide by 12 foot long wood plank, travelling at 300 mph.

The tornado missiles are summarized in the following table.

Missiles		Mass (lbs)	Horizontal Velocity (mph)	Vertical Velocity (mph)
A	Automobile	4,000	126	88.2
B	8" Dia. Armor Piercing Artillery Shell	276	126	88.2
C	1" Dia. Steel Sphere	< 1	126	126
D	4" Thick. Wood Plank 12" Wide x 12' Long	200	300	300

2.2.1.2.1 Stability of the Cask in the Vertical Position Under Wind Loading

Cask stability evaluations are performed using a conservatively low cask weight of 227,000 lbs. The cask rests in an upright position on a concrete pad. To determine an appropriate coefficient of friction between steel and concrete, the following references are cited:

Coefficient of Static Friction	References
Metal on stone: 0.30 – 0.70	Beer and Johnston, Vector Mechanics for Engineers: Static and Dynamic ⁽²³⁾
Metal on Concrete: 0.30 – 0.40	Walmer, M.E., Manual of Structural Design and Engineering Solutions ⁽²⁴⁾
Concrete to Steel: 0.40	PCI Design Handbook, 2 nd Edition ⁽²⁵⁾

The coefficient of static friction is used to calculate the maximum amount of frictional force available to prevent sliding. Once sliding begins, there is lower frictional force available, and the coefficient of kinetic friction should be used. According to the textbook⁽²³⁾, Vector Mechanics for Engineers: Static and Dynamic by F.P. Beer and E.R. Johnston, the coefficient of kinetic friction is approximately 25% smaller than the coefficient of static friction.

A broom finish will be specified for the top surface of the concrete pad. This will result in a coarser texture than a smooth, troweled finish. It is therefore concluded that a coefficient of static friction value of 0.35 is appropriate for the determination of the factor of safety against cask sliding, the kinetic coefficient of friction between the steel cask and the concrete pad is taken as 0.2625.

Cask Sliding

The wind loading on the cask body is:

$$q = 0.002558 V^2 = 0.002558 (360)^2 = 332 \text{ lb/ft}^2$$

and the projected area is

$$A = (160 \times 98 + 22.75 \times 81.25 + 32.25 \times 84.5)/144 = 140.65 \text{ ft}^2$$

Therefore, the total wind force is

$$F_{\text{wind}} = 332 \times 140.65 \approx 46,700 \text{ lbs.}$$

The friction force under the cask is

$$F_{\text{friction}} = W_{\text{cask}} \times \mu = 227,000 \times 0.35 = 79,450 \text{ lbs.}$$

A conservatively low weight of 227,000 lbs. is used for the stability analyses.

$F_{\text{friction}} > F_{\text{wind}}$, thus, the wind will not slide the cask.

Cask Tipping

The cask has an outer diameter of 84.5 inches at its base. The constant wind velocity to tip the cask is calculated by equating the tipping moment to the restoring moment:

The tipping moment due to the 360 mph wind about the bottom edge of the cask is:

$$M_{\text{tipping}} = F_{\text{wind}} \times B = 46,700 \times 97.26 = 4.54 \times 10^6 \text{ in-lb (B = 97.26", CG of the Cask)}$$

And the restoring moment due to the weight of the cask is:

$$M_{\text{restoring}} = W_{\text{cask}} \times r = 227,000 \times 42.25 = 9.59 \times 10^6 \text{ in-lb (r = 42.25", Radius of the Cask)}$$

$$M_{\text{restoring}} > M_{\text{tipping}}$$

Therefore the design basis tornado wind velocity of 360 mph will neither slide nor tip the cask.

2.2.1.2.2 Stability of the Cask in the Vertical Position Under Missile Impact

It is assumed that Missiles A, B and D impact inelastically on the cask as shown in Figure 2.2-2. Missile A (the automobile) and Missile D (the wood plank) are assumed to crush and Missile B (the rigid shell) is assumed to partially penetrate the cask wall. The cask will tend to slide if the missile strikes it below the CG (unless it is blocked in position) or tilt if the missile strikes it above the CG. Conservation of momentum is assumed for both sliding and tipping with a coefficient of restitution of zero. The energy transferred to the cask is dissipated by friction in the sliding case or transformed into potential energy as the cask CG lifts in the tipping case. When a missile strikes the side of the cask at an elevation near the CG:

In the sliding case:

$$V = \frac{mv_0}{M + m}$$

Where:

- V = cask translational velocity after impact
- v_0 = missile initial velocity
- m = mass of Missile, lbf/386.4
- M = cask mass, 227,000 lbf/386.4

When the appropriate substitutions are performed for Missile impact, the cask velocity after

impact in the sliding case, V, is summarized as follows:

	Missile	Mass (lbs)	Missile Initial Velocity v_0 (mph)	Cask Translational Velocity After Impact V (mph)
A	Automobile	4,000	126	2.182
B	8" Dia. Armor Piercing Artillery Shell	276	126	0.153
C	1" Dia. Steel Sphere	< 1	126	0
D	4" Thick. Wood Plank 12" Wide x 12' Long	204	300	0.264

Missile A therefore has a greater effect on the stability of the cask than do missiles B or D producing a velocity after impact of 2.182 mph or 38.4 in/sec.

Cask Sliding

The cask may tend to slide if the missile strikes it below the CG. Assuming no rotation and ignoring friction, the cask velocity could reach 2.182 mph or 38.4 in/sec after the impact. Therefore, the final kinetic energy is:

$$KE = 1/2(W_{\text{cask}} \times V^2)/g = 1/2 (227,000 \times 38.4^2)/386.4 = 4.33 \times 10^5 \text{ in-lb}$$

If the cask slides on the concrete pad, the cask kinetic energy after impact is absorbed by friction. The friction work can be equated to the kinetic energy. Assuming a coefficient of friction of 0.2625:

$$F_{\text{friction}} = \mu W_{\text{cask}} = 0.2625 \times 227,000 = 0.596 \times 10^5 \text{ lbs}$$

Where:

$$F_{\text{friction}} = \text{friction force}$$

$$\mu = \text{coefficient of friction}$$

The sliding distance is determined by:

$$\text{Sliding Distance } L = KE / F_{\text{friction}} = 4.33 \times 10^5 / 0.596 \times 10^5 \approx 7.3 \text{ in.}$$

The cask may tend to slide 7.3 in. if the missile strikes it below the CG of the cask.

Cask Tipping

If the entire momentum of the missile is applied to the cask, the impulse momentum would be:

$$\begin{aligned} \text{Impulse Momentum} &= (W_{\text{missile}}/g) \times (v_o) \\ &= (4000/386.4) \times (126 \times 5280 \times 12/3600) = 2.296 \times 10^4 \text{ lb-sec} \end{aligned}$$

If the impulse is applied near the top and cask pivots about a bottom corner (not sliding), therefore,

$$\text{Cask angular momentum after impact} = \text{Moment of impulse}$$

The rotational kinetic energy about corner A is (see Figure 2.2-2):

$$KE_{\text{rotation}} = 0.5 (I_{\text{cask about A}} \times \omega^2)$$

$$I_{\text{cask about A}} = I_{\text{cg}} + (W_{\text{cask}}/g) (x)^2$$

$$I_{\text{cg}} = (W_{\text{cask}}/g)(r^2 + A^2/3)/4 = (227,000/386.4)(42.25^2 + (197.25)^2/3)/4 = 2.17 \times 10^6 \text{ lb-in-sec}^2$$

$$I_{\text{cask about A}} = 2.17 \times 10^6 + (227,000/386.4)(106.04)^2 = 8.78 \times 10^6 \text{ lb-in-sec}^2$$

$$\text{Therefore, } (I_{\text{cask about A}})(\omega) = \text{Impulse} \times 215 = 2.296 \times 10^4 \times 215 = 4.94 \times 10^6 \text{ in-lb-sec}$$

$$\omega = 4.94 \times 10^6 / I_{\text{cask about A}} = 4.94 \times 10^6 / 8.78 \times 10^6 = 0.56 \text{ sec}^{-1}$$

and rotational kinetic energy is

$$KE_{\text{rotation}} = 1/2(I_{\text{cask about A}} \times \omega^2) = 1/2(8.78 \times 10^6 \times 0.56^2) = 1.38 \times 10^6 \text{ in-lb}$$

The cask tilts through a small angle before it stops. When the cask tips or pivots about point A after impact, the kinetic energy is transformed into potential energy as CG rises (Figure 2.2-2):

$$E_{\text{tipping}} = \text{Increase in Potential Energy} = \text{Kinetic Energy} = 1.38 \times 10^6 \text{ in-lb}$$

$$E_{\text{tipping}} = W_{\text{cask}} \times (x) (\sin \alpha - \sin \theta)$$

$$\text{Therefore, } \alpha = \sin^{-1} [E_{\text{tipping}} / (W_{\text{cask}} \times x) + \sin \theta]$$

$$\theta = \sin^{-1}(B/x) = \sin^{-1}(97.26/106.04) = 66.5^\circ$$

$$\alpha = \sin^{-1} [1.38 \times 10^6 / (227,000 \times 106.04) + \sin 66.5] \approx 77.0^\circ$$

So the cask tilts an angle equals to $(\alpha - \theta) = 77.0^\circ - 66.5^\circ = 10.5^\circ$

The cask is still stable since it will right itself until the CG lifts over the corner when α reaches 90° .

$$\alpha = 90^\circ \quad \alpha - \theta = 90^\circ - 66.45^\circ = 23.5^\circ$$

Therefore, the cask will not tipover.

2.2.1.2.3 Forces Applied to the Cask Due to Missile Impact

The impact forces applied to the cask as it is struck by the missiles are determined as follows:

- Missile A - (automobile) is assumed to crush 3 feet under a constant force during the impact. The loss of kinetic energy is assumed to be dissipated by crushing of the missile. The frontal area of the automobile is assumed to be 20 sq. ft.

$$F_a \times 3ft. = \frac{1}{2} [m_a v_o^2 - (M + m_a)V^2]$$

$$p'_a = F_a / 20 ft^2$$

where:

F_a = Impact force on cask by Missile A
 p_a = Impact pressure on cask by Missile A

The impact force, F_a , is determined to be 706,950 lb, and the crush pressure on the frontal area of the automobile, p_a , is 246 psi.

- Missile B - (rigid missile) does not deform under impact. The loss in kinetic energy is assumed to be dissipated as the missile partially penetrates the cask wall. The penetration force is assumed to be equal to the yield strength of the cask body material multiplied by the frontal area of the 8 in. diameter missile.

$$F_b = S_y \left(\frac{\pi}{4}\right) (8)^2$$

The impact force, F_b , is determined to be 1.558×10^6 lbs. assuming a cask body yield stress, S_y , of 31,000 psi. This force is higher than that developed by Missile A, but the

impact time duration is much smaller so that a smaller impulse is applied to the cask producing less cask movement than Missile A

- Missile C - (small rigid steel sphere) Due to its small mass, Missile C has no significant effect on the stability of the cask and is bounded by Missiles A and B.
- Missile D - Wood plank deforms and is crushed under impact. The wood is much softer than the cask material. From Reference 8, the wood with the highest density and modulus of elasticity is selected. This is hickory with a density of 51 lbs/ft³, a modulus of elasticity of 2.18×10^6 psi and a compressive strength of 8,970 psi. The wood crushing force, F_d is therefore $(8970)(4)(12) = 430,560$ lbs.

The above forces, F_a , F_b and F_d are used in the stress analysis of the cask body.

2.2.1.3 Tornado Missiles

The TN-68 cask has been evaluated for potential damage due to the four tornado missiles identified in 2.2.1.2. The effect of the missiles on the cask is summarized below and described in the following subsections.

Missile	Compressive Stress	Bending Stress	Penetration Distance, in.	Impact Force (lbs.)
A	246 psi	30,670 psi	0	706,950
B	31,000 psi	32,280 psi	1.13	1.558 x 10 ⁶
C	31,000 psi	1,640 psi	0.146	12,100
D	8,970 psi	< B	0	430,560

2.2.1.3.1 Missile A

Missile A (automobile) deforms and is crushed during the impact. The local pressure on the cask structure is less than 1% of the body yield strength. Therefore, no local penetration occurs. The shear stress in the cask wall is conservatively calculated below. It is assumed that the impact force is concentrated on a small curved section of the cask wall having dimensions $w \times L$. It is also assumed that only two edges are tending to shear (above and below the curved section). It is assumed that only 3 foot sections are shearing. Then

$$\begin{aligned} \text{Shear Area} &= 2 \times 36 \times \text{the thickness of the gamma shielding} \\ &= 2 \times 36 \times 6.0 = 432 \text{ in}^2 \end{aligned}$$

The shear stress, $\tau = \text{Force/area} = 706,950/432 = 1,637 \text{ psi}$.

The level D allowable shear stress for the gamma shielding is $0.42 S_u = 0.42 \times 70,000 = 29,400 \text{ psi}$. The shear stress is well below the allowable shear stress.

Assuming that the impact on the side of the cask is reacted by a 3 foot high section of shielding, case 18 from Table VIII of Reference 20 is used to model the impact as shown below.

$$|M_{\max}| = 3/2(wR^2)$$

The $2\pi R w$ from Table VIII, case 18 is the side impact force = 706,950 lbs.

$R = 39.25 \text{ inches}$ (mean radius of gamma shield)

Therefore, $w = F/2\pi R = 2,867$ lbs/in.

And, $|M_{\max}| = 3/2(wR^2) = 6.63 \times 10^6$ in lbs.

The bending stress on the section is:

$$\sigma_b = M \times c/I = 6.63 \times 10^6 \times (6/2)/(36 \times 6^3/12) = 30,670 \text{ psi}$$

The Level D allowable for membrane plus bending stress is $3.6S$ or S_u . For SA-266 Cl. 2 shielding material, $S = 17,500$ psi at 300°F and $S_u = 70,000$ psi. Thus the allowable stress is $3.6 \times 17,500 = 63,000$ psi. Therefore the membrane plus bending stress is acceptable.

If the automobile were to strike the top of the cask in the vertical orientation, the velocity would be 88.2 mph (70% of the horizontal impact velocity). The kinetic energy would be 12.47×10^6 in-lbs. For a crush depth of 36 inches, the impact force would be

$$F_{av} = \text{Kinetic Energy} / \text{crush distance} = 346,340 \text{ lbs.}$$

This force is less than for Missile B and is spread out over a larger area. Therefore the stresses will be lower for missile A impact than for missile B impact. The stresses from missile B impact are bounding.

2.2.1.3.2 Missile B

Missile B (rigid) partially penetrates the cask wall. The loss in kinetic energy is dissipated as strain energy in the cask wall. The force developed as the 8 in. diameter missile penetrates the cask body is calculated below. A yield strength of 31,000 psi is used for the gamma shield material at 300°F .

$$F_b = S_y \left(\frac{\pi}{4} \right) (8)^2 = 1.558 \times 10^6 \text{ lbs.}$$

From conservation of energy:

$$F_b x = \frac{1}{2} m_b v_o^2$$

Or for constant puncture force:

$$x = \frac{m_b v_o^2}{2 F_b}$$

Where x is the penetration distance.

The penetration distance is found to be 1.13 in. for perpendicular impact of the missile.

When the impact angle is not 90 degrees, the missile will rotate during impact (conservatively neglected), limiting the energy available for penetration since part of the energy will be transformed into rotational kinetic energy.

When hitting the weather protective cover, Missile B deforms the dished head before penetration begins (see Figure 2.2-2c). This will decrease the penetration distance from the above value.

If the missile were to impact the top of the cask in the vertical orientation, the missile velocity would be 88.2 mph (70% of the horizontal impact velocity of 126 mph). The kinetic energy would be:

$$\begin{aligned} \text{KE} &= 0.5 \times (276 \text{ lbs}/32.2\text{ft}/\text{sec}^2) \times (88.2 \text{ mph} \times 5280\text{ft}/\text{mi}/3600 \text{ sec}/\text{hr})^2 \times 12 \text{ in}/\text{ft} \\ &= 860,440 \text{ in lbs.} \end{aligned}$$

Ignoring the effect of the protective cover and the top neutron shield, the lid bending stresses under a top impact are evaluated. Reference 20 is used to evaluate the stresses for two boundary conditions:

1. Modeling the lid as a simply supported plate.
2. Modeling the lid as a plate with the edges fixed.

For edges simply supported, Table X, Case 2 of Reference 20 is used. The maximum stresses occur at the center, where the plate thickness is $t = 9.5$ in. The impact force, $F_b = 1.558 \times 10^6$ lbs.

The maximum stress at the center is calculated below:

$$S_r = S_t = 3W/(2\pi t^2) \times [m + (m+1)\ln(a/r_o) - (m-1)r_o^2/4a^2]$$

Where $r_o =$ uniform load radius = missile radius = 4 inches

$$m = 3.33$$

$$t = 9.5 \text{ inches}$$

$$a = 37.94 \text{ inches (effective radius for a simply supported lid at the bolt circle)}$$

$$W = F_b = 1.558 \times 10^6 \text{ lbs.}$$

Therefore, $S_r = S_t = 32,280$ psi

This is well below the Level D allowable stress of 63,000 psi.

For the second case, with the lid edges fixed, Table X, case 7 of Reference 20 is used.

The maximum stress occurs at the edge, where the plate thickness, $t = 5$ inches.

$$S_r = 3W/(2\pi t^2) (1 - r_o^2/2a^2)$$

Where $W = F_b = 1.558 \times 10^6$ lbs.

r_o = uniform load radius = missile radius = 4 inches

t = 5 inches

a = 37.94 inches

S_r = 29,590 psi.

This is also well below the allowable Level D stress of 63,000 psi.

2.2.1.3.3 Missile C (steel sphere 1" diameter)

The impact of the steel sphere can result in a local dent by penetrating into the cask surface at the yield strength, S_y , for a penetration depth, d . The contact area on the cask surface is:

$$A = \pi(2Rd - d^2)$$

Where:

R is the radius of the sphere, 0.5 inches

d is the penetration depth

The kinetic energy of the steel sphere is dissipated by displacing the cask surface material:

$$KE = \frac{1}{2}(m_c v_o^2) = S_y \int_0^d \pi(2Rd - d^2) dd$$

Where m_c = sphere mass

$$KE = 0.5(4/3)(\pi)(0.5)^3(0.28)(1/32.2)(126 \times 5280/3600)^2 = 933 \text{ in-lbs}$$

$$S_y \int_0^d \pi(2Rd - d^2) dd = S_y \pi(Rd^2 - d^3/3) = KE = 933 \text{ in-lbs}$$

For a yield strength of 31,000 psi, by trial and error:

$$d = 0.146 \text{ in.}$$

The area, A , is therefore 0.39 sq. inches. A maximum impact force of 12.1×10^3 lb. ($A \times S_y$) will be developed. It can be concluded that only local denting of the cask will result.

If the impact is at the top of the cask (ignoring the protective cover and the neutron shielding), Ref. 20, Table X, Case 4 is used to determine the stresses. The impact force is assumed to act at the center of the lid, where $p = 0$, $r_o = 0.353$ in. and $a = 37.94$ inches.

The maximum stress is:

$$S_r = S_t = 3W/(2\pi mt^2) \times [m + (m+1)\ln(a/r_o) - (m-1)r_o^2/4a^2] = 1,640 \text{ psi}$$

Since all penetrations are covered, the steel sphere will have a negligible effect on the cask.

2.2.1.3.4 Missile D (wood plank)

The weight of the plank is 204 lbs. The kinetic energy of the plank is:

$$\begin{aligned} \text{KE} &= 0.5mv^2 \\ &= (0.5) \times (204)/(32.2) \times [(300)(5280)/3600]^2 = 6.13 \times 10^5 \text{ ft} \cdot \text{lbs} = 7.359 \times 10^6 \text{ in} \cdot \text{lbs.} \end{aligned}$$

The wood is much softer than the cask material, and most of the kinetic energy will be absorbed by the wood crushing.

The wood crush force = 8,970 psi x 4 in x 12 in = 430,560 lbs.

The wood would need to crush $7.359 \times 10^6 \text{ in} \cdot \text{lbs} / 430,560 \text{ lbs} = 17.1 \text{ inch}$ to absorb 100% of the impact energy.

The wood crush force is much less than the impact force developed in the Missile B impact ($1.558 \times 10^6 \text{ lbs.}$), while the impact area is nearly the same. The cask stresses for the wood plank impact will therefore be lower than for the Missile B impact.

2.2.1.3.5 Ability of Structures to Perform Despite Failure of Structures not Designed for Tornado Loads

The TN-68 cask itself can withstand the tornado loading. Generally, the casks will be stored outside on a flat concrete slab. Therefore, there will be no structures that could collapse about the storage cask. If such structures were present at an ISFSI, further analysis would be required.

2.2.2 Water Level (Flood) Design

The cask has been evaluated for a water level of 57 ft (measured from the base of the cask) and a water drag force of 45,290 lbs. due to floods. It is demonstrated that the cask is acceptable for these conditions. If a specific site has requirements to evaluate conditions exceeding these values, further analysis is required.

2.2.2.1 Flood Elevations

It is anticipated that the storage casks will be located on flood-dry sites. However, the storage cask is designed for an external pressure of 25 psi which is equivalent to a static head of water of approximately 57 ft. This is greater than would be anticipated due to floods, regardless of the site.

2.2.2.2 Phenomena Considered in Design Load Calculations

The casks are designed to withstand loads from forces developed by the probable maximum flood including hydrostatic effects and dynamic phenomena such as momentum and drag.

2.2.2.3 Flood Force Application

Using a friction coefficient of 0.2625, a drag force greater than 45,290 lb. is required to move the cask when the cask is in an upright position (after taking into account the buoyant force on the cask). This force is equivalent to a stream of water flowing past the cask at 22.1 ft/sec.

The water velocity was calculated using the following formula:

$$F = C_D A \rho \frac{V^2}{2g}$$

where F = Drag force, 45,290 lbs.

C_D = Drag coefficient ≈ 0.7

A = Projected area, 136.1 ft²

ρ = 62.4 lb/ft³

V = water velocity, ft/sec

g = 32.2 ft/sec²

Therefore

$$V = \sqrt{\frac{2Fg}{C_D A \rho}} \quad V = 22.1 \text{ ft/sec}$$

For a lower friction coefficient, the drag force is less and the water velocity to move the cask is less.

2.2.2.4 Flood Protection

The storage cask is designed for an internal pressure of 100 psig. The metallic seals in the cask are designed to maintain helium inside of the confinement. They are also effective in preventing water in-leakage into the cask. In addition, the interspace between the confinement seals and the confinement vessel cavity are pressurized to approximately 6 atm abs and 2 atm abs, respectively, to preclude any possibility of water in-leakage.

2.2.3 Seismic Design

Seismic design criteria are dependent on the specific site location. These criteria are established

based on the general requirements stated in 10CFR Part 72.102. The design earthquake for use in the design of the casks must be equivalent to the safe shutdown earthquake (SSE) for a collocated nuclear power plant, the site of which has been evaluated under the criteria of 10CFR100, Appendix A⁽⁹⁾.

2.2.3.1 Input Criteria

The TN-68 cask is a very stiff structure. For the purpose of calculating seismic load, the cask is treated as a rigid body attached to the ground and equivalent static analysis methods are used to calculate loads and overturning moments. This assumption is valid as long as the cask does not slide due to the seismic loads.

The fundamental natural frequency of vibration for the cask is determined as shown below (Formulas for Stress and Strain⁽²⁰⁾, 4th Edition, Page 369, Case #3):

$$f = 3.89 / (WL^3/8EI)^{1/2}$$

Where:

W = Weight of Cask (227,000 lbs)

L = Height of Cask = 197.25 in.

E = Modulus of Elasticity = 28.3×10^6 psi

I = $(\pi/64)(D_o^4 - D_i^4) = (\pi/64)(84.5^4 - 69.5^4) = 1.36 \times 10^6$ in⁴

Substituting the values given above,

$$f = 52 \text{ Hz}$$

The vertical structural frequency of cask will be still higher since the cask has higher axial stiffness than the lateral stiffness. Thus the cask standing vertically on its pad has dominant lateral and vertical frequencies higher than 33 Hz (corresponding to the maximum ground acceleration, reference NUREG 1.60⁽²²⁾). Therefore, the cask can be treated as a rigid body and the maximum seismic load on the cask is the peak ground acceleration times the mass of the cask. The cask is, therefore, evaluated using an equivalent static seismic loading method, and there is no need to specify a design response spectrum or its associated time history. The factor of 1.5 (reference to NUREG 0800⁽⁶⁾, Para. 3.7.2) to account for multimode behavior need not be included in the seismic accelerations for this analysis, as the potential for sliding/uplift is due to rigid body motion, and no frequency content effects are associated with this action.

2.2.3.2 Seismic-System Analysis

Cask Sliding

If the cask is to slide due to seismic loading, the horizontal component of the seismic load must overcome the friction force between the cask base and concrete pad. The friction force is equal to the normal force due to gravity acting at the cask/ground interface multiplied by the coefficient

of friction.

The vertical seismic force is applied upward so as to decrease the normal force and hence the sliding resistance force. The equivalent static horizontal acceleration load required to initiate sliding is calculated as follows:

$$g_h \times W = \mu W (1 - 2/3 g_h)$$

where:

g_h = Fraction of horizontal acceleration value necessary to initiate sliding

W = Weight of cask on pad

μ = Coefficient of friction

For a coefficient of friction of 0.35, the equivalent static horizontal load required to initiate sliding is 0.284g.

Using a safety factor of 1.1 as recommended by ANSI/ANS-57.9⁽²⁶⁾, Section 6.17.4.1, the cask will not slide for a horizontal g loading of $0.284/1.1 = 0.26g$. The maximum vertical g loading is $2/3 (0.26)$ or 0.17g.

The two horizontal components of seismic load are combined as indicated in Section 3.7.2 of NUREG-0800. At 45° to either horizontal component, the response due to a N-S earthquake is $\sin 45^\circ \times$ N-S response and likewise for an E-W earthquake is $\sin 45^\circ \times$ E-W response. If both components are equal, the combined response is:

$$(\sin^2 45^\circ + \sin^2 45^\circ)^{1/2} \times \text{response} = \text{response in either axis.}$$

Therefore, we only need to consider a single horizontal axis for the maximum seismic response.

Cask Tipping

The cask will not tipover due to a seismic event if the stabilizing moment due to cask weight is higher than the seismic tipping moment. The vertical acceleration is assumed to be $2/3$ the horizontal acceleration in accordance with NUREG-0800. For a cylindrical cask, the horizontal g value necessary to tip the cask is calculated below:

$$M_{\text{tip}} = g_h W L_v + (2/3) g_h W L_r$$

Where:

M_{tip} = Moment necessary to tip the cask, in-lbs

g_h = Fraction of horizontal acceleration value necessary to tip the cask

W = Weight of cask on pad

L_v = Vertical distance to C.G. = 97.26 in.

L_r = Radial distance to C.G. = 42.25 in.

$$M_{\text{stab}} = W L_r$$

Where:

M_{stab} = Stabilizing moment of the cask, in-lbs.

W = Weight of cask on pad

L_r = Radial distance to CG = 42.25 in

Therefore, the g value necessary to tip the cask is found by equating M_{tip} to M_{stab} :

$$g_h W L_v + (2/3) g_h W L_r = W L_r$$

$$g_h = 42.25 / (97.26 + 0.667 \times 42.25) = 0.34$$

Using a safety factor of 1.1 as recommended by ANSI/ANS-57.9, Section 6.17.4.1, the cask will not tipover for a horizontal g loading of $0.34/1.1 = 0.31g$. The maximum vertical g loading is $2/3 (0.31)$ or $0.21g$.

Conclusion

As demonstrated by the above calculations, an applied horizontal acceleration of 0.26g (and vertical acceleration of 0.17g) or less will neither slide nor tip the cask. The load distribution is shown in Figure 2.2-1b.

For evaluation of the stresses of the cask body, a 1g lateral and 2g downward acceleration were conservatively used for seismic loads on the cask. These loads are applied while the cask is standing in a vertical position on the concrete pad and bound the specified seismic load limits.

2.2.4 Snow and Ice Loading

The decay heat of the contained fuel will maintain the storage cask outer surface temperature above 32°F throughout its service life, including the end of life, assuming an ambient temperature of -20°F. Therefore, snow or ice would melt when it comes in contact with the cask so that snow and ice loading need not be considered for the storage cask.

The temperature of the protective cover attached to the top of the cask above the lid under certain conditions could fall below 32°F and a layer of snow or ice might build up. A 50 psf (0.35 psi) snow or ice load corresponds to approximately 6 ft of snow or 1 ft of ice. However, this load is insignificant on the TN-68 since the cover is a 0.25 in. thick torispherical steel head which can withstand an external pressure over 13 psi. Therefore, the cover will maintain its intended protective function under snow or ice loading conditions.

2.2.5 Combined Load Criteria

2.2.5.1 Introduction

Sections 2.2.1 through 2.2.4, above, describe the most severe natural phenomena considered in the design of the TN-68. These phenomena have been analyzed to show that the cask is stable.

It will not tip over under any condition or slide on its pad more than about 7.3 inches. In addition, the forces and pressures applied to the cask due to these phenomena have been determined.

It should be noted that all of the above phenomena are upper bound, low probability events. In most cases, however, there is a more regular or frequent similar phenomena of lower magnitude. For instance, some small wind loading occurs often, but tornado winds are unlikely. The forces and pressures determined for the severe phenomena can therefore be used as upper bound values for all similar events.

It has been assumed that these bounding forces and pressures, with a single exception, can occur at any time and their effects are combined with those due to normal operations. The sole exception is the loading(s) due to the tornado missiles as described in Section 2.2.1.3. The missile case is evaluated in combination with others as a low probability event which is postulated only because the consequences of cask penetration might result in severe impact on the immediate environs.

2.2.5.2 TN-68 Cask Loading

A brief explanation of the cask loads due to events that will occur or can be expected to occur in the course of normal operation follows. The cask loads due to the severe natural phenomena and accidents are compared with those for similar but less severe normal events. Then loads equal to or higher than the upper bound values selected for design and analysis of the TN-68, defined as Service Loads, are described. Finally, the Service Loads are separated into two levels and superposition of simultaneous loading (combined loads) is discussed.

2.2.5.2.1 Normal Operation

During normal storage on the ISFSI pad, the cask is subjected to loading due to its own dead weight and that of its contents (fuel and basket), assembly stresses due to the bolt preload required to seat the double metallic seals and react to the internal pressure, and internal pressure due to initial pressurization and any fuel clad failure resulting in fission gas release.

Additional normal loads include wind loading which produces a distributed lateral load on one side of the cask and can also result in slight external pressure drop on other portions of the cask.

Lifting loads are applied to the cask through the trunnions and the cask dead weight is reacted through the trunnions during lifting operations.

Finally, an increased external pressure is applied to all surfaces of the cask during fuel loading when the cask is at the bottom of the spent fuel pool. Snow and ice loads apply local external pressure loading to the top of the protective cover. The cask will, of course, be subjected to the full range of thermal conditions produced by ambient variations (including insolation) and decay heat.

2.2.5.2.2 Loading Due to Severe Natural Phenomena and Accidents

The cask is subjected to dead weight loading and assembly stresses due to bolt preload and seal compression under all conditions. If it becomes necessary to unload a recently loaded hot cask, water would be slowly pumped into the cask to reduce the temperature prior to unloading. If proper controls are not maintained, an internal pressure corresponding to saturated steam pressure at the cavity wall temperature could occur which would be higher than the normal internal pressure. An evaluation of the unloading process is provided in Section 4.5.

The tornado wind loading described in Section 2.2.1 could produce higher lateral loading than any normal wind loading or flood water drag force. The external pressure drop due to the tornado wind is also more severe than due to any normal condition. Tornado missile impact described in Section 2.2.1.3 could apply a high local loading to the cask unlike any normal condition.

External pressure loading of the cask could occur due to flooding (see Section 2.2.2), or nearby explosion. The full range of thermal conditions due to ambient variations, decay heat and minor fires in the vicinity of the cask apply.

2.2.5.2.3 Thermal Conditions

The TN-68 component temperatures and thermal gradients are affected by the following thermal conditions:

- Fuel loading
- Decay heat
- Insolation
- Beginning of life unloading
- Ambient variations
- Lightning
- Minor fire
- Cask Burial

The thermal conditions which are of concern structurally are the temperature distributions in the cask and the differential thermal expansions of interfacing cask components.

2.2.5.2.4 Fuel Loading

The cask is loaded in a spent fuel pool under water. The cask is cooled by pool water; therefore, the thermal gradients established during fuel loading are negligible.

2.2.5.2.5 Decay Heat/Insolation

After the cask is loaded and removed from the pool, the cask body will gradually reach steady state conditions. Since the mass of the cask is large, the time to reach equilibrium will be approximately 1 to 2 days. The temperature gradients in the cask body have an insignificant effect on the structural integrity of the body.

Thermal analysis has been performed to determine the temperatures within the cask for different normal and accident conditions. The methods used to obtain these results are discussed in Chapter 4. The cask temperature distribution for the short-term normal condition (See Chapter 4) was used for the structural analysis.

2.2.5.2.6 Beginning of Life Unloading

This condition would occur if it were necessary to place the cask back in the pool at the beginning of life after it had been loaded and reached thermal equilibrium. Prior to placing the cask in the pool, the cask and fuel would have to be cooled by circulating water through the cask. Therefore, cold water would contact the hotter cask inside surfaces and fuel pins. This condition has been evaluated and it has been shown that the thermal gradients in the cask body are small and would have an insignificant effect on the cask body and the fuel cladding.

2.2.5.2.7 Ambient Temperature Variations

Because the cask thermal inertia is large, the cask thermal response to changes in atmospheric conditions will be relatively slow. Ambient temperature variations due to changes in atmospheric conditions i.e., sun, ice, snow, rain and wind will not affect the performance of the cask. Snow or ice will melt as it contacts the cask because the outer surface will be above 32°F for ambient temperatures as low as -20°F. The cyclical variation of insolation during a day will also create insignificant thermal gradients.

The thermal analysis is discussed in further detail in Chapter 4.

2.2.5.2.8 Lightning

Lightning will not cause a significant thermal effect. If struck by lightning on the lid, the electrical charge will be conducted by paths provided by the lid bolts to the body.

The lid metallic O-ring seals can withstand temperatures of up to 536°F without loss of sealing capability. It is not anticipated that lightning could result in the seals reaching temperatures above these values.

2.2.5.2.9 Fire

The only real source of fuel for a fire in the vicinity of the cask is the fuel tank of the tow vehicle which transports the cask to the storage pad. An evaluation was made to determine the thermal response of the cask assuming this minor fire is an engulfing fire. The details of this analysis are provided in Section 4.4. The cask will maintain its confinement integrity during and after this bounding hypothetical fire accident.

2.2.5.2.10 Buried Cask

An evaluation is made to determine the increase in cask temperature with time assuming that the cask is completely buried by dirt and debris with very low thermal conductivity. The details of this analysis are given in Section 4.4. The analysis shows that the cask will maintain its confinement integrity for a maximum burial period of 76 hours.

2.2.5.3 Bounding Loads for Design and Service Conditions

2.2.5.3.1 Dead (Weight) Loads

The only dead loads (hereafter referred to as weights) on the cask are the cask weight including the contents. The calculated weights of the individual components of the cask and the total weights are given in Table 3.2-1. The weight of the cask assembly is reacted as a contact force between cask and storage pad except when the cask is supported (lifted) by the pair of trunnions at the top of the cask during handling prior to fuel loading.

2.2.5.3.2 Lifting Loads

The cask is provided with two trunnions at the top spaced 180 degrees apart for lifting. The trunnions at the bottom of the cask are for rotation of the cask, if necessary.

The upper trunnions are single failure proof lifting devices and are evaluated for lifting for g levels equivalent to 6 times and 10 times the upper bound weight of the cask. A dynamic load factor of 1.15 is assumed in the analysis. These values are based on ANSI N14.6⁽¹¹⁾, which requires that special lifting devices for critical loads be either designed with a dual load path or capable of lifting 6 times and 10 times the cask weight without exceeding the yield and ultimate strengths of the material, respectively (twice the normal stress design factor for handling a critical load). The trunnion loads for the ANSI N14.6 analysis are shown in Figure 2.2-3 and listed in Table 2.2-2. The weight of the cask used for these analyses is a conservatively assumed maximum loaded weight of 240,000 lbs.

The local region of the cask body is conservatively evaluated for a vertical load of 6 g (i.e., 6 times the weight of the cask) which is reacted at the trunnions involved in the handling operation. The factor of 6 provides ample allowance for sudden load application during lifting.

2.2.5.3.3 Internal Pressure

The pressure inside the cavity of the storage cask results from several sources. Initially, the cavity is pressurized with helium such that the cavity pressure is about 2.2 atm abs at thermal equilibrium. The purpose of pressurizing the cavity above atmospheric pressure is to prevent in-leakage of air. The initial pressure is determined on the basis that, at minimum, a 1 atm abs pressure must exist in the cavity on the coldest day at the end of life. Pressure variations due to daily and seasonal changes in ambient temperature conditions will be small due to the large thermal capacity of the cask. Fuel clad failure results in the release of fission gas which increases cavity pressure. Chapter 7 evaluates the increases in pressure due to off-normal and accident scenarios.

Another condition when internal pressure could increase is the cool down prior to unloading. This could occur at the beginning or end of life. Unloading of fuel at the beginning of life would only be necessary due to excessive leakage past the lid seals or a severe accident, e.g. cask drop. Water will be gradually added to the cask during refilling. The inlet flow of water is controlled to ensure that the cask pressure does not exceed 90 psia (75.3 psig).

Table 2.2-1 presents a summary of internal pressures for the conditions identified. A pressure of 100 psig was chosen as the design internal pressure, since this value exceeds that of all conditions producing an internal pressure.

2.2.5.3.4 External Pressure

There are several conditions which could result in external pressure on the cask, such as a nearby explosion, debris falling on the cask and snow and ice buildup on the cask. The external pressure due to flood level is assumed to be equal to or less than 25 psi which is equivalent to a 57 ft. head of water as discussed in Section 2.2.2. This is the limiting condition for external pressure. The various external pressures are summarized in Table 2.2-1.

2.2.5.3.5 Cask Body Loads

Globally distributed loads may be applied to the cask by wind (tornado is upper bound case), flood water and seismic excitation. These loads are explained in detail and calculated in Sections 2.2.1 through 2.2.3. Table 2.2-3 lists the numerical values of these forces as calculated in the various sections. Note that bounding loads equal to the weight of the cask (1g load) in each direction (lateral and vertical) applied as inertial loads for stress analysis purposes envelope all of these distributed loads with a substantial margin. The local loads due to the tornado missile impact are unique. The calculated values from Section 2.2.1 are directly used in the cask analysis.

2.2.5.4 Design Loads

The various cask loading conditions are listed in Table 2.2-4. These loading conditions include those described in 10CFR Part 72⁽³⁾, which are categorized as normal, man-made and natural phenomena. The applied loads acting on the different cask components due to these loading conditions have been determined and are discussed in the preceding sections and are listed in Tables 2.2-1 through 2.2-3. This section describes the bases used to combine the loads for each cask component. The specific stress criteria against which each load combination will be evaluated are described in Section 3.4.

The bounding pressures and loads described above are used in the load combinations. Certain combinations are evaluations of several events (e.g. one load combination represents stresses due to tornado wind, hurricane wind, normal wind, flood water, etc.). Several loads are always present and are included in all evaluations. These are the assembly stresses due to bolt preload and metallic seal compression. Lifting loads are always reacted by the cask weight (supported on trunnions - not the storage pad). Lifting loads are not combined with those due to extreme

natural phenomena since cask operations would be halted during a flood, hurricane, etc. Dead weight loads are reacted at the bottom of the cask by the storage pad for all cases except the lifting cases.

2.2.5.4.1 Cask Body

The loading conditions for the cask body including the confinement vessel and gamma shielding are categorized based on the rules of the ASME Boiler and Pressure Vessel Code Section III, Subsection NB, for a Class 1 nuclear component. The ASME code categorizes component loadings into five service loading conditions. They include Design Conditions (same as the Primary Service) and Levels A, B, C and D Service Loadings. The code provides different stress limits for each of these service loadings.

For each of these service loading conditions, there are several applied loads acting on the cask. The Design Loads are listed in Table 2.2-5. They include internal and external pressure; lid bolt preload including the effect of the gasket reactions; distributed loads due to weight, wind, and handling, and attachment loads applied through the trunnion to the cask body.

The inertia g loads are quasistatically applied loads which are multiples of the weight of the cask and/or contents. The magnitude of the Design Loads envelop the maximum Level A Service Loads. Thermal effects are excluded, except for their influence on the preload of the lid bolts (if any) because the ASME Code does not consider them Design (i.e. primary) Loads.

The Level A Service loads are listed in Table 2.2-6 and are basically the same as the Design Loadings except that the thermal effects on the confinement vessel are included. The thermal effects consist of secondary (thermal) stresses caused by differential thermal expansion due to temperature differences caused by decay heat, solar insolation, ambient temperature variations and ambient conditions, e.g. ice, snow, wind, sun.

There are no Level B or C Service Loading Conditions. Events which occur infrequently which could be considered Level B or Level C Service Loadings are conservatively considered Level A loadings.

The loads due to Level D Service Loading Conditions, which are extremely unlikely conditions, are listed in Table 2.2-7.

Loading combinations for Normal Conditions (Design Conditions and Levels A) are given in Table 2.2-8. Loading combinations for Accident Conditions (Level D) are provided in Table 2.2-9. The loads are listed across the top of the table and the Load Combinations are designated in the first column of the table. There are six normal (Design and Level A) load combinations listed, and six accident condition (Level D) combinations. The loads which are acting simultaneously for each of these combinations are denoted by an "X" under the load column heading. For example, for Normal Condition Load Combination N1, internal pressure due to cavity pressurization, fission gas release, distributed weight, heat due to maximum normal temperatures and lid bolt preload are acting simultaneously.

2.2.5.4.2 Basket

Cask body internal and external pressures have no effect on the basket. External loads applied to the TN-68 cask do not result in basket loads unless the cask actually moves. Therefore, tornado wind and flooding produce no basket loads. The tornado missile will cause the cask to slide, however, because of the low velocity, the inertial load applied to the basket will be very small and is much less than the tipover accident impact load. Seismic loading, however, is an inertial loading as discussed in Section 2.2.3, and is applied to the basket. The seismic acceleration loading (much less than 1g acceleration) is combined with dead weight loading since the two effects occur simultaneously.

Temperature effects due to snow, minor fire and ambient temperature variations which can cause thermal transients on the outside of the cask body will not cause similar transients in the basket. The high heat capacity of the body slows the temperature response and effectively eliminates transients at the wall of the cask cavity. The steady state temperature and temperature differences throughout the basket are, however, affected by decay heat, solar insolation and ambient temperature variations.

The basket is important for control of criticality of the fuel assemblies stored in the cask. The bounding lateral and vertical inertial loadings on the basket are equal to 1g (in each direction) and have been shown to envelope the basket loadings. For the basket evaluation, an even more conservative 3g loading in the vertical direction is analyzed.

The stresses in the 304 stainless steel portions of the basket due to the primary loading, 1g in any lateral direction combined with 3g vertical (including dead weight), are determined by conservatively neglecting the tensile and bending strength of the poison plates between fuel compartment boxes. The through thickness strength of the poison plates which separate the boxes is considered. Thus the poison material is conservatively neglected in the primary load analysis where it can react some of the load. These primary stresses in the steel are evaluated at the maximum metal temperature occurring under extreme ambient conditions.

Clearance is provided between the poison and stainless steel plates to provide for differential thermal expansion. The basket design criteria described in Chapter 3 is based on Section III Subsection NG and Appendix F of the ASME Code for stress and buckling limits. The basket evaluation is provided in Chapter 3.

2.2.5.4.3 Upper Trunnions

The upper trunnions are considered to be lifting devices and are evaluated to the ANSI N14.6 requirements for lifting operations. During lifting, the trunnions are evaluated for vertical lifting reactions applied at the lifting shoulders required to support six times or ten times the maximum weight of a fully loaded cask. A dynamic amplification factor of 1.15 is also applied to the loads. When the load is equal to six times the weight, the maximum tensile stresses shall not exceed the minimum yield strength of the trunnion material. For the load equal to ten times the weight, the maximum tensile stresses shall not exceed the minimum ultimate tensile strength of the trunnion material.

In addition to the trunnions themselves, the bolts that attach the trunnions to the gamma shielding and the local region of the gamma shielding are analyzed under the same 6W and 10W reactions. The stresses in the trunnions, trunnion bolts or shielding shall not exceed the minimum yield strength of these components under the 6W loading or the minimum ultimate strength under the 10W loading.

The loads acting on the trunnions are shown in Table 2.2-2. The structural analysis of the trunnions is presented in Section 3.4.3.1.

2.2.5.4.4 Outer Shell

The outer shell is evaluated for the combined effects of inertia g loads due to lifting and internal pressure.

Outgassing from the resin between the cask body and outer shell may cause a slight pressure on the inside of the outer shell. A pressure relief valve is provided in the outer shell to assure any pressure buildup is small. The outer shell is completely supported by the resin when subjected to an external pressure. An internal pressure of 3 psi will occur due to the reduced external pressure during a tornado. An internal pressure of 25 psi is conservatively used to evaluate the outer shell.

The structural analysis of the outer shell is presented in Appendix 3A.4. A summary of results and comparison with design criteria are given in Section 3.4.4.

The combined stress due to the inertial 3g load and pressure is less than the minimum yield strength of the outer shell material.

2.3 Safety Protection Systems

2.3.1 General

The TN-68 dry storage cask is designed to provide storage of spent fuel for at least 40 years. The cask cavity pressure is always above ambient during the storage period as a precaution against the in-leakage of air which could be harmful to the fuel. Since the confinement vessel consists of a steel cylinder with an integrally-welded bottom closure, the cavity gas can escape only through the lid closure system. In order to ensure cask leak tightness, two systems are employed. A double barrier system for all potential lid leakage paths consisting of covers with multiple seals is utilized. Additionally, pressurization of monitored seal interspaces provides a continuous positive pressure gradient which guards against a release of the cavity gas to the environment and the admission of air to the cavity.

The components of the cask are classified as "Important to Safety" and "Not Important to Safety." A tabulation of the components and their classification is shown in Table 2.3-1.

The following items are considered not important to safety:

- Drain tube with all associated hardware including drain tube clamp, drain tube adapter, attachment screws, and o-ring seals. The drain tube is for operational convenience only and does not perform any safety function. The drain tube can be removed and replaced with a lance which can perform the same function.
- Quick disconnect couplings and associated o-ring seals. The couplings are for operational purposes only. These couplings do not form part of the confinement boundary.
- Pressure Monitoring equipment including pressure switches or transducers and electrical cables. If the monitoring system were not to function, no safety function of the cask would be impaired. There would be no leakage in or out of the cask.
- The top neutron shield and its attachments. The top neutron shield is used for supplemental shielding, but the accident condition dose limits are met without installing the top neutron shield.
- The key used to position the basket during normal operation. This key is for operational convenience only. No structural credit is taken for the key during normal or accident conditions.
- Paint for exterior of cask. This coating is used to prevent the cask from rusting. As part of

the surveillance activities, the paint coverage is surveyed periodically. The paint is also inspected prior to shipment at the Fabricator to ensure proper thickness and adhesion.

- Lid alignment pin. The lid alignment pin is used for ease of operation and provides no safety related function. No structural credit is taken for the pin.
- Basket rail shims. The shims are used to ensure proper spacing between the cask and the basket rails to ensure that the assumptions used in the thermal analysis are met. They provide no structural function.
- Fuel spacers. Spacers are used to support shorter fuel assemblies during normal conditions to make it easy to attach the fuel grappling tools. They provide no safety related function.
- Security wires and seals. These are used to provide evidence that the cask has not been tampered with. They provide no safety related function.
- Protective cover with bolts and o-ring seal. This cover protects the overpressure tank, top neutron shield and lid from debris and wildlife nesting and allows rain water to drain more easily from the top of the cask. It has no structural function.
- Shield ring. The shield ring is used for supplemental shielding. The accident dose rates are calculated without the shield ring. No structural credit is taken for the shield ring.

2.3.2 Protection By Multiple Confinement Barriers and Systems

2.3.2.1 Confinement Barriers and Systems

Double metallic seals are provided which guarantee tight, permanent confinement. A pressure monitoring system is used to verify the integrity of the metallic seals. There are two lid penetrations, one for draining and one for venting and pressurization. When the cask is placed in storage, a pressure greater than that of the cavity is set up in the gaps (interspaces) between the double metallic seals of the lid and the lid penetrations. A decrease in the pressure of the monitoring system is signaled by a pressure transducer/switch wired to a monitoring/alarm panel (Figure 2.3-1).

Connections to the overpressure tank are welded fittings. A quick connect coupling with a diaphragm valve is used to fill the tank.

The Helicoflex metallic face seals of the lid and lid penetrations possess long-term stability and have high corrosion resistance over the entire storage period. These high performance seals are comprised of two metal linings formed around a helically-wound spring. The sealing principle is based on plastically deforming the seal's outer lining. Permanent contact of the lining against the sealing surface is ensured by the outward force exerted by the helically-wound spring. Additionally, all metallic seal seating areas are stainless steel overlaid for improved surface control. The overlay technique has been used for Transnuclear's storage and transport casks.

The metallic seals consist of an inner spring, a lining, and a jacket. The spring is Nimonic 90 or an equivalent material. The lining and jacket are stainless steel or nickel alloy and aluminum respectively.

The review of corrosion and galvanic reactions in Section 3.4.1 demonstrates the corrosion resistance of aluminum and stainless 304. The exposure to the pool environment is short term. The long term environment of the seals is helium, except for the outside of the outer seal. That is exposed to the air under the protective cover, but it is not exposed to rain or snow. If corrosion were to occur at the crevice formed where the outer metallic lid seal contacts the sealing surface, it would be detected by the overpressure monitoring system. However, the moisture necessary for this crevice corrosion to occur is not likely to be present because of the weather cover and the decay heat from the stored fuel.

The maximum seal temperature is 212°F (Chapter 4). The neutron flux is 2.34×10^5 n/cm²s (Chapter 14) which is equivalent to less than 1.5×10^{14} n/cm² after 20 years. The temperature and neutron fluence are low enough such that for these materials, the environment is no more challenging than a non-radiation, ambient air environment.

Cefilac has conducted twice yearly leak testing of Helicoflex seals that were installed in 1973. The test fixture has been indoors, and has never been disassembled. The spring, lining, and jacket on the test seals are music wire, soft steel, and aluminum, respectively. The seal dimensions are 13 mm minor diameter x 3620 mm major diameter and 9.6 mm x 1935 mm. From 1973 to 1984, the seals were cycled 700 times between 20 and 150°C. From 1984 to present, the seals have been maintained at 20°C. The leak rates have remained below 10^{-7} Pa m³/m s for the entire test duration. Plots showing test data are attached as Figures 2.3-2 through 2.3-4.

Additionally, all metallic seal seating areas are stainless steel overlay for improved surface control. The overlay technique has been used for Transnuclear's transport casks and storage casks including the TN-24, TN-40 and TN-32 designs.

For protection against the environment, a torispherical protective cover equipped with an elastomer seal is provided above the lid. This seal is not important to safety. While the seal may harden with time due to irradiation or air exposure, this will have little effect on its ability to keep out rain and snow, because the seal is not subject to compression/decompression cycling; it is a static seal. There is no requirement for periodic inspection or replacement of the elastomer o-ring seal on the protective cover. However, if any maintenance operation requires removal of the cover, the o-ring should be inspected at that time. If there are any signs of deterioration (hardening, cracking, permanent set) it should be replaced.

The lid and cover seals described above are contained in grooves. A high level of sealing over the storage period is assured by utilizing seals in a deformation-controlled design. The deformation of the seals is constant since bolt loads assure that the mating surfaces remain in contact. The seal deformation is set by its original diameter and the depth of the groove.

Metal gasket face seal fittings, diaphragm valves and Helicoflex metallic seals are all capable of limiting leak rates to less than 1×10^{-7} ref cm³/sec.

The initial operating pressure of the monitoring system's overpressure tank is set at 6.0 atm abs minimum. Over the storage period, the pressure decreases as a result of leakage from the system and as a result of temperature reduction of the gas in the system. Since the level of permeation through the confinement vessel is negligible and leakage past the higher pressure of the monitoring system is physically impossible, a decrease in cavity pressure during the storage period occurs only as a result of a reduction in the cavity gas temperature with time. As long as the cavity pressure is greater than ambient pressure and the pressure in the monitoring system is greater than that of the cavity, no in-leakage of air nor out-leakage of cavity gas is possible.

The calculations provided in Chapter 7 define the monitoring system helium test leakage rate which ensures that no cavity gas can be released to the environment nor air admitted to the casks for the 40 year storage period. All seals are considered collectively in the analysis as the monitoring system pressure boundary. This analysis is performed in accordance with ANSI N14.5⁽¹²⁾.

As shown in Chapter 7, the monitoring system pressure is always greater than the cask cavity or atmospheric pressure. Thus, no leakage can occur from the cask cavity during the storage period. The pressure monitoring system will be set to 3.0 atm abs minimum. This is greater than the maximum cavity pressure during storage and provides sufficient time to investigate low pressure conditions. At this interseal pressure, no in leakage to the cask cavity nor out leakage from the cask cavity will occur.

2.3.2.2 Cask Cooling

To establish the heat removal capability of the TN-68 cask, several thermal design criteria are established for the normal conditions. These are:

- Confinement of radioactive material and gases must be maintained. Seal temperatures must be maintained within specified limits to satisfy the leak tight confinement function during normal and accident conditions. A maximum temperature limit of 536°F (280°C) is set for the Helicoflex seals (double metallic O-rings) in the confinement vessel closure lid.
- To maintain the stability of the neutron shield resin during normal storage conditions, a maximum temperature limit of 300°F (149°C) is set for the neutron shield.
- Maximum temperatures of the confinement structural components must not adversely affect the confinement function.
- Maintaining fuel cladding integrity during storage is another design consideration. Fuel cladding temperature limits reported in Section 3.5 are based on NRC Interim Staff Guidance memorandum ISG-11 rev 3⁽¹³⁾.

The thermal evaluation for normal conditions and hypothetical accident conditions is presented in Chapter 4.

2.3.3 Protection by Equipment and Instrumentation Selection

2.3.3.1 Equipment

Design criteria for the casks are described in Section 2.2 and summarized in Table 2.5-1.

2.3.3.2 Instrumentation

Due to the totally passive and inherently safe nature of the storage system, Important to Safety instrumentation is not necessary. Instrumentation to monitor seal interspace pressure is furnished. The pressure monitoring system is further described in Section 2.3.2.1.

2.3.4 Nuclear Criticality Safety

2.3.4.1 Control Methods for Prevention of Criticality

The design criterion for criticality is that an upper subcritical limit (USL) of 0.95 minus benchmarking bias and modeling bias will be maintained for all postulated arrangements of fuel within the cask. The fuel assemblies are assumed to stay within their basket compartment based on the cask and basket geometry.

The control method used to prevent criticality is incorporation of neutron absorbing material (boron) in the basket material.

The basket has been designed to assure an ample margin of safety against criticality under the conditions of fresh fuel in a cask flooded with fresh water. The method of criticality control is in keeping with the requirements of 10CFR72.124.

Criticality analysis is performed using the KENO-V.a Monte Carlo code⁽¹⁴⁾ along with data prepared using the NITAWL code⁽¹⁵⁾ and the SCALE 44-group cross section library. These codes and cross-section library are part of the SCALE system prepared by Oak Ridge National Laboratory for the U.S. Nuclear Regulatory Commission Office of Nuclear Regulatory Research⁽¹⁶⁾. They are widely used for criticality analysis of shipping casks, fuel storage pools and storage casks. Benchmark problems are run to verify the codes, methodology and cross section library. Examples of computer input used for criticality evaluation are included in Section 6.6.

In the criticality calculation, fuel assembly, basket, and cask geometries are modeled explicitly. Within each assembly, each fuel pin and each water rod is represented.

Reactivity analyses were performed for GE 7x7, 8x8 9x9 and 10x10 assemblies at initial lattice-average enrichment of 3.7 wt% U235. Analyses at higher enrichment and corresponding B10 areal density of the basket neutron absorber, and analyses of damaged fuel were performed on the most reactive fuel lattice, the 10x10.

The analyses assume fresh fuel composition with fresh water in the cavity, and the cask surrounded by a water reflector.

The criticality analyses are described in Chapter 6.0.

2.3.4.2 Error Contingency Criteria

Provision for error contingency is built into the criterion used in Section 2.3.4.1 above. The criterion, used in conjunction with the KENO-V.a and NITAWL codes, is common practice for licensing submittals. Because conservative assumptions are made in modeling, it is not necessary to introduce additional contingency for error.

2.3.4.3 Verification Analysis-Benchmarking

Eighty-three criticality experiments were taken from Oak Ridge National Laboratory⁽²¹⁾. The experiments which featured characteristics applicable to the TN-68 design (e.g. simple arrays, separator plates, steel reflector walls, water holes, and borated poison plates) were selected for the benchmark analyses. The methodology of Reference 21 is used which is discussed further in Section 6.5. This analysis found that there is minimal correlation between bias and any of the experimental values and therefore, no discernable trend. An upper subcritical limit (USL) of 0.95 minus benchmarking bias and modeling bias is used in the TN-68 criticality analysis.

2.3.5 Radiological Protection

Provisions for radiological protection by confinement barriers and systems are described in Section 2.3.2.1.

2.3.5.1 Access Control

The storage casks will be located in a restricted area on a site to which access is controlled. In keeping with the terminology of 10CFR72, the term restricted area refers only to an area within the controlled area. The controlled area and the site are taken to be the same. The term restricted area is defined in 10CFR20.1003⁽¹⁷⁾. The specific procedures for controlling access to the controlled area and to the restricted area are to be addressed by the license applicant's Safety Analysis Report or 10CFR72.212 analyses. The cask will not require the continuous presence of operators or maintenance personnel.

2.3.5.2 Shielding

Shielding has the objective of assuring that radiation dose rates at key locations are at acceptable levels for those locations. Three locations are of particular interest:

- (1) Immediate Vicinity of the Cask
- (2) Restricted Area Boundary
- (3) Controlled Area Boundary

Dose rates in the immediate vicinity of the cask are important in consideration of occupational exposure. Because of the passive nature of storage with this cask, occupational tasks related to the cask are infrequent and short. Personnel exposures due to operational and maintenance activities are discussed in Section 10.3.

Dose rates at the restricted area boundary should be such that people outside the restricted area need not have their radiation exposure monitored. Dose rates at the controlled area boundary should be in accordance with 10 CFR 20 Subpart D. The estimated occupational doses for personnel comply with the requirements of 10 CFR 20 Subpart C.

2.3.5.3 Radiological Alarm System

There are no credible events which result in releases of radioactive products or unacceptable increases in direct radiation. In addition, the releases postulated as the result of the hypothetical accidents described in Chapter 11 are of a very small magnitude. Therefore, radiological alarm systems are not necessary. However, as described in Section 2.3.3.1, nonsafety related pressure monitors are provided. Procedures to be followed when these alarms are activated will be specified in the ISFSI operating procedures.

2.3.6 Fire and Explosion Protection

There are no combustible or explosive materials associated with the TN-68 dry storage cask. In general, no such materials would be stored within an ISFSI controlled area. An evaluation of the cask engulfed in a fuel fire is discussed in Chapter 4.

To bound an external explosion, which might involve explosive materials which are stored or transported near the site, the cask is evaluated for an external pressure of 25 psi.

2.4 Decommissioning Considerations

The dry cask system to be utilized at the ISFSI features inherent ease and simplicity of decommissioning. At the end of its service lifetime, cask decommissioning could be accomplished by one of several options described below.

The casks, including the spent fuel stored inside, could be shipped to a suitable fuel repository for permanent storage.

The spent fuel could be removed from the ISFSI cask and shipped in a licensed shipping container to a suitable fuel repository. If desirable, cask decontamination could be accomplished through the use of conventional high pressure water sprays to further reduce contamination on the cask interior. The sources of contamination on the interior of the cask would be crud from the outside of the fuel pins and the crud left by the spent fuel pool water. The expected low levels of contamination from these sources could be easily removed with a high pressure water spray. After decontamination, the ISFSI cask could either be cut-up for scrap or partially scrapped and any remaining contaminated portions shipped as low level radioactive waste to a disposal facility.

For surface decontamination of the ISFSI cask, chemical etching using hydrochloric acid or nitric acid can be applied to remove the contaminated surface of the cask. Alternatively, electropolishing can also be used to achieve the same result.

Cask activation analyses have been performed to quantify specific activity levels of cask materials after years of storage. The following assumptions were made:

- The cask contains 68 design basis BWR assemblies.
- The neutron flux is assumed constant for 40 years, based on 7x7, 40 GWd/MTU, 10 year cooled fuel.

The cask activation analyses are presented in Chapter 14. The results of these calculations show that the TN-68 cask will be far below the specific activity limits for both long and short lived nuclides for Class A waste. Consequently, it is expected that after application of the surface decontamination process as described above, the radiation level due to activation products will be negligible and the cask could be disposed of as Class A waste. A detailed evaluation will be performed at the time of decommissioning to determine the appropriate mode of disposal.

Due to the leak tight design of the storage casks, no residual contamination is expected to be left behind on the concrete base pad. The base pad, fence, and peripheral utility structures will require no decontamination or special handling after the last cask is removed.

If the spent fuel pool is to remain functional until the ISFSI is decommissioned, it will allow the pool to be utilized to transfer fuel from the storage casks to licensed shipping containers for shipment off site if this decommissioning option is chosen.

The volume of waste material produced incidental to ISFSI decommissioning will be limited to

that necessary to accomplish surface decontamination of the casks once the spent fuel elements are removed. Furthermore, it is estimated that the cask materials will be only very slightly activated as a result of their long-term exposure to the relatively small neutron flux emanating from the spent fuel, and that the resultant activation level will be well below allowable limits for general release of the casks as noncontrolled material. Hence, it is anticipated that the casks may be decommissioned from nuclear service by surface decontamination alone.

The costs of decommissioning the ISFSI are expected to represent a small and negligible fraction of the cost of the decommissioning a Nuclear-Generating Plant.

2.5 Summary of Cask Design Criteria

The principal design criteria for the TN-68 cask are presented in Table 2.5-1. The TN-68 dry storage cask is designed to store 68 BWR spent fuel assemblies with or without channels. The maximum allowable initial lattice-average enrichment varies from 3.7 to 4.7 wt% U235 depending on the B10 areal density in the basket neutron absorber plates. The maximum bundle average burnup, maximum decay heat, and minimum cooling time are 40 GWd/MTU, 0.312 kW/assembly, and 10 years for 7x7 fuel, 60 GWd/MTU, 0.441 kW/assembly, and 7 years for all other fuel.

The maximum total heat generation rate of the stored fuel is limited to 30 kW in order to keep the maximum fuel cladding temperature below the limit necessary to ensure cladding integrity for 40 years storage⁽¹³⁾. The fuel cladding integrity is assured by the cask and basket design which limits fuel cladding temperature and maintains a nonoxidizing environment in the cask cavity⁽¹⁹⁾.

Damaged fuel that can be handled by normal means may be stored in eight peripheral compartments fitted with damaged fuel end caps designed to retain gross fragments of fuel within the compartment.

The confinement vessel (body and lid) is designed and fabricated to the maximum practicable extent as a Class I component in accordance with the rules of the ASME Boiler and Pressure Vessel Code, Section III, Subsection NB, Article NB-3200. The cask design, fabrication and testing are covered by Transnuclear's Quality Assurance Program which conforms to the criteria in Subpart G of 10CFR72.

The cask is designed to maintain a subcritical configuration during loading, handling, storage and accident conditions. Poison materials in the fuel basket are employed to maintain the upper subcritical limit of 0.9423. The TN-68 basket is designed and fabricated to the maximum practicable extent in accordance with the rules of the ASME Boiler and Pressure Vessel Code, Section III, Subsection NG, Article NG-3200.

The TN-68 cask is designed to withstand the effects of severe environmental conditions and natural phenomena such as earthquakes, tornadoes, lightning and floods. Chapter 11 describes the cask behavior under these accident conditions.

2.6 References

1. (Deleted)
2. (Deleted)
3. Licensing Requirements for the Storage of Spent Fuel in an Independent Spent Fuel Storage Installation, 10CFR Part 72, Rules and Regulations, Title 10, Chapter 1, Code of Federal Regulations - Energy, U. S. Nuclear Regulatory Commission, Washington D.C.
4. American Society of Mechanical Engineers, ASME Boiler And Pressure Vessel Code, Section III, Division 1 - Subsections NB, NF and NG, 1995 edition including 1996 addenda.
5. U.S. Nuclear Regulatory Commission Regulatory Guide 1.76, Design Basis Tornado for Nuclear Power Plants, April, 1974.
6. Standard Review Plan, NRC NUREG-0800, Rev. 2, July, 1981.
7. T. W. Singell, Wind Forces on Structures: Forces on Enclosed Structures. ASCE Structural Journal, July 1958.
8. Baumeister and Marks, Standard Handbook for Mechanical Engineers, Sixth Edition.
9. 10CFR 100, Reactor Site Criteria.
10. U.S. Nuclear Regulatory Commission, Regulatory Guide 1.92, Combining Modal Responses and Spacial Components in Seismic Response Analysis, Revision 1, February, 1976.
11. American National Standards Institute, "American National Standard for Special Lifting Devices for Shipping Containers Weighing 10,000 Pounds (4500 kg) or More for Nuclear Materials," ANSI N14.6, New York.
12. ANSI-N14.5-1997, "Leakage Tests on Packages for Shipment," February 1998.
13. USNRC Spent Fuel Project Office, Interim Staff Guidance Memo ISG-11 rev 3, Cladding Considerations for the Transportation and Storage of Spent fuel, November 2003.

14. Petrie, L.M. and Landers, N. F., KENO-V.a, An Improved Monte Carlo Criticality Program with Supergrouping, NUREG/CR-0200, Oak Ridge Laboratory, December, 1984.
15. Green, N. M., et.al., "NITAWL-S: Scale System Module for Performing Resonance Shielding and Working Library Production," NUREG/CR-0200, Oak Ridge National Laboratory, October, 1981.
16. "SCALE, A Modular Code System for Performing Standardized Computer Analyses for Licensing Evaluation", NUREG/CR-0200, Rev. 6 (ORNL/NUREG/CSD-2/R6), Vol. I-III, September 1998.
17. 10CFR 20, Standards for Protection Against Radiation.
18. (Deleted)
19. Johnson, Jr., A.B., and Gilbert, E.R., "Technical Basis for Storage of Zircaloy-Clad Spent Fuel in Inert Gases," PNL-3602, Pacific Northwest Laboratory, Richland, Wash., Sept. 1983.
20. Roark, "Formulas for Stress and Strain", 4th edition.
21. NUREG/CR-6361, "Criticality Benchmark Guide for Light-Water-Reactor Fuel in Transportation and Storage Packages," 1997.
22. U.S. Nuclear Regulatory Commission, Regulatory Guide 1.60, Rev. 1, Design Response Spectra for Seismic Design of Nuclear Plants, December, 1973.
23. Beer and Johnston, "Vector Mechanics for Engineer: Static and Dynamic", Mcgraw-Hill Book Co., 1962.
24. Walmer, M.E., "Manual of Structural Design and Engineering Solutions", Prentice-Hall, Inc., 1972.
25. PCI Design Handbook, 2nd Edition, Precast Concrete Institute, 1978.
26. ANSI/ANS-57.9-1984, "Design Criteria for an Independent Spent Fuel Storage Installation (Dry Type)".

TABLE 2.1-1

FUEL ASSEMBLY TYPES

Fuel Assembly
GE Series Designation
GE 7 x 7 Series GE2
GE 7 x 7 Series GE3
GE 8 x 8 Series GE4
GE 8 x 8 Series GE5
GE 8 x 8 Series GE-Prepres
GE 8 x 8 Series GE-Barrier
GE 8 x 8 Series GE8
GE 8 x 8 Series GE9
GE 8 x 8 Series GE10
GE 9 x 9 Series GE11
GE 10 x 10 Series GE12
GE 9 x 9 Series GE13

TABLE 2.1-2

DESIGN BASIS FUEL ASSEMBLY PARAMETERS¹

<u>Parameter</u>	<u>7 x 7</u>
Number of Fueled Rods	49
Number of Water Rods	0
Fuel Assembly Cross Section (in) ²	5.44 x 5.44
Fuel Assembly Length (in) ²	176.2
Fuel Rod Pitch (in)	0.738
Fuel Rod O.D. (in)	0.563
Clad Material	Zircaloy
Clad Thickness (in)	0.032
Fuel Pellet O.D. (in)	0.487
U ²³⁵ Bundle Average/Initial Enrichment (% wt)	3.3
U ²³⁵ Maximum Lattice Average Enrichment (% wt)	3.7
Active Fuel Length (in)	144
U Content (kg)	197.7
Assembly Weight with channel (lbs)	705

<u>Parameter</u>	<u>8 x 8</u>
Number of Fueled Rods	63
Number of Water Rods	1
Fuel Assembly Cross Section (in) ²	5.44 x 5.44
Fuel Assembly Length (in) ²	176.2
Fuel Rod Pitch (in)	0.640
Fuel Rod O.D. (in)	0.493
Clad Material	Zircaloy
Clad Thickness (in)	0.034
Fuel Pellet O.D (in)	0.416
U ²³⁵ Bundle Average/Initial Enrichment (% wt)	2.6
U ²³⁵ Maximum Lattice Average Enrichment (% wt)	Varies with basket type
Active Fuel Length (in)	146
U Content (kg)	188
Assembly Weight with channel (lbs)	705

¹ The 8x8 is the design basis fuel for thermal, shielding, and confinement analysis. Although the 7x7 has more fuel mass, it is limited to lower burnup and longer cooling times. This analysis is further detailed in Section 5.0.

² Unirradiated fuel width and length.

TABLE 2.1-3

THERMAL, GAMMA AND NEUTRON SOURCES FOR
THE DESIGN BASIS 8 x 8 GENERAL ELECTRIC FUEL ASSEMBLY

U ²³⁵ Bundle Average Initial Enrichment (% wt)	2.6
Burnup (MWD/MTU)	48,000
Specific Power (MW/assembly)	6
Cooling Time (years)	7
Decay Heat (kW/assembly)	0.441
Gamma Source (photon/sec/assembly) ¹	1.99E+15
Neutron Source (neutrons/sec/assembly)	3.17E+08

¹ This is based on the SCALE 4.4 18 group gamma library, including bremsstrahlung & gamma radiation from alpha-n reactions in a UO₂ matrix.

TABLE 2.1-4
Cooling Time as a Function of Maximum Burnup and Minimum Initial Enrichment
7x7 Fuel

REQUIRED BWR COOLING TIMES (YEARS)

Initial Enrichment (bundle ave %w)	Burnup (GWd/MTU)											
	15	20	30	32	33	34	35	36	37	38	39	40
1.0	10	10										
1.1	10	10										
1.2	10	10										
1.3	10	10										
1.4	10	10										
1.5	10	10	10	10	11	11	11					
1.6	10	10	10	10	10	11	11	11				
1.7	10	10	10	10	10	11	11	11	12			
1.8	10	10	10	10	10	11	11	11	11	12		
1.9	10	10	10	10	10	11	11	11	11	12		
2.0	10	10	10	10	10	10	11	11	11	12	12	
2.1	10	10	10	10	10	10	11	11	11	12	12	12
2.2	10	10	10	10	10	10	11	11	11	12	12	12
2.3	10	10	10	10	10	10	11	11	11	11	12	12
2.4	10	10	10	10	10	10	10	11	11	11	12	12
2.5	10	10	10	10	10	10	10	11	11	11	12	12
2.6	10	10	10	10	10	10	10	11	11	11	12	12
2.7	10	10	10	10	10	10	10	10	11	11	11	12
2.8	10	10	10	10	10	10	10	10	10	11	11	12
2.9	10	10	10	10	10	10	10	10	10	10	11	12
3.0	10	10	10	10	10	10	10	10	10	10	10	12
3.1	10	10	10	10	10	10	10	10	10	10	10	12
3.2	10	10	10	10	10	10	10	10	10	10	10	11
3.3	10	10	10	10	10	10	10	10	10	10	10	10
3.4	10	10	10	10	10	10	10	10	10	10	10	10
3.5	10	10	10	10	10	10	10	10	10	10	10	10
3.6	10	10	10	10	10	10	10	10	10	10	10	10
3.7	10	10	10	10	10	10	10	10	10	10	10	10

■ - not evaluated

Notes:

1. Total dose from gamma and neutron considered.
2. Cooling Times entered in bold and italics are cases actually run. Other values interpolated.

TABLE 2.2-1

SUMMARY OF INTERNAL AND EXTERNAL PRESSURES
ACTING ON TN-68 CASK

<u>Individual Load Conditions</u>	<u>Maximum Pressure, psig</u>
<u>Internal Pressure:</u>	
(a) Initial Cavity Pressurization	18 (2.2 atm abs)
(b) With 10% Fuel Failure	21.6 (2.5 atm abs)
(c) With 100% Fuel Failure	see condition (d)
(d) In a Minor Fire (assumed 100% fuel failure)	71.7 (5.88 atm abs)
(e) Beginning of Life Unloading	75.3 (6.1 atm abs)
(f) Cask Burial (assumes 100% fuel failure)	96.7 (6.6 atm abs)
(g) Tornado	3*
(h) Selected Bounding Pressure	100
<u>External Pressure</u>	
(a) Flood	25
(b) Snow and Ice Loading	0.35
(c) Explosion	<25
(d) Selected bounding Pressure	25

*This is due to a reduced external pressure.

TABLE 2.2-2

SUMMARY OF LIFTING LOADS USED IN UPPER TRUNNION
ANSI N14.6 ANALYSIS

<u>Handling Condition</u>	<u>Load at Cask CG (1)</u> <u>Vertical</u>
Lifting - Cask Vertical	
Yield Evaluation	1.656x 10 ⁶ lbs.
Ultimate Evaluation	2.76 0x 10 ⁶ lbs.
	<u>Load at each Trunnion (2)</u>
Yield Evaluation	0.828 x 10 ⁶ lbs.
Ultimate Evaluation	1.380x 10 ⁶ lbs.

NOTES:

1. Based on a cask weight of 240,000 lbs with 1.15 dynamic load factor.
2. Load evenly divided between one pair of upper trunnions.

TABLE 2.2-3

SUMMARY OF LOADS ACTING ON TN-68 CASK DUE TO ENVIRONMENTAL AND NATURAL PHENOMENA

Distributed Loads

Lateral Loading:

(a) Wind (external force on cask body)	332 psf
(b) Seismic (inertial force throughout system) 0.26W	59,020 lb. ⁽²⁾
Selected Bounding Load W x 1G	227,000 lb. ⁽²⁾

Vertical Loading⁽¹⁾:

(a) Seismic (inertial force throughout system) 0.17W	38,590 lb. ⁽²⁾
Selected Bounding Load W x 1G	227,000 lb. ⁽²⁾

Local Loads

Tornado Missile Loading (external force on local area of body):

(a) Lateral Load	1.558 x 10 ⁶ lb.
(b) Vertical Load	<1.558 x 10 ⁶ lb.

NOTE:

1. Does not include dead weight or lifting loads
2. A conservatively low weight is used for stability analysis. The actual weight of the cask is used for stress analysis.

TABLE 2.2-4

TN-68 CASK LOADING CONDITIONS

Normal

Assembly Loads (bolt preload and seal compression)
Pressure (internal and external)
Weight
Lifting Loads
Handling
Wind
Thermal variations (e.g. insolation, decay heat, rain, snow, ice, ambient)

Man-Made (Accident)

Fuel cladding failure (due to loading or unloading error)
Minor Fire
Explosion

Natural Phenomena (Accident)

Earthquakes
Tornadoes
Cask Burial
Flood
Lightning

TABLE 2.2-5

TN-68 CASK DESIGN LOADS
(Normal Conditions)

<u>Applied Load</u>	<u>Loading Condition</u>
Internal Pressure	(1) and (2)
External Pressure	(3)
Distributed Loads	Weight Cask Body Contents Snow Ice Wind (Tornado) Lifting
Attachment Loads	Lifting
Bolt Loads	Preload for 100 psi and metallic seal compression

- (1) Cask designed for 100 psi internal pressure which envelopes all internal pressure effects.
- (2) For normal conditions, the fission gas release is assumed to be 10%.
- (3) Cask designed for 25 psi external pressure which envelopes all external pressure effects.

TABLE 2.2-6

LEVEL A SERVICE LOADS
(Normal Conditions)

<u>Applied Load</u>	<u>Loading Condition</u>
Internal Pressure	(1) and (2)
External Pressure	(3)
Distributed Loads	Weight Cask Body Contents Snow Ice Wind (Tornado) Lifting
Attachment Loads	Lifting
Bolt Loads	Preload for 100 psi and metallic seal compression
Thermal Effects	Decay Heat Insolation Cold Rain on Hot Cask

- (1) Cask designed for 100 psi internal pressure which envelopes all internal pressure effects.
- (2) For normal conditions, the fission gas release is assumed to be 10%.
- (3) Cask designed for 25 psi external pressure which envelopes all external pressure effects.

TABLE 2.2-7

LEVEL D SERVICE LOADS
(Accident Conditions)

<u>Load</u>	<u>Cause</u>
Internal Pressure	(1) and (2)
External Pressure	(3)
Distributed Loads	Weight Cask body Contents Tornado Wind Flood Water Seismic
Local Loads	Tornado Wind Driven Missiles
Bolt Loads	Preload for 100 psi, metallic seal compression and drop impact
60 G Bottom Impact	18" Vertical Drop (Handling Accident)
65 G Side Impact	Tipover

- (1) Cask design for 100 psi internal pressure which envelopes all internal pressure effects.
- (2) Fission gas release of 100% is assumed for accident conditions.
- (3) Cask designed for 25 psi external pressure which envelopes all external pressure effects including flood water level, cask burial and explosion.

TABLE 2.2-8

NORMAL CONDITION LOAD COMBINATIONS

<u>Individual Load Combined Load</u>	Bolt Preload	1g Down	Internal Pressure 100 Psi	External Pressure 25 Psi	Thermal	6 G on Trunnion	Trunnion Local Stress
N1	X	X	X				
N2	X	X	X		X		
N3	X		X		X	X	X
N4	X	X		X			
N5	X	X		X	X		
N6	X			X	X	X	X

TABLE 2.2-9

ACCIDENT CONDITION LOAD COMBINATIONS

<u>Individual Load Combined Load</u>	Bolt Preload	Internal Pressure 100 Psi	External Pressure 25 Psi	18" BOTTOM END DROP 60 G	Tip Over Side Drop 65 G	Seismic, Tornado, Or Flood 1g-Lateral + 2g-Down
A1	X	X		X		
A2	X		X	X		
A3	X	X			X	
A4	X		X		X	
A5	X	X				X
A6	X		X			X

TABLE 2.3-1

CLASSIFICATION OF COMPONENTS

IMPORTANT TO SAFETY	NOT IMPORTANT TO SAFETY
Confinement Vessel including Lid, Flange, Inner Confinement Shell and Bottom Confinement Plate Cask Body Shell Cask Body Bottom Lid Shield Plate Lid Bolts and Threaded Inserts Lid Seals Lid Vent, Drain, and Overpressure Covers, Bolts, and Gaskets Basket Assembly including fuel compartments, poison plates, and structural plates Trunnions, Trunnion Bolts, and Trunnion Cover Screws Radial Neutron Shield Outer Shell Shim (between shield shell and flange) Basket Holddown Basket Rails	Drain Tube Hansen Couplings Pressure Monitoring System Protective Cover, Bolts, Seal, and Threaded Inserts Basket Shear Key Fuel Spacers Basket Rail Shims Security Wire & Seals Lid Alignment Pins Top Neutron Shield including Bolts and Washers Shield Ring Pressure Relief Valve (on outer shell) Basket rail studs, nuts, & washers

TABLE 2.5-1
DESIGN CRITERIA FOR TN-68 CASKS

Maximum gross weight on crane (with lift beams, without water)	120 tons
Cask height with lid removed	192.25 in.
Minimum design life	40 years
Upper subcritical limit	< 0.95- Normal < 0.95- Accident
Payload Capacity	68 BWR assemblies Including 8 damaged (acceptable assemblies listed in Table 2.1-1)
Spent Fuel Characteristics	
a) Design Basis Bundle Average Initial Enrichment	2.6%
b) Maximum Lattice Average Initial Enrichment	3.7-4.7% depending on basket type
c) Burnup (max)	40 GWD/MTU 7x7 fuel, 60 GWD/MTU all other fuel
d) Cooling time (min)	10 years 7x7 fuel, 7 years all other
e) Decay Heat	30 kW (total)
Max Clad Temperature	400°C (752°F) - Normal 570°C (1058°F) - Accident
Cask Cavity Atmosphere	Helium gas
Maximum Internal Pressure	100 psig
Daily Averaged Ambient Temperature (Min-Max) Over 24 hr. period (min-max)	-20 to 100°F
Maximum Solar Heat Load	1475 BTU/ft ² (Curved Surfaces)
Tornado Wind	360 mph (rotational and translational)
Tornado Missiles	4000 lb. auto 276 lb. (125 kg) 8 in. armor piercing shell 1 in. solid steel sphere 4" x 12" x 12' wood plank at 300 mph
Cask Drop	18" Drop onto concrete pad or equivalent end drop resulting in 60 G's
Cask Tip	Tip onto ISFSI pad equivalent side drop of 65 G's
Seismic Design Earthquake	0.26 g horizontal 0.17 g vertical
Snow and Ice	50 psf load

FIGURE 2.1-1

DECAY HEAT 7 x 7 GE FUEL ASSEMBLY
3.3 WT% U-235 MAXIMUM INITIAL BUNDLE AVERAGE ENRICHMENT,
40,000 MWD/MTU, 10 YEAR COOLED

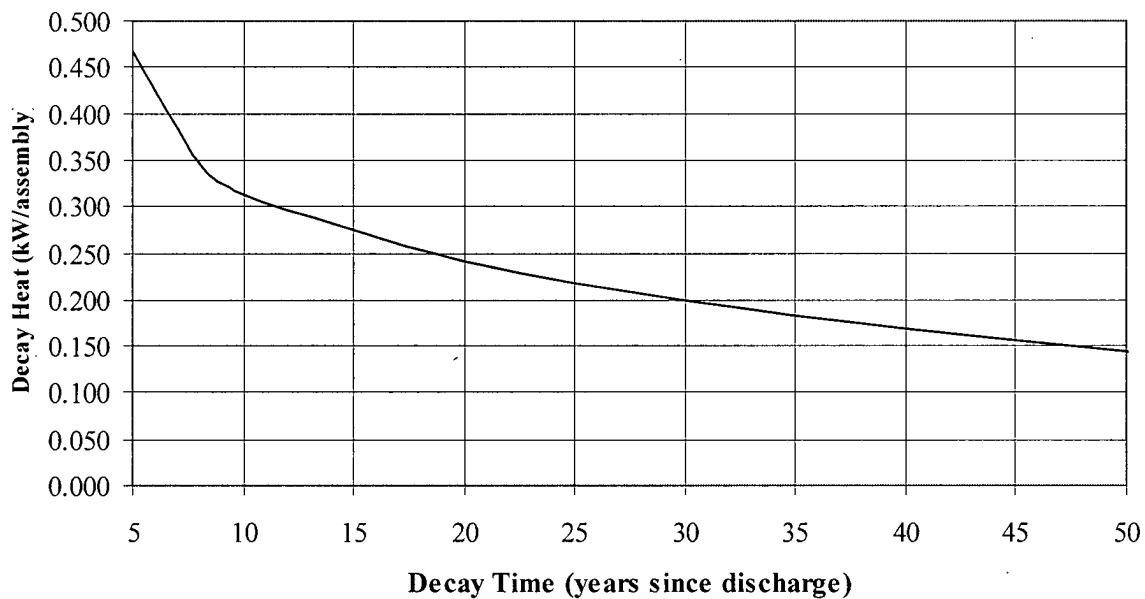


FIGURE 2.1-2

GAMMA SOURCE 7 x 7 BWR FUEL ASSEMBLY
3.3 WT% U-235 MAXIMUM INITIAL BUNDLE AVERAGE ENRICHMENT,
40,000 MWD/MTU, 10 YEAR COOLED

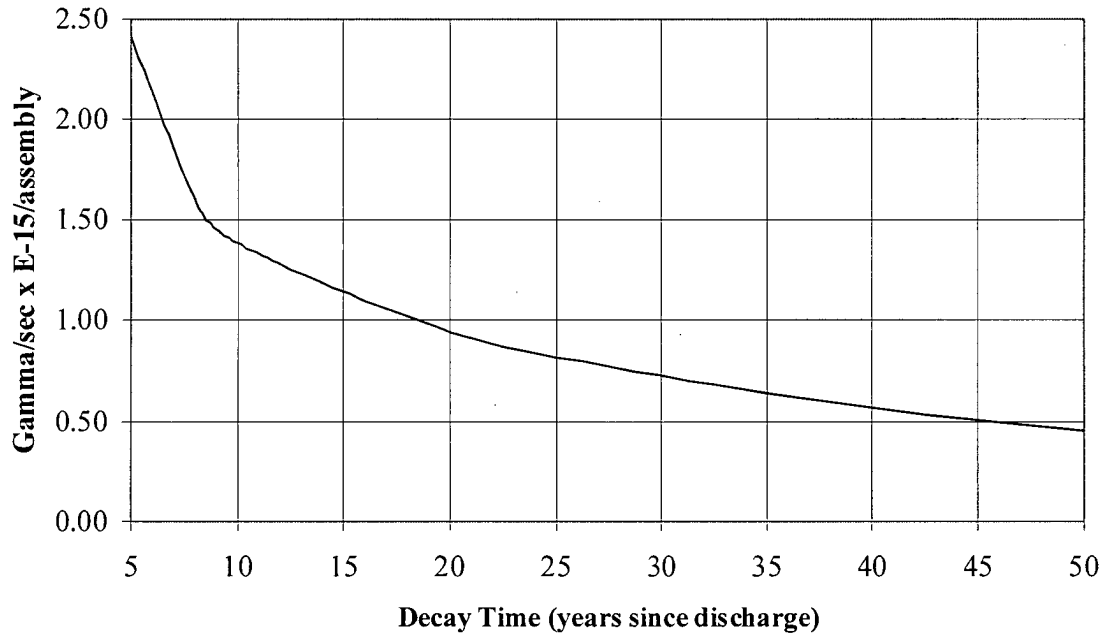


FIGURE 2.1-3

NEUTRON SOURCE 7 x 7 BWR FUEL ASSEMBLY
3.3 WT% U-235 MAXIMUM INITIAL BUNDLE AVERAGE ENRICHMENT,
40,000 MWD/MTU, 10 YEAR COOLED

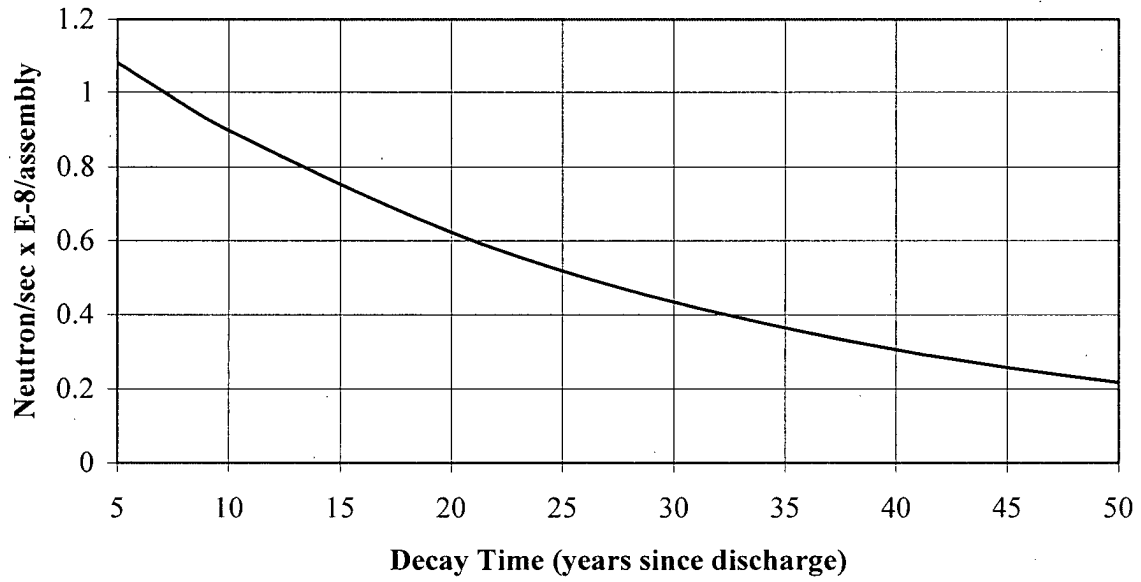
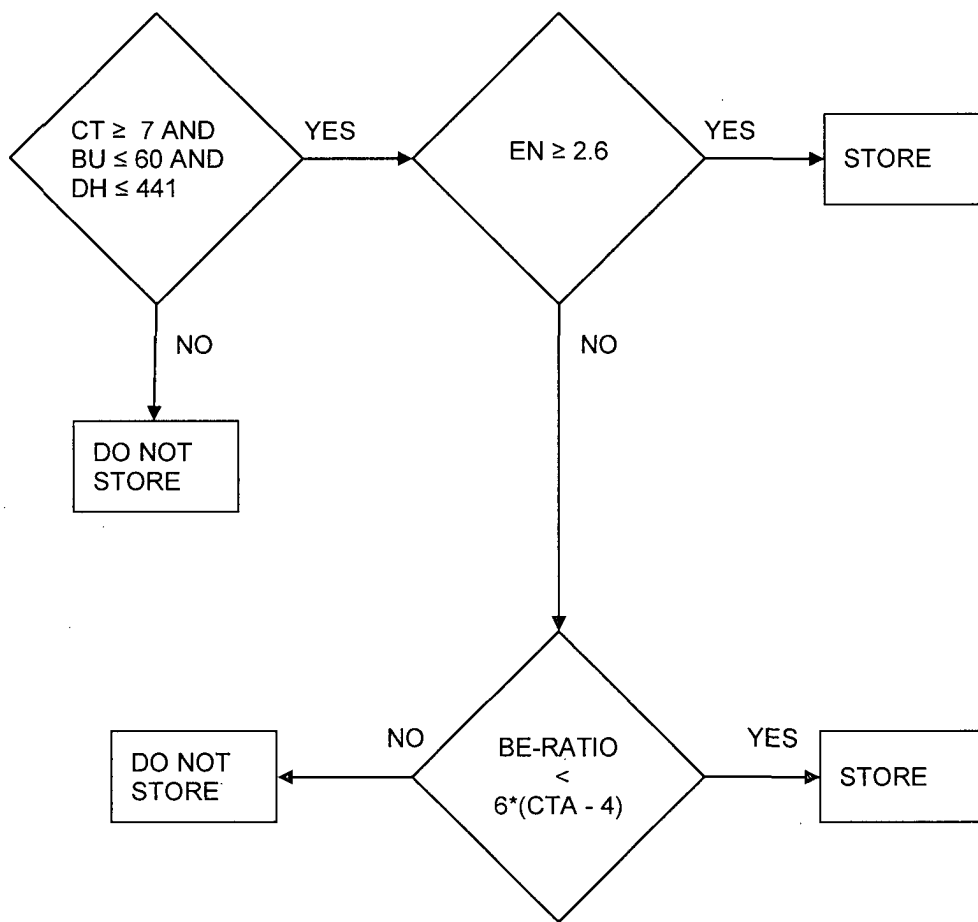


FIGURE 2.1-4

Fuel Qualification Flowchart for 8x8, 9x9, and 10x10 Fuel



CT = Cooling Time in years
CTA = CT rounded down to the nearest Integer
BU = Burnup in GWd/MTU
EN = Enrichment in wt % U235
DH = Decay Heat in Watts
BE-RATIO = Burnup to Enrichment ratio

FIGURE 2.2-1

EARTHQUAKE, WIND AND WATER LOADS



Figure Withheld Under 10 CFR 2.390

FIGURE 2.2-2

TORNADO MISSILE IMPACT LOADS

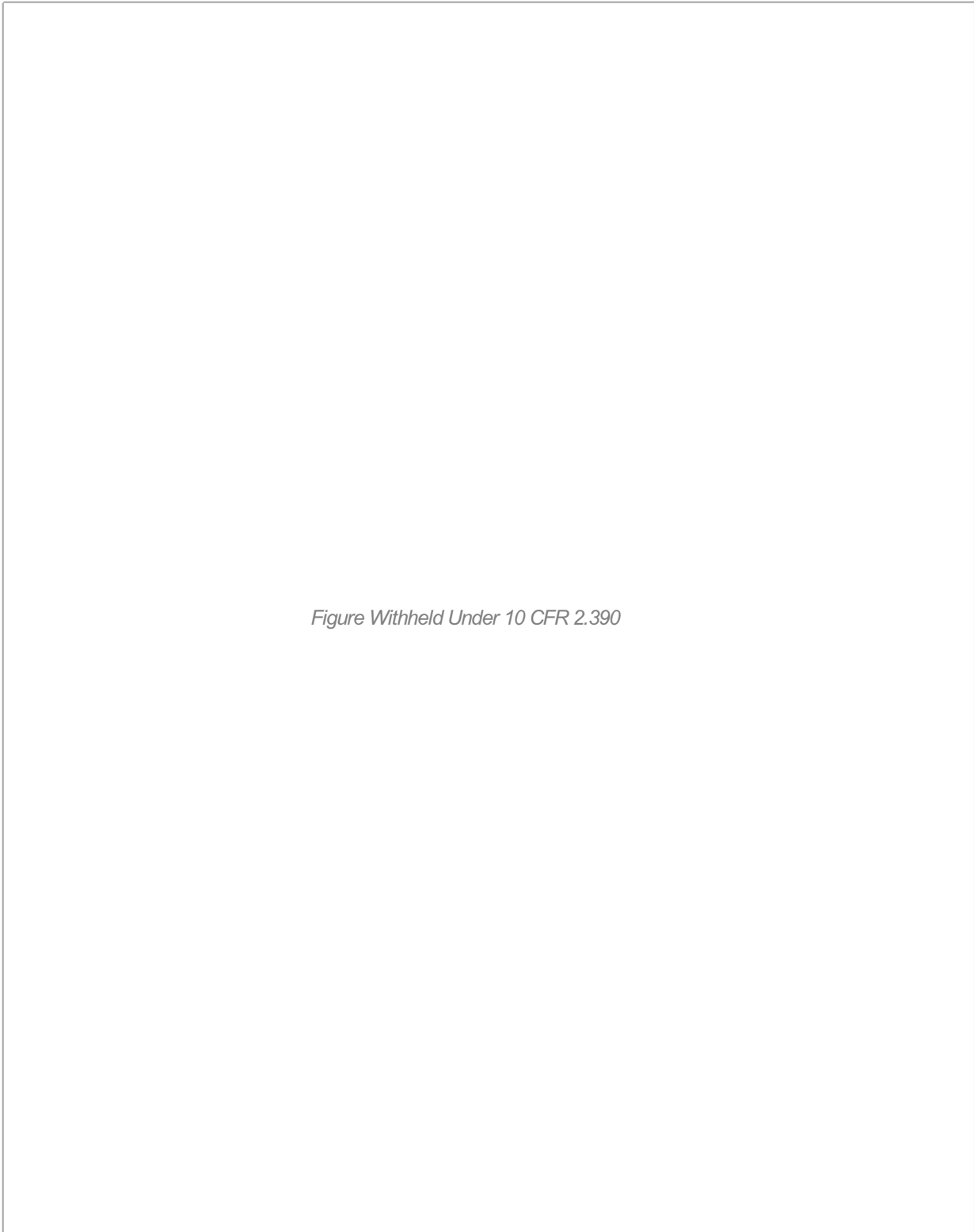


Figure Withheld Under 10 CFR 2.390

FIGURE 2.2-3
LIFTING LOADS



Figure Withheld Under 10 CFR 2.390

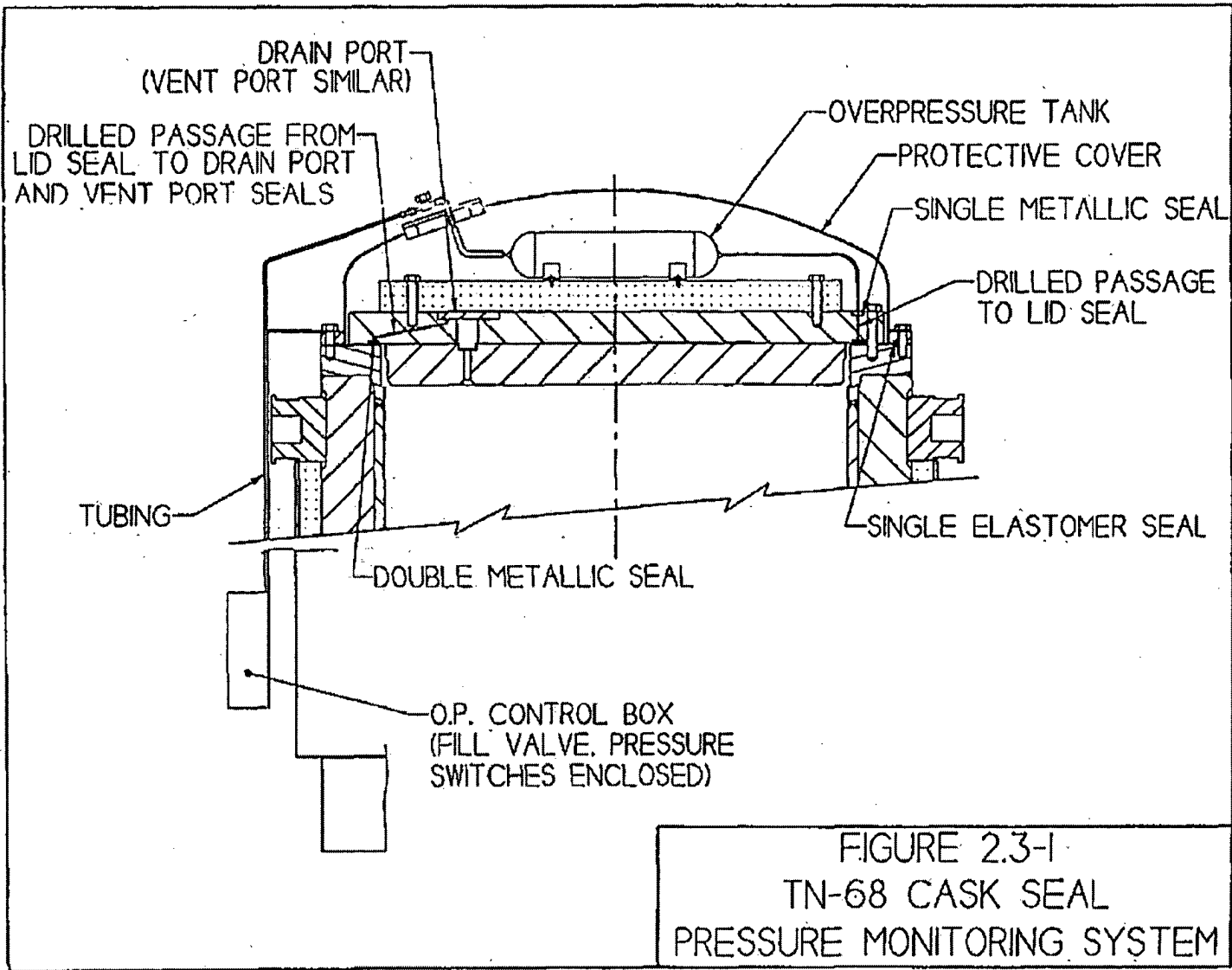


FIGURE 2.3-1
TN-68 CASK SEAL
PRESSURE MONITORING SYSTEM

FIGURE 2.3-1

PP116
 (Seal) Joints N° 2-3-4-5

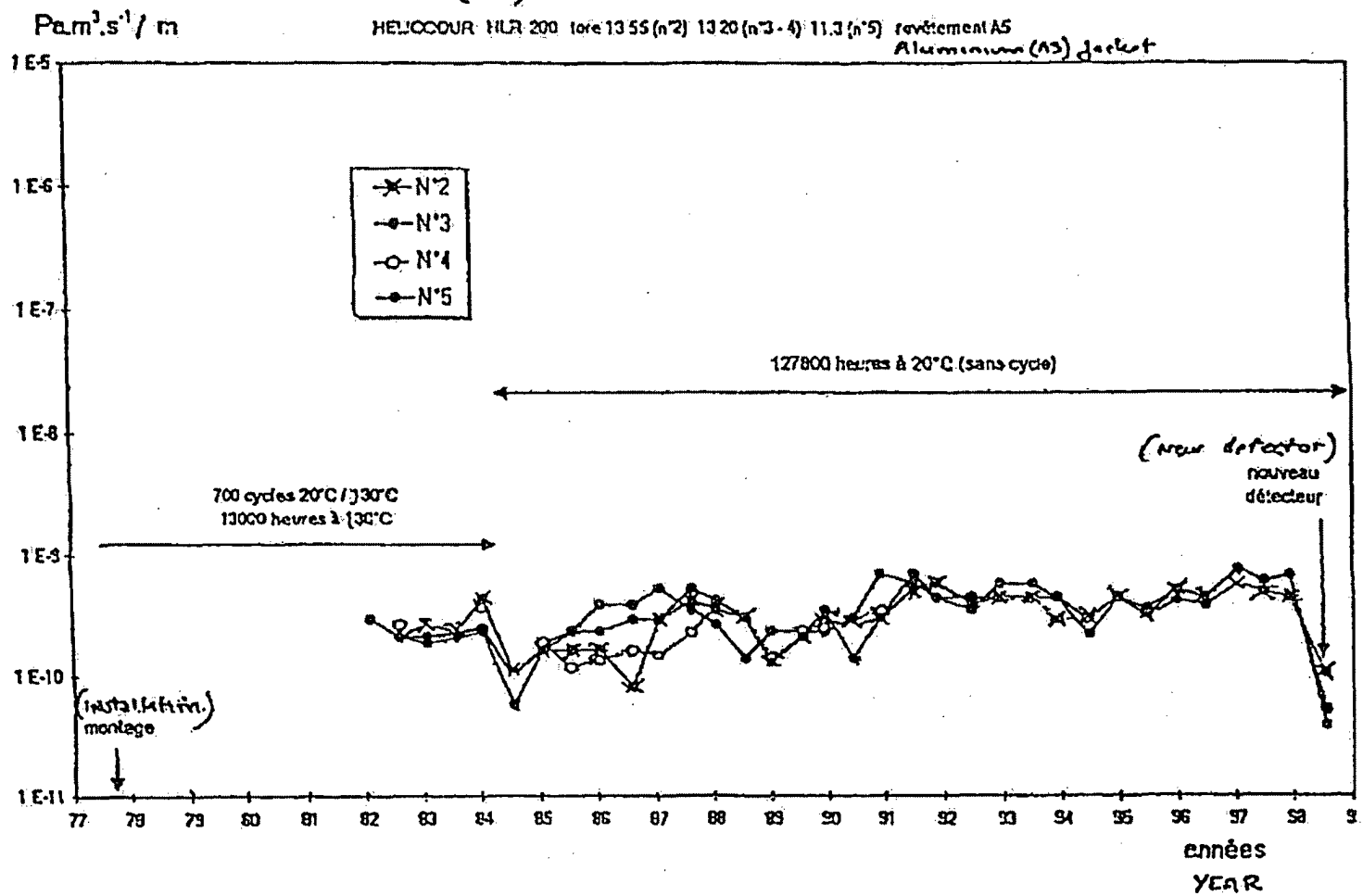


FIGURE 2.3-2
 Long Term Leak Test Results on Metallic Seals

PP 116
(Scar) Joints N°1

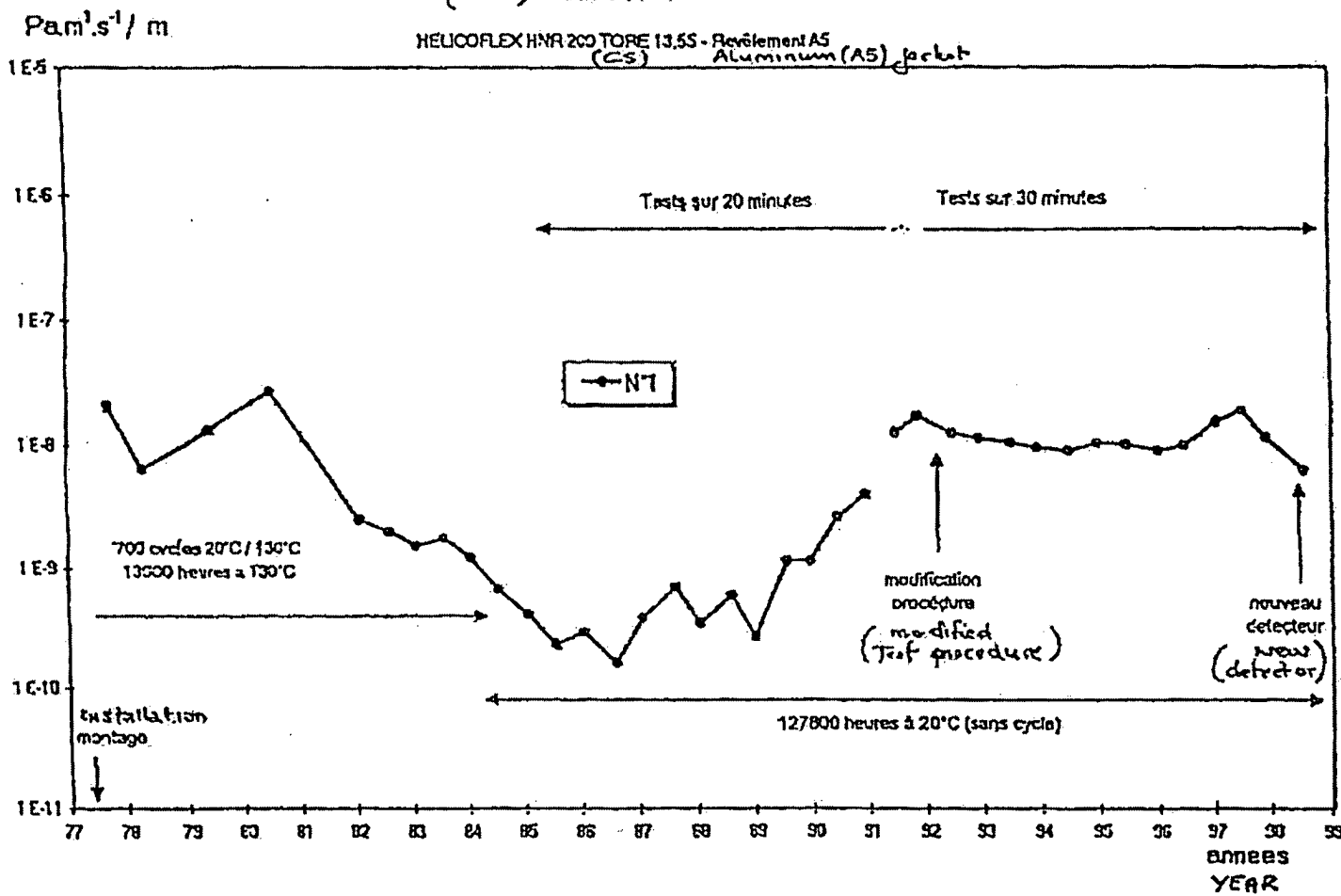


FIGURE 2.3-3
Long Term Leak Test Results on Metallic Seals

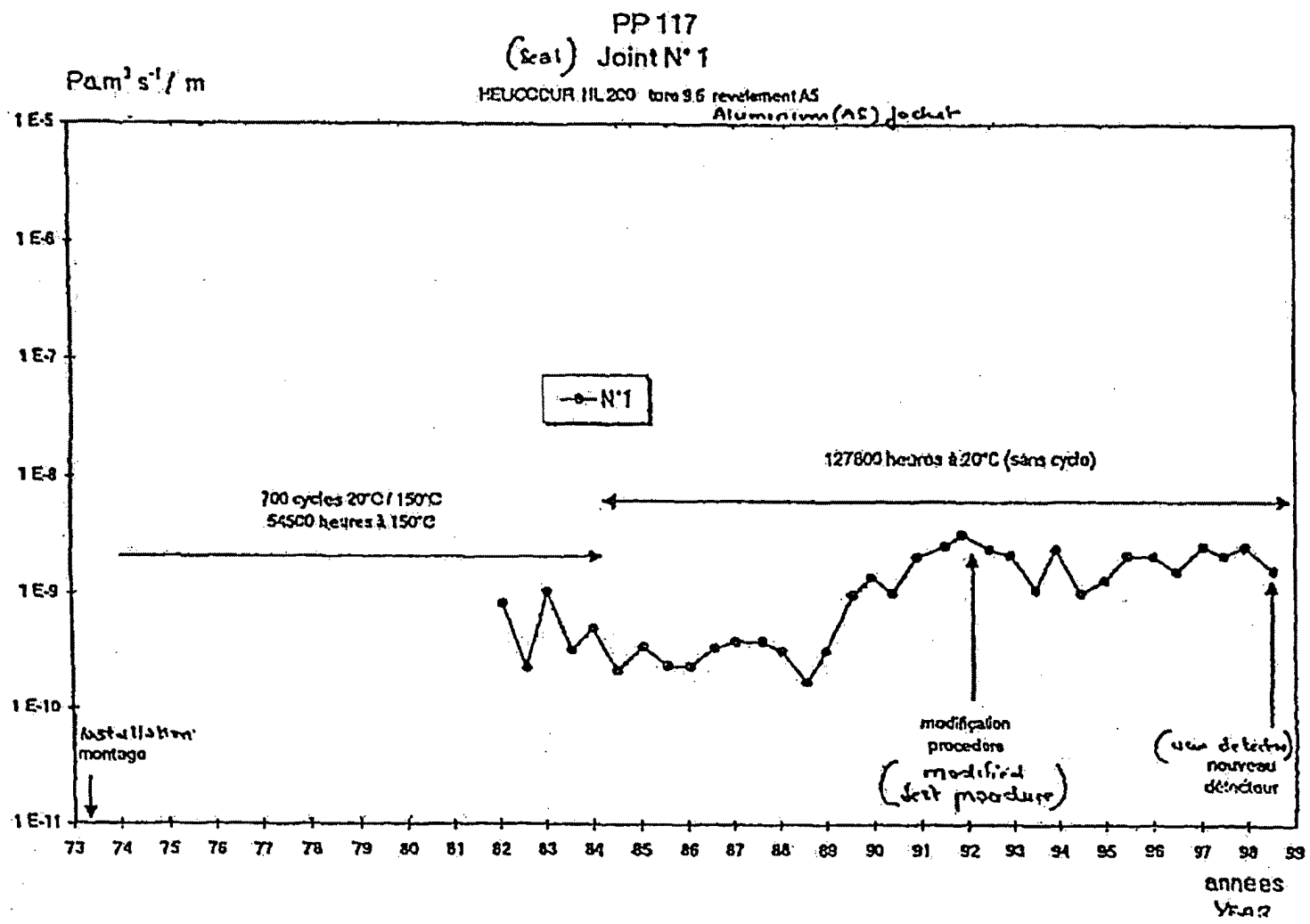


FIGURE 2.3-4
Long Term Leak Test Results on Metallic Seals

**TN-68 SAFETY ANALYSIS REPORT
TABLE OF CONTENTS**

SECTION	PAGE
3	STRUCTURAL EVALUATION
3.1	Structural Design 3.1-1
3.1.1	Discussion 3.1-1
3.1.2	Design Criteria 3.1-2
3.1.2.1	Confinement Boundary 3.1-3
3.1.2.2	Non-Confinement Structure 3.1-3
3.1.2.3	Basket 3.1-4
3.1.2.4	Trunnions 3.1-5
3.2	Weights and Centers of Gravity 3.2-1
3.3	Mechanical Properties of Materials 3.3-1
3.3.1	Cask Material Properties 3.3-1
3.3.2	Basket Material Properties 3.3-1
3.3.3	Material Properties Summary 3.3-1
3.3.4	Material Durability 3.3-1
3.4	General Standards for Casks 3.4-1
3.4.1	Chemical and Galvanic Reactions 3.4-1
3.4.1.1	Cask Interior 3.4-1
3.4.1.2	Cask Exterior 3.4-5
3.4.1.3	Lubricants and Cleaning Agents 3.4-6
3.4.1.4	Hydrogen Generation 3.4-6
3.4.1.5	Effect of Galvanic Reactions on the Performance of the Cask 3.4-7
3.4.2	Positive Closure 3.4-8
3.4.3	Lifting Devices 3.4-8
3.4.3.1	Trunnion Analysis 3.4-8
3.4.3.2	Local Stresses in Cask Body at Upper Trunnion Locations 3.4-9
3.4.3.3	Trunnion Bolt Stresses 3.4-10
3.4.4	Heat 3.4-11
3.4.4.1	Summary of Pressures and Temperatures 3.4-11
3.4.4.2	Differential Thermal Expansion 3.4-11
3.4.4.3	Stress Calculations 3.4-12
3.4.4.4	Comparison with Allowable Stresses 3.4-13
3.4.5	Cold 3.4-13
3.4.6	Fire Accident 3.4-14
3.5	Fuel Rods 3.5-1
3.5.1	Fuel Rod Temperature Limits 3.5-1
3.5-2	Thermal Stress of Fuel Cladding due to Unloading Operations 3.5-1

**TN-68 SAFETY ANALYSIS REPORT
TABLE OF CONTENTS**

SECTION	PAGE
3.6 Supplemental Information	3.6-1
3.6.1 Supplemental Information from Reference 12	3.6-1
3.6.2 Supplemental Information from Reference 18	3.6-13
3.6.3 Supplemental Information from Reference 19	3.6-17
3.7 References.....	3.7-1

**TN-68 SAFETY ANALYSIS REPORT
TABLE OF CONTENTS**

List of Tables

3.1-1	Individual Load Cases Analyzed
3.1-2	Confinement Vessel Stress Limits
3.1-3	Confinement Bolt Stress Limits
3.1-4	Non Confinement Structure Stress Limits
3.1-5	Basket Stress Limits
3.2-1	Cask Weight and Center of Gravity
3.3-1	Mechanical Properties of Body Materials
3.3-2	Temperature Dependent Body Material Properties
3.3-3	Reference Temperatures for Stress Analysis Acceptance Criteria
3.3-4	Mechanical Properties of Basket Materials
3.3-5	Temperature Dependent Basket Material Properties
3.3-6	TN-68 Cask Components and Materials
3.4-1	Upper Trunnion Section Properties and Loads
3.4-2	Upper Trunnion Stresses When Loaded by 6 and 10 Times Cask Weight
3.4-3	Upper Trunnion Loadings on TN-68 for Use in Cask Body Evaluation
3.4-4	Bijlaard Computation Sheet
3.4-5	Comparison of Actual with Allowable Stress Intensity - Confinement Vessel
3.4-6	Comparison of Actual with Allowable Stress Intensity - Gamma Shielding
3.4-7	Summary of Maximum Stress Intensity and Allowable Stress Limits for Lid Bolts
3.4-8	Comparison of Actual with Allowable Stress Intensity in Basket (Normal Conditions)
3.4-9	Comparison of Actual with Allowable Stress Intensity in Basket (Accident Conditions)
3.4-10	Comparison of Maximum Stress Intensity with Allowables in Outer Shell

**TN-68 SAFETY ANALYSIS REPORT
TABLE OF CONTENTS**

List of Figures

3.4-1	Trunnion Geometry
3.4-2	Cask Body Key Dimensions
3.4-3	Standard Reporting Locations for Cask Body
3.4-4	Weld Stress Locations
3.4-5	Potential Versus pH Diagram for Aluminum-Water System
3.4-6	Effect of pH on Corrosion of Iron in Aerated Soft Water, Room Temperature
3.5-1	Finite Element Model
3.5-2	Nodal Temperature Used for Thermal Analysis
3.5-3	Temperature Distribution Resulting from Thermal Analysis
3.5-4	Nodal Stress Intensity

CHAPTER 3

STRUCTURAL EVALUATION

3.1 Structural Design

3.1.1 Discussion

This section summarizes the structural analysis of the TN-68 storage cask. For purposes of structural analysis, the cask has been divided into four components: the cask body (consisting of confinement vessel and gamma shielding), the basket, the trunnions and the neutron shield outer shell. The following information is provided: a brief description of the components, the design bases and criteria, the method of analysis, a summary of stresses for the highest stressed locations, and a comparison with the allowable stress criteria.

The cask body is described in Section 1.2. Drawings 972-70-1, 972-70-2 and 972-70-3 show the cask body. The confinement shell, bottom and lid materials are SA-203, Grade E and SA-350 Grade LF3. The gamma shielding cylinder is SA-266, Class 2 and the bottom is SA-266 Class 2 or SA-516 Gr. 70.

In order to obtain a close fit between the confinement vessel and the gamma shielding for heat transfer, the gamma shielding is heated prior to assembly with the confinement shell. As the gamma shielding cools, a gap forms between the confinement vessel flange and the gamma shielding. This gap is filled with shims as shown on Drawing 972-70-3. The shims are machined to fill the gap and act as a backing plate for the 0.50 inch weld between the confinement flange and the gamma shield shell. The shims are typically less than 0.25 inches and no more than 0.50 inches thick and are made from SA-516, Gr. 70 material. The shims are sized so there is no more than 0.03 inch gap between the shims and the flange or the shims and the gamma shield shell.

The TN-68 confinement vessel is designed, fabricated, examined and tested in accordance with the requirements of Subsection NB of the ASME Code⁽¹⁾ to the maximum practical extent. Exceptions taken to the ASME code are specified in the TN-68 Technical Specifications. The confinement boundary consists of the inner shell and bottom plate, shell flange, lid outer plate, lid bolts, vent and drain cover plates and bolts.

Other structural and structural attachment welds are examined by the liquid penetrant or the magnetic particle method in accordance with Section V, Article 6 of the ASME Code⁽¹⁾. The magnetic particle and liquid penetrant examination acceptance standards are in accordance with Section III, Subsection NF, Paragraphs NF-5340 and NF-5350⁽¹⁾.

Seal welds are examined visually or by liquid penetrant or magnetic particle methods in accordance with Section V of the ASME Code⁽¹⁾. Electrodes, wire, and fluxes used for fabrication comply with the applicable requirements of the ASME Code, Section II, Part C⁽¹⁾.

The welding procedures, welders and weld operators are qualified in accordance with Section IX of the ASME Code⁽¹⁾.

The basket is a welded assembly of stainless steel boxes and designed to accommodate 68 fuel assemblies. The fuel compartment stainless steel box sections are attached through fusion welds to 304 SST plates sandwiched between box sections. The fusion welds are spaced intermittently along the box sections. Neutron poison plates composed of a boron-aluminum alloy or a boron carbide - aluminum metal matrix composite are sandwiched between the stainless steel walls of adjacent box sections and adjacent stainless steel plates. The 304 stainless steel members are the primary structural components. The neutron poison plates provide the heat conduction path from the fuel assemblies to the cask cavity wall, and also provide criticality control. The bottom row of plates which are 304 SST (no poison) are also sandwiched between fuel compartment box sections and provide structural support of the basket. Drawings 972-70-4 and 972-70-5 show details of the basket.

The basket is supported laterally by 6061-T6 aluminum rails (shown in Drawing 972-70-2). The rails are attached to the periphery of the basket by welded studs.

Tangential alignment between the basket and cask cavity is maintained by a key at the perimeter of the basket. This key is designed to prevent the basket from rotating in the cask cavity wall under normal lateral inertial loadings.

The two lower trunnions are cylindrical SA-105 forgings that are welded to the cask body gamma shielding. The two upper trunnions are SA-182, Gr. F6NM forgings and are designed to lift the loaded TN-68 cask vertically. The upper trunnions are bolted to the cask body with a flange connection using 12-1 1/2" diameter bolts of SA-320-L43. The lower trunnions provide capability to rotate the cask prior to loading of spent fuel. The upper trunnions are designed to meet the requirements of ANSI N14.6.⁽²⁾ The trunnions are shown in Drawing 972-70-2.

The outer shell of the neutron shield consists of a cylindrical shell section with closure plates at each end. The closure plates are welded to the outer surface of the cask body gamma shielding. The outer shell provides an enclosure for the resin-filled aluminum containers and maintains the resin in the proper location with respect to the active length of the fuel assemblies in the cask cavity. The outer shell has no other structural function. The shell is painted carbon steel.

The top neutron shield consists of a disk of commercial grade polypropylene. The top neutron shield is attached to and rests on the cask lid. It is protected from the environment by the protective cover.

3.1.2 Design Criteria

This section describes the TN-68 analyses performed under the various loading conditions identified in Section 2.2. These loadings include all of the normal events that are expected to occur regularly. In addition, they include severe natural phenomena and man-induced low probability events postulated because of their potential impact on the immediate environs. The loading from the hypothetical tipping accident that is shown not to occur, is also analyzed in this chapter.

The TN-68 loadings are summarized in Table 2.2-4 and described in Chapter 2. The loads selected for analysis of the cask are discussed in Section 2.2.5.2, 2.2.5.3 and 2.2.5.4. Numerical values of these loads are listed in Tables 2.2-2 and 2.2-3.

The TN-68 components have been evaluated using numerical analysis. Finite element models of the cask body and basket have been developed, and detailed computer analyses have been performed using the ANSYS computer program⁽³⁾. The stress analysis of the lid bolts is performed based on the methodology of NUREG/CR-6007⁽⁴⁾. Other components such as trunnions are analyzed using conventional textbook methods. Table 3.1-1 lists the specific individual load cases analyzed for each major TN-68 component. The sections describing the analyses and the tables listing the stress results, where applicable, are also indicated. TN-68 components are not subjected to any significant cyclic loads such as pressure or temperature fluctuations resulting in an appreciable fatigue usage factor. Also, in the operating temperature range, the materials selected are not subject to significant creep.

3.1.2.1 Confinement Boundary

The confinement boundary consists of the inner shell (both cylinder and bottom) and closure flange out to the seal seating surface and the lid assembly outer plate. The lid bolts and seals are also part of the confinement boundary. The confinement boundary is designed to the maximum practical extent as an ASME Class I component in accordance with the rules of the ASME Code, Section III, Subsection NB. Exceptions to the ASME Code are discussed in Chapter 7.

The stresses due to each load are categorized as to the type of stress induced, e.g. membrane, bending, etc., and the classification of stress, e.g. primary, secondary, etc. Stress limits for confinement vessel components, other than bolts, for Normal (Design and Level A) and Hypothetical Accident (Level D) Loading Conditions are given in Table 3.1-2. The stress limits used for Level D conditions, determined on an elastic basis, are based on the entire structure (confinement shell and gamma shielding material) resisting the accident load. Local yielding is permitted at the point of contact where the load is applied.

The allowable stress limits for the confinement bolts are listed in Table 3.1-3. The allowable stress limits for the lid bolts are listed separately in Tables 3A.3-3 and -4.

The allowable stress intensity value, S_m , as defined by the Code, is taken at the maximum temperature calculated for each service load condition.

3.1.2.2 Non-Confinement Structure

Certain components such as the gamma shielding, the neutron shield outer shell and the trunnions are not part of the cask confinement boundary but do have structural functions. These components, referred to as non-confinement structures, are required to react to the confinement or environmental loads and in some cases share loadings with the confinement structure. The stress limits for the non-confinement structures (excluding the basket) are given in Table 3.1-4. The top neutron shield and the radial neutron shielding including the carbon steel enclosure have not been designed to withstand all of the hypothetical accident loads. The shielding may degrade

during the fire or due to cask burial. Also there may be local damage due to tornado impacts or cask tipover. Therefore a bounding analysis assuming that the exterior neutron shielding is completely removed, has been performed. This analysis shows that the site boundary accident dose rates are not exceeded. These accidents are described in Chapter 11.

3.1.2.3 Basket

The basket is designed, fabricated and inspected in accordance with the ASME Code Subsection NG to the maximum practical extent. The following exceptions are taken:

The poison and aluminum plates are not used for structural analysis. (They are represented by coupling to simulate their through-thickness load transfer capability; see appendix 3B.2.) Therefore, the materials are not required to be code materials. The quality assurance requirements of NQA-1 or 10 CFR 72 Subpart G are imposed in lieu of NCA-3800. The basket will not be code stamped. Therefore the requirements of NCA are not imposed. Fabrication and inspection surveillance is performed by the owner and design organization in lieu of an authorized nuclear inspector.

The fuel basket rail material is not a Class 1 material. It was selected for its properties. Aluminum has excellent thermal conductivity and a high strength to weight ratio provided that temperatures do not exceed 400°F.

NUREG-3854 and 1617 allow materials other than ASME Code materials to be used in the cask fabrication. ASME Code does provide the material properties for the aluminum alloy up to 400°F and also allows the material to be used for Section III applications (Class 2 or 3) up to 400°F temperature. The construction of the aluminum rails will meet the requirements of Section III, Subsection NG.

The stainless steel basket shim (item 30, dwgs 972-70-2 & -5) is designed only to transmit compressive loads from the basket to the shell, similar to the function of the basket rail shim, item 31. The shims are an attachment to the component structure and as such are outside code jurisdiction as defined in ASME Figure NG-1131-1, callout 8, note 1.

If an automated welding process is used for the box seam welds, PT examination in accordance with Section III, Subsection NG, Para. NG-5233 will be performed in lieu of the requirements of Section III, Subsection NG, Para. NG-5231.

The stress limits for the basket are summarized in Table 3.1-5. The basket fuel compartment wall thickness is established to meet heat transfer, nuclear criticality, and structural requirements. The basket structure must provide sufficient rigidity to maintain a subcritical configuration under the applied loads. The 304 stainless steel members in the TN-68 basket are the primary structural components. The neutron poison plates are the primary heat conductors and also provide the necessary criticality control.

The basis for the 304 stainless steel fuel compartment box and fusion welds stress allowables are Section III, Division I, Subsection NG of the ASME Code. The primary membrane stress and

primary membrane plus bending stress are limited to S_m (S_m is the code allowable stress intensity) and $1.5 S_m$, respectively, at any location in the basket for Normal (Design and Level A) load conditions. The average primary shear stress across a section is limited to $0.6 S_m$. The fusion weld shear stress allowable is limited to $0.3 * 0.6 S_m = 0.18 S_m$

The hypothetical impact accidents are evaluated as short duration Level D conditions. The stress criteria are taken from Section III, Appendix F of ASME⁽¹⁾ Code. For elastic quasistatic analysis, the primary membrane stress is limited to the smaller of $2.4S_m$ or $0.7S_u$ and membrane plus bending stress intensities are limited to the smaller of $3.6S_m$ or S_u . The average primary shear stress across a section is limited to $0.42 S_u$. The fusion weld shear stress allowable is the smaller of $0.42 S_u$ or $(2 * 0.6S_m)$.

The fuel compartment walls, when subjected to compressive loadings, are also evaluated against ASME Code rules for component supports to ensure that buckling will not occur. The acceptance criteria (allowable buckling loads) are taken from ASME Code, Section III, Appendix F, paragraph F-1341.4, Plastic Instability Load. The allowable buckling load is equal to 70% of the calculated plastic instability load. The buckling analyses of the aluminum rails are considered separately. See Appendix 3B.5.4 for complete details of criteria for these conditions.

3.1.2.4 Trunnions

The design criteria for the trunnions are both unique and specific. They are specified in Section 3.4.3.1.

3.2 Weights and Centers of Gravity

The weight of the TN-68 cask and contents is 115 tons. The weights of the major individual subassemblies are listed in Table 3.2-1. The center of gravity of the cask is located on the axial centerline 97.22 inches from the base of the cask.

In most of the structural analyses, a conservatively high weight is used. However, in certain cases, such as the G load calculation and the stability analysis of the cask, a conservatively low weight and higher c.g. are used.

3.3 Mechanical Properties of Materials

3.3.1 Cask Material Properties

This section provides the mechanical properties of materials used in the structural evaluation of the TN-68 storage cask. Table 3.3-1 lists the materials selected, the applicable components, and the minimum yield, ultimate, and design stress values specified by the ASME Code. All values reported in Table 3.3-1 are for metal temperatures up to 100°F. For higher temperatures, the temperature dependency of the material properties is reported in Table 3.3-2.

Table 3.3-3 summarizes the thermal analysis results from Chapter 4. These results support the selection of cask body component design temperatures for structural analysis purposes.

3.3.2 Basket Material Properties

The material properties of the 304 stainless steel plates are taken from the ASME⁽¹⁾ Code, Section II, Part D. The material properties of the aluminum alloy (6061-T6) are also taken from the ASME Code. These properties are listed with specific references in Tables 3.3-4 and 3.3-5.

3.3.3 Material Properties Summary

Table 3.3-6 provides a table which summarizes the components of the TN-68 cask, their primary function and an overview of the general conditions (stresses, temperatures, pressures, coatings, etc) during storage. This table is intended to summarize the information provided elsewhere in the SAR.

3.3.4 Material Durability

Materials must maintain the ability to perform their safety-related functions over at least the cask's 40 year lifetime under the cask's thermal, radiological, corrosion, and stress environment.

Metallic components:

Gamma radiation has no significant effect on metals. The effect of fast neutron irradiation of metals is a function of the integrated fast neutron flux, which is on the order of 10^{14} n/cm² inside the TN-68 after 40 years. Studies on fast neutron damage in aluminum, stainless steel, and low alloy steels rarely evaluate damage below 10^{17} n/cm² because it is not significant. Extrapolation of the data available down to the 10^{14} range confirms that there will be virtually no neutron damage to any of the TN-68 metallic components.

The effect of the TN-68 temperature environment on the required structural properties is evaluated in the SAR. There is no long term degradation of metals in the TN-68 temperature environment. The effect of creep at temperature is the basis for establishing the seal temperature limits. Additional information on the seals, including construction, corrosion evaluation and long term test data, is provided in Sections 2.3.2.1 and 7.1.3.

The cask exterior carbon steel components is protected from corrosion by the paint (epoxy, acrylic urethane or equivalent). The interior is protected by the helium environment inside the cask. The aluminum, carbon steel, and stainless steel components are not subject to significant corrosion as discussed in Section 3.4.1.

Studies have been conducted to show that neither of the neutron absorber materials used in the basket will degrade significantly as both have excellent resistance to thermal and radiation alteration in the service environments of interest to this application.

Non-metallic components:

The radial neutron shield resin is a proprietary reinforced polymer. Appendix 9A provides information on the composition and the radiation and temperature resistance of the resin. Polyester is inert with respect to water, and the fire retardant mineral fill makes it self-extinguishing. Furthermore, the resin is contained in aluminum tubes inside a steel shell, so that the material is retained in place, and isolated from both water and from sources of ignition.

Elastomer o-rings or gaskets in the weather cover, quick disconnects, drain tube, and pressure relief valve are not important to safety. The quick disconnects are not part of the confinement boundary.

Stem tips on overpressure system valves are Kel-F or similar material, and are not important to safety; at the valve locations, the radiation level and temperatures are low.

Paint is subject to routine maintenance and touch-up. Radiation levels and temperature on the cask exterior are not high enough to damage the paint. This is confirmed by dry cask experience.

The top neutron shield (polypropylene) is Not Important to Safety. Polypropylene is slow burning to non-burning according to Table 24, Section 1 of the Handbook of Plastics and Elastomers⁽²³⁾. Polypropylene is inert with respect to water. Furthermore, the weather protective cover isolates the top neutron shield material from sources of ignition and from water.

3.4 General Standards for Casks

3.4.1 Chemical and Galvanic Reactions

The materials of the TN-68 cask have been reviewed to determine whether chemical, galvanic or other reactions among the materials, contents and environment might occur during any phase of loading, unloading, handling or storage. This review is summarized below:

The TN-68 cask components are exposed to the following environments:

- During loading and unloading, the casks are submerged in pool water. For BWR plants the pool water is deionized. This affects the interior and exterior surfaces of the cask body, lid and the basket. The protective cover, the top neutron shield, and the overpressure system are not submerged in the spent fuel pool. The casks are only kept in the spent fuel pool for a short period of time, typically about 6 hours to load or unload fuel, 1 - 2 hours to drain, and another 8 - 10 hours to completely dry, evacuate and backfill the cask with helium.
- During handling and storage, the exterior of the cask is exposed to normal environmental conditions of temperature, rain, snow, etc. All of the exterior surfaces with the exception of stainless steel components are protected from environmental exposure by a polyamide enamel epoxy coating. The paint is touched up periodically if there are any areas which peel or otherwise deteriorate. Therefore, the cask exterior is protected from chemical, galvanic or other reactions during storage.
- During storage, the interior of the cask is exposed to an inert helium environment. The helium environment does not support the occurrence of chemical or galvanic reactions because both moisture and oxygen must be present for a reaction to occur. The cask is thoroughly dried before storage by a vacuum drying process. It is then sealed and backfilled with helium, thus stopping corrosion. Since the cask is vacuum dried, galvanic corrosion is also precluded since there is no water present at the point of contact between dissimilar metals.
- The radial neutron shielding materials and the aluminum resin boxes are sealed during all normal operations. The amount of oxygen in the sealed region is very small. The resin material is inert after it has cured and does not affect the aluminum boxes or the carbon steel housing.

3.4.1.1 Cask Interior

The TN-68 cask materials are shown in the Parts List on Drawing 972-70-2. The confinement vessel is made from SA-203 Grade E and SA-350 LF3. This low-alloy carbon steel is uncoated.

All sealing surfaces are stainless steel clad by weld overlay.

Within the cask cavity, there are basket rails made from 6061-T6 aluminum. The cask basket is assembled from SA-240, Type 304 stainless steel boxes which are joined together by a

proprietary fusion welding process and separated by neutron poison and stainless steel plates which form a sandwich panel. The neutron poison is not welded or bolted to the stainless steel, but is held in place by the geometry of the boxes and stainless steel plates.

Potential sources of chemical or galvanic reactions are the interaction between the aluminum, aluminum-based neutron poison and stainless steel within the basket itself, and the interaction of the aluminum basket rails with the carbon steel cask cavity wall and the pool water.

Typical water chemistry in a BWR Spent Fuel pool is as follows:

pH	5.6 - 7.1
Chloride	1 - 10 ppb
Conductivity	0.7 - 1.8 μ mho
Silica	2.5 - 2.7 ppm
Pool Temperature	70 - 115°F

Behavior of Aluminum in Deionized Water

Aluminum is used for many applications in spent fuel pools. In order to understand the corrosion resistance of aluminum within the normal operating conditions of spent fuel storage pools, a discussion of each of the types of corrosion is addressed separately. None of these corrosion mechanisms are expected to occur in the short time period that the cask is submerged in the spent fuel pool.

General Corrosion

General corrosion is a uniform attack of the metal over the entire surfaces exposed to the corrosive media. The severity of general corrosion of aluminum depends upon the chemical nature and temperature of the electrolyte and can range from superficial etching and staining to dissolution of the metal. Figure 3.4-5 shows a potential -pH diagram for aluminum in high purity water at 77°F. The potential for aluminum coupled with stainless steel and the limits of pH for BWR pools are shown in the diagram to be well within the passivation domain. The passivated surface of aluminum (hydrated oxide of aluminum) affords protection against corrosion in the domain shown because the coating is insoluble, non-porous and adherent to the surface of the aluminum. The protective surface formed on the aluminum is known to be stable up to 275°F and in a pH range of 4.5 to 8.5⁽¹³⁾.

Galvanic Corrosion

Galvanic corrosion is a type of corrosion which could cause degradation of dissimilar metals exposed to a corrosive environment for a long period of time.

Galvanic corrosion is associated with the current of a galvanic cell consisting of two dissimilar conductors in an electrolyte. The two dissimilar conductors of interest in this discussion are aluminum and stainless steel or aluminum and carbon steel in deionized water. There is little galvanic corrosion in deionized water since the water conductivity is very low. There is also less galvanic current flow between the aluminum-stainless steel couple than the potential difference on stainless steel which is known as polarization. It is because of this polarization characteristic that stainless steel is compatible with aluminum in all but severe marine, or high chloride, environmental conditions¹⁵.

At points of contact between the aluminum basket rails and the carbon steel shell, some galvanic reaction may occur, with the aluminum acting as a sacrificial anode. The carbon steel shell will be protected from corrosion as a result of this reaction. The corrosion of the aluminum rails will not be sufficient to affect their thermal or mechanical performance given the water purity and short immersion time.

Pitting Corrosion

Pitting corrosion is the forming of small sharp cavities in a metal surface. The first step in the development of corrosion pits is a local destruction of the protective oxide film. Pitting will not occur on commercially pure aluminum when the water is kept sufficiently pure, even when the aluminum is in electrical contact with stainless steel. Pitting and other forms of localized corrosion occur under conditions like those that cause stress corrosion, and are subject to an induction time which is similarly affected by temperature and the concentration of oxygen and chlorides. As with stress corrosion, at the low temperatures and low chloride concentrations of a spent fuel pool, the induction time for initiation of localized corrosion will be greater than the time that the cask internal components are exposed to the aqueous environment.

Crevice Corrosion

Crevice corrosion is the corrosion of a metal that is caused by the concentration of dissolved salts, metal ions, oxygen or other gases in crevices or pockets remote from the principal fluid stream, with a resultant build-up of differential galvanic cells that ultimately cause pitting. Crevice corrosion could occur in the basket plates, around the stainless steel welds. However, due to the short time in the spent fuel pool, this type of corrosion is not expected to be significant.

Intergranular Corrosion

Intergranular corrosion is corrosion occurring preferentially at grain boundaries or closely adjacent regions without appreciable attack of the grains or crystals of the metal itself. Intergranular corrosion does not occur with commercially pure aluminum and other common work hardened aluminum alloys.

Stress Corrosion

Stress corrosion is failure of the metal by cracking under the combined action of corrosion and high stresses approaching the yield stress of the metal. During normal operations, the cask is upright and there is negligible load on the basket. The stresses on the basket plates are very small, well below the yield stress of the basket materials.

Behavior of Carbon Steel in Deionized Water

The corrosion rate of iron in aerated soft water with the range $4 \leq \text{pH} \leq 10$ is 0.01 inch/year. For 48 hour submersion during fuel loading, the total corrosion would be 5×10^{-5} inch, which is negligible. Hydrogen evolution from iron corrosion does not occur in near neutral water¹⁶. See Figure 3.4-6. Low alloy carbon steel is slightly more resistant to corrosion than iron under these conditions.

Behavior of Austenitic Stainless Steel in Deionized Water

The fuel compartments and the structural plates which support the fuel compartments are made from Type 304 stainless steel. In addition, the gasket sealing surfaces are stainless steel clad. Stainless steel does not exhibit general corrosion when immersed in deionized water. Galvanic attack can occur between the aluminum in contact with the stainless steel in the water. However, the attack is mitigated by the passivity of the aluminum and the stainless steel in the short time the pool water is in the cask. Also the low conductivity of the pool water tends to minimize galvanic reactions.

Stress corrosion cracking in the Type 304 stainless steel welds of the basket to the structural stainless steel plates is also not expected to occur, since the baskets are not highly stressed during normal operations. There may be some residual fabrication stresses as a result of welding of the stainless steel boxes and fusion welds between the boxes and stainless steel plates. Of the corrosive agents that could initiate stress corrosion cracking in the 304 stainless steel basket welds, only the combination of chloride ions with dissolved oxygen occurs in spent fuel pool water. Although stress corrosion cracking can take place at very low chloride concentrations and temperatures such as those in spent fuel pools (less than 10 ppb and 160°F, respectively), the effect of low chloride concentration and low temperature is to greatly increase the induction time, that is, the period during which the corrodent is breaking down the passive oxide film on the stainless steel surface. Below 60°C (140°F), stress corrosion cracking of austenitic stainless steel does not occur at all. At 100 °C (212 °F), chloride concentration on the order of 15% is required to initiate stress corrosion cracking¹⁸. At 288 °C (550 °F), with tensile stress at 100% of yield in BWR water containing 100 ppm O₂, time to crack is about 40 days in sensitized 304 stainless

steel¹⁹. Thus, the combination of low chlorides, low temperature and short time of exposure to the corrosive environment eliminates the possibility of stress corrosion cracking in the basket welds.

The chloride content of all expendable materials which come in contact with the basket materials are restricted and water used for cleaning the baskets is restricted to 1.0 ppm chloride.

Behavior of Aluminum Based Neutron Poison in Deionized Water

The aluminum component of the borated aluminum is a ductile metal having a high resistance to corrosion. Its corrosion resistance is provided by the buildup of a protective oxide film on the metal surface when exposed to a corrosive environment. As stated above for aluminum, once a stable film develops, the corrosion process is arrested at the surface of the metal. The film remains stable over a pH range of 4.5 to 8.5.

Tests were performed by Eagle Picher¹⁴ which concluded that borated aluminum exhibits a strong corrosion resistance at room temperature in deionized water. Satisfactory long-term usage in these environments is expected. At high temperature, the borated aluminum still exhibits high corrosion resistance in the pure water environment.

From tests on pure aluminum, it was found that borated aluminum was more resistant to uniform corrosion attack than pure aluminum.

The alternate neutron poison material is a boron carbide / aluminum composite. The billet is produced by blending of aluminum and boron carbide powders, cold isostatic compacting, and vacuum sintering. The plates are formed from the billet by rolling or extrusion. The result is a matrix of full-density aluminum with a fine dispersion of boron carbide particles throughout. The corrosion behavior is similar to that of the base aluminum alloy.

There are no chemical, galvanic or other reactions that could reduce the areal density of boron in the TN-68's neutron poison plates with either of the poison plate materials.

3.4.1.2 Cask Exterior

The exterior of the cask is carbon steel. The exterior of the cask, with the exception of the trunnion bearing surfaces is painted using an epoxy, acrylic urethane, or equivalent enamel coating with the appropriate primer. The paint should be compatible with the pool water and easy to decontaminate.

The paint is visually inspected prior to installation of the cask in the spent fuel pool and periodically during storage. Touch up painting is performed if the paint deteriorates.

3.4.1.3 Lubricants and Cleaning Agents

The following lubricants and cleaning agents may be used on the TN-68 cask:

- Never-seez or Neolube (or equivalent) is used to coat the threads and bolt shoulders of the closure bolts. Never-seez is also used to coat the contact areas of the top and bottom trunnions during transport and lifting operations to prevent impregnation of contamination.

The lubricant should be selected for compatibility with the spent fuel pool water and the cask materials, and for its ability to maintain lubricity under long term storage conditions.

- During fabrication, expendable materials are restricted to limit exposure to water leachable chlorides, halogenated compounds and sulfur and its compounds. As the cask is lowered into the spent fuel pool, the cask is sprayed with demineralized water to provide a film of clean water on the cask surfaces. The time in the pool is minimized in order to minimize cask contamination levels.

The cask body is cleaned in accordance with approved procedures to remove cleaning residues prior to shipment to the Power Station. The basket is also cleaned prior to installation in the cask. The cleaning agents and lubricants have no significant affect on the cask materials and their safety related functions.

3.4.1.4 Hydrogen Generation

During the initial passivation state, small amounts of hydrogen gas may be generated in the TN-68 cask. The passivation stage may occur prior to submersion of the cask into the spent fuel pool.

Hydrogen accumulation and the formation of a flammable mixture can be mitigated by keeping at least one cover port open when the cask is flooded to vent any hydrogen, or by purging the cavity free volume with helium or nitrogen.

The following evaluation shows that a flammable mixture will not be formed in the TN-68 during anticipated operations.

An estimate of the maximum hydrogen concentration can be made, ignoring the effects of radiolysis, recombination, and solution of hydrogen in water. Testing was conducted by Transnuclear⁽¹²⁾ to determine the rate of hydrogen generation for aluminum metal matrix composite in intermittent contact with 304 stainless steel and for aluminum 6061 in intermittent

contact with SA203 low alloy steel. The samples represent the basket rails paired with the cask cavity wall, and the neutron poison plates paired with the basket compartment tubes. The test specimens were submerged in deionized water for 12 hours at 70 °F to represent the period of initial submersion and fuel loading, followed by 12 hours at 150 °F to represent the period after the fuel is loaded, until the water is drained. The hydrogen generated during each period was removed from the water and the test vessel and measured.

The test results were

	12 hour @ 70 °F		12 hour @ 150 °F	
	cm ² hr ⁻¹ dm ⁻²	ft ³ hr ⁻¹ ft ⁻²	cm ² hr ⁻¹ dm ⁻²	ft ³ hr ⁻¹ ft ⁻²
aluminum MMC/SS304	0.517	1.696E-4	0.489	1.604E-4
low alloy steel/ Al plate	0.476	1.562E-4	0.644	2.113E-4

The total surface area of the aluminum/steel interface at the basket perimeter is 186.3 ft² and the total area of neutron absorber/compartment wall interface is 1976.4 ft². If paired aluminum and neutron absorbers are used, this surface area would double to 3953 ft². These surface areas, combined with the data at 150 °F above result in a hydrogen generation rate of

$$[(2.1 \times 10^{-4} \text{ ft}^3/\text{ft}^2\text{hr})(186.3 \text{ ft}^2)] + [(1.6 \times 10^{-4} \text{ ft}^3/\text{ft}^2\text{hr})(3953 \text{ ft}^2)] = 0.67 \text{ ft}^3/\text{hr}$$

in the TN-68. The total free volume in the cask, with fuel in place, and without water, is 211.6 ft³. The following assumptions are made to arrive at a conservative estimate of hydrogen concentration:

- The hydrogen generation rate is constant, that is, no credit is taken for the fact that less surface area is submerged as draining proceeds
- The draining rate is constant
- All generated hydrogen is released instantly to the plenum between the water and the lid, that is, no dissolved hydrogen is pumped out with the water, and no released hydrogen escapes through the open vent port.

Under these assumptions, the hydrogen concentration in the space between the water and the lid is constant during draining, and is a function of the total drain time only. For a typical drain time of 2 hours, the hydrogen concentration is $0.67 \text{ ft}^3 \text{ H}_2/\text{hr} (2 \text{ hr})/211.6 \text{ ft}^3 = 0.6\%$. For a drain time of 10 hours, much longer than expected, the concentration would be 3.2%, still well below the lower flammable limit of 4%.

Unlike welded canisters, the TN-68 cask has a bolted closure. There is no source of ignition to result in an explosion or fire.

3.4.1.5 Effect of Galvanic Reactions on the Performance of the Cask

There are no significant reactions that could reduce the overall integrity of the cask or its contents during storage. The cask and fuel cladding thermal properties are provided in Chapter 4. The emissivity of the fuel compartment is 0.3, which is typical for non-polished stainless steel surfaces. If the stainless steel is oxidized, this value would increase, improving heat

transfer. The fuel rod emissivity value used is 0.8, which is a typical value for oxidized Zircaloy. Therefore, the passivation reactions would not reduce the thermal properties of the component cask materials or the fuel cladding.

There are no reactions that would cause binding of the mechanical surfaces or the fuel to basket compartment boxes due to galvanic or chemical reactions.

There is no significant degradation of any safety components caused directly by the effects of the reactions or by the effects of the reactions combined with the effects of long term exposure of the materials to neutron or gamma radiation, high temperatures, or other possible conditions.

3.4.2 Positive Closure

Positive fastening of all access openings through the confinement boundary is accomplished by bolted closures which preclude unintentional opening. All of the openings in the TN-68 cask are through the lid of the cask. A protective cover is installed around the lid during storage. Security seals are installed in two of the protective cover bolts to ensure that no unauthorized entry into the cask has been attempted.

3.4.3 Lifting Devices

Section 3.4.3.1 provides the analysis of the trunnions, which are the only components which are used to lift the cask. Section 3.4.3.2 provides an analysis of the local stresses in the cask wall due to the effect of a 6G lifting load on the trunnions. The resulting local stresses in the cask wall are conservatively added to the normal condition stresses resulting from other load combinations. Section 3.4.3.3 provides the stress analysis of the upper trunnion flange bolts.

3.4.3.1 Trunnion Analysis

This section provides the structural analysis of the TN-68 storage cask trunnions. The upper and lower trunnion geometry is shown in Figure 3.4-1. The upper trunnions are SA-182 Gr F6NM alloy forgings and are attached to the cask body with bolted flange connections. The lower trunnions are SA-105 carbon steel forgings, and are welded to the cask body. A flat surface is machined on the cask body outer surface at each trunnion location for this purpose.

The two upper trunnions are used for lifting the cask and are designed to the requirements of ANSI N14.6⁽²⁾. They can support a loading equal to 6 times the weight of the cask without generating stresses in excess of the minimum yield strength of the material. They can also lift 10 times the weight of the cask without exceeding the ultimate tensile strength of the material. A dynamic load factor of 1.15 is used in evaluating the trunnion stresses.

The lower trunnions are used to rotate the cask from a horizontal orientation to the vertical orientation. If the cask were lifted in a horizontal orientation, all four trunnions would be used and the loading on each trunnion would be only half of the load due to the vertical lift.

Figure 3.4-1 shows the basic dimensions of the upper and lower trunnions. A cask weight of

240,000 lbs. is used in this calculation. Table 3.4-1 shows the cross sectional area and moment of inertia at shoulder cross section A-A of the upper trunnions. In addition the loads applied to this section (for 6 W and 10 W loading) to evaluate the yield and ultimate limits are also listed.

Table 3.4-2 presents a summary of the stresses at the same location to compare against the trunnion yield and ultimate strengths. Also listed at the bottom of the table are the allowable stresses (yield and ultimate strengths). All of the calculated stresses in the trunnions are acceptable. Both upper and lower trunnions are designed such that the minimum margin of safety occurs at the trunnions' shoulders.

3.4.3.2 Local Stresses in Cask Body at Upper Trunnion Locations

This section describes the analysis performed to calculate the local stresses in the cask body at the trunnion locations due to the loadings applied through the trunnions. These local effects are not included in the ANSYS stress result tables reported in Section 3.4.4. These local stresses are superimposed on the ANSYS stress results for the cases where the inertial lifting loads are reacted at the trunnions. The local stresses are calculated in accordance with the methodology of WRC Bulletin 107⁽⁵⁾ which is based on the Bijlaard analysis for local stresses in cylindrical shells due to external loadings. A summary of the trunnion loads is provided in Table 3.4-3.

The neutron shield and thin outer shell are not considered to strengthen either the trunnions or the gamma shield shell. The trunnion is approximated by an equivalent attachment so that the curves of Reference 5 can be used to obtain the necessary coefficients. These resulting coefficients are read from the reference 5 curves and inserted into blanks in a standard computation form, a sample of which is shown on Table 3.4-4. The stresses are calculated by performing the indicated multiplications and the resulting stress is inserted into the stress table at the eight stress locations, i.e., AU, AL, BU, BL, etc. Note that the sign convention for this table is defined on the figure for the load directions as shown. The membrane plus bending stresses are calculated by completing Table 3.4-4.

The cylindrical body is assumed to be a hollow cylinder of infinite length. This is conservative since end restraints reduce the local cylinder bending effects.

The trunnion and cylinder dimensions are taken from Section 1.5 drawings. The dimensions and Bijlaard parameters used are as follows:

List Of Bijlaard Parameters at Upper Trunnion Locations

<u>Parameter</u>	<u>Parameter Description</u>	<u>Parameter Value</u>
R_m	Mean radius of shell	37.88 in.
T	Wall thickness of shell	6.27 in.
$\alpha=R_m/T$	Shell Parameter	6.0
r_o	Outside radius of attachment	6.875 in.
$\beta=0.875r_o/R_m$	Attachment Parameter	0.16

The maximum primary plus bending stress intensity due to a 6 G vertical lift is 19.8 ksi. The membrane stress intensity due to this load is 7.3 ksi. These are well below the yield stress of the gamma shield cylinder material. The stress intensity due to the local trunnion loading are combined with the finite element results at the top trunnion attachment locations and presented in Section 3A.2.

3.4.3.3 Trunnion Bolt Stresses

The trunnion flange is attached to the gamma shield vessel by twelve 1.5-8UN-2A bolts of SA-320 Gr. L43 material. The bolted flange is tightly fitted into the recess in the cask body. This recess provides a bearing area between the outside perimeter of the trunnion flange and the cask body. The radial clearance between the bolt shank and trunnion flange bolt holes is large enough so that shear loads are carried by the trunnion flange-to-cask body recess interface and not the bolts. The bolts develop only the tensile load due to trunnion moment.

The bending moment at the flange interface due to 10G is equal to $1,380,000 \times 7.51 = 10,363,800$ in-lbs. From Reference 11, Case 3, (for bolt patterns symmetrical about the vertical axis and flange rotating about the bottom bolt) the maximum bolt force due to bending moment M is:

$$F_{\max} = (4/(3RN))M$$

where

R = Bolt circle radius = 6.875 in.

N = No. of bolts = 12

$$F_{\max} = 4(10,363,800)/(3 \times 6.875 \times 12) = 167,496 \text{ lbs.}$$

The bolt stress area = 1.492 in^2

Max. tensile stress = $167,496/1.492 = 112.3 \text{ ksi}$

Bolt allowable tensile stress = S_u (at 300°F) = 125 ksi

For yield load (6G), the maximum tensile stress = $(6/10)(112,263) = 67.4 \text{ ksi}$

The bolt allowable yield stress = S_y (at 300°F) = 95.7 ksi

Therefore the bolt stresses are acceptable for both 10G(ultimate) and 6G (yield) trunnion loads.

3.4.4 Heat

3.4.4.1 Summary of Pressures and Temperatures

Stress allowables for the cask components are a function of component temperature. The temperatures used to perform the structural analysis are based on actual maximum calculated temperatures or conservatively selected higher temperatures. Chapter Four summarizes significant temperatures calculated for the TN-68 cask. The design temperatures used for stress analysis acceptance criteria for the cask are provided in Table 3.3-3. These temperatures are used to establish the allowables for every normal and accident load combination evaluated in this report.

The maximum internal pressure in the cask under normal and hypothetical accident conditions is calculated in Section 7.2.2. The structural analysis of the cask is conservatively performed using 100 psi as internal pressure.

3.4.4.2 Differential Thermal Expansion

A thermal evaluation of the cask was performed in Chapter 4 to determine the maximum temperature of the cask components under normal conditions. The analysis considers maximum

decay heat and maximum solar heat loading. Analyses of the thermal effects which resulted from heating the cask from an ambient temperature (70° F) to the steady state maximum temperature are presented in Appendix 3A for the cask and Appendix 3B for the basket. The results of these calculations are presented in Tables 3A.2.3-9 and 3A.2.3-10 for the cask and Section 3B.3.4 for the basket.

The basket plates are free to expand in the axial direction, since sufficient clearance is provided between the lid and the top of the basket. As described in Section 3B.3.4, adequate clearance also exists in the aluminum and stainless steel plates, and between the basket outer diameter and cask cavity inside diameter for free thermal expansion.

3.4.4.3 Stress Calculations

The stress calculations performed on the cask and basket are presented in Appendices 3A and 3B, respectively. Finite element models of the cask body and basket have been developed, and detailed computer analyses have been performed using the ANSYS computer program⁽³⁾. The stress analysis of the lid bolts is based on the methodology of NUREG/CR-6007⁽⁴⁾. Other components such as trunnions are analyzed using conventional textbook methods. Table 3.1-1 lists the specific individual load cases analyzed for each major cask component. The SAR sections where these analyses are described and the tables listing the stress results, where applicable, are also indicated.

Section 2.2 categorizes the loads for the cask body as indicated in Tables 2.2-8 and 2.2-9 into Normal (Level A) and Hypothetical Accident (Level D) Service Loadings and lists the load combinations to be evaluated. Each combination is a set of loads that are assumed to occur simultaneously.

The cask body key dimensions are shown in Figure 3.4-2. The Standard Reporting Locations for the cask body stresses are shown in Figure 3.4-3.

3.4.4.3.1 Confinement Vessel

Table 3.4-5 lists the highest confinement shell, flange, and lid stress intensities for each service condition and identifies the load combinations and locations where these maxima occur. Also listed in the tables are the stress limits for the service conditions based on the Section 3.1.2 structural design criteria.

3.4.4.3.2 Gamma Shielding

The load combinations, for the gamma shielding cask weld locations indicated in Figure 3.4-4, are presented in Appendix 3A. Table 3.4-6 lists the highest stress intensities in cylinder, bottom and weld for each service condition and identifies the load combinations and locations where those maxima occur. The allowable stress intensity limits are also listed. It is seen that the stresses in the gamma shielding are acceptable. A 1 inch thick carbon steel shield ring may be added to the cask. The shield ring is 19 inches high and rests on the outer shell, extending up to the body flange. The weight of the shield ring is included in the weight and CG calculations as

shown in Table 3.2-1 for cask stability and lifting analyses. The shield ring does not strengthen the gamma shield cylinder, and therefore it is not included in the structural analysis of that cylinder. The cask is evaluated for a safe shutdown earthquake (SSE) of 0.26g horizontal and 0.17g vertical. Since the maximum up load is 0.17g, this is much less than the shield ring gravity weight (1g), and therefore, the shield ring will not slide up during the seismic event.

3.4.4.3.3 Lid Bolts

The stress intensities in the lid bolts as calculated in Appendix 3A.3 are summarized in Table 3.4-7. These values are well below the allowable stresses.

3.4.4.3.4 Basket

Tables 3.4-8 and 3.4-9 summarize the maximum stresses in the basket. As shown in Tables 3.4-8 and 3.4-9, the stresses in the basket are below the allowable stresses. It is shown in Chapter 2 that the cask will not tipover. It is further shown in Appendix 3D that if the cask were to tip, the maximum expected g loading on the basket including dynamic load factor would be approximately 77 g's. The analysis presented in Appendix 3B indicates that even in this extremely unlikely hypothetical accident, there is sufficient margin to ensure that the basket maintains fuel assembly geometry subcritical and allows removal of the fuel.

3.4.4.3.5 Outer Shell

The neutron shield outer shell stresses are summarized in Table 3.4-10. The shell stresses are the highest when the cask is vertical and subjected to 3G inertia load and 25 psi internal pressure (e.g. before the cask is loaded). Stresses in the shell will be much lower during normal storage of the TN-68 cask on the ISFSI pad. The shell is not analyzed under tornado missile loading, but it could be damaged by either Missile A or Missile B, as defined in Section 2.2.1. The effect of any damage to the neutron shielding is bounded by the evaluation of completely removing the neutron shield, which is evaluated in Table 5.1-2.

3.4.4.4 Comparison with Allowable Stresses

The stresses in each of the major components of the cask are compared to their allowables in Tables 3.4-5 through 3.4-10.

3.4.5 Cold

The cask has been designed for operation to ambient temperatures as low as -20°F. The confinement seals are all metallic o-rings which are not affected by temperature. The shielding materials are all solids, so there is no concern for over freezing.

The confinement vessel is made from materials selected for their low temperature fracture toughness properties. The confinement boundary materials satisfy the brittle fracture criteria of ASME B & PV code, NB-2000 and Regulatory Guides 7.11⁽²¹⁾ and 7.12⁽²²⁾.

The pressure switch/ transducer used for the overpressure system, which is not a safety related component, is selected to operate at temperatures of -20°F and above.

An evaluation has also been performed to evaluate thermal stresses due to cold rain on a hot cask. The analysis is provided below.

The cold rain is assumed at 32°F . The maximum cask temperature in unprotected flange-lid region is 212°F (see Chapter 4, table 4.3-1). It is conservatively assumed that the outer flange surface is at 32°F while the inner surface is at 212°F . Thermal stress calculation is based on a temperature differential of $212^{\circ} - 32^{\circ} = 180^{\circ}\text{F}$. The maximum flange thermal stress of 1,150 psi is calculated for 9°F temperature differential in Appendix 3A, Table 3A.2.3-10. Therefore,

Maximum thermal stresses for cold rain on hot cask = $(180/9) 1,150 = 23,000$ psi.

This stress is well below the flange material (SA 350, Grade LF3) thermal stress allowable ($3S_m = 3 \times 22,200 = 66,600$ psi at 300°F - see Table 3.3-2).

3.4.6 Fire Accident

The lid and lid bolts reach about 470°F (see Table 4.4-1). Since the lid and lid bolts have the same thermal expansion coefficients, no bolt preload will be lost and a positive (compressive) seal load is maintained during the fire accident conditions.

The maximum temperature in seal region is 470°F (See Table 4.4-1) which is lower than the maximum allowable operating temperature of 536°F for the Helicoflex seal.

The basket temperature does not change appreciably (from 595°F to 717°F , see Tables 4.3-1 and 4.4-1) while the cask temperature rises during the fire accident (from 255°F to 842°F). The gap between the outside diameter of the basket and inside diameter of the cask will increase slightly based on thermal expansion evaluation results from normal and vacuum drying conditions (Section 3B.3.4); therefore, no thermal stress will be induced in the basket.

3.5 Fuel Rods

The handling of spent fuel within the Nuclear Generating Plant will be conducted in accordance with existing fuel handling procedures. Fuel with gross cladding defects will not be considered for storage at the ISFSI.

3.5.1 Fuel Rod Temperature Limits

Fuel cladding temperature limits are 400 °C (752 °F) for normal conditions including loading operations, and 570 °C (1058 °F) for off-normal and accident conditions, based on NRC Interim Staff Guidance memorandum ISG-11 rev 3⁽⁶⁾.

That guidance also limits thermal cycling during loading operations to a maximum of 10 cycles with amplitude of 65 °C (117 °F). The TN-68 vacuum drying procedures only include one-half thermal cycle with amplitude of about 60 °F, that is, the reduction in cladding temperature at the time that helium is introduced, as shown in Figure 4.5-1(b).

3.5.2 Thermal Stress of Fuel Cladding due to Unloading Operations

To evaluate the effects of the thermal loads on the fuel cladding during unloading operations, the following assumptions are made:

- A conservatively high maximum fuel rod temperature of 622 °F (see Table 4.3-1) and quench water temperature of 50 °F are used (normally water will be taken from the spent fuel pool, average water temperature is 90 °F; using 50 °F for thermal stress analysis is conservative).
- Fuel rod is assumed simply supported at both ends.
- The outer surface temperatures of the fuel rod are conservatively assumed as shown in Fig. 3.5-2. 50 °F, 212 °F, and 622 °F temperatures occur at three equal heights.

Analysis

Steady state thermal analyses are performed using the ANSYS⁽³⁾ computer program. The finite element model is shown in Figure 3.5-1. ANSYS finite elements Plane 55 and Plane 42 (Axisymmetric) are used. The model is based on the maximum fuel rod outer diameter of 0.563 inches and a maximum clad thickness of 0.034 in. to bound all GE type fuel rods. A tube length of two inches was selected for the finite element model so that it is a long cylinder (minimum length = $3.0/\lambda = 0.22$ inches) and the maximum stresses are not affected by the assumed boundary conditions. The maximum thickness of the cylinder was selected so as to result in higher ΔT and higher thermal stresses.

Material Properties

The following material properties are used for the analysis:

Material Properties of Zircaloy

Temp °F	Conductivity ⁽⁸⁾ Btu/hr-in-°F	α ⁽⁹⁾ in/in/°F	E ⁽¹⁰⁾ (note 1) (psi)	S _y ⁽²⁴⁾ (ksi)
200	.574	3.73×10^{-6}	12.8×10^6	121.65
248	.579	3.73×10^{-6}	12.7×10^6	115.98
284	.583	3.73×10^{-6}	12.5×10^6	112.13
334	.588	3.73×10^{-6}	12.3×10^6	107.25
415	.593	3.73×10^{-6}	12.0×10^6	100.18
615	.614	3.73×10^{-6}	11.1×10^6	84.65
622	.615	3.73×10^{-6}	11.1×10^6	84.11

Note 1: The modulus of elasticity values used are taken from low burnup fuel data. Since the resulting stresses are well below the yield stress, the small changes in the value of the modulus do not have a significant effect on results.

Thermal Analysis

The steady state thermal analysis was conducted using the surface nodal temperatures as shown on Figure 3.5-2. The inside surface nodal temperatures are all assumed to be 550°F, and the outside surface nodal temperatures to conservatively represent the quench water temperature. The temperature distribution resulting from this analysis is shown on Figure 3.5-3.

Thermal Stress Analysis and Results

A thermal stress analysis using the same model was conducted using the nodal temperatures obtained from the thermal analysis. The resulting nodal stress intensity distribution is shown on Figure 3.5-4. The maximum nodal stress intensity in the fuel cladding is 18.54 ksi. This stress is less than the yield strength of Zircaloy, 84.11 ksi at 622 °F.

3.6 Supplemental Information

3.6.1 Supplemental Information from Reference 12

HYDROGEN GENERATION
FROM ALUMINIUM CORROSION
IN REACTOR CONTAINMENT SPRAY SOLUTIONS

by

N. Frid

Swedish State Power Board

and

G Karlberg, S B Sundvall

Studsvik Energiteknik AB, Sweden

ABSTRACT

The aluminium corrosion experiments in reactor containment spray solutions, under the conditions expected to prevail during LOCA in BWR and PWR, were performed in order to investigate relationships between temperature, pH and hydrogen production rates.

In order to simulate the conditions in a BWR containment, realistic ratios between aluminium surface and water volume and between aluminium surface and oxygen volume were used.

Three different aluminium alloys were exposed to spray solutions: AA 1050, AA 5052 and AA 6082.

The corrosion rates were measured for BWR solutions (deaerated and aerated) with pH 5 and 9 at 50, 100 and 150°C. The pressure was constantly 0,8 MPa. The hydrogen production rate was measured by means of gas chromatography.

In deionized BWR water the corrosion rates did not exceed about 0.05 mm/year (2 mpy) in all cases, i.e. were practically independent of temperature and pH. Hydrogen concentrations were less than 0.1 vol. % in cooled dry gas.

Corrosion rates and hydrogen production in PWR alkaline solution measured at pH 9.7 and 150°C were very high. AA 5052 alloy was the best material.

1: BACKGROUND

The main goal of experiments described in this paper was to investigate the contribution of aluminium corrosion to hydrogen production after a loss of coolant accident (LOCA) in the older Swedish BWRs where aluminium amounts are considerable.

Due to the lack of experimental data on aluminium corrosion rates in BWR spray solutions, especially at elevated temperatures, it was very difficult to calculate the contribution of this hydrogen source to the total hydrogen production after LOCA. A parametric study /1/ was performed where the

experimental data obtained by Griess and Bacarolla in 1971 /2/ were extrapolated to conditions which are expected to prevail in BWR containments after LOCA.

The hydrogen amounts obtained in this way were relatively high having negative effects on the recombiner system in terms of higher thermal loads and earlier start demands.

The problem of aluminium corrosion was found especially important when the inerted BWR containment is temporarily filled with air.

2. INTRODUCTION

A BWR station like Forsmark-1 contains about 4 000 m² of aluminium surface as the heat insulation sheet. The volume of the containment is 6 200 m³ comprising 1 000 m³ water. The spray water initially will have a pH of about 8 due to manual LiOH addition but may decrease to pH 5.6 if spraying is performed without pH adjustment. The temperature will vary between 150 and 160°C.

In the unlikely event of loss of coolant accident in a nuclear power plant the containment spray systems will be used for pressure reduction and fission product absorption. Aqueous sodium borate solutions at a pH of about 9 (BWR) or neutral water (DWR) will be used at temperatures up to 150°C. In the open literature insufficient data are published to establish highly accurate and reliable relationships between temperature and hydrogen formation rates during corrosion of aluminium alloys. Under neutral, non-borated conditions, there are even fewer available data than from alkaline solutions (1, 3).

The thermodynamic suppositions of aluminium to react with hydrogen release can be visualized in a potential-pH diagram. Macdonald and Butler (4) in a series of such diagrams show the obvious effect of temperature on the ability of the metal to form a protective passive film. Figure 1 is valid for 150°C and shows that passivity then is possible only between pH 2 and 5. At a higher pH aluminium dissolves to AlO₂⁻ with H₂ formation and oxygen consumption.

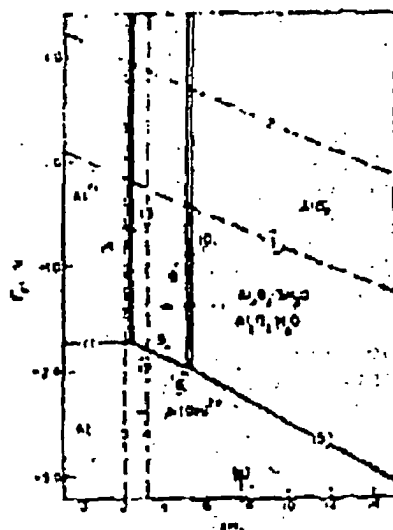


Figure 1 Potential-pH diagram for the aluminum-water system at 150°C. (a) refers to the pH of a 10^{-4} M OH⁻ solution (4).

Experimental work on corrosion of aluminium in spray solutions has been published by Griess and Bacarella (2). They used alkaline borate solutions (0.15 M NaOH + 0.28 M H₂BO₃) either with or without sodium thiosulfate (0.064 M) added in order to simulate PWR conditions. At 55°C the data indicated essentially constant corrosion rates of 130 - 190 mpy (3.3 - 4.8 mm/year) in the spray and 45 - 87 mpy (1.1 - 2.2 mm/year) on submerged specimens after a brief period of accelerated attack. At 100°C the only aluminium alloy that showed relatively good corrosion resistance was 5052 aluminium. At 140°C this alloy was the only one tested. During 24 hours the weight losses were about 20 mg/cm² in the spray and 16 mg/cm² in the solution. The 5052 alloy thus corroded much less than other aluminium alloys tested at higher temperatures but at about the same rate as the other ones at lower temperatures.

Berzins et al. (5) studied aluminium BS S1B in deionized water of pH 5 - 8 at 50°C with oxygen or nitrogen as cover gas. The mirror-bright specimens became dulled and in some cases developed a chalky film on the surface within a few days but the weight gain was low, in the order of $50 \cdot 10^{-5}$ g/cm² / 10 days (0.06 mm/year).

1. EXPERIMENTAL

The following three alloys were tested with normal delivery surface finish:

<u>Standards</u>			<u>Al</u>	<u>Mg</u>	<u>Mn</u>	<u>Si</u>
SS 4007	BS 51B	AA 1050	≥99.50			
SS 4120	BS NS4	AA 5052	97.2	2.5		
SS 4212	BS H30	AA 6082	97.4	0.5	0.7	1

Triplet specimens were exposed just once and were degreased prior to exposure. The specimens were cut from sheet to the dimensions 50 x 20 x 2 mm with a hole 7.2 mm in diameter, resulting in a specimen surface of 22.4 cm².

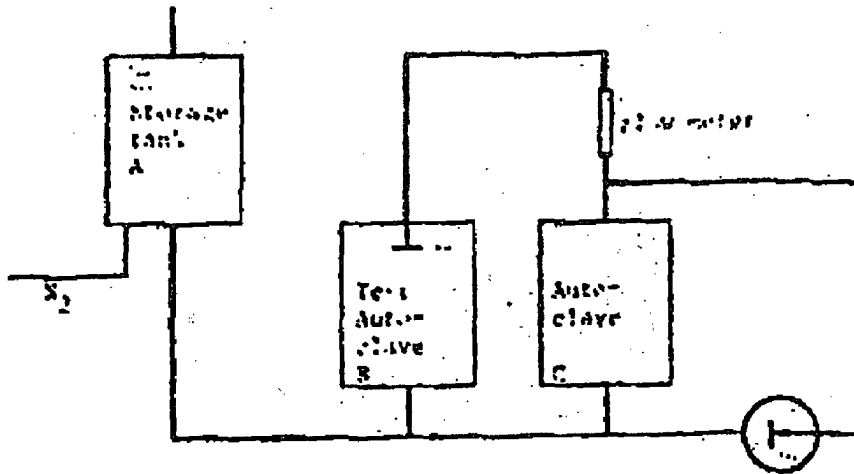


Figure 2 - Test equipment

Figure 2 shows the test equipment. Deionized water was aerated or deaerated in the vessel A. B and C were two titanium lined 37 dm³ autoclaves. Water could be pumped from C to the top of B where it was sprayed into the autoclave. B was half filled with water and half with nitrogen gas or air. The specimen holder in autoclave B had room for 48 specimens of which 24 specimens were in the spray zone above the water surface. The specimens were electrically insulated. During heating and cooling the spray was cut off and the holder put in an upper position where all specimens were above the water surface.

pH could be measured and adjusted if necessary. The temperature was 50, 100 or 150°C and the pressure constantly 0.8 MPa. Specimens were taken out from the autoclave after certain times and weighed.

The hydrogen production rate was measured by means of gas chromatography. The 5 ml gas sample from the test autoclave was cooled before the registration of hydrogen concentration.

At Forsmark 1 and Ringhals 1 the ratios between aluminium surface and water volume are 4:3 and 3.6:2.6 m²/m³ respectively. If specimens inside the autoclave gave the same conditions. In order to simulate the conditions in a containment with 5 % radiolytically formed oxygen in the gas phase we could start with aerated water. With 20 specimens in the autoclave the ratio between aluminium surface and oxygen volume was 12 m²/m³ which is comparable to the ratio between aluminium surface and oxygen volume in a reactor.

Tests were performed on the three alloys in deaerated deionized water at pH 5 and 9, in aerated water at pH 9 and in a PWR solution referred to by Griess and Bacardilla (2). In order to get the corrosion rates at different temperatures isothermal tests were run at 50, 100 and 150°C.

4. EXPERIMENTAL RESULTS

4.1 RWH solution

4.1.1 Deaerated water at pH 5

The specimens were weighed after 48, 93, 190 and 448 hours exposure in spray and water at 50, 100 and 150°C. All specimens got a grey tarnish. Their weight increases varied between $6 \cdot 10^{-4}$ and $29 \cdot 10^{-4}$ g per specimen independent of position, time, temperature and aluminium grade. Before weighing the specimens were stored in a desiccator for 24 hours. Assuming that the passive layer on the metal consists of Al₂O₃ and that the weight gain increased linearly with time with a rate of $6 \cdot 10^{-4}$ - $29 \cdot 10^{-4}$ g/specimen and 48 hours the corrosion rate was at most 0.046 mm/year (1.8 mpy).

The rate of hydrogen evolution, based on this corrosion rate, is $8 \cdot 10^{-4}$ mol H₂·m⁻²·h⁻¹.

4.1.2 Deaerated water at pH 9

The experiments were repeated at pH 9 instead of pH 5. The actual potential-pH diagrams may lead to the expectations of considerably increased corrosion rates at least at 100 and 150°C but this was not observed. The maximum weight gain at 150°C was 0.0027 g/specimen/48 hours without significant further weight gain after longer exposure times corresponding to a corrosion rate of 0.04 mm/year (1.6 mpy) independent of alloy. Once again the conservative assumption is made that the corrosion rate is equal to the rate during the first 48 hours.

The calculated rate of hydrogen evolution is $7 \cdot 10^{-4}$ mol H₂·m⁻²·h⁻¹.

4.1.3 Aerated water at pH 9

The preceding results gave about the same corrosion rates and consequently were obtained under cathodic control. Containment spraying may be performed under aerated conditions however, and Greiss and Bacarella also used aerated solutions. Because of that a series was started with aerated water. The temperature was 150°C and the exposure time 20 hours. The oxygen content in the water after this time was measured to 6.5 ppm.

Like in the earlier tests the differences in weight losses between the three alloys were small and in the magnitude of 0.08 mpy/year (3 mpy). The hydrogen evolution from aluminium corrosion was measured by means of gas chromatography. Eighteen specimens inside the autoclave produced 0.042 volume % H₂ in dry gas after 6 minutes, 0.081 % H₂ after 20 minutes, 0.096 % H₂ after 45 minutes and 0.098 % H₂ after 20 hours (see Figure 3).

The rate of hydrogen evolution, calculated from measured production and averaged over the first hour of exposure, is 0.07 mol·H₂·m⁻²·h⁻¹.

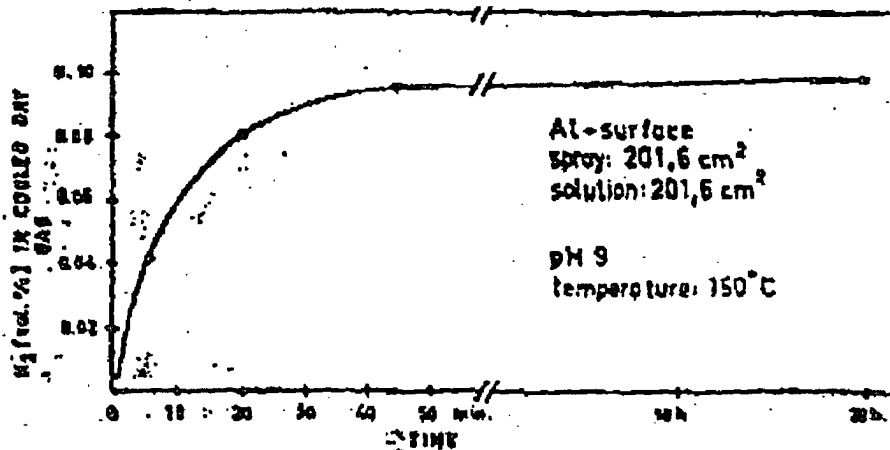


Figure 3 - Hydrogen production, measured in cooled dry gas, due to aluminium corrosion in BWR non-borated spray solution.

4.2 PWR solution

In order to demonstrate the striking difference between the behaviour of aluminium alloys in BWR water and in PWR spray solution, experiments according to those reported by Greiss and Bacarella were performed but with simultaneous registration of hydrogen evolved. The solution contained 0.15 M NaOH and 0.28 M H₃BO₃. pH was measured to 9.7 before the temperature was increased to 150°C.

After 15 minutes 18 specimens in the autoclave had produced 3.9 % H₂, after 25 minutes 5.0 % H₂ and after 35 minutes 7.8 % H₂ in cooled dry gas (see Figure 4).

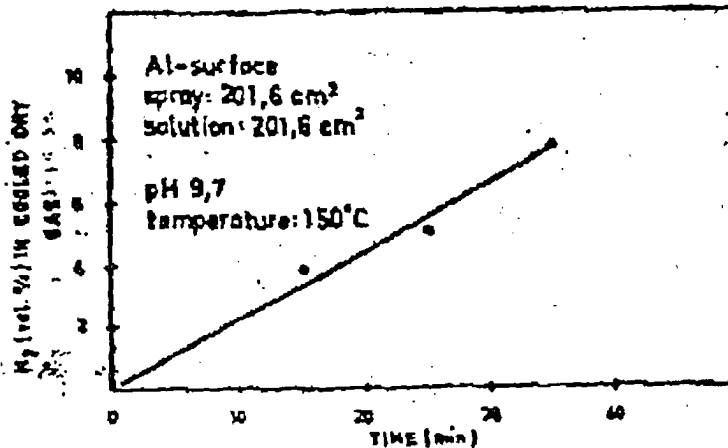


Figure 4 - Hydrogen production, measured in cooled dry gas, due to aluminium corrosion in PWR spray solution.

In this alkaline environment with high conductivity a clear difference was seen between the corrosion rates of the alloys. The mean value of AA 1050 in spray was 0.45 g/specimen/35 minutes and in water 0.46 g/specimen/35 minutes. Corresponding corrosion rate is 570 mm/year ($2.28 \cdot 10^4$ mpy). For AA 5052 and AA 6082 the corresponding values were 0.06, 0.04 (spray) and 0.25, 0.23 g/specimen/35 minutes (water), respectively. Corresponding corrosion rates are 63 mm/year ($2.5 \cdot 10^3$ mpy) for AA 5052 and 300 mm/year ($1.2 \cdot 10^4$ mpy) for AA 6082. Corrosion rates are summarized in Table 1. AA 1050 got a white appearance, AA 5052 was light brown with white spots; on specimens exposed to the spray. AA 6082 became grey and white when exposed to the spray, and brown and white when exposed in water.

The rates of hydrogen evolution, calculated from corrosion rates and measured, are given in Table 2.

5. DISCUSSION

A. The objective of hydrogen concentration measurement was to verify the reliability of hydrogen production calculations based on aluminium corrosion rates. Registration of hydrogen was performed only in two tests: for BWR solutions at pH 9, 150°C and for PWR solutions at pH 9.7, 150°C. The pressure in autoclave was 0.8 MPa.

3.6.2 Supplemental Information from Reference 18

TABLE 1

PWR solution. Corrosion rates

Alloy	Corrosion rate (mm/year)*
AA 1050	570
AA 6082	300
AA 5052	63

t = 150°C
pH 9.7

* 1 mm/year = 40 mpy

TABLE 2

PWR solution. Rates of H₂ evolution

Alloy	Calculated rate (mol H ₂ ·m ⁻² ·h ⁻¹)*
AA 1050	10.0
AA 6082	5.2
AA 5052	1.1

t = 150°C
pH 9.7

Measured rate of H₂ evolution (averaged over 35 minutes for three alloys):

$$5 \text{ mol H}_2 \cdot \text{m}^{-2} \cdot \text{h}^{-1}$$

$$* 1 \text{ mol H}_2 \cdot \text{m}^{-2} \cdot \text{h}^{-1} = 7.3 \cdot 10^{-2} \text{ SCP H}_2 \cdot \text{ft}^{-2} \cdot \text{h}^{-1}$$

Hydrogen evolved due to aluminium corrosion is distributed in the gas and water phases of the autoclaves. Hydrogen amounts and partial pressure p_{H_2} in the gas phase is easily calculated from measured concentrations in cooled dry gas using the ideal gas law.

The amount of hydrogen which is dissolved in the water phase calculated applying Henry's law.

$$P_{H_2} = H(T, p) \cdot x_{H_2}$$

where P_{H_2} - partial pressure of hydrogen in gas

x_{H_2} - mole fraction of hydrogen in liquid

$H(T, p)$ - Henry constant

Due to the fact that the Henry constant is a weak function of pressure the effect of pressure is neglected.

The Henry constant is obtained from /6/. For temperature range between 151°C and 374°C:

$$H = -9.01 \cdot 10^4 + 5.83 \cdot 10^7 / T$$

Table 3 shows the hydrogen amounts calculated with two different methods under the assumption that the passive layer on the aluminium specimens consists of Al_2O_3 .

TABLE 3

Comparison between hydrogen amounts obtained from gas chromatography measurement and calculated from aluminium corrosion rates. Aluminium surface is 403.2 cm².

Spray solution	H ₂ (mg) Gas	H ₂ (mg) Water	H ₂ (mg) Total	H ₂ (mg) 2Al+3H ₂ O + Al ₂ O ₃ +3H ₂
BWR after 20 h pH 9 t = 150°C	3.4	0.4	3.8	2.5
PWR after 35 min pH 9.7 t = 150°C	240	10	250	268

As expected the hydrogen amounts dissolved in water are very small.

Data in Table 3 indicates that calculation of hydrogen production based on corrosion rates gives reasonable results, under the assumption that corrosion products consists of Al_2O_3 .

B. In deionized water a more or less passivating film forms which results in a weight gain of the specimens, the velocity of which decreases with time. Even if one supposes that the corrosion rate is the same as during the first 24 hours the corrosion rate will not exceed 0.05 mm/year which is in good agreement with literature data at 50°C (5).

The conservative corrosion rate of 0.05 mm/year corresponds to a metal loss of 200 dm^3 /year in a station (Forsmark 1) or 540 kg/year or 20 kmol/year. The corrosion reaction



shows that after 24 hours 0.085 kmol H_2 is formed which occupies 1.9 m^3 ideally at 0°C and atmospheric pressure i.e 0.03 % of the gas volume.

Hydrogen concentration in the reactor containment can also be estimated using the measured hydrogen evolution rate i.e. 0.07 mol $H_2 \cdot m^{-2} \cdot h^{-1}$. After one hour the concentration for normal conditions would be 0.09 vol. % and no essential increase is expected based on the experimental results. Direct measurements 20 hours after start of an experiment gave a value of 0.1 vol % hydrogen.

Tests under FWR conditions on the contrary showed very high corrosion rates in good agreement with the results of Griess and Macarella.

At 150°C AA-5052 was the best material.

6. SUMMARY AND CONCLUSIONS

In BWR deionized water the three alloys in spray or water give corrosion rates of at most 0.05 mm/year (2 mpy) and hydrogen concentrations less than 0.1 %. On the contrary FWR alkaline solutions give very high corrosion rates and hydrogen contents.

One unexpected result was that aluminium corrosion rates in BWR spray solutions were practically independent of temperature and pH.

In accordance with Regulatory Guide 1.7 the corrosion rate for aluminium exposed to alkaline solution shall be 200 mpy. This value should be adjusted upward for higher temperatures early in the accident sequence.

It means, in view of presented experimental results, that applying Regulatory Guide 1.7 method to BWR non-borated solutions is extremely conservative and should not be used.

The contribution of aluminium corrosion to hydrogen production after LOCA in BWR containments is very small compared with other hydrogen sources such as zirconium-water reaction and radiolysis of water and therefore has no significant effects on combustible gas control systems.

Results of our experiment in PWR aqueous sodium borate solutions at pH 9.7 and temperature 150°C confirm Griess and Bacarella data and support the recommendation of Regulatory Guide 1.7.

ACKNOWLEDGEMENT

This work was financed by the Swedish Nuclear Power Inspectorate. The technical assistance of Mr Jörgen Gjödestål, Ingemar Larsson and Stig Lindgren is gratefully acknowledged.

REFERENCES

1. FRID, W
Statens Vattenfallverk EV-20/79
Stockholm (1979).
2. GREISS, J C and BACARELLA, A L
Nucl Technol 10, 546 (1971).
3. VAN ROOYEN, D
Hydrogen release rates from corrosion of zink
and aluminium.
Brookhaven Nat Lab, New York (1978).
BNL-NUREG-24532.
4. MACDONALD, D B and BUTLER, P
Corros Sci 13, 259 (1973).
5. BERZINS, A, EVANS, J V and LOWSON, R T
Australian Atomic Energy Commission
AAEC/E270 (1973)
ISBN 0 642 99585 0.
6. The Behaviour of Hydrogen During Accidents in
Light Water Reactors.
NUREG/CR-1561
SAND 80 - 1495.

3.6.2 Supplemental Information from Reference 18

CORROSION TYPES, INFLUENCED BY MECHANICAL FACTORS 109

Table 8.1 Spectrum of cracking phenomena in metals.

<i>Contribution of chemical and mechanical factors</i>	<i>Material</i>	<i>Environments</i>
Intergranular corrosion (without stress)	Austenitic steels	H ₂ SO ₄ ; HNO ₃ ; chloride solutions
Electrochemical stress corrosion cracking (corrosion-dominated)	Carbon steels	NaOH; NH ₄ NO ₃ ; Ca(NO ₃) ₂
	Au alloys	FeCl ₃
	Al alloys; Mg alloys	Chloride solutions
	Brass	NH ₃ ; amines
	Pure Cu	Cu(NH ₃) ₂ ⁺ ; Cu-acetate; nitrites
	Austenitic steels	Chloride solutions; H ₂ S; NaOH
Stress-sorption cracking in non-electrolytes (stress-dominated)	Ti alloys	Chloride solutions
	Inconel (74Ni 18Cr 8Ni)	NaOH
	Ferritic stainless steels	H ₂ O + H ₂ S
	Low-alloy steels	H ₂ O + H ₂ S
	Low-alloy steels	Pure H ₂ O; pure NH ₃
	Low-alloy steels	Pure H ₂
	Ti alloys	CCl ₄ ; pure alcohols; molten Cd
	Al alloys	CCl ₄ ; pure alcohols; molten Zn; Ga
	Brass; Ti alloys; Al alloys	Hg
Brittle fracture (without corrosion)	Highly stressed, embrittled metals	Inert atmospheres

according to Section 6.6.3, which occurs in the absence of applied stress, over electrochemical SCC in electrolytes and stress-sorption cracking of metals in non-electrolytes to pure brittle fracture, which occurs without the influence of corrosive influences. This spectrum is shown in Table 8.1. The order of sequence from corrosion-dominated to stress-dominated cases is uncertain, however.

Stress corrosion cracking of austenitic 18/8 steel in chloride solutions is of particular importance (Fig. 8.4). This system has therefore been investigated thoroughly, particularly by potentiostatic technique (Figs 8.5 and 8.6). It has been found that a certain time elapses before the first cracks show up. During this induction period (incubation period) a breakthrough of the passivating oxide film on the steel surface occurs. The reactions going on during the induction period are little influenced by the stress conditions of the metal. The end of the induction period is marked by the occurrence of the first crack. The length of the induction period decreases considerably



Fig. 8.4 Coffee boiler of stainless 18/8 steel showing stress corrosion cracking. The chloride content of the water in the heating jacket was originally below 50 mg l^{-1} but was increased considerably through evaporation. Courtesy of S. Henriksson, Avesta Jernverks AB.

with increasing chloride concentration and with increasing temperature. Below 60°C , SCC of austenitic steel does not occur at all. The induction period is considerably longer than the crack period, during which the cracks propagate. The induction period is therefore the dominating time factor for an austenitic material which is subjected to SCC. A cathodic current prolongs the induction period and a sufficient cathodic current prevents the occurrence of the crack period entirely. Contact of the stainless steel with a less noble metal, such as aluminium, zinc, carbon steel or lead, has the same effect.

CORROSION TYPES, INFLUENCED BY MECHANICAL FACTORS 111

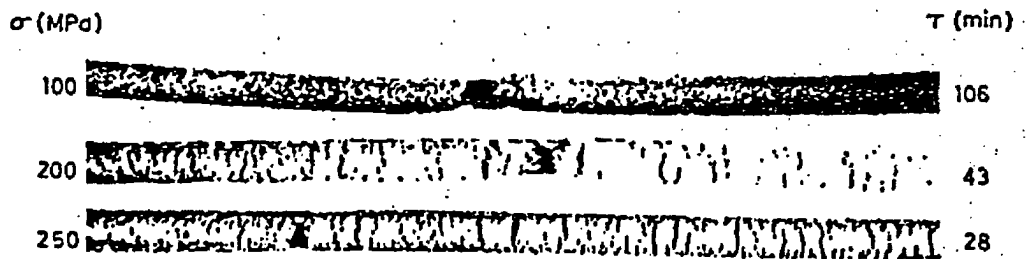


Fig. 8.5 Increase in the number of stress corrosion cracks with increasing tensile load at constant anodic polarization ($e_h = 0$ mV) of test wires, $\phi = 1.5$ mm, of austenitic steel (18 Cr:9 Ni, annealed, $\sigma_{0.2} = 310$ MPa, $\sigma_B = 820$ MPa); $\sigma =$ applied tensile stress, $\tau =$ times to fracture. The test solution consisted of 45% $MgCl_2$, b.p. $154^\circ C$, thermostated at $140^\circ C$.

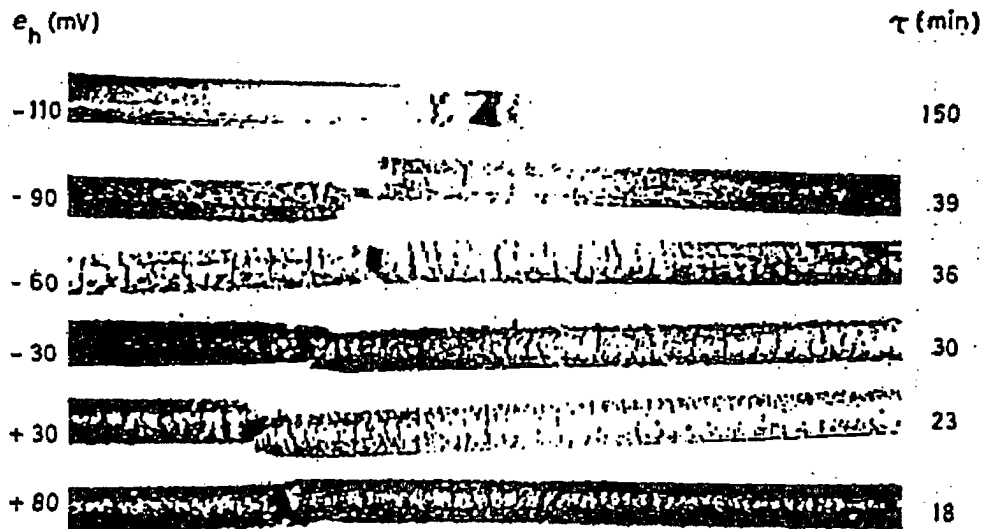


Fig. 8.6 Increase in the number of stress corrosion cracks with increasing anodic polarization of stressed ($\sigma = 305$ MPa) test wires, $\phi = 1.5$ mm, of austenitic steel (18 Cr:9 Ni, annealed, $\sigma_{0.2} = 310$ MPa, $\sigma_B = 820$ MPa); $e_h =$ test potential relative to NHE; $\tau =$ time to fracture in min. The test solution 45% $MgCl_2$, b.p. $154^\circ C$, thermostated at $140^\circ C$.

For austenitic stainless steels, the rate by which a crack propagates amounts to 0.5–1 mm/h. After the induction period has elapsed the penetration of a steel plate, a few mm thick, will therefore occur in a matter of hours. The crack propagation in austenitic steels seems to be continuous, whereas in certain other cases (Mg alloys, brass) it seems to be discontinuous (jerky).

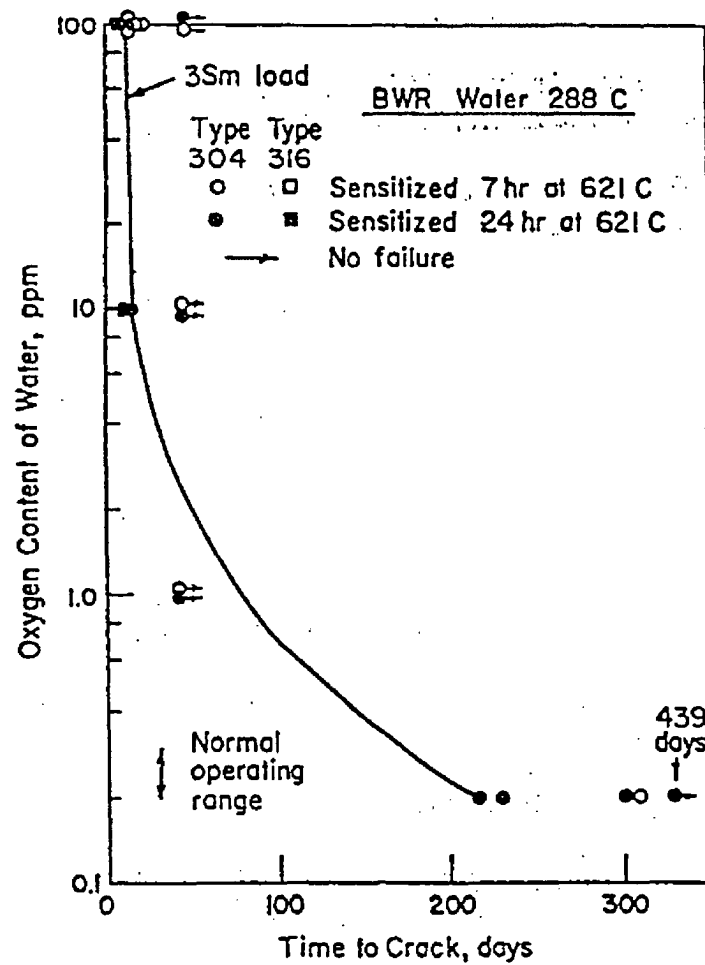
Just as in pitting, the anions causing SCC must be able to activate the metal at certain points, despite the presence of a passivating oxide film. For austenitic steels, the strongly polarizable (see Section 1.3.3) heavy halogenide ions (Cl^- , Br^- , I^-) are active in initiating SCC. Due to their general occurrence, chloride ions have the greatest practical importance. As with pitting and crevice corrosion, SCC in austenitic steels seems to be initiated at sulphide inclusions. In acid media, H_2S alone (in the absence of halogenide ions) may cause SCC in austenitic steels. Although only the anions cause SCC in austenitic steels, the cations influence the time and temperature needed for cracking to occur. Concentrated MgCl_2 solution is particularly efficient and is therefore often used in laboratory testing (Figs 8.5 and 8.6). This is probably so because (a) Mg^{2+} is strongly hydrolysed, giving an acid solution and (b) concentrated MgCl_2 has an exceptionally high activity coefficient (> 1), reducing the pH still further. Chlorides of oxidizing cations, such as Hg^{2+} , Cu^{2+} and Fe^{3+} , do not cause SCC but just pitting. This is true also of a very high anodic polarization. In practice, common chlorides, such as those of Na, K and Ca, are usually the cause of SCC. At moderate temperatures (100°C), the locally required chloride concentration seems to be fairly high (about 15% Cl^-), but several powers of ten lower at higher temperatures. Local increase of concentration may easily occur in apparatus in operation, e.g. due to local boiling. To this must be added the chloride-enriching effect of the corrosion current, which in the induction period, may be generated by pitting or crevice corrosion, which also, by hydrolysis of dissolved Cr^{3+} and Mo^{3+} ions, leads to local acidification. At high temperatures and in the presence of crevices, SCC in austenitic materials (e.g. in steam generators) may be observed at chloride concentrations well below 1 p.p.m. (1 mg/l).

Besides chloride ions, oxygen or some other oxidizing agent for the maintenance of the cathode process must be present in the solution in order that SCC of stainless steel shall occur. Oxidizing inhibitors as chromate may counteract SCC by passivation, however. If the oxygen content increases, a smaller amount of chloride is necessary to cause crack formation. In contrast, if the chloride concentration increases, less oxygen is necessary. It has therefore been suggested that the product of chloride concentration and oxygen concentration must attain a certain minimum for SCC to occur. The presence of pure hydrogen or nitrogen above the solution eliminates SCC of austenitic steels entirely. On the other hand, the active metal exposed within the advancing crack reacts with the acidified crack solution and hydrogen is evolved. It therefore seems possible that embrittlement due to atomic hydrogen plays a part in the SCC of austenitic steels. As we shall see below, hydrogen is usually of decisive importance in the stress cracking of ferritic steels.

Practically all austenitic Fe-Cr-Ni alloys are susceptible to SCC in chloride media. The ferritic alloys are less susceptible to cracking in

3.6.3 Supplemental Information from Reference 19

Sensitized Stainless Steel: Effect of Dissolved Oxygen on Time-to-Cracking



Effect of dissolved oxygen level on time-to-cracking of sensitized stainless steel specimens stressed to 3 Sm in water at 288 °C (Sm = 90% of yield stress at 288 °C).

3.7 References

1. American Society of Mechanical Engineers, ASME Boiler and Pressure Vessel Code, Sections II, III, V and IX, 1995 including 1996 addenda.
2. American National Standards Institute, ANSI N14.6, American National Standard for Special Lifting Devices for Shipping Containers Weighing 10,000 Pounds or More for Nuclear Materials, 1986.
3. ANSYS Engineering Analysis System, Users Manual for ANSYS Rev. 6.0, Swanson Analysis Systems, Inc., Houston, PA, 2001.
4. NUREG/CR-6007 "Stress Analysis of Closure Bolts for Shipping Casks", By Mok, Fischer, and Hsu, Lawrence Livermore National Laboratory, 1992.
5. WRC Bulletin 107, March 1979 Revision "Local Stresses in Spherical and Cylindrical Shells Due to External Loadings."
6. USNRC Spent Fuel Project Office, Interim Staff Guidance Memo ISG-11 rev 3, "Cladding Considerations for the Transportation and Storage of Spent Fuel," November 2003.
7. PNL-4835, "Technical Basis for Storage of Zircaloy Clad Spent Fuels in Inert Gases.
8. Rust, J. "Nuclear Power Plant Engineering", Haralson Publishing Company, Georgia, 1979.
9. NUREG/CR-0497 "MATPRO-Verson 11: A Handbook of Materials Properties for Use in the Analysis of Light Water Reactor Fuel Rod Behavior", By EG&G, Inc., 2/1979.
10. Dynamic Impact Effects on Spent Fuel Assemblies, By Chun, Witte, and Schwartz, Lawrence Livermore National Laboratory, 10/1987.
11. Machine Design, August 17, 1967, "Eccentrically Loaded Joints", Richard T. Berger.
12. Hydrogen Generation Analysis Report for TN-68 Cask Materials, Test Report No. 61123-99N, Rev 0, Oct 23, 1998, National Technical Systems
13. Brooks and Perkins , Boral Product Performance Report 624.

14. Baratta, et al. Evaluation of Dimensional Stability and Corrosion Resistance of Borated Aluminum, Final Report submitted to Eagle-Picher Industries, Inc. by the Nuclear Engineering Department, Pennsylvania State University.
15. Pacific Northwest Laboratory Annual Report - FY 1979, Spent Fuel and Fuel Pool Component Integrity, May, 1980.
16. H. H. Uhlig, Corrosion and Corrosion Control, 2nd ed., Wiley 1971
17. BNL-NUREG-24532, Hydrogen Release Rates from Corrosion of Zinc and Aluminum, 1978
18. G. Wranglen, An Introduction to Corrosion and Protection of Metals, Chapman and Hall, 1985, pp. 109-112.
19. A.J. McEvily, Jr., ed., Atlas of Stress Corrosion and Corrosion Fatigue Curves, ASM Int'l, 1995, p. 185.
20. Aluminum Association Catalog, Aluminum Standards and Data, 1990.
21. Regulatory Guide 7.11, "Fracture Toughness criteria of Base Material for ferritic steel shipping Cask Confinement Vessels With a Maximum Wall thickness of 4 Inches (0.1m).
22. Regulatory Guide 7.12, "Fracture Toughness criteria of Base Material for ferritic steel shipping Cask Confinement Vessels With a Wall thickness Greater Than 4 Inches (0.1m), But not Exceeding 12 Inches (0.3m).
23. Harper, Charles A., ed., Handbook of Plastics and Elastomers, McGraw-Hill, 1975.
24. K.J. Geelhood and C.E. Beyer, PNNL Stress/Strain Correlation for Zircaloy, March 2005.

TABLE 3.1-1

INDIVIDUAL LOAD CASES ANALYZED

COMPONENT/ ANALYSIS	LOADING	SAR SECTION	INDIVIDUAL STRESS RESULT TABLES
CASK BODY			
Bolt Preload	Preload	3A.2.3.1	3A.2.3-1 3A.2.3-2
Gravity	1G down	3A.2.3.1	3A.2.3-3 3A.2.3-4
Internal Pressure (1)	100 PSI	3A.2.3.1	3A.2.3-5 3A.2.3-6
External Pressure (1)	25 PSI	3A.2.3.1	3A.2.3-7 3A.2.3-8
Thermal Stress	Short Term Temperatures	3A.2.3.1	3A.2.3-9 3A.2.3-10
Lifting	6G on Upper Trunnions	3A.2.3.1 3.4.3	3A.2.3-11 3A.2.3-12 Section 3.4-3
Seismic Load (1)	2G Down + 1G lateral	3A.2.3.1 2.2.3	3A.2.3-17 3A.2.3-18
Tipover	1G Side Drop	3A.2.3.2	3A.2.3-13 3A.2.3-14 3A.2.3-15 3A.2.3-16
LID BOLTS			
Preload	Preload Tension	3A.3	---
Thermal Effects	Differential Expansion	3A.3	---
Torquing	Preload Torsion	3A.3	---
Pressure	100 psi	3A.3	---
Impact	Tip Over - 65 G	3A.3	---

TABLE 3.1-1(Continued)⁽³⁾

INDIVIDUAL LOAD CASES ANALYZED

COMPONENT/ ANALYSIS	LOADING	SAR SECTION	INDIVIDUAL STRESS RESULTS TABLES
BASKET			
Bounding Side Load (2)	1 G Lateral	3B.3.2	3B.3-1 through 3B.3-4
Bounding Down Load (2)	3 G Down	3B.3.3	---
Hypothetical Accident	End Drop	3B.4.1	---
Hypothetical Accident	Tipover	3B.4.2	3B.4-1 through 3B.4-4
TRUNNIONS			
Lifting	6 g and 10 g	3.4.3	3.4-2

NOTES:

1. The above pressures and bounding loads conservatively envelope all possible pressure effects as well as tornado wind load, flood water load and seismic load.
2. The bounding loads selected for basket evaluation are extremely conservative. These loads are more severe than any loads that will actually be applied to the basket.
3. Local loads and stresses due to tornado driven missiles are evaluated in Chapter 2, Section 2.2.1.3.

TABLE 3.1-2

CONFINEMENT VESSEL STRESS LIMITS ⁽³⁾

CLASSIFICATION	STRESS INTENSITY LIMIT ⁽³⁾
Normal (Level A) Conditions(1)	
P_m	S_m
P_1	$1.5 S_m$
$(P_m \text{ or } P_1) + P_b$	$1.5 S_m$
Shear Stress	$0.6 S_m$
Bearing Stress	S_y
$(P_m \text{ or } P_1) + P_b + Q$	$3 S_m$
$(P_m \text{ or } P_1) + P_b + Q + F$	S_a
Hypothetical Accident (Level D)(2)	
P_m	Smaller of $2.4 S_m$ or $0.7 S_u$
P_1	Smaller of $3.6 S_m$ or S_u
$(P_m \text{ or } P_1) + P_b$	Smaller of $3.6 S_m$ or S_u
Shear Stress	$0.42 S_u$

NOTES:

1. Classifications and Stress Intensity Limits are as defined in ASME B&PV Code, Section III, Subsection NB.
2. Stress intensity limits are in accordance with ASME B&PV Code, Section III, Appendix F.
3. When using materials data from ASME B&PV Code Section II, Part D Tables other than 2A, S values may be substituted for S_m values in these expressions.

TABLE 3.1-3

CONFINEMENT BOLT STRESS LIMITS ⁽¹⁾⁽⁵⁾

CLASSIFICATION	STRESS INTENSITY LIMIT
Normal (Level A) Conditions ⁽²⁾	
Average Tensile Stress	2 S _m
Maximum Combined Stress	3 S _m
Bearing Stress	S _y
Hypothetical Accident (Level D) ⁽³⁾	
Average Tensile Stress	Smaller of S _y or 0.7 S _u
Average Shear Stress	Smaller of 0.4 S _u or 0.6 S _y
Maximum Combined Stress	S _u
Combined Shear & Tension	$R_t^2 + R_s^2 < 1^{(4)}$

NOTES

1. The stress analysis of the lid bolt is performed in accordance with NUREG/CR-6007⁽⁴⁾ described in Appendix 3A.3. The stress limits for the lid bolt are listed separately in Tables 3A.3-3 and -4.
2. Classification and stress limits are as defined in ASME B&PV Code, Section III, Subsection NB.
3. Stress limits are in accordance with ASME B&PV Code, Section III, Appendix F.
4. R_t : Ratio of average tensile stress to allowable average tensile stress
R_s : Ratio of average shear stress to allowable average shear stress
5. All stresses include the effect of tensile and torsional loads due to bolt preloading.

TABLE 3.1-4

NON CONFINEMENT STRUCTURE STRESS LIMITS

CLASSIFICATION	STRESS INTENSITY LIMIT (3)
Normal (Level A) Conditions (1)	
P_m	S_m
P_l	$1.5 S_m$
$(P_m + P_l) + P_b$	$1.5 S_m$
$(P_m + P_l) + P_b + Q$	$3 S_m$
Shear Stress	$0.60 S_m$
Bearing Stress	S_y
Hypothetical Accident (Level D)(2)	
P_m	Smaller of $2.4 S_m$ or $0.7 S_u$
P_l	Smaller of $3.6 S_m$ or S_u
$(P_m + P_l) + P_b$	Smaller of $3.6 S_m$ or S_u
Shear Stress	$0.42 S_u$

NOTES:

1. Classifications and stress intensity limits are as defined in ASME B&PV Code, Section III, Subsection NB.
2. Stress intensity limits are in accordance with ASME B&PV Code, Section III, Appendix F.
3. When using materials data from ASME B&PV Code, Section II, Part D Tables other than 2A, S values may be substituted for S_m values in these expressions.

TABLE 3.1-5⁽⁴⁾

BASKET STRESS LIMITS

CLASSIFICATION	STRESS INTENSITY LIMIT (3)
Normal (Level A) Conditions (1)	
P_m	S_m
P_l	$1.5 S_m$
$(P_m + P_l) + P_b$	$1.5 S_m$
$(P_m + P_l) + P_b + Q$	$3 S_m$
$(P_m + P_l) + P_b + Q + F$	S_a
Shear Stress	$0.6 S_m$
Hypothetical Accident (Level D)(2)	
P_m	Smaller of $2.4 S_m$ or $0.7 S_u$
P_l	Smaller of $3.6 S_m$ or S_u
$(P_m + P_l) + P_b$	Smaller of $3.6 S_m$ or S_u
Shear Stress	Smaller of $0.42 S_u$ or $2(0.6 S_m)$

NOTES

1. Classifications and stress intensity limits are as defined in ASME B&PV Code, Section III, Subsection NG.
2. Limits are in accordance with ASME B&PV Code, Section III, Appendix F.
3. When using materials data from ASME B&PV Code, Section II, Part D Tables other than 2A, S values may be substituted for S_m values in these expressions.
4. Stability is also evaluated under compressive loading. See Section 3B.5.

TABLE 3.2-1

CASK WEIGHT AND CENTER OF GRAVITY

COMPONENT	NOMINAL WEIGHT (lbs. x 1000)	CENTER OF GRAVITY (Inches)*
Body	94.4	101.1
Bottom	15.6	4.875
Lid and Lid Bolts	12.3	192.25
Neutron Shield Aluminum Boxes	2.5	93.25
Resin	13.9	93.25
Outer Shell	11.2	93.25
Resin Disk	0.9	199.25
Trunnions - Upper	0.8	173.25
- Lower	0.9	27.41
Protective Cover	0.8	203.7
Basket and Rails	25.9	91.75
Shield Ring	1.4	182.75
Basket Hold Down Ring	1.4	180.5
Fuel Assemblies	47.9	91.75
Overpressure Tank, Drain Tube	0.1	205.6
Cask Weight w/o Protective Cover and Resin Disk	228.3	96.38
Weight on Storage Pad	230.0	97.22**

* Center of Gravity is measured along the axial centerline from the base of the cask; 97.26 is conservatively used for stability analysis.

** For the damaged fuel configuration, the weight of damaged fuel extensions and end caps is added to the basket, the holddown ring weight is reduced, and the eight damaged fuel assemblies are raised about 0.25 inch. The net effect is to reduce the weight by 65 lb and to lower the center of gravity to 97.16 inches.

Summary of weight used for Analysis:

- | | |
|---------------------------------------|--------------|
| 1. Stability of Cask | 227,000 lbs. |
| 2. Accident G Load Calculations | 229,600 lbs. |
| 3. Trunnion and Local Stress Analysis | 240,000 lbs. |
| 4. Cask Body Analysis | 240,000 lbs. |

TABLE 3.3-1

MECHANICAL PROPERTIES OF BODY MATERIALS (NOTE 1)

Material Specification (Nominal Composition)	Application	Minimum Yield Strength S_y , psi	Minimum Ultimate Strength S_u , psi	Design Stress Value, Psi (Note 2)	Data Source (Note 3)
ASME SA-350, Grade LF3 (3 ½ Ni)	Flange Confinement Lid	37,500	70,000	$S_m=23,300$	Table 2A
ASME SA-203, Grade E (3-1/2 Ni)	Confinement Lid Confinement Shell	40,000	70,000	$S_m=23,300$	Table 2A
ASME SA-266, Class 2 (C-Si)	Gamma Shielding	36,000	70,000	$S= 20,000$	Table 1A
ASME SA-516, Gr. 70 (C-Mn-Si)	Outer Shell Lid Shield Plate, Protective Cover	38,000	70,000	$S= 20,000$	Table 1A
ASME SA-105, (C-Si)	Lower Trunnion	36,000	70,000	$S= 17,500$	Table 1A
ASME SA-182 Gr. F6 NM (13 Cr – 4 Ni)	Upper Trunnion	90,000	115,000	$S_m= 32,900$	Table 2A
ASME SA-540 Gr. B24 Cl. 1 (2Ni-3/4 Cr-1/3 Mo)	Lid Bolts	150,000	165,000	$S_m= 50,000$	Table 4
ASME SA-320, Grade L43 (1 ¼ Ni-3/4 Cr - ¼ Mo)	Upper Trunnion Bolts	105,000	125,000	$S_m= 35,000$	Table 4

TABLE 3.3-1(continued)

MECHANICAL PROPERTIES OF BODY MATERIALS (NOTE 1)

NOTES:

1. Mechanical properties listed are for metal temperatures up to 100°F to provide a baseline comparison of all structural materials.
Temperature dependent properties required for structural analysis are provided in Table 3.3-2.
2. Values listed are the stress parameters which form the basis for structural analysis acceptance criteria.
S refers to the ASME allowable stress for Class 2 or Class 3 components,
 S_m refers to the ASME design stress intensity for Class 1 components, and S_y
refers to minimum yield strength.
3. Data are taken from tables in ASME Section II, Part D, 1998 including 2000 Addenda, unless otherwise noted.

TABLE 3.3-2

TEMPERATURE DEPENDENT BODY MATERIAL PROPERTIES (SHEET 1 OF 4)

COEFFICIENTS OF THERMAL EXPANSION (NOTE 1)

Material/Temp., °F	100	150	200	250	300	350	400	450	500	550	600
SA350,SA320, SA540, SA203 (Note 2)	6.5	6.6	6.7	6.8	6.9	7.0	7.1	7.2	7.3	7.3	7.4
SA105,SA266 and SA516 (Note 2)	6.5	6.6	6.7	6.8	6.9	7.0	7.1	7.2	7.3	7.3	7.4
SA182 Gr F6NM (Note 2)	6.0	6.1	6.2	6.2	6.3	6.4	6.4	6.4	6.5	6.5	6.5

NOTES:

1. Values listed are the mean coefficients of thermal expansion $\times 10^{-6}$ (in./in.°F) from 70°F to the indicated temperature.
2. Source of data is ASME Section II, Part D, 1998 including 2000 Addenda, Table TE-1.

TABLE 3.3-2

TEMPERATURE DEPENDENT BODY MATERIAL PROPERTIES (SHEET 2 OF 4)

MODULUS OF ELASTICITY, E (NOTE 1)

MATERIAL/ TEMPERATURE °F	70	200	300	400	500	600
SA-203, SA-320, SA-540 and SA-350 (Note 2)	27.8	27.1	26.7	26.1	25.7	25.2
SA-105, SA-266 And SA-516 (Note 2)	29.5	28.8	28.3	27.7	27.3	26.7
SA-182 Gr F6 NM (Note 2)	29.2	28.5	27.9	27.3	26.7	26.1

NOTES:

1. Values listed are the modulus of elasticity x 10⁶ psi for the indicated temperature.
2. Source of data is ASME SECTION II, Part D, 1998 including 2000 addenda, Table TM-1.

TABLE 3.3-2

TEMPERATURE DEPENDENT BODY MATERIAL PROPERTIES (SHEET 3 OF 4)

MATERIAL	STRESS PARAMETER (NOTE 1)	100°F	200°F	300°F	400°F	500°F	600°F	DATA SOURCE (NOTE 2)
SA-350, Gr. LF3	S _m	23.3	22.8	22.2	21.5	20.2	(Note 4)	Table 2A Table Y-1 Table U
	S _y	37.5	34.3	33.2	32.0	30.4	28.2	
	S _u	70.0	70.0	70.0	70.0	70.0	70.0	
SA-203, Grade E	S _m	23.3	23.3	23.3	22.9	21.6	(Note 4)	Table 2A Table Y-1 Table U
	S _y	40.0	36.6	35.4	34.2	32.5	30.0	
	S _u	70.0	70.0	70.0	70.0	70.0	70.0	
SA-266 Class 2	S	20.0	20.0	20.0	20.0	19.6	18.4	Table 1A Table Y-1 Table U
	S _y	35.0	32.1	31.0	29.9	28.5	26.8	
	S _u	70.0	70.0	70.0	70.0	70.0	70.0	
SA-516 Grade 70	S	20.0	20.0	20.0	20.0	20.0	19.4	Table 1A Table Y-1 Table U
	S _y	38.0	34.8	33.6	32.5	31.0	29.1	
	S _u	70.0	70.0	70.0	70.0	70.0	70.0	
SA-105	S	20.0	20.0	20.0	20.0	19.6	18.4	Table 1A Table Y-1 Table U
	S _y	36.0	33.0	31.8	30.8	29.3	27.6	
	S _u	70.0	70.0	70.0	70.0	70.0	70.0	
SA-182 Gr. F6 NM	S _m	38.3	38.3	38.3	37.9	36.6	35.0	Table 2A Table Y-1 Table U
	S _y	90.0	86.5	84.6	82.8	80.8	78.5	
	S _u	115.0	115.0	115.0	113.6	109.7	105.1	
SA-540 Gr. B24, CL.1 (Bolt)(Note3)	S _m	50.0	47.8	46.2	44.8	43.4	41.4	Table 4 3S _m Table 3
	S _y	150.0	143.4	138.6	134.4	130.2	124.2	
	S _u	165.0	165.0	165.0	165.0	165.0	165.0	
SA-320, Gr. L43 (Bolt)(Note3)	S _m	35.0	33.0	31.9	30.6	29.5	28.1	Table 4 3S _m Table 3
	S _y	105.0	99.0	95.7	91.8	88.5	84.3	
	S _u	125.0	125.0	125.0	125.0	125.0	125.0	

TABLE 3.3-2

TEMPERATURE DEPENDENT BODY MATERIAL PROPERTIES (SHEET 4 OF 4)

NOTES FOR SHEET 3 OF 4:

1. Values listed are the stress parameters which form the basis for structural analysis acceptance criteria. S refers to the ASME allowable stress for Class 2 or Class 3 components, or Section VIII, Division 1. S_m refers to the ASME design stress intensity for Class 1 components, and S_y refers to minimum yield strength.
2. Data is taken from ASME Section II, Part D, 1998 including 2000 addenda.
3. For bolting materials, $S_y \geq 3 S_m$.
4. Properties are not available at 600F in ASME Section II, Part D.

TABLE 3.3-3

REFERENCE TEMPERATURES FOR
STRESS ANALYSIS ACCEPTANCE CRITERIA*

Component	Max. Calculated Temperature, °F	Selected Design** Temperature, °F
Cask Body	314	400
Cask Lid	212	400
Lid Bolts	212	300
Trunnions	227	300
Upper Trunnion Bolts	227	300

* For thermal stress due to fire accident, see Section 3.4.6.

** Temperatures specified are used to determine allowable stresses. They are not a maximum use temperature for the material.

TABLE 3.3-4

MECHANICAL PROPERTIES OF BASKET MATERIALS (NOTE 1)

Material Specification (Nominal Composition)	Minimum Yield Strength S_y , psi	Minimum Ultimate Strength S_u , psi	Design Stress Value, psi (Note 2)	Data Source (Note 3)
ASME SA-240, Type 304 (Basket Plates)	30,000	75,000	$S_m = 20,000$	Table 2A
ASME SB 221, 6061-T6 Aluminum (Aluminum Rails)	35,000	38,000	$S = 10,900$	Table 1B

NOTES

1. Mechanical properties listed are for metal temperatures up to 100°F to provide a baseline comparison of all structural materials.

Temperature dependent properties required for structural analysis are provided in Table 3.3-5.

2. Values listed are the stress parameters which form the basis for structural analysis acceptance criteria.

S refers to the ASME allowable stress for Class 2 or Class 3 components, S_m refers to the ASME design stress intensity for Class 1 components, and S_y refers to minimum yield strength.

3. Data is taken from tables in ASME Section II, Part D, 1998 including 2000 addenda unless otherwise noted.

TABLE 3.3-5

TEMPERATURE DEPENDENT BASKET MATERIAL PROPERTIES (SHEET 1 OF 3)

COEFFICIENTS OF THERMAL EXPANSION (Note 1)

TEMPERATURE, °F											
MATERIAL	100	150	200	250	300	350	400	450	500	550	600
SA 240, TYPE 304	8.6	8.8	8.9	9.1	9.2	9.3	9.5	9.6	9.7	9.8	9.8
SB-221, 6061-T6 ALUMINUM	12.4	12.7	13.0	13.1	13.3	13.4	13.6	13.8	13.9	14.1	14.2

1. Values listed are the mean coefficients of thermal expansion x 10⁻⁶ (in./in.°F from 70°F to the indicated temperature).
2. Source of data is ASME Section II, Part D, 1998 including 2000 addenda.

TABLE 3.3-5

TEMPERATURE DEPENDENT BASKET MATERIAL PROPERTIES (SHEET 2 OF 3)

MODULI OF ELASTICITY, E (Note 1)

TEMPERATURE, °F						
MATERIAL	70	200	300	400	500	600
SA-240, TYPE 304 STAINLESS STEEL	28.3	27.6	27.0	26.5	25.8	25.3
SB-221, 6061-T6 ALUMINUM	10.0	9.6	9.2	8.7	8.1	

NOTES:

1. Values listed are the moduli of elasticity x 10^6 psi for the indicated temperature.
2. Source of data is ASME Section II, Part D, 1998 including 2000 addenda.

TABLE 3.3-5

TEMPERATURE DEPENDENT BASKET MATERIAL PROPERTIES (SHEET 3 OF 3)

DESIGN STRESS PARAMETERS

		TEMPERATURE, °F						
MATERIAL	STRESS PARAMETER (KSI) (NOTE 1)	100	200	300	350	400	500	DATA SOURCE
ASME SA-240 Type 304	S_y	30.0	25.0	22.4	21.6	20.7	19.4	Table Y-1 (NOTE 2)
	S_u	75.0	71.0	66.2	65.1	64.0	63.4	Table U
	S_m	20.0	20.0	20.0	19.4	18.7	17.5	TABLE 2A
ASME SB-221 Alloy 6061-T6 (Aluminum)	S_y	35.0	33.7	27.4	20.0	13.3		TABLE Y-1
	S_u	38.0	35.5	28.7	22.4	16.0		NOTE 3
	S	10.9	10.9	7.9	6.3	4.5		TABLE 1B

NOTES:

1. Values listed are the stress parameters which form the basis for structural analysis acceptance criteria.
2. S_m refers to the ASME design stress intensity for Class 1 components, and S_y refers to minimum yield strength. S_u refers to minimum ultimate strength.
3. S_u is available in ASME Section II, Part D only at room temperature. For elevated temperatures, S_u was obtained by ratioing S_u data in Aluminum Association "Aluminum Standards and Data" 1990. (Reference 20)

Table 3.3-6
TN-68 Cask Components and Materials
Sheet 1 of 3

Materials and Components of TN-68 Cask					
Primary Function	Component	Drawing	Safety Class.	Codes/Standards	Material
Containment	Lid	972-70-2 It.2	A	ASME Subsection NB	SA-350, LF3 or SA-203 Gr. E
	Inner Containment	972-70-2 It.3	A	ASME Subsection NB	SA-203 Gr. E
	Bottom Containment	972-70-2 It.5	A	ASME Subsection NB	SA-203 Gr. E
	Flange	972-70-2 It.35	A	ASME Subsection NB	SA-350, LF3
	Lid Bolt (48)	972-70-2 It.14	A	ASME Subsection NB	SA-540 Gr. B24 Cl. 1
	Lid Seal	972-70-2 It.16	A		Double Metallic O-Ring
	Drain Port Cover	972-70-2 It.22	A	ASME Subsection NB	SA-240, Type 304
	Vent Port Cover	972-70-2 It.23	A	ASME Subsection NB	SA-240, Type 304
	Threaded Insert	972-70-2 It. 45	A		304 SST
	Vent & Drain Port Cover Seal	972-70-2 It.24	A		Double Metallic O-Ring
	Vent & Drain Port Cover Bolts	972-70-2 It.25	A	ASME Subsection NB	SA-193 Gr. B7
Criticality	Poison Plates	972-70-2 It.33	A		Borated Aluminum or Boron Carbide /Aluminum Metal Matrix Composite
	Control	Basket Rail Type 1	972-70-2 It.28	A	B221, 6061-T6 Aluminum
		Basket Rail Type 2	972-70-2 It.29	A	B221, 6061-T6 Aluminum
	Basket Shim	972-70-2 It.30	A		SA-240 Type 304, SA-336 Type 304, or SA-351 CF-3
	Fuel Compartment	972-70-2 It.32	A	ASME Subsection NG	SA-240 Type 304
	Structural Plates	972-70-2 It.34	A	ASME Subsection NG	SA-240 Type 304
	Basket Holddown	972-70-2 It.39	A	ASME Subsection NF	SA-240 Type 304
Shielding	Gamma Shield	972-70-2 It. 1	A	ASME Subsection NF	SA-266 Class 2
	Shield Plate	972-70-2 It.8	B	ASME Subsection NF	SA-105 or SA-516, Gr. 70
	Bottom	972-70-2 It.4	A	ASME Subsection NF	SA-516 Gr. 70 or SA-266 Cl. 2
	Radial Neutron Shield	972-70-2 It. 9	B		Borated Polyester Resin
	Outer Shell	972-70-2 It. 10	B		SA-516 Gr. 70
	Soc. Head Cap Screw	972-70-2 It. 47	B		304 SST
	Shim	972-70-2 It. 36	A		SA-516 Gr. 70
Top Neutron Shield	972-70-2 It. 12	B		Polypropylene	
Heat Transfer	Radial Neutron Shield Box	972-70-2 It. 13	B		6063-T5 Aluminum
	Poison Plates	972-70-2 It. 33	A		Borated Aluminum or Boron Carbide /Aluminum Metal Matrix Composite
	Basket Rail Shim	972-70-2 It. 31	B		6061-T6 Aluminum
	Basket Rail Type 1	972-70-2 It.28	A		B221, 6061-T6 Aluminum
	Basket Rail Type 2	972-70-2 It.29	A		B221, 6061-T6 Aluminum
	Basket Shim	972-70-2 It.30	A		SA-240 Type 304, SA-336 Type 304, or SA-351 CF-3
Structural Integrity	Gamma Shield	972-70-2 It.1	A	ASME Subsection NF	SA-266 Class 2
	Bottom	972-70-2 It.4	A	ASME Subsection NF	SA-516 Gr. 70 or SA-266 Cl. 2
Operations Support	Upper Trunnion	972-70-2 It. 6	A	ANSI N14.6	SA-182 Gr. F6NM
	Lower Trunnion	972-70-2 It. 7	B		SA-105
	Protective Cover	972-70-2 It. 11	C		SA-516 Gr. 70
	Protective Cover Bolt	972-70-2 It. 15	C		SA-193 Gr. B7
	Protective Cover Seal	972-70-2 It.17	C		Elastomer
	Top Neutron Shield Bolt	972-70-2 It.20	C		SA-193 Gr. B7
	Trunnion Bolt	972-70-2 It. 37	A		SA-320 L43
	Fuel Spacer	972-70-2 It. 38	C		Aluminum
	Shear Key	972-70-2 It. 40	A		SA-203 Gr. E
	Pressure Relief Valve	972-70-2 It. 41	C		SST
	Security Wire	972-70-2 It. 42	C		304 SST
	Security Wire Seal	972-70-2 It. 43	C		Lead
	Flat Washer	972-70-2 It. 46	C		SST
	Threaded Insert	972-70-2 It. 44	C		304 SST
	Quick Disconnect Couplings	972-70-3	C		SST
Lid Alignment Pin	972-70-2 It 27	C		A479, Type 316	
Leakage Monitoring Secondary Seal	Overpressure Port Cover	972-70-2 It. 18	C		SA-240 Type 304
	Overpressure Port Cover Seal	972-70-2 It. 19	C		Single Metallic O-ring
	Pressure Monitoring System	972-70-2 It. 21	C		Carbon Steel/Stainless Steel
	Overpressure Port Cover Bolts	972-70-2 It. 26	C		SA-193 Gr. B7

Table 3.3-6
TN-68 Cask Components and Materials
Sheet 2 of 3

Materials and Components of TN-68 Cask (cont.)				
Primary Function	Component	Strength (ksi)	Coating	Welding/Weld Filler Metal
Containment	Lid	70	SST Cladding on Sealing Surfaces; Epoxy Paint on External Surfaces	Per Section III, NB and Section IX
	Inner Containment	70	None	Per Section III, NB and Section IX
	Bottom Containment	70	None	Per Section III, NB and Section IX
	Flange	70	SST Cladding on Sealing Surfaces; Epoxy Paint on External Surfaces	Per Section III, NB and Section IX
	Lid Bolt (48)	165	Nuclear Grade Neolube or equiv.	N/A
	Lid Seal		None	N/A
	Drain Port Cover	75	None	N/A
	Vent Port Cover	75	None	N/A
	Threaded Insert	300	None	N/A
	Vent & Drain Port Cover Seal		None	N/A
	Vent & Drain Port Cover Bolts		Nuclear Grade Neolube or equiv.	N/A
	Criticality Control	Poison Plates		None
Basket Rail Type 1		38	None	N/A
Basket Rail Type 2		38	None	N/A
Basket Shim		75	None	Per Section III, NG and Section IX
Fuel Compartment		75	None	Per Section III, NG and Section IX
Structural Plates		75	None	Per Section III, NG and Section IX
Basket Holddown		75	None	Per Section III, NG and Section IX
Shielding	Gamma Shield	70	Epoxy Paint on Exterior	Per Section IX
	Shield Plate	70	None	Per Section IX
	Bottom	70	Epoxy Paint on Exterior	Per Section IX
	Radial Neutron Shield		None	
	Outer Shell	70	Epoxy Paint on Exterior	
	Soc. Head Cap Screw	70	None	
	Shim	70	None	
Top Neutron Shield		None		
Heat Transfer	Radial Neutron Shield Box		None	
	Poison Plates		None	
	Basket Rail Shim	38	None	
	Basket Rail Type 1	38	None	
	Basket Rail Type 2	38	None	
Basket Shim	75	None		
Structural Integrity	Gamma Shield	70	Epoxy Paint on Exterior	
	Bottom	70	Epoxy Paint on Exterior	
Operations Support	Upper Trunnion	115	Nuclear Grade Neolube or equiv.	
	Lower Trunnion	70	Epoxy Paint on Exterior	
	Protective Cover	70	Epoxy Paint on Exterior	
	Protective Cover Bolt		Nuclear Grade Neolube or equiv.	
	Protective Cover Seal		None	
	Top Neutron Shield Bolt		None	
	Trunnion Bolt	125	Nuclear Grade Neolube or equiv.	
	Fuel Spacer		None	
	Shear Key	70	None	
	Pressure Relief Valve		None	
	Security Wire		None	
	Security Wire Seal		None	
	Flat Washer		None	
	Threaded Insert		None	
Quick Disconnect Couplings		None		
Lid Alignment Pin		None		
Leakage Monitoring Secondary Seal	Overpressure Port Cover	75	None	
	Overpressure Port Cover Seal		None	
	Pressure Monitoring System		Epoxy Paint on Exterior	
	Overpressure Port Cover Bolts		Nuclear Grade Neolube or equiv.	

Table 3.3-6
TN-68 Cask Components and Materials
Sheet 3 of 3

Materials and Components of TN-68 Cask (cont.)									
Primary Function	Component	Stress		Normal Temp (deg F)**			Pressure		
		Normal Cond.	Accident Cond.	Min	Max	20 yr ***	Min (psig)	Max (psig)	Gas (type)
Containment	Lid	4.5	5.5	-20	212	204	0	100	Helium
	Inner Containment	25.8	53.3	-20	319	223	0	100	Helium
	Bottom Containment			-20	309	218	0	100	Helium
	Flange	3.1	29.6	-20	212	204	0	100	Helium
	Lid Bolt (48)	40.7	25	-20	212	204	0	100	Helium
	Lid Seal			-20	212	204	0	100	Helium
	Drain Port Cover			-20	212	204	0	100	Helium
	Vent Port Cover			-20	212	204	0	100	Helium
	Threaded Insert			-20	212	204	0	100	Helium
	Vent & Drain Port Cover Seal			-20	212	204	0	100	Helium
	Vent & Drain Port Cover Bolts	26	47.4	-20	212	204	0	100	Helium
Criticality	Poison Plates*			-20	595	359			
Control	Basket Rail Type 1	0.15	1	-20	382	258			
	Basket Rail Type 2	0.15	1	-20	382	258			
	Basket Shim	0.15	1	-20	350	258			
	Fuel Compartment*			-20	595	359			
	Structural Plates*	0.58	6.03	-20	595	359			
	Basket Holddown*			-20	595	359			
Shielding	Gamma Shield	25.3	55.3	-20	314	211			
	Shield Plate	2.8	5.4	-20	212	204			
	Bottom			-20	248	218	3	5	Air
	Radial Neutron Shield			-20	295	211			
	Outer Shell	4.5	9.1	-20	255	185	3	5	Air
	Soc. Head Cap Screw Shim			-20	255	185			
	Top Neutron Shield			-20	211	204			
Heat Transfer	Radial Neutron Shield Box			-20	295	211			
	Poison Plates			-20	595	359			
	Basket Rail Shim			-20	350	258			
	Basket Rail Type 1	0.15	1	-20	350	258			
	Basket Rail Type 2	0.15	1	-20	350	258			
	Basket Shim	0.15	1	-20	350	258			
Structural Integrity	Gamma Shield			-20	314	211			
	Bottom			-20	248	218	3	5	Air
Operations Support	Upper Trunnion	10.65		-20	227	223	3	5	Air
	Lower Trunnion			-20	284	223	3	5	Air
	Protective Cover			-20	176	185	3	5	Air
	Protective Cover Bolt	17		-20	176	204	3	5	Air
	Protective Cover Seal			-20	176	204			
	Top Neutron Shield Bolt			-20	211	204			
	Trunnion Bolt			-20	227	223			
	Fuel Spacer			-20	330	258			
	Shear Key			-20	362	258			
	Pressure Relief Valve			-20	225	211			
	Security Wire			-20	212	204			
	Security Wire Seal			-20	212	204			
	Flat Washer			-20	212	204			
	Threaded Insert			-20	212	204			
	Quick Disconnect Couplings			-20	212	204			
	Lid Alignment Pin			-20	212	204			
Leakage Monitoring Secondary Seal	Overpressure Port Cover			-20	211	204			
	Overpressure Port Cover Seal			-20	211	204			
	Pressure Monitoring System			-20	212	185	3	5	Air
	Overpressure Port Cover Bolts			-20	212	204			

* A value of 565 deg F is obtained during short-term drying.

** See SAR Tables 4.3-1, 4.3-2, and 4.4-1 for Additional Temperature Information

*** based on initial 21.2 kW thermal load

TABLE 3.4-1

UPPER TRUNNION SECTION PROPERTIES AND LOADS

ITEM	SECTION A-A
Cross Section Area, In ²	29.3
Area Moment Of Inertia, In ⁴	279.83
Yield Condition* Shear Force, Lbs	828,000
Yield Condition* Bending Moment, In- Lbs	1,705,680
Ultimate Condition ** Shear Force, Lbs.	1,380,000
Ultimate Condition ** Bending Moment, In-Lbs	2,842,800

* Trunnion Loads to Support (6 * 1.15) times Cask Weight

** Trunnion Loads to Support (10 * 1.15) times Cask Weight

TABLE 3.4-2

UPPER TRUNNION STRESSES WHEN LOADED
BY 6 AND 10 TIMES CASK WEIGHT

STRESS	YIELD LIMIT (ksi)
	SECTION A-A
Shear Stress	28.3
Bending Stress	29.8
Stress Intensity	63.9
Allowable Stress, S_y	84.6
	ULTIMATE LIMIT (ksi)
Shear Stress	47.1
Bending Stress	49.6
Stress Intensity	106.5
Allowable Stress	115.0

NOTE:

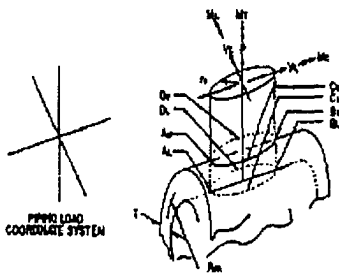
1. Sections A-A is shown on Figure 3.4-1.

TABLE 3.4-3

UPPER TRUNNION LOADINGS ON TN-68 FOR USE IN CASK BODY EVALUATION

Loading Description	Inertial Load	Max. Trunnion Load / Trunnion (Load Shared by 2 Top Trunnions)
Lifting Cask Vertical	$(6 * 1.15) G$	$V_L = 828,00 \text{ lbs.}$ $M_L = 6,218 \text{ in-kips}$

1. APPLIED LOADS
 RADIAL LOAD P _____ LB. VESSEL THICKNESS T _____ IN. $T = \frac{D \cdot P}{2 \cdot S}$
 CIRC. MOMENT M_c _____ IN-LB. ATTACHMENT RADIUS R _____ IN. $M_c = \frac{P \cdot R^2}{2}$
 LOAD MOMENT M_L _____ IN-LB. VESSEL RADIUS R_v _____ IN.
 TORSION MOMENT M_t _____ IN-LB.
 SHEAR LOAD V_x _____ LB.
 SHEAR LOAD V_y _____ LB.



NOTE: ENTER ALL FORCE VALUES IN ACCORDANCE WITH SIGN CONVENTION

FROM FIG.	READ CURVES FOR	COMPUTE ABSOLUTE VALUES OF STRESS AND ENTER RESULT	STRESSES - IF LOAD IS OPPOSITE THAT SHOWN, REVERSE SIGNS SHOWN								
			σ_x	σ_y	σ_z	τ_{xy}	τ_{yz}	τ_{zx}	τ_{xy}	τ_{yz}	
3C AND 4C	$\frac{M_c}{D \cdot T}$	$\frac{M_c}{D \cdot T}$	+	+	+	+	+	+	+	+	
1C AND 2C-1	$\frac{M_L}{R}$	$\frac{M_L}{R}$	+	-	+	-	+	-	+	-	
3A	$\frac{M_c}{D \cdot T}$	$\frac{M_c}{D \cdot T}$					-	-	+	+	
3A	$\frac{M_L}{R}$	$\frac{M_L}{R}$					-	+	+	-	
3B	$\frac{M_c}{D \cdot T}$	$\frac{M_c}{D \cdot T}$	-	-	+	+					
1B OR 1B-1	$\frac{M_L}{R}$	$\frac{M_L}{R}$	-	+	+	-					
ADD ALGEBRAICALLY FOR SUMMATION OF 1. STRESSES σ_1											
3C AND 4C	$\frac{M_c}{D \cdot T}$	$\frac{M_c}{D \cdot T}$	+	+	+	+	+	+	+	+	
1C-1 AND 2C	$\frac{M_L}{R}$	$\frac{M_L}{R}$	+	-	+	-	+	-	+	-	
4A	$\frac{M_c}{D \cdot T}$	$\frac{M_c}{D \cdot T}$					-	-	+	+	
2A	$\frac{M_L}{R}$	$\frac{M_L}{R}$					-	+	+	-	
4B	$\frac{M_c}{D \cdot T}$	$\frac{M_c}{D \cdot T}$	-	-	+	+					
2B OR 2B-1	$\frac{M_L}{R}$	$\frac{M_L}{R}$	-	+	+	-					
ADD ALGEBRAICALLY FOR SUMMATION OF 2. STRESSES σ_2											
SHEAR STRESS DUE TO TORSION M_t			$\tau_{xy} = \tau_{yz} = \tau_{zx} = \frac{M_t}{R \cdot T}$	+	+	+	+	+	+	+	
SHEAR STRESS DUE TO LOAD V_x			$\tau_{xy} = \frac{V_x}{A}$	+	+	-	-				
SHEAR STRESS DUE TO LOAD V_y			$\tau_{yz} = \frac{V_y}{A}$					+	+	-	-
ADD ALGEBRAICALLY FOR SUMMATION OF SHEAR STRESSES τ_1											

LONGITUDINAL σ_1
 PRESSURE STRESS $\frac{P \cdot R}{T}$ _____
 LONGITUDINAL BENDING STRESS _____
 TOTAL MEMBRANE STRESS _____
 TOTAL SURFACE STRESS _____

CIRCUMFERENTIAL σ_2

NOZZLE NO. _____
 PIPING LOAD CODE _____
 ANALYSIS POINT _____

COMPUTATION SHEET FOR LOCAL STRESSES IN CYLINDRICAL SHELLS	

BILLIARD COMPUTATION SHEET

TABLE 3.4-4

TABLE 3.4-5

COMPARISON OF ACTUAL WITH ALLOWABLE STRESS INTENSITY
CONFINEMENT VESSEL

Service Condition	Component	Stress Category	Stress Resultant Table	Maximum Stress Intensity (ksi)	Allowable Stress Intensity (ksi)
Normal Condition	Shell	P_m	3A.2.5-12 Location 16	—	22.9 (S_m)
		$P_m + P_b$	3A.2.5-12 Location 16	20.0	34.35 ($1.5S_m$)
	Flange	P_m	—	—	21.5 (S_m)
		$P_m + P_b$	3A.2.5-7 Location 20	1.0	32.25 ($1.5S_m$)
	Lid	P_m	—	—	21.5 (S_m)
		$P_m + P_b$	3A.2.5-7 Location 22	2.0	32.25 ($1.5S_m$)
Accident Condition	Shell	P_m	3A.2.5-21 Location 11	37.0	49.0 ($0.7S_u$)
		$P_m + P_b$	3A.2.5-21 Location 11	53.0	70.0 (S_u)
	Flange	P_m	—	—	49.0 ($0.7S_u$)
		$P_m + P_b$	3A.2.5-26 Location 19	30.0	70.0 (S_u)
	Lid	P_m	—	—	49.0 ($0.7S_u$)
		$P_m + P_b$	3A.2.5-18 Location 22	5.0	70.0 (S_u)

Note: If the primary plus bending stress for a particular component meets the primary membrane stress allowable, only the Normal Condition primary plus bending stress is reported

TABLE 3.4-6

COMPARISON OF ACTUAL WITH ALLOWABLE STRESS INTENSITY
GAMMA SHIELDING

Service Condition	Component	Stress Category	Stress Resultant Table	Maximum Stress Intensity (ksi)	Allowable Stress Intensity (ksi)
Normal Condition	Cylinder	P_m	3A.2.5-7 Location 36	—	20.0 (S)
		$P_m + P_b$	3A.2.5-7 Location 36	20.0**	30.0 (1.5S)
	Bottom	P_m	—	—	20.0 (S)
		$P_m + P_b$	3A.2.5-7 Location 23	16.0	30.0 (1.5S)
	Welds	P_m	—	—	17.5 (S)
		$P_m + P_b$	3A.2.5-7 Location 38	2.0	30.0 (1.5S)
Accident Condition	Cylinder	P_m	3A.2.5-26 Location 32	11.0	49.0 (0.7S _u)
		$P_m + P_b$	3A.2.5-26 Location 32	54.0	70.0 (S _u)
	Bottom	P_m	3A.2.5-26 Location 25	11.0	49.0 (0.7S _u)
		$P_m + P_b$	3A.2.5-26 Location 25	60.0	70 (3.6S _u)
	Welds	P_m	—	—	49.0 (0.7S _u)
		$P_m + P_b$	3A.2.5-26 Location 37	21.0	70.0 (3.6S _u)

Note: If the primary plus bending stress for a particular component meets the primary membrane stress allowable, only the Normal Condition primary plus bending stress is reported. Local loads and stresses due to tornado driven missiles are evaluated in chapter two, section 2.2.1.3.

** For this maximum combined stress including secondary stress (thermal), the maximum allowable stress is $3S_m$. It is conservative to use allowable stress of $1.5S_m$. Gamma shielding is SA-266 Class 2 or SA-516 Gr. 70 or SA-105. The lowest value of allowable stress is used in these evaluations.

TABLE 3.4-7

SUMMARY OF MAXIMUM STRESS INTENSITY
AND ALLOWABLE STRESS LIMITS FOR LID BOLTS

STRESS CATEGORY	SERVICE CONDITION	CALCULATED STRESS (ksi)	ALLOWABLE STRESS (ksi)
Tensile	Level A	25.0	92.4 (2/3 S _Y)
	Level D	25.0	115.5 (0.7 S _u)
Shear	Level A	10.7	55.4 (0.4S _y)
	Level D	10.7	69.3 (0.4S _u)
Combined S.I.	Level A	40.7	124.7 (0.9S _y)
	Level D	(not required)	(not required)
Interaction Equation: $R_t^2 + R_s^2 \leq 1$	Level A	0.11	
	Level D	0.07	

TABLE 3.4-8

COMPARISON OF ACTUAL WITH ALLOWABLE STRESS INTENSITY IN BASKET
(NORMAL CONDITIONS)

Loading	Stress Category	Max.Stress (ksi)	Allowable Stress (ksi)	Reference Section/ Table
304 Stainless Steel Plate				
1G Lateral	P_m	0.36	14.76 ($S_m \times 0.9$)	Table 3B.3-1 (0° Drop)
	$P_m + P_b$	0.63	22.14 ($1.5 S_m \times 0.9$)	Table 3B.3-1 (0° Drop)
3G Vertical	P_m	0.30	14.76 ($S_m \times 0.9$)	Sect. 3B.3.3
Stainless Steel Fusion Weld				
1G Lateral	τ	0.055	2.95 ($0.6 S_m \times 0.3$)	Table 3B.3-1 (45° Drop)
3G Vertical	τ	0.05	2.95 ($0.6 S_m \times 0.3$)	Sect. 3B.3.3
6061-T6 Aluminum Rail				
1G Lateral	P_m	0.11	4.5 (S_m)	Table 3B.3-2 (Location 1)
	$P_m + P_b$	0.15	6.75 ($1.5 S_m$)	Table 3B.3-2 (Location 1)
3G Vertical	P_m	0.05	4.5 (S_m)	Sect. 3B.3.3

TABLE 3.4-9

COMPARISON OF ACTUAL WITH ALLOWABLE STRESS INTENSITY IN BASKET
(ACCIDENT CONDITIONS)

Loading	Stress Category	Max. Stress (ksi)	Allowable Stress (ksi)	Max. Allowable G load	Max. Calculated G Load	Reference Section/Table
304 Stainless Steel Plate / Box						
60 G End Drop	P_m	6.03 (60G)	39.36 (2.4 S_m)	392	60	Sect. 3B.4.1
Side drop Stress Analysis	P_m	0.36 (1G)	39.36 (2.4 S_m)	109	77	Table 3B.4-1 (0° Drop)
	$P_m + P_b$	0.63 (1G)	59.04 (S_u)	94	77	Table 3B.4-1 (0° Drop)
Side drop Buckling Analysis				92	77	Sect. 3B.5.2
Stainless Steel Fusion weld						
60 G End Drop	τ	0.92 (60G)	19.68 (0.6 $S_m \times 2$)	1283	60	Sect. 3B.4.1
Side Drop Stress Analysis	τ	0.055 (1G)	19.68 (0.6 $S_m \times 2$)	358	77	Table 3B.4-1 (45° Drop)
6061-T6 Aluminum Rail						
60 G End Drop	P_m	1.0 (60G)	10.8 (2.4 S_m)	648	60	Sect. 3B.4.1
Side Drop Stress analysis	P_m	0.10 (1G)	10.8 (2.4 S_m)	98	77	Table 3B.4-2 (Location 1)
	$P_m + P_b$	0.15 (1G)	16.0 (S_u)157	107	77	Table 3B.4-2 (Location 1)
Side Impact Buckling Analysis				100	77	Sect. 3B.5.4

TABLE 3.4-10

COMPARISON OF MAXIMUM STRESS INTENSITY
WITH ALLOWABLES IN OUTER SHELL

LOAD	Maximum Stress Intensity (ksi)	Allowable Stress (ksi)
25 psi Internal Pressure	4.5	$S_y = 33.6$
25 psi + 3G Down Cask Vertical	9.1	$S_y = 33.6$
25 psi + 3G Down Cask Horizontal	7.0	$S_y = 33.6$

Figure Withheld Under 10 CFR 2.390

FIGURE 3.4-1
TRUNNION GEOMETRY

Figure Withheld Under 10 CFR 2.390

**FIGURE 3.4-2
CASK BODY KEY DIMENSIONS**

Rev. 0 2/00

Figure Withheld Under 10 CFR 2.390

FIGURE 3.4-3
STANDARD REPORTING
LOCATIONS FOR CASK BODY

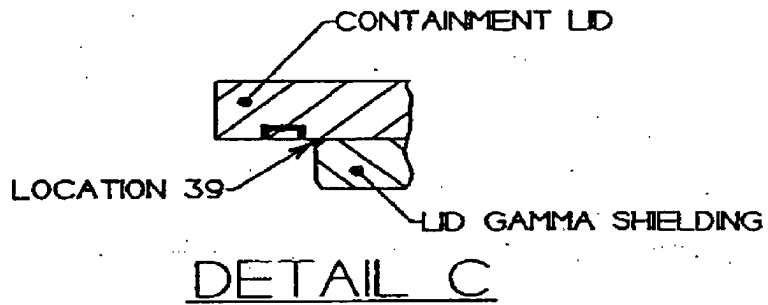
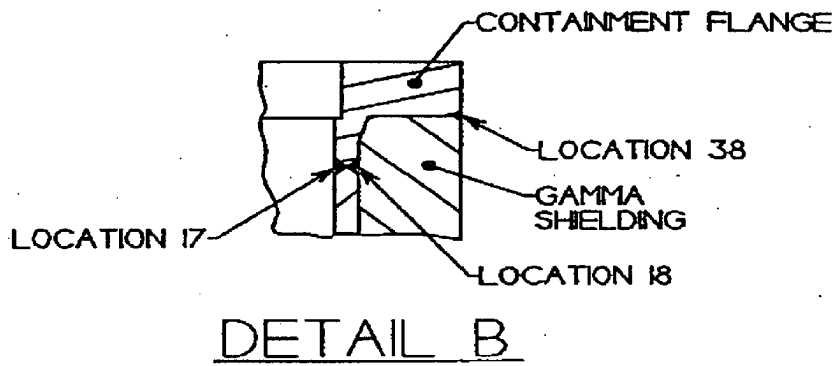
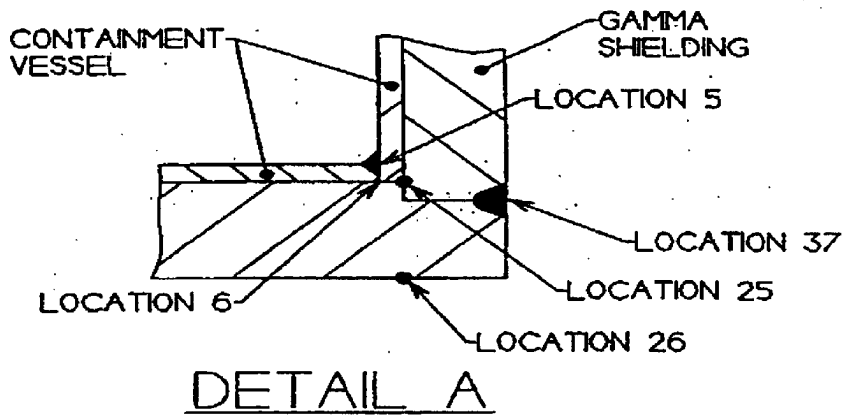
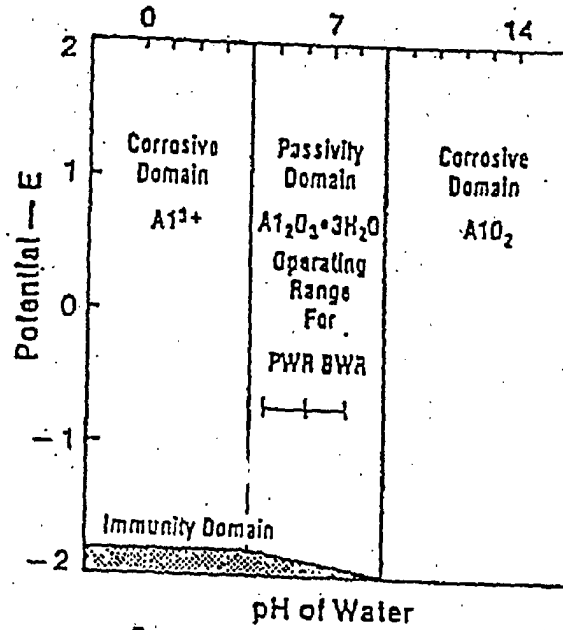


FIGURE 3.4-4
WELD STRESS LOCATIONS

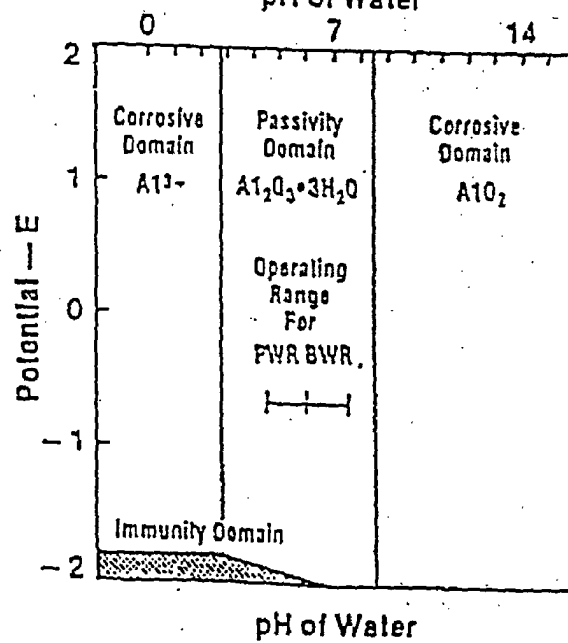
FIGURE 3.4-5

POTENTIAL VERSUS pH DIAGRAM FOR ALUMINUM-WATER SYSTEM

At 25°C (77°F):



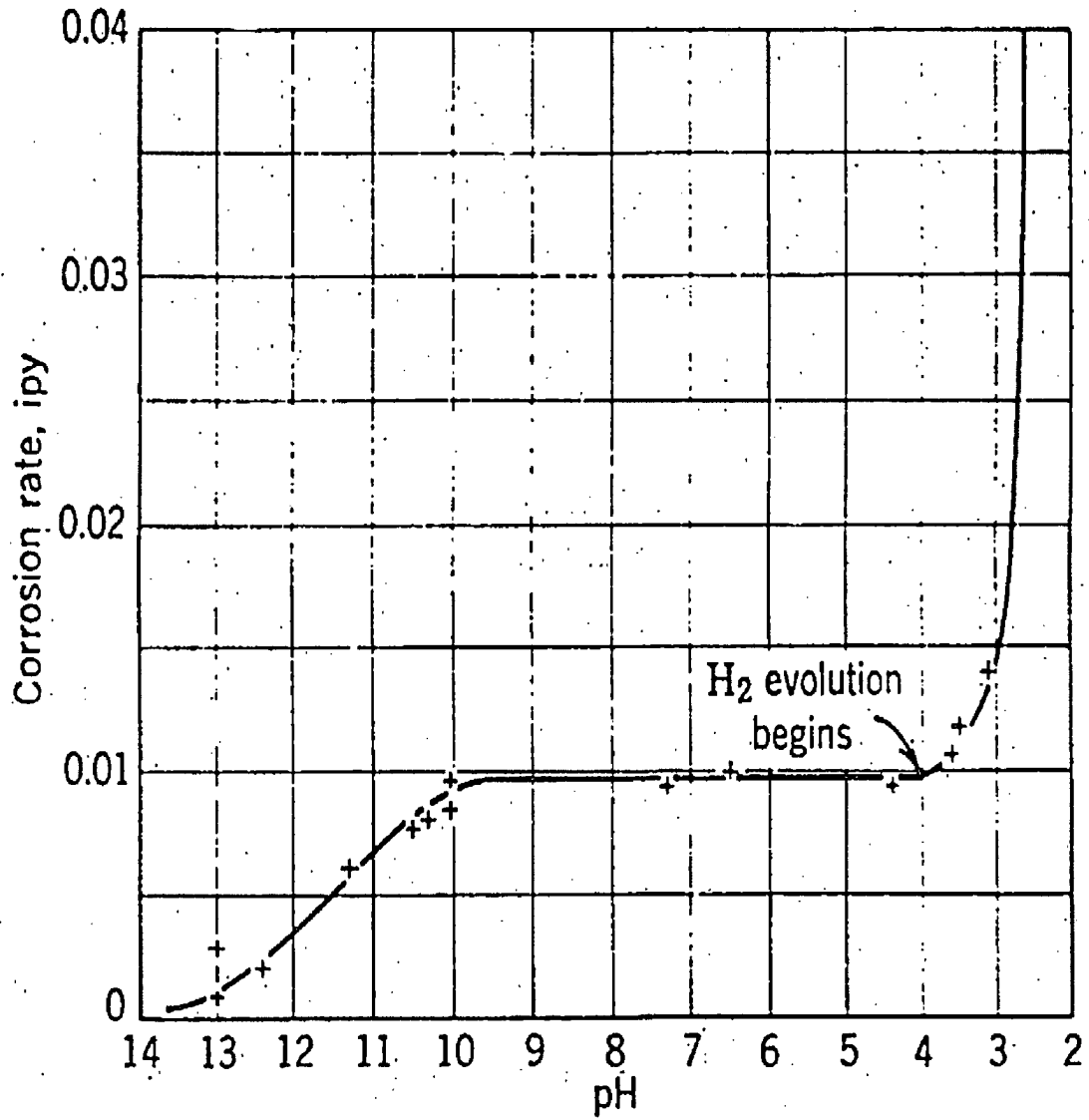
At 60°C (140°F):



Source: Reference 13

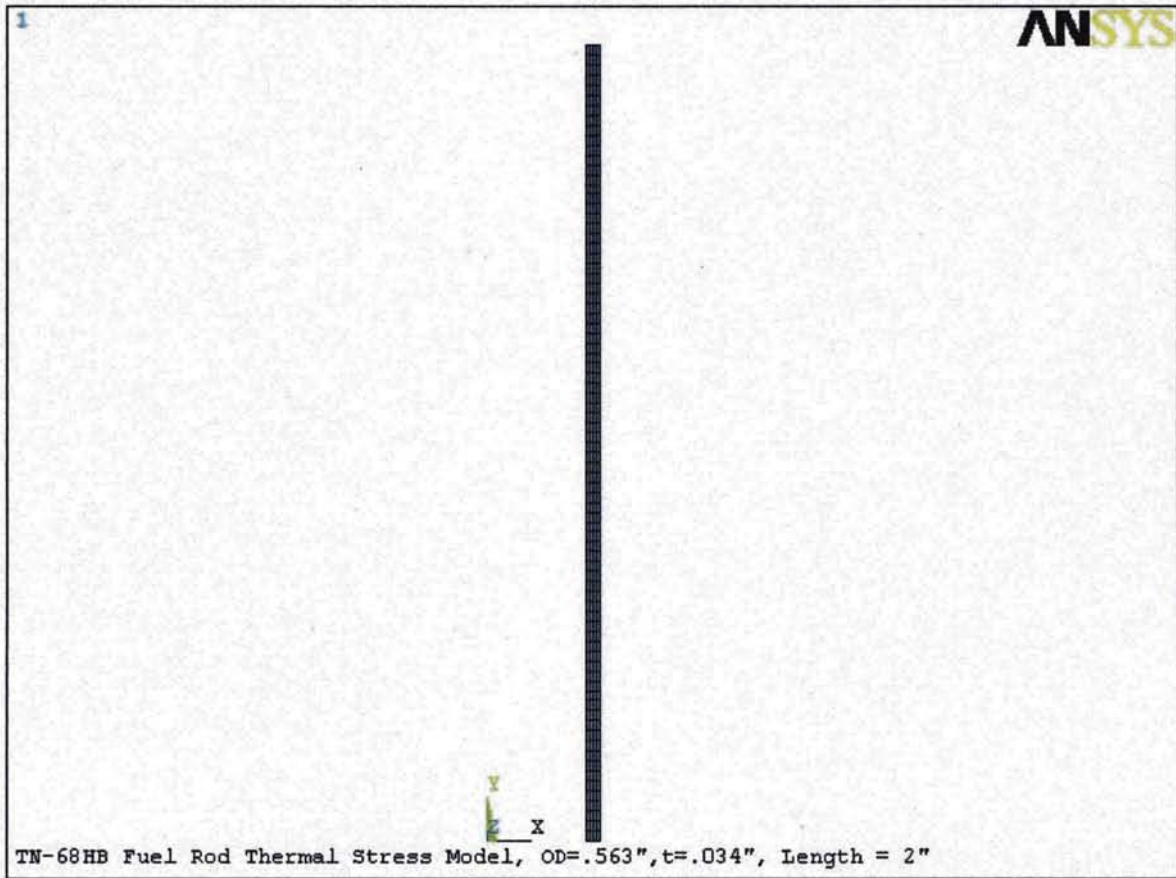
FIGURE 3.4-6

EFFECT OF pH ON CORROSION OF IRON IN AERATED SOFT WATER,
ROOM TEMPERATURE



Source: Reference 16

Figure 3.5-1
Finite Element Model



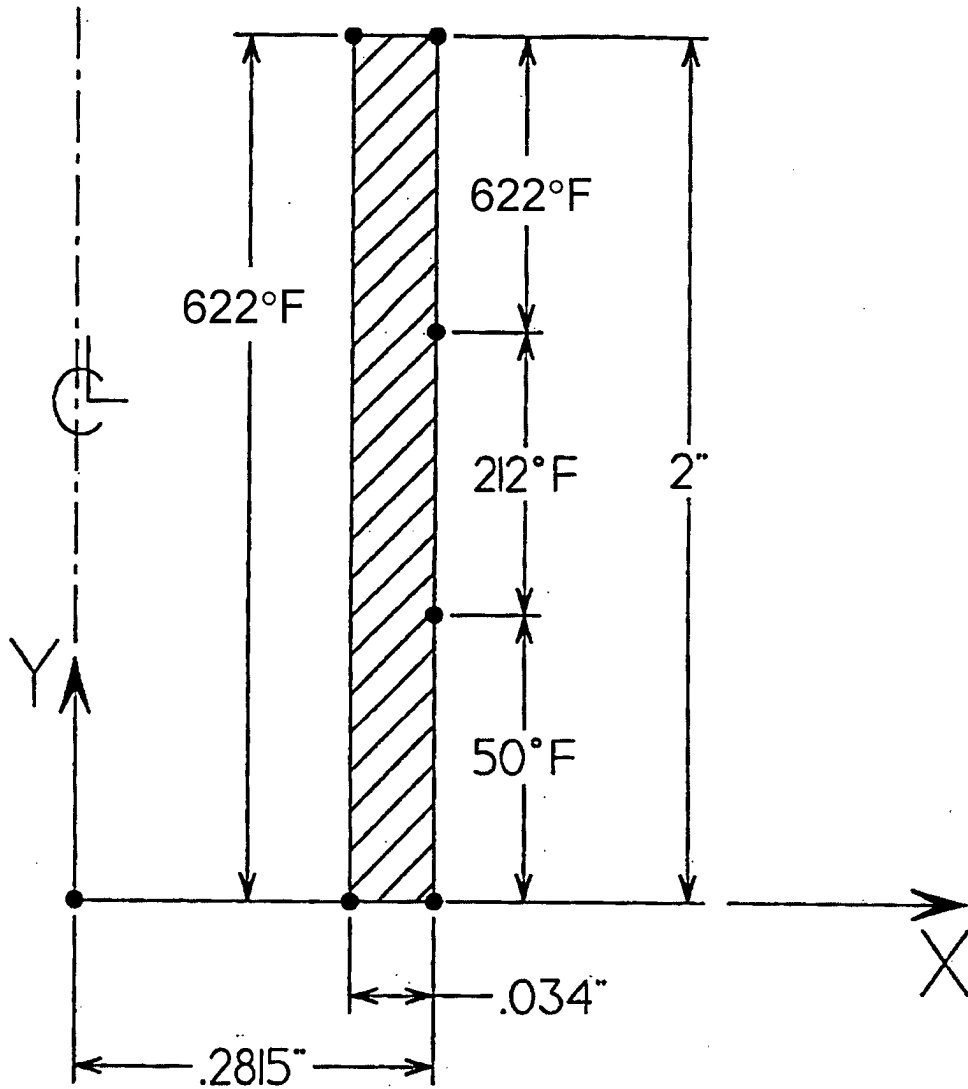


FIGURE 3.5-2
 NODAL TEMPERATURE USED
 FOR THERMAL ANALYSIS

Figure 3.5-3
 Temperature Distribution Resulting From Thermal Analysis

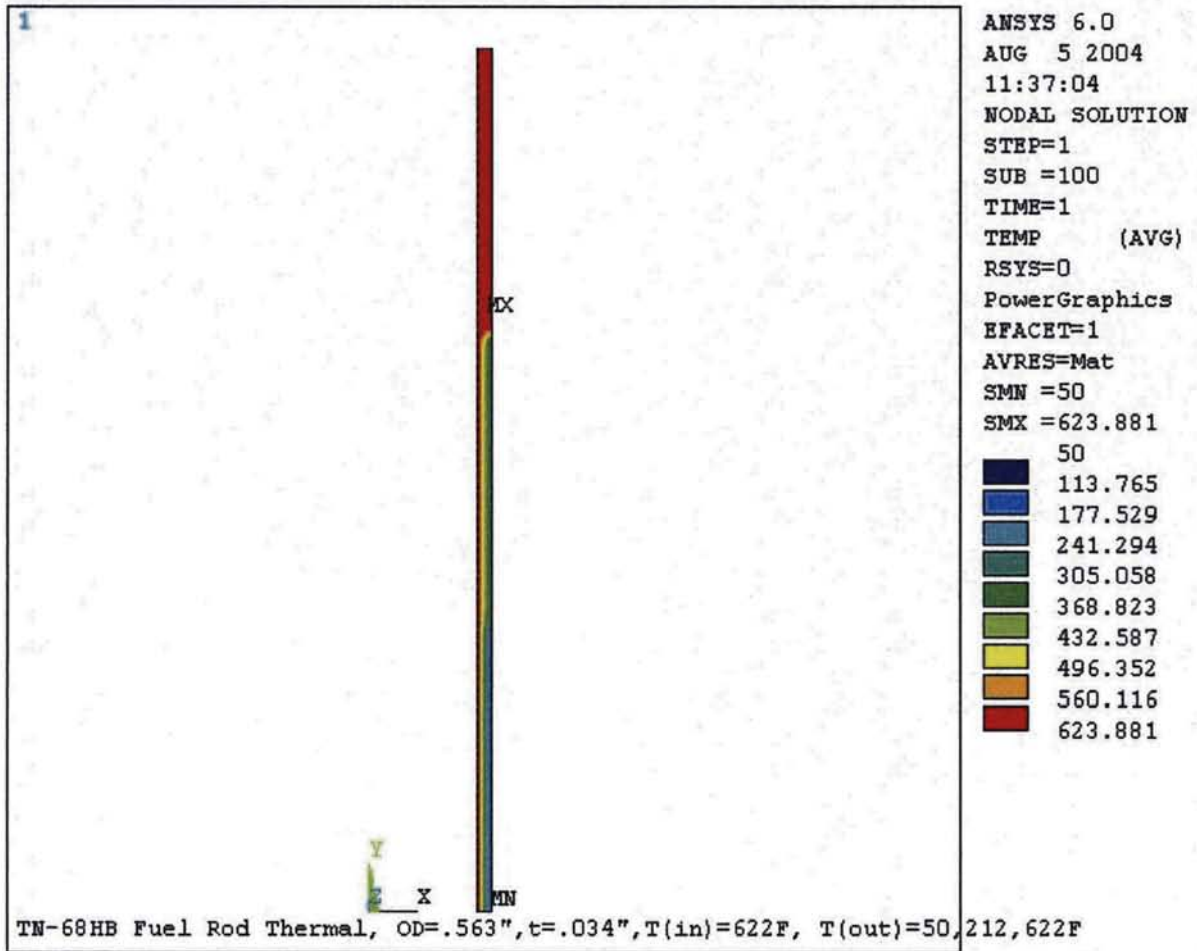
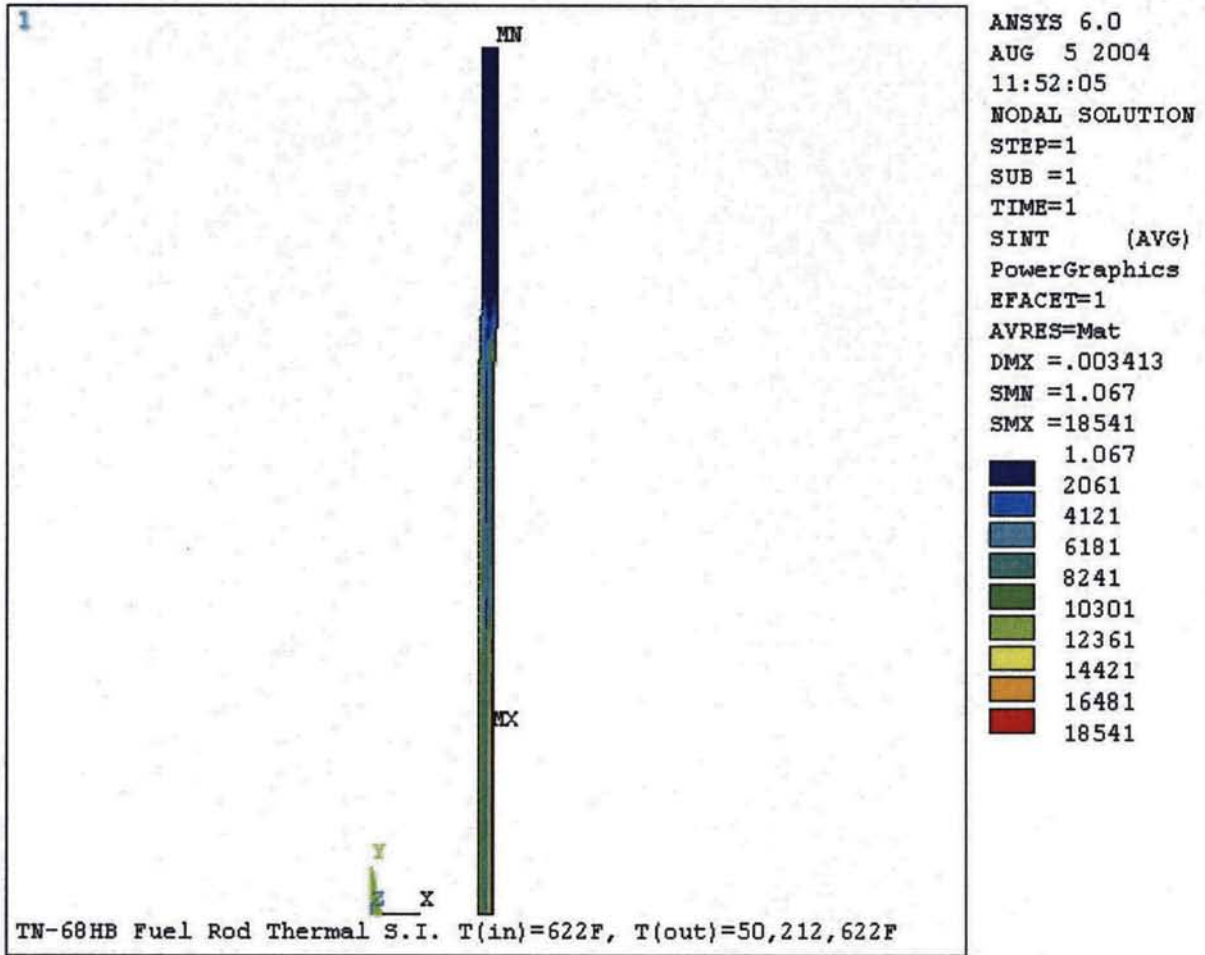


Figure 3.5-4
Nodal Stress Intensity



**TN-68 SAFETY ANALYSIS REPORT
TABLE OF CONTENTS**

SECTION	PAGE
Appendix 3A	STRUCTURAL ANALYSIS OF THE TN-68 STORAGE CASK BODY
3A.1	Introduction..... 3A.1-1
3A.2	Cask Body Structural Analysis 3A.2-1
3A.2.1	Description..... 3A.2-1
3A.2.2	ANSYS Cask Model..... 3A.2-1
3A.2.3	Individual Load Cases..... 3A.2-2
3A.2.3.1	Normal Conditions..... 3A.2-2
3A.2.3.2	Accident Conditions..... 3A.2-5
3A.2.3.3	Summary of Individual Load Cases..... 3A.2-6
3A.2.3.4	Fire Accident..... 3A.2-7
3A.2.4	Additional Cask Body Analyses 3A.2-8
3A.2.4.1	Trunnion Local Stresses..... 3A.2-8
3A.2.4.2	Tornado Missile Impact..... 3A.2-8
3A.2.4.3	Impact on a Trunnion..... 3A.2-9
3A.2.5	Evaluation (Load Combinations Vs. Allowables) 3A.2-11
3A.3	Lid Bolt Analyses 3A.3-1
3A.3.1	Introduction..... 3A.3-1
3A.3.2	Bolt Load Calculations 3A.3-2
3A.3.3	Load Combinations..... 3A.3-6
3A.3.4	Bolt Stress Calculations..... 3A.3-7
3A.3.5	Results..... 3A.3-9
3A.3.6	Minimum Engagement Length, L_e For Bolt and Flange..... 3A.3-9
3A.3.7	Conclusions..... 3A.3-10
3A.4	Outer Shell 3A.4-1
3A.4.1	Description..... 3A.4-1
3A.4.2	Materials Input Data 3A.4-1
3A.4.3	Applied Loads..... 3A.4-1
3A.4.4	Method of Analysis..... 3A.4-2
3A.4.5	Results..... 3A.4-3
3A.5	References..... 3A.5-1

**TN-68 SAFETY ANALYSIS REPORT
TABLE OF CONTENTS**

List of Tables

3A.2.3-1	Bolt Preload (Shell Elements)
3A.2.3-2	Bolt Preload (Solid Elements)
3A.2.3-3	One (1) G Down (Shell Elements)
3A.2.3-4	One (1) G Down (Solid Elements)
3A.2.3-5	Internal Pressure - 100 PSI (Shell Elements)
3A.2.3-6	Internal Pressure - 100 PSI (Solid Elements)
3A.2.3-7	External Pressure - 25 PSI (Shell Elements)
3A.2.3-8	External Pressure - 25 PSI (Solid Elements)
3A.2.3-9	Thermal Stress (Shell Elements)
3A.2.3-10	Thermal Stress (Solid Elements)
3A.2.3-11	Six (6) G on Trunnion (Shell Elements)
3A.2.3-12	Six (6) G on Trunnion (Solid Elements)
3A.2.3-13	One (1) G Side Drop - Contact Side (Shell Elements)
3A.2.3-14	One (1) G Side Drop - Contact Side (Solid Elements)
3A.2.3-15	One (1) G Side Drop - Side Opposite Contact (Shell Elements)
3A.2.3-16	One (1) G Side Drop - Side Opposite Contact (Solid Elements)
3A.2.3-17	Seismic Load - 2G Down + 1G Lateral (Shell Elements)
3A.2.3-18	Seismic Load - 2G Down + 1G Lateral (Solid Elements)
3A.2.5-1	Normal Condition Load Combinations
3A.2.5-2	Bolt Preload + 100 PSI Internal Pressure + 1G Down (Shell Elements)
3A.2.5-3	Bolt Preload + 100 PSI Internal Pressure + 1G Down (Solid Elements)
3A.2.5-4	Bolt Preload + 100 PSI Internal Pressure + 1G Down + Thermal (Shell Elements)
3A.2.5-5	Bolt Preload + 100 PSI Internal Pressure + 1G Down + Thermal (Solid Elements)
3A.2.5-6	Bolt Preload + 100 PSI Internal Pressure + Thermal + 6G Up + Trunnion Local Stress (Shell Elements)
3A.2.5-7	Bolt Preload + 100 PSI Internal Pressure + Thermal + 6G Up + Trunnion Local Stress (Solid Elements)
3A.2.5-8	Bolt Preload + 1G Down + 25 PSI External Pressure (Shell Elements)
3A.2.5-9	Bolt Preload + 1G Down + 25 PSI External Pressure (Solid Elements)
3A.2.5-10	Bolt Preload + 1G Down + 25 PSI External Pressure + Thermal (Shell Elements)
3A.2.5-11	Bolt Preload + 1G Down + 25 PSI External Pressure + Thermal (Solid Elements)
3A.2.5-12	Bolt Preload + 25 PSI External Pressure + Thermal + 6G Up + Trunnion Local Stress (Shell Elements)
3A.2.5-13	Bolt Preload + 25 PSI External Pressure + Thermal +6G Up + Trunnion Local Stress (Solid Elements)
3A.2.5-14	Accident Condition Load Combinations
3A.2.5-15	Bolt Preload + 60G Down End Drop + 100 PSI Internal Pressure (Shell Elements)
3A.2.5-16	Bolt Preload + 60G Down End Drop + 100 PSI Internal Pressure (Solid Elements)
3A.2.5-17	Bolt Preload + 60G Down End Drop + 25 PSI External Pressure (Shell Elements)
3A.2.5-18	Bolt Preload + 60G Down End Drop + 25 PSI External Pressure (Solid Elements)
3A.2.5-19	Bolt Preload + Tipover(65G) + 100 PSI Internal Pressure - Opposite Contact Side (Shell Elements)

**TN-68 SAFETY ANALYSIS REPORT
TABLE OF CONTENTS**

3A.2.5-20	Bolt Preload + Tipover(65G) + 100 PSI Internal Pressure - Opposite Contact Side(Solid Elements)
3A.2.5-21	Bolt Preload + Tipover(65G) + 100 PSI Internal Pressure - Contact Side(Shell Elements)
3A.2.5-22	Bolt Preload + Tipover(65G) + 100 PSI Internal Pressure - Contact Side(Solid Elements)
3A.2.5-23	Bolt Preload + Tipover(65G) + 25 PSI External Pressure - Opposite Contact Side (Shell Elements)
3A.2.5-24	Bolt Preload + Tipover(65G) + 25 PSI External Pressure - Opposite Contact Side (Solid Elements)
3A.2.5-25	Bolt Preload + Tipover(65G) + 25 PSI External Pressure - Contact Side (Shell Elements)
3A.2.5-26	Bolt Preload + Tipover(65G) + 25 PSI External Pressure - Contact Side (Solid Elements)
3A.2.5-27	Bolt Preload + 100 PSI Internal Pressure + Seismic(Tornado, Flood) (Shell Elements)
3A.2.5-28	Bolt Preload + 100 PSI Internal Pressure + Seismic(Tornado, Flood) (Solid Elements)
3A.2.5-29	Bolt Preload + 25 PSI External Pressure+ Seismic(Tornado, Flood) (Shell Elements)
3A.2.5-30	Bolt Preload + 25 PSI External Pressure+ Seismic(Tornado, Flood) (Solid Elements)
3A.3-1	Design Parameters for Lid Bolt Analysis
3A.3-2	Bolt Data (Ref. 10, Table 5.1)
3A.3-3	Allowable Stresses in Closure Bolts for Normal Conditions
3A.3-4	Allowable Stresses in Closure Bolts for Accident Conditions
3A.4-1	Stress In Outer Shell and Closure Plates

**TN-68 SAFETY ANALYSIS REPORT
TABLE OF CONTENTS**

List of Figures

3A.1-1	Cask Body Key Dimensions
3A.2-1	Cask Body - Finite Element Model
3A.2-2	Cask Body - Bottom Corner
3A.2-3	Cask Body - Top Corner
3A.2-4	Cask Lid to Shield Plate Connection
3A.2-5	Fourier Coefficients for 1 g Lateral
3A.2-6	Bolt Preload and Seal Reaction
3A.2-7	Design Internal Pressure (100 PSIG)
3A.2-8	External Pressure Loading (25 PSIG)
3A.2-9	1g Down Loading
3A.2-10	Lifting: 6g Vertical Up
3A.2-11	1g Lateral
3A.2-12	Standard Reporting Locations for Cask Body
3A.2-13	Weld Stress Locations
3A.2-14	Fourier Series Approximation of the Footprint Pressure for the Side Drop
3A.2-15	Trunnion Geometry
3A.3-1	TN-68 Cask Lid Closure Arrangement
3A.3-2	TN-68 Cask Lid Bolt
3A.4-1	Cask Outer Shell and Connection with Cask Body
3A.4-2	Finite Element Model Outer Shell
3A.4-3	Finite Element Model Bottom Corner
3A.4-4	Finite Element Model Top Corner
3A.4-5	Internal Pressure (25 psi)
3A.4-6	3G Down

APPENDIX 3A

STRUCTURAL ANALYSIS OF THE TN-68 STORAGE CASK BODY

3A.1 Introduction

This appendix presents the structural analysis of the TN-68 storage cask body which consists of the cask body, the trunnions and the outer shell. Analyses are performed to evaluate the various cask components under the loadings described in Section 2.2.5.

The detailed calculations for the cask body are presented in Section 3A.2 and the lid bolt analysis is reported in Section 3A.3. The calculations for the outer shell are reported in Section 3A.4. The trunnions are analyzed in Chapter 3, Section 3.4.3.

The design criteria used in the analyses of the cask components are in accordance with the ASME Code, Section III, Subsection NB⁽¹⁾. The material properties used are those obtained from the ASME Code, Section II, Part D⁽²⁾. Key dimensions of the storage cask are shown in Figure 3A.1-1.

3A.2 Cask Body Structural Analysis

3A.2.1 Description

The cask body as shown in Figure 3A.1-1 consists of:

1. A 1 1/2 in. thick inner vessel with a welded flat bottom, a flange welded at the top, and a lid bolted to the flange by 48, 1.875 in. diameter high strength bolts and sealed with two metallic o-rings. This is the confinement vessel, the primary confinement boundary of the cask.
2. A thick cylindrical vessel with a welded flat bottom surrounding the confinement. This vessel and a steel disk welded to the lid inner surface provide the gamma shielding.

The lid and the flange are carbon steel forgings as are the gamma shielding components. The cask body is designed as a Class 1 component in accordance with the rules of the ASME Code. A static, linear elastic analysis is performed on the cask body so that combinations of loads can be obtained by superposition of individual loads. The stresses and deformations due to the applied loads are generally determined using the ANSYS computer program⁽³⁾. A 2D ANSYS model was specifically developed for this purpose. Exceptions include the analyses of the local effects at the trunnion and of the lid bolt locations, as well as effects of local loads due to tornado missile impacts.

3A.2.2 ANSYS Cask Model

A two dimensional ANSYS model is used to evaluate the stresses in the cask body due to the individual load cases. The finite elements used in the model are the axisymmetric shell element, SHELL 61, and the axisymmetric harmonic element, PLANE 25. Both of these elements consider axisymmetric and non-axisymmetric loadings.

The cylindrical confinement shell and bottom are modeled using SHELL 61 elements. The remainder of the cask body is modelled with PLANE 25 elements except for the lid bolts which are modelled with the two dimensional elastic beam, BEAM 3. The finite element model of the cask body is shown in Figure 3A.2-1.

Figure 3A.2-2 shows an enlarged view of the bottom corner with the weld joining the gamma shielding flat bottom to cylinder simulated by coupling nodes 236-107 and 280-108.

The weld connecting the gamma shielding cylinder to the confinement flange is simulated by coupling nodes 63-328 and 64-329 as shown in Figure 3A.2-3. The gamma shielding is heated prior to assembly with the confinement shell and flange for ease of installation. During cooldown, a gap may result between the flange and the gamma shield shell. The gap is filled with shim plates made from SA-516, Grade 70 plate. The plates are fit between the gamma shield shell and the flange behind the weld. These shim plates are not modeled. The weld between the gamma shield and the flange is not affected by the shims. Also shown in this figure are the lid bolts connecting the lid to the confinement flange. The connection is simulated by

coupling nodes 505, 506 and 507 of the bolts to the corresponding nodes 81, 74, and 67 of the flange; and nodes 501, 502 and 503 of the bolts to the corresponding nodes 438,439, and 440 of the lid. In this manner the threaded portion of the bolt is fixed to the flange while the bolt head is fixed to the top surface of the lid. In order to prevent the lid from moving into the flange, nodes 79 and 395 are also coupled in the axial or Y direction. The enlarged view in Figure 3A.2-4 shows the coupling of nodes 394-383 and 395-384 which simulates the weld connecting the confinement lid to the gamma shielding disk.

The pairs of nodes listed above, with the exception of nodes 79-395, are coupled in the X, Y and Z directions. The coupling of nodes 79-395 is in the Y direction only. Nodes 80-396 and 82-398 are also coupled in Y-direction. These are accomplished using constraint equations. The reactions at these nodes are monitored during the analysis to insure that tensile forces between the flange and the lid are not developed.

Appropriate boundary conditions are applied to prevent rigid body motion and to show that the system of forces applied to the cask in each of the individual load cases is in equilibrium. Generally a node at the center of the vessel bottom is held in all directions and all nodes at the center line are held in the X direction. Node 78 (Figure 3A.2-3) is held in the Z direction to avoid rigid body motion.

3A.2.3 Individual Load Cases

Individual load cases are evaluated to determine the stress contribution due to specific individual loads. Stress results are reported in this Appendix for each individual load. Since the individual load cases are linearly elastic, their results can be ratioed and/or superimposed as required in order to obtain the load combinations characteristic of the particular loading condition.

3A.2.3.1 Normal Conditions

The following individual loads are analyzed using the ANSYS model described in the previous section: (These loads are defined in Chapter 2, section 2.2.5.4.1)

1. Bolt preload and seal seating pressure.
2. Internal pressure loading.
3. External pressure loading.
4. 1 g down with cask standing in a vertical position on the concrete storage pad.
5. 6 g lifting (Cask Vertical) load.
6. Worst normal thermal condition.
7. 1 g lateral and 2 g down bounding loads for tornado wind, flood water, and seismic loads on the cask standing in a vertical position on the concrete pad. The 2 g bounding load includes 1.0 g dead weight and 0.17 g seismic load.

Loadings for Cases 1 through 6 are axisymmetric. In Case 7, Fourier series representation of the nonaxisymmetric loads are required. Each discrete load acting on the cask body is expanded into a Fourier series and is input into ANSYS as a series of load steps. Each load step contains all of the terms from the applied loads having the same mode number. The number of terms in the

Fourier series required to adequately represent a load varies with the type of load (concentrated or distributed) and the degree of accuracy required. In this case, the load applied by the internals to the inside wall of the confinement is assumed to be a distributed load varying sinusoidally in the arc 90° to 270° and acting on the total length of the cavity. Figure 3A.2-5 shows that only a few terms of the series are required to get a satisfactory representation of the load.

Since Case 7 is asymmetric, the resulting stresses are asymmetric. Therefore, in order to properly characterize the stress condition in the cask body, results are obtained at the two worst diametrically opposite locations and reported for the location where they are maximum.

The individual loads are described in the following paragraphs:

1. Bolt Preload and Seal Seating Pressure

A lid bolt preload corresponding to 35,000 psi (actual lid bolt preload stress is 25,000 psi, however, lid bolt preload corresponding to 35,000 psi is used for all load combinations) direct stress in the bolt shank is simulated by specifying an initial strain in the elements representing the bolts. A portion of this strain becomes elastic preload strain in the bolts, and a portion becomes strain in the clamped parts. The required initial strain value of 0.001309 in/in (in the bolts) was determined by trial and error.

The selected bolt preload is sufficient to insure a full seating of the metallic seals under a maximum design internal pressure of 100 psig. The metallic seal seating load is 1,399 lb./in./seal⁽⁴⁾ or 2,798 lb./in. for 2 seals. This load is simulated by applying a pressure of 3,498 psi on an annular ring on both the confinement lid and flange surfaces as shown in Figure 3A.2-6.

2. Internal Pressure Loading

A conservative design pressure of 100 psig is used as the maximum pressure acting in the confinement vessel cavity as shown in Figure 3A.2-7.

3. External Pressure Loading

A pressure of 25 psig is used as the maximum external pressure acting on the outer surface of the cask body as shown in Figure 3A.2-8.

4. 1 g Down

The cask is stored vertically on the concrete storage pad as shown in Figure 3A.2-9, with the following loads acting on it:

- a. A distributed vertical down inertia force of 1 g acting at each finite element in the model. For practical purposes, the resultant of all these forces is shown acting at the C.G. of the cask. Note that the resin, the outer shell and the trunnions are not

included in the model. They are accounted for by increasing the density of the gamma shielding.

- b. Since the internals are not included in the model, their loading effects are simulated by a distributed pressure acting on the inside bottom surface of the cask cavity.
- c. All nodes on the outside bottom surface of the cask are fixed in the axial directions.

5. Lifting: 6 g Vertical Up

The cask is oriented vertically in space held by the 2 top trunnions and subjected to a vertical down load of 6 g, as shown on Figure 3A.2-10.

The inertia force acting on the cask elements and the pressure from the internals on the confinement bottom inner surface are as described in Case 4 multiplied by a factor of 6. The total cask weight (including internals) is replaced by forces applied to the 2 top trunnions so that the system of forces acting on the cask is again in equilibrium. A cask weight of 240,000 lb. is used in the calculations. The two trunnion forces F_{TR} are replaced by a total force:

$$F_Y = 6.0 \times (240,000) \times 1.15 = 1,656,000 \text{ lbs}$$

A 15% additional load is included to cover the dynamic effects of lifting. This force acting in the Y direction on the outer surface node 319 (location 36, Figure 3A.2-12) of the gamma shielding at the trunnion location. Superimposed on this solution are the local trunnion effects at two locations around the circumference which are determined by using the Bijlaard method. The trunnion flange and bolt stresses are determined using hand calculations.

6. Worst Temperature Distribution in the Cask Body

Thermal analyses of the cask under normal and off-normal storage conditions are performed in Chapter 4. An average daily ambient temperature of 100 °F is considered for the maximum off-normal storage temperature and -20 °F for the minimum off-normal storage temperature. Normal ambient storage temperatures are bounded by these two maximum and minimum off-normal temperatures. The temperature profiles in the cask, which are calculated from the thermal stress analyses in Chapter 4, are imposed to the ANSYS stress model of Figure 3A.2-1 for calculation of the thermal stresses.

7. 1 g Lateral and 2 g Down Bounding Loads - Cask Standing in a Vertical Orientation on the Pad.

The $\sin\theta$ and $\cos\theta$ terms of the Fourier series are used to represent the 1 g lateral load acting at the CG of each finite element of the model. The lateral load applied by the internals to the inside surface of the confinement is assumed to vary sinusoidally on a 180° arc as shown in Figures 3A.2-5, and the same Fourier representation applies. The 2 g down load is applied simultaneously (as described in item 4, above) with the 1 g lateral load. The cask is held at the bottom and no tilting or sliding is allowed (See Figure 3A.2-11). This load combination is an upper bound loading for tornado wind, flood water, seismic loads, etc. (See Table 2.2-3).

3A.2.3.2 Accident Conditions

This section evaluates the effects of a hypothetical drop or tipover of the cask on the ISFSI storage pad. The following cases are evaluated:

- An 18 inch end drop onto a concrete storage pad. This is the maximum height the cask will be lifted during transport to the storage location.
- A tipover of the cask onto a concrete storage pad.
- Fire Accident

The stability of the TN-68 storage cask in the upright position on the ISFSI concrete storage pad is demonstrated in Section 2.2 of this SAR. The effects of tornado wind and missiles, flood water and earthquakes are also described in Section 2.2. It is shown in this section that the cask will not tip over under the bounding natural phenomena specified.

The storage pad is the hardest concrete surface outside of the containment building. The cask is generally oriented vertically and is never lifted higher than 18 in. once it leaves the containment building. Therefore this case is an upper bound drop event since impact onto a softer surface would result in lower cask deceleration and a lower impact force. The 18 in. drop and tip over of the cask impact G loads are presented in Appendix D. Postulated end drops at specific sites which exceed 18 inches will be evaluated on a site specific basis to ensure that the g loading on the cask does not exceed 60 g's. If the cask is to be rotated after loading or handled horizontally at a specific site, evaluations shall be performed to verify that the equivalent side drop g loading of 65 g's is not exceeded. For example, if the cask needs to be lifted 3 feet at a specific site, impact limiters could be used to ensure that the end drop g loading does not exceed 60 g's.

The stress analysis results for two hypothetical impact accidents are reported in this section. These are the 60 g bottom end drop onto the storage pad (18 inch drop), and a 65 g side drop which envelops the tip over case. As explained in Chapter 2, these accidents have a very low probability of occurrence, but in view of their potential impact on the environs, a detailed analysis was performed. Thermal stresses cause by a fire accident are also evaluated in this section.

Cask Body Stress Analysis

A conservative 60 g bottom drop onto the concrete pad was analyzed. The ANSYS model in Section 3A.2.2 was used to evaluate the stresses in the cask body due to the drop. The 60 g bottom drop individual load case is simply 60 times the 1g vertical load case described previously.

A 65 g side drop was also analyzed. The applied load is asymmetric and a Fourier series representation of the loading is required. Figure 3A.2-14 shows the degree of approximation obtained when the series is truncated after 13 terms and the foot print of the external impact force is approximated by a rectangular strip along the cask length. The inertia force due to internals is applied as a cosine pressure distribution inside the cask. This pressure is represented by 3 terms of the Fourier series (Figure 3A.2-5). The side impact analysis results, at the selected locations, are reported in Table 3A.2.3-13 through 3A.2.3-16 for a side load of 1 g. Since a linear analysis was performed, the stresses for the 65 g load case will be 65 times the 1g load case results.

3A.2.3.3 Summary of Individual Load Cases

Stress results for these individual loads are reported in Tables 3A.2.3-1 through 3A.2.3-18. Figure 3A.2-12 shows the locations on the cask body, where stress results are reported. These locations are divided into two groups, confinement and non-confinement. Stress intensities at nodal locations on the inner and outer surfaces of each cask body component are reported in these tables.

These results are provided to indicate the relative significance of the individual loads. These point-wise results are combined in Section 3A.2.5 with the results of several hand computations to provide results for the various load combinations which are compared to the design criteria in Chapter 3.

In order to check the reasonableness of the finite element models response, some simple close-form calculations are conducted. While these simple results are unlikely to duplicate the complex area of model and complex loading conditions, they can be used to verify the stresses in simple areas away from discontinuities.

- Bolt Preload

Bolt tensile stress = Strain * Modulus of Elasticity

$$= .001309 \times 27.8 \text{ E } 10^6 = 36,390 \text{ psi}$$

This is close to the simulated preload of 35,000 psi by the computer run which takes into account the flange and lid stiffnesses.

- Internal Pressure (100 psig)

$$\text{Membrane stress intensity in a cylinder} = \frac{P * r_m}{t} + \frac{P}{2}$$

$$= [(100 * 38.5 / 7.5) + (100/2)] = 513 \text{ psi}$$

Average of stress intensities at locations 11 and 32 (Figure 3A.2-12) from computer output at Tables 3A.2.3-5 and 3A.2.3-6 = $\frac{1}{2} (589 + 416) = 503$ psi. This is close to the hand-calculated stress intensity.

- Normal Thermal Condition

$$\text{Thermal stress in a cylinder} = \frac{E * \alpha * \Delta T}{2(1 - \mu)}$$

$$\Delta T \text{ between locations 11 and 32} \cong 210 - 201 = 9^\circ\text{F}$$

$$\text{Thermal stress} = (28.6\text{E}6 * 6.7\text{E}-6 * 9) / (2 * 0.7) = 1232 \text{ psi}$$

Average stress intensity at locations 11 and 32 from computer output (Tables 3A.2.3-9 and 3A.2.3-10) = $\frac{1}{2} (1220 + 1699) = 1460$ psi. This is close to the hand-calculated intensity.

The above comparison indicates that the finite element response to various simple loads is reasonable.

3A.2.3.4 Fire Accident

The lid and lid bolts reach about 485°F (see Table 4.4-1). Since the lid and lid bolts have the same thermal expansion coefficients, no bolt preload will be lost and a positive (compressive) seal load is maintained during the fire accident conditions.

The maximum temperature in seal region is 485°F (See Table 4.4-1) which is much lower than the maximum allowable operating temperature of 536°F for the Helicoflex seal.

The basket temperature does not change appreciably while the cask temperature rises during the fire accident (See Table 4.4-1). The gap between the outside diameter of the basket and inside diameter of the cask will slightly increase (See Section 3B.3.4), therefore, no thermal stress will be induced in the basket.

3A.2.4 Additional Cask Body Analyses

Additional analyses of the cask body were performed using classical methods rather than the ANSYS finite element method. These analyses determine the maximum stresses at local points on the body: (a) due to the trunnion reactions (while lifting the cask) and (b) in the locations where tornado missile impact might occur.

3A.2.4.1 Trunnion Local Stresses

The local stresses in the cask body outer gamma shielding at the trunnion locations due to the loadings applied through the trunnions are described in Section 3.4.3. These local effects are not included in the ANSYS stress result tables reported above in Section 3A.2.3. The local stresses must be superimposed on the above stress results for the cases where the inertial lifting loads are reacted at the trunnions. The local stresses are calculated in accordance with the methodology of WRC Bulletin 107⁽⁶⁾ which is based on the Bijlaard analysis for local stresses in cylindrical shells due to external loadings.

The maximum membrane and membrane plus bending stress intensities due to a vertical lift (6 G) are 7.3 ksi and 19.8 ksi, respectively. These local stresses are combined with the finite element results from Section 3A.2.3 at the same locations (15,16,35, and 36 of Figure 3A.2-12) and compared with the allowables in Section 3A.2.5.

3A.2.4.2 Tornado Missile Impact

According to NUREG-1536 (Reference 12), the cask systems are not required to survive missile impacts without permanent deformations. The stresses due to tornado missiles are presented in chapter 2 in section 2.2.1.3. It is seen from the summary table that the maximum stress of 32.3 ksi occurs due to missile B (8 inches diameter rigid missile). The maximum wall penetration of 1.13 inches is also caused by missile B. This maximum stress is conservatively added to the highest stress (irrespective of its location) due to combined effect of bolt preload, 1 G down, 25 psi external pressure and thermal loads in Table 3A.2.5-11 which is 13 ksi (at location 23). It may be noted that this stress is almost entirely due to thermal gradient and the stresses due to other loads are negligible. Therefore, the wall thickness reduction due to 1.13 inch penetration will have no significant effect on these stresses.

Thus, the maximum combined stress due to tornado missiles, preload, gravity, external pressure and thermal load = $32.3 + 13 = 45.3$ ksi. This stress is less than even the accident membrane allowable of 49 ksi ($0.7 S_w$). It is further seen from Table 3.4-6 that stresses due to this load combination are less than reported for stress combinations with tip-over load and therefore are not bounding.

3A.2.4.3 Impact on a Trunnion

This section describes the analysis of the storage cask tipping over and impacting against the ISFSI concrete pad with the cask oriented so that an upper trunnion contacts the pad. The analyses of the trunnions and cask body under Normal conditions (when the trunnions are used to lift the cask) are reported in Section 3.4.3. This analysis is a variation of the Hypothetical Tipping Accident analyzed in 3A.2.3 to consider the particular case of the cask contacting the pad on a trunnion.

The upper trunnion could strike the pad during tipover, but the consequences would be minimal. The contact area between the cask and pad would initially be equal to the projected end area of the trunnion. The trunnion would punch into the pad for a few inches until the neutron shield and then the forged gamma shield strike the concrete pad. At this point the contact area between the cask and pad would be the full side area of the cask (as analyzed in Section 3A.2.3.2).

From Figure 3A.2-15, the projected trunnion area is $(\pi/4)(11.25^2 - 7.60^2)$ or 54.04 in^2 . For a 4,200 psi concrete compressive strength, the impact force on the end of the trunnion would be $(54.04)(4,200) = 226,968 \text{ lbs}$.

The center of the trunnion is 173.25 in. above the corner of the cask (the pivot point). The 226,968 lb. impact force would apply a torque or moment about the pivot point of $(226,968)(173.25)$ or $39.32 \times 10^6 \text{ in.-lb}$. The moment of inertia of the cask about the corner pivot point is $I_p = 8.77 \times 10^6 \text{ lb.-in.-sec}^2$. The rotational deceleration that would occur as the trunnion punches into the concrete can be determined from the relationship $\text{Torque} = I \alpha$ or $\alpha = \text{Torque}/I$. The rotational deceleration, α , = $39.32 \times 10^6 \text{ in.-lb}/8.77 \times 10^6 \text{ lb.-in.-sec}^2$ or $4.483 \text{ radians/sec}^2$.

The translational deceleration at any distance (d) from the pivot point is equal to $(d) \times \alpha$. The deceleration at the CG where $d = 105.72 \text{ in.}$ from Figure 2.2-2 is $(105.72)(4.483) = 473.9 \text{ in./sec}^2$. This is a deceleration at the CG of $473.9/386 = 1.23g$. Therefore, the peak CG deceleration of the cask during initial trunnion impact after tipover is much less than 65 g deceleration conservatively determined in Section 3A.2.3 for full side impact. Therefore the stress analysis cases for the cask body (except for the local gamma shielding stresses due to the trunnion loads) and basket conservatively assuming 65 g deceleration bound those for the 1.26g trunnion impact case.

The trunnion is attached to the gamma shielding of the cask body using a flanged connection with 12-1.5 in. diameter high strength bolts. The compressive stress in the trunnion due to the trunnion impact force would be $226,968/[(\pi/4)(9.75^2 - 7.6^2)]$ or 7.8 ksi. The minimum wall thickness of the gamma shielding at the flat machined for the trunnions is 5.09 in. Therefore the shear stress around the plug of gamma shield material behind the 17 inch diameter trunnion flange is $226,968/(\pi \times 17.0 \times 5.09)$ or 0.9 ksi. The bearing stress under the flange is $226,968/\pi(8.5)^2$ or 1.0 ksi.

The local and discontinuity stresses in the gamma shell are computed using Ref. 8 (shell subjected to radial load P uniformly distributed over small area A).

$$\text{Area, } A = \pi(8.5)^2 = 227 \text{ in}^2$$

$$\text{Shell thickness, } t = 5.09 \text{ in.}$$

$$\text{Shell mean radius, } R = 36.25 + 5.09/2 = 38.80 \text{ in.}$$

$$P = 226,968 \text{ lbs}$$

$$A/R^2 = 227/38.80^2 = 0.15$$

$$R/t = 38.80/5.09 = 7.62$$

From Ref. 8, Table XIII, Case 7

$$S'_2 (t^2)/P \approx .6 \text{ and } S_2(Rt)/P \approx 2.0$$

Where S'_2 is hoop bending stress and
 S_2 is hoop membrane stress

$$S'_2 = \frac{.6 (226,968)}{(5.09)^2} = 5,256 \text{ psi} = 5.3 \text{ ksi}$$

$$S_2 = \frac{2.0 \times 226,968}{38.80 \times 5.09} = 2,299 \text{ psi} = 2.3 \text{ ksi}$$

Combined hoop stress, $\sigma_H = 5.3 + 2.3 = 7.6 \text{ ksi}$

Assuming Conservatively, Longitudinal Stress = Hoop Stress = 7.6 ksi

Shear Stress = 0.9 ksi

Therefore, the maximum Stress Intensity = 8.5 ksi

The allowable stress intensities for non confinement structure in Table 3.1-4 for Level D loads can be used to evaluate these Hypothetical Accident stresses, in the gamma shielding.

S_u and S_m for the SA-266 gamma shielding at 400°F is 70 ksi and 20.6 ksi, respectively. The membrane plus bending allowable, $P_m + P_b$, is the smaller of $3.6S_m$ or S_u , which is 70 ksi. The allowable shear stress is $0.42 S_u$ or 29.4 ksi.

The 0.9 ksi shear stress is well below the 29.4 ksi shear limit. The maximum combined stress intensity is 8.5 ksi is also well below the allowable of 70 ksi. Therefore tipping of the cask onto a trunnion results in acceptable stresses.

3A.2.5 Evaluation (Load Combinations Vs. Allowables)

The TN-68 cask loading conditions are listed in Section 2.2.5, Table 2.2-4. The individual loads acting on the various cask components due to these loading conditions have been applied to the cask and the resulting stresses are reported in Tables 3A.2.3-1 through Table 3A.2.3-18.

The loading conditions listed in Table 2.2-4 are categorized according to the rules of the ASME Code, Section III, Subsection NB for Class 1 nuclear components. These categories include Normal (Design and Level A) and Hypothetical Accident (Level D) loading conditions. See Tables 2.2-5 through 2.2-7 for these categories. Next, the load combinations are determined based on those loads that can occur simultaneously. The individual loads of each combination are indicated in Tables 2.2-8 and 2.2-9.

The stress intensities for the combined load cases are evaluated using ANSYS postprocessor and hand calculations at the locations indicated in Figure 3A.2-12 and compared to the stress limits associated with each service loading. The normal condition load combinations are summarized in Table 3A.2.5-1. Stresses due to normal condition load combinations are presented in Tables 3A.2.5-2 through 3A.2.5-13. The accident condition load combinations are summarized in Table 3A.2.5-14. Stresses due to accident condition load combinations are presented in Tables 3A.2.5-15 through 3A.2.5-30.

Tables 3A.2.5-1 and 3A.2.5-14 provide matrices of the individual loads and how they are combined to determine the cask body stresses for the specified normal and accident conditions. The thermal stresses are actually secondary stresses that could be evaluated using higher allowables than for primary stresses. They are conservatively added to the primary stresses and the combined stresses are evaluated using primary stress allowables. Finally, for those load combinations that include trunnion reactions, the local stresses at the trunnion locations found by the Bijlaard method are superimposed on the ANSYS combined stresses at the stress reporting locations near the trunnions. In nearly all of the locations selected the stress intensities thus calculated are less than the membrane allowable stress. At the two locations (locations 25, 32, and 34, Figure 3A.2-12) where the maximum combined stress intensities (membrane plus bending) exceed the membrane allowable stress, the stresses are linearized and membrane and bending stresses are separated for comparison with the allowables.

3A.3 Lid Bolt Analyses

3A.3.1 Introduction

The TN-68 cask lid closure arrangement is shown in Figure 3A.3-1. The 5.0 inch thick lid is bolted directly to the end of the confinement vessel flange by 48 high strength alloy steel 1.875 inch diameter bolts. Close fitting alignment pins ensure that the lid is centered in the vessel.

The lid bolt is shown in Figure 3A.3-2. The bolt material is SA-540 Gr. B24 class 1 which has a minimum yield strength of 150 ksi at room temperature.

This section analyzes the ability of the cask closure to maintain a leak tight seal under normal and accident conditions. Also evaluated in this section, are the bolt thread and internal thread stresses. The stress analysis is performed in accordance with NUREG/CR-6007⁽¹⁰⁾.

The following evaluations are documented in this section:

- Lid bolt torque
- Bolt preload
- Gasket seating load
- Pressure load
- Temperature load
- Impact load
- Thread engagement length evaluation
- Bearing stress
- Load combinations for normal and accident conditions
- Bolt stresses and allowables

The following loads are used in the lid bolt analysis:

Cask cavity pressure	= 100 psig
Impact loads: bottom end drop	= 60 g
Tip over drop	= 65 g

The design parameters of the lid closure are summarized in Table 3A.3-1. The lid bolt data and material allowables are presented in Tables 3A.3-2 to 3A.3-4. The following load cases are considered in the analysis. A maximum temperature of 300°F is used in the lid bolt region during normal and accident conditions.

Load Case #1:	Preload + Temperature Load (normal condition)
Load Case #2:	Pressure Load (Normal Condition)
Load Case #3:	Pressure + Gasket Load + Impact Load (accident condition)

3A.3.2 Bolt Load Calculations

Symbols and terminology for this analysis is taken from NUREG/CR-6007 and are reproduced in Table 3A.3-1.

A. Lid Bolt Torque

The desired maximum preload stress in lid bolts is 25,000 psi

For a 1 7/8" - 8UN - 2A bolt,

Tensile Stress Area = 2.414 in² (see Table 3A.3-1)

$F_a = 25,000 \times \text{Stress Area} = 25,000 \times 2.414 = 60,350 \text{ lbs.}$

The torque required to achieve this preload is (Ref. 10, Section 4.0):

$Q = K D_b F_a = 0.1 (1.875) (60,350) = 11,315 \text{ in.- lbs.} = 943 \text{ ft.- lbs.}$

A bolt torque range of 840 to 940 ft-lbs. has been selected.

Using the minimum torque,

$F_a = 840 \times 12 / (0.1 \times 1.875) = 53,760 \text{ lbs, and}$
Preload stress = $53,760 / 2.414 = 22,270 \text{ psi.}$

B. Bolt Preload (Ref. 10, Table 4.1)

$F_a = Q / K D_b = 11,315 / 0.1 (1.875) = 60,350 \text{ lbs}$

Residual torsional moment, $M_{tr} = 0.5Q = .5(11,315) = 5,657 \text{ in. lb.}$

Residual tensile bolt force, $F_{ar} = F_a = 60,350 \text{ lbs}$

C. Gasket Seating Load (Seal - Helicoflex HND 229, Aluminum Jacket -Ref 4)

The diameter of inner seal, $D_{is} = 71.3 \text{ in.}$

The diameter outer seal, $D_{os} = 72.9 \text{ in.}$

The force to seat the seals is 1399 lbs./in (245 N/mm) (Ref. 4) times the circumference of the seal.

The force required to seat the seals is:

$$\text{Inner } \pi (71.3) (1399) = 313,370 \text{ lbs.}$$

$$\text{Outer } \pi (72.9) (1399) = 320,402 \text{ lbs.}$$

Total, $F_a = 633,772$ lbs.

Therefore, The gasket seating load is:

$$F_a/48 = 633,772/48 = 13,204 \text{ lb./bolt}$$

D. Pressure Loads (Ref. 10, Table 4.3)

Axial force per bolt due to internal pressure is:

$$F_a = \frac{\pi D_{lg}^2 (p_{li} - P_{lo})}{4 N_b}$$

D_{lg} for outer seal (conservative) = 72.9 in.

$$F_a = \frac{\pi (72.9)^2 (100 - 0)}{4 (48)} = 8,696 \text{ lbs/bolt}$$

Fixed edge closure lid force,

$$F_f = \frac{D_{lb} (P_{li} - P_{lo})}{4} = \frac{75.88(100)}{4} = 1897 \text{ lb/in}$$

Fixed edge closure lid moment,

$$M_f = \frac{(P_{li} - P_{lo}) D_{lb}^2}{32} = \frac{100 \times (75.88)^2}{32} = 17,993 \text{ in-lb/in}$$

Shear bolt force per bolt,

$$F_s = \frac{\pi E_l t_l (P_{li} - P_{lo}) D_{lb}^2}{2 N_b E_c t_c (1 - N_w)} = \frac{\pi (27.8 * 10^6) (5.0) (100) (75.88)^2}{2 (48) (27.8 * 10^6) (7.5) (0.7)} = 17,945 \text{ lbs/bolt}$$

This shear force is taken by the lid shoulder during the tipover accident.

E. Temperature Loads

The lid bolt material is SA-540GR.B24 Cl. 1, 2Ni ¼ Cr 1/3 Mo. This is Group E in the thermal coefficients of expansion tables in Reference 2. The lid is SA-350 Gr. LF3, 3 ½ Ni, which is in Group E also. The flange is also made of SA-350 Grade LF3. Thus, bolts, lid and flange have same coefficient of thermal expansion (6.78×10^{-6} in/in-°F at 300°F). Therefore, heating to the maximum isothermal temperature will have no effect on the loads.

F. Impact Loads (Ref. 10, Table 4.5)

Non-Prying tensile bolt force, per bolt (F_a)

$$F_a = \frac{1.34 \sin(\xi) \text{DLF ai}(W_l + W_c)}{N_b} = \frac{1.34 \times \sin(\xi) (1.2) \text{ ai}(89500)}{48} = 2,998.3 \text{ ai} \sin(\xi) \text{ lb/bolt}$$

Shear bolt force

$$F_s = \frac{\cos(\xi) \text{ ai} W_l}{N_b} = \frac{(12,100) \text{ ai} \cos(\xi)}{48} = 252.1 \text{ ai} \cos(\xi)$$

Shear force is taken by the lid shoulder during accident condition drops.

$$F_s = 0$$

Fixed-edge closure lid force (F_f)

$$F_f = \frac{1.34 \sin(\xi) \text{DLF ai}(W_l + W_c)}{\pi D_{lb}} = \frac{1.34 \sin(\xi) (1.2) \text{ ai}(89,500)}{\pi(75.88)}$$
$$= 604 \text{ ai} \sin(\xi)$$

Fixed-edge closure lid moment (M_f)

$$M_f = \frac{1.34 \sin(\xi) \text{DLF ai}(W_l + W_c)}{8\pi} = \frac{1.34 \sin(\xi) (1.2) \text{ ai}(89500)}{8\pi}$$
$$= 5726 \text{ ai} \sin(\xi)$$

Loads for bottom end drop

$$\text{ai} = 60 \text{ g}$$

In case of bottom impact, the non-prying and prying bolt forces are zero.

$$F_a = 0 \quad F_f = 0 \quad M_f = 0$$

Loads for tipover

Maximum tip over G load = 65

For the lid bolt load calculations, it is assumed that cask is oriented 10° below horizontal at the end of tipover with 65 g. maximum rigid-body acceleration. This is very conservative since the impacting end of the cask is not expected to indent into the concrete enough to result in a 10° angle.

$$F_a = 2998.3 (65) (\sin 10^\circ) = 33,911 \text{ lbs/bolt}$$

$$F_f = 614 (65) (\sin 10^\circ) = 6,831 \text{ lbs/in}$$

$$M_f = 5726 (65) (\sin 10^\circ) = 64,761 \text{ in.-lb/in}$$

The individual lid bolts are summarized in the following table.

LID BOLT INDIVIDUAL LOAD SUMMARY

Load Type	Condition	Non-Prying Tensile Force, F_a (lb)	Torsional Moment, M_t (in.-lb)	Prying Force, F_f (lb/in.)	Prying Moment, M_f (in.-lb/in.)
Preload	Residual	60,350	5,657	0	0
Pressure	100 Psig Internal	8,696	0	1,897	17,993
Gasket	Seating Load	13,204	0	0	0
Impact	End Drop (60 G)	0	0	0	0
	Tipover (65 G)	33,911	0	6,831	64,761
Thermal	300°F	0	0	0	0

3A.3.3 Load Combinations (Ref. 10, Table 4.9)

A summary of normal and accident load combinations is presented in the following table.

LID BOLT NORMAL AND ACCIDENT LOAD COMBINATIONS

Load Case	Combination Description	Non-Prying Tensile Force, F_a (lb)	Torsional Moment, M_t (in-lb)	Prying Force, F_f (lb/in)	Prying Moment, M_f (in-lb/in)
1	Preload + Temp Load (Normal)	60,350	11,315**	0	0
2	Pressure (Normal)	8696	0	1,897	17,993
3	Pressure + Tip over (Accident)	42,607	0	8,728	82,754

** 100% torque is used as M_t in load combination and stress calculations.

The maximum bending bolt moment generated by the applied load is evaluated as follows:

Bending Moment Bolt, M_{bb} (Ref. 10, Table 2.2)

$$M_{bb} = (\pi \times D_{ib}/N_b) [K_b/(K_b + K_l)] M_f$$

The K_b and K_l are defined in reference 10, Table 2.2, by substituting the values given above,

$$K_b = 0.68 \times 10^6 \text{ and } K_l = 11.29 \times 10^6$$

$$\text{Therefore, } M_{bb} = 0.282 M_f,$$

For normal condition, $M_f = 17,933 \text{ in.-lb}$

Substituting the value given above,

$$M_{bb} = 5,074 \text{ in.-lb/bolt}$$

3A.3.4 Bolt Stress Calculations (Ref.10, Table 5.1)

A. Average Tensile Stress

$$\text{Normal Condition} \quad S_{b_a} = 1.2732 \frac{(60,350)}{(1.753)^2} = 25,000 \text{ psi} = 25.0 \text{ ksi}$$

$$\text{Accident Condition} \quad S_{b_a} = 1.2732 \frac{(60,350)^{**}}{(1.753)^2} = 25,000 \text{ psi} = 25.0 \text{ ksi}$$

** The bolt preload is calculated to withstand the worst case load combination and to maintain a clamping (compressive) force on the closure joint, both under normal and accident conditions. Based upon the load combination results (see Table on pg. 3A.3-6), it is shown that a positive (compressive) load is maintained on the clamped joint for all load combinations. Therefore, in both normal and accident load cases, the maximum non-prying tensile force of 60,350 lbs from preload + temperature load is used for bolt stress calculations.

B. Bending Stress

$$S_{bb} = \frac{10.186 M_{bb}}{(D_{ba})^3} \quad M_{bb} = 5,074 \text{ in-lb}$$

$$S_{bb} = 10.186 (5,074)/1.753^3 = 9,595 \text{ psi} = 9.6 \text{ ksi}$$

C. Shear Stress

Average shear stress caused by shear bolt force (Fs)

$$S_{BS} = 0$$

Maximum shear stress caused by the torsional moment (Mt)

$$S_{bt} = \frac{5.093 M_t}{(D_{ba})^3} = 5.093 \frac{(11,315)}{(1.753)^3} = 10,698 \text{ psi} = 10.7 \text{ ksi}$$

D. Maximum Stress Intensity Caused By Tension + Shear + Bending + Torsion

$$S_{bi} = [(S_{b_a} + S_{bb})^2 + 4(S_{b_s} + S_{bt})^2]^{0.5}$$

For normal condition;

$$S_{bi} = [(25,000 + 9,595)^2 + 4(0 + 10,698)]^{0.5} = 40,677 \text{ Psi} = 40.7 \text{ ksi}$$

E. Stress Ratios

$$R_t^2 + R_s^2 < 1$$

For normal conditions: (Ref. Table 3A.3-3)

$$R_t = 25,000/92,400 = 0.27, \quad R_s = 10,698/55,400 = 0.19$$

$$R_t^2 + R_s^2 = (0.27)^2 + (0.19)^2 = 0.11 < 1.0 \quad \text{O.K.}$$

For accident conditions: (Ref. Table 3A.3-4)

$$R_t = 25,000/115,500 = 0.22$$

$$R_s = 10,698/69,300 = 0.15$$

$$R_t^2 + R_s^2 = (0.22)^2 + (0.15)^2 = 0.07 < 1.0 \quad \text{O.K.}$$

F. Bearing Stress (Under Bolt Head)

Maximum Axial Force = 60,350 Lbs.

Bolt head corresponding to 2 1/4" dia. Bolt is used for 1 7/8" dia. Shank due to higher bearing load in transport. The total bearing area under the 2 1/4" Hex bolt head is 5.54 in.² The bearing stress is:

$$\text{Bearing Stress} = 60,350/5.54 = 10,894 \text{ psi} = 10.9 \text{ ksi}$$

3A.3.5 Results

A summary of the stresses is listed in the following table:

SUMMARY OF STRESSES AND ALLOWABLES

Stress Type	Normal Condition	Accident Condition
Avg. Tensile (ksi) Allowable (ksi)	25.0 92.4	25.0 115.5
Shear (ksi) Allowable (ksi)	10.7 55.4	10.7 69.3
Combined (ksi) Allowable (ksi)	40.7 124.7	(Not Required per Reference 10)
Interaction E.Q. $R_t^2 + R_s^2 < 1$	0.11	0.07
Bearing (ksi) Allowable (ksi) (S_y of lid material)	10.9 35.4	(Not Required per Reference 10)

The calculated bolt stresses are all less than the specified allowable stresses.

3A.3.6 Minimum Engagement Length, L_e For Bolt And Flange (Ref. 11, Page 1149)

$$L_e = \frac{2A_t}{3.146K_{n_{max}} \left[\frac{1}{2} + .57735n(E_{s_{min}} - K_{n_{max}}) \right]}$$

Bolt: 1 7/8" - 8UN - 2A

Material: SA - 540 GR. B24 Cl.1

$S_u = 165$ ksi $S_y = 135$ ksi (at room temperature)

Flange Material: SA - 350 GR. LF3

$S_u = 70$ ksi $S_y = 37.5$ ksi (at room temperature)

A_t : Tensile Stress Area = 2.414 in²

n: Number Of Threads = 8

$K_{n \text{ Max}}$: Maximum Minor Diameter Of Internal Threads = 1.765 in

$E_{s \text{ Min}}$: Minimum Pitch Diameter Of External Threads = 1.7838 in

$D_{s \text{ min}}$: Minimum Major Dia. Of External Threads = 1.8577"

Substituting the values given above,

$$L_e = \frac{2 \times 2.414}{3.1416 \times 1.765 [0.5 + .57735 \times 8 (1.7838 - 1.765)]} = 1.484 \text{ in}$$

$$J = \frac{A_s \times \text{Tensile Strength of External Thread Material}}{A_n \times \text{Tensile Strength of Internal Thread Material}}$$

A_s : Shear Area External Threads = $3.1416 n L_e K_{n \text{ max}} [1/2n + .57735 (E_{s \text{ min}} - K_{n \text{ max}})]$

A_n : Shear Area, Internal Threads = $3.1416 n L_e D_{s \text{ min}} [1/2n + .57735(D_{s \text{ min}} - E_{n \text{ max}})]$

$$A_s = 3.1416 \times 8 \times 1.484 \times 1.765 [1/(2 \times 8) + .57735 (1.7838 - 1.765)] = 4.829 \text{ in.}^2$$

$E_{n \text{ max}}$: Max. Pitch Dia. of Internal Threads = 1.8038"

$$A_n = 3.1416 \times 8 \times 1.484 \times 1.8577 [1/(2 \times 8) + .57735 (1.8577 - 1.8038)] = 6.487 \text{ in.}^2$$

$$J = \frac{4.829 \times 165.0}{6.487 \times 70.0} = 1.755$$

Therefore, the minimum required engagement length, $Q = J L_e = 1.755 \times 1.484 = 2.605 \text{ in.}$

The actual minimum engagement length = 2.79 in. > 2.605 in. O.K.

3A.3.7 Conclusions

1. Bolt stresses meet the acceptance criteria of NUREG/CR-6007 "Stress Analysis of Closure Bolts for Shipping Casks".
2. A positive (compressive) load is maintained during normal and accident condition loads as bolt preload is higher than the applied loads.
3. The bolt and flange thread engagement length is acceptable.

3A.4 Outer Shell

This section presents the structural analysis of the outer shell of the TN-68 storage cask. The outer shell consists of a cylindrical shell section and closure plates at each end which connect the cylinder to the cask body. The normal loads acting on the outer shell are due to internal and external pressure and the normal handling operations. Membrane stresses and bending due to the pressure difference and handling loads are determined. These stresses are compared to the allowable stress limits in Section 3.1 to assure that the design criteria are met.

3A.4.1 Description

The outer shell is constructed from low-alloy carbon steel and is welded to the outer surface of the cask body gamma shielding. The cylindrical shell section and the closure plates are 0.75 in. thick. Pertinent dimensions are shown in Fig. 3A.4-1 and Drawing 972-70-1.

3A.4.2 Materials Input Data

The outer shell cylindrical section and closure plates are SA 516-GR 70. The material properties are taken from the ASME⁽²⁾ Code, Section II, Part D. The yield strength of the material is also obtained from the code at a temperature of 300°F.

3A.4.3 Applied Loads

It is assumed that a pressure of 25 psi may be applied to the inside or outside of the outer shell. This bounding assumption envelopes the actual expected pressures described in Section 2.2.5.

The handling loads acting on the outer shell are a result of lifting. The loads applied to the shell as a result of these operations consist of the values given in Section 2.2.5. The weight or inertia load can include all of the weights of the outer shell, neutron resin shield, and aluminum containers. The most severe Normal Service (Design and Level A) Condition load is assumed 3 g inertia load in the vertical lifting orientation. The shell is also analyzed for 3 g loading when the cask is oriented horizontally to ensure it is not damaged during delivery.

- Cask in the Vertical Orientation
 - Stress due to 25 psi pressure
 - Stress due to 3G inertia load (lifting)

- Cask in the Horizontal Orientation
 - Stress due to 25 psi pressure
 - Stress due to 3G inertia load

3A.4.4 Method of Analysis

ANSYS Model

A finite element model is built for the structural analysis of the outer shell and closure plates. The outer shell and closure plates are modeled with ANSYS Plane 42 elements. The element is used as an axisymmetric element. Double nodes are created at weld locations. The partial penetration welds are simulated by coupling the nodes where weld existed. The basic geometry of the outer shell and weld sizes used for analysis are shown in Figure 3A.4-1. The finite element model is shown in Figures 3A.4-2, -3, and -4.

A. Cask in the Vertical Orientation

- Stresses due to 25 psi Pressure

An external pressure of 25 psi will not induce any load or stress in the outer shell since it is in contact with and supported by the resin filled aluminum containers.

An internal pressure of 25 psi is used as the maximum pressure acting in the inner surface of the outer shell as shown on Figure 3A.4-5. The maximum stress intensity for this load case is 4.5 ksi.

- 3G Down

The weight of the resin and aluminum containers is modeled as an additional pressure on the bottom inner surface as shown on Figure 3A.4-6. The maximum stress intensity for this load case is 9.1 ksi.

B. Cask in the Horizontal Orientation

The stress due to 25 psi internal pressure is same as for the vertical orientation. The stress due to 3G inertia load conservatively assumes that the weight of the outer shell, resin, and aluminum containers is uniformly distributed over the 160 in. length and at a 45° angle only. Therefore, the equivalent pressure applied to the outer shell is:

Weight of outer shell: 11.2 kips
Weight of resin: 13.9 kips
Weight of alum. Containers: 2.5 kips

$$P_{\text{equipment}} = (11.2 + 13.9 + 2.5)(3)(1000)(360)/(\pi)(96.5)(160)(45) \approx 14 \text{ psi}$$

The stress results from this 14 psi load is approximately assumed that this pressure is acting like the internal pressure and applied on the full 360° inner surface of the outer shell. Therefore, the stress due to the this 3G inertia load can be ratioed from the 25 psi internal pressure case and is:

$$\sigma = 4,468 (14)/25 = 2,502 \text{ psi (2.5 ksi)}$$

C. Maximum Combined Stress Intensities

Based on the above calculations the stress intensities are summarized in the following table:

Loading	Stress Intensities
25 psi Internal Pressure	4.5 ksi
25 psi + 3G Down (Cask in Vertical Orientation)	9.1 ksi
25 psi + 3G Down (Cask in Horizontal Orientation)	7.0 ksi

3A.4.5 Results

The stresses acting on the outer shell and closure plates are also listed in Table 3A.4-1. They are compared with the allowable values in Table 3.4-10.

3A.5 References

1. American Society of Mechanical Engineers, ASME Boiler and Pressure Vessel Code, Section III, 1995 including 1996 addenda.
2. American Society of Mechanical Engineers, ASME Boiler and Pressure Vessel Code, Section II, Part D, 1998 including 2000 addenda.
3. ANSYS Engineering Analysis System, Users Manual for ANSYS Revision 6.0, Swanson Analysis Systems, Inc., Houston, PA, 2001.
4. High Performance Sealing, Metal Seals Helicoflex Catalog, Helicoflex Co., Boonton, N.J., ET 507 E 5930.
5. (Deleted)
6. WRC Bulletin 107, March 1979 Rev: "Local Stresses in Spherical and Cylindrical Shells Due to External Loadings."
7. (Deleted)
8. Roark, R.J.: "Formulas for Stress & Strain", 4th Edition, McGraw-Hill Book Co.
9. (Deleted)
10. NUREG/CR-6007, "Stress Analysis of Closure Bolts for Shipping Cask."
11. Machinery Handbook, 21st Ed.
12. NUREG-1536, "Standard Review Plan for Dry Cask Storage Systems," January 1997.
13. American Society of Mechanical Engineers, ASME Boiler and Pressure Vessel Code, Section III, 1998 including 2000 addenda.
14. American Society of Mechanical Engineers, ASME Boiler and Pressure Vessel Code, Section II, Part D, 1998 including 2000 addenda.

TABLE 3A.2.3-1

BOLT PRELOAD (SHELL ELEMENTS)

LOCATION		NODAL STRESS INTENSITY (PSI)
INNER BOTTOM PLATE	1	1
	2	1
	3	1
	4	1
	5	12
	6	11
INNER SHELL	7	12
	8	12
	9	12
	10	12
	11	12
	12	12
	13	10
	14	13
	15	44
	16	27
	17	13
	18	10

TABLE 3A 2.3-2

BOLT PRELOAD (SOLID ELEMENTS)

LOCATION		NODAL STRESS INTENSITY (PSI)
FLANGE	19	528
	20	418
LID	21	13
	22	141
OUTER BOTTOM PLATE	23	1
	24	1
	25	16
	26	1
GAMMA SHIELDING CYLINDER	27	3
	28	3
	29	3
	30	3
	31	3
	32	3
	33	5
	34	2
	35	57
	36	43
WELDS	37	1
	38	121
	39	301

TABLE 3A 2.3-3

ONE (1) G DOWN (SHELL ELEMENTS)

LOCATION		NODAL STRESS INTENSITY (PSI)
INNER BOTTOM PLATE	1	26
	2	21
	3	28
	4	17
	5	90
	6	66
INNER SHELL	7	72
	8	70
	9	61
	10	61
	11	44
	12	44
	13	27
	14	27
	15	20
	16	18
	17	17
	18	8

TABLE 3A.2.3-4

ONE (1) G DOWN (SOLID ELEMENTS)

LOCATION		NODAL STRESS INTENSITY (PSI)
FLANGE	19	39
	20	10
LID	21	51
	22	84
OUTER BOTTOM PLATE	23	23
	24	25
	25	98
	26	64
GAMMA SHIELDING CYLINDER	27	79
	28	69
	29	63
	30	64
	31	47
	32	46
	33	29
	34	30
	35	23
	36	16
WELDS	37	87
	38	12
	39	96

TABLE 3A.2.3-5

INTERNAL PRESSURE - 100 PSI (SHELL ELEMENTS)

LOCATION		NODAL STRESS INTENSITY (PSI)
INNER BOTTOM PLATE	1	301
	2	136
	3	239
	4	74
	5	1419
	6	737
INNER SHELL	7	493
	8	456
	9	601
	10	544
	11	589
	12	532
	13	590
	14	535
	15	524
	16	417
	17	638
	18	500

TABLE 3A.2.3-6

INTERNAL PRESSURE - 100 PSI (SOLID ELEMENTS)

LOCATION		NODAL STRESS INTENSITY (PSI)
FLANGE	19	1057
	20	713
LID	21	1398
	22	2335
OUTER BOTTOM PLATE	23	1031
	24	1419
	25	2532
	26	738
GAMMA SHIELDING CYLINDER	27	295
	28	296
	29	578
	30	439
	31	565
	32	416
	33	567
	34	421
	35	520
	36	310
WELDS	37	869
	38	775
	39	2478

TABLE 3A.2.3-7

EXTERNAL PRESSURE - 25 PSI (SHELL ELEMENTS)

LOCATION		NODAL STRESS INTENSITY (PSI)
INNER BOTTOM PLATE	1	75
	2	45
	3	61
	4	32
	5	345
	6	164
INNER SHELL	7	123
	8	130
	9	151
	10	151
	11	148
	12	148
	13	148
	14	149
	15	128
	16	125
	17	159
	18	141

TABLE 3A.2.3-8

EXTERNAL PRESSURE - 25 PSI (SOLID ELEMENTS)

LOCATION		NODAL STRESS INTENSITY (PSI)
FLANGE	19	280
	20	172
LID	21	351
	22	584
OUTER BOTTOM PLATE	23	261
	24	357
	25	629
	26	186
GAMMA SHIELDING CYLINDER	27	75
	28	73
	29	146
	30	111
	31	143
	32	105
	33	143
	34	106
	35	131
36	79	
WELDS	37	219
	38	189
	39	620

TABLE 3A.2.3-9

THERMAL STRESS (SHELL ELEMENTS)

LOCATION		NODAL STRESS INTENSITY (PSI)	
		HOT	COLD
INNER BOTTOM PLATE	1	7916	8591
	2	8753	9553
	3	7345	8044
	4	7940	8747
	5	2715	3078
	6	936	878
INNER SHELL	7	911	1080
	8	981	1091
	9	1064	1200
	10	830	973
	11	1080	1220
	12	814	954
	13	1005	1143
	14	888	1030
	15	584	921
	16	1304	1447
	17	754	639
	18	1382	1561

TABLE 3A.2.3-10

THERMAL STRESS (SOLID ELEMENTS)

LOCATION		NODAL STRESS INTENSITY (PSI)	
		HOT	COLD
FLANGE	19	806	475
	20	1150	994
LID	21	12	7
	22	269	252
OUTER BOTTOM PLATE	23	12715	13191
	24	1106	1179
	25	3806	4962
	26	393	176
GAMMA SHIELDING CYLINDER	27	420	629
	28	999	1108
	29	1061	935
	30	1198	1161
	31	1388	1269
	32	1738	1699
	33	827	719
	34	1237	1209
	35	854	759
	36	657	706
WELDS	37	2090	2054
	38	1142	1254
	39	750	713

TABLE 3A.2.3-11

SIX (6) G ON TRUNNION (SHELL ELEMENTS)

LOCATION		NODAL STRESS INTENSITY (PSI)
INNER BOTTOM PLATE	1	801
	2	12
	3	704
	4	167
	5	1974
	6	1329
INNER SHELL	7	505
	8	551
	9	431
	10	435
	11	561
	12	562
	13	695
	14	633
	15	815
	16	672
	17	757
	18	942

TABLE 3A.2.3-12

SIX (6) G ON TRUNNION (SOLID ELEMENTS)

LOCATION		NODAL STRESS INTENSITY (PSI)
FLANGE	19	581
	20	794
LID	21	353
	22	626
OUTER BOTTOM PLATE	23	1931
	24	2465
	25	3712
	26	1223
GAMMA SHIELDING CYLINDER	27	850
	28	590
	29	445
	30	534
	31	607
	32	607
	33	800
	34	676
	35	118
	36	1243
WELDS	37	1215
	38	426
	39	847

TABLE 3A.2.3-13

ONE (1) G SIDE DROP - CONTACT SIDE (SHELL ELEMENTS)

LOCATION		NODAL STRESS INTENSITY (PSI)
INNER BOTTOM PLATE	1	212
	2	202
	3	243
	4	228
	5	230
	6	363
INNER SHELL	7	487
	8	164
	9	703
	10	297
	11	813
	12	359
	13	687
	14	274
	15	430
	16	169
	17	346
	18	190

TABLE 3A.2.3-14

ONE (1) G SIDE DROP - CONTACT SIDE (SOLID ELEMENTS)

LOCATION		NODAL STRESS INTENSITY (PSI)
FLANGE	19	444
	20	417
LID	21	17
	22	17
OUTER BOTTOM PLATE	23	137
	24	69
	25	917
	26	79
GAMMA SHIELDING CYLINDER	27	291
	28	395
	29	490
	30	707
	31	605
	32	829
	33	534
	34	753
	35	301
	36	445
WELDS	37	322
	38	111
	39	229

TABLE 3A.2.3-15

ONE (1) G SIDE DROP - SIDE OPPOSITE CONTACT (SHELL ELEMENTS)

LOCATION		NODAL STRESS INTENSITY (PSI)
INNER BOTTOM PLATE	1	102
	2	93
	3	101
	4	88
	5	57
	6	107
INNER SHELL	7	100
	8	48
	9	174
	10	119
	11	252
	12	177
	13	164
	14	108
	15	83
	16	49
	17	72
	18	78

TABLE 3A.2.3-16

ONE (1) G SIDE DROP - SIDE OPPOSITE CONTACT (SOLID ELEMENTS)

LOCATION		NODAL STRESS INTENSITY (PSI)
FLANGE	19	111
	20	114
LID	21	41
	22	22
OUTER BOTTOM PLATE	23	58
	24	9
	25	245
	26	54
GAMMA SHIELDING CYLINDER	27	68
	28	60
	29	116
	30	170
	31	184
	32	244
	33	141
	34	195
	35	67
36	71	
WELDS	37	82
	38	39
	39	24

TABLE 3A.2.3-17

SEISMIC LOAD - 2 G DOWN + 1G LATERAL (SHELL ELEMENTS)

LOCATION		NODAL STRESS INTENSITY (PSI)
INNER BOTTOM PLATE	1	652
	2	650
	3	265
	4	265
	5	164
	6	344
INNER SHELL	7	174
	8	157
	9	72
	10	83
	11	26
	12	33
	13	27
	14	39
	15	32
	16	46
	17	65
	18	74

TABLE 3A.2.3-18

SEISMIC LOAD - 2 G DOWN + 1G LATERAL (SOLID ELEMENTS)

LOCATION		NODAL STRESS INTENSITY (PSI)
FLANGE	19	118
	20	97
LID	21	184
	22	203
OUTER BOTTOM PLATE	23	529
	24	543
	25	893
	26	161
GAMMA SHIELDING CYLINDER	27	229
	28	102
	29	109
	30	119
	31	7
	32	109
	33	29
	34	105
	35	36
36	86	
WELDS	37	519
	38	115
	39	248

TABLE 3A.2.5-1

NORMAL CONDITION LOAD COMBINATIONS

<u>INDIVIDUAL LOAD COMBINED LOAD</u>	<u>BOLT PRELOAD</u>	<u>1G DOWN</u>	<u>INTERNAL PRESSURE 100 PSI</u>	<u>EXTERNAL PRESSURE 25 PSI</u>	<u>THERMAL</u>	<u>6G ON TRUNNION</u>	<u>TRUNNION LOCAL STRESS</u>	<u>STRESS TABLE NO.</u>
N1	X	X	X					3A.2.5-2 3A.2.5-3
N2	X	X	X		X			3A.2.5-4 3A.2.5-5
N3	X		X		X	X	X	3A.2.5-6 3A.2.5-7
N4	X	X		X				3A.2.5-8 3A.2.5-9
N5	X	X		X	X			3A.2.5-10 3A.2.5-11
N6	X			X	X	X	X	3A.2.5-12 3A.2.5-13

TABLE 3A.2.5-2

BOLT PRELOAD +100 PSI INTERNAL PRESSURE + 1G DOWN
(SHELL ELEMENTS)

LOCATION		COMBINED STRESS INTENSITY (KSI)
INNER BOTTOM PLATE	1	0.3
	2	0.2
	3	0.3
	4	0.1
	5	1.4
	6	0.9
INNER SHELL	7	0.5
	8	0.5
	9	0.6
	10	0.6
	11	0.6
	12	0.6
	13	0.6
	14	0.6
	15	0.6
	16	0.5
	17	0.7
	18	0.5

TABLE 3A.2.5-3

BOLT PRELOAD + 100 PSI INTERNAL PRESSURE + 1G DOWN
(SOLID ELEMENTS)

LOCATION		COMBINED STRESS INTENSITY (KSI)
FLANGE	19	0.8
	20	0.8
LID	21	1.4
	22	2.4
OUTER BOTTOM PLATE	23	1.1
	24	1.5
	25	2.7
	26	0.8
GAMMA SHIELDING CYLINDER	27	0.3
	28	0.3
	29	0.6
	30	0.5
	31	0.6
	32	0.5
	33	0.6
	34	0.5
	35	0.6
36	0.4	
WELDS	37	1.0
	38	0.7
	39	2.2

TABLE 3A.2.5-4

BOLT PRELOAD + 100 PSI INTERNAL PRESSURE + 1G DOWN + THERMAL
(SHELL ELEMENTS)

LOCATION		COMBINED STRESS INTENSITY (KSI)	
		HOT	COLD
INNER BOTTOM PLATE	1	8.2	8.9
	2	8.6	9.4
	3	7.5	8.2
	4	7.9	8.7
	5	1.6	1.7
	6	0.6	0.1
INNER SHELL	7	0.9	0.8
	8	0.9	0.8
	9	0.8	0.9
	10	0.6	0.7
	11	0.9	0.9
	12	0.7	0.7
	13	1.0	0.8
	14	0.9	0.8
	15	0.2	0.4
	16	1.1	1.2
	17	0.9	0.8
	18	1.7	1.7

TABLE 3A.2.5-5

BOLT PRELOAD + 100 PSI INTERNAL PRESSURE + 1G DOWN + THERMAL
(SOLID ELEMENTS)

LOCATION		COMBINED STRESS INTENSITY (KSI)	
		HOT	COLD
FLANGE	19	1.3	1.1
	20	1.2	1.2
LID	21	1.4	1.4
	22	2.1	2.1
OUTER BOTTOM PLATE	23	13.7	14.1
	24	0.3	0.3
	25	6.3	7.4
	26	0.9	0.8
GAMMA SHIELD CYLINDER	27	0.5	0.8
	28	1.2	1.4
	29	0.9	0.8
	30	1.5	1.5
	31	1.2	1.0
	32	1.9	1.9
	33	0.6	0.5
	34	1.4	1.4
	35	0.7	0.7
36	1.0	1.1	
WELDS	37	2.0	2.0
	38	1.8	1.9
	39	1.4	1.4

TABLE 3A.2.5-6

BOLT PRELOAD + 100 PSI INTERNAL PRESSURE + THERMAL + 6G UP + TRUNNION
 LOCAL STRESS
 (SHELL ELEMENTS)

LOCATION		COMBINED STRESS INTENSITY (KSI)	
		HOT	COLD
INNER BOTTOM PLATE	1	9.0	9.7
	2	8.6	9.4
	3	8.2	8.9
	4	8.1	8.9
	5	0.7	0.5
	6	1.3	1.2
INNER SHELL	7	0.3	0.4
	8	0.3	0.4
	9	0.3	0.4
	10	0.1	0.4
	11	0.3	0.3
	12	0.2	0.2
	13	0.3	0.1
	14	0.3	0.1
	15	20.4 ⁽¹⁾	20.4 ⁽³⁾
	16	20.1 ⁽²⁾	20.3 ⁽⁴⁾
	17	0.8	0.5
	18	0.8	0.7

Note : 1. P_m at Location 15 = 12.9 ksi
 2. P_m at Location 16 = 12.7 ksi
 3. P_m at Location 15 = 13.0 ksi
 4. P_m at Location 16 = 12.9 ksi

TABLE 3A.2.5-7

BOLT PRELOAD + 100 PSI INTERNAL PRESSURE + THERMAL + 6G UP + TRUNNION
 LOCAL STRESS
 (SOLID ELEMENTS)

LOCATION		COMBINED STRESS INTENSITY (KSI)	
		HOT	COLD
FLANGE	19	1.3	0.8
	20	0.4	0.4
LID	21	1.1	1.1
	22	1.6	1.6
OUTER BOTTOM PLATE	23	15.6	16.1
	24	2.8	2.7
	25	9.9	11.1
	26	2.2	2.0
GAMMA SHIELD CYLINDER	27	0.4	0.2
	28	1.3	1.6
	29	0.4	0.2
	30	2.1	2.1
	31	0.5	0.4
	32	2.6	2.6
	33	0.4	0.4
	34	2.1	2.1
35	20.5 ⁽¹⁾	20.5 ⁽³⁾	
36	21.1 ⁽²⁾	21.2 ⁽⁴⁾	
WELDS	37	2.1	2.1
	38	1.4	1.5
	39	0.7	0.7

Note : 1. P_m at Location 35 = 13.1 ksi
 2. P_m at Location 36 = 13.7 ksi
 3. P_m at Location 35 = 13.1 ksi
 4. P_m at Location 36 = 13.7 ksi

TABLE 3A.2.5-8

BOLT PRELOAD + 1G DOWN + 25 PSI EXTERNAL PRESSURE
(SHELL ELEMENTS)

LOCATION		COMBINED STRESS INTENSITY (KSI)
INNER BOTTOM PLATE	1	0.1
	2	0.1
	3	0.1
	4	0.1
	5	0.5
	6	0.1
INNER SHELL	7	0.2
	8	0.2
	9	0.2
	10	0.2
	11	0.2
	12	0.2
	13	0.2
	14	0.2
	15	0.2
	16	0.1
	17	0.2
	18	0.2

TABLE 3A.2.5-9

BOLT PRELOAD +1G DOWN + 25 PSI EXTERNAL PRESSURE
(SOLID ELEMENTS)

LOCATION		COMBINED STRESS INTENSITY (KSI)
FLANGE	19	0.9
	20	0.5
LID	21	0.4
	22	0.6
OUTER BOTTOM PLATE	23	0.3
	24	0.4
	25	0.6
	26	0.2
GAMMA SHIELDING CYLINDER	27	0.2
	28	0.2
	29	0.2
	30	0.2
	31	0.2
	32	0.2
	33	0.2
	34	0.2
	35	0.2
36	0.1	
WELDS	37	0.2
	38	0.4
	39	1.0

TABLE 3A.2.5-10

BOLT PRELOAD + 1G DOWN + 25 PSI EXTERNAL PRESSURE + THERMAL
(SHELL ELEMENTS)

LOCATION		COMBINED STRESS INTENSITY (KSI)	
		HOT	COLD
INNER BOTTOM PLATE	1	7.8	8.5
	2	8.8	9.6
	3	7.3	8.0
	4	7.9	8.8
	5	3.2	3.5
	6	1.0	1.0
INNER SHELL	7	1.0	1.2
	8	1.2	1.3
	9	1.2	1.4
	10	1.0	1.1
	11	1.2	1.4
	12	1.0	1.1
	13	1.1	1.3
	14	1.0	1.2
	15	0.7	1.0
	16	1.4	1.5
	17	0.7	0.8
	18	1.5	1.6

TABLE 3A.2.5-11

BOLT PRELOAD +1G DOWN + 25 PSI EXTERNAL PRESSURE + THERMAL
(SOLID ELEMENTS)

LOCATION		COMBINED STRESS INTENSITY (KSI)	
		HOT	COLD
FLANGE	19	0.2	0.5
	20	0.7	0.5
LID	21	0.4	0.4
	22	0.8	0.8
OUTER BOTTOM PLATE	23	12.5	12.9
	24	1.4	1.5
	25	3.3	4.4
	26	0.4	0.3
GAMMA SHIELD CYLINDER	27	0.5	0.8
	28	0.9	1.0
	29	1.2	1.0
	30	1.3	1.2
	31	1.5	1.4
	32	1.6	1.6
	33	0.9	0.8
	34	1.2	1.1
	35	0.8	0.7
	36	0.6	0.7
WELDS	37	2.2	2.1
	38	0.8	0.9
	39	1.7	1.7

TABLE 3A.2.5-12

BOLT PRELOAD + 25 PSI (EXT. P) + THERMAL + 6G UP + TRUNNION LOCAL STRESS
(SHELL ELEMENTS)

LOCATION		COMBINED STRESS INTENSITY (KSI)	
		HOT	COLD
INNER BOTTOM PLATE	1	8.6	9.3
	2	8.8	9.6
	3	7.9	8.6
	4	8.1	8.9
	5	1.1	1.5
	6	0.6	0.3
INNER SHELL	7	0.7	0.8
	8	0.7	0.8
	9	0.8	1.1
	10	0.7	1.0
	11	0.6	0.9
	12	0.5	0.8
	13	0.4	0.8
	14	0.4	0.8
	15	20.3 ⁽¹⁾	20.6 ⁽³⁾
	16	20.5 ⁽²⁾	20.8 ⁽⁴⁾
	17	0.1	0.3
	18	0.6	0.7

Note : 1. P_m at Location 15 = 12.9 ksi
 2. P_m at Location 16 = 13.1 ksi
 3. P_m at Location 15 = 13.2 ksi
 4. P_m at Location 16 = 13.4 ksi

TABLE 3A.2.5-13

BOLT PRELOAD + 25 PSI (EXT. P) + THERMAL + 6G UP + TRUNNION LOCAL STRESS
(SOLID ELEMENTS)

LOCATION		COMBINED STRESS INTENSITY (KSI)	
		HOT	COLD
FLANGE	19	0.7	0.6
	20	0.6	0.5
LID	21	0.7	0.7
	22	1.3	1.3
OUTER BOTTOM PLATE	23	14.3	14.8
	24	1.0	0.9
	25	6.8	8.0
	26	1.3	1.1
GAMMA SHIELD CYLINDER	27	0.5	0.3
	28	0.9	1.2
	29	0.9	0.7
	30	1.9	1.8
	31	1.2	1.0
	32	2.3	2.3
	33	0.8	0.7
	34	1.8	1.8
35	20.6 ⁽¹⁾	20.5 ⁽³⁾	
36	21.0 ⁽²⁾	21.0 ⁽⁴⁾	
WELDS	37	1.8	1.8
	38	0.6	0.7
	39	2.5	2.4

Note : 1. P_m at Location 35 = 13.2 ksi
 2. P_m at Location 36 = 13.6 ksi
 3. P_m at Location 35 = 13.1 ksi
 4. P_m at Location 36 = 13.6 ksi

TABLE 3A.2.5-14

ACCIDENT CONDITION LOAD COMBINATIONS

INDIVIDUAL LOAD COMBINED LOAD	BOLT PRELOAD	INTERNAL PRESSURE 100 PSI	EXTERNAL PRESSURE 25 PSI	18" BOTTOM END DROP 60G	TIP OVER SIDE DROP 65G	SEISMIC, TORNADO, OR FLOOD 1G-LATERAL+ 2G-DOWN	STRESS TABLE NO.
A1	X	X		X			3A.2.5-15 3A.2.5-16
A2	X		X	X			3A.2.5-17 3A.2.5-18
A3	X	X			X		3A.2.5.19 3A.2.5.20 3A.2.5.21 3A.2.5.22
A4	X		X		X		3A.2.5.23 3A.2.5.24 3A.2.5.25 3A.2.5.26
A5	X	X				X	3A.2.5.27 3A.2.5.28
A6	X		X			X	3A.2.5.29 3A.2.5.30

TABLE 3A.2.5-15

BOLT PRELOAD + 60G DOWN END DROP + 100 PSI INTERNAL PRESSURE
(SHELL ELEMENTS)

LOCATION		COMBINED STRESS INTENSITY (KSI)
INNER BOTTOM PLATE	1	1.3
	2	1.4
	3	1.5
	4	1.3
	5	4.1
	6	4.8
INNER SHELL	7	4.5
	8	4.4
	9	3.9
	10	3.9
	11	2.9
	12	2.9
	13	1.9
	14	1.9
	15	1.4
	16	1.3
	17	1.1
	18	0.9

TABLE 3A.2.5-16

BOLT PRELOAD + 60 G DOWN END DROP + 100 PSI INTERNAL PRESSURE
(SOLID ELEMENTS)

LOCATION		COMBINED STRESS INTENSITY (KSI)
FLANGE	19	1.9
	20	0.8
LID	21	1.7
	22	2.6
OUTER BOTTOM PLATE	23	0.4
	24	2.9
	25	8.3
	26	3.4
GAMMA SHIELDING CYLINDER	27	4.7
	28	4.2
	29	4.2
	30	4.1
	31	3.1
	32	3.1
	33	2.1
	34	2.0
	35	1.6
36	1.2	
WELDS	37	6.1
	38	0.5
	39	3.6

TABLE 3A.2.5-17

BOLT PRELOAD + 60G DOWN END DROP + 25 PSI EXTERNAL PRESSURE
(SHELL ELEMENTS)

LOCATION		COMBINED STRESS INTENSITY (KSI)
INNER BOTTOM PLATE	1	1.7
	2	1.3
	3	1.8
	4	1.1
	5	5.8
	6	3.9
INNER SHELL	7	4.4
	8	4.4
	9	3.8
	10	3.8
	11	2.8
	12	2.8
	13	1.8
	14	1.8
	15	1.2
	16	1.1
	17	1.2
	18	0.6

TABLE 3A.2.5-18

BOLT PRELOAD + 60G DOWN END DROP + 25 PSI EXTERNAL PRESSURE
(SOLID ELEMENTS)

LOCATION		COMBINED STRESS INTENSITY (KSI)
FLANGE	19	3.2
	20	1.0
LID	21	3.4
	22	5.5
OUTER BOTTOM PLATE	23	1.7
	24	1.2
	25	5.4
	26	4.0
GAMMA SHIELDING CYLINDER	27	4.8
	28	4.2
	29	3.9
	30	3.9
	31	2.9
	32	2.9
	33	1.9
	34	1.9
	35	1.5
	36	0.9
WELDS	37	5.1
	38	1.0
	39	6.7

TABLE 3A.2.5-19

BOLT PRELOAD + TIP OVER (65G) + 100 PSI INTERNAL PRESSURE
OPPOSITE CONTACT SIDE (SHELL ELEMENTS)

LOCATION		COMBINED STRESS INTENSITY (KSI)
INNER BOTTOM PLATE	1	6.7
	2	6.1
	3	6.5
	4	5.8
	5	4.1
	6	6.2
INNER SHELL	7	7.0
	8	3.6
	9	11.8
	10	8.0
	11	16.6
	12	11.7
	13	11.2
	14	7.3
	15	5.9
	16	3.7
	17	5.2
	18	5.3

TABLE 3A.2.5-20

BOLT PRELOAD + TIP OVER (65g) + 100 PSI INTERNAL PRESSURE
OPPOSITE CONTACT SIDE (SOLID ELEMENTS)

LOCATION		COMBINED STRESS INTENSITY (KSI)
FLANGE	19	6.8
	20	7.7
LID	21	4.1
	22	2.9
OUTER BOTTOM PLATE	23	3.7
	24	2.0
	25	13.5
	26	2.8
GAMMA SHIELDING CYLINDER	27	4.6
	28	3.7
	29	8.1
	30	10.6
	31	12.6
	32	15.5
	33	9.6
	34	12.3
	35	4.6
36	4.3	
WELDS	37	4.5
	38	1.9
	39	0.7

TABLE 3A.2.5-21

BOLT PRELOAD + TIP OVER (65G) + 100 PSI INTERNAL PRESSURE
CONTACT SIDE (SHELL ELEMENTS)

LOCATION		COMBINED STRESS INTENSITY (KSI)
INNER BOTTOM PLATE	1	13.8
	2	13.1
	3	15.7
	4	14.8
	5	15.3
	6	22.8
INNER SHELL	7	32.1
	8	11.1
	9	46.3 ⁽¹⁾
	10	19.5
	11	53.3 ⁽²⁾
	12	23.5
	13	45.1 ⁽³⁾
	14	18.1
	15	28.4
	16	11.5
	17	23.1
	18	12.5

Note: (1) P_m at location 9 = 31.9 ksi
 (2) P_m at location 11 = 37.2 ksi
 (3) P_m at location 13 = 31.1 ksi

TABLE 3A.2.5-22

BOLT PRELOAD + TIP OVER (65g) + 100 PSI INTERNAL PRESSURE
CONTACT SIDE (SOLID ELEMENTS)

LOCATION		COMBINED STRESS INTENSITY (KSI)
FLANGE	19	28.5
	20	27.3
LID	21	1.1
	22	3.4
OUTER BOTTOM PLATE	23	8.9
	24	4.6
	25	57.2 ⁽¹⁾
	26	4.7
GAMMA SHIELDING CYLINDER	27	19.3
	28	25.5
	29	32.6
	30	45.6
	31	40.1
	32	53.6 ⁽²⁾
	33	35.5
	34	48.6 ⁽³⁾
	35	20.3
	36	28.6
WELDS	37	20.2
	38	7.0
	39	12.8

Note: (1) P_m at location 25 = 10.6 ksi

(2) P_m at location 32 = 10.8 ksi

(3) P_m at location 34 = 10.0 ksi

TABLE 3A.2.5-23

BOLT PRELOAD + TIP OVER (65G) + 25 PSI EXTERNAL PRESSURE
OPPOSITE CONTACT SIDE (SHELL ELEMENTS)

LOCATION		COMBINED STRESS INTENSITY (KSI)
INNER BOTTOM PLATE	1	6.7
	2	6.1
	3	6.6
	4	5.7
	5	3.7
	6	7.1
INNER SHELL	7	6.4
	8	3.0
	9	11.3
	10	7.7
	11	16.3
	12	11.4
	13	10.5
	14	7.0
	15	5.3
	16	3.1
	17	4.6
	18	5.0

TABLE 3A.2.5-24

BOLT PRELOAD + TIP OVER (65g) + 25 PSI EXTERNAL PRESSURE
OPPOSITE CONTACT SIDE (SOLID ELEMENTS)

LOCATION		COMBINED STRESS INTENSITY (KSI)
FLANGE	19	8.0
	20	7.9
LID	21	2.6
	22	1.7
OUTER BOTTOM PLATE	23	3.8
	24	0.5
	25	16.6
	26	3.7
GAMMA SHIELDING CYLINDER	27	4.5
	28	4.0
	29	7.5
	30	11.2
	31	11.9
	32	16.0
	33	9.2
	34	12.8
	35	4.4
	36	4.7
WELDS	37	5.6
	38	2.9
	39	2.5

TABLE 3A.2.5-25

BOLT PRELOAD + TIP OVER (65G) + 25 PSI EXTERNAL PRESSURE
CONTACT SIDE (SHELL ELEMENTS)

LOCATION		COMBINED STRESS INTENSITY (KSI)
INNER BOTTOM PLATE	1	13.8
	2	13.1
	3	15.8
	4	14.8
	5	14.8
	6	23.7
INNER SHELL	7	31.4
	8	10.5
	9	45.4
	10	19.2
	11	52.5 ⁽¹⁾
	12	23.2
	13	44.4
	14	17.8
	15	27.8
	16	11.0
	17	22.3
	18	12.2

Note: (1) P_m at location 11 = 36.5 ksi

TABLE 3A.2.5-26

BOLT PRELOAD + TIP OVER (65g) + 25 PSI EXTERNAL PRESSURE
CONTACT SIDE (SOLID ELEMENTS)

LOCATION		COMBINED STRESS INTENSITY (KSI)
FLANGE	19	29.6
	20	27.5
LID	21	1.4
	22	0.9
OUTER BOTTOM PLATE	23	9.0
	24	4.5
	25	60.4 ⁽¹⁾
	26	5.4
GAMMA SHIELDING CYLINDER	27	19.0
	28	25.8
	29	31.8
	30	46.1
	31	39.4
	32	54.1 ⁽²⁾
	33	34.7
	34	49.2 ⁽³⁾
	35	19.6
	36	29.0
WELDS	37	21.2
	38	7.5
	39	15.7

Note: (1) At location 25, $P_m=10.8$ ksi
 (2) At location 32, $P_m=11.1$ ksi
 (3) At location 34, $P_m=10.5$ ksi

TABLE 3A.2.5-27

BOLT PRELOAD + 100 PSI INTERNAL PRESSURE + SEISMIC (TORNADO, FLOOD)
(SHELL ELEMENTS)

LOCATION		COMBINED STRESS INTENSITY (KSI)
INNER BOTTOM PLATE	1	0.7
	2	0.8
	3	0.3
	4	0.3
	5	1.3
	6	1.1
INNER SHELL	7	0.5
	8	0.5
	9	0.7
	10	0.6
	11	0.6
	12	0.6
	13	0.6
	14	0.6
	15	0.6
	16	0.5
	17	0.7
	18	0.6

TABLE 3A.2.5-28

BOLT PRELOAD + 100 PSI INTERNAL PRESSURE + SEISMIC (TORNADO, FLOOD)
(SOLID ELEMENTS)

LOCATION		COMBINED STRESS INTENSITY (KSI)
FLANGE	19	0.9
	20	0.9
LID	21	1.3
	22	2.3
OUTER BOTTOM PLATE	23	1.2
	24	1.9
	25	3.5
	26	0.6
GAMMA SHIELDING CYLINDER	27	0.4
	28	0.3
	29	0.7
	30	0.6
	31	0.6
	32	0.6
	33	0.6
	34	0.6
	35	0.6
36	0.5	
WELDS	37	1.4
	38	0.8
	39	2.0

TABLE 3A.2.5-29

BOLT PRELOAD + 25 PSI EXTERNAL PRESSURE + SEISMIC (TORNADO, FLOOD)
(SHELL ELEMENTS)

LOCATION		COMBINED STRESS INTENSITY (KSI)
INNER BOTTOM PLATE	1	0.7
	2	0.7
	3	0.3
	4	0.3
	5	0.5
	6	0.2
INNER SHELL	7	0.3
	8	0.3
	9	0.2
	10	0.2
	11	0.2
	12	0.2
	13	0.2
	14	0.2
	15	0.2
	16	0.1
	17	0.2
	18	0.2

TABLE 3A.2.5-30

BOLT PRELOAD + 25 PSI EXTERNAL PRESSURE + SEISMIC (TORNADO, FLOOD)
(SOLID ELEMENTS)

LOCATION		COMBINED STRESS INTENSITY (KSI)
FLANGE	19	0.9
	20	0.5
LID	21	0.6
	22	0.7
OUTER BOTTOM PLATE	23	0.7
	24	0.6
	25	0.4
	26	0.4
GAMMA SHIELDING CYLINDER	27	0.3
	28	0.2
	29	0.2
	30	0.1
	31	0.2
	32	0.1
	33	0.2
	34	0.1
	35	0.2
	36	0.1
WELDS	37	0.4
	38	0.3
	39	1.2

TABLE 3A.3-1

DESIGN PARAMETERS FOR LID BOLT ANALYSIS

-	D _b	Nominal diameter of closure bolt; 1.875 in
-	K	Nut factor for empirical relation between the applied torque and achieved preload, used 0.1 for neolube
-	Q	Applied torque for the preload (in-lb)
-	D _{lb}	Closure lid dia at bolt circle, 75.88 in
-	D _{lg}	Closure lid dia at the seal (outer) = 72.90 in.
-	E _c	Young's modulus of cask wall material, 28 x 10 ⁶ Psi
-	E _l	Young's modulus of lid material, 27.8 x 10 ⁶ Psi
-	N _b	Total number of closure bolts, 48
-	N _{ul}	Poisson's ratio of closure lid, 0.3
-	P _{ei}	Inside pressure of cask, 100 Psig
-	D _{lo}	Closure Lid Dia at outer edge, 79.88 in
-	P _{li}	Pressure inside the closure lid, 100 Psig
-	t _c	Thickness of cask wall, 6.0 + 1.5 = 7.5 in
-	t _l	Thickness of lid, 9.5/5.0 in
-	l _b	Thermal coeff of expansion bolt material, 6.27 x 10 ⁻⁶ at R.T., 6.78 x 10 ⁻⁶ in/in-°F at 300°F
-	l _c	Thermal coeff of expansion, cask 6.27 x 10 ⁻⁶ at R.T., 6.78 x 10 ⁻⁶ in/in-°F at 300°F
-	l _l	Thermal coeff of expansion, lid 6.27 x 10 ⁻⁶ R.T., 6.78 x 10 ⁻⁶ in/in °F at 300 °F
-	E _b	Young's modulus of bolt material, 27.8 x 10 ⁶ Psi
-	ai	Maximum rigid-body impact acceleration (g) of the cask
-	DLF	Dynamic load factor to account for any difference between the rigid body acceleration and the acceleration of the contents and closure lid = 1.2
-	W _c	weight of contents = 46,920 (fuel) + 30,320(basket) ** = 77,240 lbs.
-	W _l	weight of lid = 12,074 lbs., say 12,100 lbs
-	W _{c+W_l}	77,240 + 12,074 = 89,314 lbs., say 89,500 lbs.
-	xi	Impact angle between the cask axis and target surface
-	S _{yl}	Yield strength of closure lid material
-	S _{ul}	Ultimate strength of closure lid, 70,000 psi
-	S _{yb}	Yield strength of bolt material (see Table 3A.3-3)
-	S _{ub}	Ultimate strength of bolt material (see Table 3A.3-4)
-	P _{lo}	Pressure outside the lid
-	L _b	Bolt length between the top and bottom surfaces of closure 5.0 in.

** Conservatively using higher basket weight for lid bolt analysis.

TABLE 3A.3-2

BOLT DATA (Ref.10, Table 5.1)

Bolt: 1 7/8" - UN8 - 2A

N: no of threads per inch = 8

p: Pitch = 1/8" = .125 in.

D_b: Nominal Diameter = 1.875 in.

D_{ba}: Bolt diameter for stress calculations = D_b - .9743p = 1.875 - .9743 (.125) = 1.753 in

Stress Area = $\pi/4 (1.753)^2 = 2.414 \text{ in}^2$

TABLE 3A.3-3

ALLOWABLE STRESSES IN CLOSURE BOLTS FOR NORMAL CONDITIONS

(MATERIAL: SA-540 Gr. B24 CL.1)

Temperature (°F)	Yield Stress (1) (ksi)	Normal Condition Allowables		
		F _{tb} (2,4) (ksi)	F _{vb} (3,4) (ksi)	S.I (5) (ksi)
100	150	100.0	60.0	135.0
200	143.4	95.6	57.4	129.1
300	138.6	92.4	55.4	124.7
400	134.4	89.6	53.8	121.0
500	130.2	86.8	52.1	117.2
600	124.2	82.8	49.7	111.8

Notes:

1. Yield stress values are from ASME Code, Section II, Table Y-1 (Ref.2)
2. Allowable Tensile stress, $F_{tb} = 2/3 S_y$
3. Allowable shear stress, $F_{vb} = 0.4 (S_y)$
4. Tension and shear stresses must be combined using the following interaction equation:

$$\frac{(f_{tb})^2}{(F_{tb})^2} + \frac{(f_{vb})^2}{(F_{vb})^2} \leq 1.0$$
5. Stress intensity from combined tensile, shear and residual torsion loads, $S.I. < 0.9 (S_y)$

TABLE 3A.3-4

ALLOWABLE STRESSES IN CLOSURE BOLTS FOR ACCIDENT CONDITIONS

(MATERIAL: SA-540 Gr. B24 Cl.1)

Temperature (°F)	Yield Stress (1) (ksi)	Accident Condition Allowables		
		0.6 S _y (3) (ksi)	F _{tb} (2,4) (ksi)	F _{vb} (3,4) (ksi)
100	150.0	90.0	115.5	69.3
200	143.4	86.0	115.5	69.3
300	138.6	83.2	115.5	69.3
400	134.4	80.6	115.5	69.3
500	130.2	78.1	115.5	69.3
600	124.2	74.5	115.5	69.3

Notes:

1. Yield and tensile stress values are from ASME Code, (Ref.2) Table Y-1, Note that S_u is 165 KSI at all temperatures of interest.
2. Allowable tensile stress, F_{tb} is the smaller of 0.7 S_u or S_y where: 0.7 S_u = 0.7 (165) = 115.5 ksi.
3. Allowable shear stress, F_{vb} is smaller of 0.42 S_u or 0.6 S_y, where: 0.42 S_u = 0.42 (165.) = 69.3 ksi.
4. Tension and shear stresses must be combined using the following interaction equation:

$$\frac{(f_{tb})^2}{(F_{tb})^2} + \frac{(f_{vb})^2}{(F_{vb})^2} \leq 1.0$$

TABLE 3A.4-1

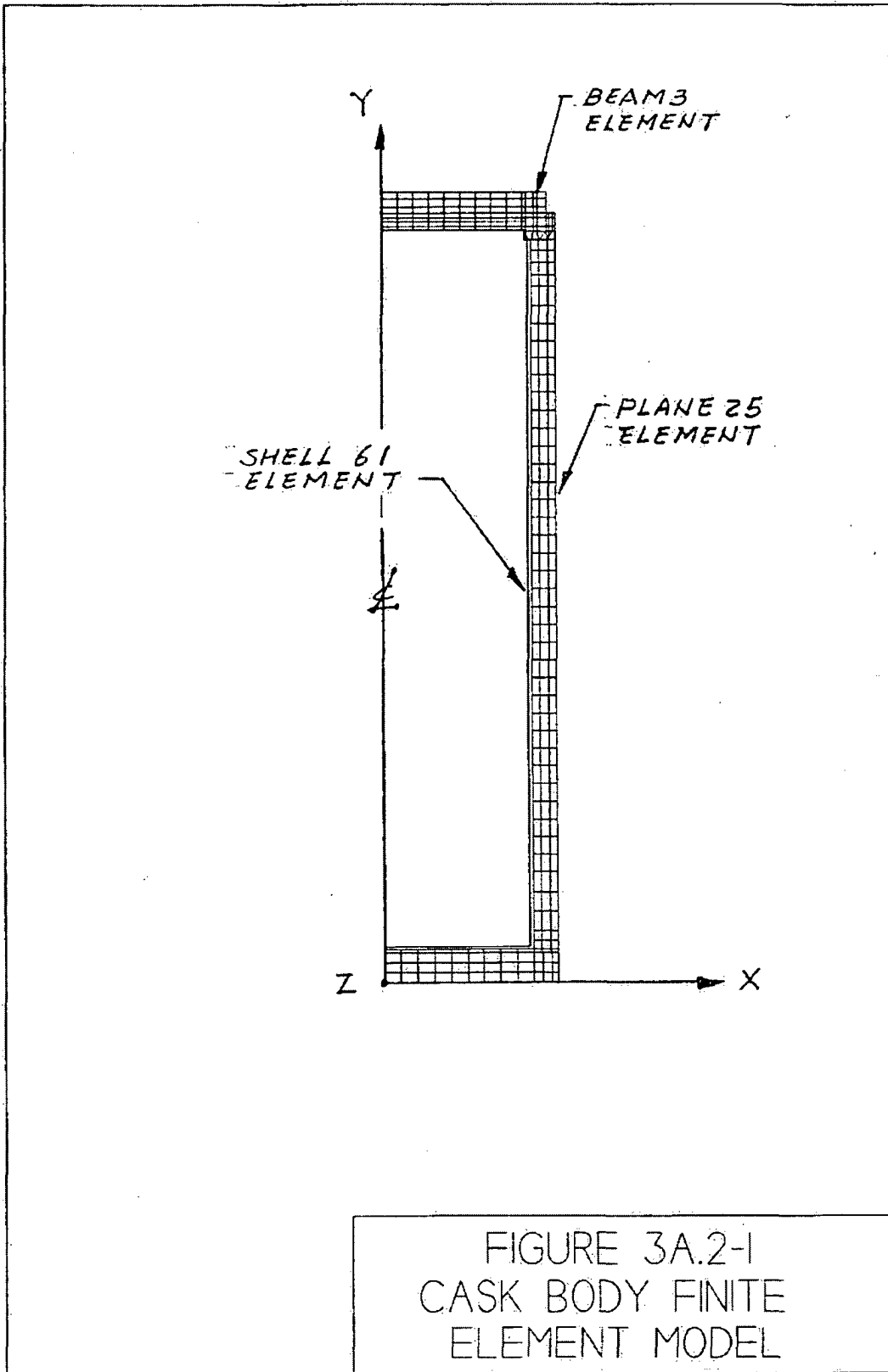
Stress In Outer Shell and Closure Plates

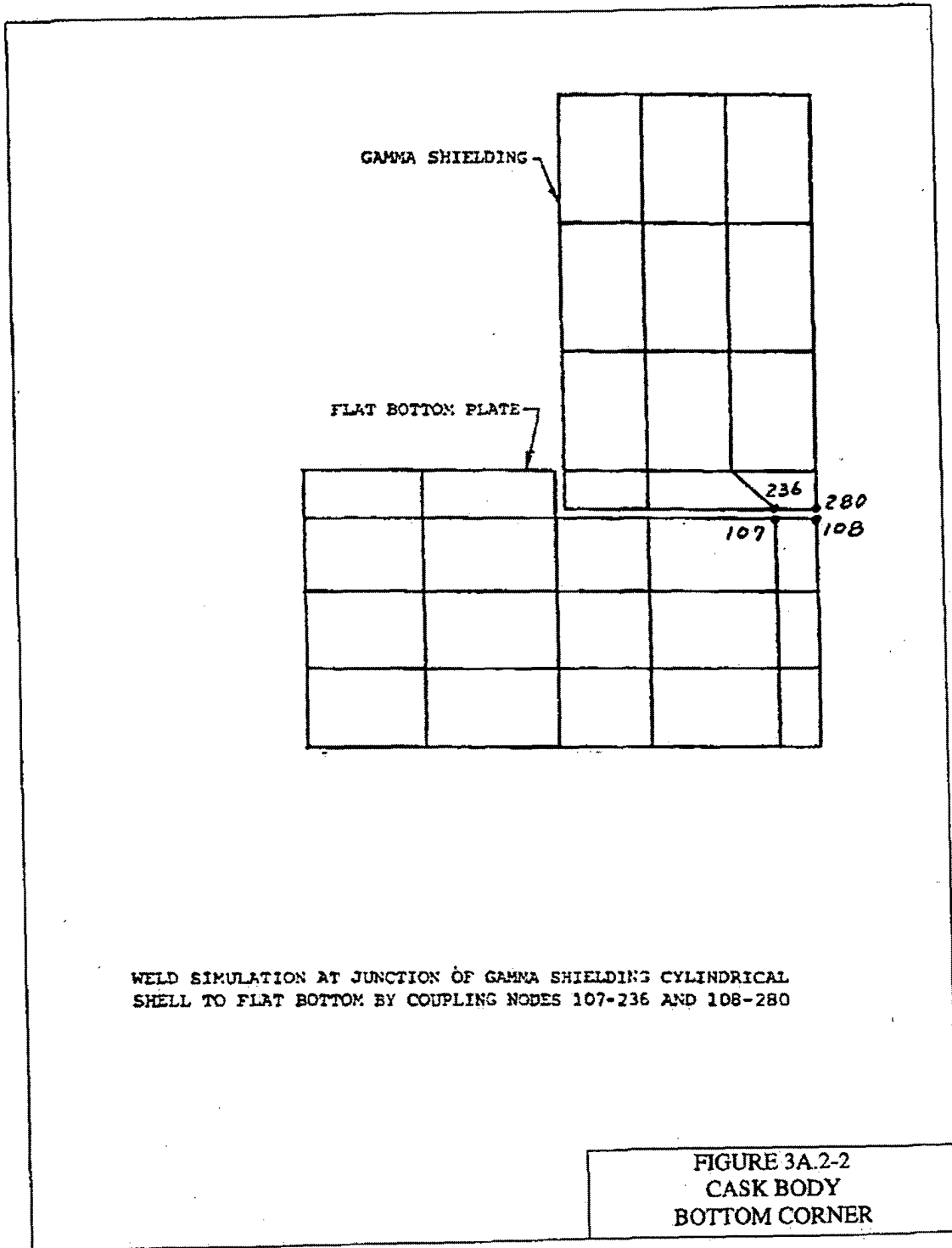
LOADING	LOCATIONS	STRESS INTENSITIES (ksi)
25 psi internal pressure	Juncture of outer Shell and top plate	4.5
25 psi + 3 G down Cask Vertical	Juncture of outer Shell and top plate	9.1
25 psi + 3G down Cask Horizontal	Outer Shell	7.0

Note: The allowables are listed in Chapter 3, Table 3.4-10

Figure Withheld Under 10 CFR 2.390

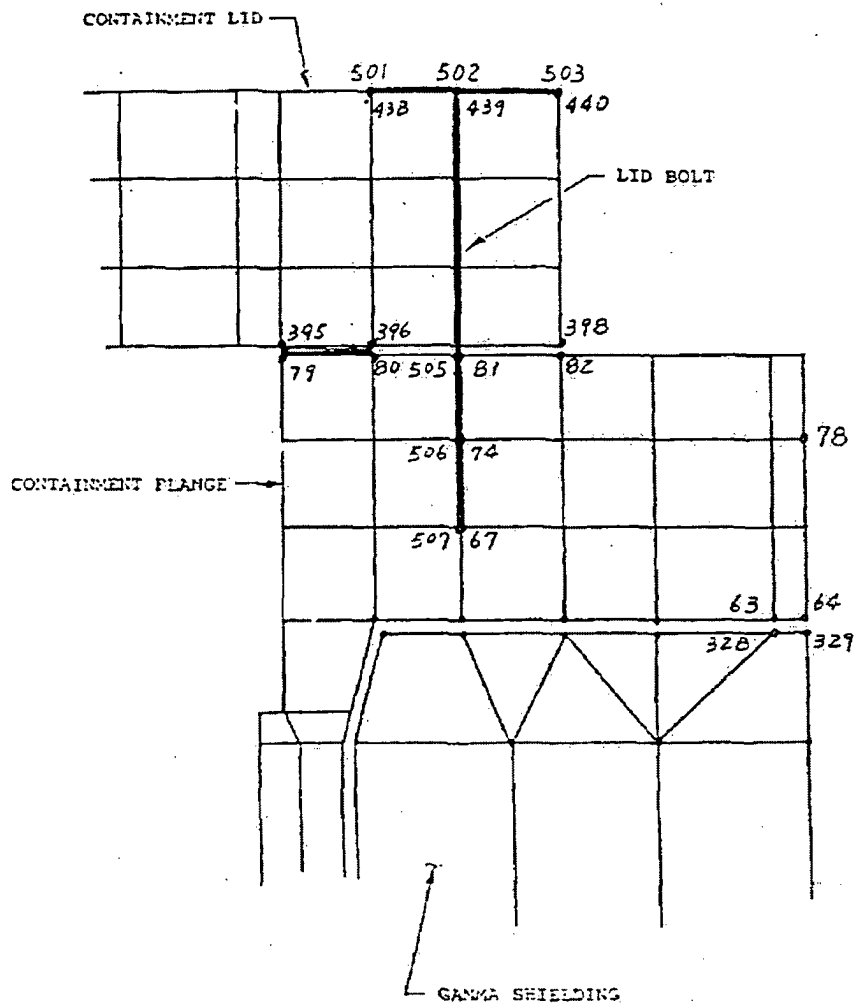
FIGURE 3A.H
CASK BODY KEY DIMENSIONS





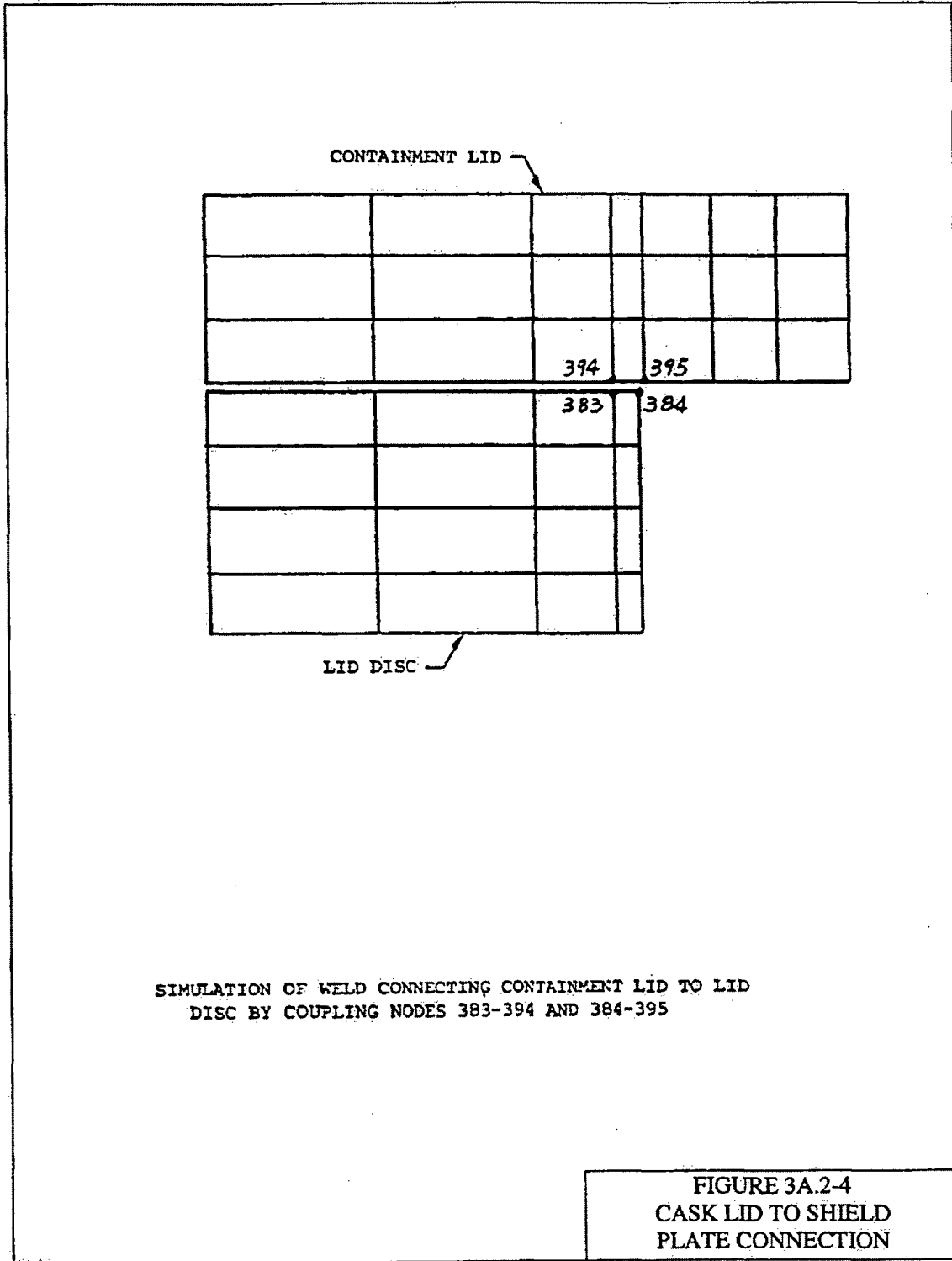
WELD SIMULATION AT JUNCTION OF GAMMA SHIELDING CYLINDRICAL SHELL TO FLAT BOTTOM BY COUPLING NODES 107-236 AND 108-280

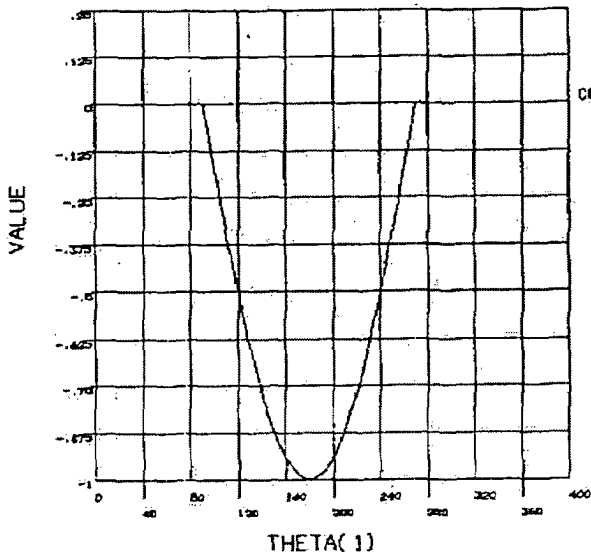
FIGURE 3A.2-2
 CASK BODY
 BOTTOM CORNER



LID BOLTS CONNECTING PRIMARY LID TO CONTAINMENT FLANGE
AND WELD ATTACHING GAMMA SHIELDING TO FLANGE

FIGURE 3A.2-3
CASK BODY
TOP CORNER





FOURIER COEFFICIENTS

MODE	COEFF	ISYM
0.0000	-0.3182	1.0000
1.0000	0.5000	1.0000
1.0000	0.0000	-1.0000
2.0000	-0.2124	-1.0000
2.0000	0.0000	-1.0000
3.0000	0.0000	1.0000
3.0000	0.0000	-1.0000
4.0000	0.0426	1.0000
4.0000	0.0000	-1.0000
5.0000	0.0000	1.0000
5.0000	0.0000	-1.0000
6.0000	-0.0283	1.0000
6.0000	0.0000	-1.0000
7.0000	0.0000	1.0000
7.0000	0.0000	-1.0000
8.0000	0.0203	1.0000
8.0000	0.0000	-1.0000
9.0000	0.0000	1.0000
9.0000	0.0000	-1.0000
10.0000	-0.0066	1.0000
10.0000	0.0000	-1.0000

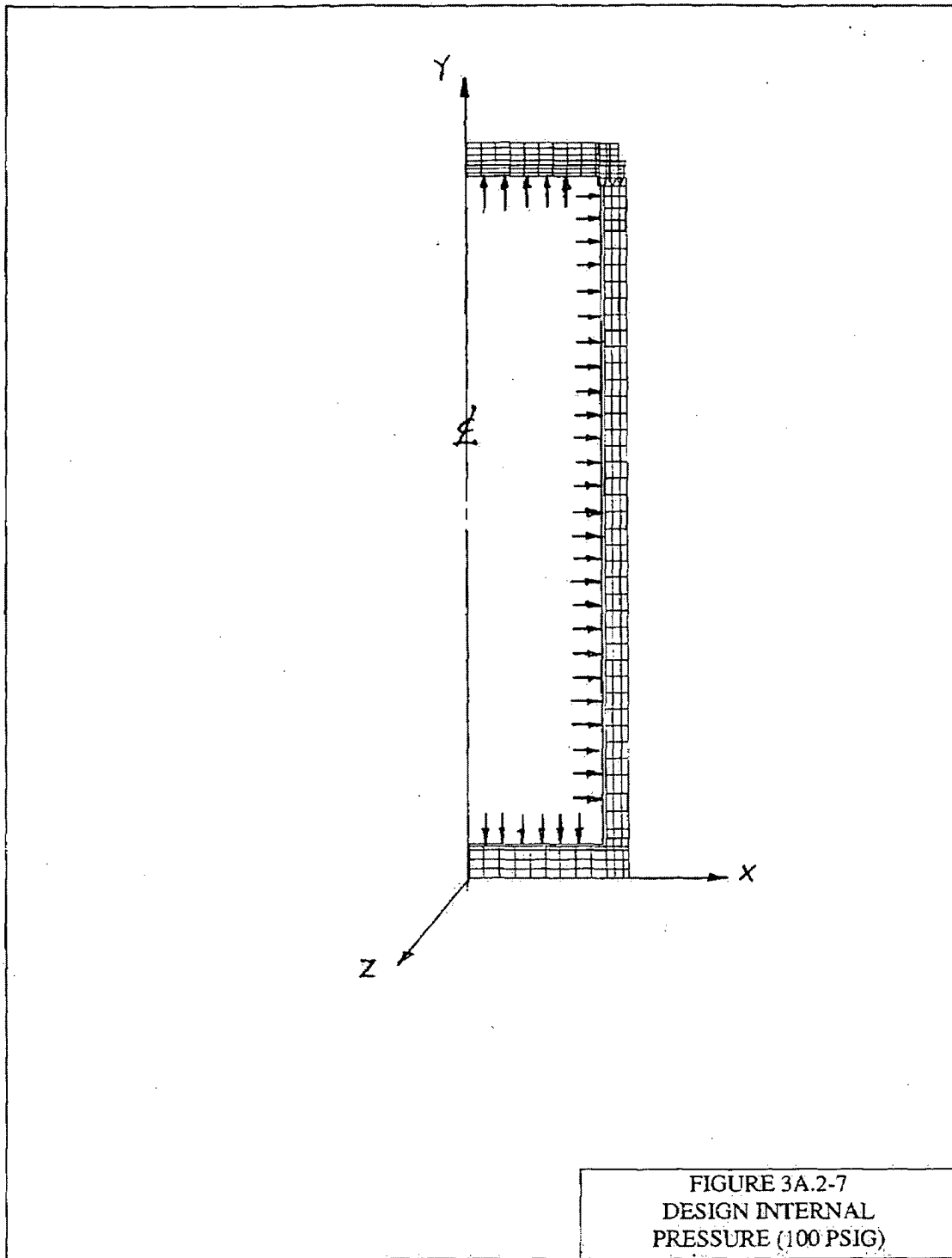
FOURIER OUTPUT CURVE FOR COS FUNCTION OVER 90-270 DEGREES

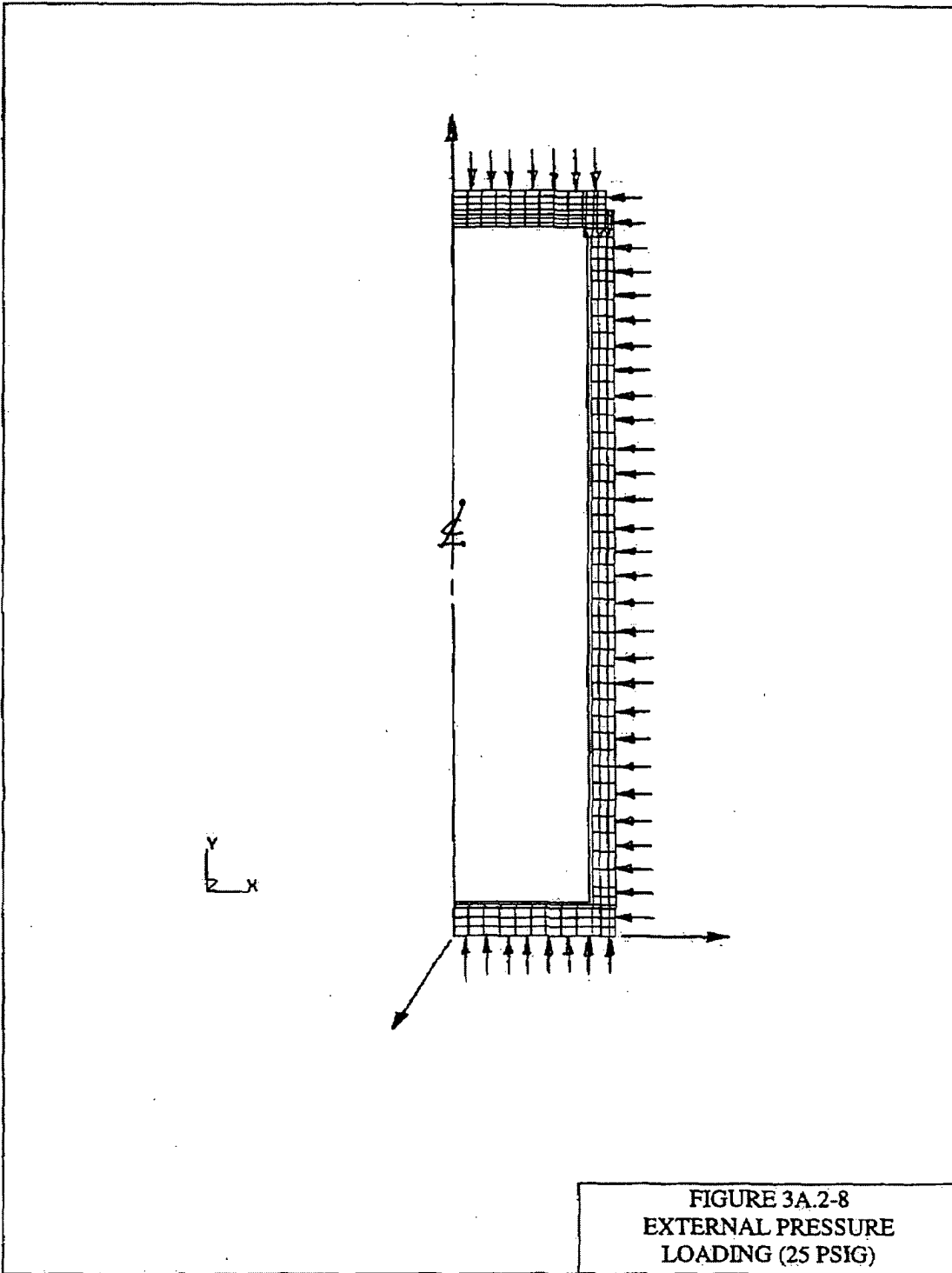
FIGURE 3A.2-5
FOURIER COEFFICIENTS FOR
1G LATERAL

Figure Withheld Under 10 CFR 2.390

** The actual lid bolt preload stress is 25,000 psi, however, lid bolt preload corresponding to 35,000 psi is used for all load combinations.

**FIGURE 3A.2-6
BOLT PRELOAD
AND
SEAL REACTION**





W- TOTAL WEIGHT OF CASK
 (BASED ON 240,000 LBS.)
 -TOTAL WEIGHT OF INTERNALS
 (BASED ON 77,240 LBS)
 - 162,760 LBS.

P_i - PRESSURE ON CONTAINMENT BOTTOM
 INNER SURFACE DUE TO WEIGHT OF
 INTERNALS

$$\frac{77,240}{\pi (35.5^2)}$$

- 19.509 psi

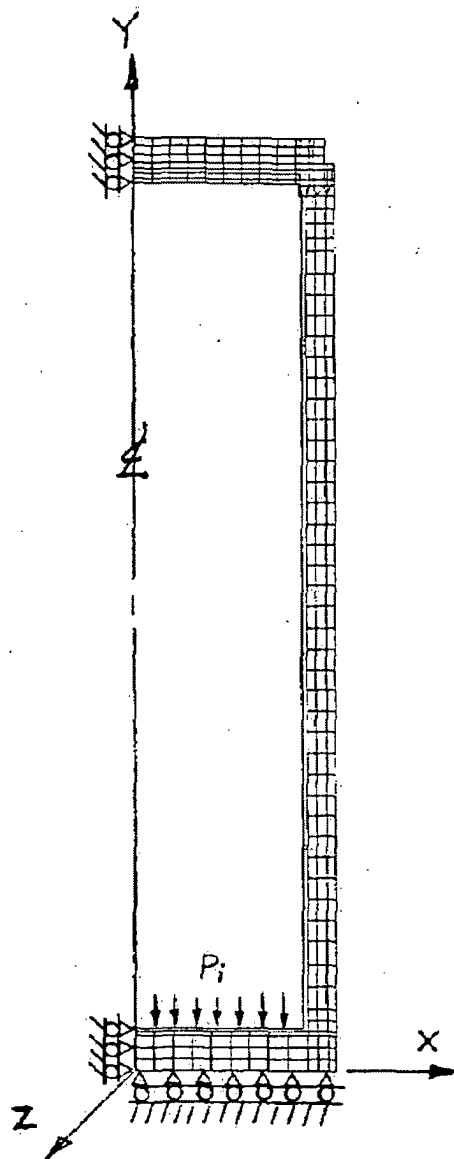
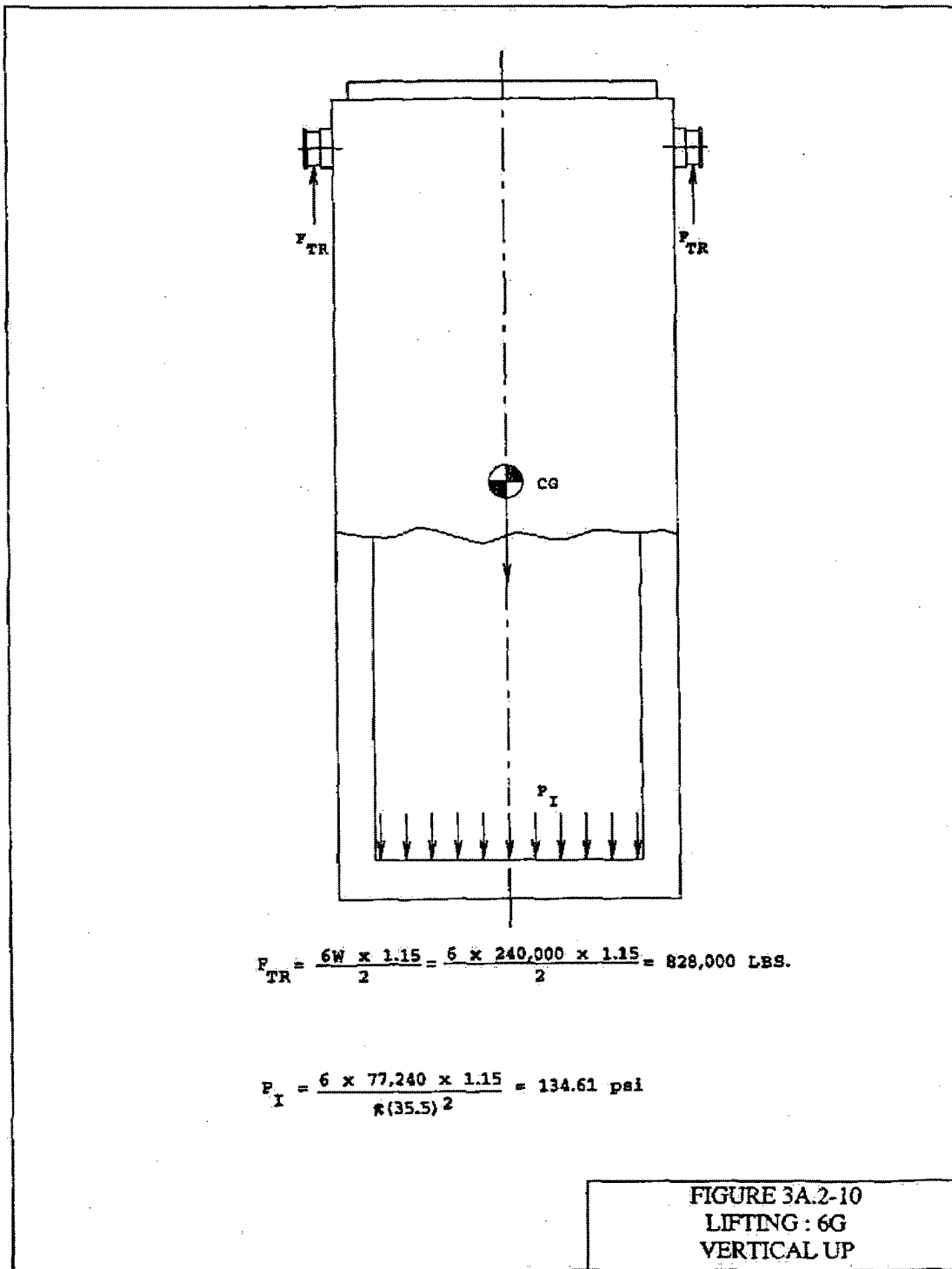


FIGURE 3A.2-9
 I_g DOWN LOADING



$$F_{TR} = \frac{6W \times 1.15}{2} = \frac{6 \times 240,000 \times 1.15}{2} = 828,000 \text{ LBS.}$$

$$P_I = \frac{6 \times 77,240 \times 1.15}{\pi(35.5)^2} = 134.61 \text{ psi}$$

FIGURE 3A.2-10
LIFTING : 6G
VERTICAL UP

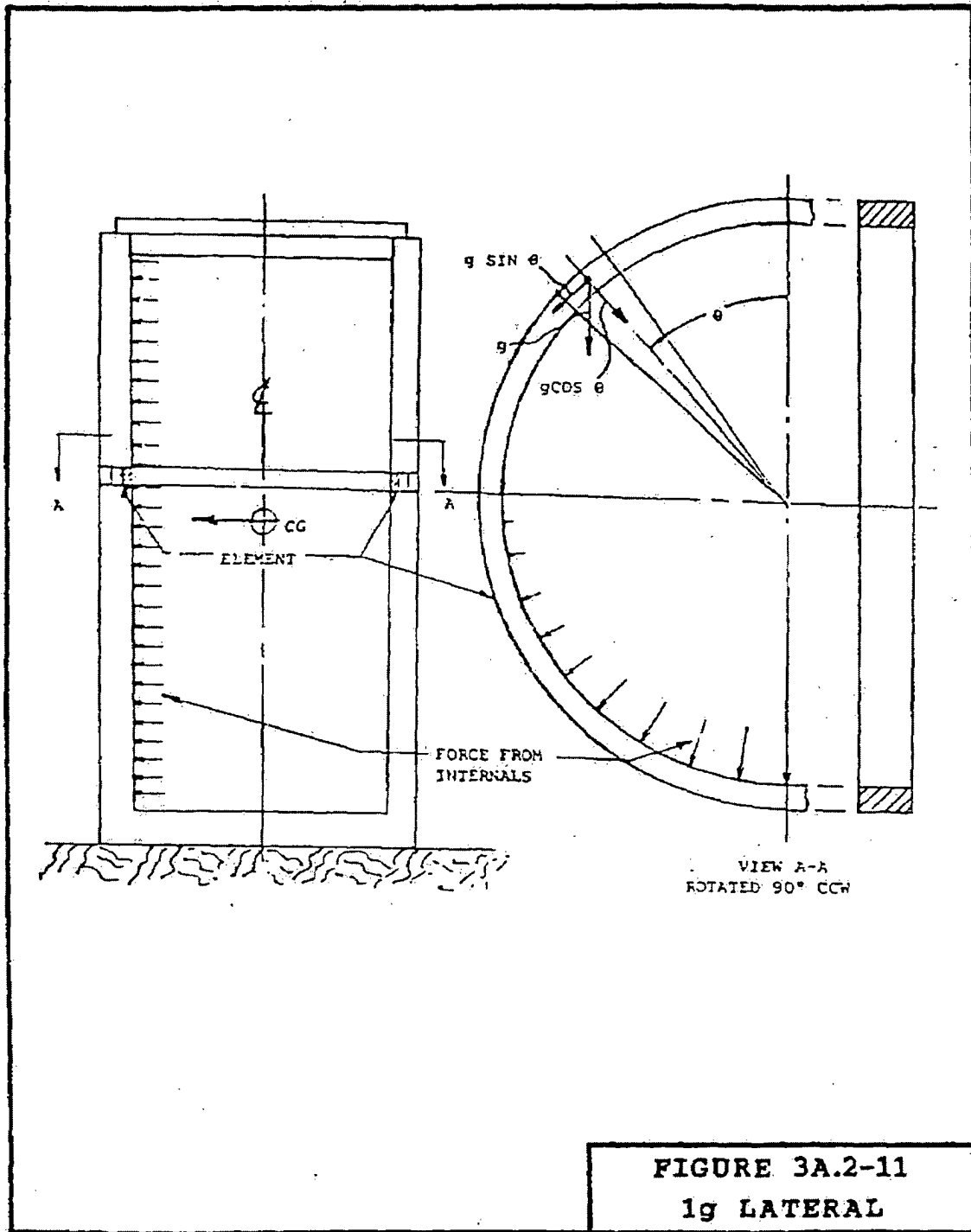
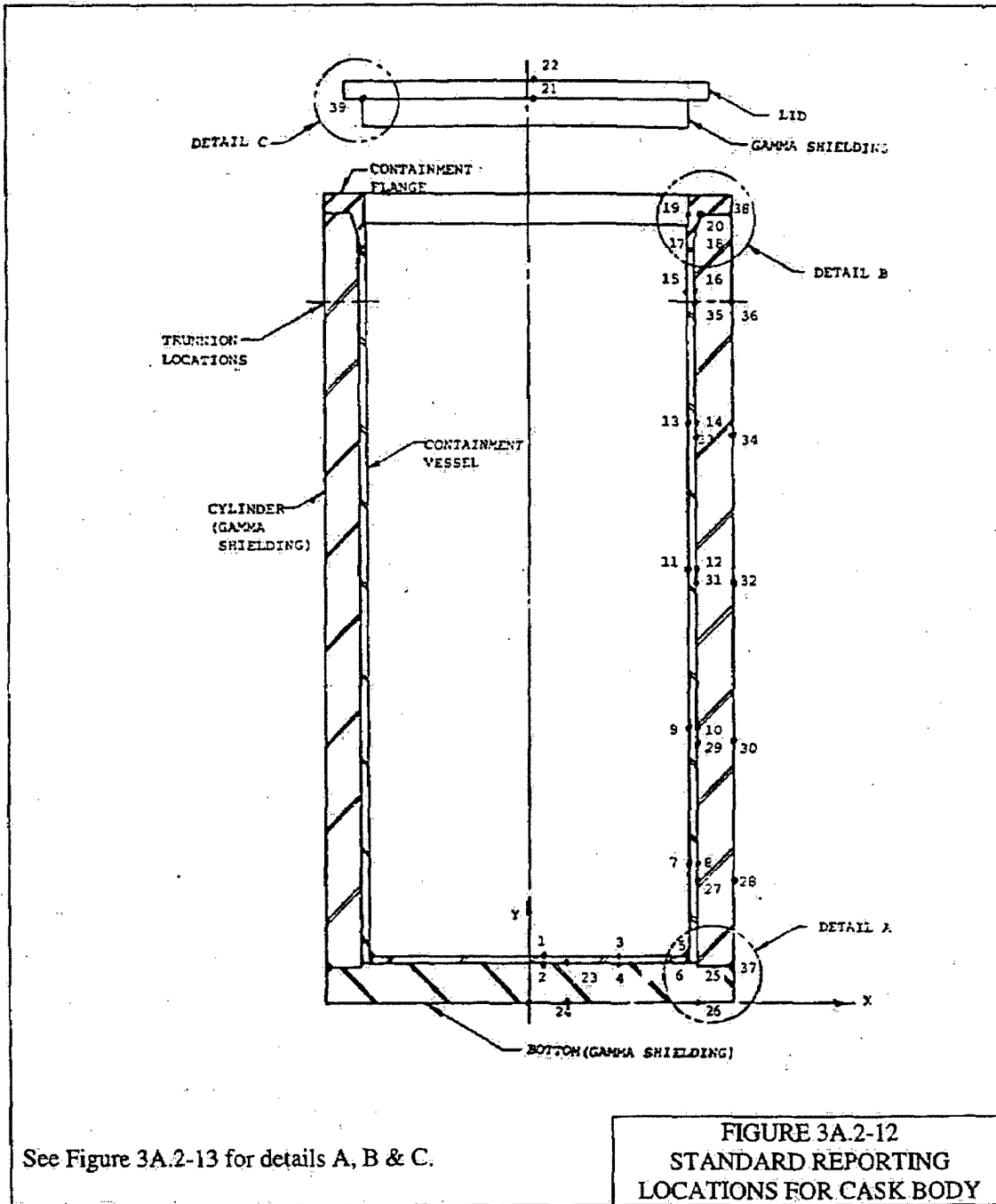
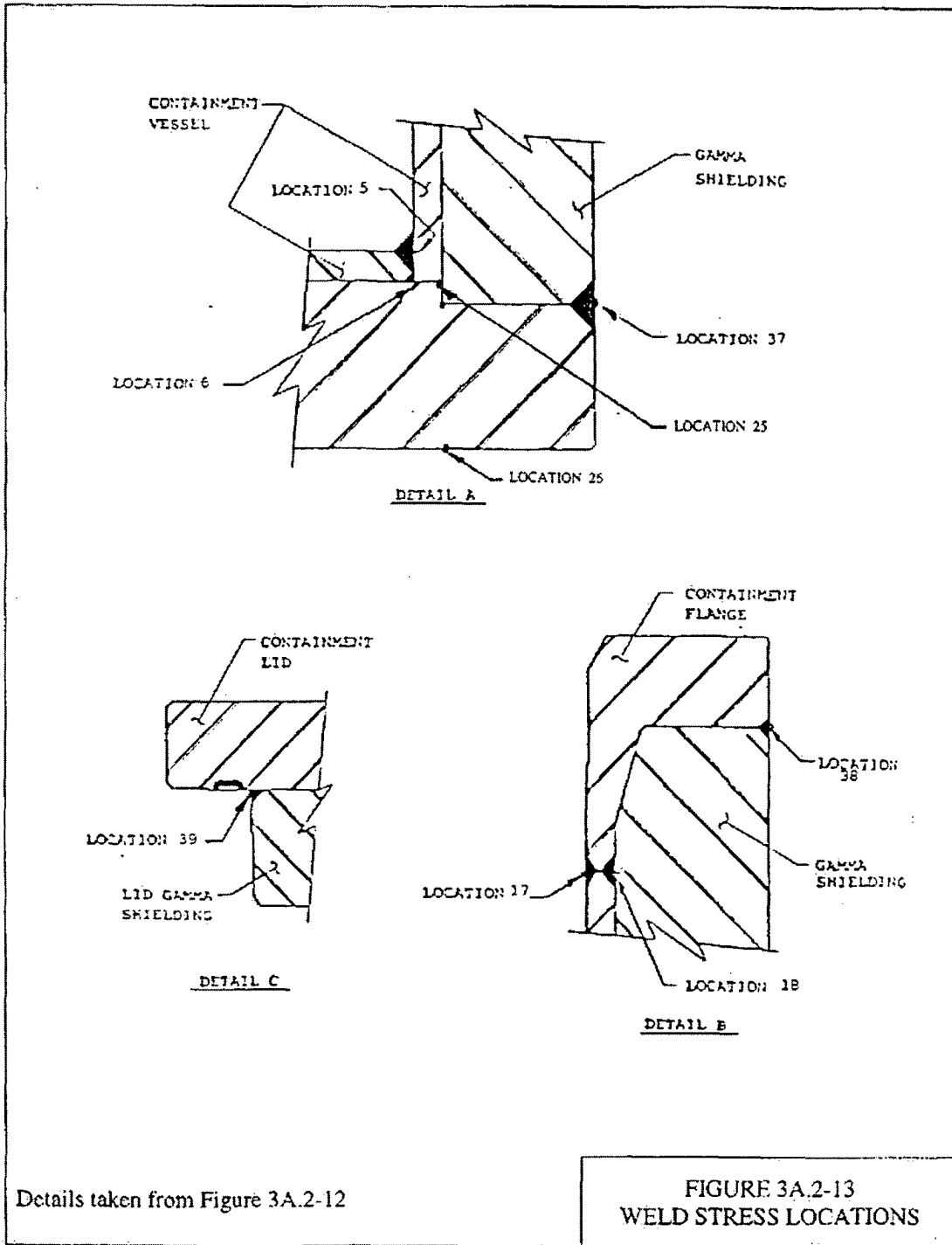
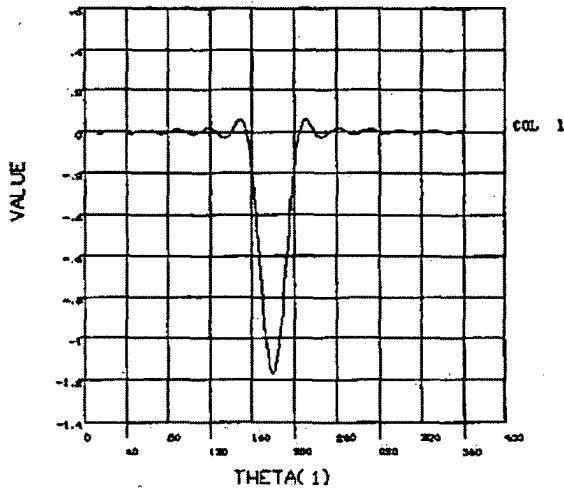


FIGURE 3A.2-11
1g LATERAL







FOURIER COEFFICIENTS

MODE	COEFF	ISYM
0.0000	-0.0851	1.0000
1.0000	0.1681	1.0000
1.0000	0.0000	-1.0000
2.0000	-0.1620	1.0000
2.0000	0.0000	-1.0000
3.0000	0.1523	1.0000
3.0000	0.0000	-1.0000
4.0000	-0.1391	1.0000
4.0000	0.0000	-1.0000
5.0000	0.1233	1.0000
5.0000	0.0000	-1.0000
6.0000	-0.1053	1.0000
6.0000	0.0000	-1.0000
7.0000	0.0860	1.0000
7.0000	0.0000	-1.0000
8.0000	-0.0661	1.0000
8.0000	0.0000	-1.0000
9.0000	0.0465	1.0000
9.0000	0.0000	-1.0000
10.0000	-0.0278	1.0000
10.0000	0.0000	-1.0000
11.0000	0.0107	1.0000
11.0000	0.0000	-1.0000
12.0000	0.0042	1.0000
12.0000	0.0000	-1.0000

FOURIER OUTPUT FOR COS FUNCTION OVER 165-195 DEGREES

FIGURE 3A.2-14
FOURIER SERIES APPROXIMATION
OF THE FOOTPRINT PRESSURE FOR
THE SIDE DROP

Figure Withheld Under 10 CFR 2.390

FIGURE 3A.2-15
TRUNNION GEOMETRY

Figure Withheld Under 10 CFR 2.390

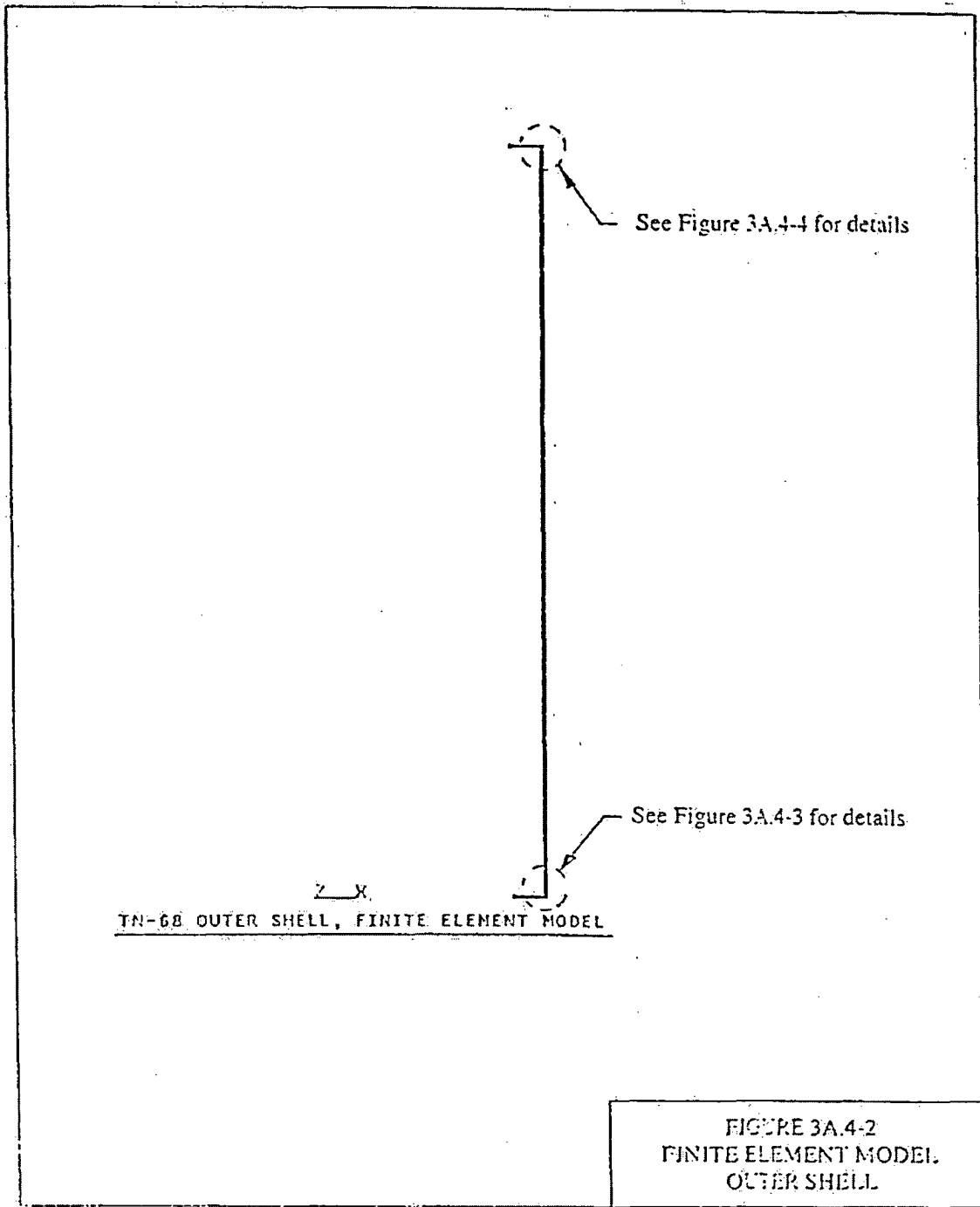
**FIGURE 3A.3-1
TN-68 CASK LID CLOSURE ARRANGEMENT**

Figure Withheld Under 10 CFR 2.390

**FIGURE 3A.3-2
TN-68 CASK LID BOLT**

Figure Withheld Under 10 CFR 2.390

FIGURE 3A.4-1
CASK OUTER SHELL AND
CONNECTION WITH CASK BODY



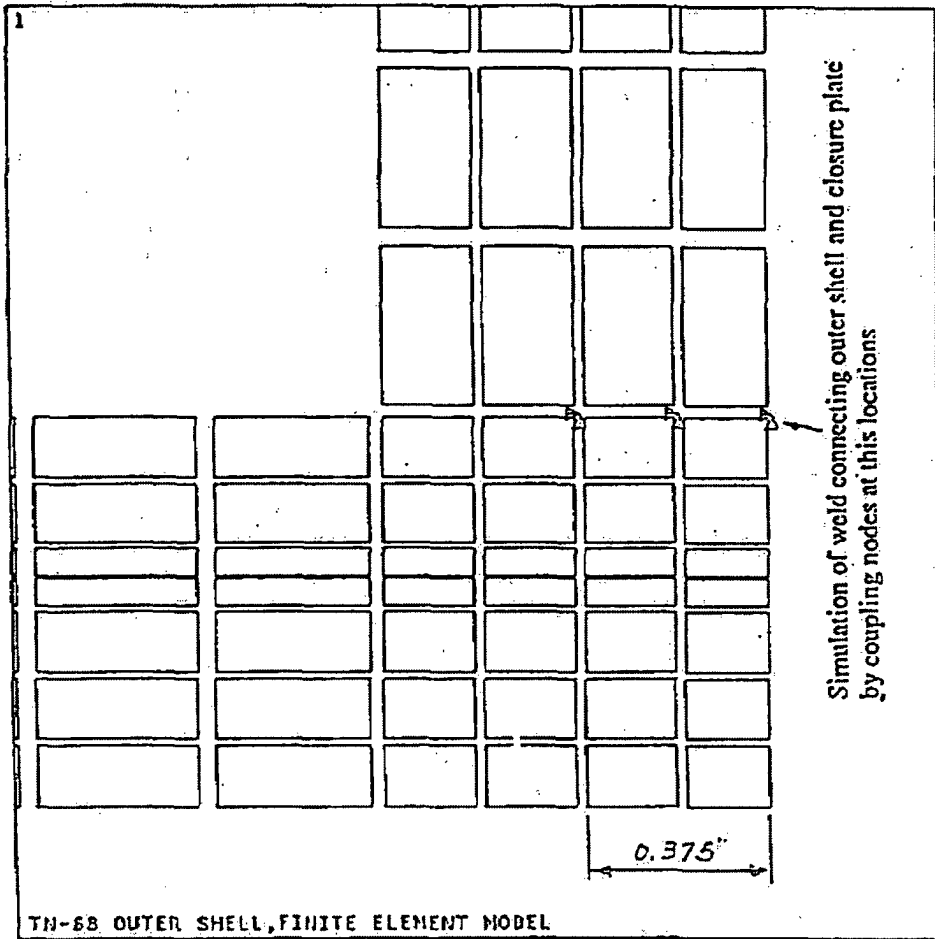


FIGURE 3A.4-3
FINITE ELEMENT MODEL
BOTTOM CORNER

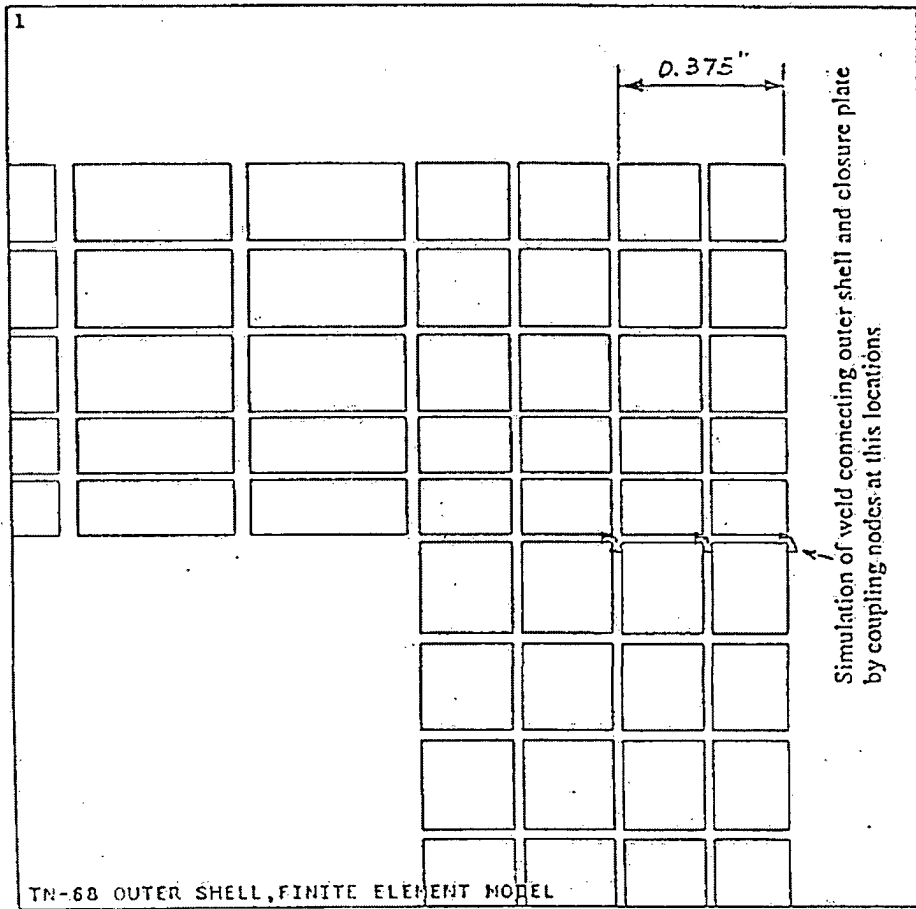
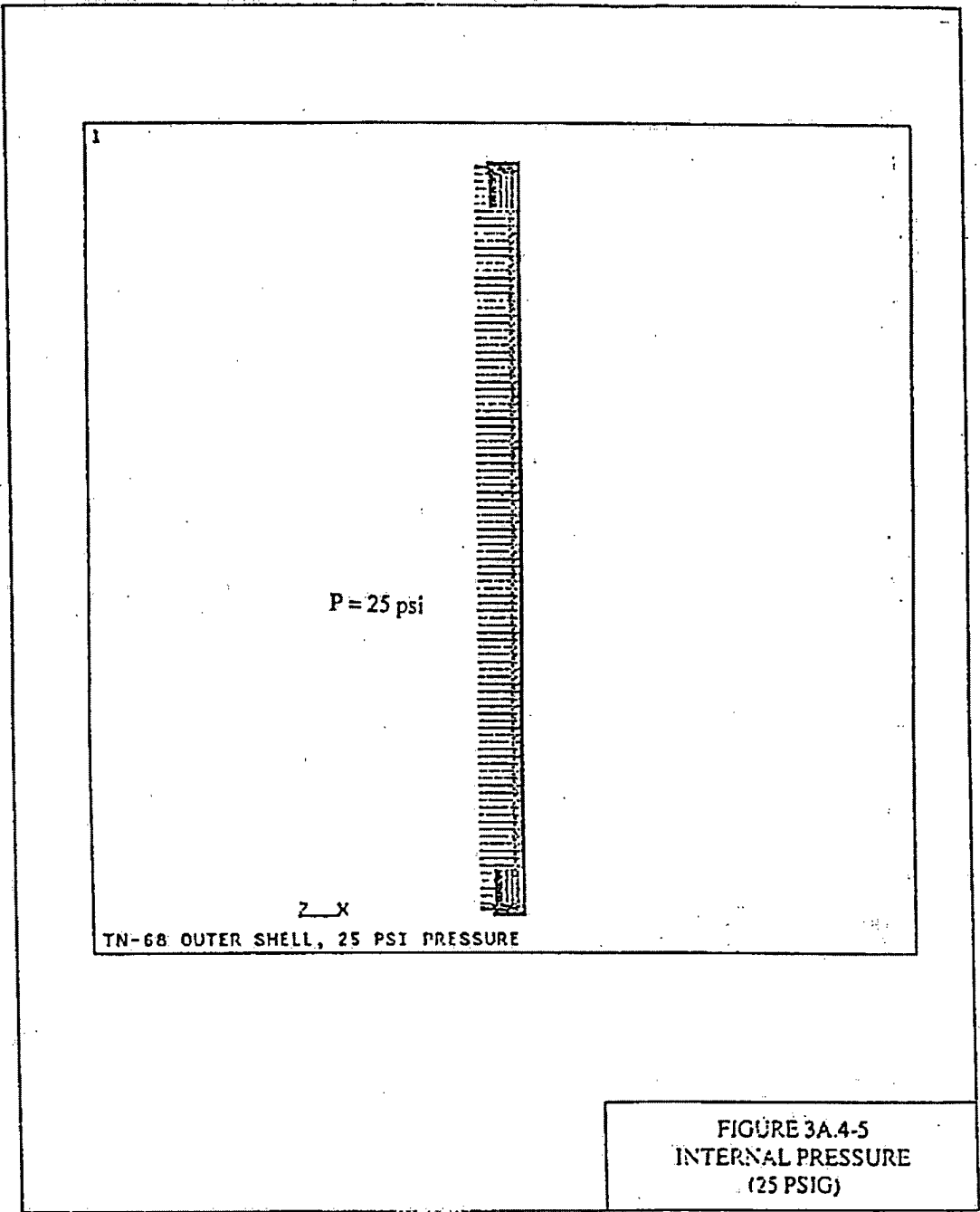
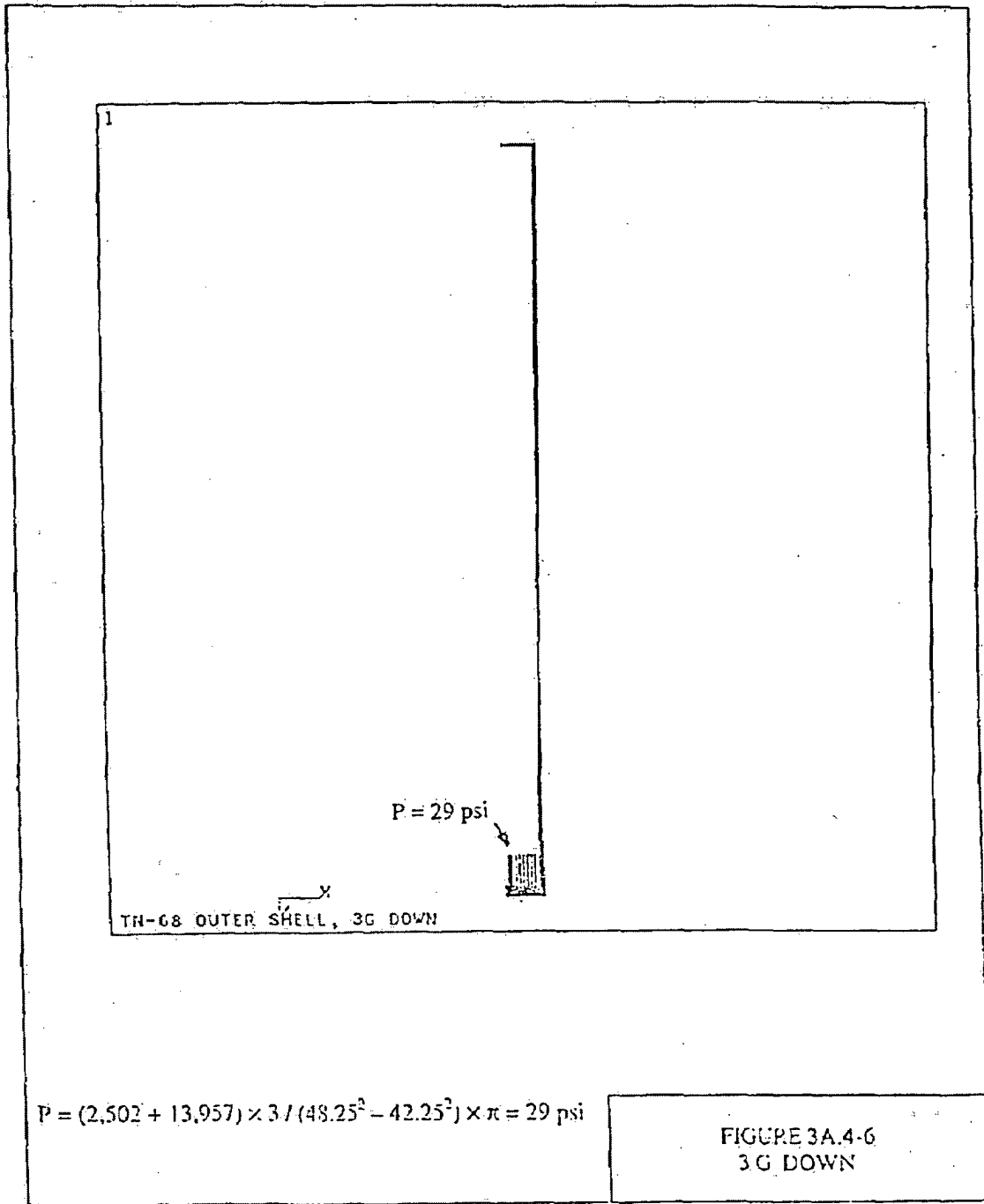


FIGURE 3A.4-4
FINITE ELEMENT MODEL
TOP CORNER





**TN-68 SAFETY ANALYSIS REPORT
TABLE OF CONTENTS**

SECTION	PAGE
 Appendix 3B STRUCTURAL ANALYSIS OF THE TN-68 BASKET	
3B.1 Introduction.....	3B.1-1
3B.1.1 Geometry.....	3B.1-1
3B.1.2 Weight.....	3B.1-2
3B.1.3 Temperature.....	3B.1-2
 3B.2 Basket Finite Element Model Development (For Side Impact Analysis).....	 3B.2-1
 3B.3 Basket Under Normal Condition Loads.....	 3B.3-1
3B.3.1 Description.....	3B.3-1
3B.3.2 Basket Analysis Under 1G Side Load.....	3B.3-1
3B.3.3 Basket Analysis Under Vertical Load.....	3B.3-2
3B.3.4 Basket Thermal Expansion Analysis.....	3B.3-3
3B.3.5 Design Criteria.....	3B.3-6
3B.3.6 Evaluation.....	3B.3-7
 3B.4 Basket Under Accident Condition Loads - Stress Analysis.....	 3B.4-1
3B.4.1 Basket Analysis Under 60 g Bottom End Drop.....	3B.4-1
3B.4.2 Basket Analysis Under Tipover Side Impact.....	3B.4-2
3B.4.3 Design Criteria For Impact Accident.....	3B.4-2
3B.4.4 Evaluation.....	3B.4-3
 3B.5 Basket Under Accident Condition Loads-Buckling Analysis.....	 3B.5-1
3B.5.1 Analysis of Basket To Determine the Buckling Loads.....	3B.5-1
3B.5.2 Analysis Results.....	3B.5-3
3B.5.3 Evaluation.....	3B.5-5
3B.5.4 Analysis of the Aluminum Rails to Determine the Buckling Loads.....	3B.5-5
3B.5.5 Evaluation.....	3B.5-8
 3B.6 Summary of Basket Structural Analysis.....	 3B.6-1
3B.6.1 Stresses Due To Normal Condition Service.....	3B.6-1
3B.6.2 Stresses Due To Accident Condition.....	3B.6-2
 3B.7 References.....	 3B.7-1

**TN-68 SAFETY ANALYSIS REPORT
TABLE OF CONTENTS**

List of Tables

3B.3-1	Summary of Basket Stress Analysis - Normal Condition (1G Side Load)
3B.3-2	Linearized Stress Intensities of Aluminum Rail - Normal Condition (0° Side Load)
3B.3-3	Linearized Stress Intensities of Aluminum Rail - Normal Condition (30° Side Load)
3B.3-4	Linearized Stress Intensities of Aluminum Rail - Normal Condition (45° Side Load)
3B.4-1	Summary of Basket Stress Analysis - Accident Condition (Side Drop)
3B.4-2	Linearized Stress Intensities of Aluminum Rail - Accident Condition (0° Side Drop)
3B.4-3	Linearized Stress Intensities of Aluminum Rail - Accident Condition (30° Side Drop)
3B.4-4	Linearized Stress Intensities of Aluminum Rail - Accident Condition (45° Side Drop)

**TN-68 SAFETY ANALYSIS REPORT
TABLE OF CONTENTS**

List of Figures

3B.1-1	Representative Basket Wall Panel
3B.2-1	Axial View of Basket
3B.2-2	Geometry for ANSYS Model
3B.2-3	Finite Element Model and Element Types
3B.2-4	Basket Finite Element Model - Stainless Steel Boxes
3B.2-5	Basket Finite Element Model - Stainless Steel Plates
3B.2-6	Basket Finite Element Model - Aluminum Rails
3B.3-1	Loading and Boundary Conditions - 0° Drop
3B.3-2	Loading and Boundary Conditions - 30° Drop
3B.3-3	Loading and Boundary Conditions - 45° Drop
3B.3-4	Membrane Stress Intensity (SS Plate) - 0 Degree Drop
3B.3-5	Membrane + Bending Stress Intensity (SS Plate) - 0 Degree Drop
3B.3-6	Membrane Stress Intensity (SS Box) - 0 Degree Drop
3B.3-7	Membrane + Bending Stress Intensity (SS Box) - 0 Degree Drop
3B.3-8	Membrane Stress Intensity (SS Plate)-30 Degree Drop
3B.3-9	Membrane + Bending Stress Intensity (SS Plate) - 30 Degree Drop
3B.3-10	Membrane Stress Intensity (SS Box) - 30 Degree Drop
3B.3-11	Membrane + Bending Stress Intensity (SS Box) - 30 Degree Drop
3B.3-12	Membrane Stress Intensity (SS Plate)- 45 Degree Drop
3B.3-13	Membrane + Bending Stress Intensity (SS Plate) - 45 Degree Drop
3B.3-14	Membrane Stress Intensity (SS Box) - 45 Degree Drop
3B.3-15	Nodal Stress Intensity (SS Plate) - 45 Degree Drop
3B.3-16	Nodal Stress Intensity (Aluminum Rails) - 0 Degree Drop
3B.3-17	Nodal Stress Intensity (Aluminum Rails) - 30 Degree Drop
3B.3-18	Membrane + Bending Stress Intensity (Aluminum Rails) - 45 Degree Drop
3B.3-19	Basket Stress Due to 3G Vertical Load
3B.3-20	Stress Report Location (Big Rail)
3B.3-21	Stress Report Location (Small Rail)
3B.3-22	Extraction of Partial Basket Model (Fusion Welds)
3B.3-23	Basket Partial Model (Fusion Welds)
3B.3-24	Basket Full Model (Fusion Welds)
3B.3-25	Locations of Basket Support Plates
3B.5-1	Drop Orientation
3B.5-2	Finite Element Model Simulation
3B.5-3	Finite Element Model Geometry
3B.5-4	Finite Element Model Plot
3B.5-5	Loading Conditions
3B.5-6	Boundary Conditions
3B.5-7	0° Drop Buckling Analysis - ANSYS Computer Plot
3B.5-8	10° Drop Buckling Analysis - ANSYS Computer Plot
3B.5-9	20° Drop Buckling Analysis - ANSYS Computer Plot
3B.5-10	30° Drop Buckling Analysis - ANSYS Computer Plot
3B.5-11	45° Drop Buckling Analysis - ANSYS Computer Plot

APPENDIX 3B

STRUCTURAL ANALYSIS OF THE TN-68 BASKET

3B.1 Introduction

This appendix presents the structural analysis of the TN-68 fuel support basket. The basket is a welded assembly of stainless steel boxes and designed to accommodate 68 fuel assemblies. The fuel compartment stainless steel box sections are attached together locally by fusion welds to 304 stainless steel plates sandwiched between the stainless steel walls of adjacent box sections. The basket contains 68 compartments for proper spacing and support of the fuel assemblies.

The basket structure is open at each end and therefore, longitudinal fuel assembly loads are directly on the cask body and not on the fuel basket structure. The fuel assemblies are laterally supported in the stainless steel structural boxes, and the basket is laterally supported by the rails and the inner shell of the cask.

The deformations and stresses induced in the basket structure due to the applied lateral loads are determined using the ANSYS computer program⁽¹⁾. The most severe loading for which the basket is evaluated is the hypothetical tipover accident as described in Section 3A.2.3.2. A 60 g vertical loading on the basket is also evaluated to represent a hypothetical end drop accident. Also a 3 g loading is applied to the basket in the vertical directions and 1 g loading is applied to the lateral direction as a bounding load to represent Level A (normal) Conditions. The inertial loads of the fuel assemblies are applied as equivalent densities on the stainless steel boxes. Quasistatic stress analyses are performed with applied loads in equilibrium with the reactions at the periphery of the basket. The calculated stresses in the basket structure are compared with the stress limits to demonstrate that the established design criteria are met.

3B.1.1 Geometry

The details of the TN-68 basket are shown on TN Drawing Nos. 972-70-4, and -5. As described above, the basket structure consists of an assembly of stainless steel boxes or cells joined by fusion welds and separated by stainless steel and poison plates. The stainless box, stainless steel plate and poison plate between fuel compartments is effectively a sandwich panel. The panel consists of one 0.3125 in. thick 304 stainless steel plate and one 0.3125 in. thick poison plate sandwiched between two 0.1875 in. thick 304 stainless boxes. The 304 stainless steel members are the primary structural components. The poison plates provide the heat conduction path from the fuel assemblies to the cask cavity wall, and also provide criticality control.

A representative basket wall panel between fuel compartments is shown in Figure 3B.1-1. The panel plates are welded together at discrete locations (1 fusion weld every 12.17 inches) along their length. The adjacent fuel compartment stainless steel walls are fusion welded to both adjacent box sections. This method of construction forms a very strong honeycomb-like structure of boxes. The open dimension of each fuel compartment cell or box is 6.0 in. x 6.0 in. which provides a minimum of 1/8 in. clearance around the fuel assemblies. The pitch of the cells

is approximately 6.69 in. The overall basket length including spacer, (164 in. + 13.25 in.) 177.25 in., is less than the cask cavity length to allow for loading the fuel assemblies, thermal expansion and tolerance stackup.

Structural rails oriented parallel to the axis of the cask are attached to the periphery of the basket to establish and maintain basket orientation, to prevent twisting of the basket assembly, and to support the edges of those plates adjacent to the rails, which would otherwise be free to slide tangentially around the cask cavity wall under lateral inertial loadings.

3B.1.2 Weight

A value of 705 lb. is assumed for the weight of each fuel assembly including fuel channels. Under lateral inertial loading each assembly is assumed to be uniformly supported across the width and along the length of the basket wall. The inertia of the basket structure (weight of the basket x g load) is also included in the analysis.

3B.1.3 Temperature

Thermal analyses are performed to obtain the temperature distributions in the basket for various conditions. These analyses are presented in Chapter 4. The effects of axial and radial thermal expansion of the basket are evaluated in Section 3B.3.4.

3B.2 Basket Finite Element Model Development (For Side Impact Analysis)

The basket model is an extremely large and complex ANSYS model. Because of the number of plates in the basket and the size of the basket, certain modeling approximations are necessary. The basket structure construction is repetitive symmetry (1 fusion weld every 12.17 inches along the length). It is practical to model only a single transverse slice (12.17 inches length) using a three-dimensional finite element model. The elements used in the model to represent the plates are Shell 63 quadrilateral shell elements and the rails are modeled by Solid 45 3D structural solid elements. For conservatism, the poison plates are not assumed to carry the structural load (except through the thickness support) and are not included in the model, but their weight (inertial load) is included in the stress calculation.

The fuel compartment corners and basket periphery are carefully modeled to define each plate connection. The connections between stainless steel boxes, stainless boxes and poison plates, stainless steel boxes and aluminum rails are made by node couplings. The nodes at the locations of fusion welds are coupled in all degrees of freedom (the fusion welds are rigidly connected the stainless steel boxes and stainless steel plates together at these nodes). The nodes of various plates are coupled together in the out of plane direction so that they will bend in unison under surface pressure or other lateral loading and to simulate the through thickness support provided by the poison plates. Figures 3B.2-1 and 2 show the typical basket panel ANSYS finite element model simulation. The component assembly model computer plot is shown on Figure 3B.2-3 and the individual component computer plots are shown on Figures 3B.2-4 to 3B.2-6.

3B.3 Basket Under Normal Condition Loads

3B.3.1 Description

The poison plates in the TN-68 basket are heat conductors and provide the necessary criticality control. The 304 stainless steel members are the primary structural components.

The poison plate strength is neglected (except for through thickness load transfer capability) under primary loading where the poison plate can share the load with the 304 stainless steel. This analysis approach produces conservatively high calculated values of primary stresses in the stainless steel components. The primary stress analysis of the basket under the bounding loads for Level A is described below.

3B.3.2 Basket Analysis Under 1 g Side Load

Finite Element Model

The ANSYS finite element model described in Section 3B.2 is used to perform the structural analysis of the basket.

Loading

The basket is analyzed for 0°, 30°, and 45° lateral loads to bound the possible maximum stress cases. The lateral load orientation angles are defined in Figures 3B.3-1, 3B.3-2, and 3B.3-3.

All analysis is based on 1g acceleration. The loading due to poison plates and fuel assembly weight are applied as equivalent densities. The poison plate weight is distributed on all four sides of stainless steel boxes, and the fuel assembly weights are distributed on the top panel of the SST-AL-SST sandwich for the 0° lateral load orientation and proportionally distributed on the top & side panels for the 30° and 45° lateral load orientations.

Boundary Conditions

The boundary condition at each point of contact between the basket and cask body cavity depends on the direction of the applied inertial load. As the basket is forced in a particular lateral direction, it separates from the cask wall on one side and reacts against the wall on the other side. At the locations where the basket loses contact with the wall, no restraint or support is provided in the model. For vertical inertial loading on a horizontal cask and basket, contact is lost between the basket and cask wall at the top half of the structure. The load distributions and boundary conditions are shown on Figures 3B.3-1 through 3B.3-3.

Material Properties

The material properties of the 304 stainless steel plates are taken from ASME⁽²⁾ Code, Section II, Part D. The material properties of the aluminum alloy (6061-T6) are also taken from the ASME

Code. These properties are listed with specific reference in Chapter 3. Chapter 4 shows the temperature distribution at various locations of the basket and rails. The maximum calculated temperatures for the various sections of the basket and rails are also summarized in Chapter 4. Based on this thermal analysis, the maximum basket temperature is 595°F and the maximum rail temperature is 382°F. The structural analysis of the basket and rails conservatively assumes a uniform temperature of 600°F for basket and 400°F for the rails.

Analysis and Stress Results

Analyses using the basket system model are performed for the 0°, 30°, and 45° lateral load orientations relative to the basket plates as indicated in Figures 3B.3-1 through 3B.3-3. In all cases, the analyses for the individual loads are performed using the linear elastic method so that ratios can be used to obtain stress results for specified loads. Detailed stress, displacements, and forces in the finite element model are available in ANSYS output files. These results were postprocessed. The nodal stress intensities and deformed geometry for 0°, 30°, and 45° load cases are plotted in Figures 3B.3-4 through 3B.3-18. The stress intensities shown in figures are calculated based on an average fuel assembly weight of 705 lb (the entire fuel assembly weight is conservatively assumed to act on 144" basket length only) and are summarized in Tables 3B.3-1 to 3B.3-4. These maximum stresses are evaluated below to verify that the design criteria are met.

3B.3.3 Basket Analysis Under Vertical Load

Under vertical loads, the fuel assemblies and basket are forced against the bottom of the cask. It is important to note that, for any vertical or near vertical loading, the fuel assemblies react directly against the bottom of the cask cavity and not through the basket structure as in lateral loading.

3 g Vertical Load - 304 Stainless Steel

The analysis of the basket subjected to the 3 g bounding vertical load (bounds all Level A, Normal Conditions) for the panels with poison plate is shown in Figure 3B.3-19. A full length of compartment wall (164 in. long) with a span length of 6.375 in. is evaluated for compressive loading. A maximum compressive force of (3 × 163) 489 lbs. occurs at the bottom of the wall. Stresses are conservatively calculated by assuming all of the load is taken by the 304 stainless steel. Therefore

$$\sigma = \text{Total Compressive Load/Cross Section of 304SS} = 489 \text{ lbs}/2.39 \text{ in.}^2 = 205 \text{ psi} \approx 0.21 \text{ ksi}$$

There are cutouts in 4 locations at the bottom of the basket for lifting. In addition there are drain slots (1.0" wide × 1.0" high) at the bottom of the basket. For these locations, an analysis of the vertical g loadings has been evaluated for each box section.

$$\text{Total weight of one box section (164" long)} = 163 \text{ lbs} \times 4 = 652 \text{ lbs}$$

$$\sigma = \text{Total Compressive Load/Cross Section of 304SS} = (652 \times 3) \text{ lbs}/6.49 \text{ in.}^2 = 301 \text{ psi} \approx 0.3 \text{ ksi}$$

Based on the above results it is concluded that the stresses in the stainless steel panel due to the 3 g vertical load are insignificant (much less than the allowable stress of 14.76 ksi, Section 3B.3.5).

Stainless Steel Fusion Weld

Under the vertical load, each fusion weld is designed to support a panel including one 0.3125" thick × 10.4" high × 6.1875" span poison plate and one 0.3125" thick × 1.75" high × 6.1875" span stainless steel, therefore, the total weight of this panel is:

$$W = (0.3125" \times 10.4" \times 6.1875") \times 0.1 \text{ lb/in.}^3 + (0.3125" \times 1.75" \times 6.1875") \times 0.29 \text{ lb/in.}^3 = 3 \text{ lbs}$$

Under 3 g vertical load, the shear stress, $\tau = 3W/A = 3(3)/[\pi(0.5)^2/4] = 46 \text{ psi} \approx 0.05 \text{ ksi}$

This shear is much less than the allowable shear stress of 2.95 ksi (Section 3B.3.5).

3 g Vertical Load - Aluminum Rails

Under vertical load, each rail is designed to support its own weight. The weight and areas of the rail are:

	Area (in. ²)	Weight (164" long), lbs
Small Rail (Figure 3B.3-21)	8.78	145
Large Rail (Figure 3B.3-20)	16.34	270

Therefore, the maximum compressive stress under 3 g vertical load is:

$$\sigma_1 = 145 \times 3/8.78 = 49.54 \text{ psi} \approx 0.05 \text{ ksi}$$

$$\sigma_2 = 270 \times 3/16.34 = 49.57 \text{ psi} \approx 0.05 \text{ ksi}$$

These compressive stresses are much less than the allowable stress of 4.5 ksi (Section 3B.3.5)

3B.3.4 Basket Thermal Expansion Analysis

The thermal analyses of the basket under various conditions are described in Chapter 4. The temperatures from those thermal analyses are used to evaluate the effects of axial and radial thermal expansion in the basket components.

Thermal Expansion between Fuel Assembly / Basket / Cask

In order to prevent thermal stress, adequate clearance is provided between the basket outer diameter and cask cavity inside diameter, basket axial length and cask cavity length, and fuel assembly axial length and cask cavity length for free thermal expansion. Expansion is checked for three cases with the 30 kW design basis heat load:

- 1) Long term normal condition, 100°F ambient, 0.10 inch hot gap at perimeter of basket (Section 4.3.5, Table 4.3-1 "Average temp at hottest cross section")
- 2) Vacuum drying at 30 hours, with radial gap between basket and cask wall (Section 4.5.1, Table 4.5-2, "Avg temperature at hottest cross section, 0.1 inch hot gap")
- 3) Vacuum drying at 30 hours, no radial gap between basket and cask wall (Section 4.5.1, Table 4.5-2 "Avg temperature at hottest cross section, 0.0 hot gap")

Case 2 is the bounding condition for internal basket and fuel temperatures, and therefore it is the bounding case for axial expansion of the fuel and the basket relative to the cask, pairs B and C in the table below. Case 3 pair A demonstrates that if the basket comes into contact with the cavity wall, as assumed in Section 4.5.1, the resulting drop in the basket temperature will result in an equilibrium condition with a small radial gap between the basket and shell.

Summary of gaps between adjacent components of the TN-68 Storage Cask

Pair	Differential Expansion Between Components	Material	Long Term 100°F Ambient Case 1		Vacuum w/radial gap Case 2		Vacuum no radial gap Case 3	
			Avg Temp (°F)	Min Gap (in)	Avg Temp (°F)	Min Gap (in)	Avg Temp (°F)	Min Gap (in)
A	Basket OD	SA-240 Type 304	479	0.011	--	Note 1	433	0.02
		Aluminum Rail	366		--		258	
	Cask ID	SA-203 Gr. E	316		--		252	
B	Fuel Assembly length	Zircaloy/ 304 S.S.	622	0.362 Note 2	752	0.158 Note 2	--	Note 3
	Cask Cavity length	SA-203 Gr. E	316		223		--	
C	Basket length	SA-240 Type 304	479	0.317	534	0.101	--	Note 3
		Aluminum Poison plate	366		400		--	
	Cask Cavity length	SA-203 Gr. E	316		223		--	

Notes:

1. The gap is not calculated because this case assumes by definition that a radial gap exists, as the basis for calculating the maximum temperatures of basket components and fuel.
2. Includes consideration of 0.36 inch of axial free space taken up by damaged fuel end caps
3. This is not the bounding case for axial expansion, because contact of the basket perimeter with the cavity wall results in reduced basket and fuel temperatures.

Thermal Expansion between the Basket Stainless Steel Support Plates and Aluminum Poison Plates

The TN-68 basket design includes gaps in both the transverse and axial directions to accommodate differential thermal expansion between the basket stainless steel plate and the neutron absorber plate. The following evaluation demonstrates that these gaps are adequate for the bounding normal condition for cask internal temperatures, vacuum drying with a radial gap between the basket and cask, case 2 above. All plates are assumed to be at the average temperature, 568°F, of the longest absorber plate calculated using a cross-section model with no axial heat transfer (Section 4.5.1).

Thermal Expansion Between Basket Stainless Steel and Poison Plates (Radial Direction)

There are four (4) different lengths of basket plates in the radial direction; the thermal expansion calculations are based on nominal plate length. The differential thermal expansions between stainless steel and poison plates at these four different locations are:

$$\Delta_1 = 66.94 \times (14.136 - 9.8) \times 10^{-6} \times (568-70) = 0.145 \text{ inch}$$

$$\Delta_2 = 53.81 \times (14.136 - 9.8) \times 10^{-6} \times (568-70) = 0.116 \text{ inch}$$

$$\Delta_3 = 40.44 \times (14.136 - 9.8) \times 10^{-6} \times (568-70) = 0.087 \text{ inch}$$

$$\Delta_4 = 13.69 \times (14.136 - 9.8) \times 10^{-6} \times (568-70) = 0.03 \text{ inch}$$

Therefore, at these locations, minimum spaces of 0.15 in., 0.13 in., 0.1 in., and 0.05 in. are provided between stainless steel and poison plates (poison plate will be cut short) to allow free thermal expansion.

Thermal Expansion Between Basket Stainless Steel and Poison Plates (Axial Direction)

There are thirteen (13) poison plate sections (see Figure 3B.2-1) along the axial direction, the nominal height of the poison plate is 10.4", therefore, the maximum differential thermal expansion between the poison and stainless steel plates at 568°F is:

$$\Delta = 10.4 \times (14.136 - 9.8) \times 10^{-6} \times (568-70) = 0.022 \text{ inch}$$

Therefore, a minimum clearance of 0.023" is provided to permit free thermal expansion.

Based on the above calculations, adequate clearances have been provided for thermal expansion. Thus no thermal stress will be induced in the baskets.

Conclusion

Based on the above calculation, adequate clearances have been provided for thermal expansion. Thus no thermal stress will be induced in the basket.

3B.3.5 Design Criteria

The basis for the 304 stainless steel fuel compartment box section stress allowables is Section III, Subsection NG of the ASME⁽³⁾ Code. The primary membrane stress intensity and primary membrane plus bending stress intensities are limited to S_m (S_m is the Code allowable stress intensity) and $1.5 S_m$, respectively, at any location in the basket for Level A (Normal Service) load combinations. The average primary shear stress across a section is limited to $0.6S_m$.

The ASME Code provides a basic $3 S_m$ limit on primary plus secondary stress intensity for Level A conditions. That limit is specified to prevent ratcheting of a structure under cyclic loading and to provide controlled linear strain cycling in the structure so that a valid fatigue analysis can be performed. The Code also provides guidance in the application of plastic analyses which can be performed to demonstrate shakedown (absence of ratcheting) and to determine stresses for fatigue evaluation. Ratcheting and fatigue cannot occur in the basket since thermal cycling will not occur in this basket design. The numerical values of primary stress intensity limits are list in the following table.

TN-68 Basket Structural Design Criteria for Level A Conditions

Numerical Values of Primary Stress Intensity Limits			
	304 SS at 600°F (ksi)	SB 221, 6061-T6 Aluminum Rails at 400°F, (ksi)	ASME Reference
Membrane Stress Intensity $P_m (S_m)$	14.76 *	4.50	Subsection NG NG-3221.1
Membrane + Bending Stress Intensity $P_m + P_b (1.5 S_m)$	22.14*	6.75	Subsection NG NG-3221.2
Shear Stress at 600°F (Fusion Weld) $\tau (0.6 S_m)$	2.95**	-----	Subsection NG NG-3227.2 Table NG-3352-1

* The allowables were reduced ($\times 0.9$) to include the quality factor for full penetration based on progressive MT or PT examination (NG-3352)

** The allowables were reduced ($\times 0.3$) to include the quality factor for fusion weld based on visual examination (NG-3352)

3B.3.6 Evaluation

Stainless Boxes and Stainless Plates

Tables 3B.3-1 lists the stress intensities for the 1 G side load in the basket due to 0°, 30°, and 45° drop orientations. Note that these stresses have been calculated elastically (assuming structurally ineffective poison plates). The highest membrane stress intensity is 0.36 ksi. The highest membrane plus bending stress intensity is 0.63 ksi. These stresses are well below the allowable membrane stress intensity of 14.76 ksi and the allowable membrane plus bending stress intensity 22.14 ksi based on a basket temperature of 600°F.

Stainless Steel Fusion Welds

The ANSYS computer code is used to calculate the shear stresses at the fusion welds. Two drop orientations are analyzed. A partial finite element model for the 0° drop analysis was constructed with the following modifications using the finite element model described in Section 3B.2.

0° side impact

- Figure 3B.3-22 shows the full basket model and the section where the partial models will be extracted and modified for fusion weld shear stress calculations.
- Removed all aluminum rail elements (SOLID45). Also removed all the shell elements, except one center vertical row of elements as shown in Figure 3B. 3-23 for 0° side impact orientation. All the boundary conditions and couplings at the unused nodes were removed.
- Symmetry boundary conditions were applied at the cut surfaces.
- Removed the couplings at the fusion welds and replaced them with Elastic Pipe Element (PIPE16) of 0.5" outer dia. and 0.25 " thickness. The diameter of pipe elements for the 0° side impact model at the symmetry boundaries was reduced to 0.3536" (thickness = 0.1768) for 1/2 section area.
- All material properties, real constants and couplings of the reduced models are the same as described in Section 3B.3.2. The element and node numbers are, however, compressed in the partial models.

The maximum shear force in pipe element due to 1g load = 8.5 lb

Therefore, average shear stress = $8.5 / (\pi/4 \times 0.5^2) = 43$ psi

45° Side Impact

A full model was considered better than a partial model for a 45 degree side drop, because it avoids complex symmetry boundary conditions at two cut sections needed for a partial model.

The ANSYS full finite element model and material properties were taken from Section 3B.3. The couplings at the fusion weld locations of the model are replaced with Elastic Pipe Element

(PIPE16) of 0.5" outer diameter and 0.25" thickness. The finite element model and boundary conditions are shown in Figure 3B.3-24.

1g resultant load was applied using a factor of -0.707 in X-direction and 0.707 in Y-direction. The detailed resulting stresses and displacements are given in ANSYS file.

The maximum shear force in pipe element due to 1g load = 10.7 lb

Therefore,
$$\text{Avg. Shear Stress} = 10.7 / (\pi/4 \times 0.5^2) = 55 \text{ psi}$$

It is seen that the maximum average shear stress of 55 psi occurs in the fusion welds during a 45 degree-oriented side drop under 1g load.

The allowables at 600° F are:

Allowable = $0.3 \times 0.6 \times 16.4 = 2.95 \text{ ksi}$

Therefore, Normal Condition Allowable 'g' load = $2.95 / 0.055 = 54$

Aluminum Rails

The maximum nodal stress intensities of the aluminum rails due to 0°, 30°, and 45° drop orientations are plotted in Figures 3B.3-16 through 3B.3-18. However, the final results of interest for comparison to design criteria are membrane and bending stress intensities. The stress components are processed to obtain the averaged membrane stress across each cross section and the linearized membrane plus bending stress. The cross section for averaging and linearization is defined by a path consisting of two ends or surface points (model nodes). The stress components through the section are linearized by the ANSYS postprocessor and separated into constant membrane stresses, P_m , and bending stresses, P_b , which varies linearly between the end points. The values of the principal stresses are determined from the stress components, and the membrane and membrane plus bending stress intensities are calculated from these principal stresses. The critical sections in Figures 3B.3-20 and -21 are selected because of high nodal stresses at these locations and also for a potential of high linearized membrane and membrane plus bending stress intensities. The small rail (item 30, drawing no. 972-70-5) is not selected for a detailed evaluation as this rail acts just like a shim and is not subjected to any bending or column action.

Table 3B.3-2 lists the linearized stress intensities at each of the critical cross sections as shown on Figures 3B.3-20 and 21 for the 0° side load. The maximum membrane stress intensity in the basket is 0.11 ksi at location 1 and the maximum membrane plus bending stress intensity is 0.15 ksi also at location 1. These stress values are much less than the allowables for general membrane stress intensity of 4.5 ksi and membrane plus bending stress intensity of 6.75 ksi.

Table 3B.3-3 lists the linearized stress intensities at each of the critical cross sections as shown on Figures 3B.3-20 and 21 for the 30° side load. The maximum membrane stress intensity in the basket is 0.08 ksi at location 1 and the maximum membrane plus bending stress intensity is 0.11

ksi also at location 1. These stress values are less than the allowables for general membrane stress intensity of 4.5 ksi and membrane plus bending stress intensity of 6.75 ksi.

Table 3B.3-4 lists the linearized stress intensities at each of the critical sections as shown on Figures 3B.3-20 and 21 for the 45° side load. The maximum membrane stress intensity in the basket is 0.06 ksi at location 1 and the maximum membrane plus bending stress intensity is 0.08 ksi also at location 1. These stress values are also less than the allowables for general membrane stress intensity of 4.5 ksi and membrane plus bending stress intensity of 6.75 ksi.

Based on the results of these analyses, it is concluded that:

1. The maximum stresses in the 304 stainless steel (fuel compartment) both in the stainless steel plates and stainless steel boxes of the basket, are well below the specified allowable stresses under normal service condition (1 g side load and 3g vertical load).
2. The maximum shear stress in the fusion welds is low under the 1 g side load and 3 g vertical load above.
3. The maximum membrane and membrane plus bending stress intensities of the aluminum rails are low.
4. The basket is structurally adequate and it will properly support and position the fuel assemblies under normal loading conditions.

3B.4 Basket Under Accident Condition Loads - Stress Analysis

3B.4.1 Basket Analysis Under 60 g Bottom End Drop

Appendix 3D presents the dynamic impact analysis of the TN-68 cask during a hypothetical end drop and tip over accidents. The maximum calculated impact g load for an 18 in. vertical drop is 37 g. This section evaluates the basket stresses for a 60 g vertical load which is a conservative representation of the end drop. Appendix 3B.3.3 presents the analysis of the basket due to a 3 g vertical load neglecting the strength contribution from the poison plates (weight of poison plate is included in the calculation). It is conservatively assumed that all the load is taken by the 304 stainless steel. Therefore, the maximum compressive stress due to the 60 g end drop is:

$$\sigma_1 = \text{Total Comp. Load/Cross Section of 304SS} = (163 \times 60) \text{ lbs}/2.39 \text{ in.}^2 = 4,092 \text{ psi} \approx 4.1 \text{ ksi}$$

There are cutouts in 4 locations at the bottom of the basket for lifting. In addition there are drain slots (1" wide \times 1.0" high) at the bottom of the basket. For these locations, an analysis of the vertical g loadings has been performed for each box section.

$$\text{Total weight of one box section (164" long)} = 163 \text{ lbs} \times 4 = 652 \text{ lbs}$$

$$\text{Total area} = (2.39 \text{ in.}^2 \times 4) \times (17.3/25.5) = 6.49 \text{ in.}^2$$

$$\sigma_2 = \text{Total Comp. Load/Cross Section of 304SS} = (652 \times 60) \text{ lbs}/6.49 \text{ in.}^2 = 6,028 \text{ psi} \approx 6.03 \text{ ksi}$$

These stresses are less than the Level D membrane stress intensity limit for 304 stainless steel of 39.36 ksi (Section 3B.4.3).

Stainless Steel Fusion Weld

Under the vertical load, each fusion weld is designed to support a panel including one 0.3125" thick \times 10.4" high \times 6.1875" span poison plate and one 0.3125" thick \times 1.75" high \times 6.1875" span stainless steel, therefore, the total weight of this panel is:

$$W = (0.3125" \times 10.4" \times 6.1875") \times 0.1 \text{ lb./in.}^3 + (0.3125" \times 1.75" \times 6.1875") \times 0.29 \text{ lb./in.}^3 = 3 \text{ lbs}$$

$$\text{Under 60 g end impact, the shear stress, } \tau = 60W/A = 60(3)/[\pi(0.5)^2/4] = 917 \text{ psi} \approx 0.92 \text{ ksi}$$

This shear is much less than the allowable shear stress of 19.68 ksi (Section 3B.4.3).

60 g Vertical Load - Aluminum Rails

Under vertical load, each rail is designed to support its own weight. The weight and area of the rails are:

	Area (in. ²)	Weight (164" long), lbs
Small Rail (Figure 3B.3-21)	8.78	145
Big Rail (Figure 3B.3-20)	16.34	270

Therefore, the maximum compressive under 60 g end impact load is:

$$\begin{aligned}\sigma_1 &= 145 \times 60 / 8.78 = 990.9 \text{ psi} \approx 1.0 \text{ ksi} \\ \sigma_2 &= 270 \times 60 / 16.34 = 991.4 \text{ psi} \approx 1.0 \text{ ksi}\end{aligned}$$

These compressive stresses are much less than the membrane allowable stress of 10.8 ksi (Section 3B.4.3).

3B.4.2 Basket Analysis Under Tipover Side Impact

This section describes the analysis of the TN-68 basket in the unlikely event of cask tipover on a concrete pad. The design criteria established for the TN-68 basket for the hypothetical accident condition are described in Section 3B.4.3. These criteria were selected to ensure that the basket is structurally adequate under the tipover impact loads. The results from the analyses presented in this section are evaluated against the design criteria in Section 3B.4.3.

To determine the structural adequacy of the basket due to the cask tipover accident, the same drop orientations as described in Section 3B.3.2 are used to evaluate the basket stresses. Since those individual load cases are linear and elastic, their results can be ratioed and superimposed as required in order to perform the normal and hypothetical accident load combinations. Tables 3B.4-1 through 3B.4-4 list the maximum "membrane" & "membrane plus bending" stress intensities of the basket and rails due to 1g at 0°, 30°, and 45° side impacts. These stress intensities are compared with the Level D allowables to calculate the corresponding maximum allowable g loads.

3B.4.3 Design Criteria For Impact Accident

The stress criteria are taken from Section III, Appendix F of ASME⁽³⁾ Code. The hypothetical impact accidents are evaluated as short duration Level D conditions. For elastic analysis, the primary membrane stress is limited to the smaller of $2.4S_m$ or $0.7S_u$ and membrane plus bending stress intensities are limited to the smaller of $3.6S_m$ or S_u . The average primary shear stress across a section is limited to the smaller of $0.42 S_u$ or $2 \times 0.6S_m$.

The fuel compartment walls, when subjected to compressive loadings, are also evaluated against ASME Code rules for component supports to ensure that buckling will not occur. The acceptance criteria (allowable buckling loads) are taken from ASME Code, Section III, Appendix F, paragraph F-1341.4, Plastic Instability Load. The allowable buckling load is equal to 70% of the calculated plastic instability load. The numerical values of Level D stress limits are listed in the following table.

TN-68 Basket Structural Design Criteria for Level D Conditions

Numerical Values of Primary Stress Intensity Limits			
	304 SS at 600°F (ksi)	SB 221, 6061-T6 Aluminum Rails at 400°F, (ksi)	ASME Reference
Membrane Stress Intensity P_m , (smaller of $2.4S_m$ or $0.7S_u$)	39.36	10.8	Appendix F F-1331.1a
Membrane + Bending Stress Intensity, $P_m + P_b$ (smaller of $3.6S_m$ or S_u)	59.04	16.0	Appendix F F-1331.1c
Shear Stress (Fusion Weld) τ , (smaller of $0.42 S_u$ or $2 \times 0.6S_m$)	19.68	----	Appendix F F-1331.1d or NG-3225

3B.4.4 Evaluation

Based on the above analyses and results list in Tables 3B.4-1 through 3B.4-4, it is concluded that:

1. The maximum allowable G load for the stainless steel basket assembly is 94G. This G load is much higher than the calculated G load of 77 as described in Appendix D.
2. The maximum allowable G load for the aluminum rails is 98G.

3B.5 Basket Under Accident Condition Loads - Buckling analysis

3B.5.1 Analysis of Basket to Determine the Buckling Loads

Additional analyses are performed in this section to evaluate the outer basket plate stability when the lateral inertial loading is applied at various angles relative to the plates. Analyses are performed for 0, 10, 20, 30, and 45 degree drop angles (Figure 3B.5-1).

The basic structural element of the basket is considered to be a wall between fuel compartments which consists of 0.3125" thick stainless steel plate sandwiched between two 0.1875" thick stainless steel plates (the strength of poison plate is neglected from buckling load calculation, but its own weight is included). The overall dimensions of this outer basket wall are 6.1875" high and 12.17" wide (12.25" is used in the model, see Figures 3B.5-2 and 3B.5-3).

Finite Element Model

In order to calculate the buckling load, a three-dimensional ANSYS finite element model is constructed using a Shell 43 plastic large strain shell element. Shell 43 is well suited to model nonlinear, flat or warped, thin to moderately thick shell structures. The element has six degrees of freedom at each node: translations in the nodal x, y, and z directions and rotations about the nodal x, y, and z axes. The nodes at the locations of fusion welds are coupled for all degrees of freedom (the fusion welds rigidly connect the stainless steel boxes and stainless steel plates at these nodes). The nodes of various plates are coupled together in the out of plane direction so that they will bend in unison under surface pressure loading and to simulate the through thickness support provided by the poison plates. The finite element model is shown on Figure 3B.5-4.

Geometric Nonlinearities

Since the structure experiences large deformations before buckling, the large displacement option of ANSYS is used for all the analyses. The deflections during each load step are used to continuously redefine the geometry of the structure, thus producing a revised stiffness matrix. Therefore, buckling can be analyzed with the large deflection option. If the rate of change in deflection (per iteration) is observed, an estimation of the stability of the structure can be made. In particular, if the change of displacement at any node is increasing, the loading is above critical and the structure will eventually buckle.

Material Nonlinearities

The basket is constructed from 304 stainless steel. A bilinear stress strain relationship is used to simulate the correct nonlinear material behavior. The following elastic and inelastic material properties are used in the analysis:

Mechanical Properties of SA-240 Type 304 SS

	500°F	600°F
Modulus of Elasticity (psi)	25.8×10^6	25.3×10^6
Yield Strength (psi)	19,400	18,400
Ultimate Strength (psi)	63,500	63,400
Tangent Modulus (psi)	110,457	112,705

Loadings

The loadings on the panel model (Figure 3B.5-2, Location 1) were appropriately transferred from full size basket loadings. The loads used in 0, 10, 20, 30, and 45 degree drop analyses are summarized in the following table. Maximum loads of 200g were applied in each analysis. The automatic time stepping program option "Autots" was activated. This option lets the program decide the actual size of the load-substep for a converged solution. The program stops at the load substep when it fails to result in a converged solution. The last load step, with a converged solution, is the plastic instability load for the model. Figures 3B.5-5 shows the loading conditions.

Summary of Loads for Different Drop Orientations Analysis

$(F_y = F \cos\theta, P_x = P \sin\theta)$

Drop Orientation (Degree)	1G load (12.25" Length) (Weight including all SS & poison plates above the bottom panel, rails, and 9 fuel assemblies**)		200 G Load Computer Run	
	Axial Load F_y (lbs)	Trans. Load P_x (psi)	F_y (lbs)	P_x (psi)
0	675	0	135,000	0
10	665	0.148	133,000	29.6
20	634	0.29	126,800	58.0
30	585	0.425	117,000	85
45	477	0.601	95,400	120.2

** This assumption is very conservative for drop orientation other than 0 degree, for example, for 30 and 45 degree drops the bottom panel only supports 7 fuel assemblies instead of 9 fuel assemblies.

Boundary Conditions

The ANSYS finite element model conservatively assumes that both ends of column are hinged. The boundary conditions are shown on Figure 3B.5-6. However, the stainless steel (0.3125" thick × 1.75" wide) and poison plates forming the panel extend beyond the panel and connect into other panels so that moments can be developed at the top and bottom panel edges. These reactive end moments will keep the ends from rotating during buckling. Reference to "Formulas for Stress and Strain" by Raymond Roark⁽⁵⁾, Fourth Edition, Table XV indicates that:

Load Case No. (From Table XV of Roark)	Loading and Edge Condition	Formula for Critical Load (P)
2	End Load Both Ends Hinged	$P = (1)(\pi^2EI/L^2)$
3	End Load Both Ends Fixed	$P = (4)(\pi^2EI/L^2)$

Based on the formulas described above, the end conditions selected for the ANSYS model (both end hinged) are conservative and the calculated allowable compressive load has a large margin of safety.

3B.5.2 Analysis Results

ANSYS Finite Element Analysis Results

The plastic instability load and allowable buckling load for 0,10, 20, 30, and 45 degree orientation drops at 500°F and 600°F basket temperatures are summarized in the following tables. Based on the design criteria described in Section 3B.4.3, the allowable buckling load is equal to 70% of the calculated plastic instability load. Displacement and nodal stress intensity plots for 0, 10, 20, 30, and 45 degree orientation drops (500°F) at the last converged load step are shown on Figures 3B.5-7 through 3B.5-11.

Plastic Instability Load and Allowable Buckling Load

Drop Orientation (Degree)	Plastic Instability Load (G)	Allowable Buckling Load (G)
	Bottom Compartment At 500 °F (Location 1)	Bottom Compartment At 500 °F
0	153	107
10	144	100
20	139	97
30	138	96
45	144	100

Additional analysis is performed at location 2 (Figure 3B.5-2), conservatively using the same loading as in Location 1, based on 30 degree drop orientation (lowest allowable buckling load) and basket temperature of 600°F and the result is listed in the following table.

Plastic Instability Load and Allowable Buckling Load
(Figure 3B.5-2, Location 2)

Drop Orientation (Degree)	Plastic Instability Load, 600°F (G)	Allowable Buckling Load (G)
30	132	92

Result From Hand Calculation

As an order of magnitude check, the allowable buckling load based on 500°F temperature and 0 degree drop orientation is calculated below and compared to the ANSYS analysis results. As given in ASME⁽⁴⁾ Code, Subsection NF, Paragraph NF-3322-1(c)(2)(a)(Level A Condition) and modified as per Appendix F, Paragraph F-1334 (Level D Condition), the compressive stress limit for the accident condition (Level D) when KL/r is less than 120 and $S_u > 1.2 S_y$ is:

$$F_a = 2 \times S_y [0.47 - (KL/r)/444]$$

Where:

$$K = 0.65$$

$$L = 6.0''$$

$$S_y = 19,400 \text{ psi (at 500°F)}$$

$$S_u = 63,400 \text{ psi (at 500°F)}$$

$$I = b h^3/12 = 0.3038 \text{ in}^4$$

$$A = 5.12 \text{ in}^2$$

$$r = (I/A)^{1/2} = 0.2436 \text{ in}$$

$$KL/r = 0.65 \times 6.0/0.2436 = 16.1$$

Substituting the values given above,

$$F_a = 2 \times 19,400 [0.47 - (16.1)/444] = 16,829 \text{ psi}$$

The maximum allowable force is $16,829 \times 5.12 = 86,164 \text{ lb}$, therefore, the maximum allowable G load is:

$$G = 86,164 / 675 = 128$$

This value is reasonably close to the solution given by the ANSYS result (107 G).

3B.5.3 Evaluation

Based on the results of this analysis, it is concluded that the maximum allowable buckling load is 96g based on a stainless steel temperature of 500°F (Reference to Chapter 4, the maximum basket temperature at the outer basket panel is less than 471°F, therefore, use of 500°F is conservative). This G load is higher than 77 G shown in the Appendix D cask impact analysis. The G load at the hottest part of the basket (595°F) is located at the center of the basket (see Chapter 4). The ANSYS run at this location (Figure 3B.5-2, location 2) based on 600°F temperature, results in an allowable G load of 92. Therefore, the compressive and bending stresses developed in the stainless steel cannot cause the panel to buckle due to the tipover impact load.

3B.5.4 Analysis of the Aluminum Rails to Determine the Buckling Loads

The maximum membrane and bending stresses in the aluminum rails from the drop analyses (see Section 3B.4) at the most highly stressed location in the vertical member of the rail are listed below (1 G):

Location (Figure 3B.3-20)	Maximum Membrane S.I. (psi)	Maximum Bending S.I. (psi)
2 (Table 3B.3-2)	90	11**
3 (Table 3B.3-2)	51	8**

** These bending stress intensities are obtained through linearization of the cross section using ANSYS postprocessor

Criteria to Ensure Stability Under Compressive Loading

As given in ASME⁽⁴⁾ Code, Subsection NF, Paragraph NF-3322-1(c)(1)(a) and modified per Appendix F, Paragraph F-1334, the compressive stress limit for the accident condition (Level D) when KL/r is less than C_c :

$$F_a = \frac{1.4 [1 - (KL/r)^2 / (2 C_c^2)] S_y}{5/3 + [3 (KL/r) / (8 C_c)] - [(KL/r)^3 / (8 C_c^3)]}$$

Where:

$$C_c = [(2 \pi^2 E)/S_y]^{1/2}$$

$$K = 1$$

$$L = 6.6" \text{ (location 2), } 4.8" \text{ (Location 3)}$$

$$S_y = 13,300 \text{ psi (at } 400^\circ\text{F)}$$

$$S_u = 16,000 \text{ psi (at } 400^\circ\text{F)}$$

$$E = 8.7 \times 10^6 \text{ (at } 400^\circ\text{F)}$$

$$I = b h^3/12 = 1(0.75)^3/12 = 0.0351 \text{ in}^4$$

$$A = 1.0 \times 0.75 = 0.75 \text{ in}^2$$

$$r = (I/A)^{1/2} = 0.216 \text{ in}$$

$$KL/r = 1 \times 6.6/0.216 = 30.55$$

$$C_c = [(2 \pi^2 \times 8.7 \times 10^6)/13,300]^{1/2} = 113.63$$

$$F_a = \frac{1.4 [1 - (30.55)^2 / (2 \times 113.63^2)] (13,300)}{5/3 + [3 (30.55) / (8 \times 113.63)] - [(30.55)^3 / (8 \times 113.63^3)]} = 10,168 \text{ psi}$$

For L = 4.8 in

$$KL/r = 1 \times 4.8/0.216 = 22.22$$

$$C_c = [(2 \pi^2 \times 8.7 \times 10^6)/13,300]^{1/2} = 113.63$$

$$F_a = \frac{1.4 [1 - (22.22)^2 / (2 \times 113.63^2)] (13,300)}{5/3 + [3 (22.22) / (8 \times 113.63)] - [(22.22)^3 / (8 \times 113.63^3)]} = 10,502 \text{ psi}$$

Based on the above calculations, the allowable compressive stresses for the locations 2 & 3 are listed in the following table:

Location (Figure 3B.3-20)	Allowable Compressive Stress (F_a , psi)	Calculated Compressive Stress (1 G, psi)
2	10,168	90
3	10,502	51

Criteria To Prevent Failure Under Combined Loading (Compression + Bending)

For combined axial compression and bending, equations 20 and 21 of Paragraph NF-3322.1 (e) (1) apply.

$$f_a / F_a + C_{mx} (f_b) / (1 - f_a / F_e) F_b \leq 1.0 \text{ -----(1)}$$

and

$$f_a / (1.4)(0.6) S_y + f_b / F_b \leq 1.0 \text{ -----(2)}$$

The allowable stresses for the above equations are determined as follows:

	Allowable Stress	ASME Code Reference
F _a	10,168 psi (Location 2) 10,502 psi (Location 3)	NF-3322-1(c)(1)(a)
F _b	0.66 S _y ** = 8,788 psi	F-1334.5 (c)
C _{mx}	0.6	NF-3322.1 (e) (1) (b)
Note	The allowable stress F _a is multiplied by 1.4, which is the minimum factor allowed by Paragraph F-1334.	

** Conservatively use Level A allowable for Level D load calculations

The value of F_e is calculated by the formula below per Paragraph F-1334.5 (b):

$$F_e = \pi^2 (E) / (1.3) (KL/r)^2$$

Where:

K is conservatively taken as 1

L is the free length of the member, 6.6 in. (Location 2), 4.8 in. (Location 3)

r is the radius of gyration, in.

E is the modulus of elasticity, 8.7×10^6 psi

This formula gives the following results for F_e :

Location	F_e (psi)
2 (L = 6.6", r = 0.216 in.)	70,771
3 (L = 4.8", r = 0.216 in.)	133,778

The interaction equations were evaluated based on:

Location 2 (Assume 100 g)

$$f_a / F_a + C_{mx} (f_b) / (1 - f_a / F_e) F_b = [(90 \times 100) / 10,168] + [0.6 \times (11 \times 100)] / [(1 - 90 \times 100 / 70,771) \times 8,778] = 0.971 \leq 1$$

$$f_a / (1.4)(0.6) S_y + f_b / F_b = [(90 \times 100) / (1.4 \times 0.6 \times 13,300)] + (11 \times 100) / 8,778 = 0.931 \leq 1$$

Location 3 (Assume 100 g)

$$f_a / F_a + C_{mx} (f_b) / (1 - f_a / F_e) F_b = [(51 \times 100) / 10,502] + [0.6 \times (8 \times 100)] / [(1 - 51 \times 100 / 133,778) \times 8,778] = 0.542 \leq 1$$

$$f_a / (1.4)(0.6) S_y + f_b / F_b = [(51 \times 100) / (1.4 \times 0.6 \times 13,300)] + [(8 \times 100) / 8,778] = 0.547 \leq 1$$

3B.5.5 Evaluation

Based on the result of this analysis, it concluded that the buckling load for aluminum rails is at least 100 G under a side drop. This G load is much higher than the 77 G load shown on Appendix D cask impact analysis. Therefore, the compressive and bending stresses developed in the aluminum rails due to the tipover impact load cannot cause the rails to buckle.

3B.6 Summary of Basket Structural Analysis

3B.6.1 Stresses Due to Normal Condition Service

The following table summarized the normal condition basket structural analysis:

Stress Summary of Normal Condition Structural Analysis

Loading	Stress Category	Max. Stress (ksi)	Allowable Stress (ksi)	Reference Section/ Table
304 Stainless Steel Plate				
1G Lateral	P_m	0.36	14.76 ($S_m \times 0.9$)	Table 3B.3-1 (0° Drop)
	$P_m + P_b$	0.63	22.14 ($1.5 S_m \times 0.9$)	Table 3B.3-1 (0° Drop)
3G Vertical	P_m	0.30	14.76 ($S_m \times 0.9$)	Sect. 3B.3.3
Stainless Steel Fusion Weld				
1G Lateral	τ	0.055	2.95 ($0.6 S_m \times 0.3$)	Table 3B.3-1 (45° Drop)
3G Vertical	τ	0.05	2.95 ($0.6 S_m \times 0.3$)	Sect. 3B.3.3
6061-T6 Aluminum Rail				
1G Lateral	P_m	0.11	4.5 (S_m)	Table 3B.3-2 (Location 1)
	$P_m + P_b$	0.15	6.75 ($1.5 S_m$)	Table 3B.3-2 (Location 1)
3G Vertical	P_m	0.05	4.5 (S_m)	Sect. 3B.3.3

Based on the results shown on the above table, all of the calculated stresses in the basket and rails are acceptable.

3B.6.2 Stresses Due to Accident Condition

The following table summarized the accident condition basket structural analysis:

Stress Summary of Accident Condition Structural Analysis

Loading	Stress Category	Max. Stress (ksi)	Allowable Stress (ksi)	Max. Allowable G load	Max. Calculated G Load	Reference Section/Table
304 Stainless Steel Plate						
60 G End Drop	P_m	6.03 (60G)	39.36 (2.4 S_m)	392	60	Sect. 3B.4.1
Side drop Stress Analysis	P_m	0.36 (1G)	39.36 (2.4 S_m)	109	77	Table 3B.4-1 (0° drop)
	$P_m + P_b$	0.63 (1G)	59.04 (S_u)	94	77	Table 3B.4-1 (0° drop)
Side drop Buckling Analysis				92	77	Sect. 3B.5.2
Stainless Steel Fusion weld						
60 G End Drop	τ	0.92 (60G)	19.68 (0.6 $S_m \times 2$)	1283	60	Sect. 3B.4.1
Side Drop Stress Analysis	τ	0.055 (1G)	19.68 (0.6 $S_m \times 2$)	358	77	Table 3B.4-1 (45° drop)
6061-T6 Aluminum Rail						
60 G End Drop	P_m	1.0 (60G)	10.8 (2.4 S_m)	648	60	Sect. 3B.4.1
Side Drop Stress analysis	P_m	0.11 (1G)	10.8 (2.4 S_m)	98	77	Table 3B.4-2 (Location 1)
	$P_m + P_b$	0.15 (1G)	16.0 (S_u)	107	77	Table 3B.4-2 (Location 1)
Side Impact Buckling Analysis				100	77	Sect. 3B.5.4

Based on this analysis, the basket and rails are structurally adequate up to 94 G (limited by 0° side drop), this G load is higher than the calculated G load of 77 from tip over impact analysis described in Appendix D. The basket and rails will remain in place and maintain separation of adjacent fuel assemblies.

3B.7 References

1. ANSYS Engineering Analysis System User's Manual, Rev. 6.0, 2001. |
2. ASME B&PV Code, Section II, Part D, 1998 including 2000 Addendum. |
3. ASME B&PV Code, Section III Appendices and Subsection NG, 1995 including 1996 Addendum.
4. ASME B&PV Code, Section III, Subsection NF, 1995 including 1996 Addendum.
5. Roark, R. "Formulas for Stress and Strain" Fourth Edition.
6. ASME B&PV Code, Section III, Appendix F, 1995 including 1996 Addendum. |

Table 3B.3-1
 Summary of Basket Stress Analysis - Normal Condition
 (1G Side Load)

Drop Orientation (Degree)	Component	Stress Category	Max. Stress (1G) (ksi)	Allowable Stress (ksi)	Reference Figures
0	S.S. Plate	P_m	0.24	14.76	3B.3-4
		$P_m + P_b$	0.63	22.14	3B.3-5
	S.S. Box	P_m	0.36	14.76	3B.3-6
		$P_m + P_b$	0.38	22.14	3B.3-7
	Fusion Weld	τ	0.043	2.95	Fig. 3B.3-23
30	S.S. Plate	P_m	0.21	14.76	3B.3-8
		$P_m + P_b$	0.47	22.14	3B.3-9
	S.S. Box	P_m	0.28	14.76	3B.3-10
		$P_m + P_b$	0.35	22.14	3B.3-11
45	S.S. Plate	P_m	0.17	14.76	3B.3-12
		$P_m + P_b$	0.40	22.14	3B.3-13
	S.S. Box	P_m	0.23	14.76	3B.3-14
		$P_m + P_b$	0.31	22.14	3B.3-15
	Fusion Weld	τ	0.055	2.95	Fig. 3B.3-24

Table 3B.3-2
 Linearized Stress Intensities of Aluminum Rail - Normal Condition
 (0° Side Load)

Location (Figures 3B.3-20 & 21)	Stress Category	Max. S.I. 1G (ksi)	Allowable S.I. (ksi)
1	P_m	0.11	4.5
	$P_m + P_b$	0.15	6.75
2	P_m	0.09	4.5
	$P_m + P_b$	0.10	6.75
3	P_m	0.05	4.5
	$P_m + P_b$	0.06	6.75
4	P_m	0.02	4.5
	$P_m + P_b$	0.03	6.75
5	P_m	0.01	4.5
	$P_m + P_b$	0.02	6.75

Table 3B.3-3
 Linearized Stress Intensities of Aluminum Rail - Normal Condition
 (30° Side Load)

Location (Figures 3B.3-20 & 21)	Stress Category	Max. S.I. 1G (ksi)	Allowable S.I. (ksi)
1	P_m	0.08	4.5
	$P_m + P_b$	0.11	6.75
2	P_m	0.08	4.5
	$P_m + P_b$	0.09	6.75
3	P_m	0.04	4.5
	$P_m + P_b$	0.05	6.75
4	P_m	0.03	4.5
	$P_m + P_b$	0.03	6.75
5	P_m	0.02	4.5
	$P_m + P_b$	0.02	6.75

Table 3B.3-4
 Linearized Stress Intensities of Aluminum Rail - Normal Condition
 (45° Side Load)

Location (Figures 3B.3-20 & 21)	Stress Category	Max. S.I. 1G (ksi)	Allowable S.I. (ksi)
1	P_m	0.06	4.5
	$P_m + P_b$	0.08	6.75
2	P_m	0.06	4.5
	$P_m + P_b$	0.07	6.75
3	P_m	0.04	4.5
	$P_m + P_b$	0.04	6.75
4	P_m	0.02	4.5
	$P_m + P_b$	0.02	6.75
5	P_m	0.02	4.5
	$P_m + P_b$	0.03	6.75

Table 3B.4-1
Summary of Basket Stress Analysis - Accident Condition
(Side Drop)

Drop Orientation (Degree)	Component	Stress Category	Max. Stress (1G) (ksi)	Allowable Stress (ksi)	Max. Allowable G Load
0	S.S. Plate	P_m	0.24	39.36	164
		$P_m + P_b$	0.63	59.04	94
	S.S. Box	P_m	0.36	39.36	109
		$P_m + P_b$	0.38	59.04	155
	Fusion Weld	τ	0.043	19.68	458
30	S.S. Plate	P_m	0.21	39.36	187
		$P_m + P_b$	0.47	59.04	126
	S.S. Box	P_m	0.28	39.36	141
		$P_m + P_b$	0.35	59.04	169
45	S.S. Plate	P_m	0.17	39.36	232
		$P_m + P_b$	0.40	59.04	148
	S.S. Box	P_m	0.23	39.36	171
		$P_m + P_b$	0.231	59.04	256
	Fusion Weld	τ	0.055	19.68	358

Table 3B.4-2
 Linearized Stress Intensities of Aluminum Rail - Accident Condition
 (0° Side Drop)

Location (Figures 3B.3-20 & 21)	Stress Category	Max. S.I. 1G (ksi)	Allowable S.I. (ksi)	Max. Allowable G Loads
1	P_m	0.11	10.8	98
	$P_m + P_b$	0.15	16.0	107
2	P_m	0.09	10.8	120
	$P_m + P_b$	0.10	16.0	160
3	P_m	0.05	10.8	216
	$P_m + P_b$	0.06	16.0	267
4	P_m	0.02	10.8	540
	$P_m + P_b$	0.03	16.0	533
5	P_m	0.01	10.8	1080
	$P_m + P_b$	0.02	16.0	800

Table 3B.4-3
 Linearized Stress Intensities of Aluminum Rail - Accident Condition
 (30° Side Drop)

Location (Figures 3B.3-20 & 21)	Stress Category	Max. S.I. 1G (ksi)	Allowable S.I. (ksi)	Max. Allowable G Loads
1	P_m	0.08	10.8	135
	$P_m + P_b$	0.11	16.0	146
2	P_m	0.08	10.8	135
	$P_m + P_b$	0.09	16.0	178
3	P_m	0.04	10.8	270
	$P_m + P_b$	0.05	16.0	320
4	P_m	0.03	10.8	360
	$P_m + P_b$	0.03	16.0	533
5	P_m	0.02	10.8	540
	$P_m + P_b$	0.02	16.0	800

Table 3B.4-4
 Linearized Stress Intensities of Aluminum Rail - Accident Condition
 (45° Side Drop)

Location (Figures 3B.3-20 & 21)	Stress Category	Max. S.I. 1G (ksi)	Allowable S.I. (ksi)	Max. Allowable G Loads
1	P_m	0.06	10.8	180
	$P_m + P_b$	0.08	16.0	200
2	P_m	0.06	10.8	180
	$P_m + P_b$	0.07	16.0	229
3	P_m	0.04	10.8	270
	$P_m + P_b$	0.04	16.0	400
4	P_m	0.02	10.8	540
	$P_m + P_b$	0.02	16.0	800
5	P_m	0.02	10.8	540
	$P_m + P_b$	0.03	16.0	533

Figure Withheld Under 10 CFR 2.390

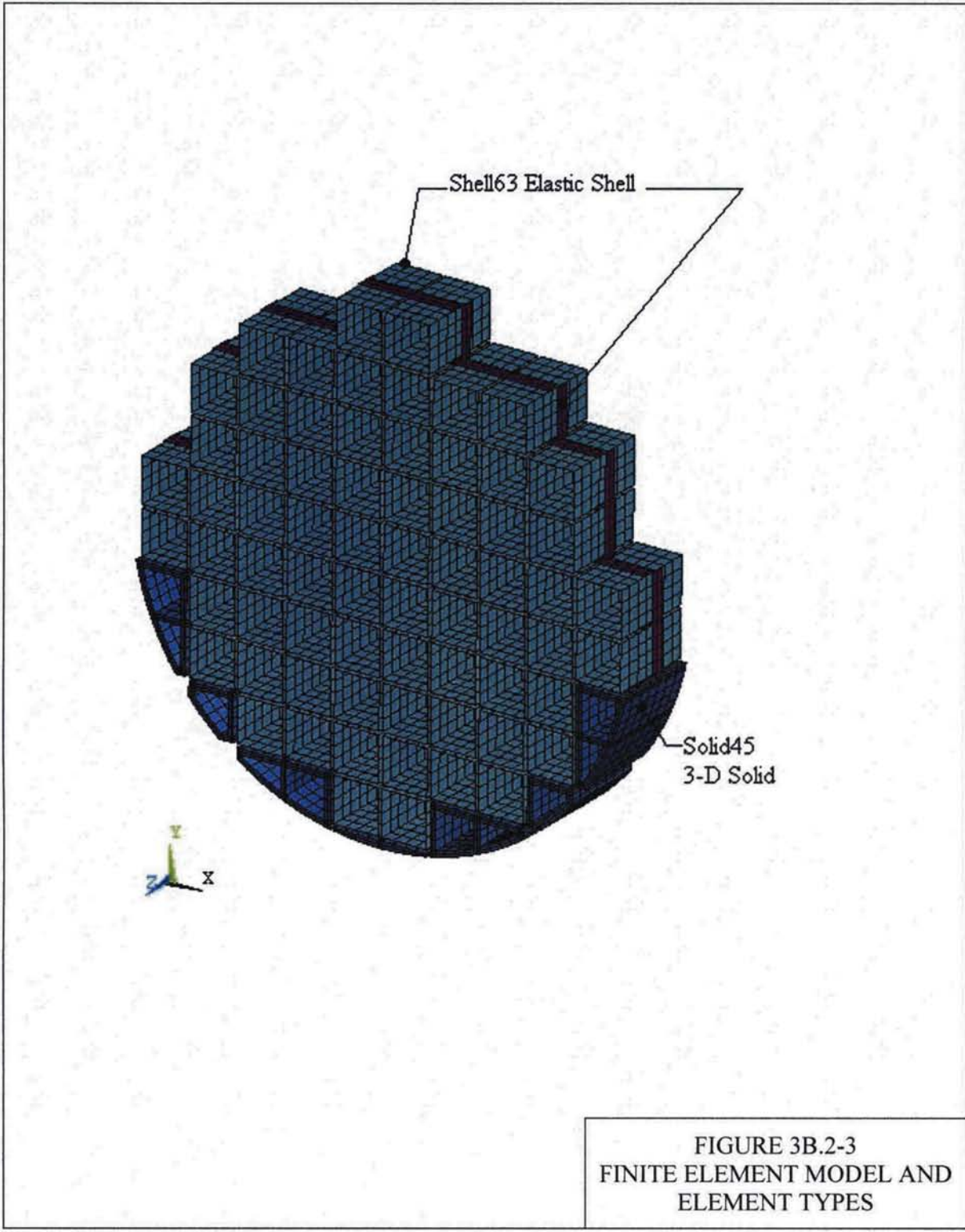
**Figure 3B.1-1
REPRESENTATIVE BASKET
WALL PANEL**

Figure Withheld Under 10 CFR 2.390

FIGURE 3B.2-1
AXIAL VIEW OF BASKET

Figure Withheld Under 10 CFR 2.390

FIGURE 3B.2-2
GEOMETRY FOR ANSYS
MODEL



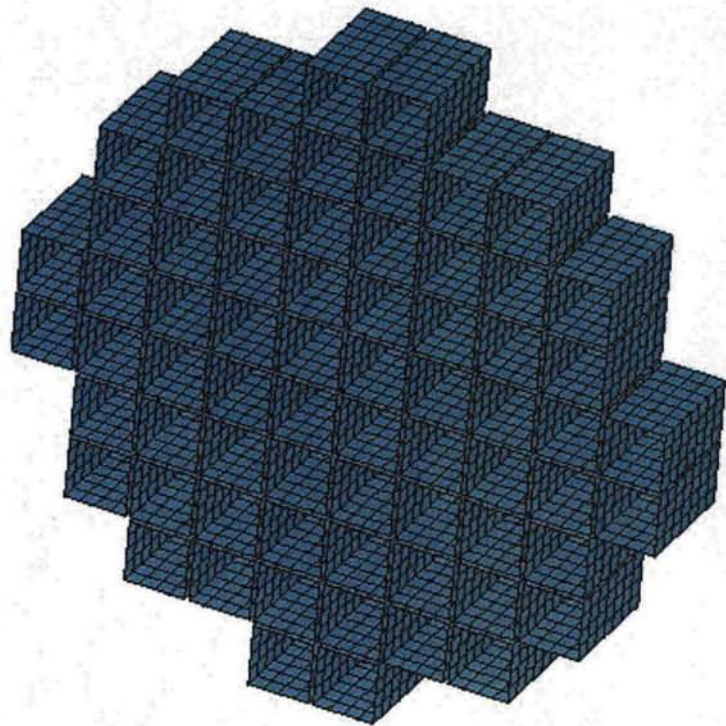


FIGURE 3B.2-4
BASKET FINITE ELEMENT
MODEL- STAINLESS STEEL
BOXES

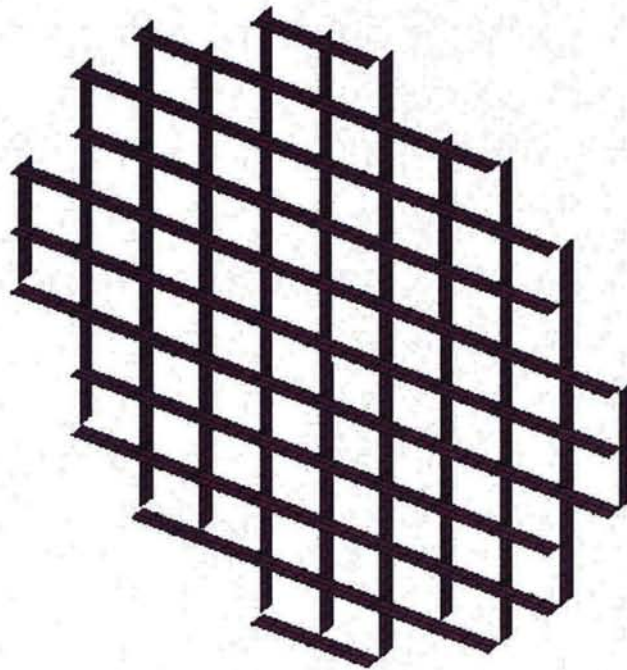


FIGURE 3B.2-5
BASKET FINITE ELEMENT
MODEL- STAINLESS STEEL
PLATES

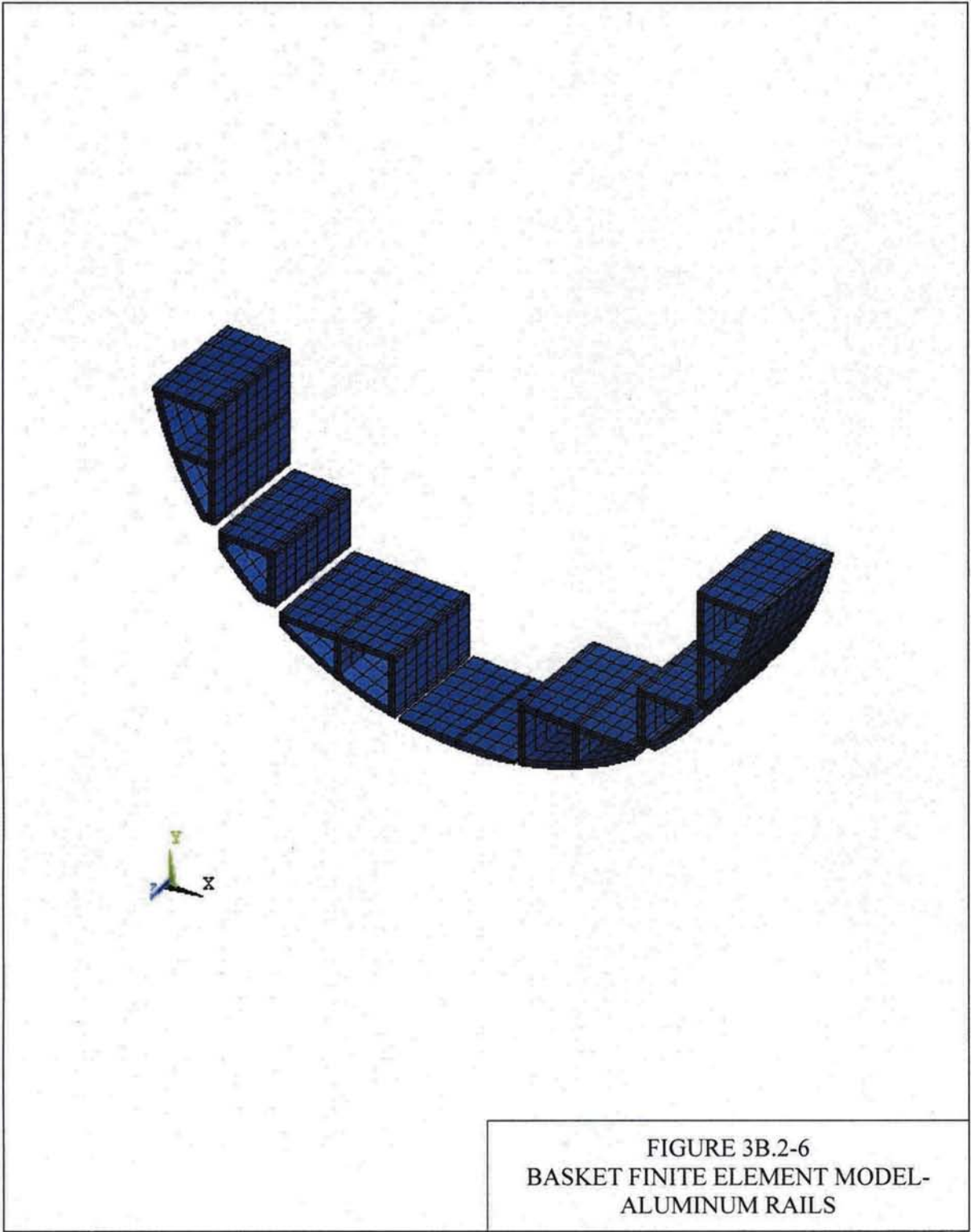


FIGURE 3B.2-6
BASKET FINITE ELEMENT MODEL-
ALUMINUM RAILS

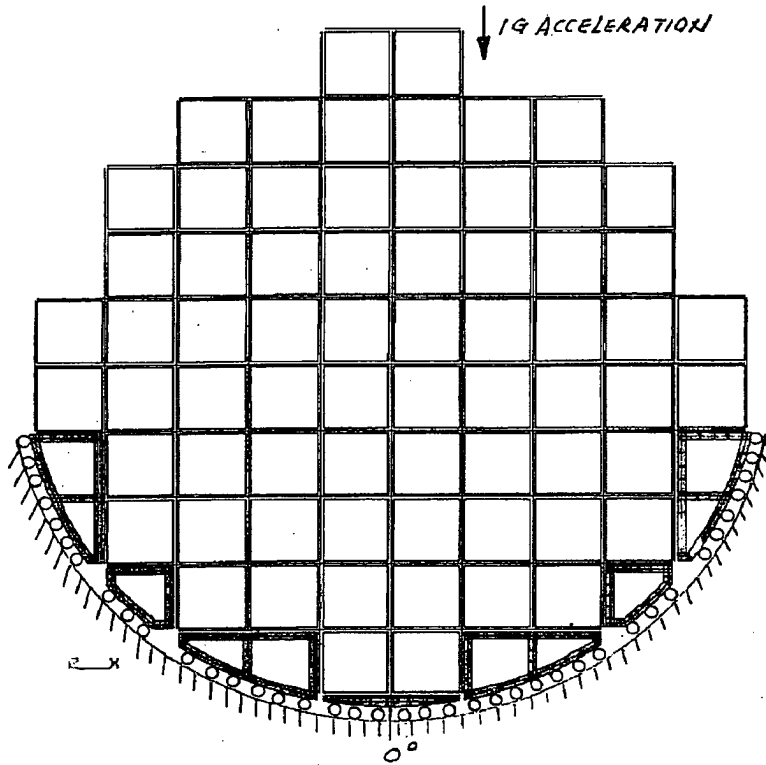
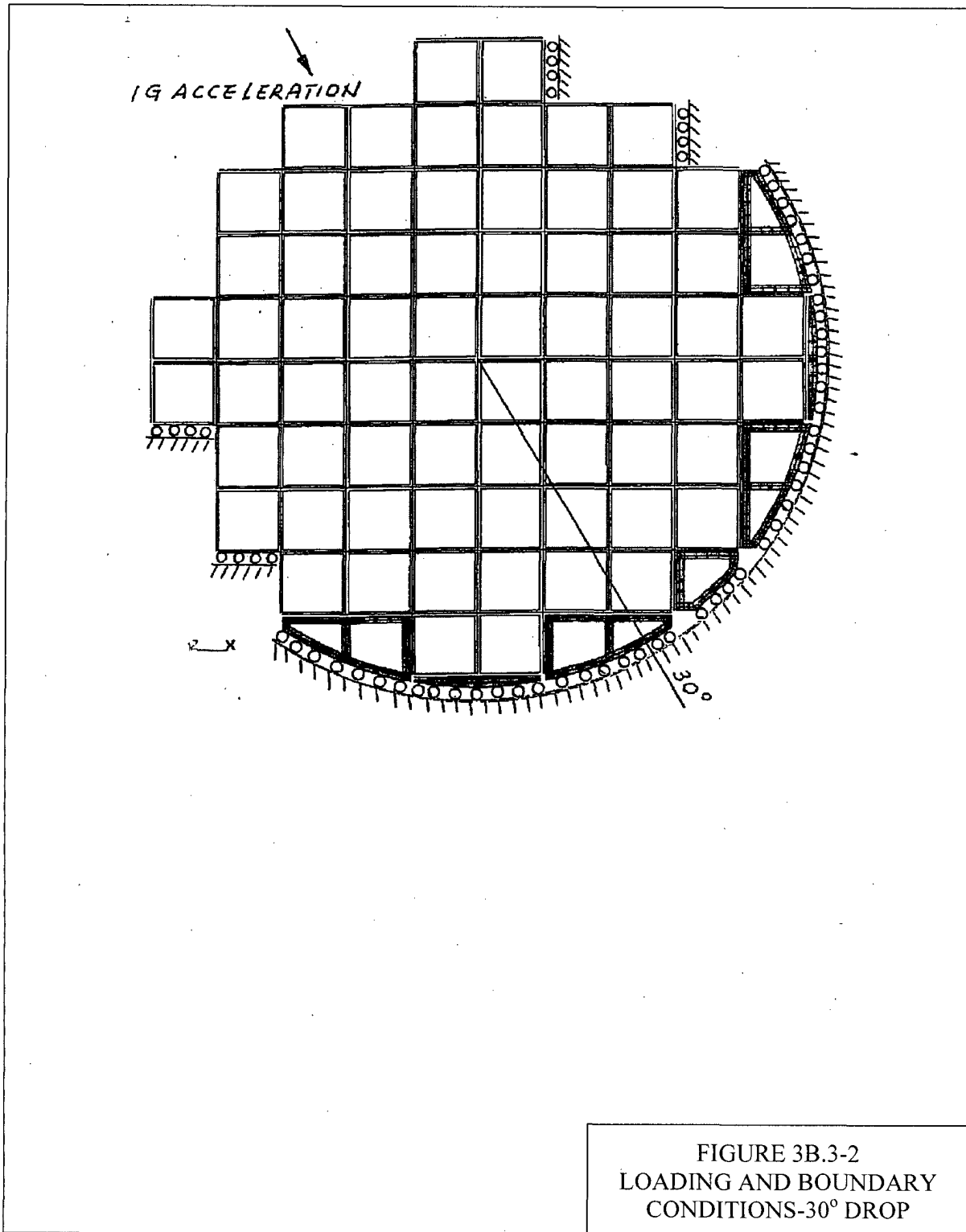


FIGURE 3B.3-1
LOADING AND BOUNDARY
CONDITIONS-0° DROP



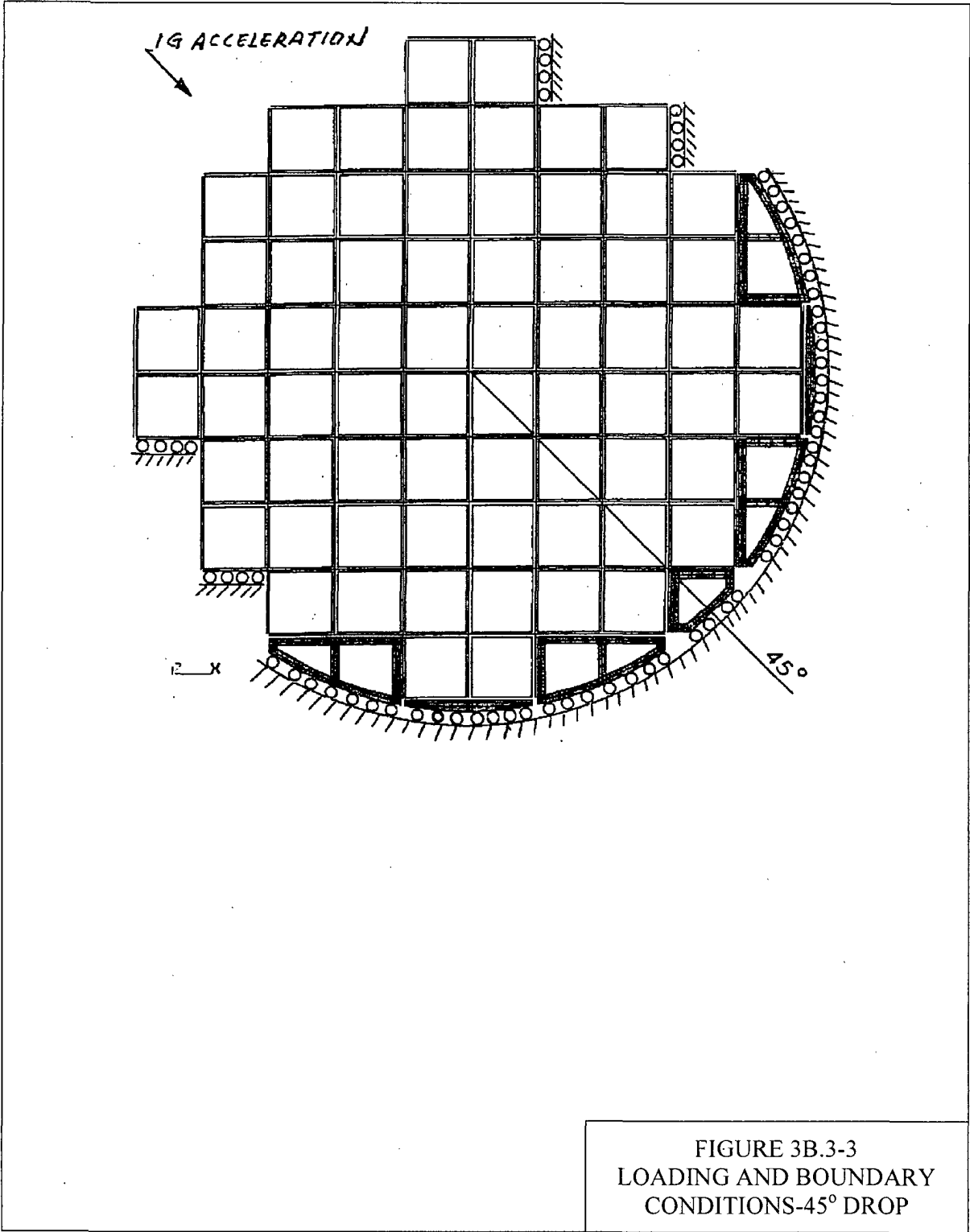


FIGURE 3B.3-3
LOADING AND BOUNDARY
CONDITIONS-45° DROP

Figure 3B.3-4
 Membrane Stress Intensity (SS Plate)-0 Degree Drop

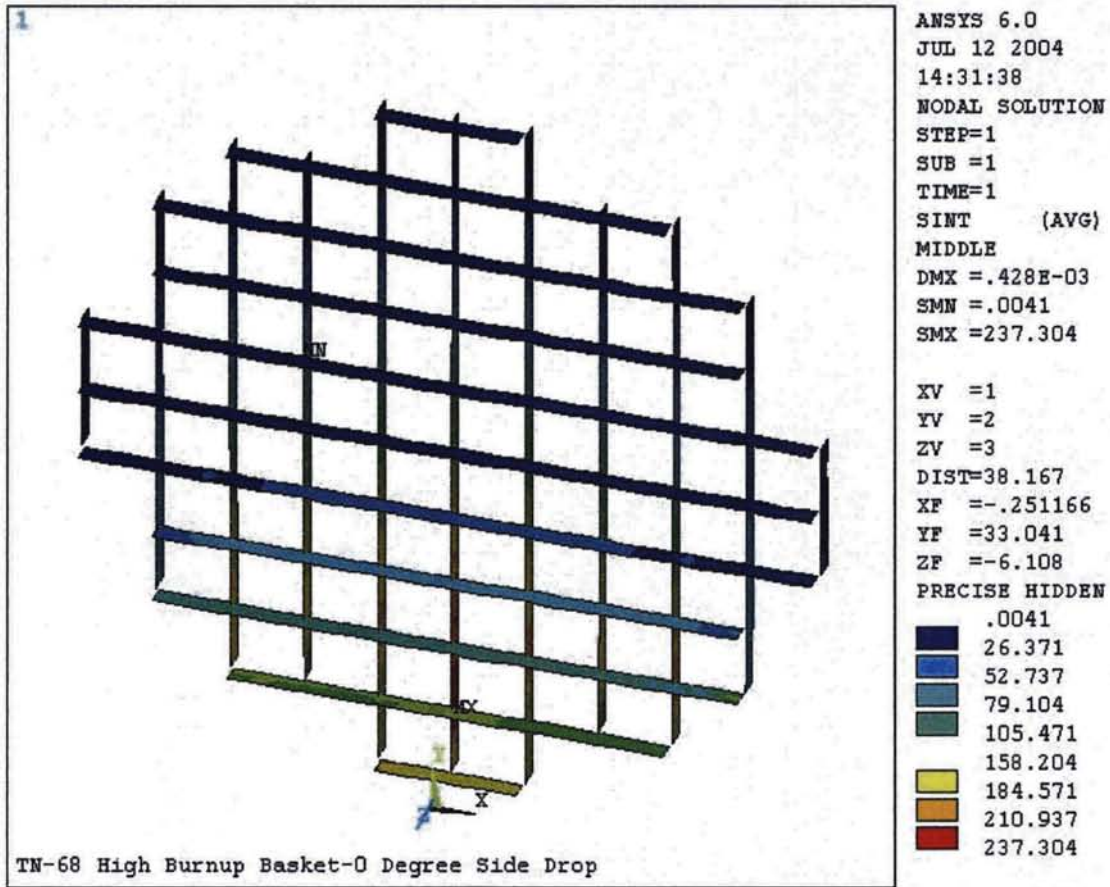


Figure 3B.3-5
 Membrane + Bending Stress Intensity (SS Plate)-0 degree Drop

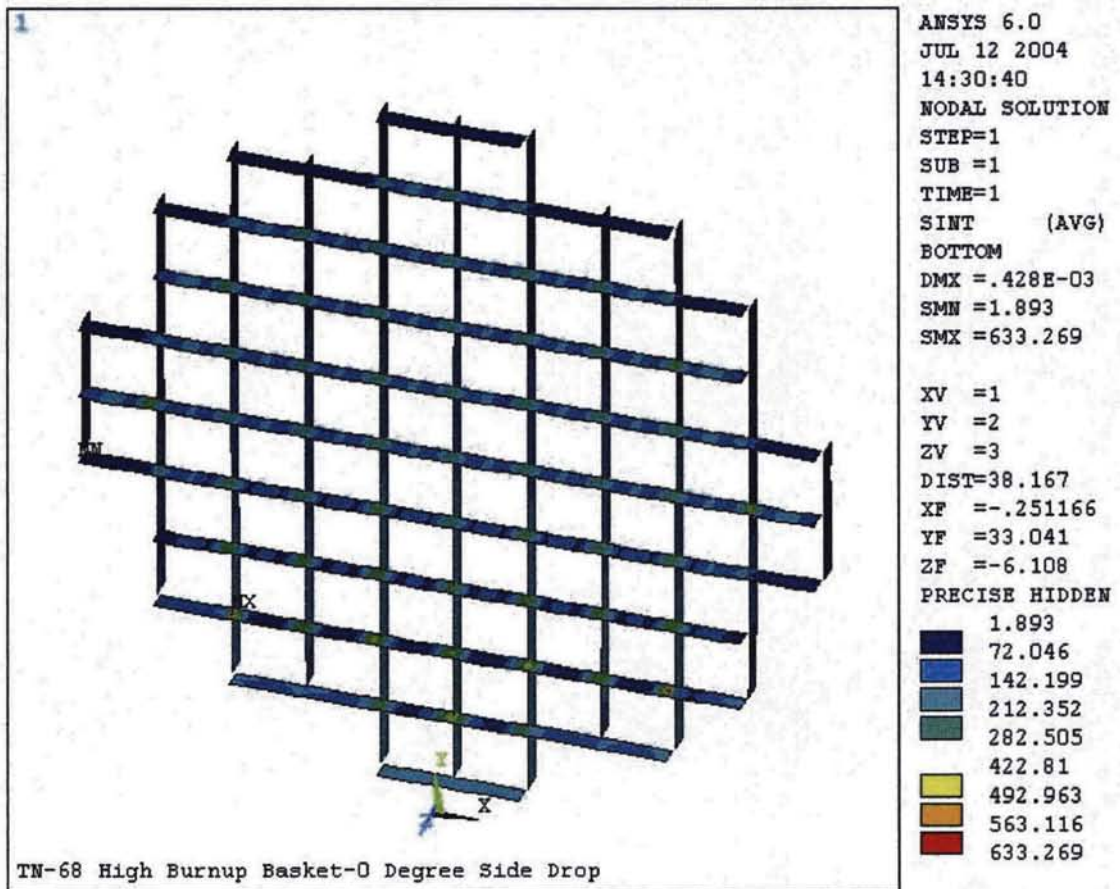


Figure 3B.3-6
Membrane Stress Intensity (SS Box)-0 Degree Drop

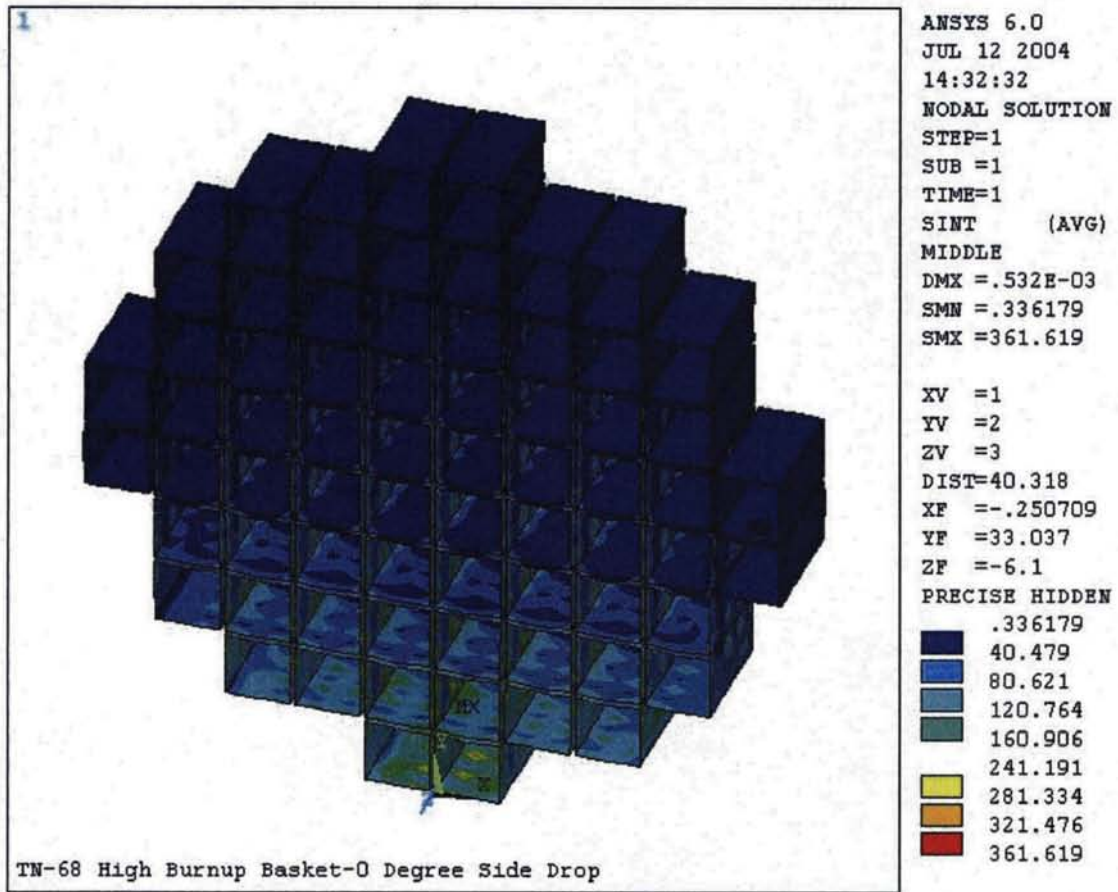


Figure 3B.3-7
Membrane + Bending Stress Intensity (SS Box)-0 Degree Drop

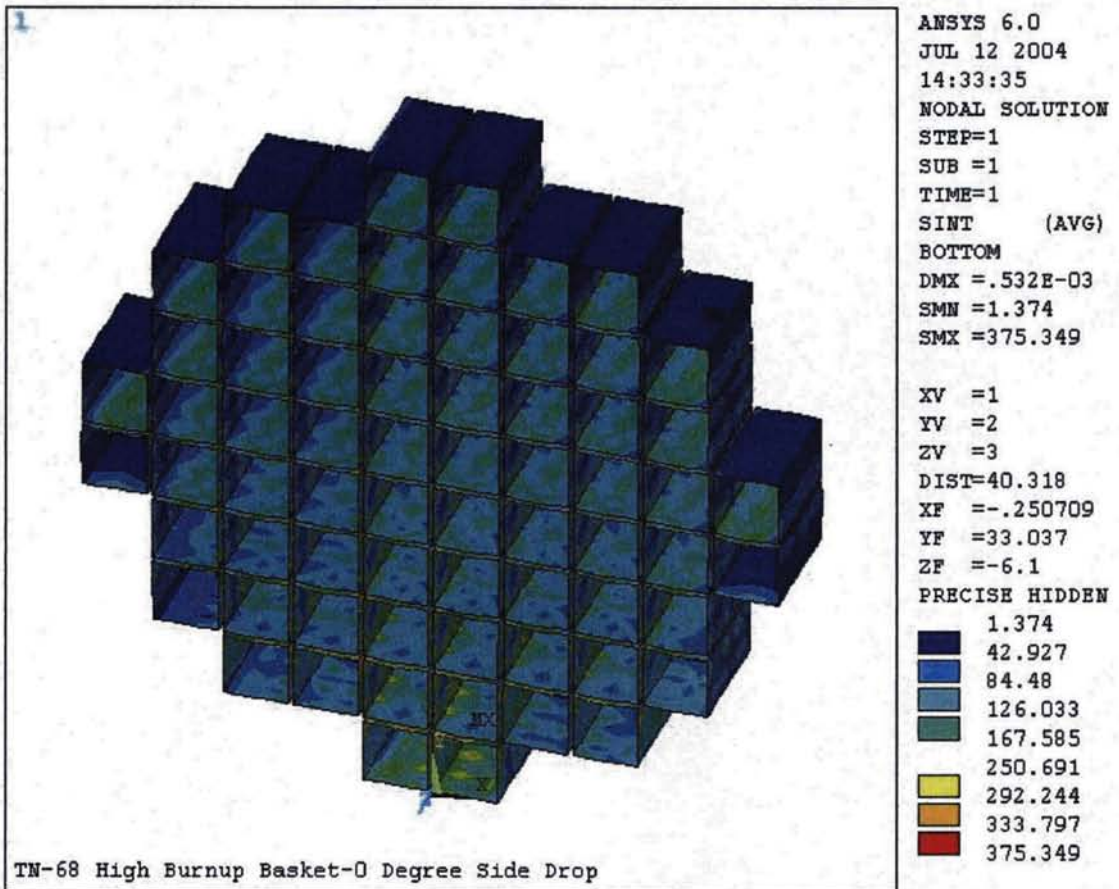


Figure 3B.3-8
Membrane Stress Intensity (SS Plate)-30 Degree Drop

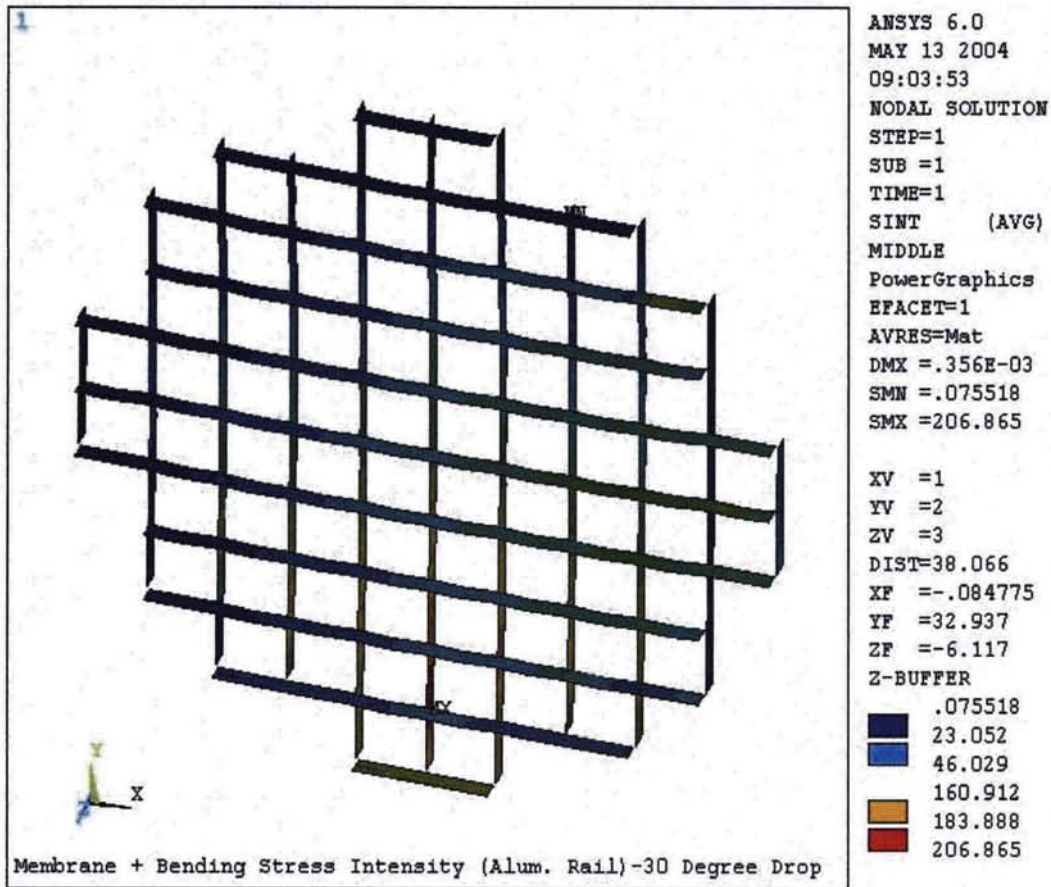


Figure 3B.3-9
Membrane + Bending Stress Intensity (SS Plate)-30 degree Drop

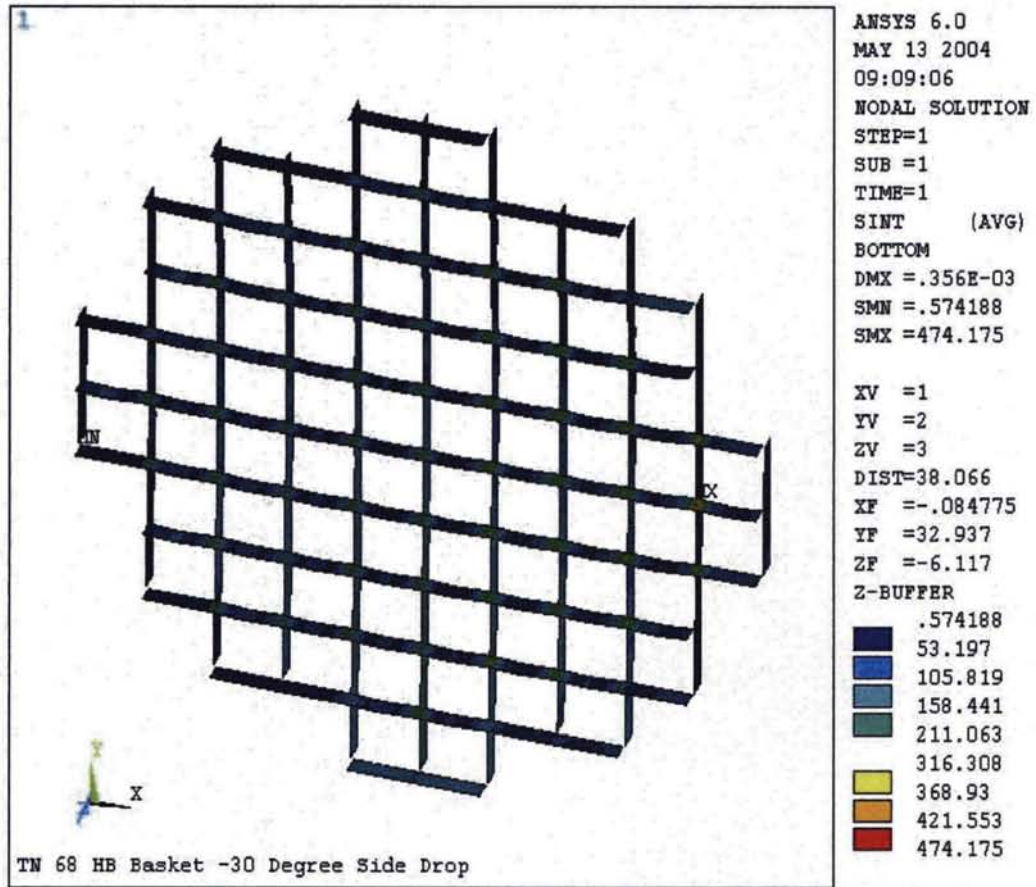


Figure 3B.3-10
Membrane Stress Intensity (SS Box)-30 Degree Drop

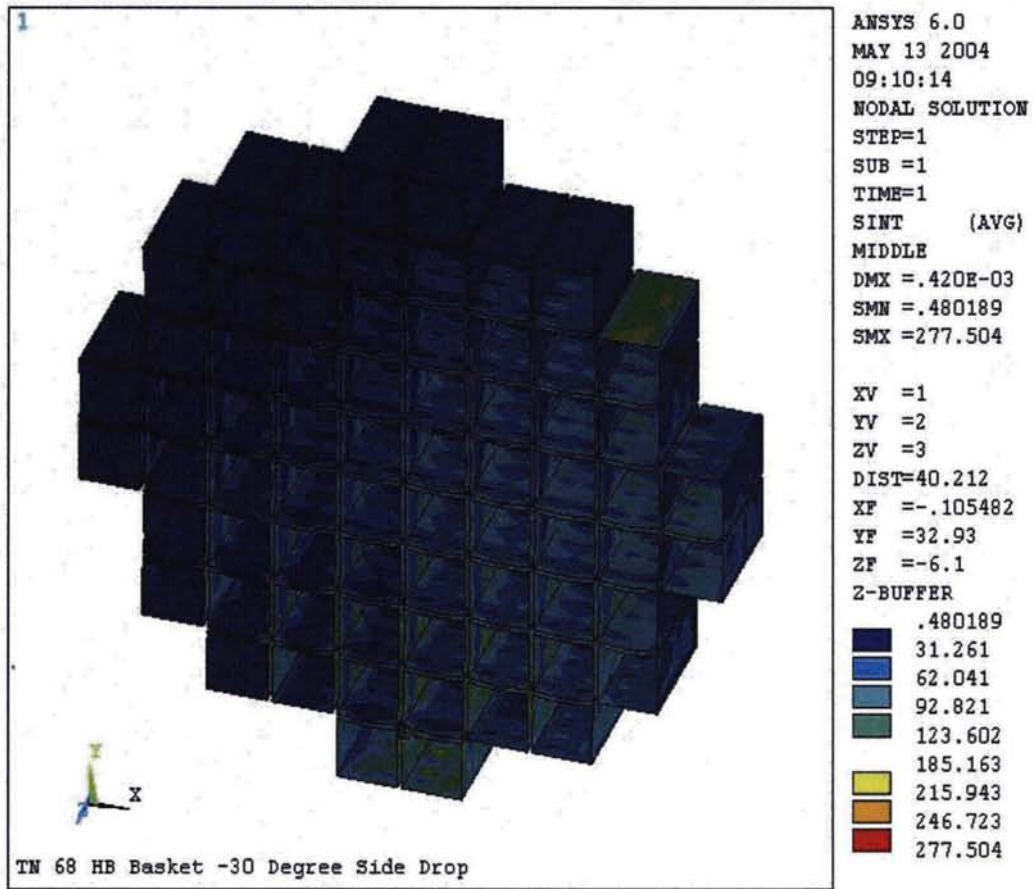


Figure 3B.3-11
Membrane + Bending Stress Intensity (SS Box)-30 Degree Drop

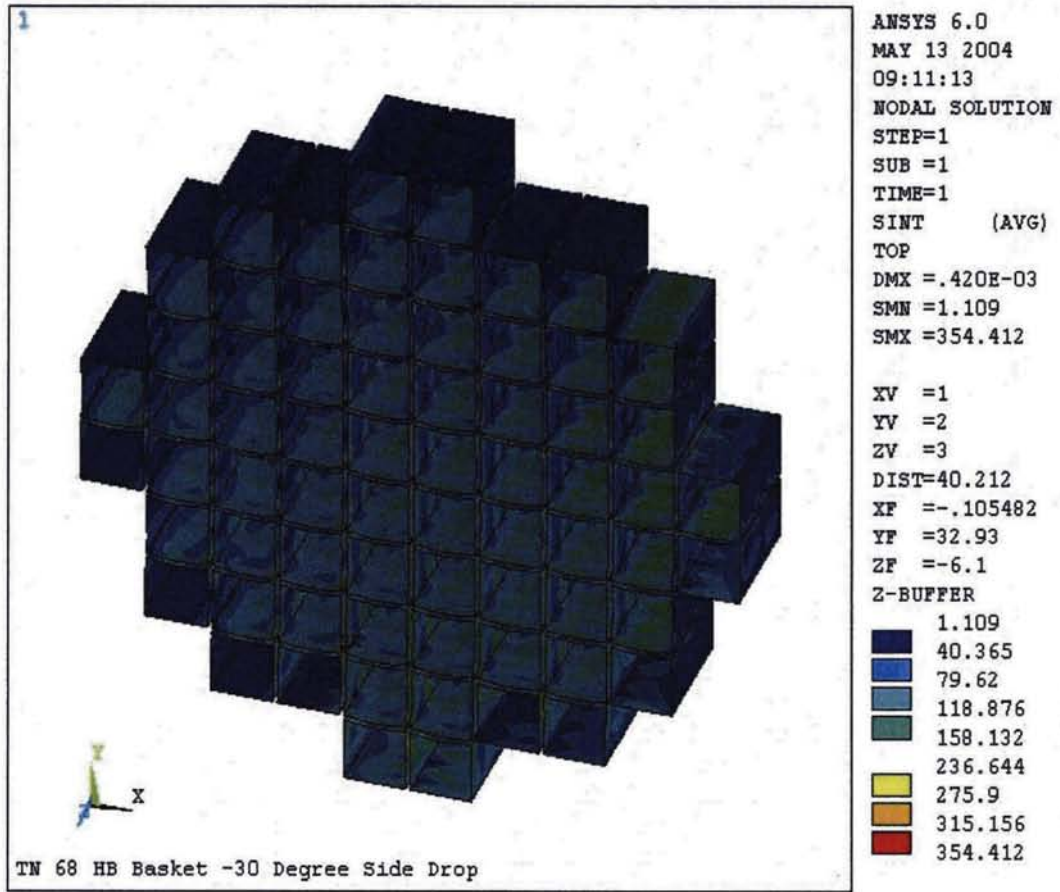


Figure 3B.3-12
Membrane Stress Intensity (SS Plate)-45 Degree Drop

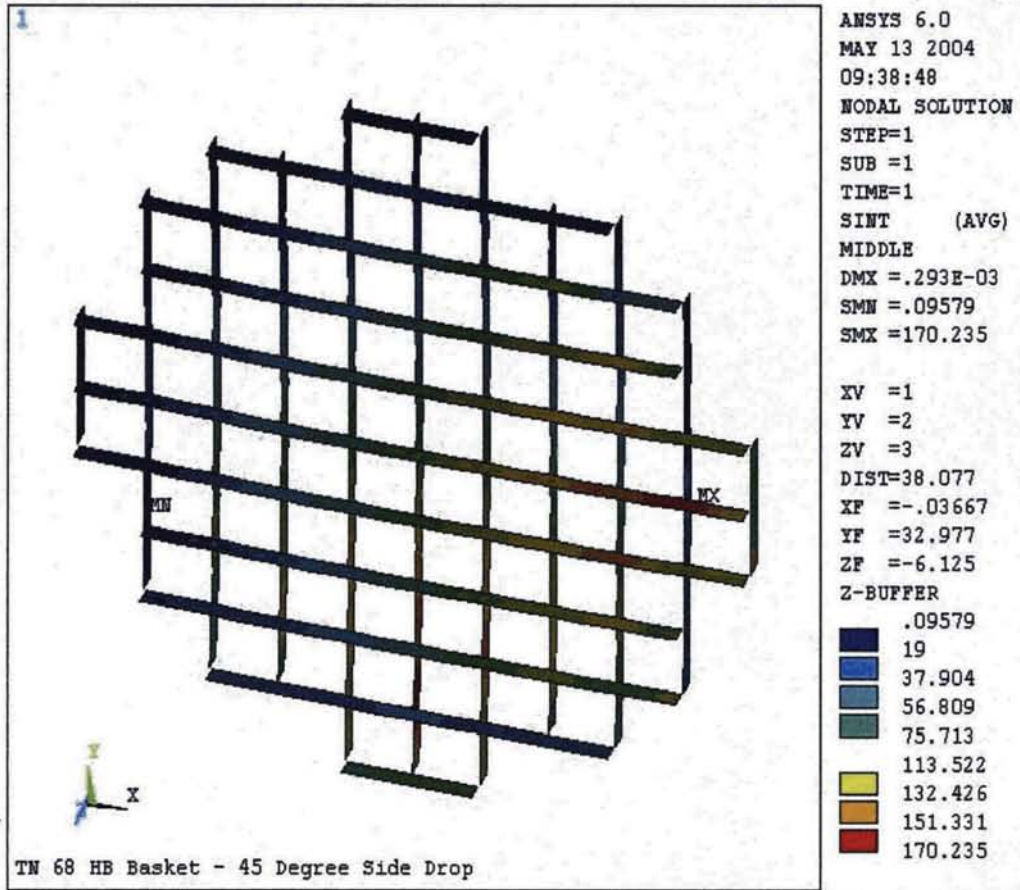


Figure 3B.3-13
 Membrane + Bending Stress Intensity (SS Plate)-45 Degree Drop

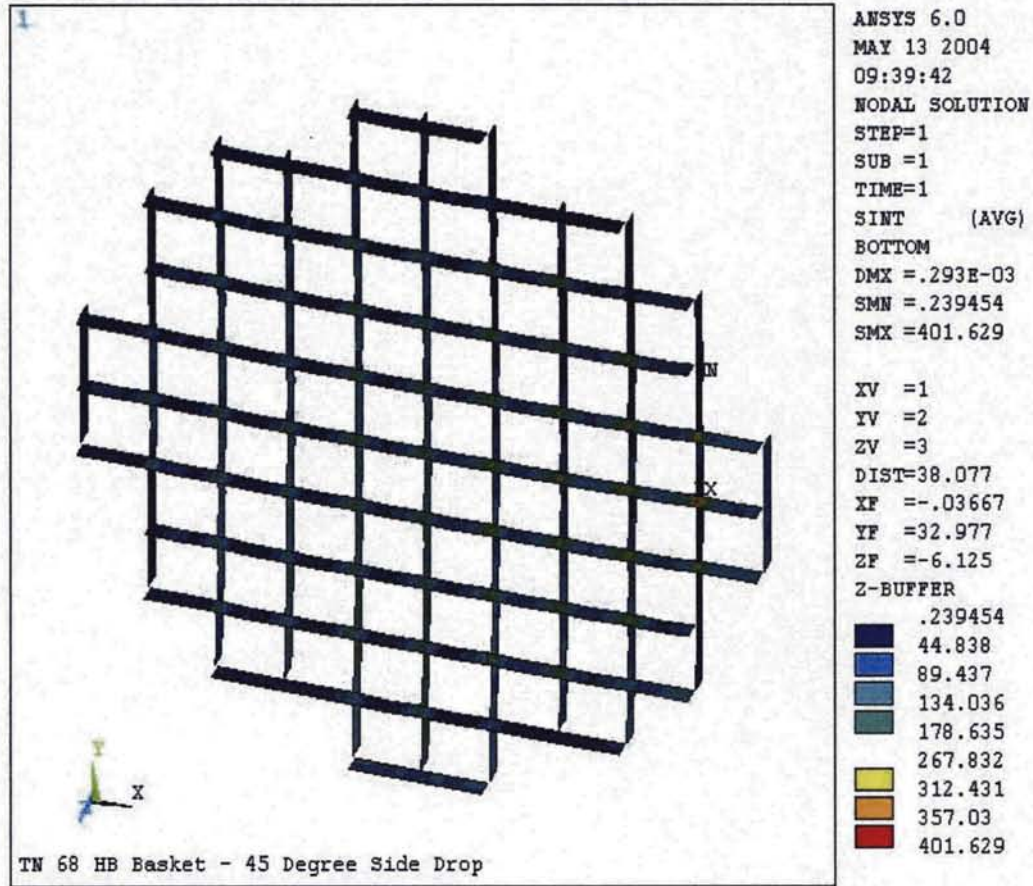


Figure 3B.3-14
Membrane Stress Intensity (SS Box)-45 Degree Drop

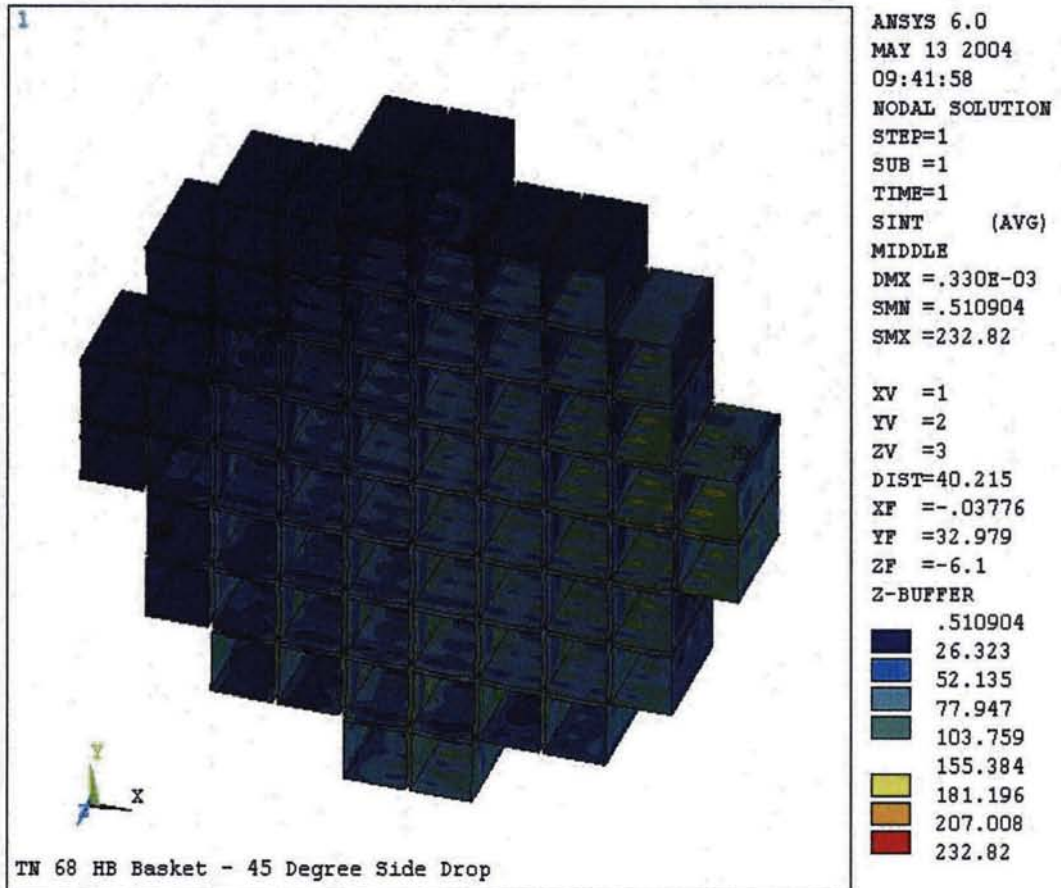


Figure 3B.3-15
Membrane + Bending Stress Intensity (SS Box)-45 Degree Drop

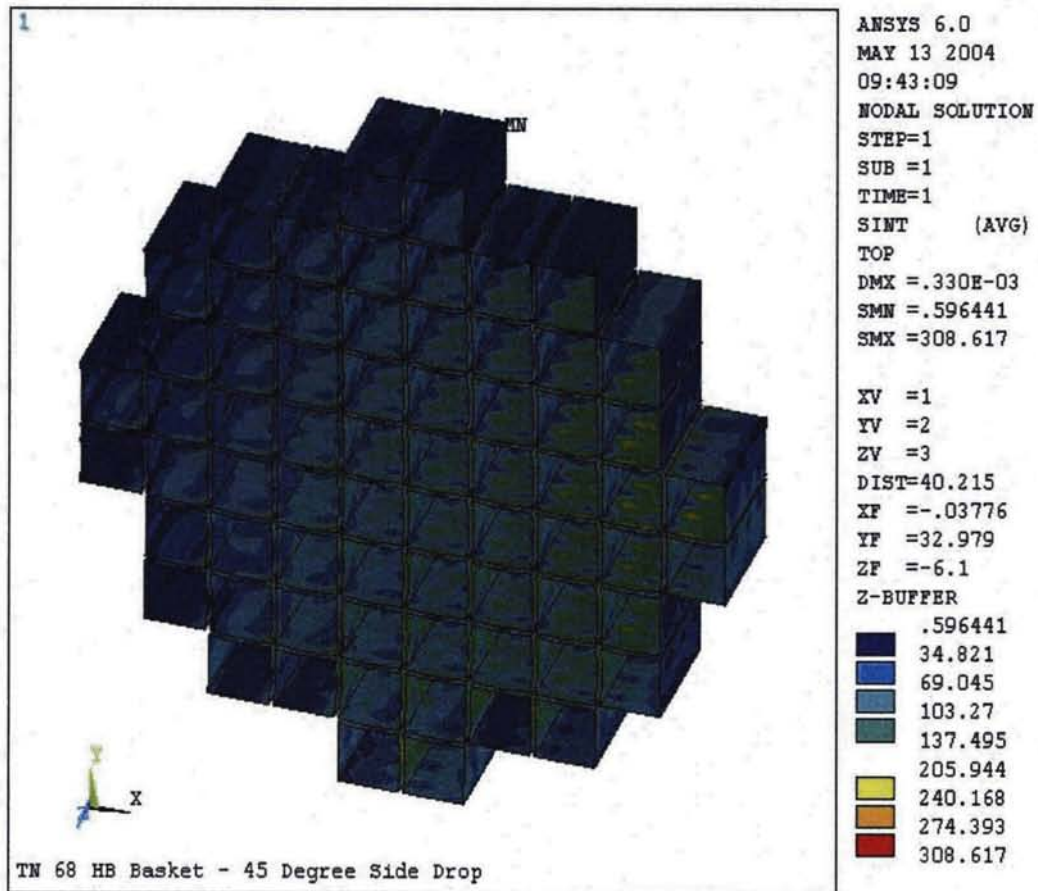


Figure 3B.3-16
Nodal Stress Intensity (Aluminum Rails)-0 Degree Drop

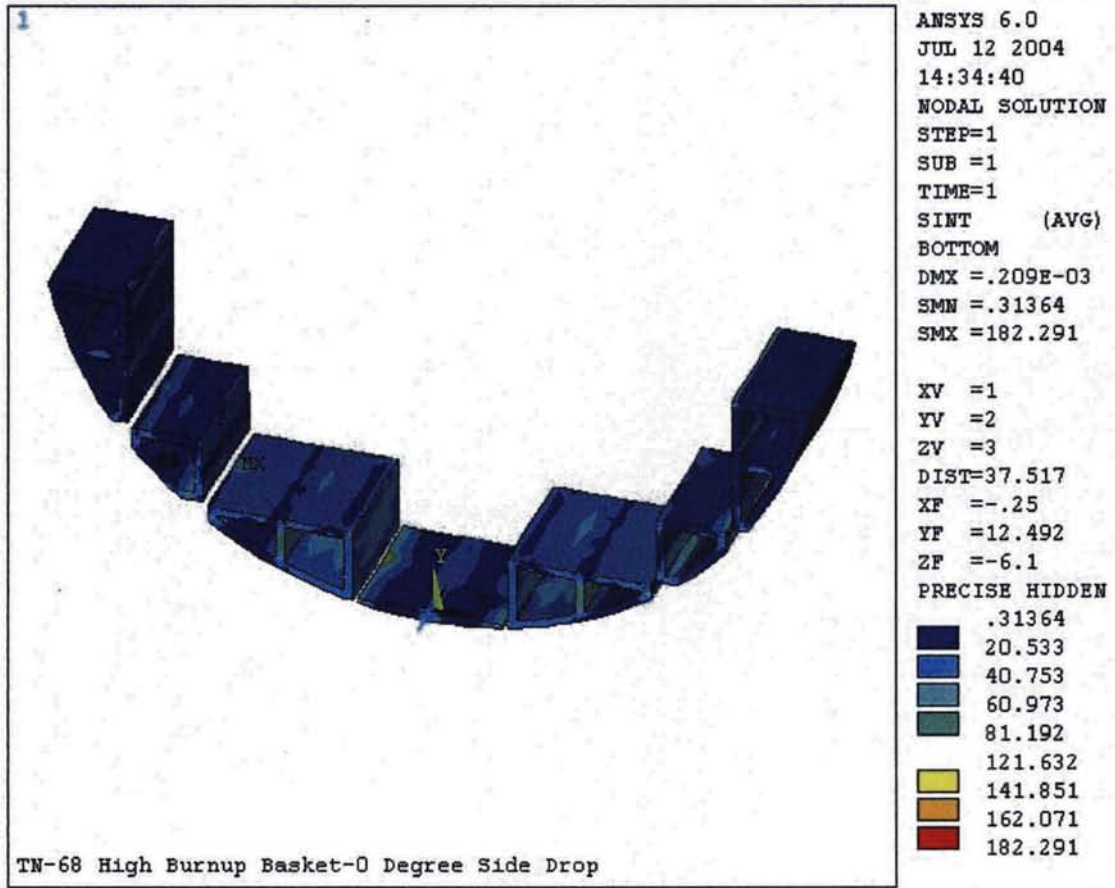


Figure 3B.3-17
Nodal Stress Intensity (Aluminum Rails)-30 Degree Drop

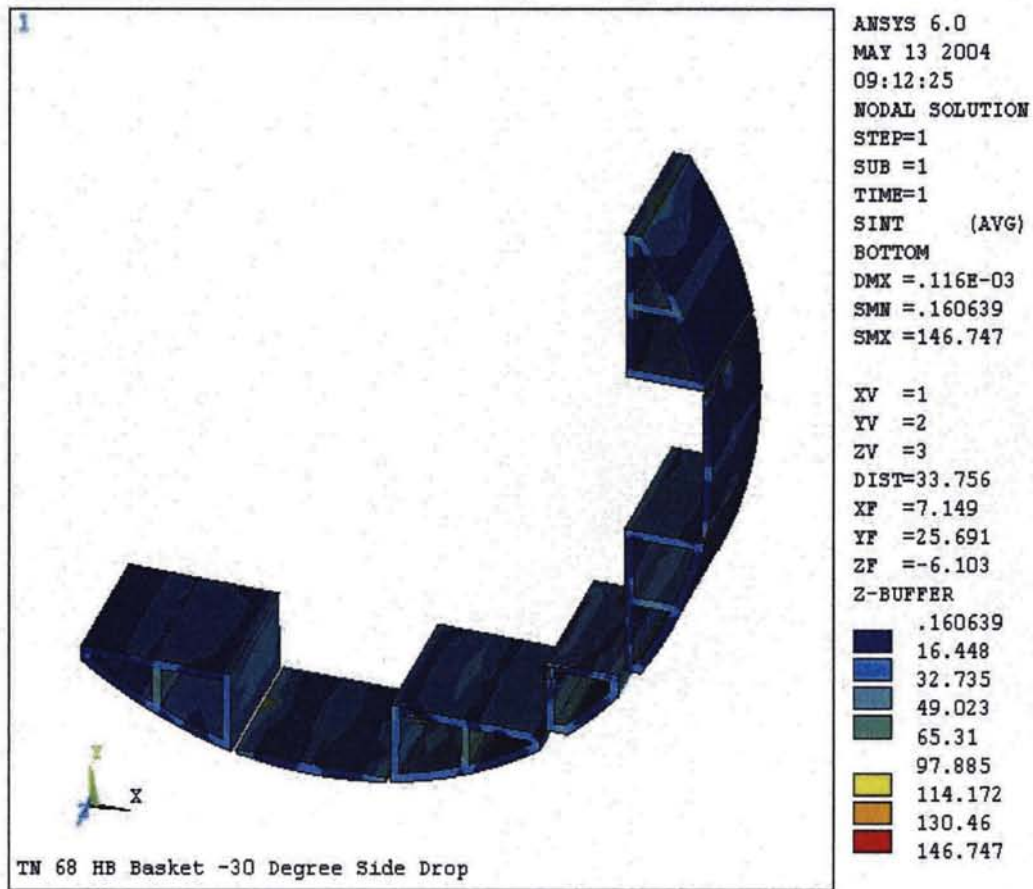


Figure 3B.3-18
Nodal Stress Intensity (Aluminum Rails)-45 Degree Drop

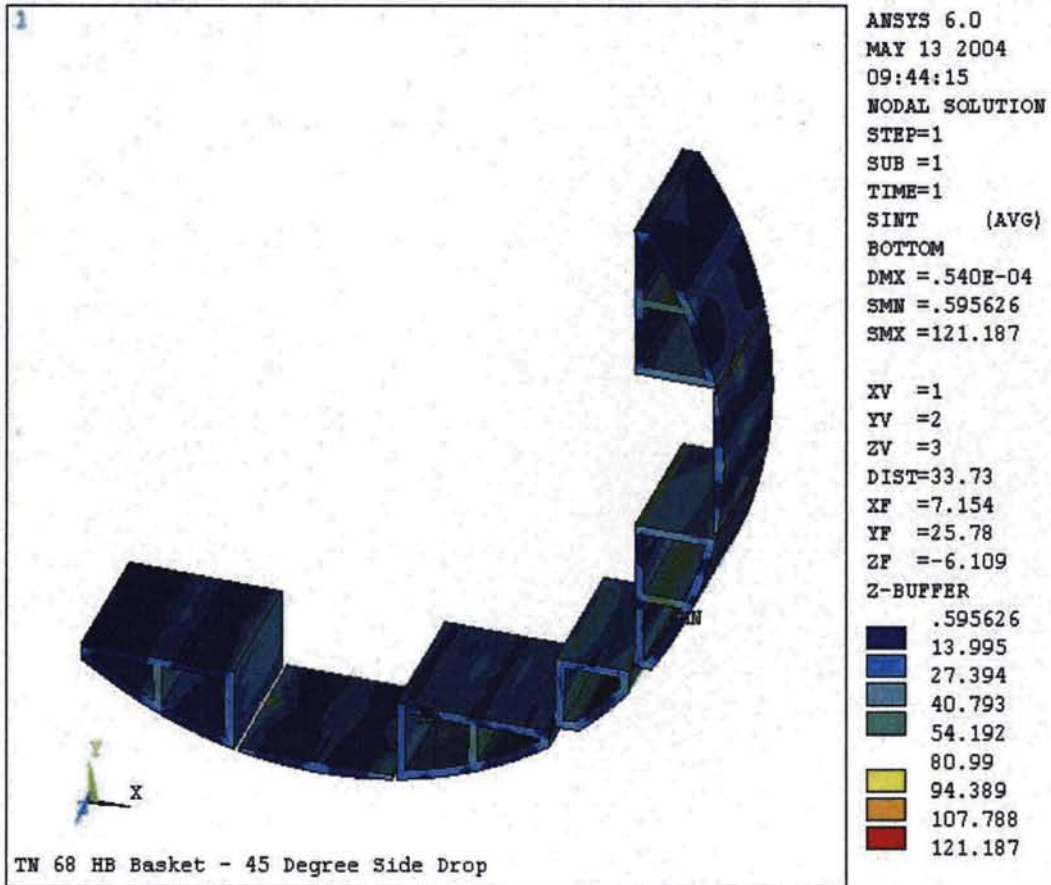
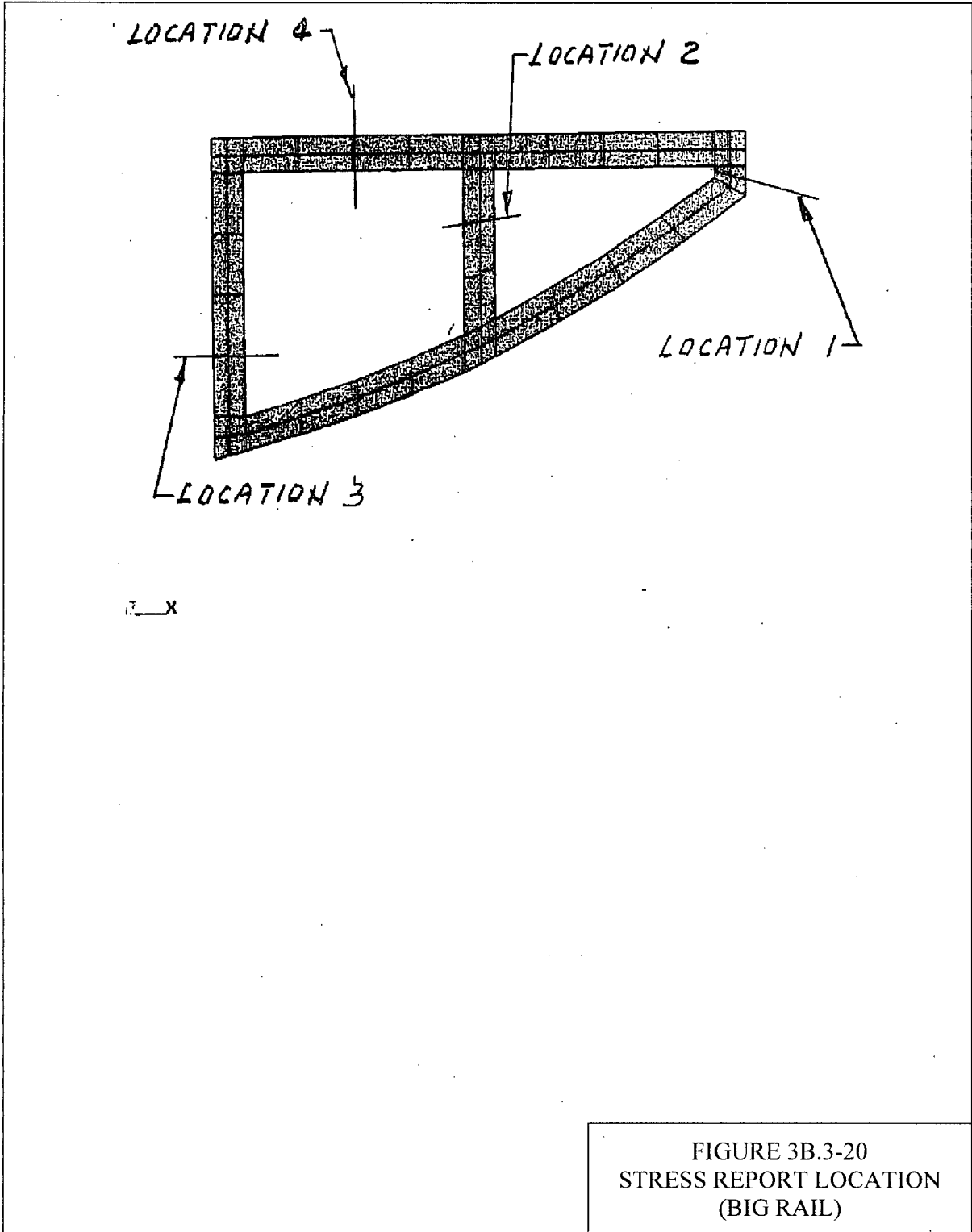


Figure Withheld Under 10 CFR 2.390

FIGURE 3B.3-19
BASKET STRESS DUE TO 3G
VERTICAL END DROP



LOCATION 5

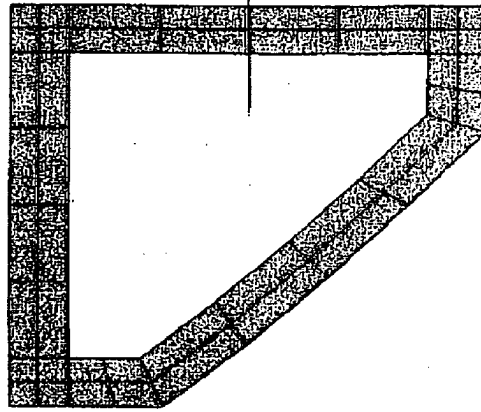
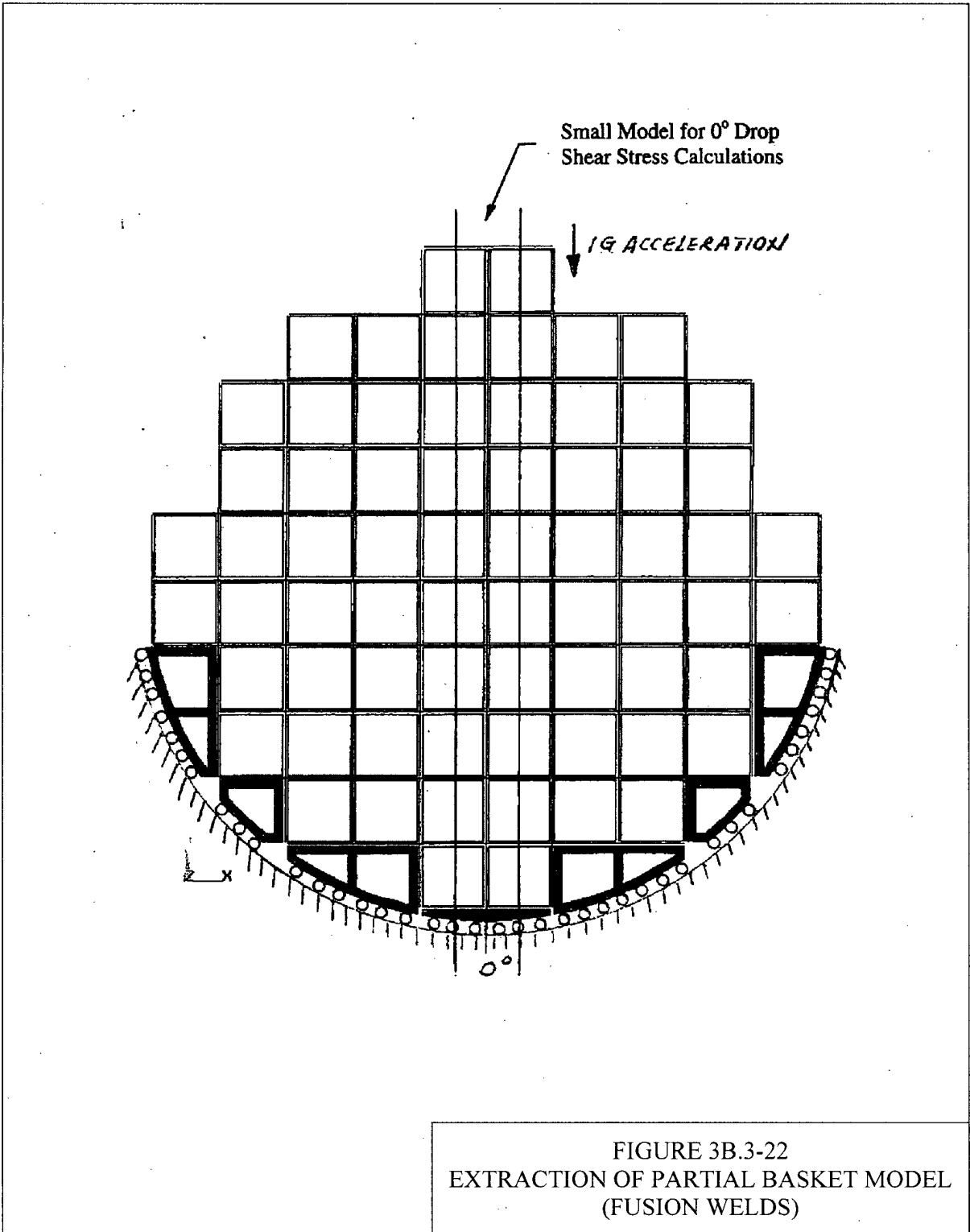
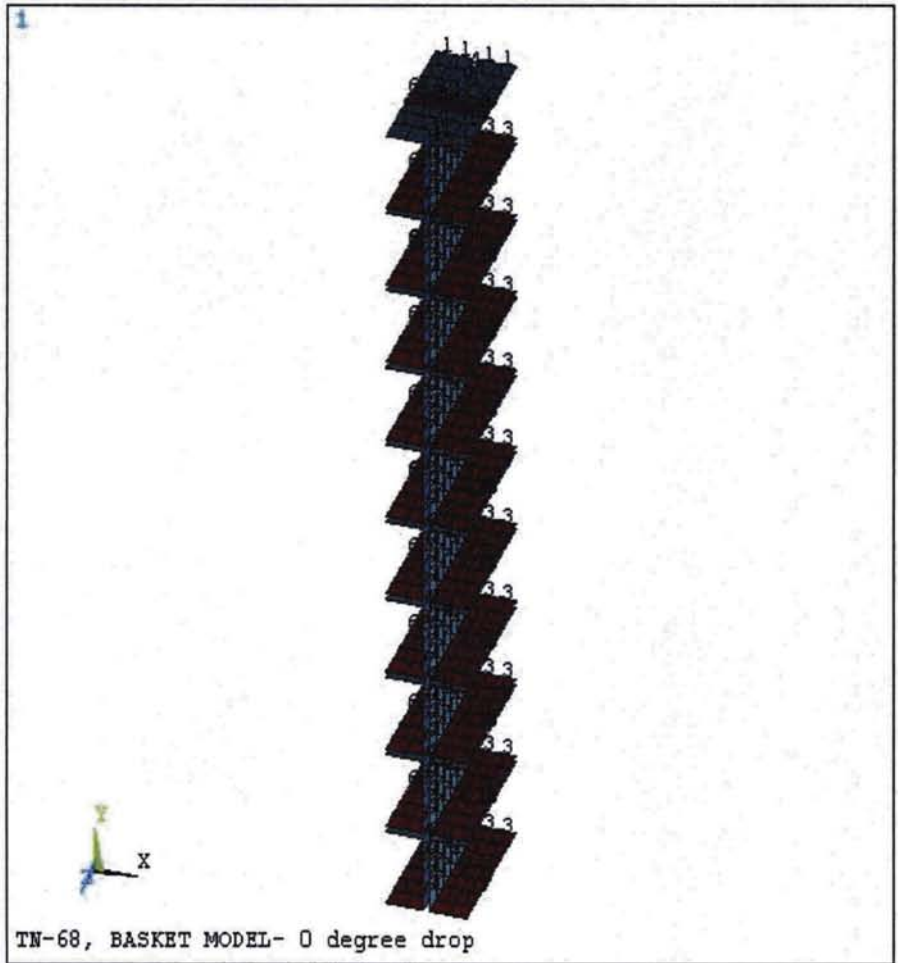


FIGURE 3B.3-21
STRESS REPORT LOCATION
(SMALL RAIL)





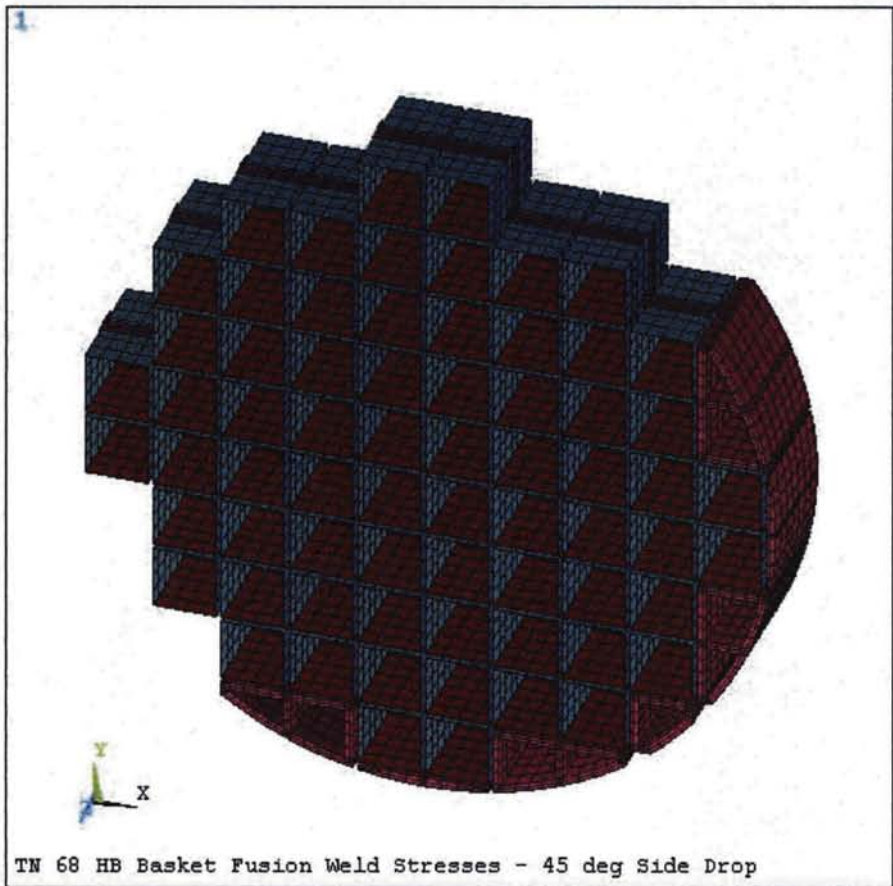
```

ANSYS 6.0
JUL 16 2004
15:08:52
ELEMENTS
PowerGraphics
EFACET=1
MAT NUM

XV =1
YV =2
ZV =3
DIST=35.124
XF =-.25
YF =33.188
ZF =-6.125
Z-BUFFER

```

FIGURE 3B.3-23
BASKET PARTIAL MODEL
(FUSION WELDS)



ANSYS 6.0
JUL 16 2004
15:18:11
ELEMENTS
PowerGraphics
EFACET=1
MAT NUM

XV =1
YV =2
ZV =3
DIST=41.365
XF =.341249
YF =32.596
ZF =-6.1
Z-BUFFER

FIGURE 3B.3-24
BASKET FULL MODEL
(FUSION WELDS)

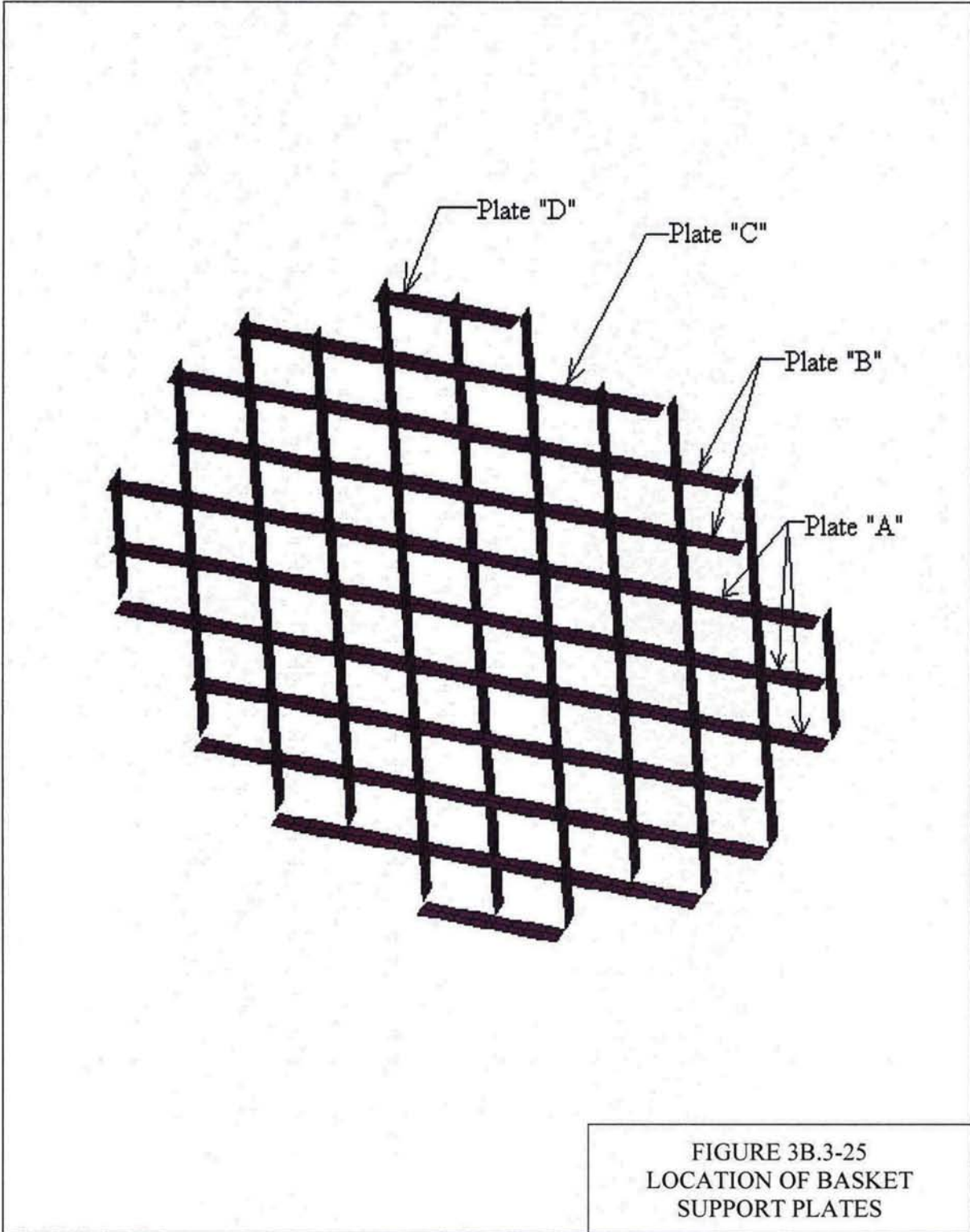


FIGURE 3B.3-25
LOCATION OF BASKET
SUPPORT PLATES

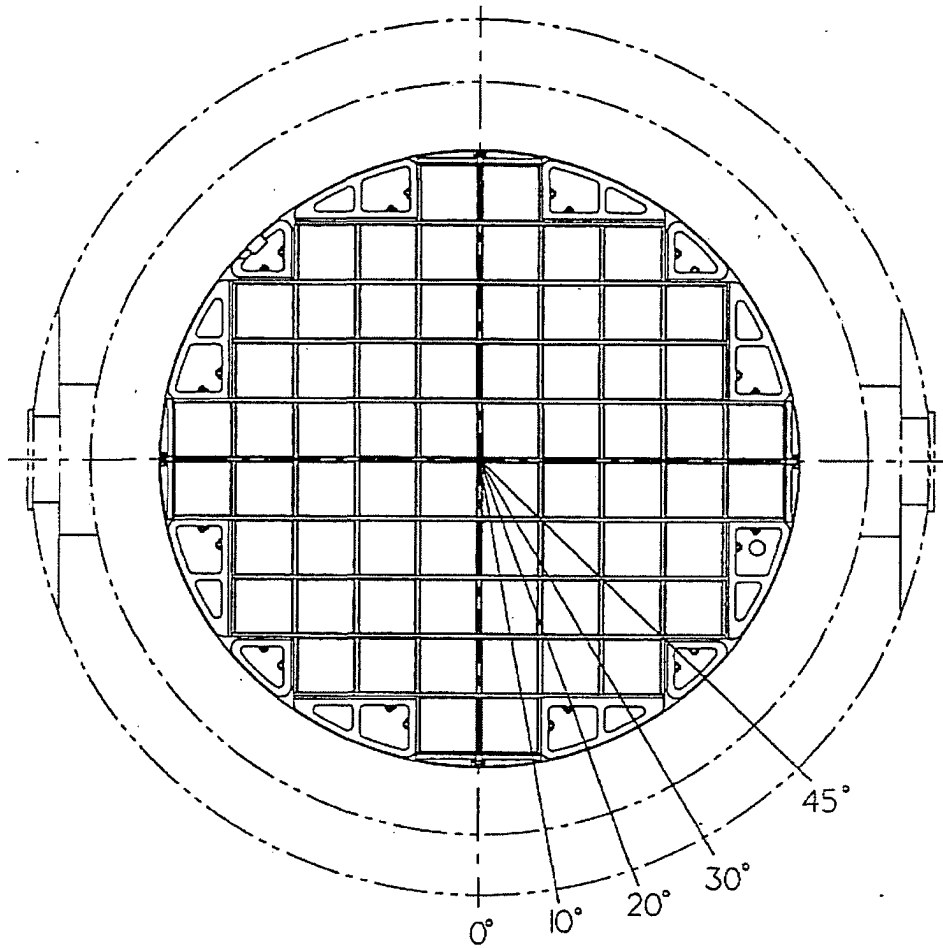


FIGURE 3B.5-1
DROP ORIENTATION

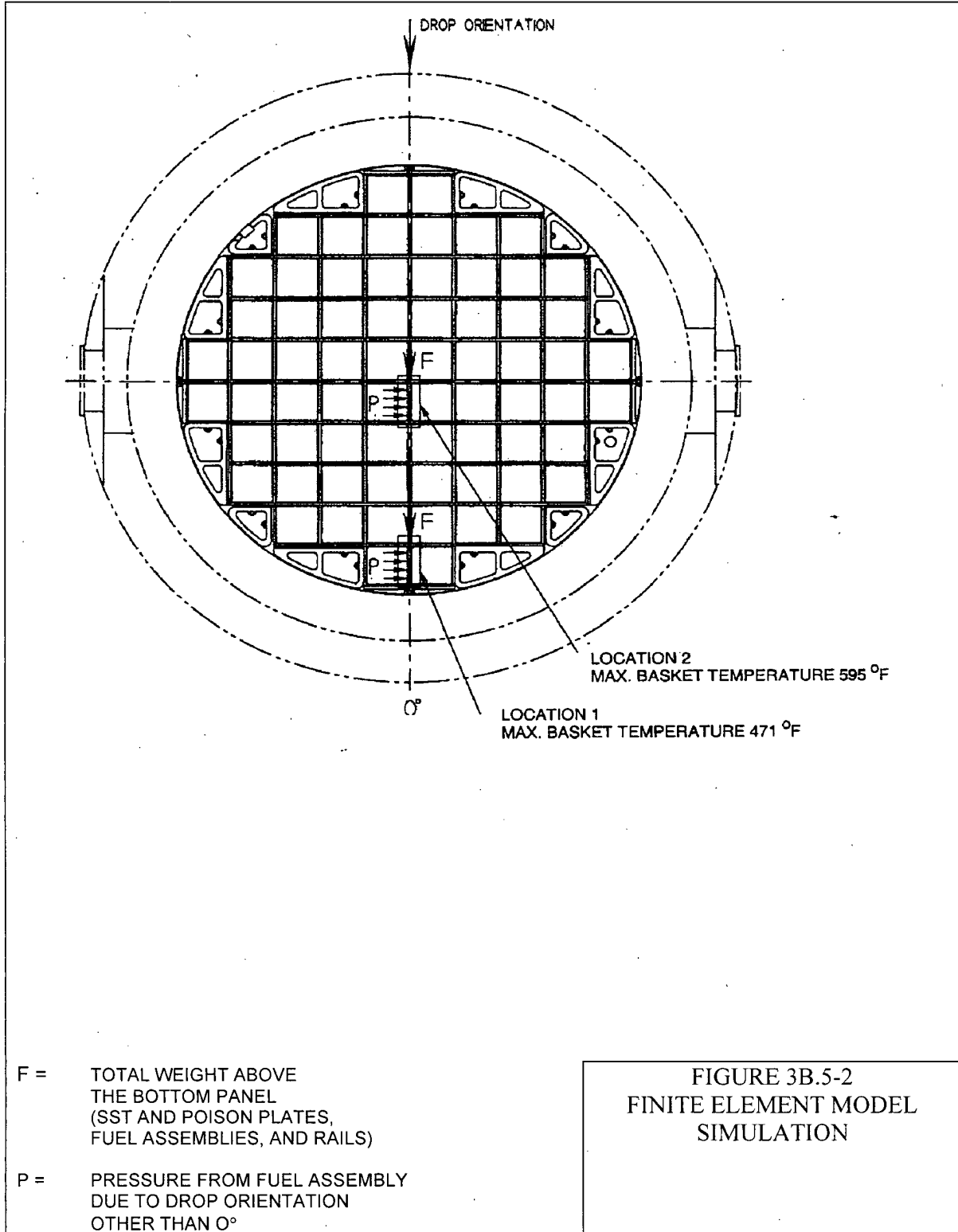
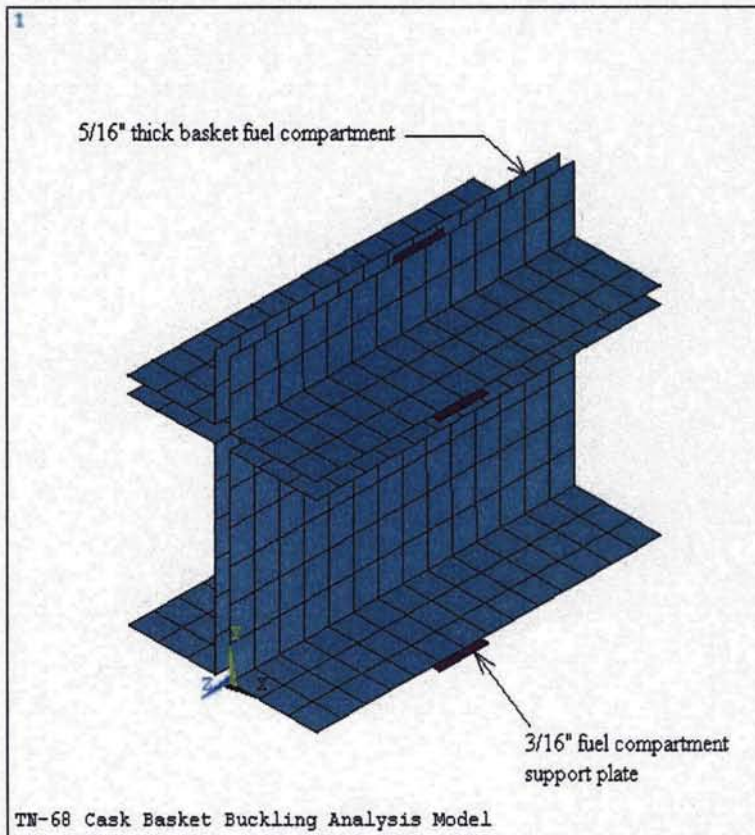


Figure Withheld Under 10 CFR 2.390

**FIGURE 3B.5-3
FINITE ELEMENT MODEL
GEOMETRY**



```

ANSYS 6.0
JUL 6 2004
08:16:06
ELEMENTS
PowerGraphics
EFACET=1
REAL NUM

XV =1.051
YV =.899049
ZV =1.042
*DIST=9.568
*XF =-.25068
*YF =4.307
*ZF =-5.831
A-ZS=.134323
Z-BUFFER

```

FIGURE 3B.5-4
FINITE ELEMENT MODEL
PLOT

F- TOTAL WEIGHT ABOVE
THE BOTTOM PANEL
(SST AND POISON PLATES,
FUEL ASSEMBLIES, AND RAILS)

P- PRESSURE FROM FUEL ASSEMBLY
DUE TO DROP ORIENTATION
OTHER THAN 0°

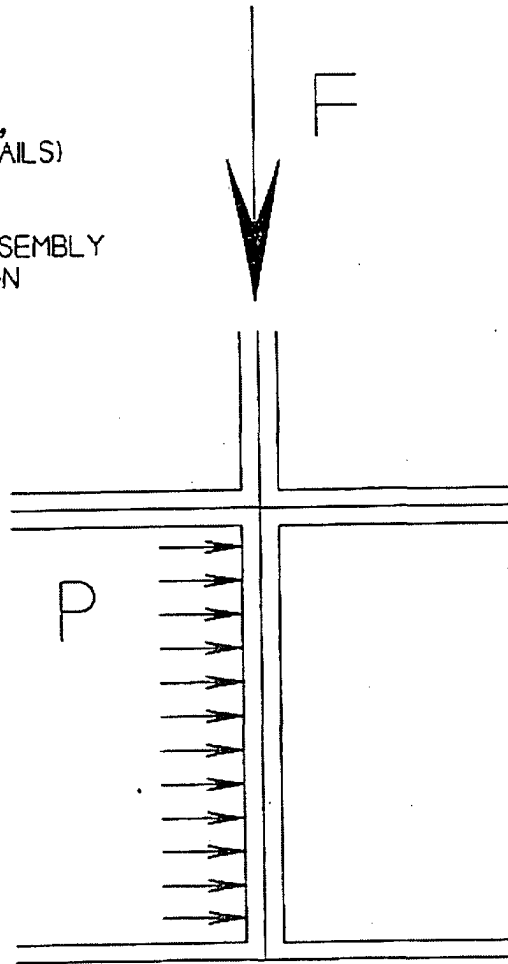


FIGURE 3B.5-5
LOADING CONDITIONS

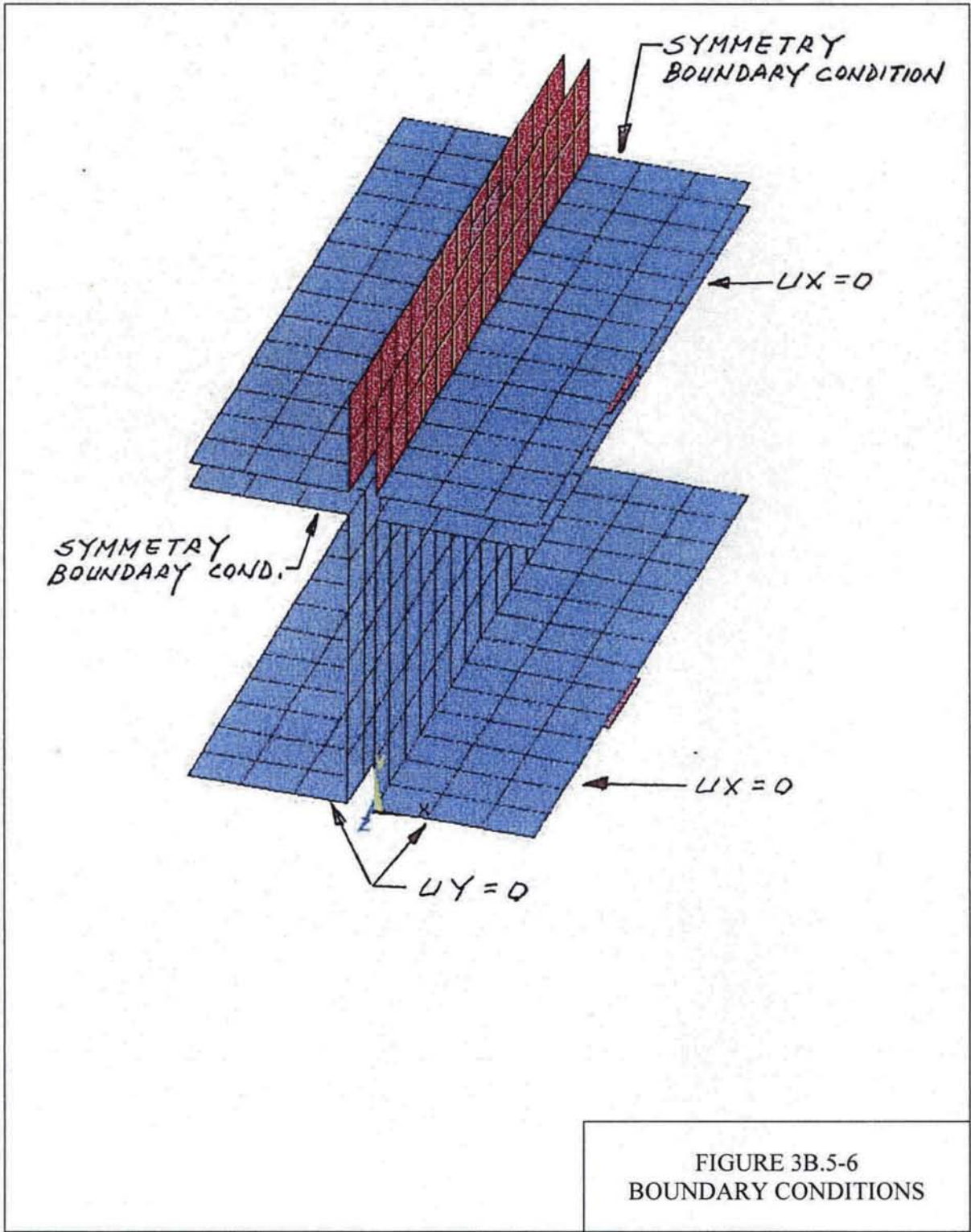


FIGURE 3B.5-6
BOUNDARY CONDITIONS

Figure 3B.5-7
0° Drop Buckling Analysis - ANSYS Computer Plot

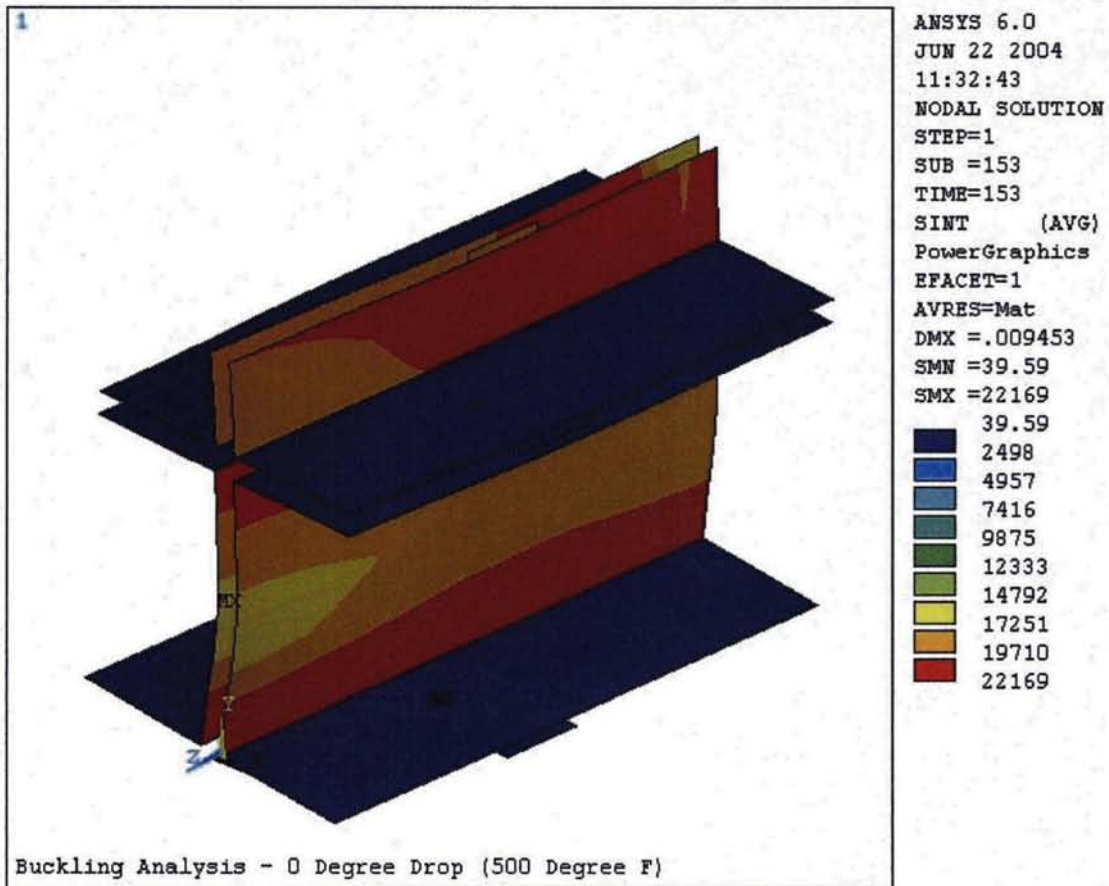


Figure 3B.5-8
10° Drop Buckling Analysis - ANSYS Computer Plot

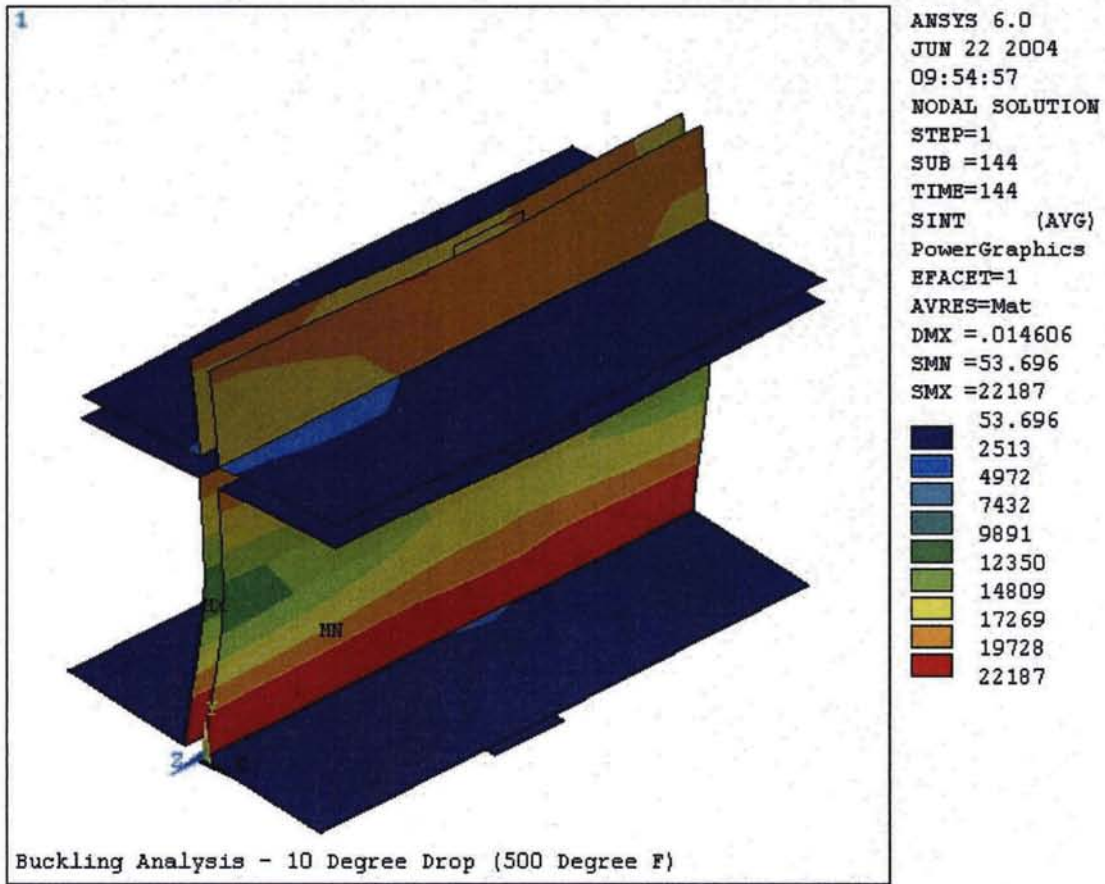


Figure 3B.5-9
20° Drop Buckling Analysis - ANSYS Computer Plot

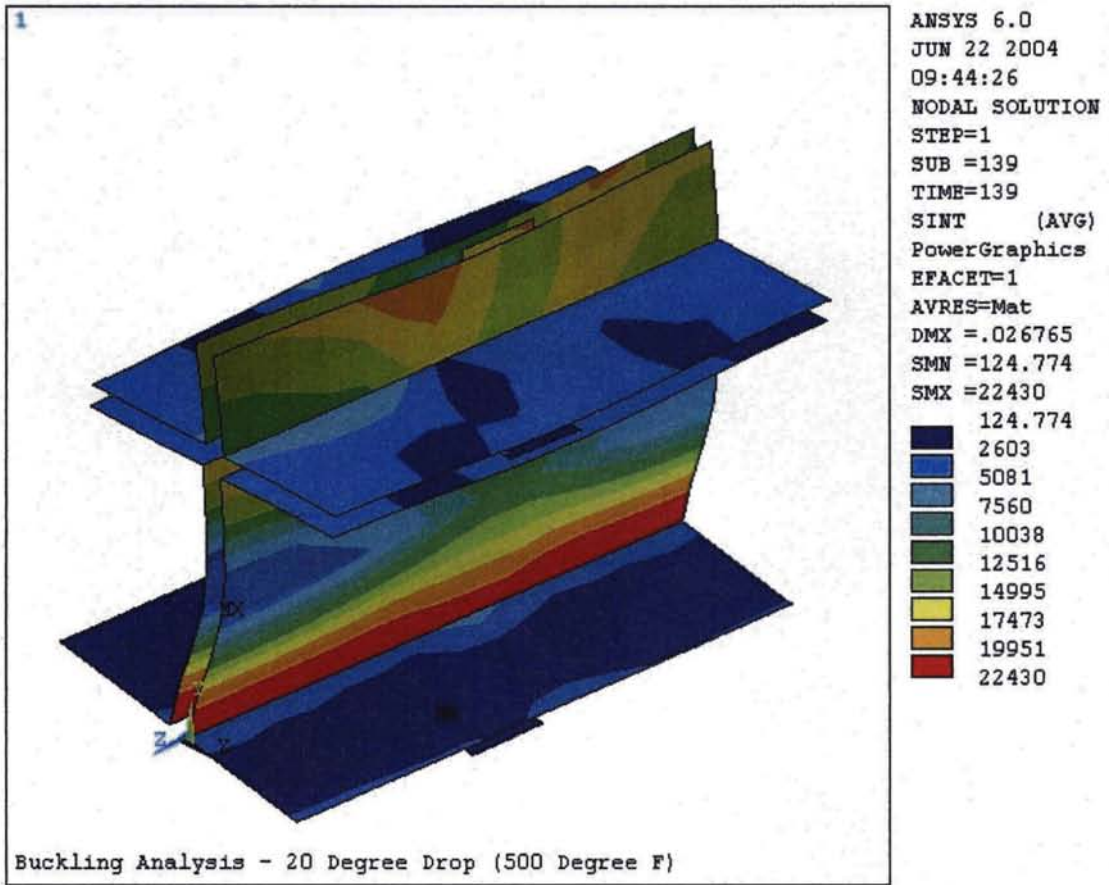


Figure 3B.5-10
30° Drop Buckling Analysis - ANSYS Computer Plot

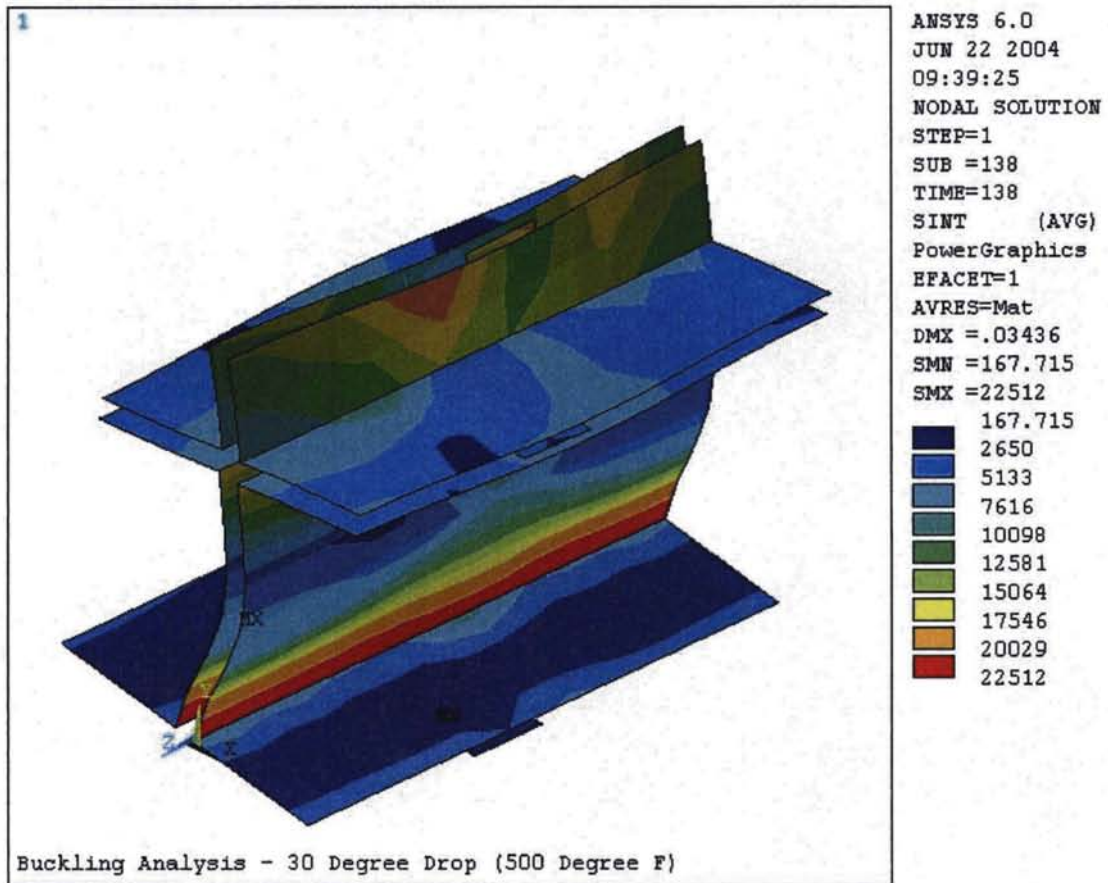
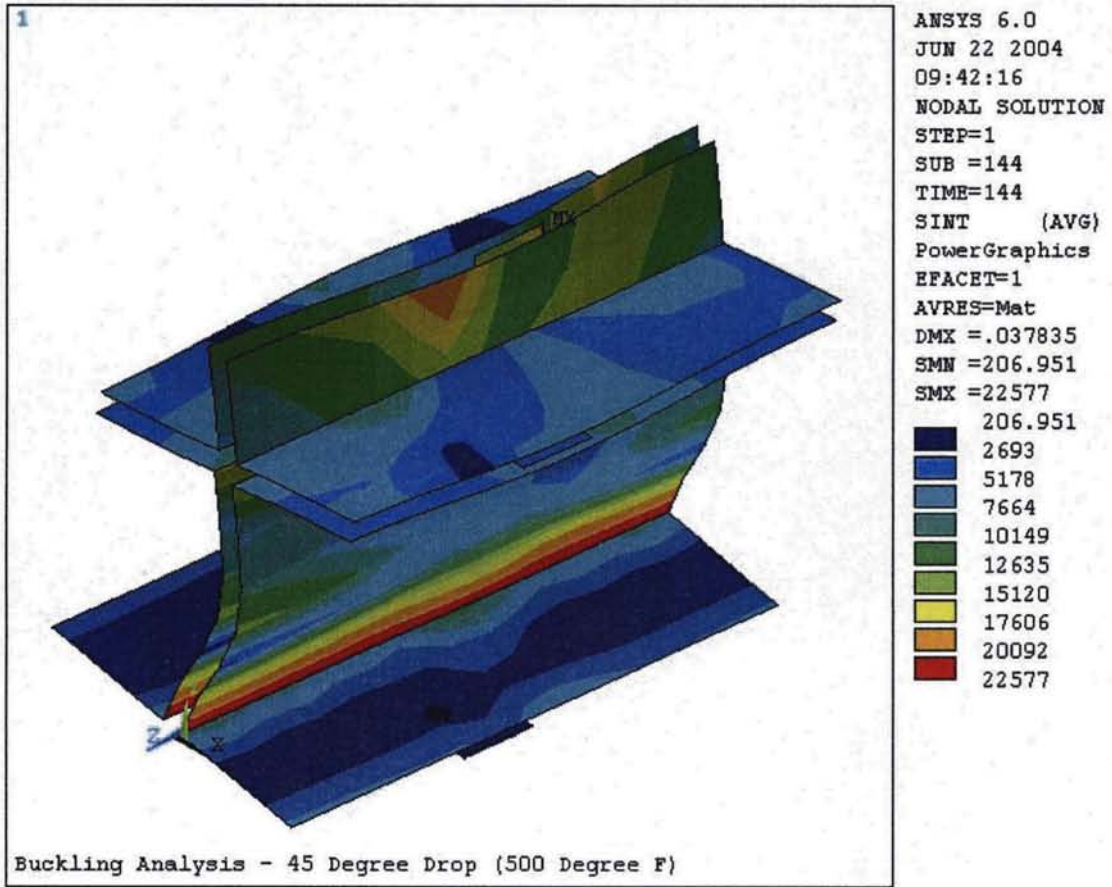


Figure 3B.5-11
45° Drop Buckling Analysis - ANSYS Computer Plot



**TN-68 SAFETY ANALYSIS REPORT
TABLE OF CONTENTS**

SECTION	PAGE
Appendix 3C	MODAL ANALYSIS OF THE TN-68 BASKET
3C.1	Introduction.....3C.1-1
3C.1.1	Modal Analysis.....3C.1-1
3C.1.2	Results.....3C.1-2
3C.1.3	Conclusion.....3C.1-4
3C.2	References.....3C.2-1

**TN-68 SAFETY ANALYSIS REPORT
TABLE OF CONTENTS**

List of Figures

3C.1-1	Basket Finite Element Model for Modal Analysis
3C.1-2	Boundary Condition - 0° Modal Analysis
3C.1-3	0° Modal Analysis - First Mode (204 Hz)
3C.1-4	0° Modal Analysis - Second Mode (225 Hz)
3C.1-5	0° Modal Analysis - Third Mode (237 Hz)
3C.1-6	0° Modal Analysis - Fourth Mode (242 Hz)
3C.1-7	30° Modal Analysis - First Mode (195 Hz)
3C.1-8	30° Modal Analysis - Second Mode (253 Hz)
3C.1-9	30° Modal Analysis - Third Mode (258 Hz)
3C.1-10	30° Modal Analysis - Fourth Mode (264 Hz)
3C.1-11	45° Modal Analysis - First Mode (181 Hz)
3C.1-12	45° Modal Analysis - Second Mode (232 Hz)
3C.1-13	45° Modal Analysis - Third Mode (272 Hz)
3C.1-14	45° Modal Analysis - Fourth Mode (281 Hz)
3C.1-15	Maximum Dynamic Amplification Factor for a Triangular Load

APPENDIX 3C

MODAL ANALYSIS OF TN-68 BASKET

3C.1 Introduction

This appendix presents the modal analysis of the TN-68 fuel support basket. The TN-68 basket is analyzed for an 18 in. end drop and tipover accident in Appendix 3B using equivalent static methods. The equivalent static loads for the drop evaluations of the TN-68 basket are determined by multiplying the peak rigid body accelerations (analyzed in Appendix D) by the corresponding dynamic load factor (DLF). The purpose of this analysis is to determine the fundamental frequencies of the basket which have the most significant effect on the response of the basket tipover side impact. Based on the fundamental frequencies of the basket structure at temperatures calculated for a 21.2 kW load, the dynamic amplification factor is determined from the spring mass model described in Appendix D. For the basket at temperatures associated with a 30 kW thermal load, the dynamic amplification factor is determined from Figure 3C.1-15 which is taken from NUREG/CR-3966⁽³⁾.

3C.1.1 Modal Analysis

Finite Element Model

The ANSYS⁽¹⁾ finite element model described in Appendix 3B is used to perform the modal analysis. The supporting rails are removed from the finite element model and boundary conditions are directly applied to the panels. It is reasonable to remove the supporting rails because the coupling of rail nodes to the panel nodes would have resulted in stiffer panels and higher frequency modes. The basket finite element model is shown on Figure 3C.1-1.

Material Properties

Material properties based on a basket temperature of 500°F for 21.2 kW and 600 °F for 30 kW are input as described in Appendix 3B. Weight densities are changed to mass densities ($\rho_m = \rho_w / 386.4$).

Boundary Conditions

Boundary conditions applied to the model are as follows: restraint of the bottom half of the perimeter in the direction parallel to the drop angle vector, and restraint the direction perpendicular to the drop angle vector on the remainder of the perimeter. These boundary conditions are chosen to eliminate modes of vibration that are incompatible with the orientation of the drop. For instance, side to side modes are not important for the 0° drop, because they are restrained by the rails and cask wall and, more importantly, because they have no modal weight in the drop direction, and therefore are not activated by the drop. For 30 and 45 degree drops, boundary conditions are modified by rotating the perimeter support nodes for the drop angle and then applying the appropriate displacement boundary conditions in the rotated coordinate system.

Also for 30 and 45 degree drops, the modal weight is associated with both horizontal and vertical panels of the basket. Typical boundary conditions for the 0° modal analysis are shown on Figure 3C.1-2.

3C.1.2 Results

Modes and Frequencies From ANSYS Analysis

The first six mode frequencies resulting from the different drop orientation ANSYS modal analyses are tabulated below:

ANSYS Modal Analysis Results

Mode	Frequency		
	0°	30°	45°
1	204	195	181
2	225	253	232
3	237	258	272
4	242	264	281
5	246	266	282
6	247	268	292

Results From Hand Calculations

For the first mode shape of each drop, the deformed shape of the central basket panels resemble s a simple-simple supported beam.

As an order of magnitude check, the frequency of the fundamental mode of vibration for the simple-simple supported beam is calculated below and compared to the frequency of the first mode of 0° ANSYS modal analysis result. Reference 2, page 369, case 6, "Single span, end supported, uniform load W", lists the following equation for the fundamental frequency:

$$f = 3.55 / (5WL^3/384EI)^{1/2}$$

Where:

$$\begin{aligned} W &= 5.1577 \text{ lbs.} \\ L &= 6.1875 \text{ in.} \\ E &= 25.8 \times 10^6 \text{ psi} \\ I &= 0.001462 \text{ in.}^4 \end{aligned}$$

Substituting the values given above,

$$F = 173 \text{ Hz}$$

This value is reasonably close to the solution given by ANSYS for the basket. The actual support conditions for the basket are somewhere in between simple-simple and fixed-fixed supports. A fixed-fixed beam's fundamental frequency is approximately double that of a simple-simple supported beam. Therefore, we should expect the ANSYS solution to be somewhere between these values.

Basket with 30 kW Thermal Load

The above fundamental frequency equation is used to ratio basket frequency between the frequency calculated from ANSYS (basket with fuel up to 21.2 kW) and basket with high burn up fuel.

$$f = 3.55 / (5WL^3/384EI)^{1/2}$$

f_1 = Fundamental frequency of basket (w/fuel up to 21.2 kW) calculated from ANSYS

f_2 = Fundamental frequency of basket (w/high burn up fuel)

E_1 = Modulus of elasticity of basket Plate at 500°F = 25.8x10⁶ psi (w/fuel up to 21.2 kW)

E_2 = Modulus of elasticity of basket Plate at 600°F = 25.3x10⁶ psi (w/fuel up to 30 kW)

W_1 = Uniform load on basket plate. This is proportional to basket plate equivalent densities calculated based on total fuel assembly weight distributed on 164 inch basket length

W_2 = Uniform load on basket plate. This is proportional to basket plate equivalent densities calculated based on total fuel assembly weight distributed on 144 inch basket length (active fuel length)

Using the above frequency equation and simplifying,

$$f_1^2 / f_2^2 = (E_1 / E_2) (W_2 / W_1)$$

$$f_2 = f_1 [(E_2/E_1) (W_1/W_2)]^{1/2}$$

The fundamental frequencies for the 30 kW load are calculated using the above relationship:

	0-degree Drop Orientation	30-degree Drop Orientation	45-degree Drop Orientation
f_1 from Section 3C.1.2	204 Hz	195 Hz	181 Hz
E_1 at 500°F	25.8 x 10 ⁶ psi	25.8 x 10 ⁶ psi	25.8 x 10 ⁶ psi
E_2 at 600°F	25.3 x 10 ⁶ psi	25.3 x 10 ⁶ psi	25.3 x 10 ⁶ psi
D_1	4.006 lb/in ³	3.1125 lb/in ³	2.219 lb/in ³
D_2	4.634 lb/in ³	3.579 lb/in ³	2.524 lb/in ³
Factor [(E_2/E_1) (D_1/D_2)] ^{1/2}	0.9207	0.9235	0.9285
$f_2 = \text{Factor} * f_1$	187	180	168

The dynamic load factor is a function of the rise time of the applied load, the duration of the load, the shape of the load, and the natural period of the structure. DYNA computer program as

described in Appendix 3D is used to predict the impact duration during the tipover analysis. Based on the results in the Appendix 3D, the impact duration is 0.003 sec and the pulse shape is triangle.

From Figure 3C.1-15 (from reference 3), the dynamic load factor is calculated as follows:

$$\begin{aligned}t &= \text{impact duration} = 0.003 \\T &= 1/f = 1/187 = 0.005348 \\t/T &= 0.003/0.005348 = 0.56\end{aligned}$$

Therefore, the dynamic load factor is approximately 1.32. This dynamic load factor is similar to the dynamic load factor calculated from the LS-DYNA dynamic analysis described in Appendix 3D.5.2.

3C.1-3 Conclusion

The first four (4) mode shapes of the 0, 30, and 45 degree modal analyses (basket with fuel assembly up to 21.2 kW) are plotted on Figures 3C.1-3 through 3C.1-14. Except for the first mode shapes of each drop orientation, the mode shapes are neither symmetric nor have significant modal deflection in the direction of the drop angle. Therefore, the frequencies of these modes with substantial modal weight in the direction of the drop - for angles 0°, 30°, and 45° are 204 Hz, 195 Hz, and 181 Hz, respectively.

3C.2 References

1. ANSYS Engineering Analysis System User's Manual, Rev. 5.2, Vol. 1 to 4, 1995.
2. Roark, R. "Formulas for Stress and Strain" Fourth Edition.
3. NUREG/CR-3966 "Methods for Impact Analysis of Shipping Containers" by T.A. Nelson and R.C. Chun.

Figure 3C.1-1
Basket Finite Element Model for Modal Analysis

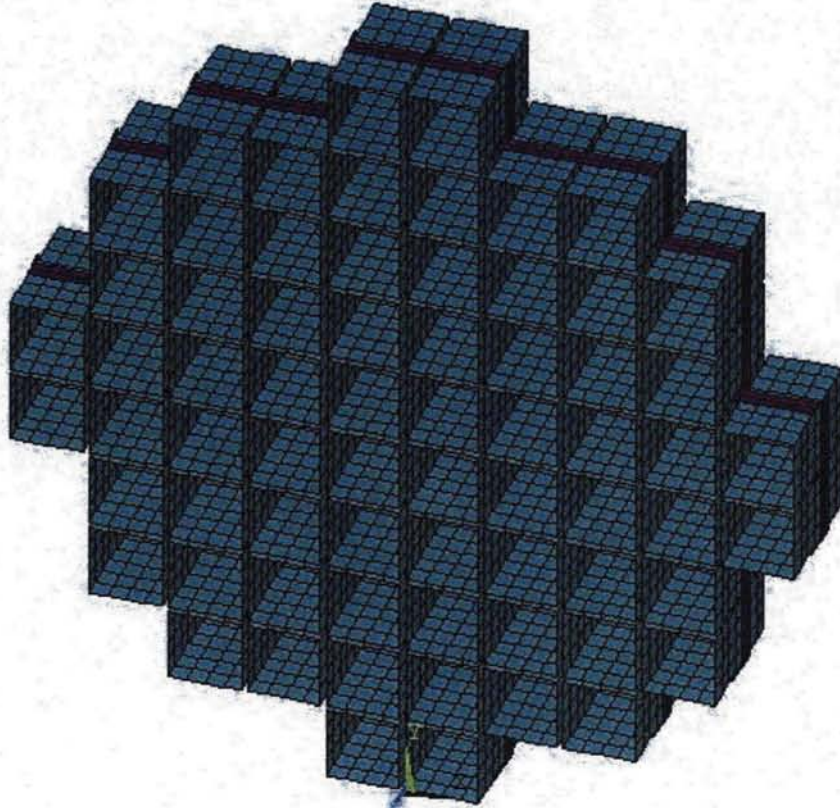


Figure 3C.1-2
Boundary Condition – 0° Modal Analysis

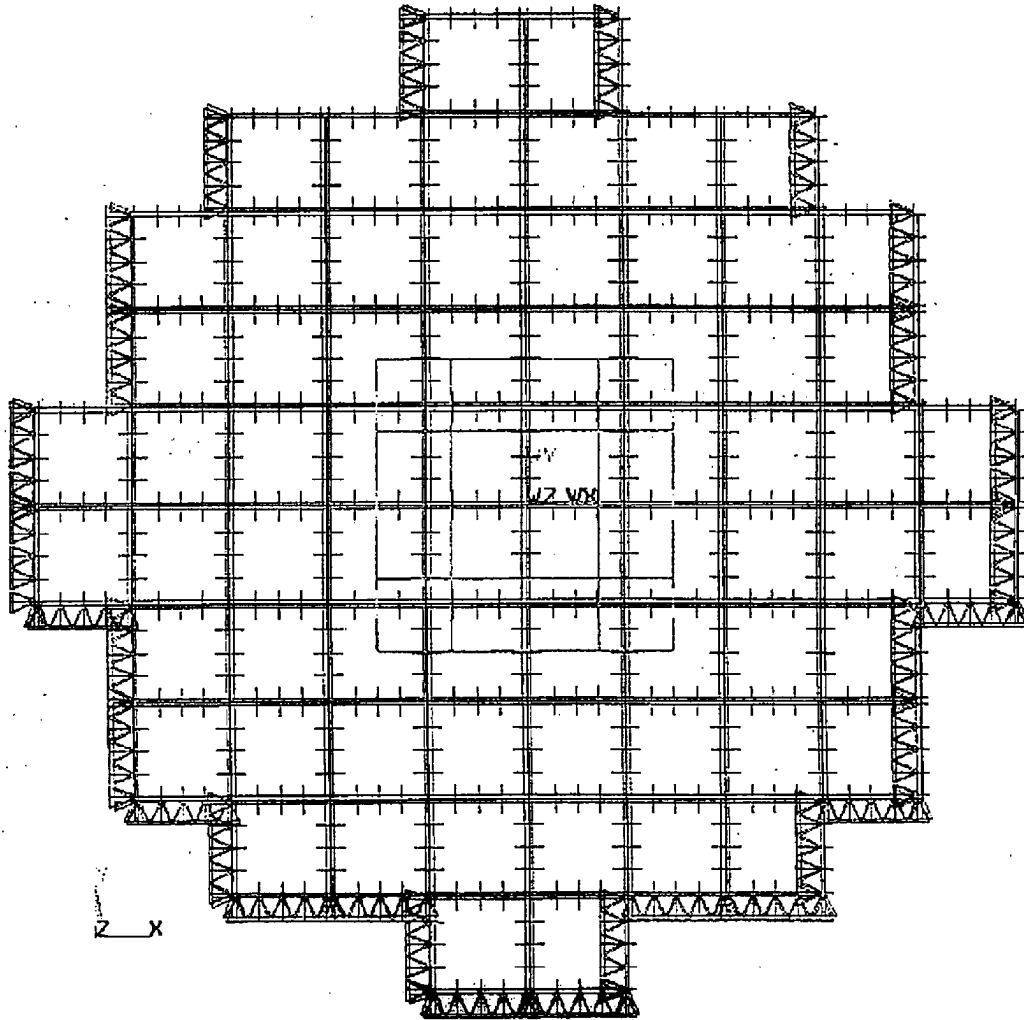


Figure 3C.1-3
0⁰ Modal Analysis -First Mode (204 HZ)

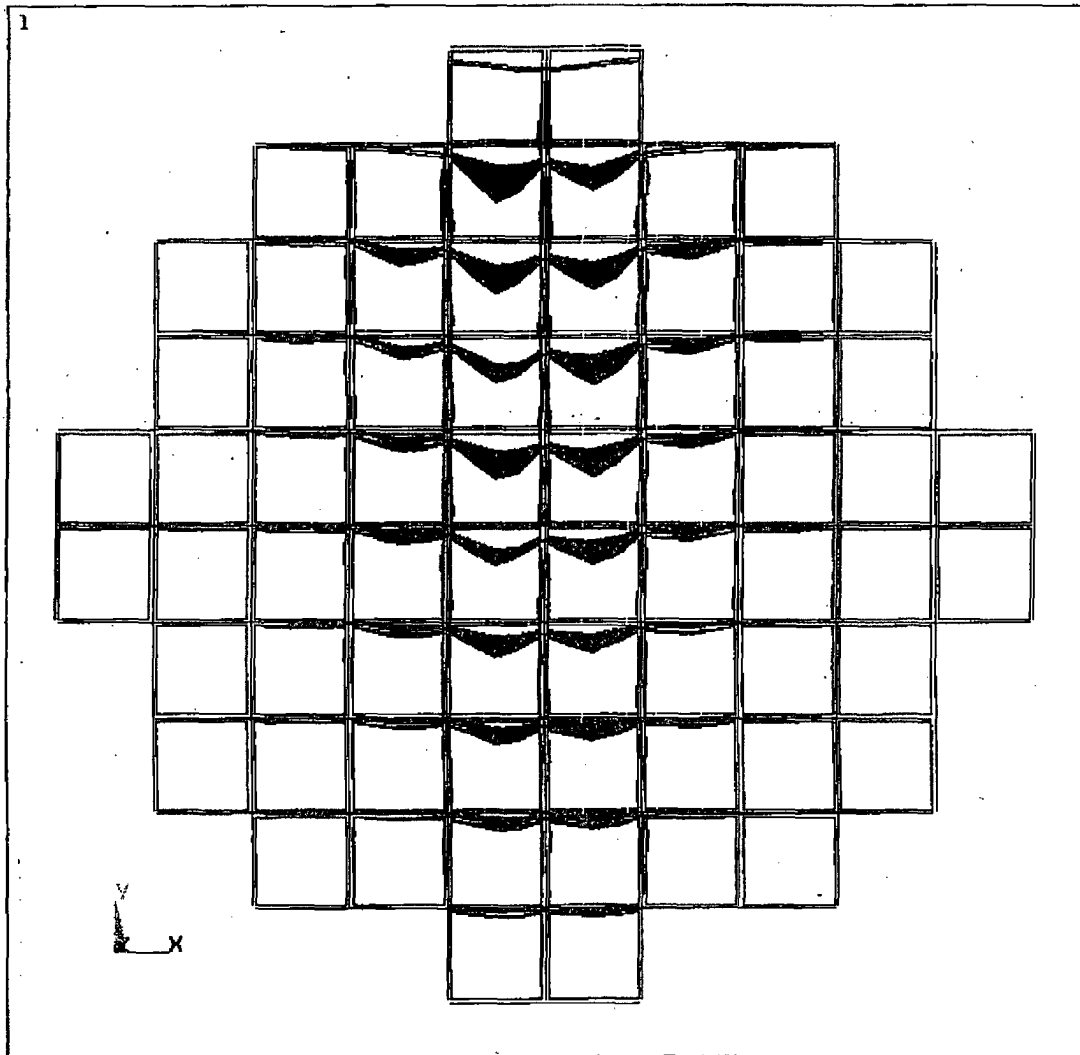


Figure 3C.1-4
0° Modal Analysis – Second Mode (225 HZ)

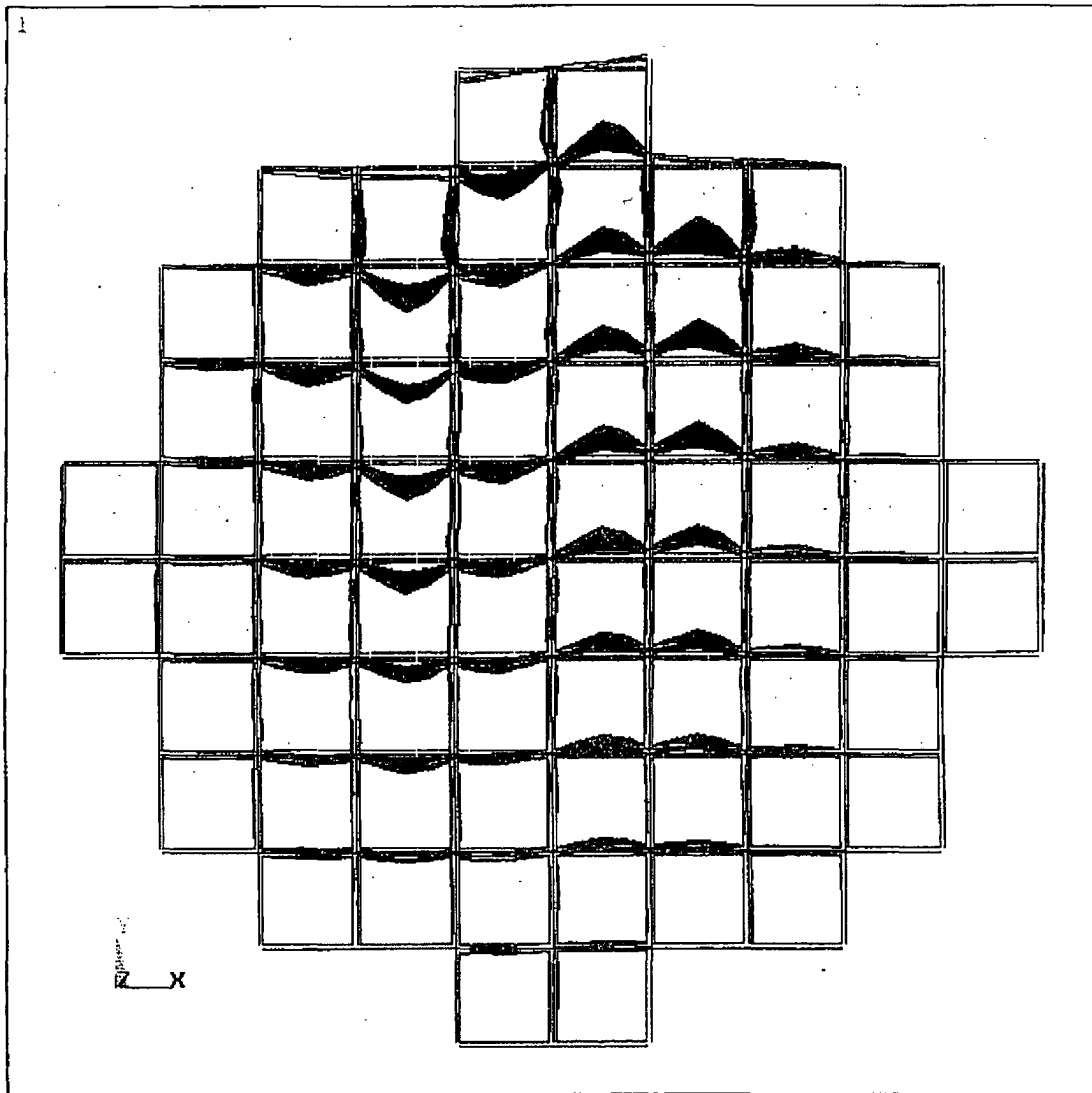


Figure 3C.1-5
0° Modal Analysis - Third Mode (237 HZ)

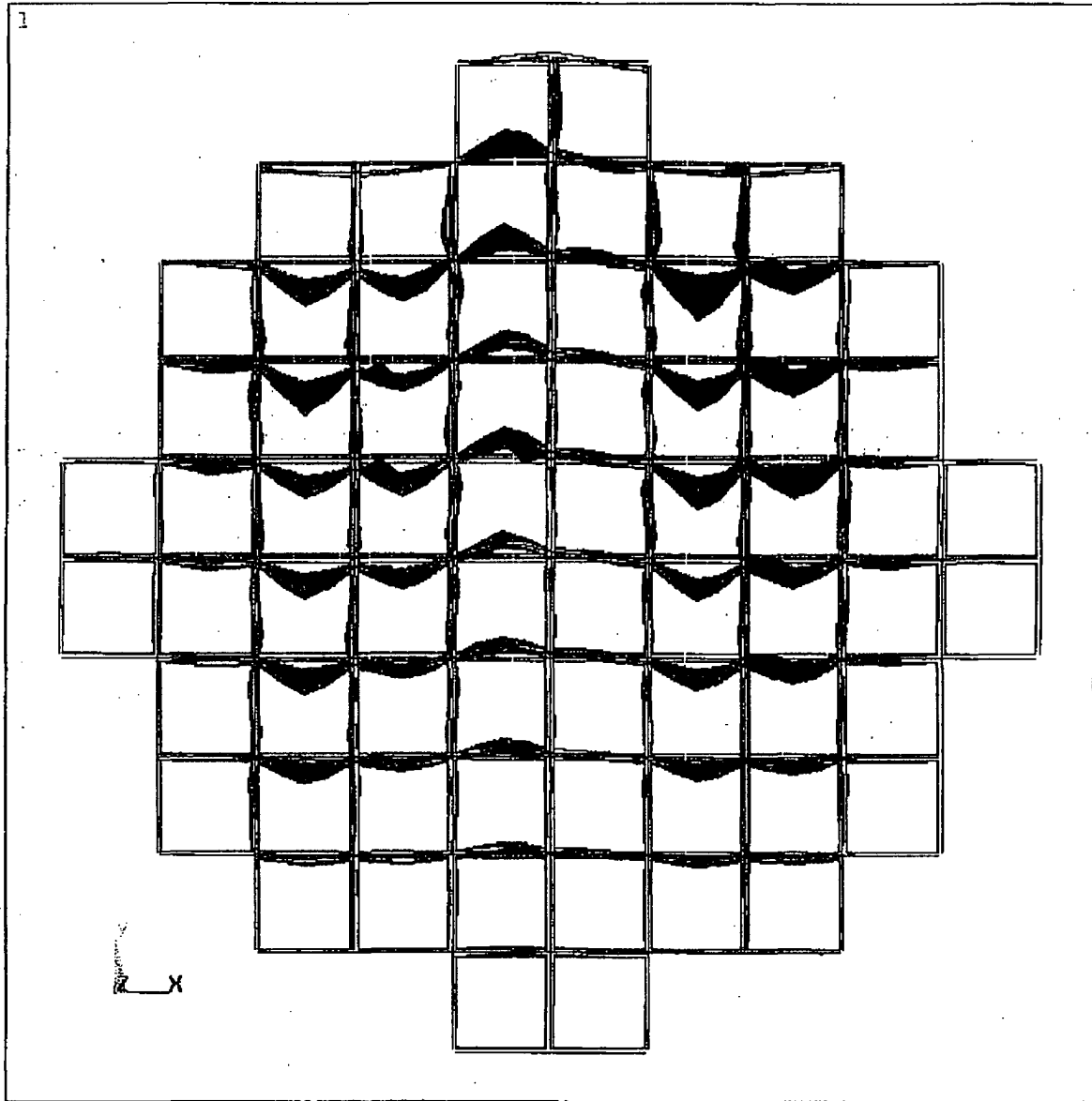


Figure 3C.1-6
0° Modal Analysis – Fourth Mode (242 HZ)

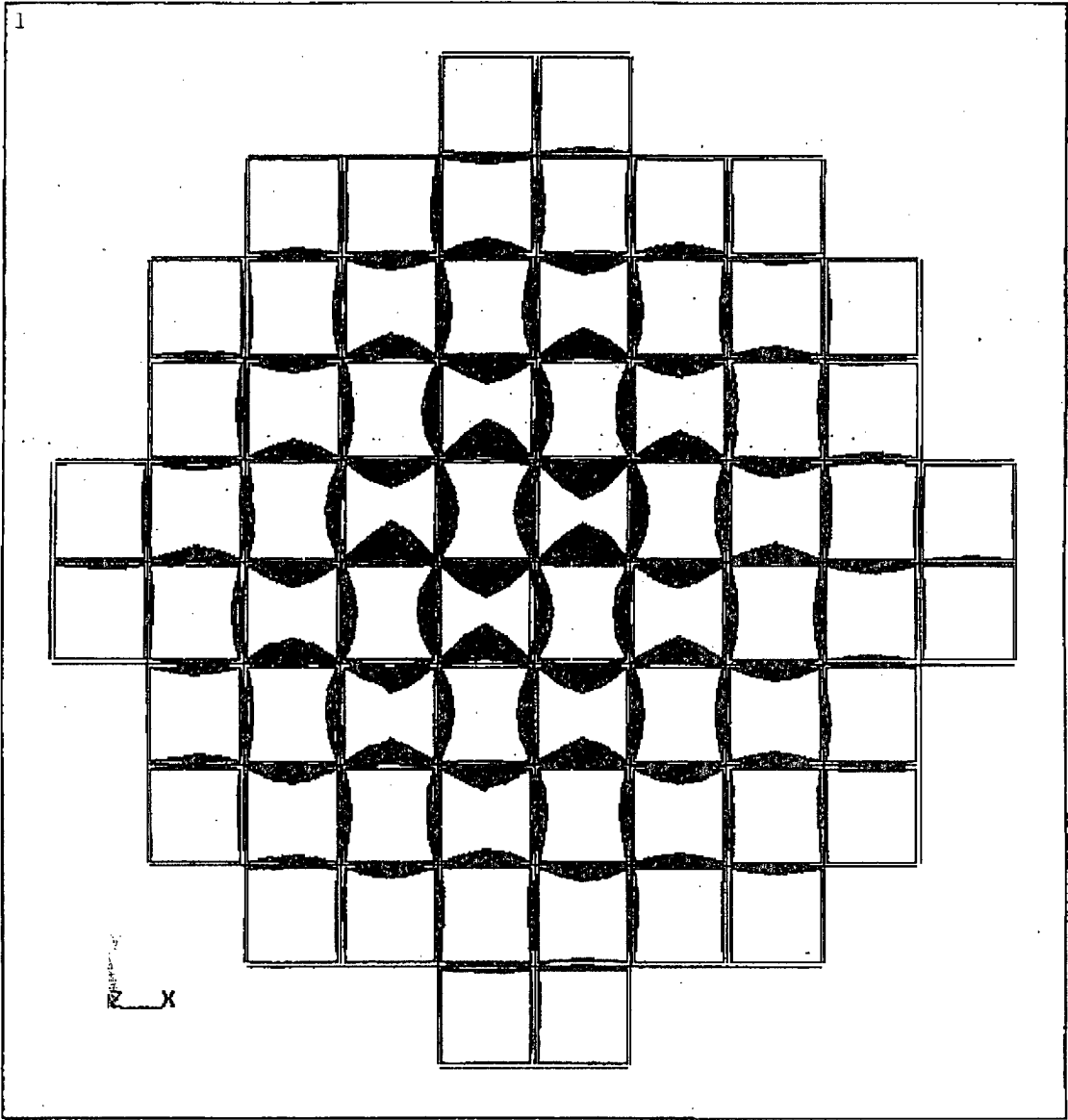


Figure 3C.1-7
30° Modal Analysis – First Mode (195 HZ)

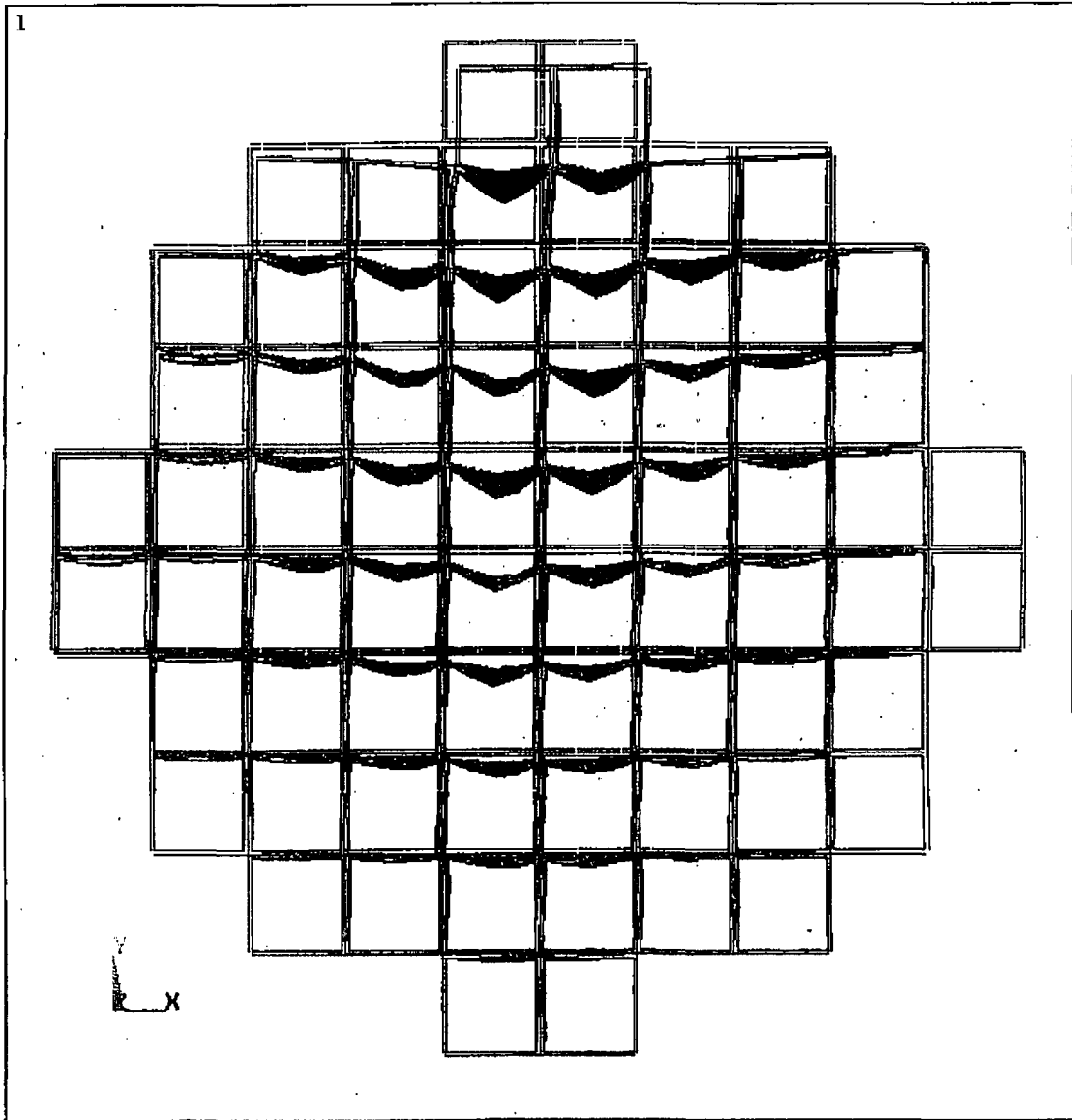


Figure 3C.1-8
30° Modal Analysis – Second Mode (253 HZ)

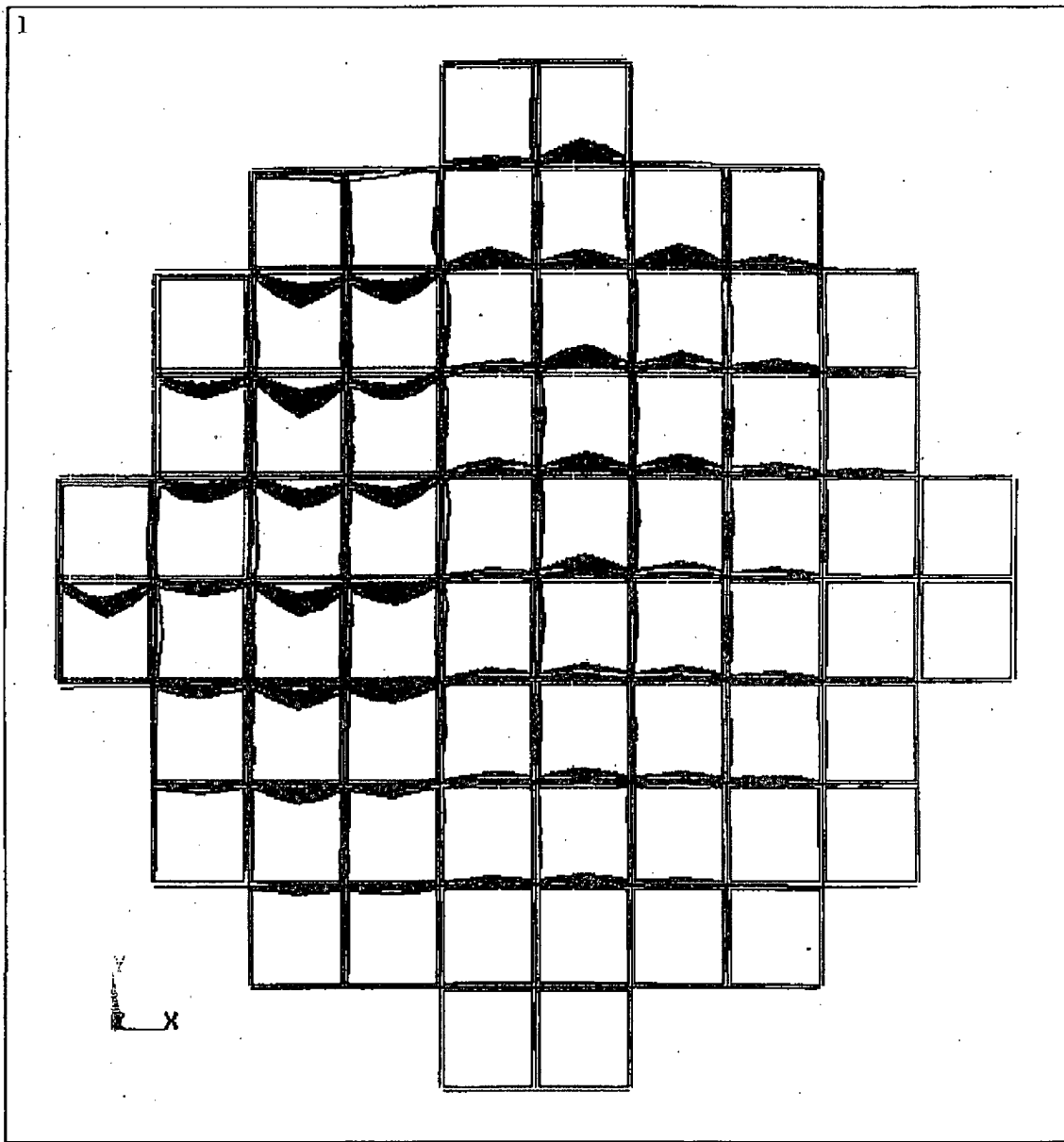


Figure 3C.1-9
30° Modal Analysis – Third Mode (258 HZ)

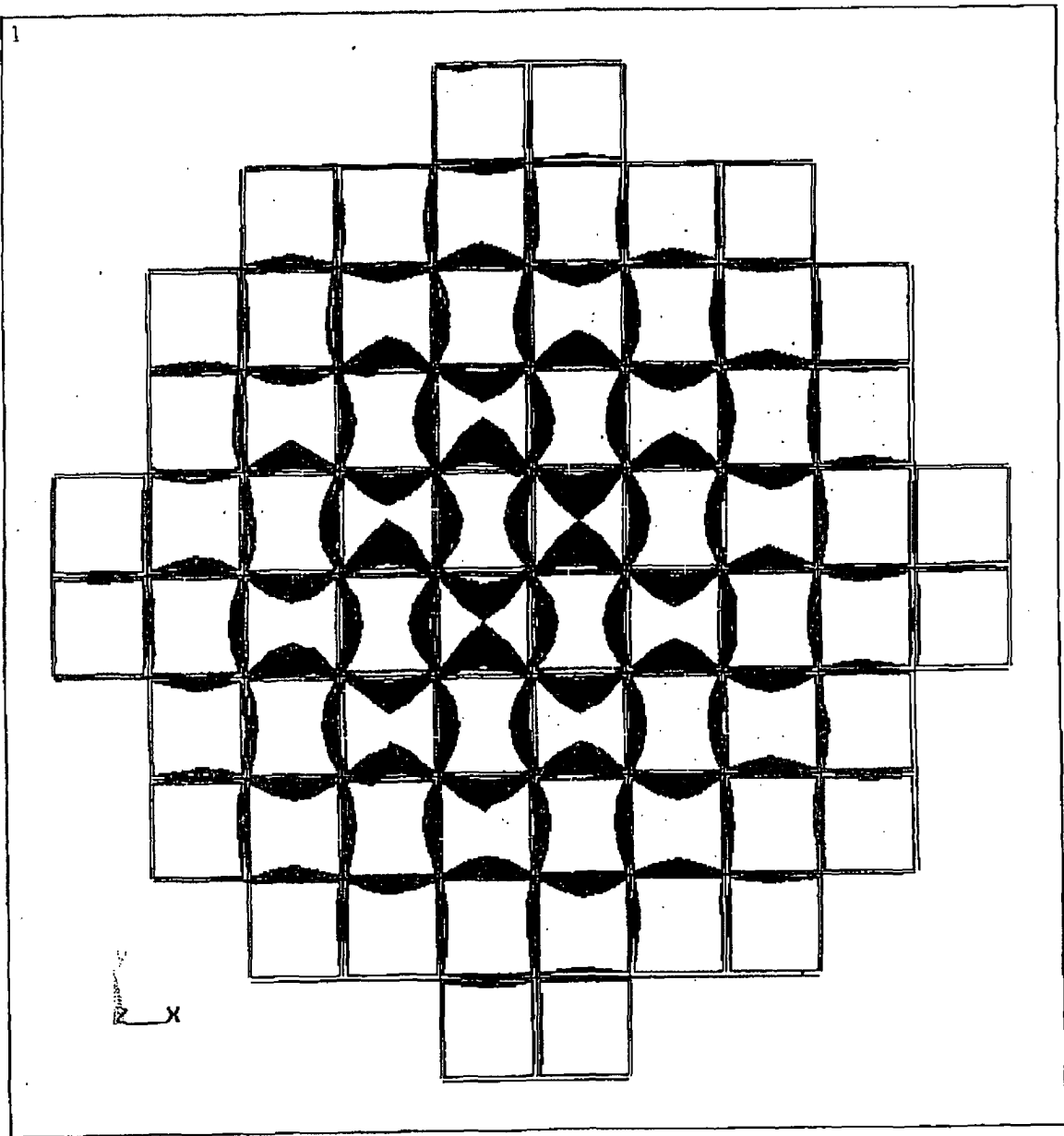


Figure 3C.1-10
30° Modal Analysis – Fourth Mode (264 HZ)

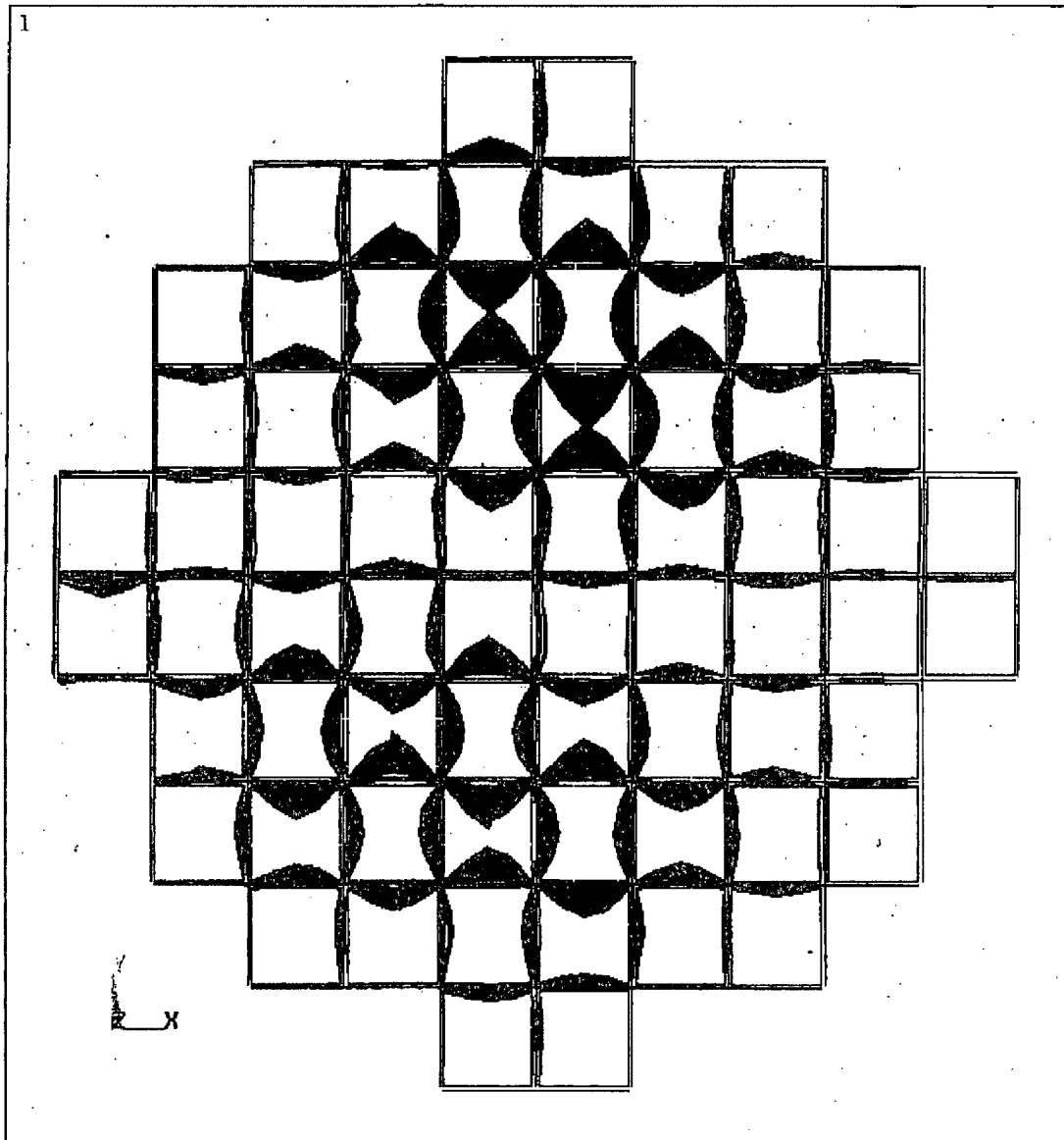


Figure 3C.1-11
45° Modal Analysis – First Mode (181 HZ)

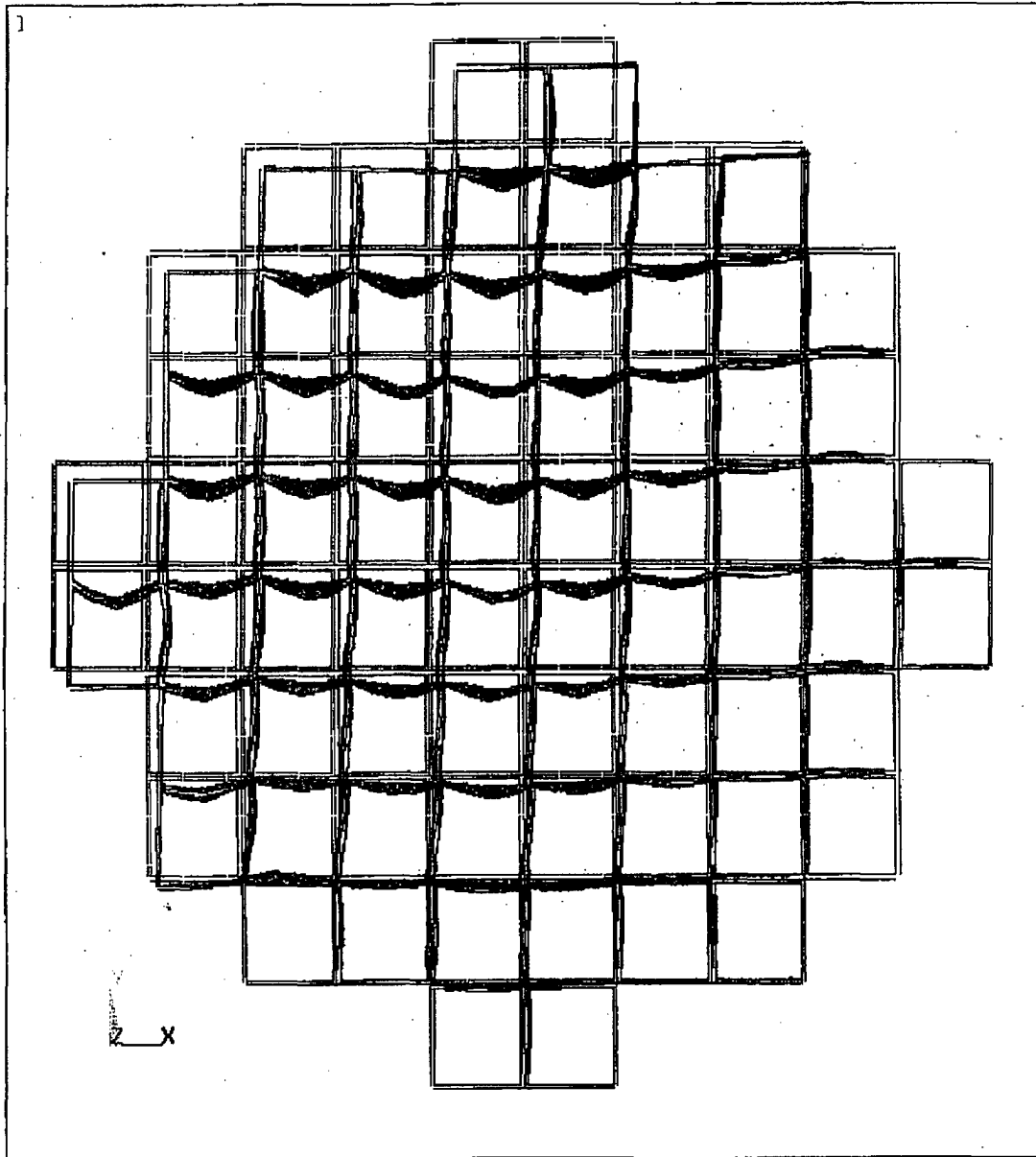


Figure 3C.1-12
45° Modal Analysis – Second Mode (232 HZ)

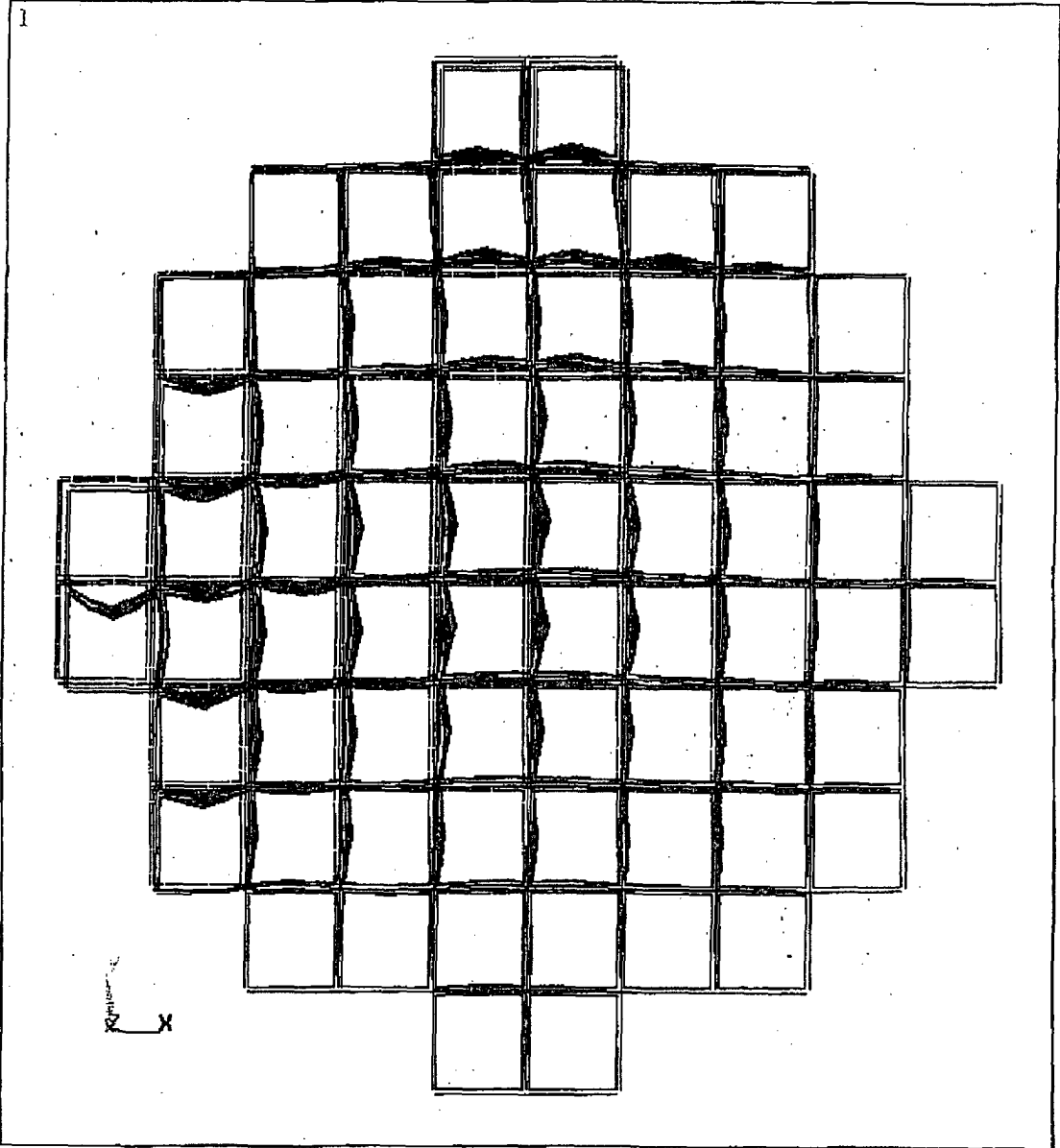


Figure 3C.1-13
45° Modal Analysis – Third Mode (272 HZ)

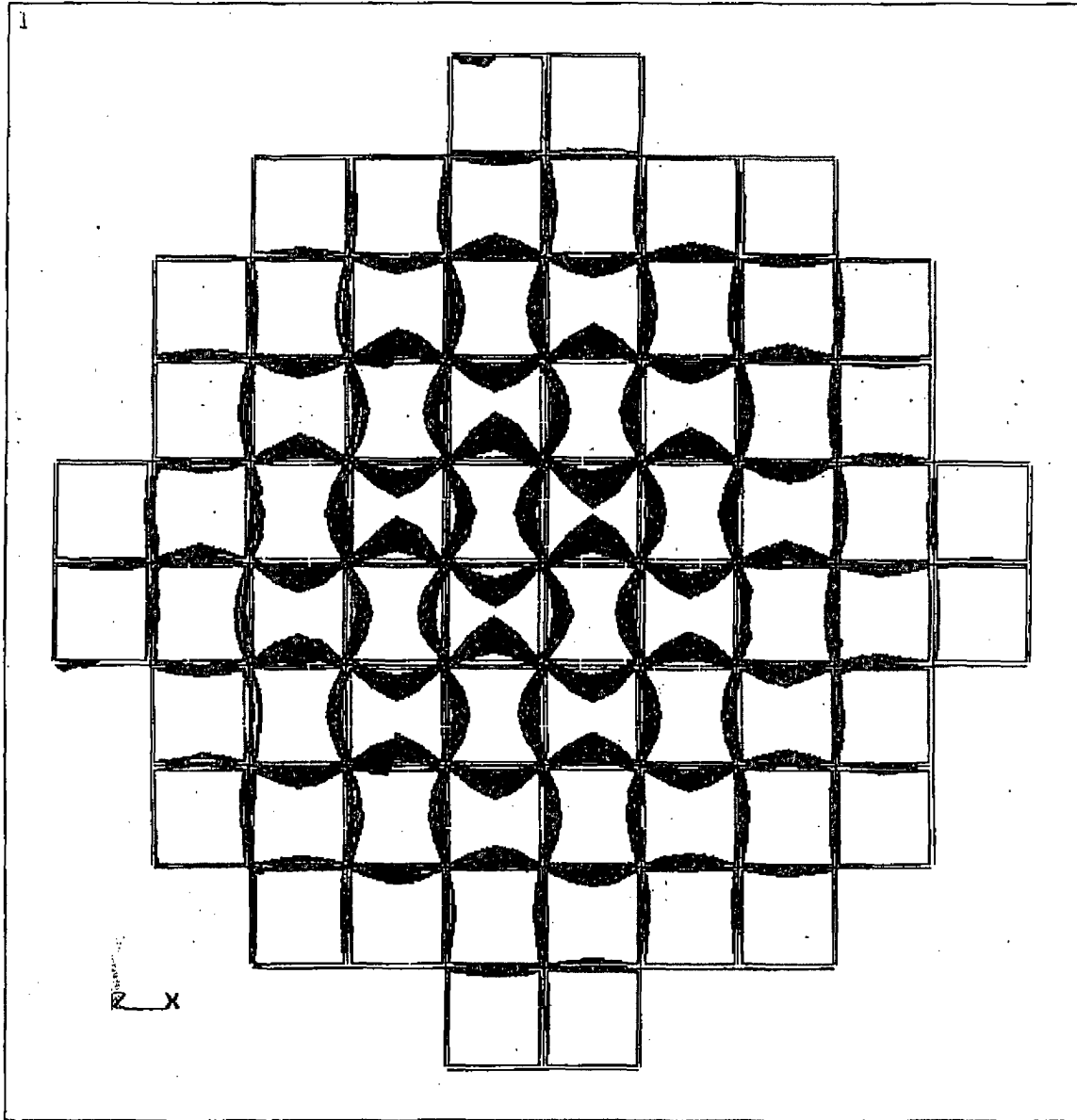


Figure 3C.1-14
45° Modal Analysis – Fourth Mode (281 HZ)

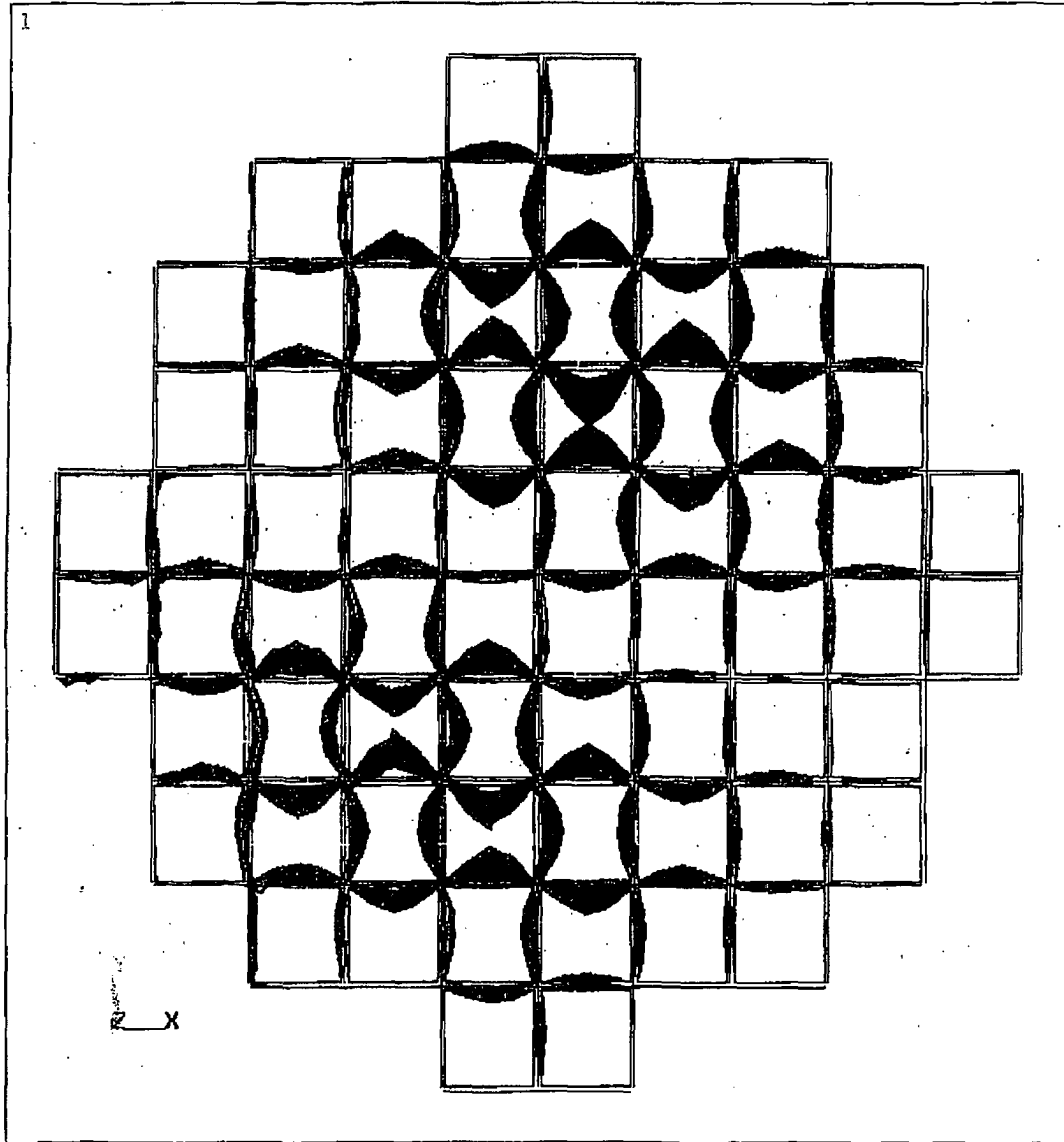
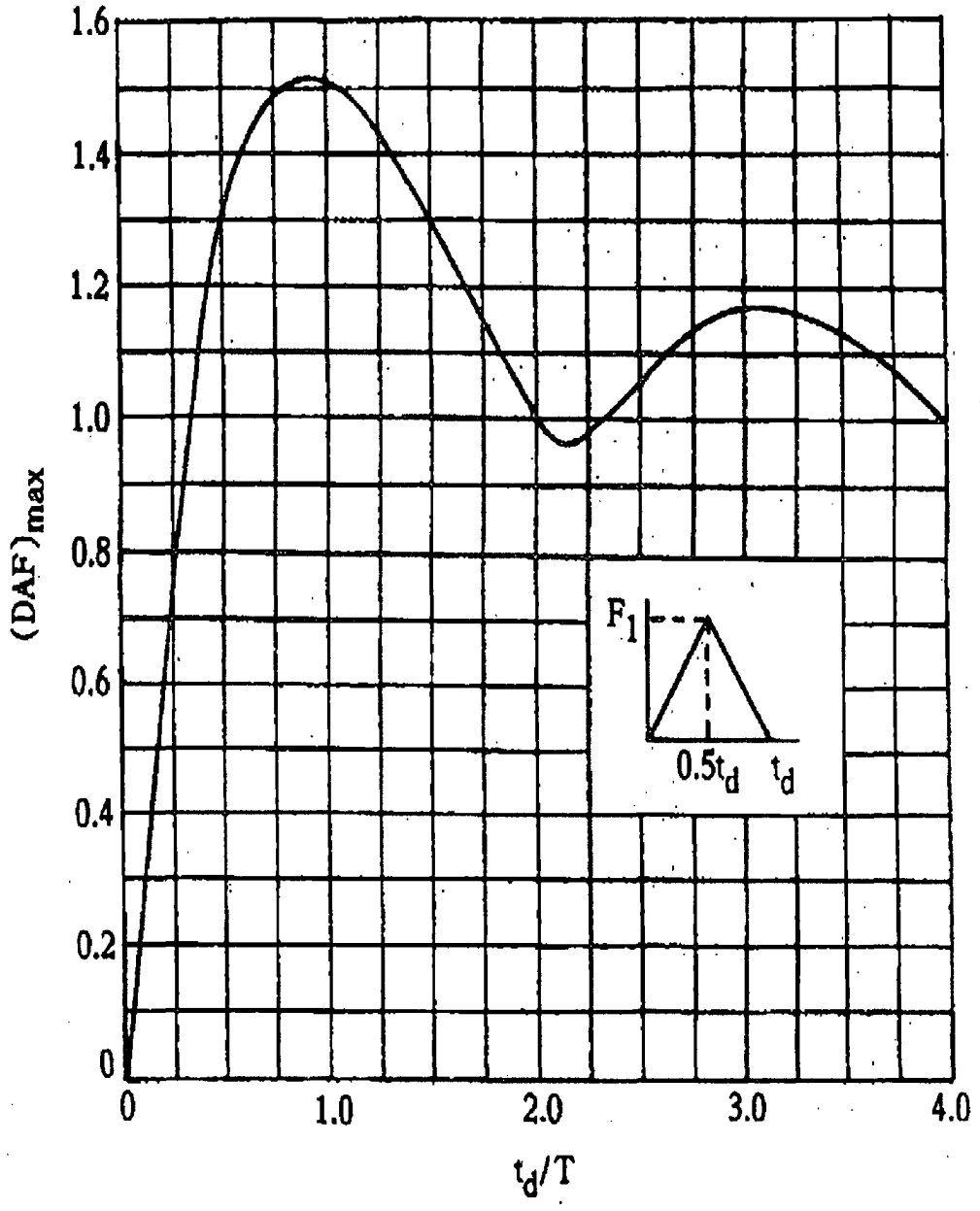


Figure 3C.1-15
Maximum Dynamic Amplification Factor for a Triangular Load



TN-68 SAFETY ANALYSIS REPORT
TABLE OF CONTENTS

SECTION	PAGE
Appendix 3D	TIPOVER AND END DROP ANALYSES OF TN-68 STORAGE CASK
3D.1	Tipover Analysis of TN-68 Storage Cask..... 3D.1-1
3D.2	Finite Element Model For Analysis..... 3D.2-1
3D.2.1	TN-32 Model 3D.2-1
3D.2.2	TN-68 Model 3D.2-1
3D.2.3	BNFL Model..... 3D.2-2
3D.3	Description of Tipover Analysis..... 3D.3-1
3D.3.1	Analysis Program..... 3D.3-1
3D.3.2	Material Properties..... 3D.3-1
3D.3.3	Loading and Boundary Conditions 3D.3-4
3D.4	Tipover Analysis Verification..... 3D.4-1
3D.4.1	Analysis Assumptions..... 3D.4-1
3D.4.2	Experimental Validation 3D.4-1
3D.4.3	TN-32 Tipover Analysis Validation 3D.4-2
3D.4.4	DaDisp Program Validation..... 3D.4-4
3D.5	TN-68 Tipover Analysis Results 3D.5-1
3D.5.1	Results of TN-68 Tipover Analysis..... 3D.5-1
3D.5.2	Dynamic Amplification Calculation..... 3D.5-1
3D.6	Summary of G Loads For Cask and Basket Side Impact Analyses..... 3D.6-1
3D.6.1	Equivalent Side Drop G Load For The Cask to Envelop The Tipover Accident 3D.6-1
3D.6.2	Equivalent Side Drop G Load For The Basket to Envelop The Tipover Accident..... 3D.6-1
3D.7	End Drop Analysis of TN-68 Storage Cask..... 3D.7-1
3D.7.1	General Approach..... 3D.7-1
3D.7.2	Cask and Concrete Pad/Soil Description..... 3D.7-2
3D.7.3	End Impact Analysis 3D.7-2
3D.8	References..... 3D.8-1

**TN-68 SAFETY ANALYSIS REPORT
TABLE OF CONTENTS**

List of Figures

3D.2-1	Weight and Dimensions of TN-32 Cask
3D.2-2	TN-32 Cask - Finite Element Model (1)
3D.2-3	TN-32 Cask - Finite Element Model (2)
3D.2-4	TN-32 Cask - Finite Element Model (3)
3D.2-5	TN-68 Cask Finite Element Model (1)
3D.2-6	TN-68 Cask Finite Element Model (2)
3D.2-7	TN-68 Cask Finite Element Model (3)
3D.2-8	Weight and Dimensions of TN-68 Cask
3D.2-9	Finite Element Grid for Cask Drop on Concrete Slab
3D.2-10	Finite Element Model of BNFL Full Scale Drop Test #4
3D.3-1	TN-32 Cask - Symmetry Boundary Conditions
3D.3-2	TN-32 Cask - Modal Analysis
3D.3-3	TN-32 Cask - Modal Analysis of the Approximate Basket Model
3D.3-4	TN-68 Cask Modal Analysis
3D.3-5	TN-68 Cask - Modal Analysis of the Approximate Basket Model
3D.3-6	BNFL Full Scale Drop Test #4 - Cask Modal Analysis
3D.3-7	Damping Ratio Data Reproduced from References 13 and 14
3D.3-8	Tipover Analysis Damping Coefficients
3D.4-1	BNFL Cask End Drop - Stress Plot
3D.4-2	BNFL Cask End Drop - Displacement Plot
3D.4-3	BNFL Cask End Drop - Displacement Time History
3D.4-4	BNFL Cask End Drop - Acceleration Time History (TN Analysis)
3D.4-5	BNFL Full Scale Drop Test #4 - Acceleratin Time History (Test Data)
3D.4-6	TN-32 Cask Tipover Analysis - Acceleration Time History
3D.4-7	Verification of DADisp Program - Sine Wave Pulse
3D.4-8	18" Billet Side Drop Test Data From Channel A3 - Unfiltered and Filtered at 450 Hz (Performed by TN)
3D.4-9	18" Billet Side Drop Test Data From Channel A3 - Unfiltered and Filtered at 450 Hz (Performed by LLNL)
3D.5-1	TN-68 Cask Tipover Analysis - Displacement Time History Along the Length of the Cask
3D.5-2	TN-68 Cask Tipover Analysis - Displacement Plot (E=28.3E6 psi)
3D.5-3	TN-68 Cask Tipover Analysis - Von Mises Stress Plot (E=28.3E6 psi)
3D.5-4	TN-68 Cask Tipover Analysis - Acceleration Time History (E=28.3E6 psi)
3D.5-5	TN-68 Cask Tipover Analysis - Acceleration Time History (E=30E6 psi)
3D.5-6	Single Degree of Freedom Model
3D.5-7	Dynamic Amplification Factor (E = 28.3E6)
3D.5-8	Ratio of Max. Cask/Basket Displacement vs. Time (E=28.3E6 psi)

APPENDIX 3D

TIPOVER AND END DROP ANALYSES OF TN-68 DRY STORAGE CASK

3D.1 Tipover Analysis of TN-68 Storage Cask

The purpose of this analysis is to determine the peak rigid body accelerations of the TN-68 storage cask under tipover accident. The rigid body accelerations are predicted analytically using the LS-DYNA3D explicit nonlinear dynamic analysis finite element program⁽¹⁾. The methodology used in performing the analysis is based on work done at Lawrence Livermore National Labs⁽²⁾ where an analysis methodology was developed and verified through comparisons with test data⁽³⁾.

Benchmarking of the analyses presented herein are achieved through comparison with the Lawrence Livermore National Labs analyses as well as true scale end drop tests performed by BNFL⁽⁴⁾. The results of the analyses are used as input to the detailed static analyses presented in Appendix 3A and 3B. Quasi-static analyses of the cask internal basket structure (presented in Appendix 3B) are performed by computing dynamic application factors based on the acceleration magnitude, duration and shape (See Section 3D.5.2).

3D.2 Finite Element Model For Analysis

In order to validate the accuracy of the TN-68 tipover analysis, two analyses are performed. First, a tipover analysis of the TN-32 cask is performed and compared with the LLNL⁽²⁾ results based on the TN-32 cask geometry. Second, analyses are performed on the BNFL⁽⁴⁾ end drop cask configuration and compare with the test data⁽⁷⁾.

The finite element models of the TN-32 and TN-68 casks are developed in a similar manner to those models represented in Reference 2. The cask and basket meshes are simplified and totally independent of each other with surface-to-surface contact elements transferring load between the two components. Contact elements are also used between the cask and concrete pad and between the concrete pad and the soil. Details on the TN-32, TN-68 and BNFL cask models are provided in the following subsections.

3D.2.1 TN-32 Model

The TN-32 finite element model is made up of four components: cask body, cask internals, concrete and soil. Each of these components is modeled using 3-D 8-node brick elements. The finite element models were developed in ANSYS 5.3⁽⁹⁾ and transferred to LS-DYNA through the ANSYS-LS-DYNA interface. Modifications were made to the LS-DYNA input to add the material definition and state variables since they are not available through the ANSYS translator. The geometries of the cask and basket have been simplified since the purpose of the analysis is to predict the rigid body response of the cask. Features on the cask such as the trunnions, neutron shield and weather cover are neglected in terms of stiffness but their weight is lumped into the density of the cask. The geometry of the cask body used in the analysis is illustrated in Figure 3D.2-1. Figures 3D.2-2 through 4 illustrate the finite element model of the cask, basket, concrete, and soil. Mesh sizes in this analysis are in reasonable agreement with those represented in Reference 2. The concrete material is modeled with all elements having a constant length of 10 inches since the concrete material law can be dependent on mesh size. Boundary conditions and material properties used in the analysis are discussed in Section 3D.3.

The purpose of this model is to predict the rigid body response of the cask body under impact loading. More detailed analysis models are used to evaluate the cask and basket using quasi-static analyses based on the loads developed from these analyses.

3D.2.2 TN-68 Model

The TN-68 finite element model is illustrated in Figures 3D.2-5 through 7. The model is developed based on the geometry illustrated in Figure 3D.2-8. The mesh size and contact definition is the same as used in the TN-32 finite element model. Boundary conditions and material properties used in the analysis are also discussed in Section 3D.3.

3D.2.3 BNFL Model

The BNFL analysis is performed using a similar model to that used in EPRI's validation of its methodology for analysis of spent-fuel cask drop and tipover events⁽⁴⁾.

Figure 3D.2-9 illustrates the geometry used in EPRI's analysis validation. Figure 3D.2-10 illustrates the finite element model used in the validation analysis. A one-quarter segment was used in the LS-DYNA analysis since it is limited to 3-D analysis. Symmetry boundary conditions are used at 0 and 90 degrees. Material properties were extracted from the EPRI report with the exception of the concrete which used the material behavior described in Section 3D.3.2.

3D.3 Description of Tipover Analysis

3D.3.1 Analysis Program

The LS-DYNA⁽¹⁾ finite element program was used for the analyses presented in this Appendix. Model generation was performed using the ANSYS⁽⁵⁾ finite element program. Data filtering was performed using the DADisp⁽⁶⁾ software.

LS-DYNA is a general purpose, explicit finite element program used to model the nonlinear dynamic response of three-dimensional models. Applications of LS-DYNA include crash worthiness, sheet metal forming, high velocity impact, explosive phenomena, drop tests, etc.

ANSYS is a general purpose program capable of solving structural, mechanical, electrical, electromagnetic, electronic, thermal, fluid, and biomedical problems. It has extensive preprocessing (model generation), solution, postprocessing, and graphics capabilities.

DADisp is an interactive graphics worksheet which is used to manipulate data. It is a visually oriented software package for the display, management, analysis and presentation of scientific and technical data. The filtering package is a menu-driven module for FIR and IIR digital filter design and analysis.

3D.3.2 Material Properties

The material properties required to perform the analysis include the modulus of elasticity (E), Poisson's ratio (ν) and material density (ρ) for the cask, internals and soil. The concrete requires a more detailed material model since all the significant nonlinear deformations occur in the concrete. Material properties used for the concrete and soil are based on those developed at Lawrence Livermore National Laboratory⁽²⁾.

Soil Material

The Lawrence Livermore National Laboratory report indicates that the stiffness of the soil has little impact on the peak accelerations predicted in the cask. Thus for the purpose of the TN-32 and TN-68 analyses, the same soil model is assumed as was used in the Livermore report. The soil material properties assumed for the analyses are:

$$E = 6,000 \text{ psi}$$

$$\nu = 0.3$$

$$\rho = 0.225E-3 \text{ lb-sec}^2/\text{in}^4$$

Cask Material

The same modulus of elasticity used in the LLNL report is used for the TN-32 and TN-68 tipover analyses. The density of the cask was adjusted to match the mass properties of those entities not explicitly modeled. The material properties used for the casks are as follows:

TN-32 Cask $E = 30 \text{ E6 psi}$

TN-68 Cask $E = 30 \text{ E6 psi}$ (Case #1, material property same as TN-32)

TN-68 Cask $E = 28.3 \text{ E6 psi}$ (Case #2, material property based on TN-68 cask body design temperature of 300°F)

$\nu = 0.3$

TN-32 Cask $\rho = 0.865\text{E-3 lb-sec}^2/\text{in}^4$

TN-68 Cask $\rho = 0.942\text{E-3 lb-sec}^2/\text{in}^4$

Note that the density of each cask has been adjusted so that the weight of the TN-32 cask minus the basket and fuel is 166,200 lbs. For the TN-68 Cask (minus the basket and fuel) the weight is 155,600 lbs.

Fuel/Basket Material

The fuel and basket were modeled as a set of hollow cylinders inside the cask walls (similar manner to those models represented in Reference 2). The material properties of the fuel/basket were defined to match the correct weight and approximate the stiffness of the basket. The cask and basket finite element model meshes are totally independent of each other with surface-to-surface contact elements transferring load between the two components. Because the cask stiffness is so much greater than the basket stiffness this simplification is reasonable. The modulus of elasticity used for the basket is adjusted such that the fundamental frequency of the approximate basket matches the fundamental frequency of the detailed basket analysis. Material properties used for the basket are as follows:

TN-32 Basket $E = 8.1\text{E6 psi}$

TN-68 Basket $E = 23.5\text{E6 psi}$

$\nu = 0.3$

TN-32 basket $\rho = .863\text{E-3 lb-sec}^2/\text{in}^4$

TN-68 basket $\rho = .87E-3 \text{ lb-sec}^2/\text{in}^4$

Again the density of the basket has been adjusted to account for the weight of the fuel. The weight of the basket plus fuel for TN-32 cask is 65,800 lbs. The weight of basket plus fuel for the TN-68 cask is 74,000 lbs.

Concrete Material

The concrete pad is modeled using material law 16 in LS-DYNA which was developed specifically for granular type materials. The data used in the analysis was originally developed by LLNL for the Shippingport Station Decommissioning Project in 1988. This model was also used in the LLNL⁽²⁾ cask drop analyses. Material constants were input into Material Model 16 Mode II.B in DYNA. A summary of the input used in the analyses is as follows:

$$\rho = 2.09675E-4 \text{ lb-sec}^2 / \text{in}^4$$

$$\nu = .22$$

$$a_0 = 1,606 \text{ psi}$$

$$a_1 = 0.418$$

$$a_2 = 8.35E-5 \text{ psi}^{-1}$$

$$b_1 = 0$$

$$a_{of} = 0.0 \text{ psi}$$

$$a_{if} = 0.385$$

<u>Effective Plastic Strain</u>	<u>Scale Factor, η</u>
0	0
0.00094	0.289
0.00296	0.465
0.00837	0.629
0.01317	0.774
0.0234	.893
0.04034	1.0
1.0	1.0

The maximum principal stress tensile failure cutoff is set at 870 psi. Strain rate effects were neglected in the analysis. Dilger suggests in Reference 8 that the major impact of strain rate effects

is in the softening part of the stress-strain curve. Since the purpose of these analyses are primarily to predict the peak accelerations, we can neglect the strain rate effects on the material behavior.

The pressure-volume behavior of the concrete is modeled with a tabulated pressure vs. volumetric strain rate relationship using the equation of state feature in LS-DYNA.

<u>Volumetric strain (ϵ)</u>	<u>Pressure (psi)</u>
0	0
-0.006	4,600
-0.0075	5,400
-0.01	6,200
-0.012	6,600
-0.02	7,800
-0.038	10,000
-0.06	12,600
-0.0755	15,000
-0.097	18,700

An unloading bulk modulus of 700,000 psi is used and is assumed to be constant at any volumetric strain (Reference 2).

One percent reinforcement is assumed in the concrete pad to account for the pad reinforcement. The 1% reinforcement is also used in analyses presented in EPRI report NP-7551 (Reference 10). The material properties used for the reinforcing bars are as follows:

$E = 30E6$ psi

$\nu = 0.3$

Yield Stress = 30,000 psi

Tangent Modulus = 30E4 psi

3D.3.3 Loading and Boundary Conditions

TN-32 Modal Analysis

Modal analyses are performed on the cask and basket assemblies to assess their vibratory characteristics. Boundary conditions are limited to symmetry boundaries illustrated in Figure 3D.3-1. ANSYS's Solid45 eight node brick elements are used in these modal analyses. The full subspace modal extraction technique using the generalized Jacobi iteration algorithm is used to calculate the natural frequencies and mode shapes. This method is highly accurate and is

commonly used for small to medium sized problems. Rigid body modes are ignored when interpreting the results of the modal analyses. The first modes of vibration for the TN-32 cask and basket are illustrated in Figures 3D.3-2 and 3D.3-3. The first mode frequency for the cask is 188 Hz and the approximate basket model is 137 Hz.

TN-68 Modal Analysis

Similar plots are made to illustrate the results of the TN-68 modal analysis. The first modes of vibration for the TN-68 cask and basket are illustrated in Figures 3D.3-4 and 3D.3-5. The first mode frequency for the cask is 146 Hz and the approximate basket model is 200 Hz. The 200 Hz matches the first mode of the detailed model of the TN-68 basket assembly (204Hz) analyzed in Appendix 3C. A summary of the cask's first 5 modes is as follows:

TN-68 Cask Mode	Frequency (Hz)
1	146
2	229
3	270
4	317
5	349

Five modes of the cask exist below the 350 Hz filtering level, thus the response predicted by the tipover analysis (Section 3D.5, Figure 3D.5-4) includes more than the rigid body response of the cask. Thus, the 350 Hz level of filtering is conservative.

BNFL Modal Analysis

In order to quantify the damping ratio, a modal analysis is performed of the BNFL cask model. Figure 3D.3-6 illustrates the first mode response of the cask. The fundamental frequency of the cask is 86 Hz.

DYNA Analysis

For the tipover analyses, an angular velocity is applied based on a non-mechanistic cask tipover accident. The center of rotation is set at the edge of the cask bottom located at the center of the coordinate system as illustrated in Figure 3D.3-1. DYNA calculates the initial velocity components associated with each node for this rotational motion. Loads applied to the two casks are listed below:

TN-32 Tipover	-	1.729 Radians/sec
TN-68 Tipover	-	1.816 Radians/sec

A ½ model is used in both analyses, with symmetry boundary conditions used to simulate the full structure. Non-reflecting boundaries were used around the soil non-symmetry boundaries to prevent artificial stress waves from reflecting from the boundaries of the soil. Figure 3D.3-1 also illustrates the boundary conditions used in the finite element model.

The BNFL end drop analysis is simulated by giving an initial velocity to the cask. The 5 foot drop is represented by a 215.3 in/sec initial velocity.

Damping

The true damping characteristics of the cask impact event are very hard to quantify. Typical values for reinforced concrete structures subjected to dynamic loads are in the 5 to 10% range (See References 13 and 14, Figures in these references are reproduced in Figure 3D.3-7). During the tipover drop events, the concrete, cask and soil absorb energy as a result of damping. Since the response of the concrete is nonlinear, a single damping ratio can not be defined. In order to define a relatively uniform damping ratio over a range of frequencies, damping is defined proportional to both the stiffness and mass matrices. Known as Rayleigh damping (Reference 12), two factors can be defined relative to mass and stiffness proportional damping to provide a range of damping. A uniform damping rate of 5% of critical is assumed between the frequencies of 50 and 1000 Hz in developing the initial damping coefficients. Since the damping ratio must be assumed, both an upper and lower bound ratio of damping is used in the preliminary analyses. However, based on the results presented in Reference 2, the 6% critical damping results appear to be most realistic. Figure 3D.3-8 illustrates two sets of damping curves used in TN-68 preliminary analyses. Based on the analysis results presented in 3D.5, it concluded that using 6.1% critical damping for TN-68 tipover analysis is realistic and conservative. The corresponding critical damping ratios (relative to the cask response) and natural frequencies of the casks are summarized in the following table:

Cask Design	α Damping Constant	β^{**} Stiffness Damping Constant	Natural Frequency	Damping Ratio
BNFL	100	1.5E-5	86 Hz	10%
TN-32	122	1.5E-5	188 Hz	6%
TN-68	100	1.5E-5	146.5 Hz	6.1%

** The value of β is kept constant because it influences the high frequency response (natural frequency > 1000 Hz).

3D.4 Tipover Analysis Verification

3D.4.1 Analysis Assumptions

Several assumptions were required to perform this analysis. These are summarized as follows:

- 1) Coefficient of Friction of .25 was assumed between all sliding surfaces.
- 2) Nonlinear material response of the cask internals and soil, if any, is neglected.
- 3) Reinforcement in the concrete pad is assumed to be 1% of the pad volume.
- 4) Strain rate effects on all material properties are neglected.

The negligible effects of these simplifying assumptions is justified through the comparison of the analytical results with experimental tests.

3D.4.2 Experimental Validation

Validation of the accuracy of the finite element model is obtained through experimental verification. Two analyses are used as verification. First analyses performed on the BNFL end drop cask configuration provide excellent agreement with test data in References 4 and 7. Second the results of the TN-32 tipover analyses provide reasonable agreement with LLNL results presented in Reference 2.

The BNFL analysis is performed using a similar model to that used in EPRI's validation of its methodology for analysis of spent-fuel cask drop and tipover events⁽⁴⁾. Material properties are extracted from the EPRI report with the exception of the concrete, which used the material behavior described in Section 3D.3. Summaries of the cask and soil properties are:

	E (psi)	v	ρ (lb-sec ² /in ⁴)
Cask	30E6	0.3	2.08E-3
Soil	82,000	0.45	0.180E-3

A 10% damping value is used in the analysis as described previously in Section 3D.3.3. In order to quantify the damping ratio, a modal analysis is performed of the cask model. Figure 3D.3-6 illustrates the first mode response of the cask. The fundamental frequency of the cask is 86 Hz.

Since this is reasonably close to the TN-32 and TN-68 cask frequencies, a similar dynamic response to the TN-32 and TN-68 casks is expected. Results from the analysis are illustrated in Figures 3D.4-1 through 4. Figure 3D.4-1 illustrates the Von Mises stress distribution predicted in the cask during the peak impact. Figure 3D.4-2 illustrates the displacement of the cask 0.01 seconds after impact. A history of the cask bottom displacement is illustrated in Figure 3D.4-3. The predicted acceleration history at the location of the acceleration gauges (48 inches up from the bottom of the cask) is illustrated in Figure 3D.4-4. Test data at the same location is illustrated in Figure 3D.4-5. A summary of a comparison of the two data sets is as follows:

Comparison of BNFL End Drop Analysis

	Test Data	Transnuclear DYNA Analysis
Peak Acceleration (350 Hz Filter)	112-121 G	130 G
Duration of Pulse	0.004 sec	0.0035 sec
Pulse Shape	Triangle	Triangle

Excellent correlation is achieved for the end drop analysis.

3D.4.3 TN-32 Tipover Analysis Validation

Figure 3D.4-6 illustrates the result for the TN-32 tipover analysis. The following table lists the LLNL and Transnuclear analysis results.

Comparison of TN-32 Tipover Analysis

	LLNL DYNA Analysis	Transnuclear DYNA Analysis
Peak Acceleration (350 Hz Filter)	66.7 g	67 g
Duration of Pulse	0.003 sec	0.003 sec
Pulse Shape	Triangle	Triangle

Excellent correlation is achieved for the tipover analysis.

(This page intentionally left blank.)

3D.4.4 DADisp Program Validation

The DADisp worksheet data can be manipulated both with FIR (Finite Impulse Response) and IIR (Infinite Impulse Response) filter. The Butterworth filter used in this analysis is characterized for its large number of coefficients, small pass band ripple and slow roll off.

Verification of the DADisp program is achieved through two example analyses. First, a sine wave pulse is defined with noise attached to it. The pulse is then filtered down to just the sine wave (Figures 3D.4-7). Second, data from Reference 2 is imported into DADisp and filtered in a similar manner as performed in Reference 2 (Figure 3D.4-8). Figure 3D.4-9 illustrates the comparative results from Reference 2.

3D.5 TN-68 Tipover Analysis Results

The following table highlights the results from the two analyses. The table presents peak accelerations in the tipover analysis due to two different moduli of elasticity. Detailed results on the two analyses are presented in the following sections.

Results of TN-68 Tipover Analysis

Load Case	Modulus of Elasticity (E)	Damping Ratio	Peak G	Dynamic Load Factor	Duration	Pulse Shape
1	30 E6 (psi)	6.1%	66	1.31	0.003 sec	Triangle
2	28.3 E6 (psi)	6.1%	65	1.32	0.003 sec	Triangle
3	28.3 E6 (psi)	2.3%	65	1.29	0.003 sec	Triangle

3D.5.1 Results of TN-68 Tipover Analysis

Two conditions are evaluated for the TN-68 tipover analysis. Changes in cask modulus of elasticity are evaluated. Plots are chosen for these analyses to illustrate the overall cask response and to highlight their differences.

Figures 3D.5-1 through 3D.5-4 illustrate the results for the TN-68 tipover analysis for the 28.3E6 psi modulus cask and the 6.1% damping case. Figure 3D.5-1 illustrates how the displacement increases along the length of the cask. The top curve illustrates the vertical displacement at the origin of rotation while the bottom curve illustrates the vertical displacement of the far edge of the lid. Figure 3D.5-2 illustrates the distribution in the cask at the maximum response time of .0124 seconds after impact. Figure 3D.5-3 illustrates the peak stresses in the cask immediately after impact of 34 ksi. Figure 3D.5-4 shows the acceleration time history.

Figure 3D.5-5 illustrates the time history of the increased cask modulus of 30E6 psi. Differences caused by the modulus are small.

3D.5.2 Dynamic Amplification Calculation

Since the basket is not modeled in detail in the transient dynamic analysis it is necessary to transfer the loads from the dynamic analysis model to the detailed model of the basket. The basket structure is designed using a quasi-static analysis using a dynamic magnification factor computed from the transient dynamic analysis. The value of dynamic magnification is representative of the

amplification of the displacement of the basket relative to the displacement in the cask (Reference 12). The displacement history of the basket can be calculated from the displacement history of the cask using a simple spring-mass model, where the frequency of the simplified model matches the fundamental frequency of the basket. The following 5 step procedure is used to calculate the dynamic amplification factor:

- The displacement time history from LS-DYNA is downloaded into ANSYS. A spring-mass model is developed in ANSYS (see Figure 3D.5-6). A conservative assumption of no damping is made.
- The LS-DYNA displacement time history is applied as base motion to the spring-mass model in a transient dynamic analysis.
- The base displacement history (Input from LS-DYNA) is divided by the amplified time history of the free mass (Output response from the ANSYS analysis).
- The maximum ratio of base to free mass displacement is extracted. This is the dynamic magnification factor for the spring-mass frequency (set equal to the basket fundamental frequency).

This magnification factor can also be applied to the acceleration history, since for an undamped system, the product of the mass times the total acceleration must be equal in magnitude to the elastic spring force. Where the elastic spring force is equal to the stiffness times the maximum displacement. See Reference 12 for derivation of the dynamic magnification factor. This methodology is conservative since no damping is assumed between the cask and basket.

Dynamic amplification effects are developed for TN-68 cask using the spring mass model as described above. Figure 3D.5-7 illustrates the displacement response of the cask and single degree of freedom model along with the ratio of the two quantities. The ratio of these 2 curves is the dynamic amplification factor. A factor of 1.32 is predicted for the TN-68 tipover analysis (based on 6.1% damping ratio and $E = 28.3E6$ psi tipover analysis) when conservatively no damping is accounted for.

As an alternative, the vertical displacements for the far corner of basket and the cask point directly underneath the basket were selected from the LS-DYNA transient analysis. A ratio of these displacements predicts an amplification factor of 1.19 (Figure 3D.5-8). This indicates the conservatism of the 1.32 value predicted by the single degree of freedom analysis described above.

3D.6 Summary of G Loads For Cask and Basket Side Impact Analyses

3D.6.1 Equivalent Side Drop G Load For The Cask to Envelop The Tipover Accident

The tipover analysis of TN-68 results in the following decelerations:

Peak Deceleration = 65 G For $E = 28.3 \times 10^6$ psi at Cask Design Temp. of 300°F

Peak Deceleration = 66 G For $E = 30 \times 10^6$ psi at Room Temperature

It is assumed that using 65 G's for an equivalent side drop analysis of the cask is very conservative based on:

- A. The tipover analysis conservatively neglects the outer shell, resin and aluminum boxes. During the drop, these components will deform and absorb energy. Thus the actual deceleration will be less than the above calculated G loads.
- B. During the tipover drop accident, the G loads vary from minimum to the maximum value along the length, from bottom end to the top surface of the lid. However, for the cask static stress analysis, a uniform 65 G load along its entire length is conservatively assumed. This and all other assumptions made in the static analysis of the cask result in a peak stress intensity of about 60,000 psi (Chapter 3). The dynamic analysis indicates a peak stress of about 34,000 psi (see Figure 3D.5-3 of this Appendix). This shows that the overall effect of all the assumptions made in the static analysis for tipover drop are very conservative and there is an approximately 50% additional margin of safety in the cask stresses.

3D.6.2 Equivalent Side Drop G Load For The Basket to Envelop The Tipover Accident

The actual G load at the end of the cask lid is less than the calculated G loads. Both the 66 G and 65 G occurs at the top of the lid, and the G load at the top of the basket will be approximately the ratio of the basket height to the cask height (173.75/197.25), or about 58 G. Therefore, for the basket static stress analysis, it is reasonable to use the G load of 58 from the cask tipover analysis.

The dynamic load factor calculated from Section 3D.5.2 is about 1.32, thus the basket structural analysis should model the side impulse as a steady-state acceleration equal to 77 G ($58 \times 1.32 = 77$).

3D.7 End Drop Analysis of TN-68 Storage Cask

This section evaluates the effects of an 18 in. end drop of the TN-68 cask on the ISFSI concrete storage pad. The impact analysis is based on the methodology of EPRI NP-4830⁽⁹⁾ and NP-7551⁽¹⁰⁾. This section considers the mass and geometry of the cask but assumes it to be rigid compared to the concrete storage pad. The storage pad properties and the cask geometry are used to determine the pad hardness parameter. The report provides graphs that show the force on the cask as a function of storage pad hardness. Scale model drop testing at Sandia National Laboratories and full scale cask drop testing in England have recently been performed in an attempt to "benchmark" the EPRI methodology. The results of the tests⁽¹¹⁾ (end drops) show excellent correlation with the predicted results.

3D.7.1 General Approach

The EPRI reports give Force (applied to the cask) vs. Deformation (of the target) curves for different magnitudes of target hardness. The target hardness is defined as a set of parameters times the area of the impact surface. This impact area usually depends of the deformation. The following procedure is used to determine the maximum deceleration of the cask and deformation of the target:

1. A small target deformation is taken.
2. The geometry of the cask relative to the target is used to compute the impact area for the given deformation.
3. The target hardness is then computed for this target area.
4. The data in the EPRI report is used to determine the force associated with the deformation.
5. The energy absorbed in the increments of deformation is evaluated as the area under the force vs. deformation curve..
6. The deformation is increased and steps 2 through 5 are repeated.
7. This process is continued until the absorbed energy is equal to the cask weight times the drop height. This is the final solution for the force and deformation.

For an end drop analysis, the impact area is constant. Therefore, repeating steps 2 through 5 is not necessary.

3D.7.2 Cask And Concrete Pad/Soil Description

The geometry of the cask is shown on TN drawing 972-70-1. The technical data used for cask and concrete slab/soil are :

- W = Weight of cask = 226,000 lbs (slightly low weight gives higher G load)
- R = Cask outer radius = 42.25 in.
- A = cask foot print area = $\pi (42.25)^2 = 5,607.94 \text{ in.}^2$
- E_c = Concrete elastic modulus = 3.6E6 psi
- σ_u = Ultimate concrete strength = 6,000 psi
- ν_s = Poisson's ratio of concrete = 0.22
- h_c = Concrete pad thickness = 36 inches
- S_y = Rebar yield strength = 60,000 psi
- E_s = Sub-soil modulus = 32,600 psi (in hand calculation, high value gives higher G load)
- ν_s = Poisson's ratio of soil = 0.3
- M_u = 3,014,388 in-lb/ft, is based on pad thickness of 36 in., #11 rebar @ 12 in. spacing (normal), 2 in. cover (normal).

3D.7.3 End Impact Analysis

The results of the EPRI reports are presented in term of a target hardness number (S). In general this is given by:

$$S = \frac{M_u \sigma_u A}{W^2 \delta_c}$$

Where

- M_u = Ultimate moment capacity of 1 foot section of slab = 3,014,388 in-lb/ft
- σ_u = Ultimate concrete strength = 4,200 psi
- A = Area of impact surface, in²
- W = Weight of cask = 226,000 lbs.
- δ_c = Deflection of cask under weight of cask (1G), in.

For the end drop, the area A = Area of the cask

$$A = \pi R^2 = \pi (42.25)^2 = 5,607.94 \text{ in}^2$$

The deflection (δ_c) is given as:

$$\delta_c = \frac{W}{2 Rk} (1 - e^{-\beta R} \cos \beta R)$$

Where

$$k = \frac{\pi E_s}{1 - \nu_s^2} = \frac{\pi (32,600)}{1 - 0.3^2} = 112,545 \text{ psi/in}$$

$$D_c = \frac{E_c h^3}{12 (1 - \nu_c^2)} = \frac{3.6 (10)^6 (36)^3}{12 (1 - 0.22^2)} = 14,709 \times 10^6 \text{ in-lbs}$$

$$\beta = \left(\frac{E_s}{4 D_c} \right)^{1/4} = \left(\frac{32,600}{4 \times 14,709 \times 10^6} \right)^{1/4} = 0.02728$$

$$\begin{aligned} \delta_c &= \frac{W}{2 Rk} (1 - e^{-\beta R} \cos \beta R) = \frac{226,000}{2 \times 42.25 \times 112,545} (1 - e^{-0.02728 \times 42.25} \cos 0.02728 \times 42.25) \\ &= 0.0207 \text{ in.} \end{aligned}$$

Then,

$$S = \frac{M_u \sigma_u A}{W^2 \delta_c} = \frac{3,014,388 \times 6,000 \times 5,607.94}{226,000^2 \times 0.0207} \approx 95,930$$

The force-deformation curve is obtained by interpolating the data shown on Figure 14 of the EPRI report (reference 9). Conservatively using Figure 22 of reference 9 for a 20 in. drop height, the peak force is 39G (times weight) and the displacement at the end of elastic phase is 0.81 in.

It is noted that the above G load is based on the assumption that cask is rigid. To account for actual cask primary mode of response, Reference 11 recommends a conservative dynamic load factor of 1.5 be used for structural evaluation.

Therefore, the maximum acceleration is $39 \times 1.5 = 58.5$ G. For conservatism, 60 G's is used for the structural analyses of the cask and basket due to an 18 in. cask end drop.

3D.8 References

1. "LS-DYNA3D User's Manual (Nonlinear Dynamic Analysis of Structures in Three Dimensions)," August 1, 1995 Version 936, Livermore Software Technology Corporation.
2. Witte, M. et. Al "Evaluation of Low-Velocity Impact Testing of Solid Steel Billet onto Concrete Pads and Application to Generic ISFSI Storage Cask for Tipover and Side Drop." Lawrence Livermore National Laboratory. UCRL-ID-126295, Livermore, California. March 1997.
3. Witte, M. et. Al., Letter forwarding data diskettes containing the drop and tipover tests, NTFS97-76/MW, June 4. 1997
4. "Validation of EPRI Methodology of Analysis of Spent-Fuel Cask Drop and Tipover Events," EPRI TR-108760, August 1997, Prepared by ANATECH Corp., San Diego, CA.
5. ANSYS User's Manual, Revision 5.3, Ansys Inc., P.O. Box 65, Houston, PA 15342-0065.
6. DADisp Worksheet User Manual, DSP Development Corporation, March 1996
7. A. J. Sparkes, J.E. Gillard, P.A. Sims, "Full-Scale Drop Tests for Benchmarking Concrete Pads for Dry Spent Fuel Storage Casks," AEA Technology, Report No. AEA-D&W-0622, July 1993.
8. "Ductility of Plain and Confined Concrete Under Different Strain Rates", By W.H. Dilger, ACI Journal, Jan-Feb, 1984.
9. "The Effect of Target Hardness on the Structural Design of Concrete Storage Pads for Spent-Fuel Casks", EPRI NP-4830, October 1986.
10. "Structural Design of Concrete Storage Pads for Spent-Fuel Cask", EPRI NP-7551, August 1991.
11. Y.R. Rashid, R.J. James and O. Ozer, "Validation of EPRI Methodology for Analysis of Cask Drop and Tipover Accidents at Spent Fuel Storage Facilities.
12. Clough and Penzien, "Dynamics of Structures" McGraw Hill, 2nd Edition 1993.
13. R.B. Matthiesen, "Observations of Strong Motions From Earthquakes", ASCE Convention and Exposition, Portland, Oregon, April 1980.
14. R.C. Dove, et. Al., "Seismic Tests on Models of Reinforced-Concrete Category I Buildings, Structural Mechanics in Reactor Technology, SMIRT 8, Brussels, Belgium, 1985.

Figure 3D.2-1
Weight and Dimension of TN-32 Cask
(Weights of Trunnions, Neutron Shield, and Protective Cover are Included in the Cask)

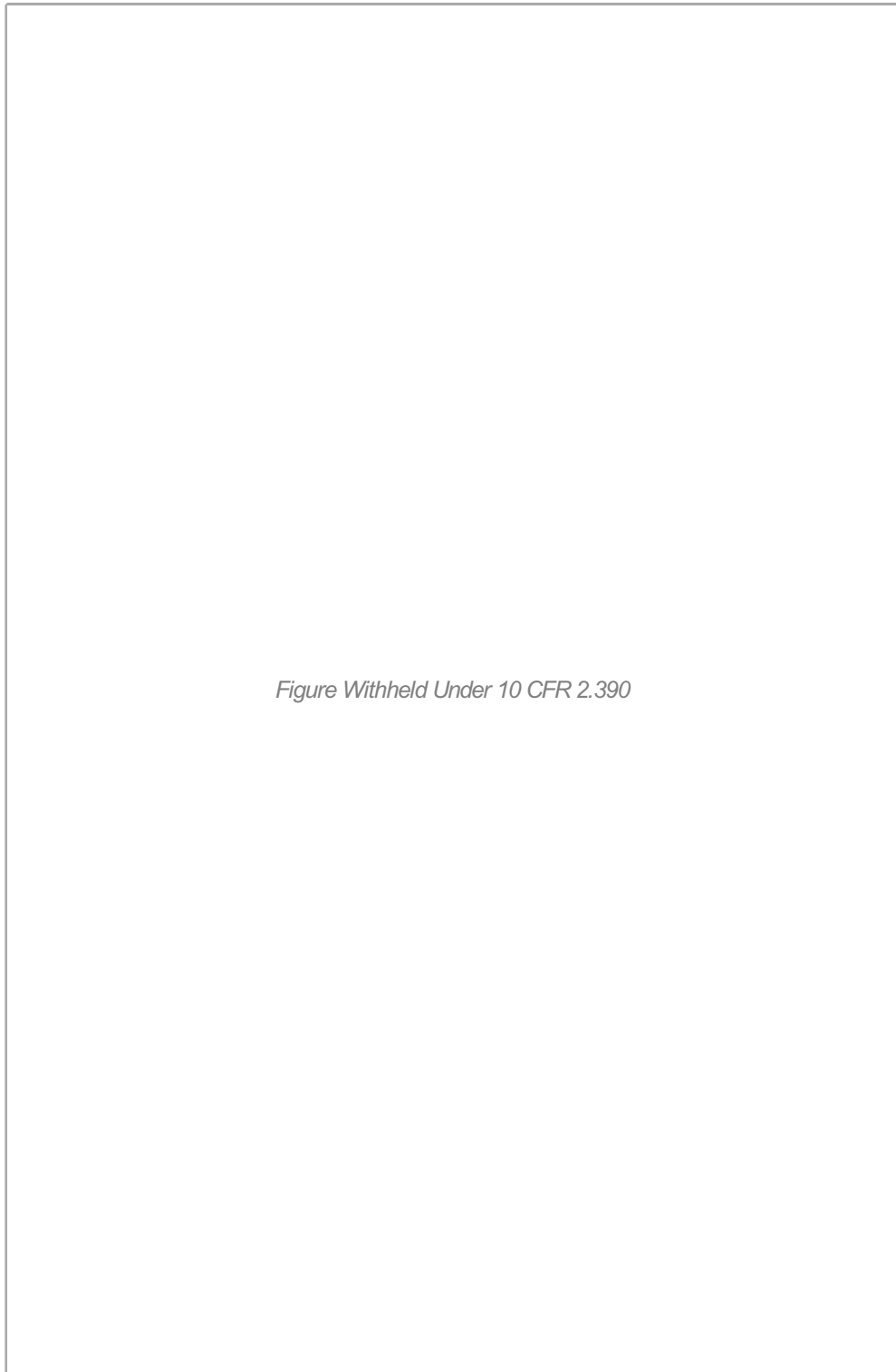


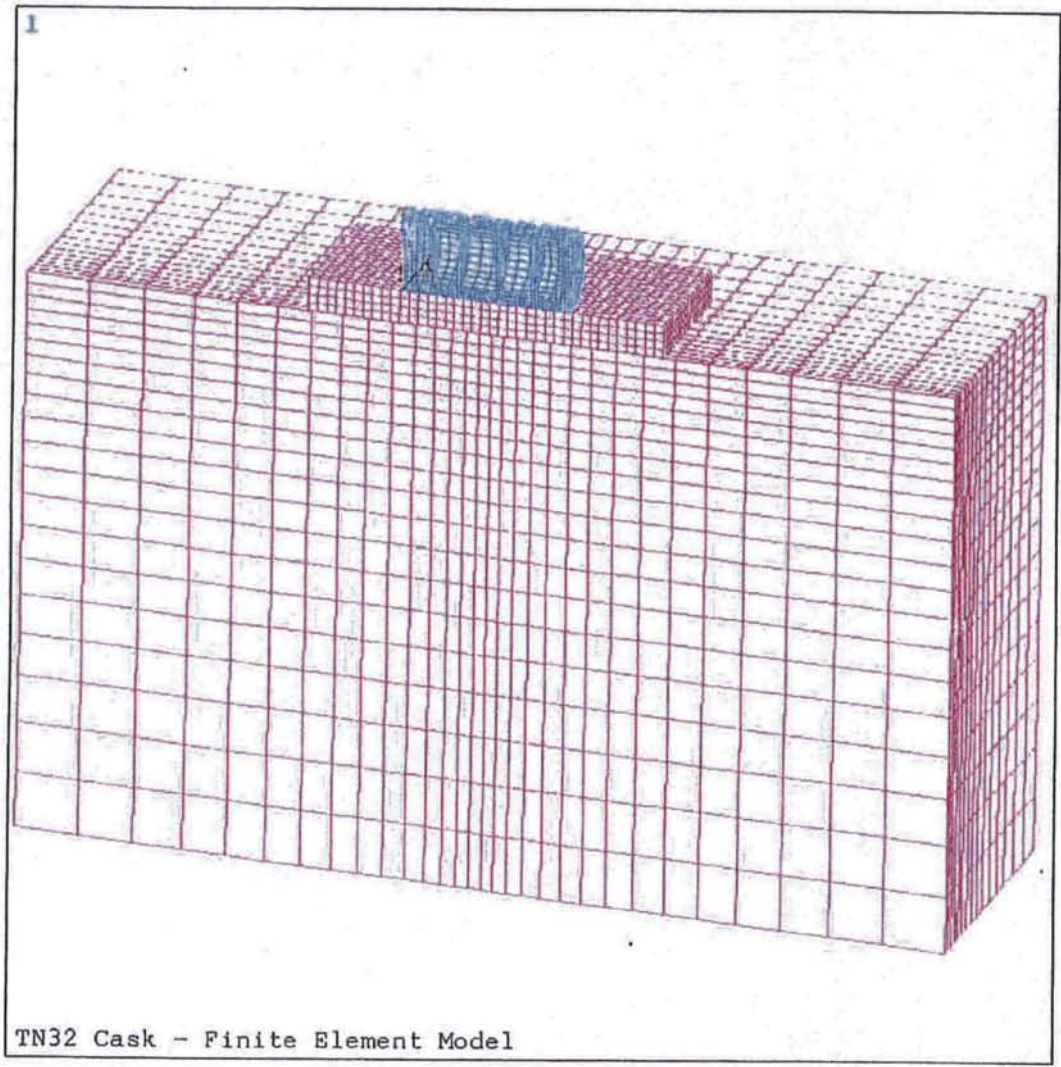
Figure Withheld Under 10 CFR 2.390

Figure 3D.2-2
TN-32 Cask - Finite Element Model (1)



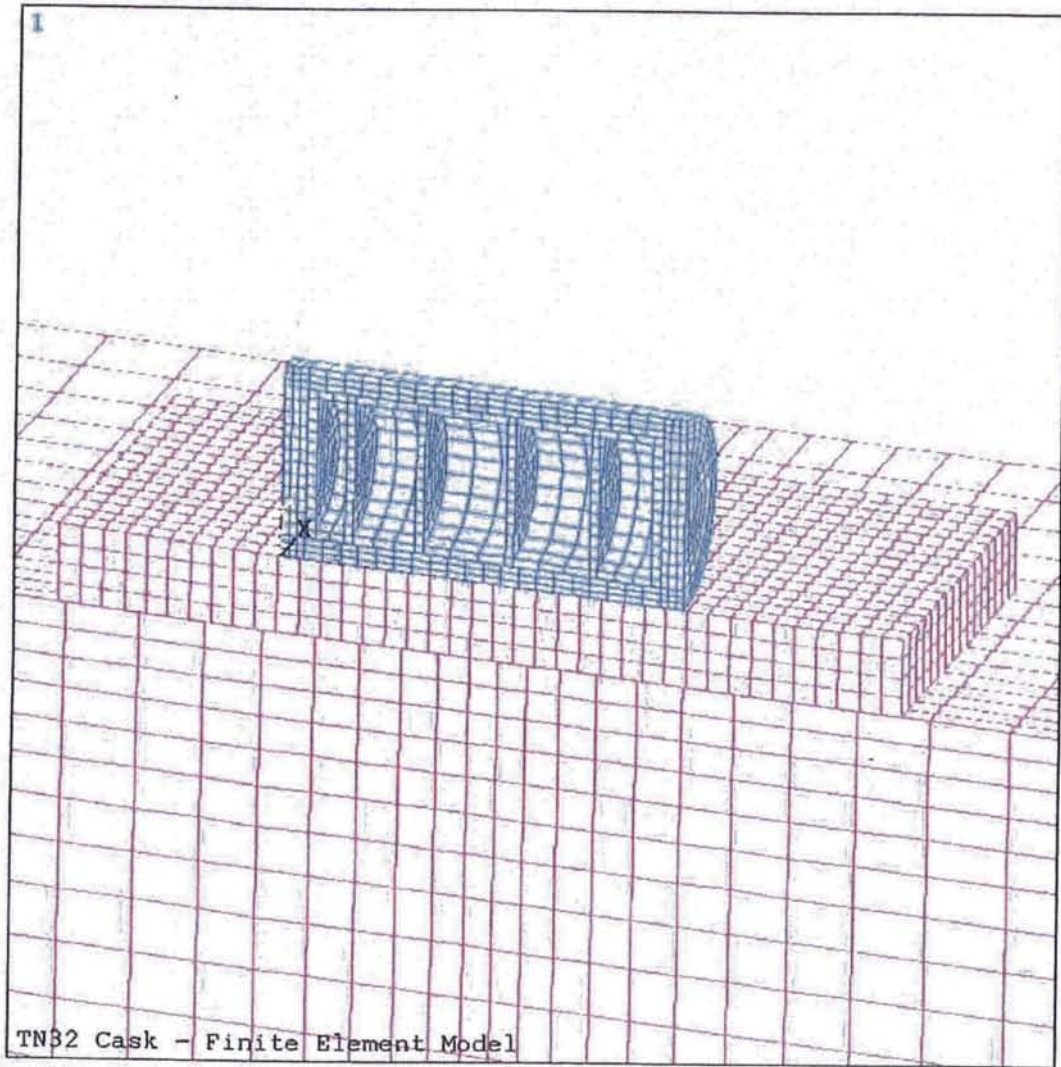
```
ANSYS 5.3  
DEC 15 1997  
09:39:54  
VOLUMES  
MAT NUM  
  
XV =-.8855  
YV =.3698  
ZV =.2814  
*DIST=535.644  
*XF =140.372  
*YF =-307.641  
*ZF =105.862  
A-ZS=-.6148  
Z-BUFFER
```

Figure 3D.2-3
TN-32 Cask - Finite Element Model (2)



```
ANSYS 5.3  
DEC 15 1997  
09:39:16  
ELEMENTS  
MAT NUM  
  
XV =-.8855  
YV =.3698  
ZV =.2814  
*DIST=535.644  
*XF =140.372  
*YF =-307.641  
*ZF =105.862  
A-ZS=-.6148  
Z-BUFFER
```

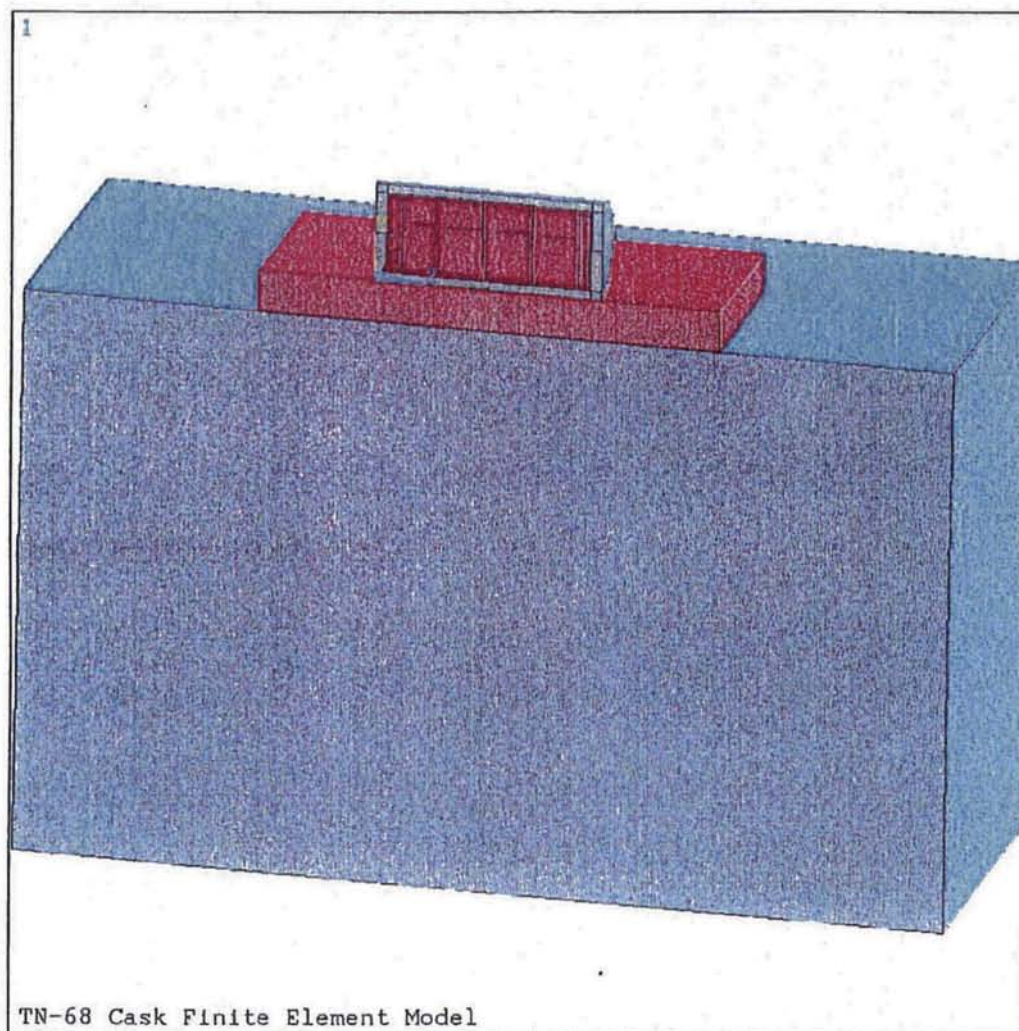
Figure 3D.2-4
TN-32 Cask - Finite Element Model (3)



ANSYS 5.3
DEC 15 1997
09:38:10
ELEMENTS
MAT NUM

XV =-.8855
YV =.3698
ZV =.2814
*DIST=226.744
*XF =221.9
*YF =-67.681
*ZF =47.069
A-ZS=-.6148
Z-BUFFER

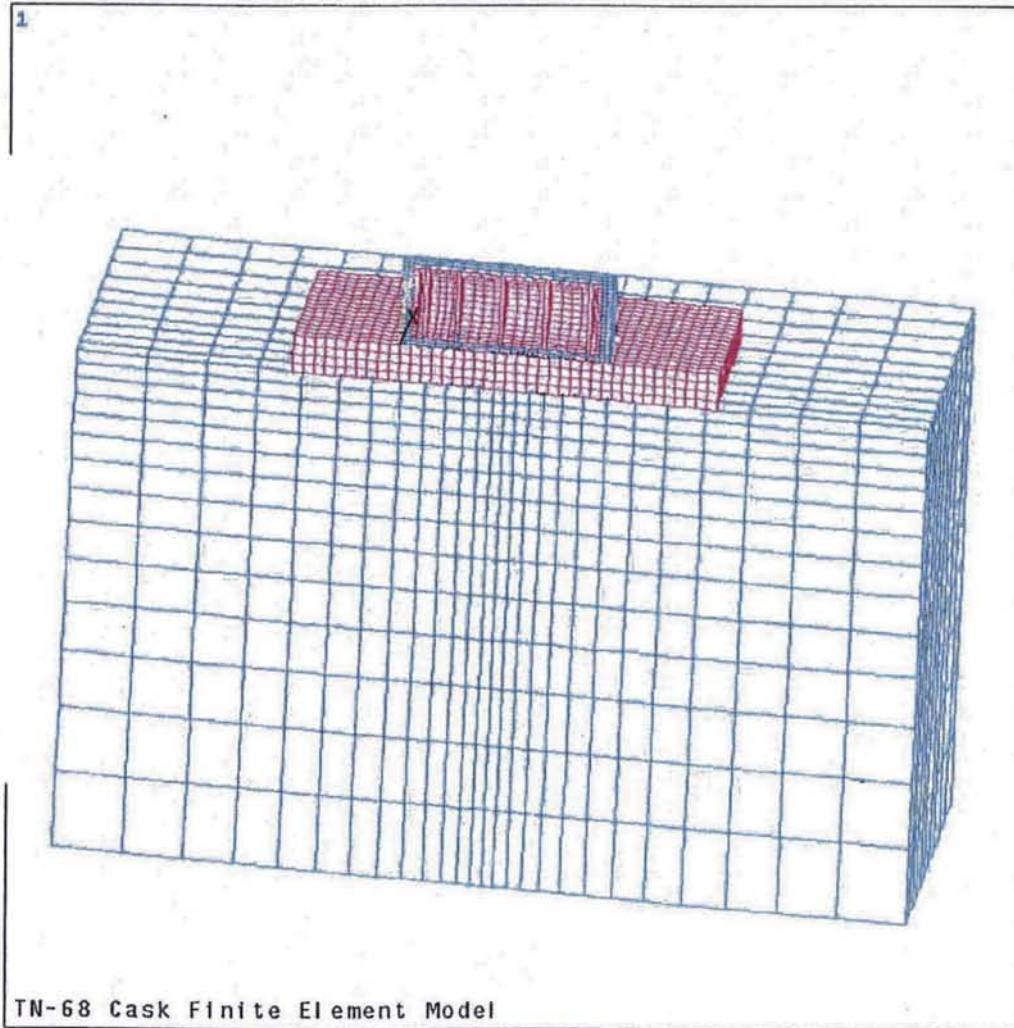
Figure 3D.2-5
TN-68 Cask - Finite Element Model (1)



ANSYS 5.3
DEC 15 1997
15:06:46
VOLUMES
MAT NUM

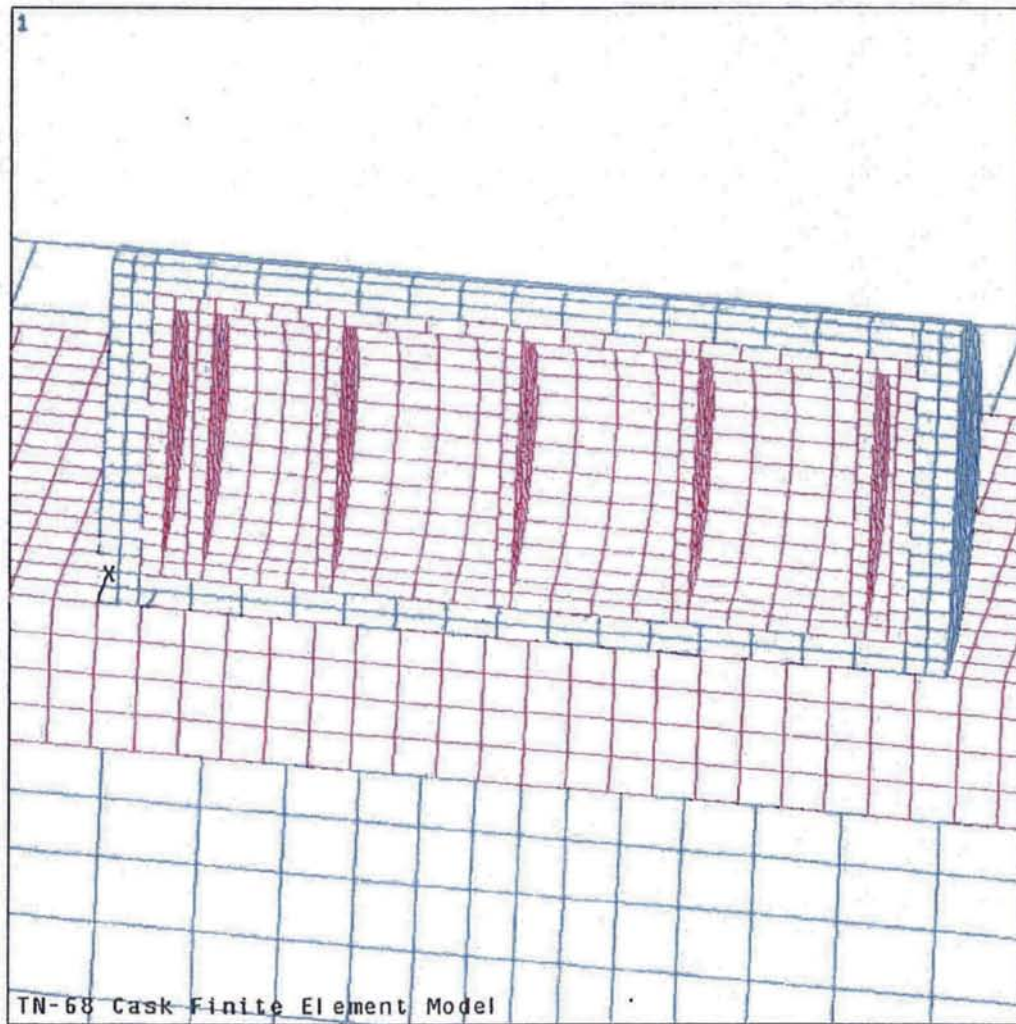
XV =-.9243
YV =.3163
ZV =.2135
*DIST=426.277
*XF =140.067
*YF =-251.069
*ZF =98.952
A-ZS=-.9631
Z-BUFFER

Figure 3D.2-6
TN-68 Cask - Finite Element Model (2)



```
ANSYS 5.3  
DEC 15 1997  
11:10:43  
ELEMENTS  
MAT NUM  
  
XV =-.919  
YV =.3778  
ZV =.113  
DIST=471.415  
XF =150  
YF =-222.75  
ZF =100  
A-ZS=-2.421  
PRECISE HIDDEN
```

Figure 3D.2-7
TN-68 Cask - Finite Element Model (3)



ANSYS 5.3
DEC 15 1997
11:11:30
ELEMENTS
MAT NUM

XV = -.919
YV = .3778
ZV = .113
*DIST=116.075
*XF = 214.059
*YF = -57.908
*ZF = 69.851
A-ZS=-2.421
PRECISE HIDDEN

Figure 3D.2-8
Weight and Dimensions of TN-68 Cask
(Weights of Trunnions, Neutron Shield, and Protective Cover are Included in the Cask)



Figure Withheld Under 10 CFR 2.390

Figure 3D.2-9
Finite Element Grid for Cask Drop on Concrete Slab

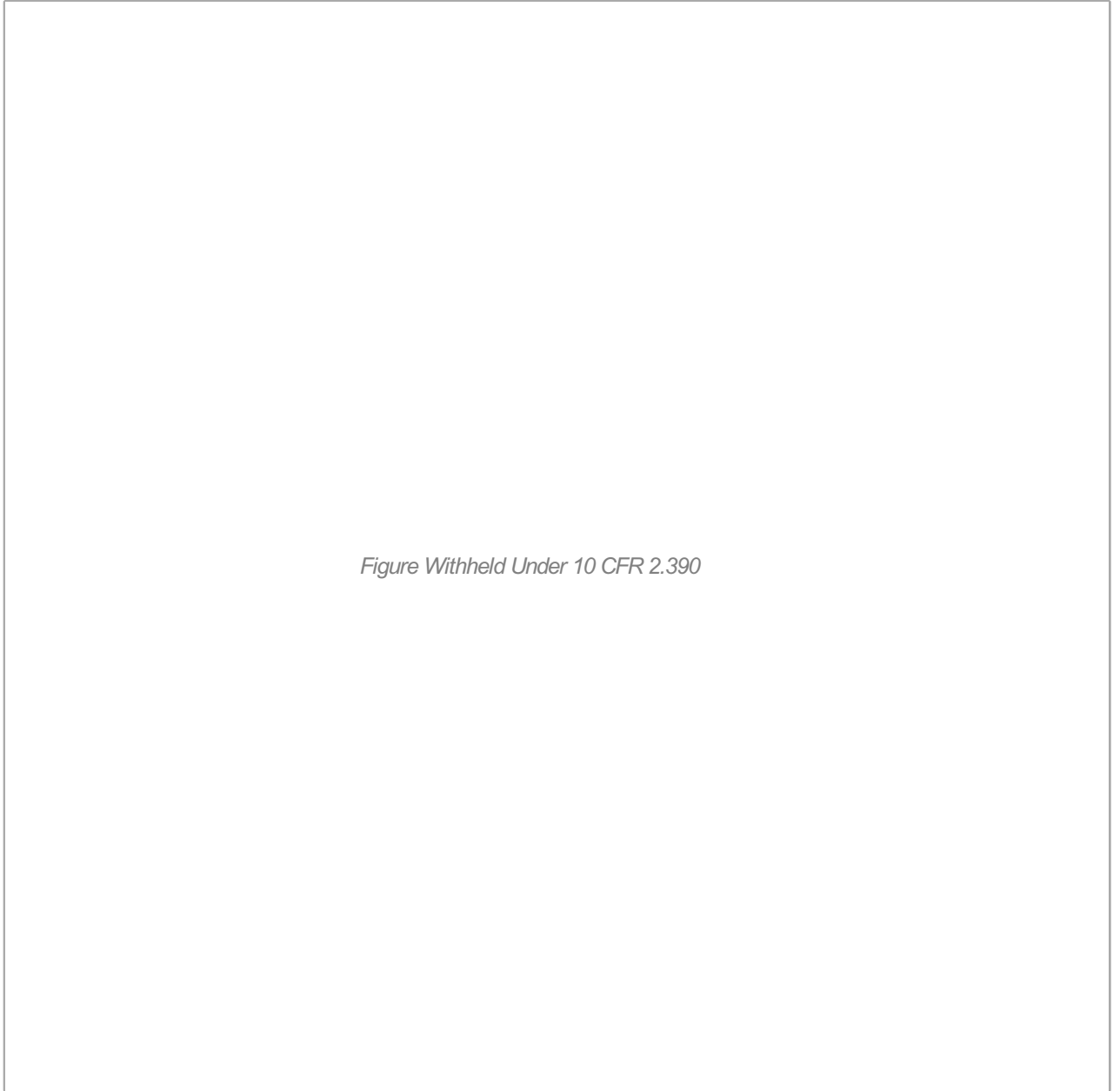
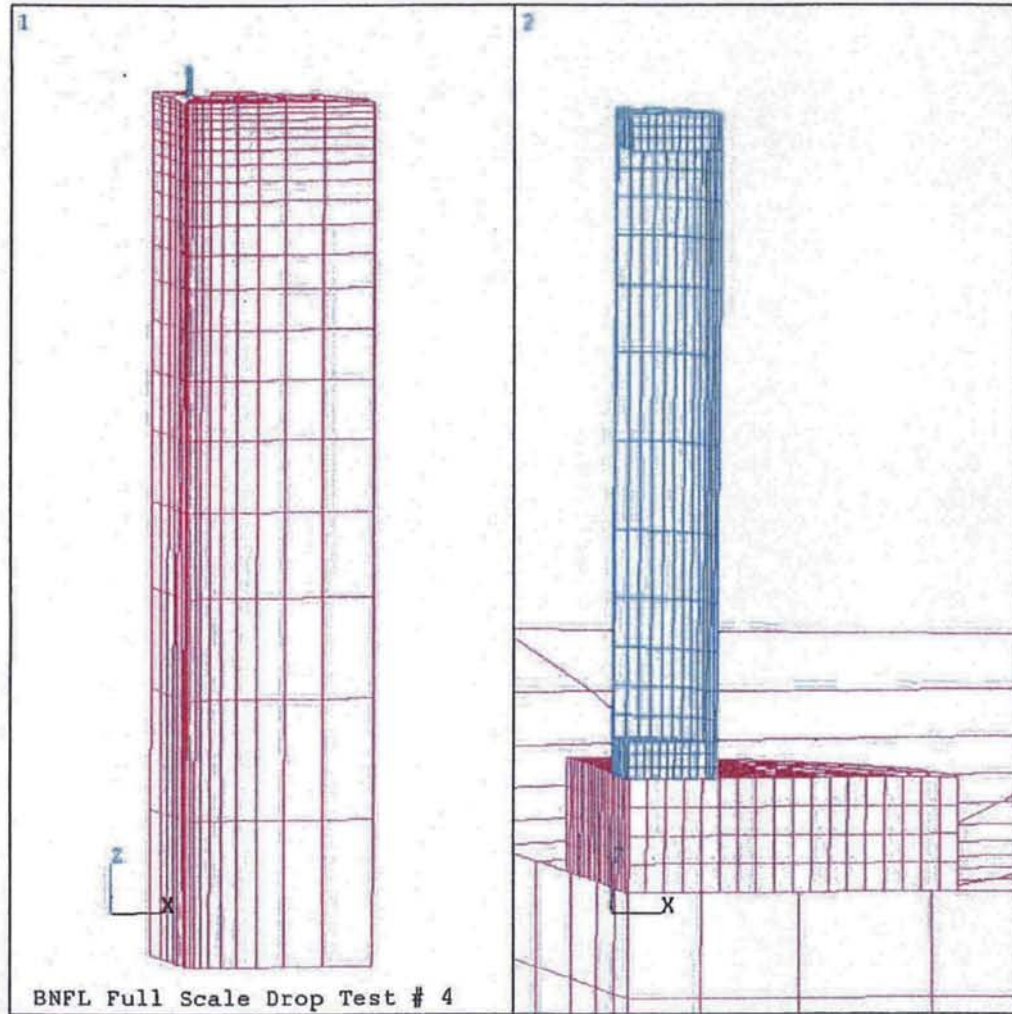


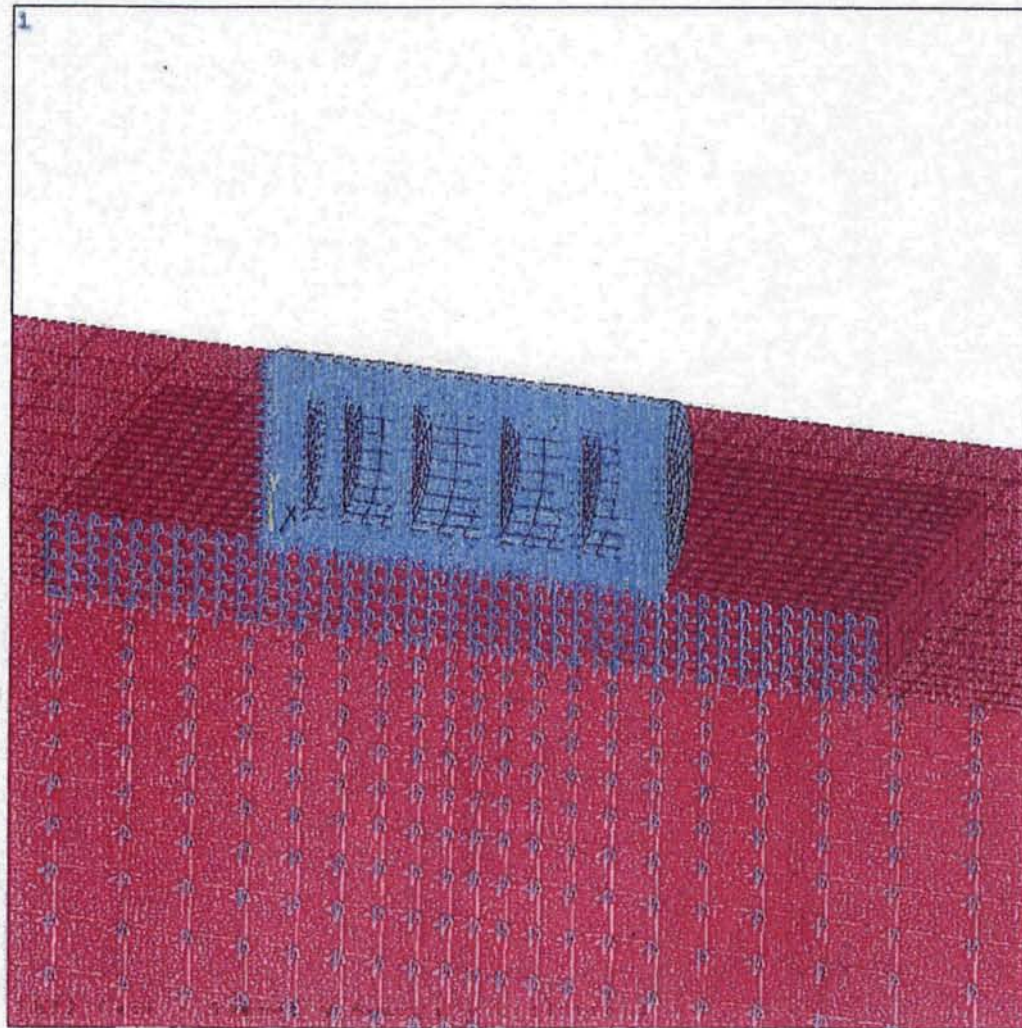
Figure Withheld Under 10 CFR 2.390

Figure 3D.2-10
Finite Element Model of BNFL Full Scale Drop Test #4



ANSYS 5.3
DEC 15 1997
07:12:29
ELEMENTS
MAT NUM

Figure 3D.3-1
TN-32 Cask - Symmetry Boundary Conditions



```
ANSYS 5.3  
DEC 15 1997  
09:36:45  
ELEMENTS  
MAT NUM  
U  
XV =-.8855  
YV =.3698  
ZV =.2814  
*DIST=226.744  
*XF =221.9  
*YF =-67.681  
*ZF =47.069  
A-ZS=-.6148  
Z-BUFFER
```

Figure 3D.3-2
TN-32 Cask - Modal Analysis

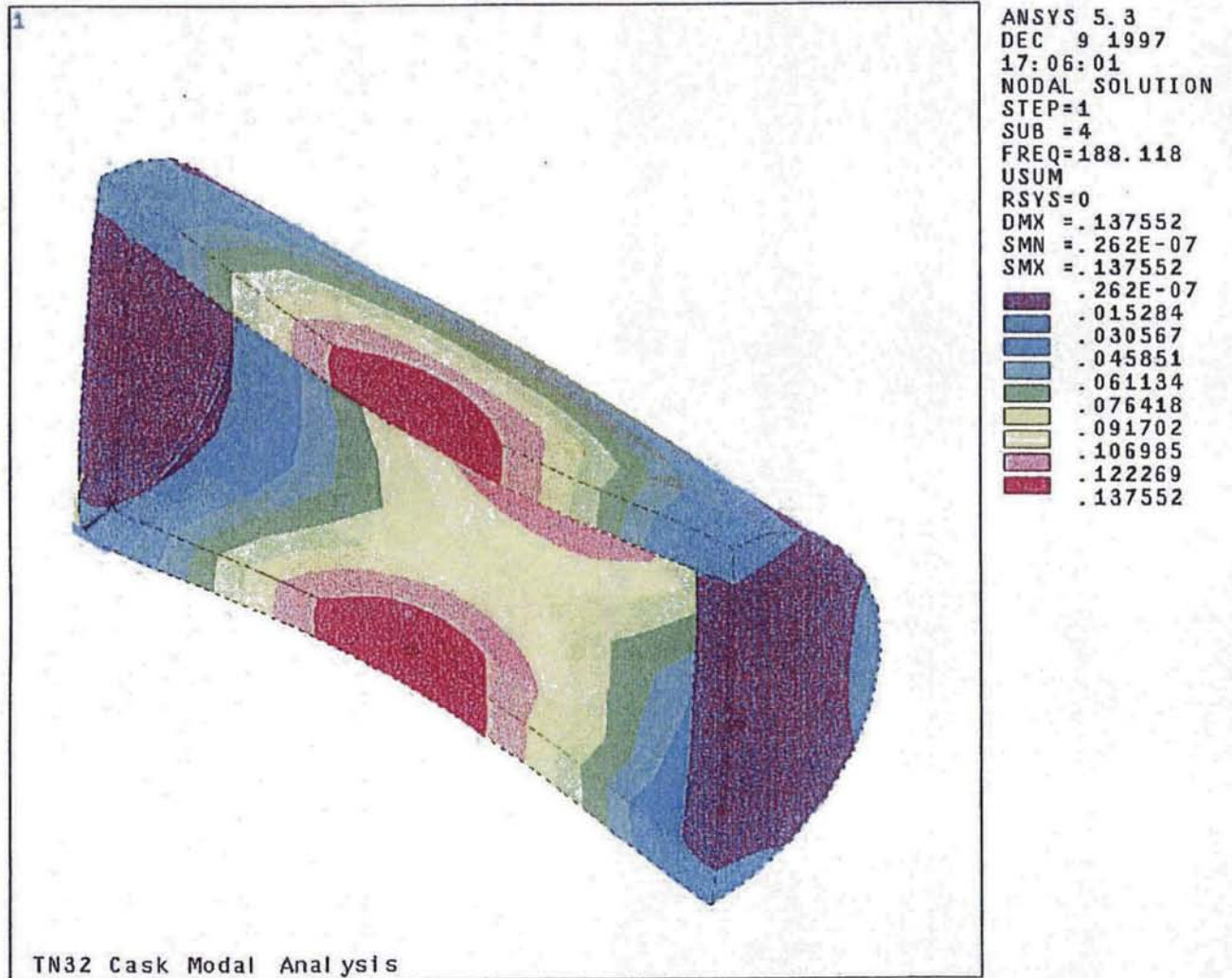


Figure 3D.3-3
TN-32 Cask - Modal Analysis of the Approximate Basket Model

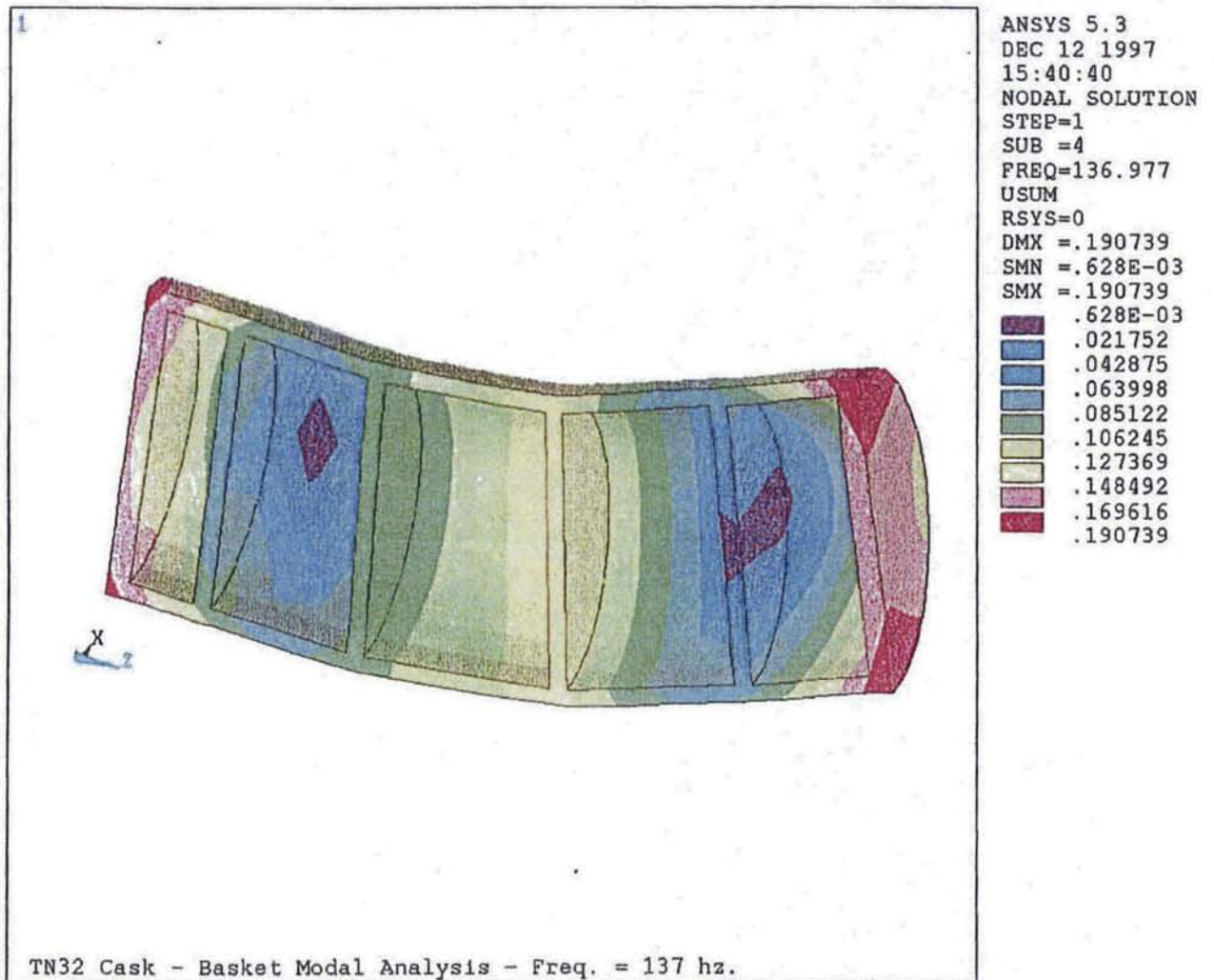


Figure 3D.3-4
TN-68 Cask Modal Analysis

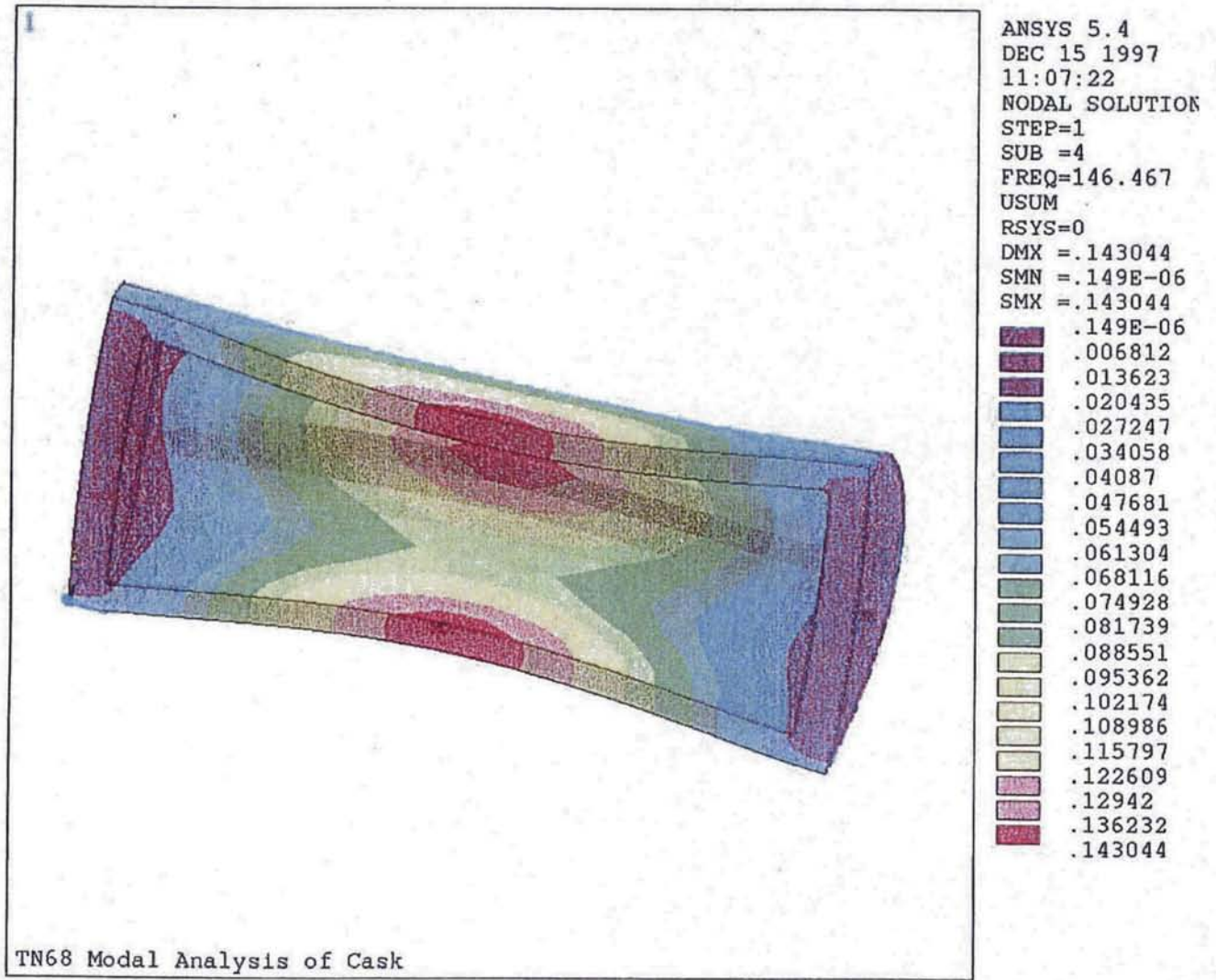


Figure 3D.3-5
TN-68 Cask - Modal Analysis of the Approximate Basket Model

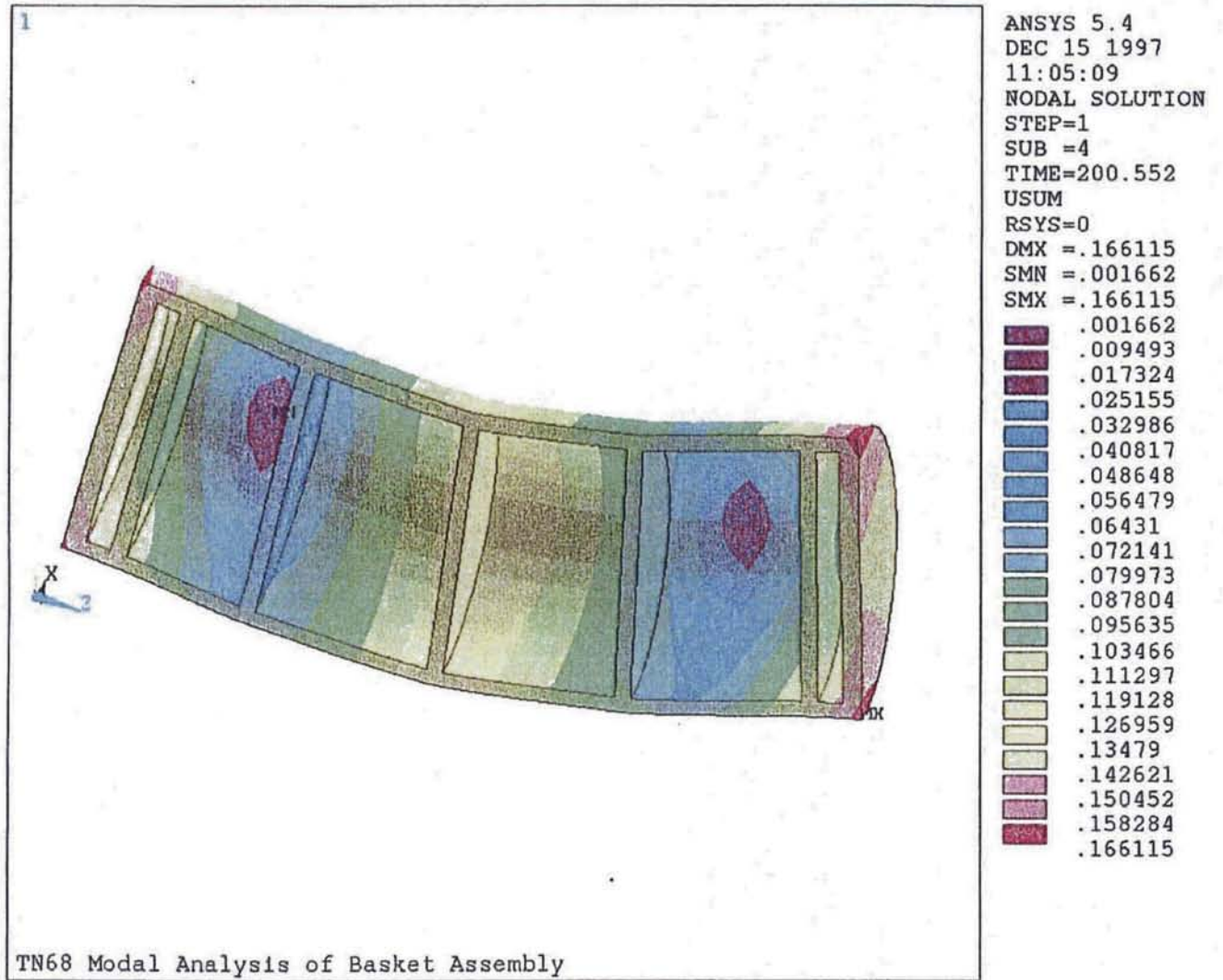


Figure 3D.3-6
BNFL Full Scale Drop Test #4 - Cask Modal Analysis

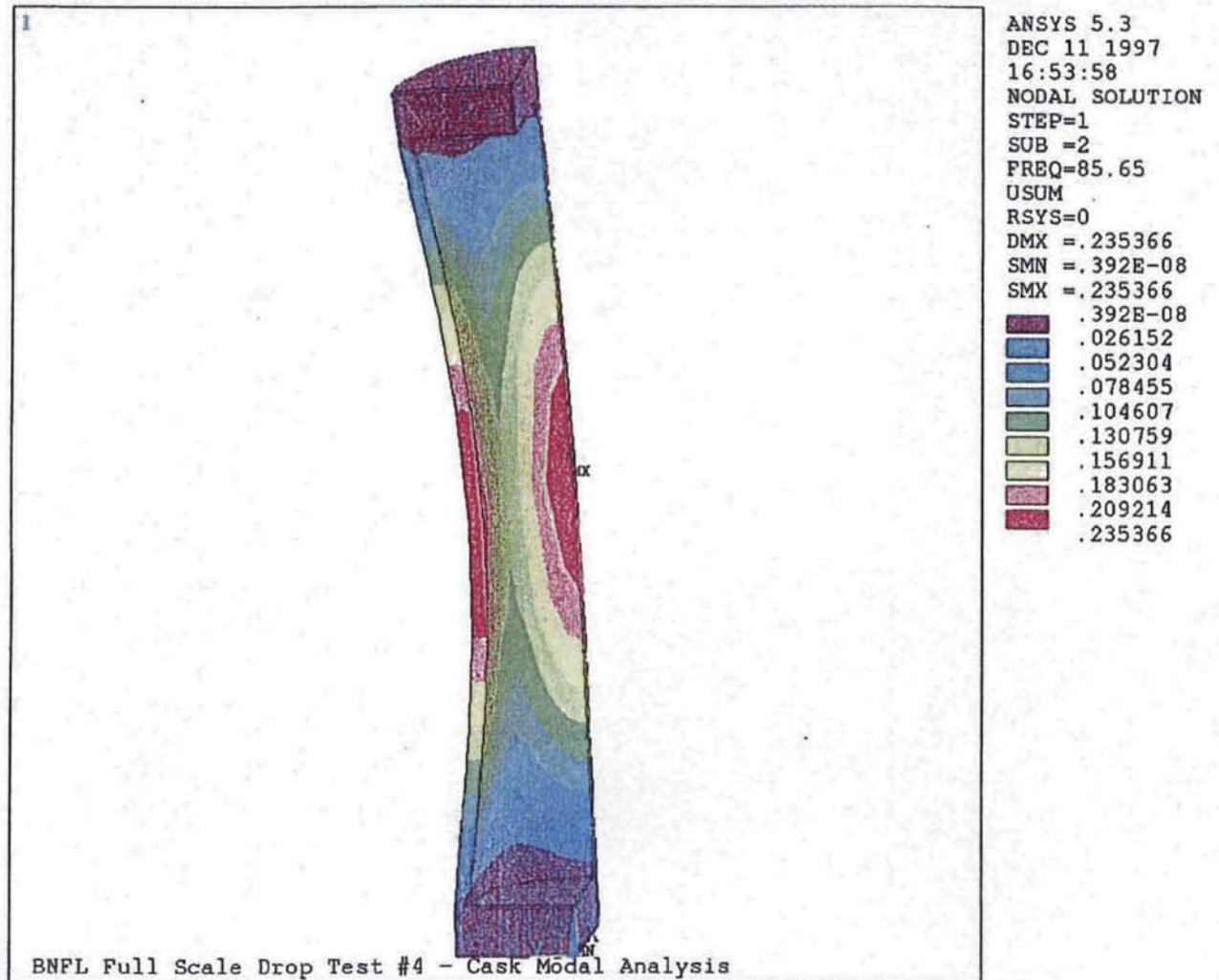
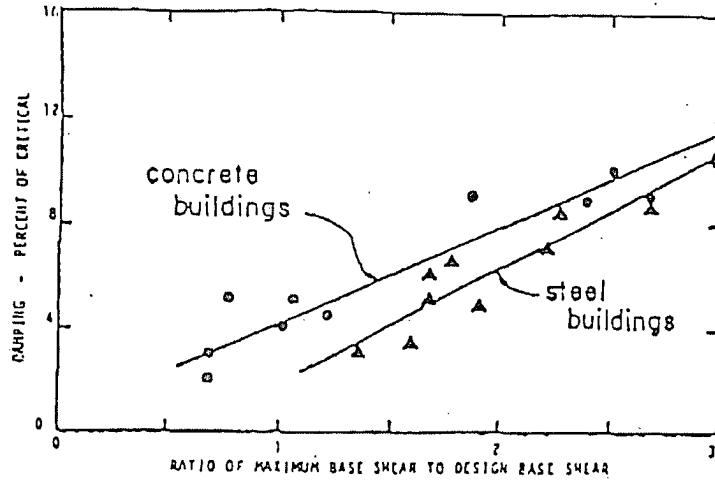
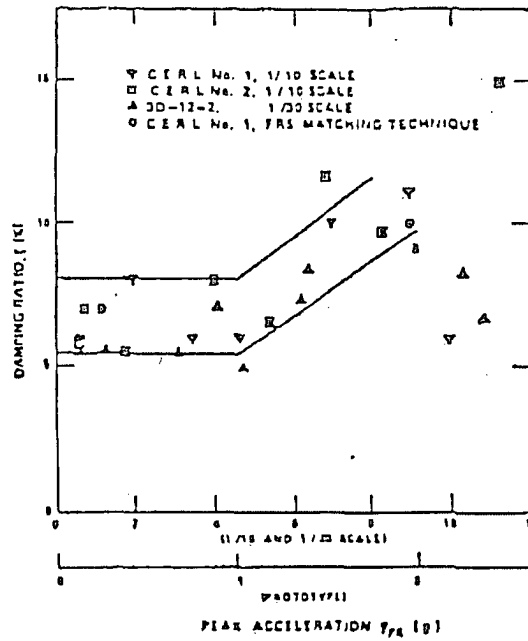


Figure 3D.3-7
 Damping Ratio Data Reproduced From References 13 and 14



Relationship of Effective First Mode Damping to Maximum Base Shear that Occured During the San fernando Earthquake (FROM REF. 13)



Measured Damping Ratios for Reinforced Concrete Category I Buildings (FROM REF. 14)

Figure 3D.3-8
Tipover Analysis Damping Coefficients

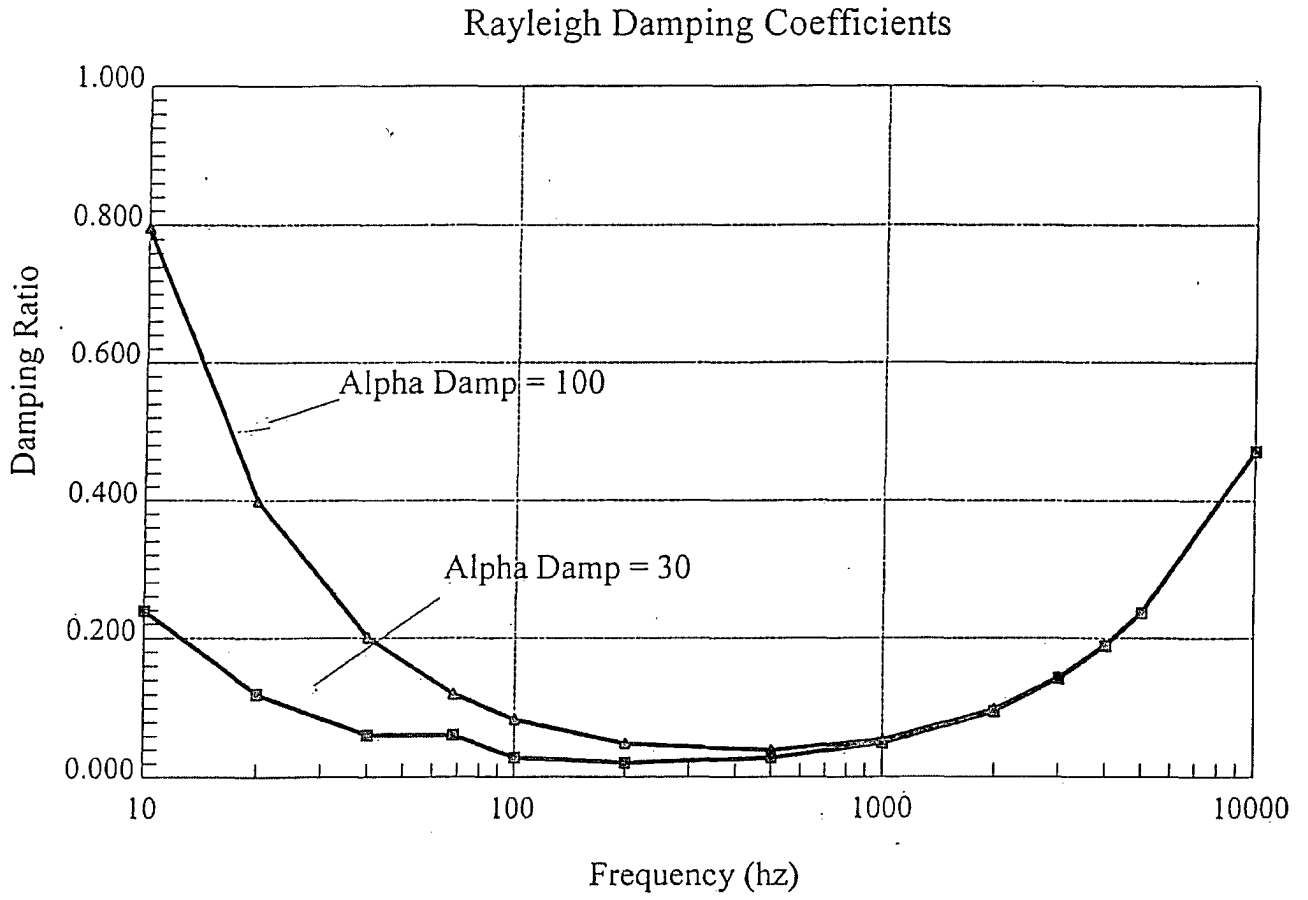


Figure 3D.4-1
BNFL Cask End Drop - Stress Plot

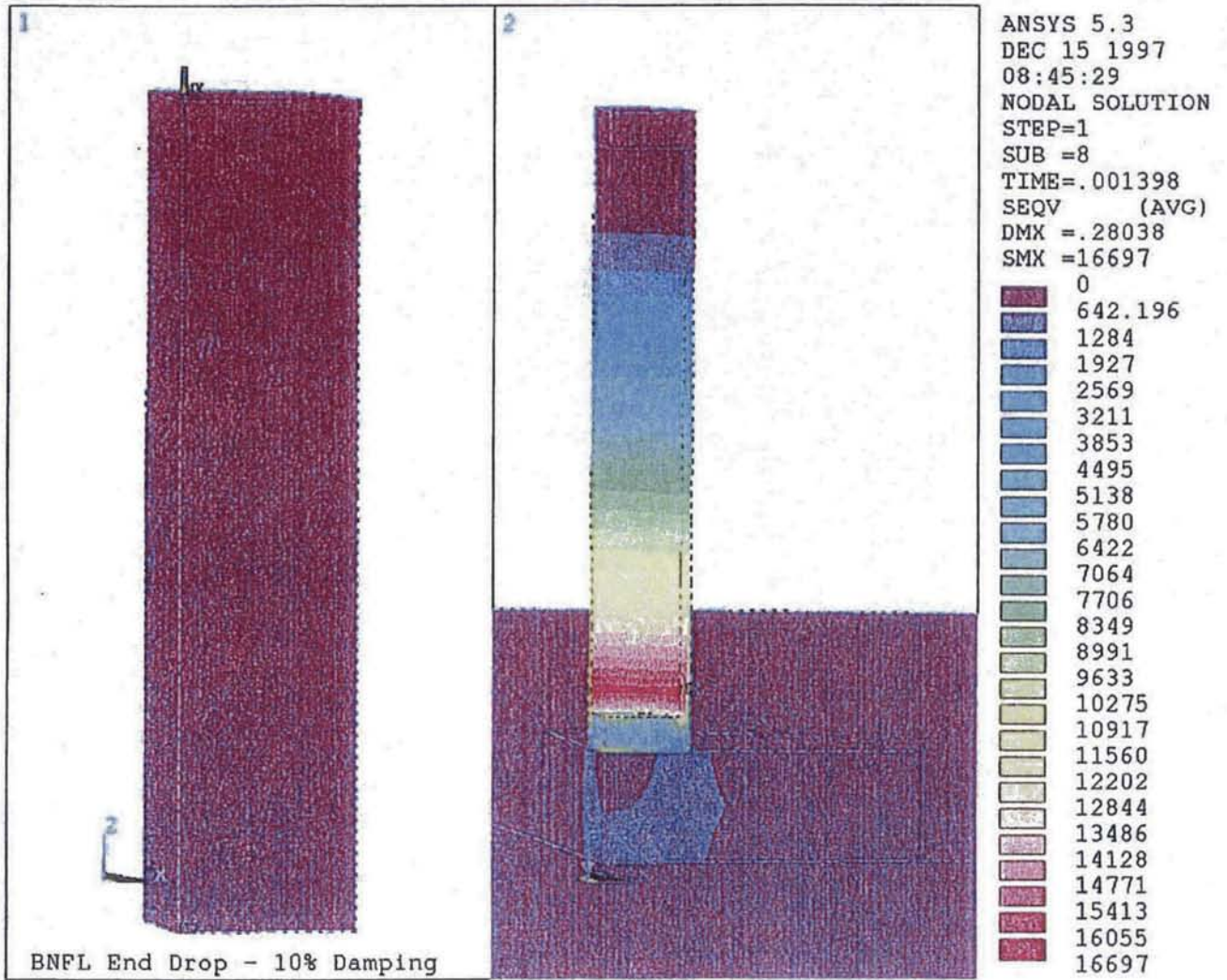


Figure 3D.4-2
BNFL Cask End Drop - Displacement Plot

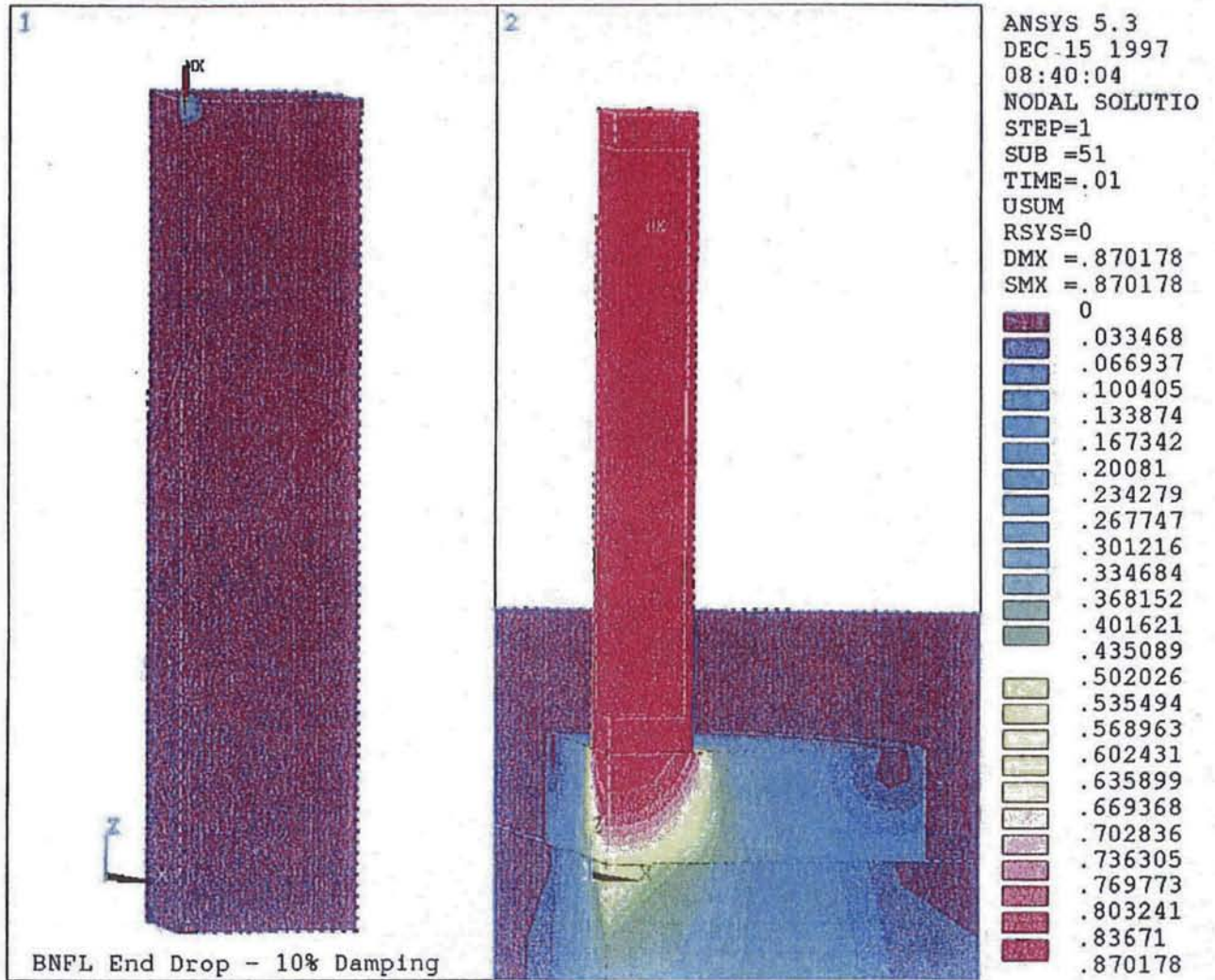
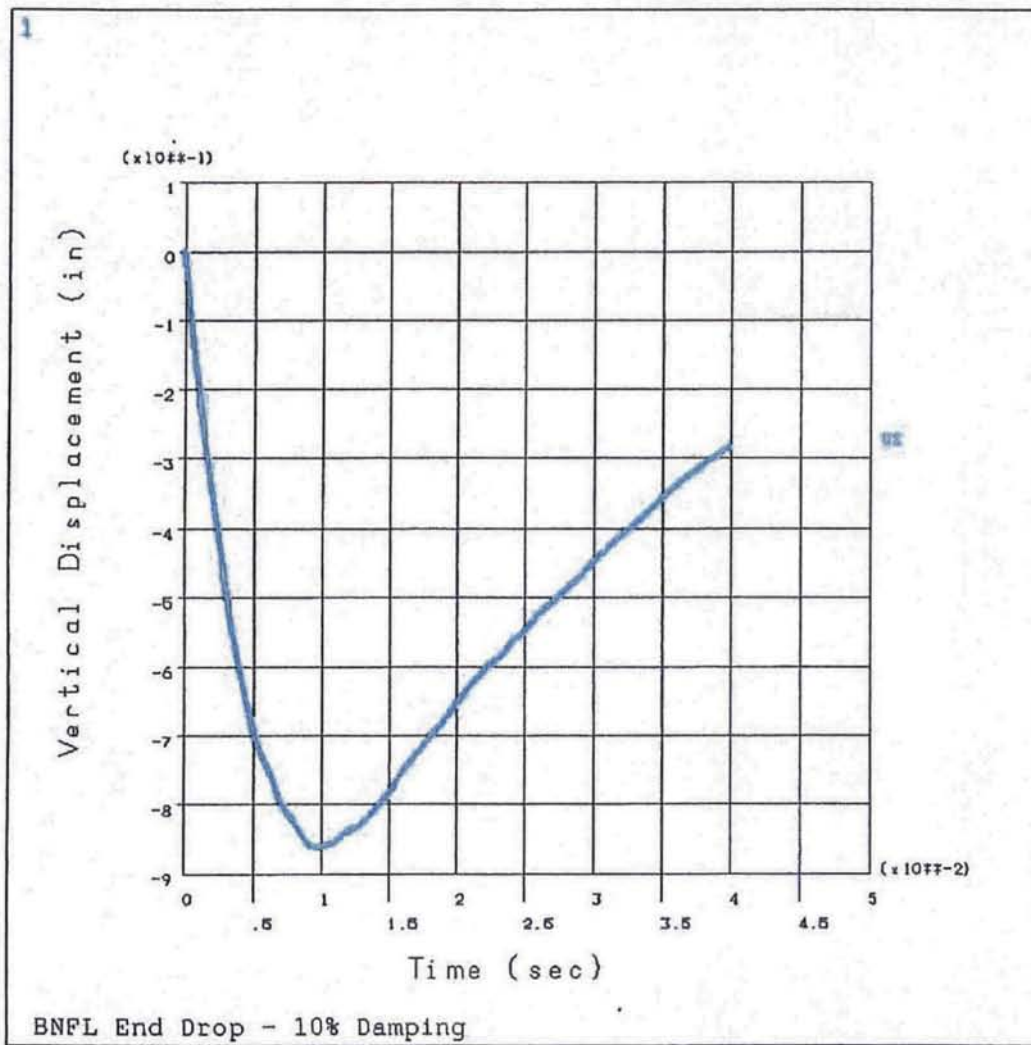


Figure 3D.4-3
BNFL Cask End Drop - Displacement Time History



ANSYS 5.3
DEC 15 1997
09:10:24
POST26

ZV =1
DIST=.75
XF =.5
YF =.5
ZF =.5
Z-BUFFER

Figure 3D.4-4
BNFL Cask End Drop - Acceleration Time History (TN Analysis)

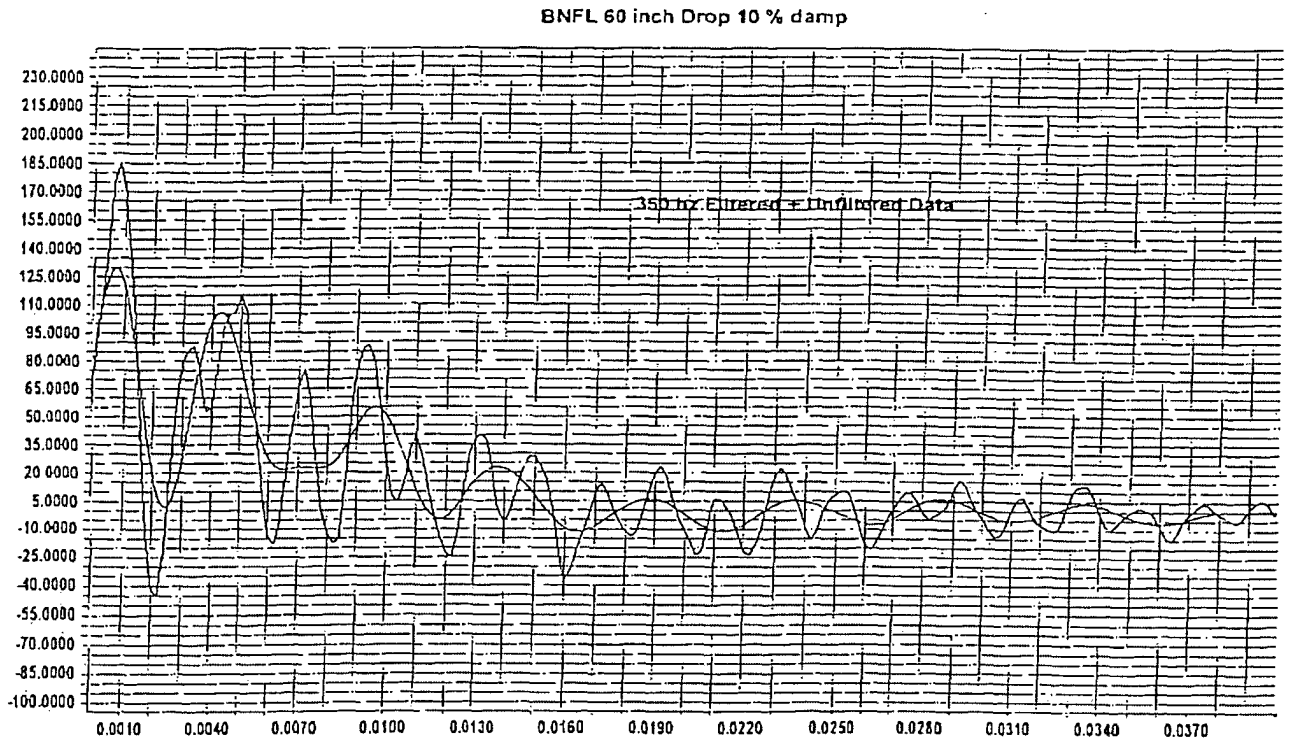


Figure 3D.4-5
BNFL Full Scale Drop Test #4 - Acceleration Time History (Test Data)

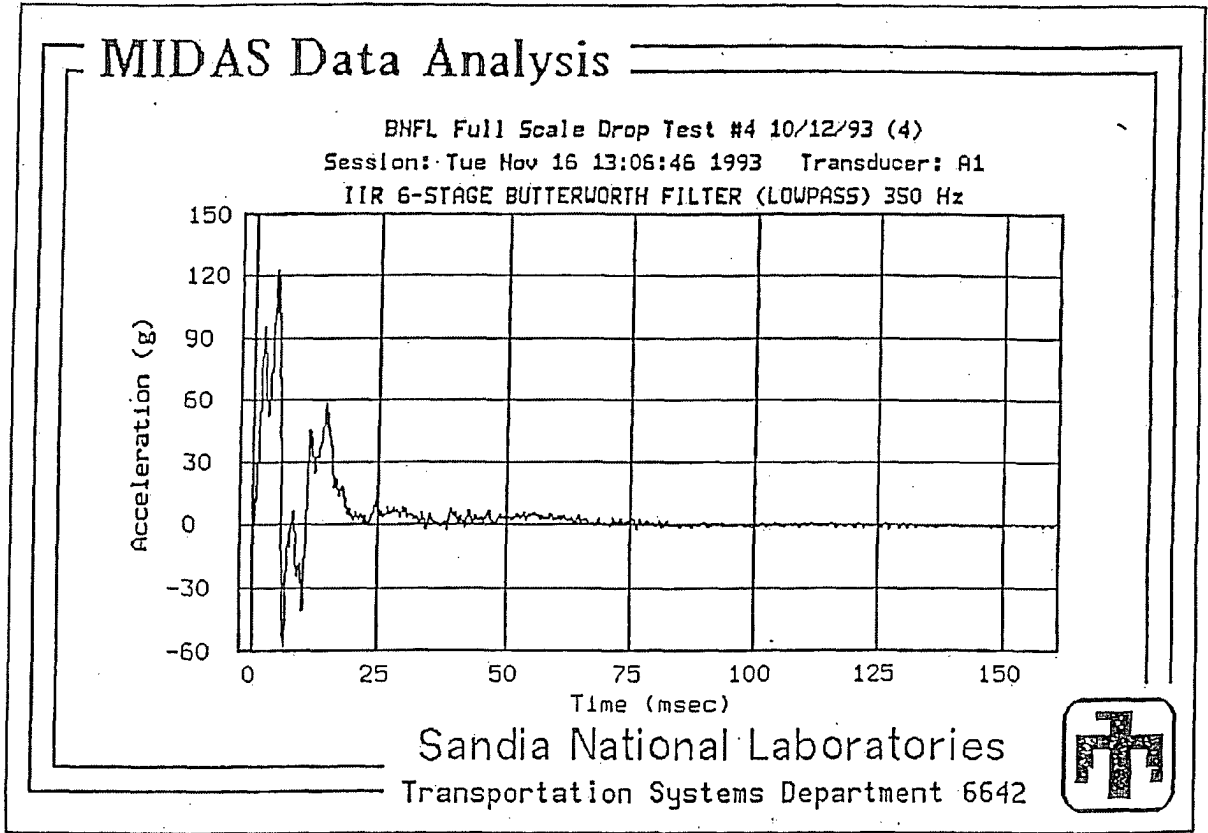


Figure 3D.4-6
TN-32 Cask Tipover Analysis - Acceleration Time History

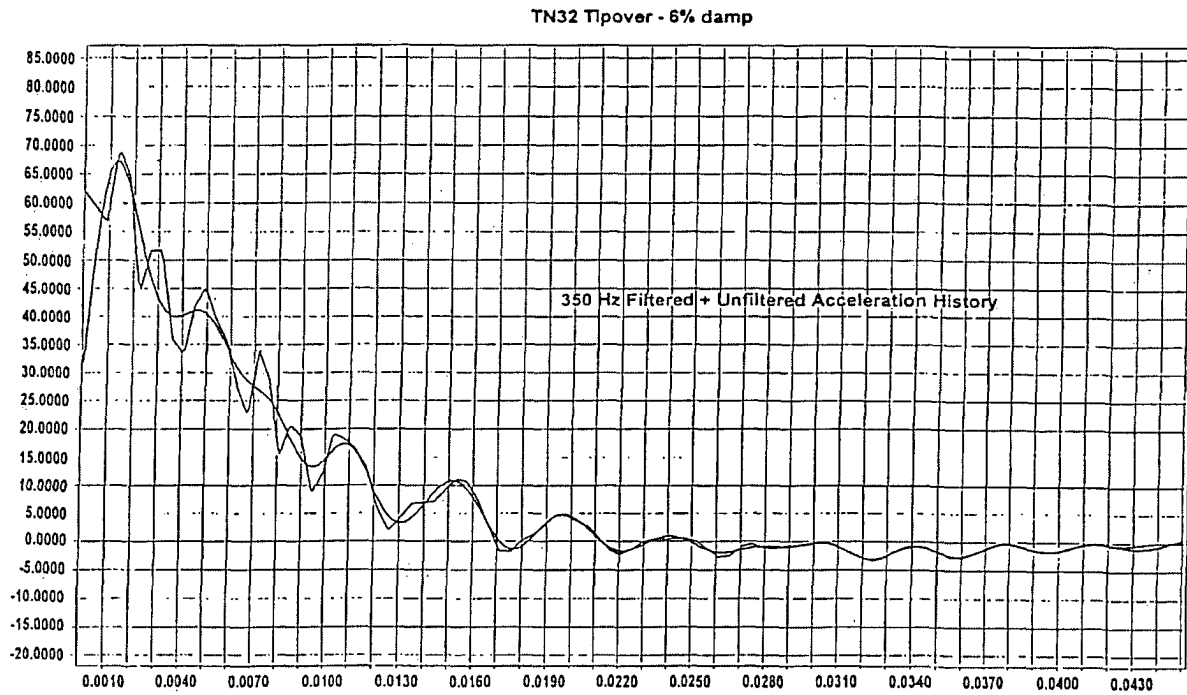


Figure 3D.4-7
Verification of DADisp Program - Sine Wave Pulse

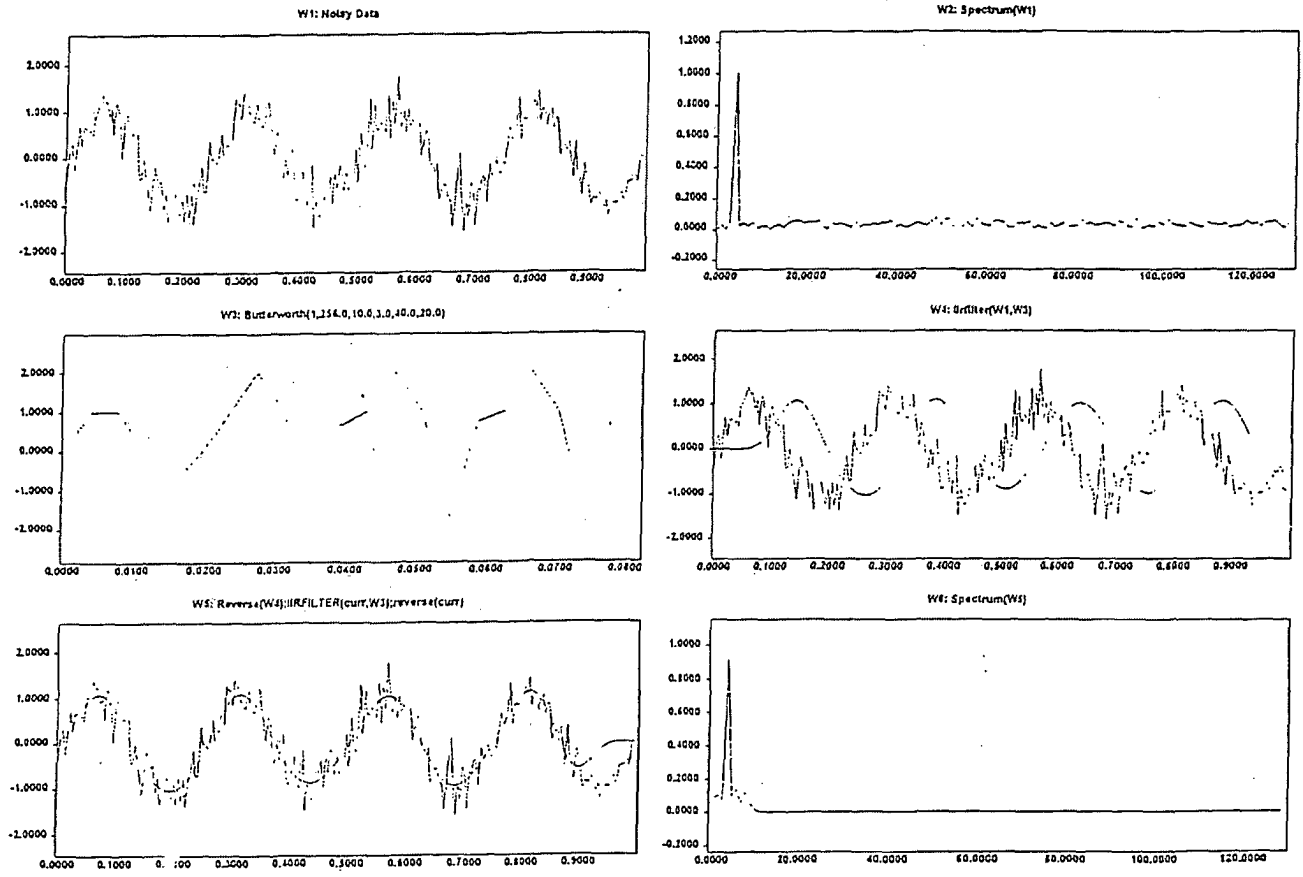


Figure 3D.4-8
18" Billet Side Drop Test Data From Channel A3 - Unfiltered and Filtered at 450 Hz
(Performed by TN)

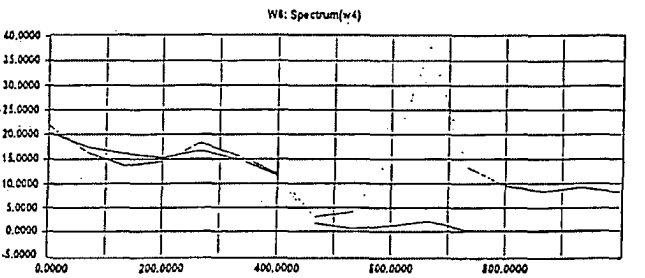
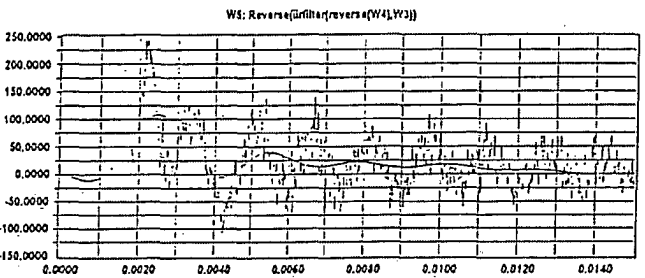
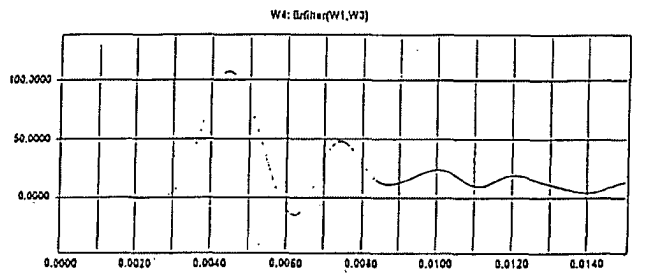
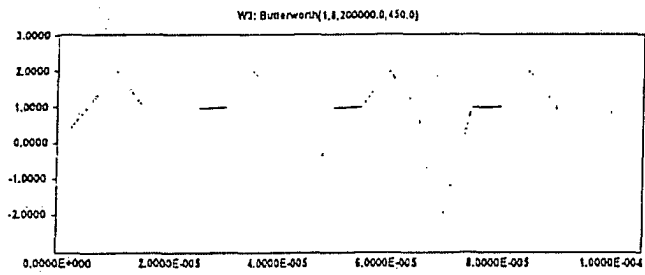
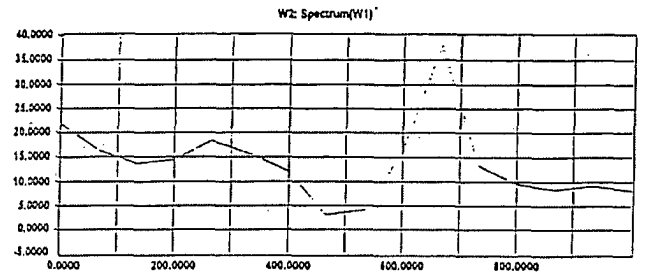
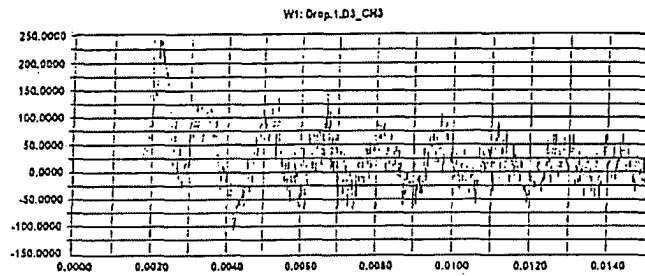
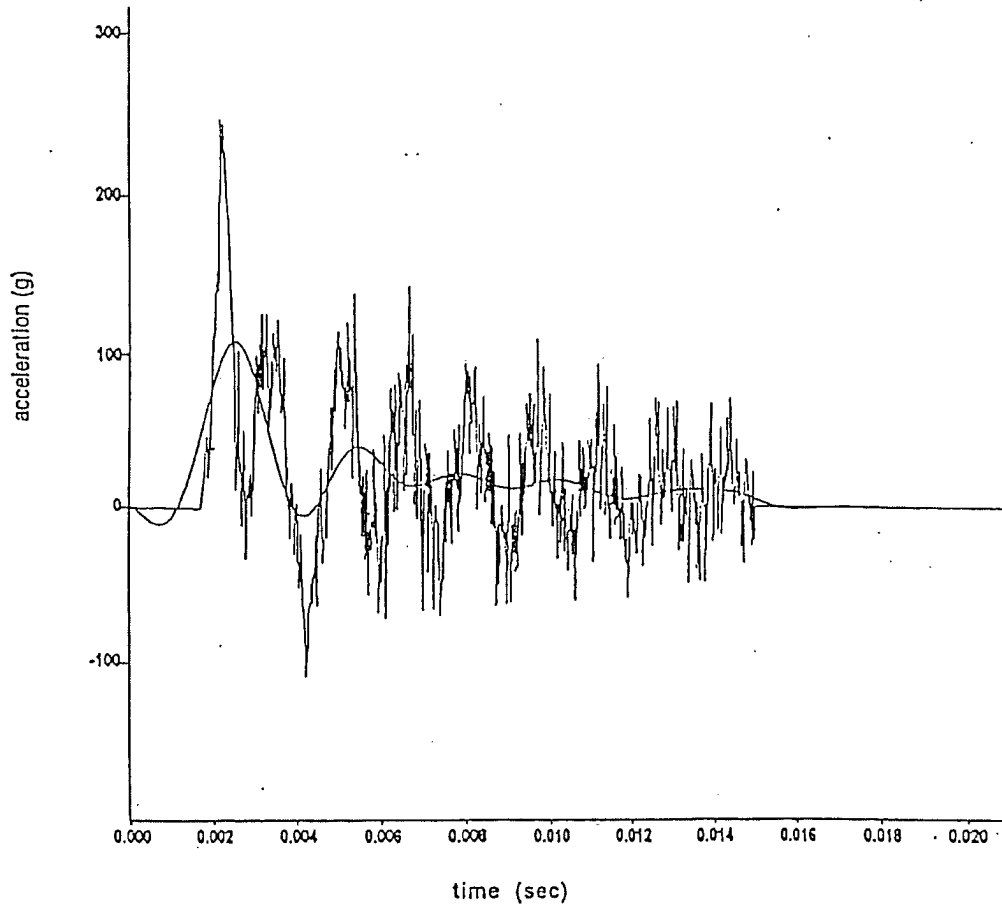


Figure 3D.4-9

18" Billet Side Drop Test Data From Channel A3 - Unfiltered and Filtered at 450 Hz
(Performed by LLNL)



Test #3, 18" billet side drop, test data from channel A3: unfiltered and filtered at 450 Hz, maximum acceleration = 108.2g

Figure 3D.5-1

TN-68 Cask Tipover Analysis - Displacement Time History Along The Length of The Cask

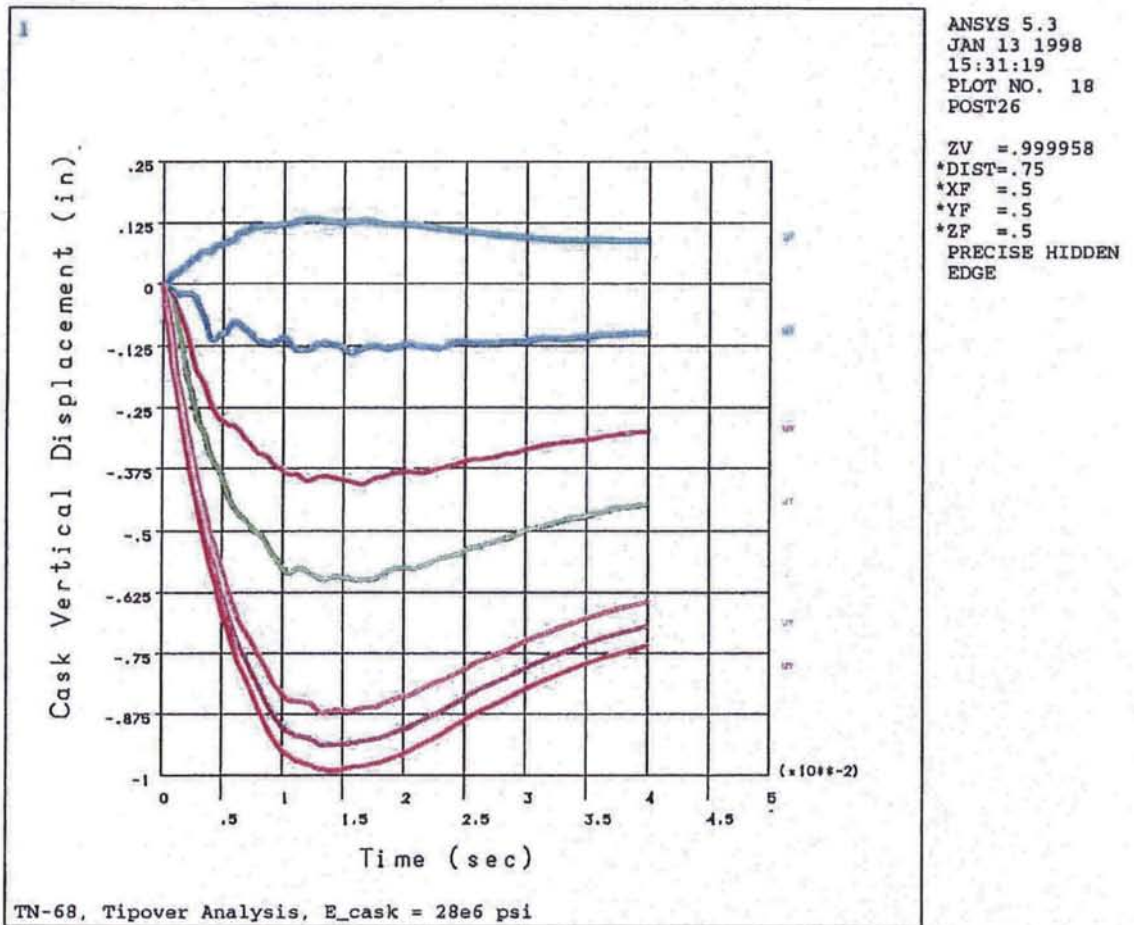


Figure 3D.5-2
TN-68 Cask Tipover Analysis - Displacement Plot (E = 28.3E6 psi)

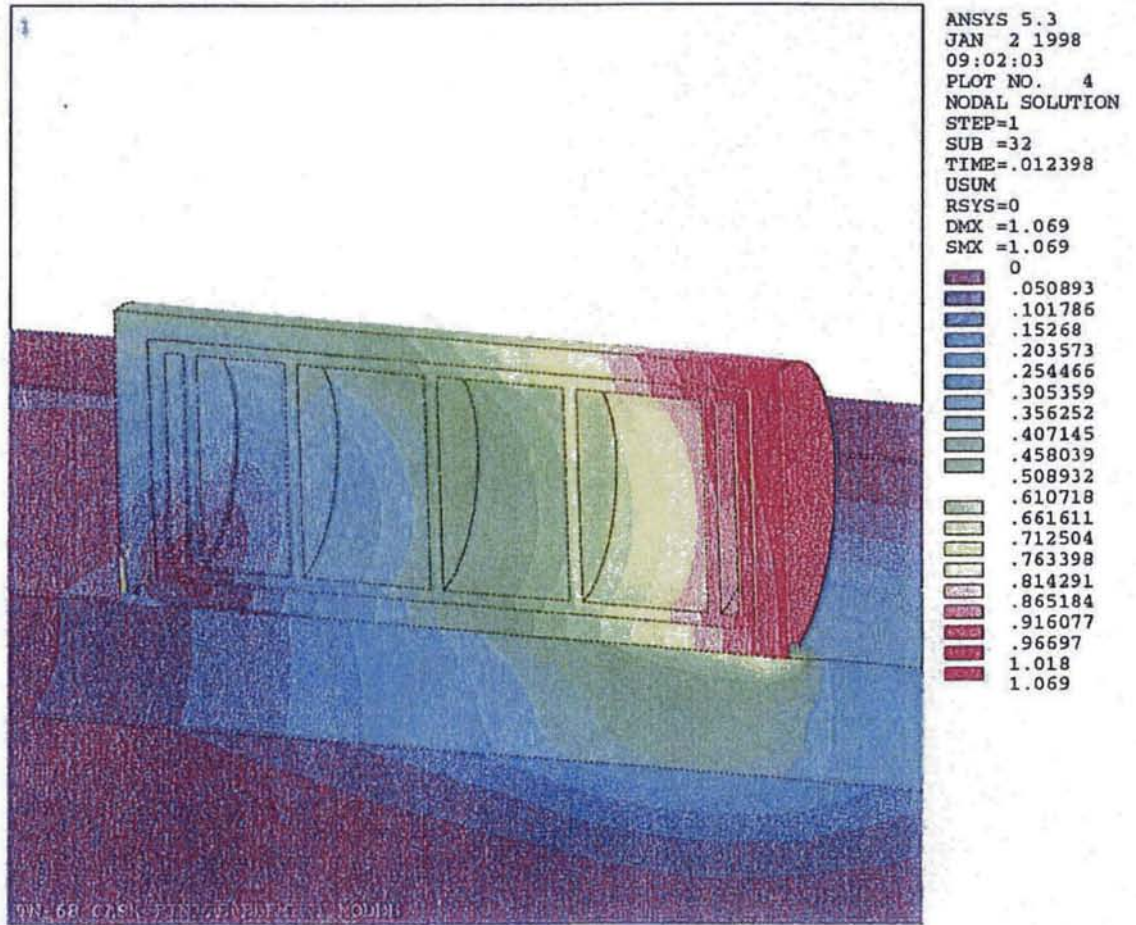


Figure 3D.5-3
TN-68 Cask Tipover Analysis - Von Mises Stress Plot (E = 28.3E6 psi)

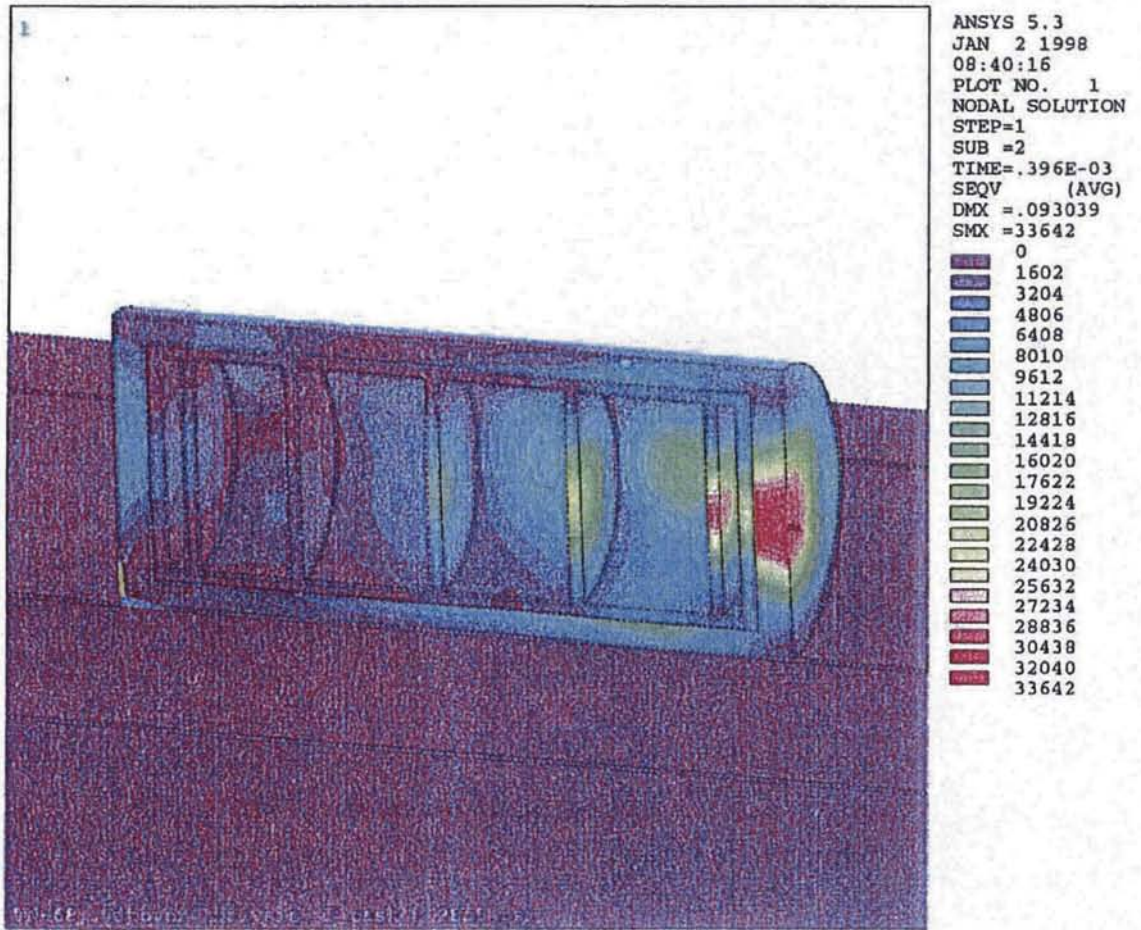


Figure 3D.5-4
TN-68 Cask Tipover Analysis - Acceleration Time History (E = 28.3E6 psi)

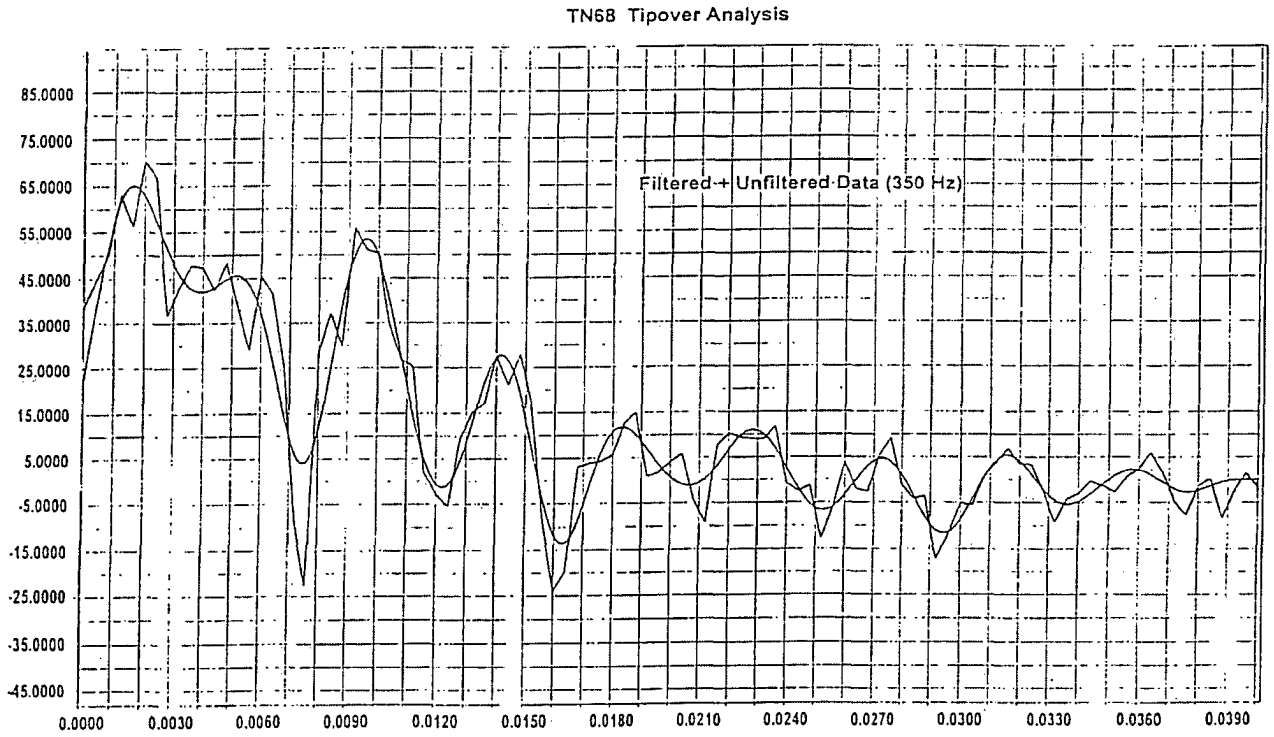


Figure 3D.5-5
TN-68 Cask Tipover Analysis - Acceleration Time History (E = 30E6 psi)

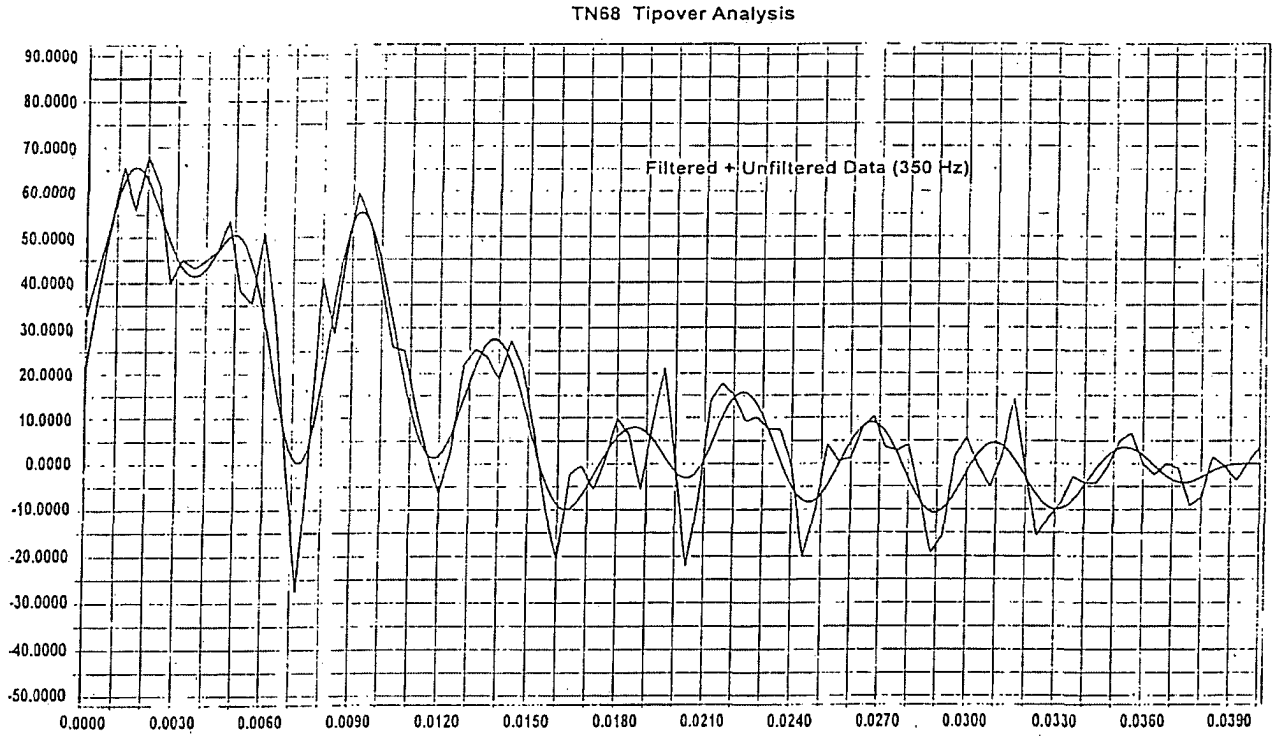
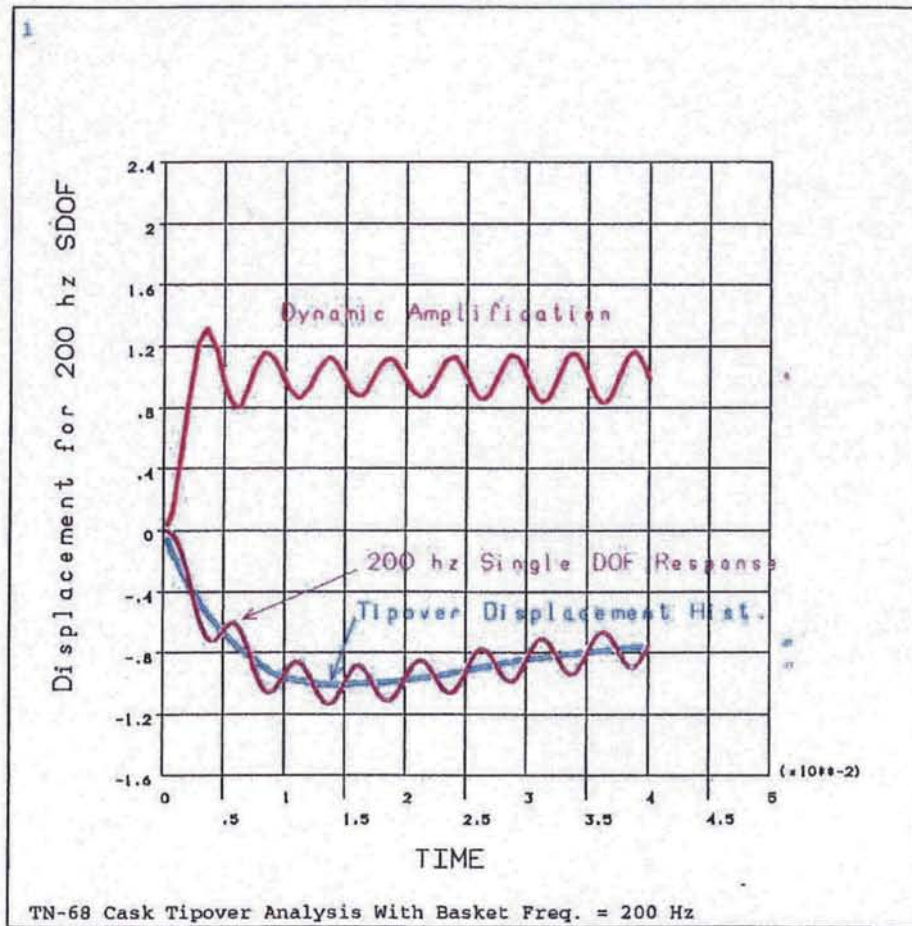


Figure 3D.5-6
Single Degree of Freedom Model



ANSYS 5.3
DEC 15 1997
15:11:06
ELEMENTS
TYPE NUM
U
ZV =1
DIST=55
YF =-50
Z-BUFFER

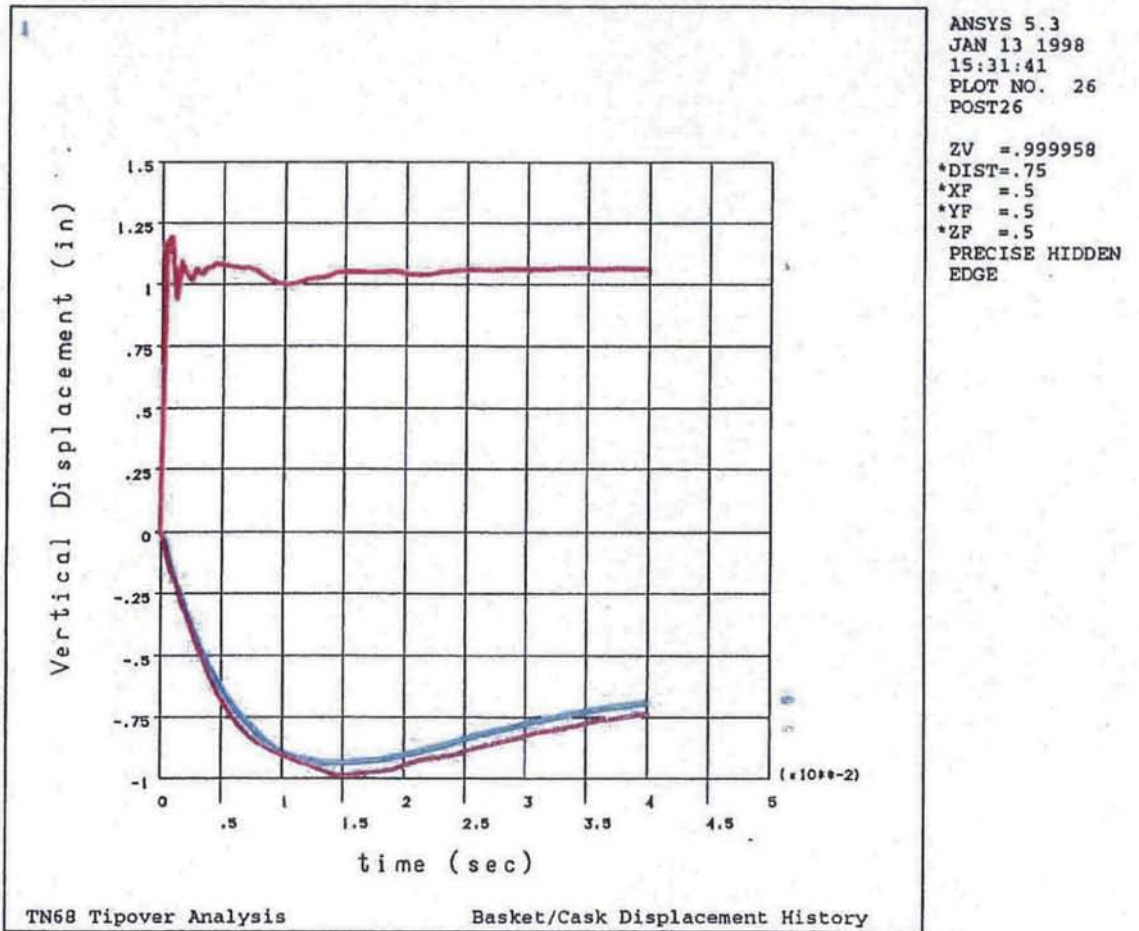
Figure 3D.5-7
Dynamic Amplification Factor ($E = 28.3E6$)



ANSYS 5.3
DEC 10 1997
14:59:48
PLOT NO. 8
POST26

ZV =1
DIST=.75
XF =.5
YF =.5
ZF =.5
Z-BUFFER

Figure 3D.5-8
Ratio of Max. Cask/Basket Displacement vs. Time (E = 28.3E6)



**TN-68 SAFETY ANALYSIS REPORT
TABLE OF CONTENTS**

SECTION	PAGE
Appendix 3E FRACTURE TOUGHNESS EVALUATION OF TN-68 CASK	
3E.1 Introduction.....	3E-1
3E.1.1 Fracture Toughness Evaluation of Confinement Boundary.....	3E-1
3E.1.2 Fracture Toughness Evaluation of Gamma Shield	3E-2
3E.1.3 References.....	3E-13

**TN-68 SAFETY ANALYSIS REPORT
TABLE OF CONTENTS**

List of Figures

- 3E-1 Locations of Fracture Toughness Evaluations (TN-68 Gamma Shield)
3E-2 Charpy V-Notch Test Results for SA-266 Gr. 2

APPENDIX 3E

FRACTURE TOUGHNESS EVALUATION OF TN-68 CASK

3E.1 Introduction

This appendix documents the fracture toughness requirements of the TN-68 confinement boundary and also calculates the allowable flaw sizes of the gamma shield and welds. The results of the flaw sizes can be used to develop an appropriate inspection program and select an appropriate inspection technique to properly inspect the cask. It can also be used as an initial screening criteria to disposition any indications which are detected during inspection.

The analysis is first performed for conditions corresponding to a 21.2 kW cask thermal load and is then scaled to conditions at 30 kW.

3E.1.1 Fracture Toughness Evaluation of Confinement Boundary

The TN-68 confinement boundary material is a ferritic steel and is therefore subject to fracture toughness requirements in order to assure ductile behavior at the lowest service temperature (LST) of -20°F . The confinement boundary materials (including lid bolts) are selected to meet the fracture toughness criteria of ASME Code Section III, Division 3⁽¹⁾, Subsection WB. The cask shell & bottom plate are 1.5 inches thick, the flange is 7.5 inches thick, and the lid plate is 5 inches thick. Therefore, by interpolating between values provided in Table WB-2331.2-1 of the Section III, Subsection WB (Para. WB-2300), the nil ductility transition temperatures (T_{NDT}) of the confinement boundary materials are:

- Shell and bottom plates: -80°F
- Flange: -133°F
- Lid plate: -126°F

In addition to determining the nil ductility transition temperature, Charpy v-notch testing shall be performed at a temperature no greater than 60°F above the T_{NDT} . The acceptance criteria is that the material exhibit at least 35 mils lateral expansion and not less than 50 ft-lbs absorbed energy. This testing is sufficient to ensure that the confinement boundary materials will not be susceptible to brittle fracture at -20°F .

The fracture toughness requirements of the lid bolts will meet the criteria of ASME Code, Section III, Division 3, Subsection WB (Para. WB-2333). Charpy v-notch testing shall be performed at -20°F . The acceptance criteria is that the material exhibit at least 25 mils lateral expansion (Table WB-2333-1).

3E.1.2 Fracture Toughness Evaluation of gamma shield

The gamma shield shell is forged from SA-266 Grade 2 material. The bottom shield plate is constructed from either SA-105 forging or SA-516 Grade 70 material, and top shield plate (plate welded to the bottom of the lid) is constructed from either SA-266 Grade 2 material, or SA-516 Grade 70 material. The main function of the gamma shield is to provide shielding. It is not part of the confinement, and its shielding properties are not temperature dependent.

In storage, the gamma shielding is not subjected to any significant loads. The worst case loading is due to the non-mechanistic tipover. The TN-68 cask is shown not to tipover during storage due to normal, off-normal or accident events. Nevertheless, a tipover event is evaluated. If the cask were to tipover at an ambient temperature of -20°F, it would not crack due to its reasonable fracture toughness at low temperature. However, even if it were to crack, there would be no breach of confinement, since the confinement materials have exceptional fracture toughness at low temperatures.

Furthermore, if the cylindrical gamma shielding were to crack, there is no credible mechanism for the shielding to separate from itself or the confinement. In order for this to occur, the 6 inch thick shell must become completely severed, and there would need to be a sufficient axial force to overcome the frictional forces holding the confinement vessel and the gamma shielding together resulting from the shrink fit. The top shield plate is welded to the lid and is captured by the confinement vessel. Even, if it is postulated that the weld fails completely, the shield plate will still remain inside the confinement boundary and will not lose its shield capability. The one exception is the weld of the gamma shield shell to the bottom plate. In this region, if the weld were to completely fail, the bottom plate could become detached and have an impact on the shielding capability of the cask.

Preliminary charpy test data of the same material (SA-266) from a similarly sized shield shell has been provided by one of the material manufacturers for the shield shell, and the results are tabulated below.

Charpy V-Notch Test – Results for SA-266 Gr. 2

Temperature	Specimen No.	Absorbed Energy (ft-lbs) Avg. of 3 specimens
0°C (32°F)	V1	63
	V2	60
-10°C (14°F)	V3	56
	V4	50
-20°C (-4°F)	V5	45
	V6	40
-30°C (-22°F)	V7	18
	V8	20
-40°C (-40°F)	V9	17
	V10	10

The TN-68 cask is designed for an ambient temperature of -20°F. As can be seen from the materials testing, even at temperatures as low as -20°F the gamma shielding has relatively good charpy impact properties. It is unlikely that the gamma shield would reach -20°F, since the heat load of the fuel would keep the cask temperatures elevated.

Shipping casks are often shipped empty or loaded with non-fuel components. Therefore, it is appropriate to neglect the heat load of the cask contents in determining the minimum service temperature. Unlike shipping casks, storage casks are not subjected to severe impact loads at severe temperatures. During storage, the casks are stationary and do not tipover due to seismic loads, tornado missiles and high winds.

Despite the fact that the shielding material is not part of the confinement boundary and it is unlikely that the gamma shield would reach -20°F, a fracture of the gamma shield will have no safety implications. However, Transnuclear has performed a fracture mechanics evaluation of the TN-68 Dry Storage Cask gamma shield based on a service temperature of -20°F. The work includes the following:

- Methodology
- Loadings
- Material fracture toughness
- Fracture toughness criteria
- Primary stress criteria
- Allowable flaw calculations
- Conclusions
- NDE Inspection Plan

Methodology

The allowable flaw sizes were performed using linear elastic fracture mechanics (LEFM) methodology from Section XI of ASME⁽²⁾ Code Section (1989). Flaws in the welds, if they occur, are welding defects, rather than initiated cracks. There is not an active mechanism for crack initiation and growth at any of the weld locations. Thus, the calculated allowable flaw sizes can be used during fabrication.

Loadings

The following table lists the maximum membrane and bending stresses at the gamma shield under normal and accident conditions for TN-68 contents up to 21.2 kW. Figure 3E-1 shows the selected locations on the gamma shield numbered 1 through 6 for fracture toughness analysis. These locations were selected to be representative of the stress distribution in the gamma shield with special attention given to areas subject to high stresses and weld locations. The maximum stress may occur at a different location for different load combinations (bolt preload, pressure, temperature, lifting load, fabrication stress, end drop, and tipover side drop).

Summary of Stress Components (21.2 kW)
(TN-68 Gamma Shield)

Location (Fig. 3E-1)	Normal Condition				Accident Condition				Residual Stress (ksi)
	Axial Stress (ksi)		Hoop Stress (ksi)		Axial Stress (ksi)		Hoop Stress (ksi)		
	σ_m	σ_b	σ_m	σ_b	σ_m	σ_b	σ_m	σ_b	
1	-0.06	0.53	1.34	0.21	-2.43	4.55	8.73	3.11	8.0
2	0.56	0.16	0.57	0.09	10.56	3.97	-1.22	0.18	36.0
3	0.31	0.96	2.87	0.75	-11.5	17.5	-8.0	48.5	0
4	0.26	0.53	0.32	0.64	-6.62	13.15	-1.31	1.75	0
5	-0.55	2.28	-0.08	1.86	-4.34	0.57	4.25	0.15	0
6	-0.50	0.29	0.28	0.2	0.5	2.15	-3.33	0.03	8.0

The gamma shield welds at locations 1 and 6 are partially stress relieved. However, the lower gamma shield welded to the bottom shield plate (location 2) does not undergo stress relief. Weld residual stress is included in the calculations for all weld locations. The weld residual stress is reduced due to the stress relief at all weld locations except the weld at location 2.

Weld residual stresses are steady state secondary stresses. The ASME Code does not prescribe limits for weld residual stresses. These stresses are displacement (or strain) controlled, and are self equilibrating through the weld thickness. For the purpose of this calculation, residual stresses will be conservatively assumed to be a constant tensile magnitude of 36 ksi at location 2. This value corresponds to the minimum specified yield stress of the base material (SA-266, Gr. 2). For other welds, which have been stress relieved, it is conservatively assumed that not all of the weld residual stress is relieved during the stress relief process. A stress value of 8 ksi has been included for welds at locations 1 & 6 for fracture toughness evaluations. This is similar to the procedure used in evaluation of reactor pressure vessel to account for the potential for remaining residual stress after post weld heat treatment.

The K due to residual stresses is applied with a safety factor of 1, as recommended in ASME, Section XI, Appendix H, Paragraph H-7300. Therefore, the total K_1 (applied) is determined from membrane, bending, and residual stresses.

Material Fracture Toughness

The gamma shield shell is a forged cylinder, nominally 6 inches thick by 180.15 inches long, made from SA-266, Gr. 2 material. The welding at the top flange and bottom plate may be performed using SAW, FCAW, or SMAW processes.

The results of the Charpy testing tabulated above are used. Figure 3E-2 shows a summary of the Charpy impact data used. The actual data points are shown along with a smoothed line that connects the average values at each test temperature. This data demonstrates that a lower bound Charpy impact value of 18 ft-lbs is appropriate for an exposure temperature of -20°F.

The Charpy impact measurement may be transformed into a fracture toughness value by using the empirical relation below (Ref.3):

$$K_{id} = [5E(C_v)]^{1/2} = 51,960 \text{ psi} \cdot (\text{in})^{1/2}$$

Where

K_{id} = Dynamic Fracture Toughness, psi \cdot (in)^{1/2}

E = Modulus of Elasticity, 30×10^6

C_v = Charpy Impact Measurement, 18 ft-lbs

For conservatism, the above calculated K_{id} was reduced by another 10% to 47 ksi- $(\text{in})^{1/2}$ (corresponding to 15 ft-lbs charpy values at -20°F) for fracture toughness evaluations.

Both the FCAW and SMAW electrodes used in the gamma shield weldments are alloyed with manganese, nickel, chromium, and vanadium. They are essentially matching filler metals for alloys such as ASME SA-533 Gr. B, the most commonly used reactor pressure vessel steel. The higher alloy content of the FCAW and SMAW electrodes and their typical usage in applications where good toughness is required indicate that the expected fracture toughness values for the FCAW and SMAW weld fillers are as good as or better than that of the SA-266 material. Use of the fracture properties from the wrought material for locations at or near the weld joints is conservative.

Fracture Toughness Criteria

Using the rule of Section XI, IWB-3613, the limiting fracture toughness values are reduced by a factor of $\sqrt{10}$ for the normal condition and $\sqrt{2}$ for the accident condition, to define the limiting allowable $K_{allowable}$. That is,

$$K_{allowable} \leq K_{ia} / (\sqrt{10}) = 14.86 \text{ ksi} \cdot \sqrt{\text{in}} \text{ for normal conditions}$$

$$K_{allowable} \leq K_{ic} / (\sqrt{2}) = 33.2 \text{ ksi} \cdot \sqrt{\text{in}} \text{ for accident conditions}$$

Where:

K_{ia} = the available fracture toughness based on crack arrest

K_{ic} = the available fracture toughness based on crack initiation

The K_{ia} value is conservatively used for fracture toughness evaluation for both normal and accident conditions.

Primary Stress Criteria

ASME Section XI, IWB-3610 requires that any flaw evaluation include verification that the primary stress limits of ASME Code Section III continue to be met for the flawed component. The following formula is conservatively assumed that the available cross section is equal to the original thickness minus the allowable flaw depth.

$$a_{all} = t(1 - S/S_{all})$$

Where:

a_{all} = allowable flaw depth based on ASME Code Section III limits

t = original local thickness

S = maximum calculated local stress intensity

S_{all} = allowable stress intensity per ASME Section III.

All stresses are considered to be pure tensile membrane stresses and that the stresses will increase linearly with decreasing wall thickness.

Allowable Flaw Size Calculation

Using the above load definitions and fracture toughness, a series of allowable flaw size calculations was performed using the Structural Integrity Associates computer program pc-CRACK™ (Ref. 4).

- Surface Flaws

For purpose of analysis, the postulated surface flaws are oriented in both the axial and circumferential direction. The cracks selected for each location are shown in the above table. The results of the pc-CRACK calculations are shown in the following table.

- Subsurface Flaws

The above discussion addressed the determination of allowable flaw sizes for flaws that are connected to the surface of the shield shell. The shell or weld could also contain subsurface defects.

An evaluation of allowable subsurface defects was performed using the same linear elastic fracture mechanics (LEFM) techniques as were described above for surface defects. For this case, a center cracked panel (CCP) model was used to evaluate an assumed length flaw. The flaw must be sufficiently embedded such that treatment as a subsurface flaw is justified. In general, if a flaw is closer to the surface than 0.4 of its half-depth, it must be considered a surface flaw.

The results of the pc-CRACK calculations are shown in the following table.

Allowable Surface Flaws Depth (inches)
(TN-68 Gamma Shield)

Location	Normal Condition		Accident Condition	
	⊥ to Axial Stress	⊥ to Hoop Stress	⊥ to Axial Stress	⊥ to Hoop Stress
1	-- (0.39)	-- (0.39)	-- (0.44)	-- (0.44)
2	0.32	0.27	0.34	0.29
3	-- (4.55)	2.05	-- (1.26)	0.192
4	5.79 (4.03)	5.54 (4.03)	-- (2.84)	-- (2.84)
5	-- (4.01)	3.24	-- (4.18)	2.23
6	0.5	0.46	0.48 (0.38)	0.48 (0.38)

Allowable Sub-Surface Flaws (Embedded) Depth (inches)

Location	Normal Condition		Accident Condition	
	⊥ to Axial Stress	⊥ to Hoop Stress	⊥ to Axial Stress	⊥ to Hoop Stress
1	-- (0.39)	-- (0.39)	-- (0.44)	0.44
2	0.71	0.72	0.4	0.8
3	--	4.38	5 (1.26)	0.41
4	-- (4.03)	-- (4.03)	6.06 (2.84)	-- (2.84)
5	-- (4.01)	-- (4.01)	-- (4.18)	-- (4.18)
6	-- (0.63)	-- (0.63)	-- (0.38)	-- (0.38)

Note:

“—” Indicates that the allowable flaw depth is not limited by fracture mechanics calculation.

“()” Indicates that the allowable flaw depth is limited by primary stress criteria.

Specific conservatisms included in the above analysis are listed below:

- All factors of safety on applied stress required by ASME Section XI (1989 Edition) were included in the evaluation.
- Weld residual stresses were treated as constant tensile stresses normal to the flaw orientation. Flaws were assumed to be long (infinitely long or full circumference)
- Lower bound material properties were used.

Stresses in the TN-68 cask gamma shield are also calculated based on cask contents up to 30 kW. The following table lists the maximum membrane and bending stresses at the gamma shield under normal and accident conditions for storing 30 kW.

Summary of Stress Components (for TN-68 Cask with 30 kW)
(TN-68 Gamma Shield)

Location (Fig. 3E-1)	Normal Condition				Accident Condition				Residual Stress (ksi)
	Axial Stress (ksi)		Hoop Stress (ksi)		Axial Stress (ksi)		Hoop Stress (ksi)		
	σ_m	σ_b	σ_m	σ_b	σ_m	σ_b	σ_m	σ_b	
1	-0.69	0.83	0.7	0.32	-3.03	4.81	-7.75	3.21	8.0
2	1.15	0.09	2.03	0.10	11.25	3.64	0.22	0.07	36.0
3	0.29	1.56	2.53	0.91	-11.8	17.15	-9.34	49.12	0
4	0.75	1.14	0.93	0.15	-6.28	12.68	-0.6	1.24	0
5	-0.64	1.72	-0.29	1.40	-4.43	0.02	4.04	0.81	0
6	-0.27	0.09	-0.08	0.25	0.75	2.37	-3.67	0.09	8.0

The different between the stresses in this table and previous calculated stress table based on 21.2 kW are very small. Therefore, the flaw sizes from the stresses calculated from the TN-68 cask with 30 kW contents are scaled from the previous table by using the following formula (only flaw sizes limited by fracture mechanic calculations are ratioed).

$$a_1 = a_2 \times (\sigma_1/\sigma_2)^2$$

Where a_1 = Flaw size for the stresses based on TN-68 cask with high burn up fuel
 a_2 = Flaw size for the stresses based on TN-68 cask with fuel up to 21.2 kW
 σ_1 = Stresses calculated based on TN cask with fuel up to 21.2 kW
 σ_2 = Stresses calculated based on TN cask with high burn up fuel

The results are listed in the flowing table.

Allowable Surface Flaws Depth (inches) for TN-68 Cask with 30 kW Fuel
(TN-68 Gamma Shield)

Location	Normal Condition		Accident Condition	
	⊥ to Axial Stress	⊥ to Hoop Stress	⊥ to Axial Stress	⊥ to Hoop Stress
1	-- (0.39)	-- (0.39)	-- (0.44)	-- (0.44)
2	0.31	0.25	0.335	0.27
3	-- (4.55)	2.27	-- (1.26)	0.199
4	1.01 (4.03)	4.38 (4.03)	-- (2.84)	-- (2.84)
5	-- (4.01)	--	-- (4.18)	1.835
6	0.496	0.495	0.44 (0.38)	0.545 (0.38)

Allowable Sub-Surface Flaws Depth (inches) for TN-68 Cask with 30 kW Fuel
(TN-68 Gamma Shield)

Location	Normal Condition		Accident Condition	
	⊥ to Axial Stress	⊥ to Hoop Stress	⊥ to Axial Stress	⊥ to Hoop Stress
1	-- (0.39)	-- (0.39)	-- (0.44)	0.44
2	0.68	0.66	0.39	0.74
3	--	4.85	6.288 (1.26)	0.42
4	-- (4.03)	-- (4.03)	6.3 (2.84)	-- (2.84)
5	-- (4.01)	-- (4.01)	-- (4.18)	-- (4.18)
6	-- (0.63)	-- (0.63)	-- (0.38)	-- (0.38)

Note:

- Indicates that the allowable flaw depth is not limited by fracture mechanics calculation.
- () Indicates that the allowable flaw depth is limited by primary stress criteria.

Conclusions

The gamma shield is not part of the confinement boundary. Cracks postulated in the gamma shield will not propagate into the confinement boundary due to the geometry of the cask. If the gamma shield were to fracture along the length or around the circumference or around the weld between the gamma shield and top flange, there is no credible mechanism which would result in the gamma shielding separating from the confinement boundary. The top shield plate is welded to the lid and is captured by the confinement vessel. Therefore, if the weld were to completely fail the shield plate will still remain inside the confinement boundary and will not lose its shielding capability. Therefore, even if a fracture were to occur in the gamma shield shell or the weld between the gamma shield and top flange or top shield plate or weld between top shield plate and lid, there would be no safety significance, since confinement would be maintained, and shielding would not be impaired. The one exception is in the region of the weld of the gamma shield shell to the bottom plate. In this region, if the weld were to completely fail, the bottom plate could become detached and have an impact on the shielding capability of the cask.

NDE Inspection Plan

The results of the fracture toughness analysis shows that the flaws in the gamma shield shell and top and bottom shield plates which would result in unstable crack growth or brittle fracture are larger than those generally observed in forged steel and plate components. No special examination requirements on the gamma shield shell, top and bottom shield plates are required.

The flaw sizes in the welds which could result in brittle fracture at -20°F will be detected by NDE methods. The welds at locations 1 if it were to completely fail, would be no safety significance. Therefore, only PT or MT of the final is be specified.

If the bottom plate weld were to completely fail, the bottom plate could become detached and have an impact on the shielding capability of the cask. The minimum allowable flaw sizes for surface and subsurface are 0.25 in. and 0.39 in., respectively. Therefore, the following NDE will be used to ensure defects of the minimum flaw sizes calculated are detected and repaired prior to used for fuel storage.

- PT or MT at weld preparation surfaces (base metal)
- PT or MT at root pass
- PT or MT for each 0.375 inches of weld
- PT or MT at final surface

The weld at location 6, if it were to completely fail, could result in a drop of the shield plug into the cask cavity. Therefore the NDE requirements specified for the location 6 weld will be the same as that specified for the location 2 weld above.

The liquid penetrant or magnetic particle method will be in accordance with Section V, Article 6 of ASME Code.

3E.1.3 References

1. ASME Section III, Division 3, Containment System and transport Packaging for spent Nuclear Fuel and High Level Radioactive waste.
2. ASME Code Section XI, 1989.
3. NUREG/CR-1815, Recommendations for Protecting Against Failure by Brittle Fracture in Ferritic Steel Shipping containers up to four Inches Thick.
4. Structural Integrity Associates, pc-CRACK™ for Windows, Version 3.0, March 27, 1997.

Figure 3E-1
Locations of Fracture Toughness Evaluations
(TN-68 Gamma Shield)

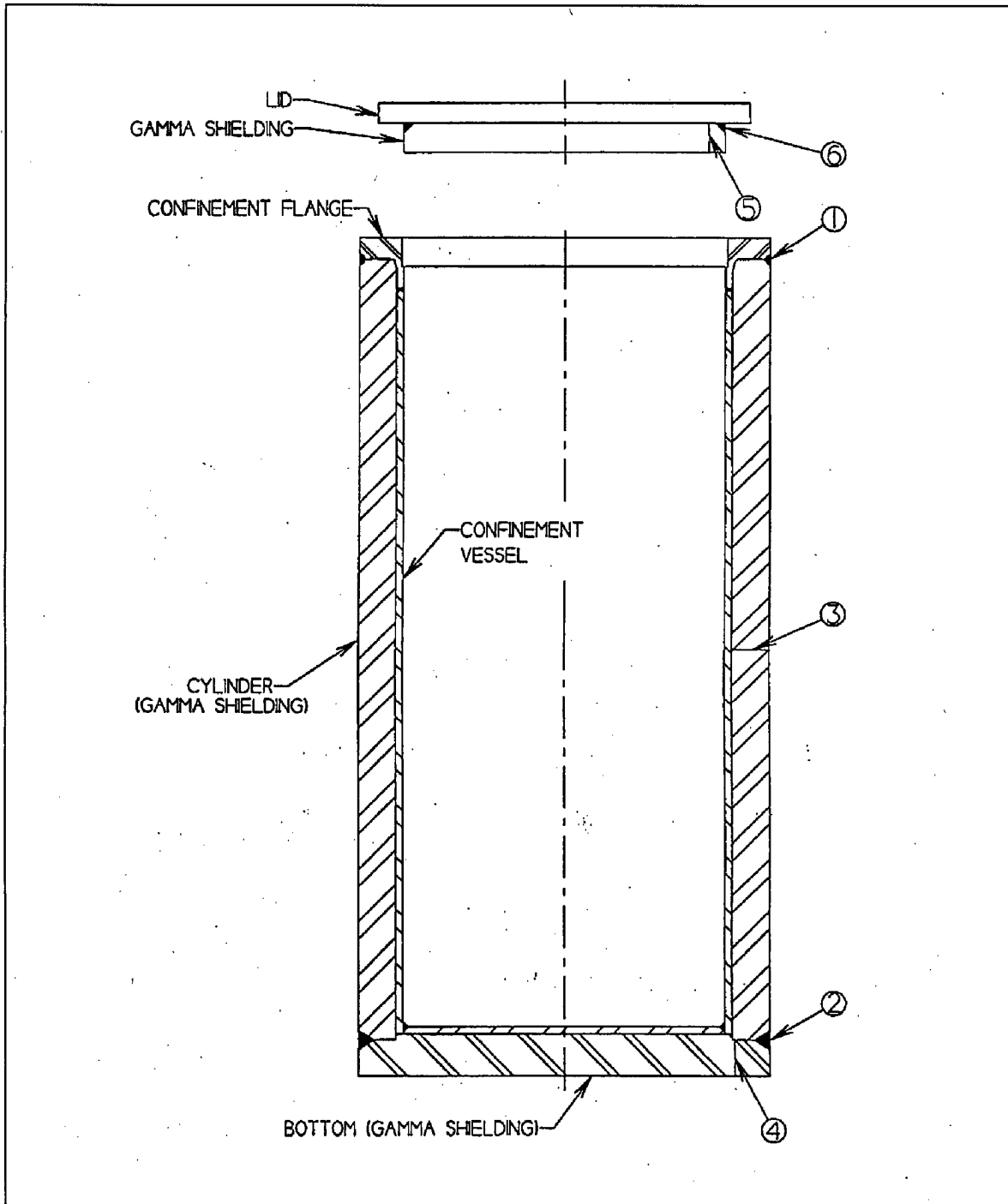


Figure 3E-2
Charpy V-Notch Test -Results for SA-266 Gr. 2

